

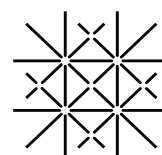
Abstract Volume 13th Swiss Geoscience Meeting

Basel, 20th – 21st November 2015

Modelling the Earth

sc | nat 

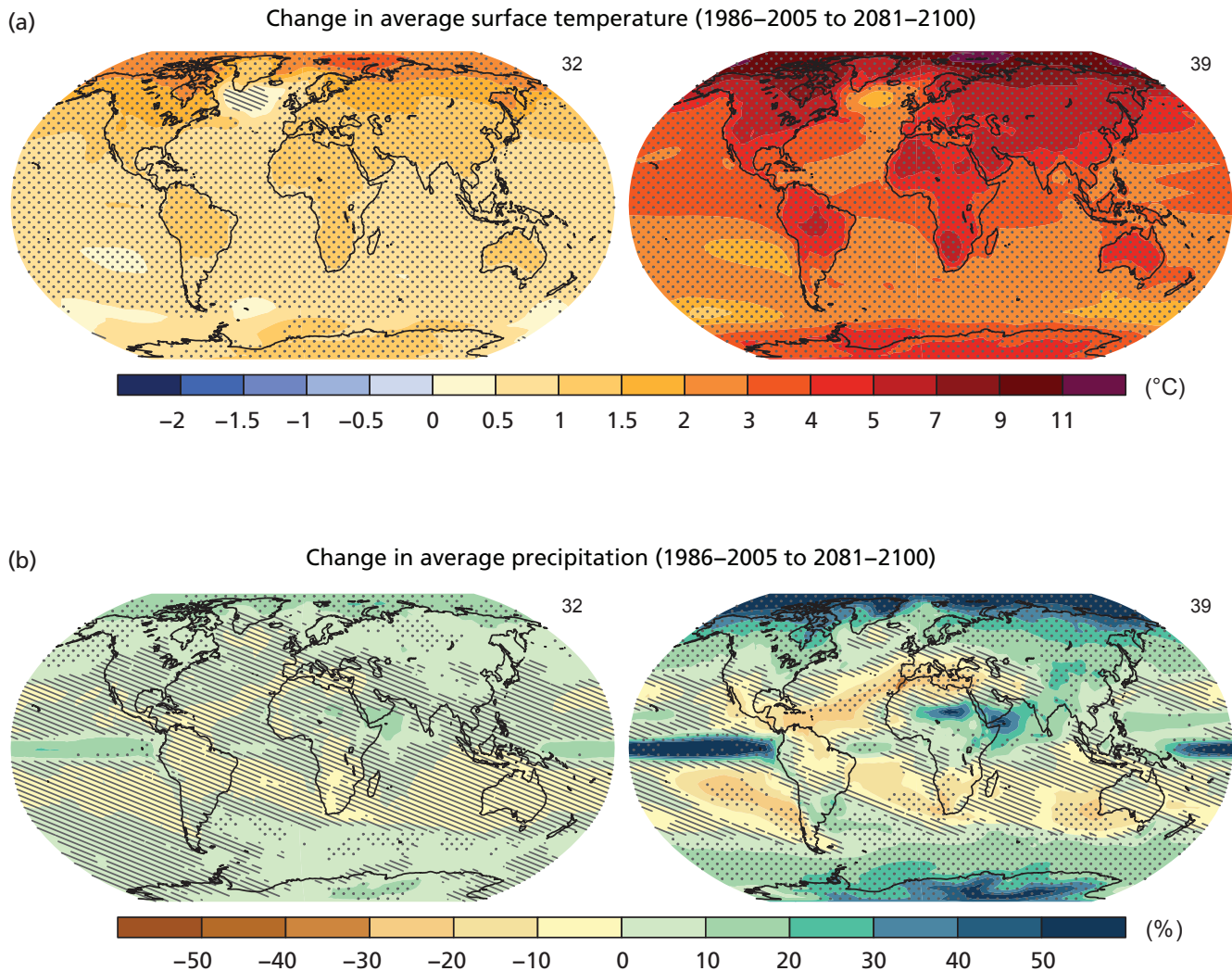
Swiss Academy of Sciences
Akademie der Naturwissenschaften
Accademia di scienze naturali
Académie des sciences naturelles



University
of Basel

RCP 2.6

RCP 8.5



Legend for cover pictures:

The cover pictures are details of the figure above showing projected temperature and precipitation changes by the end of the 21st century under a strong climate mitigation scenario (left) and a business-as-usual scenario (right): Coupled Model Intercomparison Project Phase 5 (CMIP5) multi-model mean projections (i.e., the average of the model projections available) for the 2081–2100 period under the RCP2.6 (left) and RCP8.5 (right) scenarios for (a) change in annual mean surface temperature and (b) change in annual mean precipitation, in percentages. Changes are shown relative to the 1986–2005 period. The number of CMIP5 models used to calculate the multi-model mean is indicated in the upper right corner of each panel. Stippling (dots) indicates regions where the projected change is large compared to natural internal variability (i.e., greater than two standard deviations of internal variability in 20-year means) and where at least 90% of the models agree on the sign of change. Hatching (diagonal lines) indicates regions where the projected change is small compared to natural internal variability (i.e., less than one standard deviation of natural internal variability in 20-year means). (Source: Adapted from Figure SPM.8 of IPCC, 2013: *Summary for Policymakers*. In: *Climate Change 2013: The Physical Science Basis. Contribution of Working Group I to the Fifth Assessment Report of the Intergovernmental Panel on Climate Change* [Stocker, T.F., D. Qin, G.-K. Plattner, M. Tignor, S.K. Allen, J. Boschung, A. Nauels, Y. Xia, V. Bex and P.M. Midgley (eds.)]. Cambridge University Press, Cambridge, United Kingdom and New York, NY, USA, pp. 1–30, doi:10.1017/CBO9781107415324.004.)

13th Swiss Geoscience Meeting, Basel 2015

Table of contents

Organisation	2
--------------	---

Abstracts

1.	Structural Geology, Tectonics and Geodynamics	4
2.	Mineralogy, Petrology, Geochemistry	48
3.	Gemmology	96
4.	Palaeontology	118
5.	Stratigraphy	144
6.	- - -	
7.	Geothermal Energy, CO ₂ Sequestration and Shale Gas	166
8.	Geomorphology	194
9.	Quaternary environments: landscapes, climate, ecosystems, human activity during the past 2.6 million years	228
10.	Cryospheric Sciences	260
11.	Hydrology, Limnology and Hydrogeology	294
12.	- - -	
13.	The International Year of Soils: open session on soil security	334
14.	Biogeochemistry of aquatic and terrestrial realms	334
15.	Atmospheric Processes and Interactions with the Biosphere	354
16.	Phenology and seasonality	
17.	Earth Observation addressing key Earth System processes	354
18.	Geoscience and Geoinformation - From data acquisition to modelling and visualisation	372

Organisation

Host Institution

Department of Environmental Sciences of the University of Basel

Patronnage

Platform Geosciences, Swiss Academy of Sciences

Local Organizing Committee

Stefanie von Fumetti

Christian de Capitani

Christian Meyer

Moritz Lehmann

Helge Niemann

Jacob Zopfi

Franz Conen

Joelle Glanzmann

Karin Liesenfeld

Leander Franz (President SGM 2015)

Coordination

Pierre Dèzes

Participating Societies and Organisations

Federal Office of Topography (swisstopo)
 Forum for Climate and Global Change (ProClim–)
 International Geosphere-Biosphere Programme, Swiss Committee (IGBP)
 International Union of Geodesy and Geophysics, Swiss Committee (IUGG)
 International Union of Geological Sciences, Swiss Committee (IUGS)
 Kommission der Schweizerischen Paläontologischen Abhandlungen (KSPA)
 National Research Programme “Sustainable Use of Soil as a Resource” (NRP 68)
 Swiss Association of Energy Geoscientists (SASEG)
 Swiss Commission on Atmospheric Chemistry and Physics (ACP)
 Swiss Commission for Phenology and Seasonality (CPS)
 Swiss Commission for Remote Sensing (SCRS)
 Swiss Committee for Stratigraphy (Platform Geosciences/SCNAT)
 Swiss Gemmological Society (SGG-SSG)
 Swiss Geodetic Commission (SGC)
 Swiss Geological Society (SGG/SGS)
 Swiss Geological Survey (swisstopo)
 Swiss Geomorphological Society (SGGm/SSGm)
 Swiss Geophysical Commission (SGPK)
 Swiss Geotechnical Commission (SGTK)
 Swiss Geothermal Society (GEOTHERMIE.CH)
 Swiss Hydrogeological Society (SGH)
 Swiss Hydrological Commission (CHy)
 Swiss Paleontological Society (SPG/SPS)
 Swiss Snow, Ice and Permafrost Society (SIP)
 Swiss Society for Hydrology and Limnology (SGHL / SSHL)
 Swiss Society for Quaternary Research (CH-QUAT)
 Swiss Society of Mineralogy and Petrology (SMPG / SSMP)
 Swiss Soil Science Society (SSSS)
 Swiss Tectonics Studies Group (Swiss Geologiocal Society)

1. Structural Geology, Tectonics and Geodynamics

Guido Schreurs, Neil Mancktelow, Paul Tackley

Swiss Tectonics Studies Group of the Swiss Geological Society

TALKS:

- 1.1 Belgrano T., Herwegh M., Berger A.: Brittle reactivation of a mylonitic shear zone network: Inherited controls on fault geometry, architecture and hydrothermal activity
- 1.2 Dielforder A., Berger A., Herwegh M.: The accretion of foreland basin deposits and its effect on early orogenic processes: insights from the north-central European Alps, Switzerland
- 1.3 Fabbri S.C., Herwegh M., Schlunegger F., Volken S., Möri A., Hübscher Ch., Weiss B.J., Schmelzbach C., Horstmeyer H., Anselmetti F. S.: Neotectonic Fault Structures, Sedimentary Infill and Bedrock Topography of Lake Thun
- 1.4 Frehner M. (2015 Paul Niggli Medallist – Invited talk): 3D fold growth in transpression
- 1.5 Houlié N., Woessner J., Rothacher M., Giardini D.: Strain rate and stress field of Switzerland
- 1.6 Hovakimyan S., Moritz R., Tayan R., Harutyunyan M., Rezeau H.: Structural controls, metal distribution and fluid characteristics of the giant Tertiary Kadjaran porphyry Cu-Mo deposit, Tethys metallogenic belt, Armenia, Lesser Caucasus
- 1.7 Lechmann A.K., Burg J.-P., Faridi M.: Late Miocene to Quaternary volcanism in NW Iran Azerbaijan: new geochemical and geochronological data
- 1.8 Masson H., Steck A.: The Maggia-Sambuco nappe : stratigraphy, correlations and tectonic consequences (Central Alps)
- 1.9 Peters M., Herwegh M., Poulet T., Regenauer-Lieb K., Veveakis M.: Boudinage and folding as the same energy bifurcation of elasto-visco-plastic rocks
- 1.10 Sørensen K., Korstgård J.A., Glassley W.E.: A Nagssugtoqidian (W Greenland) crustal profile
- 1.11 Zwaan F., Schreurs G.: Effects of transtension and inherited structures on continental rift interaction in 4D analogue models

POSTERS:

- P 1.1 Abednego M., Blascheck P., Mosar J., Nussbaum C., Joswig M., Bossart P.: Focal Mechanism Analysis of Seismic Events from Microseismic Monitoring in Mont Terri Rock Laboratory, St-Ursanne (JU) : A Workflow
- P 1.2 Aliyev F., Kangarli T., Mosar J.: Analysis of earthquakes focal zones in relation to tectonic structures of the Greater Caucasus (Azerbaijan)
- P 1.3 Akçar N., Yavuz V., Ivy-Ochs S., Nyffenegger F., Fredin O., Schlunegger F.: Rearward landsliding in sensitive clays: February 2011 massive failures at the Çöllolar coalfield, eastern Turkey
- P 1.4 Beaussier S., Gerya T., Burg J.P.: Lateral change in subduction polarity: Insight from 3D thermo-mechanical numerical modeling
- P 1.5 Buchs N., Epard J.-L.: The Nidar Ophiolite and its surrounding units in the Indus Suture Zone (NW Himalaya, India): new field data and interpretations
- P 1.6 Cioldi S., Moulas E., Tajcmanová L., Burg J.-P.: Duration of inverted metamorphic sequence formation across the Himalayan Main Central Thrust (MCT), Sikkim
- P 1.7 Duretz T., Mohn G., Schenker F.L., Schmalholz S.M.: Multi-layer lithospheric extension: implications for Mesozoic rifting in the Alps
- P 1.8 Duretz T., Schmalholz S. M.: Multi-layer extension: implications for the development of ductile shear zones
- P 1.9 Gamkrelidze I., Koiava K., Mosar J.: Geological Structure of Georgia and Geodynamic Evolution of the Caucasus
- P 1.10 Giuntoli F., Manzotti P., Engi M., Ballèvre M.: Structural and metamorphic subdivision of the central Sesia Zone (Aosta Valley, Italy)
- P 1.11 Gruber M., Sommaruga A., Mosar J.: Evidence for Liassic to Dogger synsedimentary normal faulting in the Western Swiss Molasse Basin based on seismic interpretation
- P 1.12 Guerit L., Dominguez S., Malavieille J., Castelltort S.: Deformation of an experimental drainage network in oblique collision
- P 1.13 Humair F., Bauville A., Jean-Epard L., Schmalholz S.: Numerical investigation of the transition between folding and thrusting: applications to the Swiss Jura and Canadian Foothills foreland fold-and-thrust belts
- P 1.14 Jaquet Y., Schmalholz S., Duretz T.: Formation of necking zones during lithospheric rifting
- P 1.15 Kelevitz K., Houlie N., Giardini D., Rothacher M.: Mapping the subsurface with seismic and GPS data
- P 1.16 Kilian R., Morales L., Peters M.: Rheology during high temperature granular flow – inferences from microstructures
- P 1.17 Lu Gang, Winkler W., Willett S., von Quadt A., Fellin M.G., Rahn M., Brack P.: Cenozoic volcanoclastic signatures in sandstones of the Central and Southern Alps: their age, derivation and geodynamic significance – A project layout

- P 1.18 Madritsch H., Naef H., Heuberger S., Meier B.: Tectonics of northern Switzerland's Permo-Carboniferous Trough as inferable from revised and densified 2D-seismic reflection data
- P 1.19 Magott R., Fabbri O., Fournier M.: Shallow interplate seismicity vs. intraplate Wadati-Benioff zone intermediate-depth seismicity: Insights from a structural analysis of Alpine high-pressure ophiolite-hosted pseudotachylytes (Corsica, France)
- P 1.20 Mandal S.K., Fellin M.G., Burg J.-P., Maden C.: Phanerozoic surface history of southern Peninsular India from apatite (U-Th-Sm)/He data
- P 1.21 Mauvilly J., Koiava K., Irakli Gamkrelidze Mosar J.: Tectonics in the Greater Caucasus: a N-S section along the Georgian Military Road – Georgia
- P 1.22 Schmitt N., Grassi R., Miller S.A., Perrochet L., Valley B., Mosar J.: Fault anatomy of the La Sarraz strike-slip fault system
- P 1.23 Normand R., Simpson G., Bahroudi A.: Extreme surface uplift rates revealed by late quaternary marine terraces in the Iranian Makran
- P 1.24 Richter B., Stünitz H., Heilbronner R.: Stresses and pressures at the quartz-coesite transition in deformation experiments
- P 1.25 Schenker F.L., Ambrosi C., Scapozza C., Castelletti C., Maino M.: Preliminary results of the Swiss National Map, sheet Osogna (no. 1293,1:25'000)
- P 1.26 Schmid T., Frehner M.: Parasitic folds with wrong vergence: How asymmetries can be inherited
- P 1.27 Thielmann M.: Thermal localization in a heterogeneous lithosphere
- P 1.28 von Däniken P., Frehner M.: 3D fold geometry at Panixer pass
- P 1.29 Wex S., Mancktelow N., Hawemann F., Camacho A., Pennacchioni G.: Inverted localization of deformation in the “dry” middle crust across the Woodroffe Thrust, Central Australia
- P 1.30 El Hadj Youcef Brahim, Mohamed Chadi, Rami Djefla: About the Autochthony of Constantinois Neritic Shelf (NE Algeria)

1.1

Brittle reactivation of a mylonitic shear zone network: Inherited controls on fault geometry, architecture and hydrothermal activity

Thomas Belgrano¹, Marco Herwegh¹, Alfons Berger¹

¹ *Institute of Geological Sciences, University of Bern, Baltzerstrasse 3, CH-3012 Bern, Switzerland
(thomas.belgrano@students.unibe.ch)*

A late Neogene strike-slip fault and its resident fossil and active hydrothermal systems at Grimsel Pass (Aar Massif, Central Swiss Alps) are mapped and structurally characterised to delineate the structural controls on hydrothermal flow in a crystalline basement fault. We map the fault system, here termed the “Grimsel Breccia Fault” and model it in 3D, using the distinctive mineralisation and active thermal fluid discharge (the highest documented in the Alps) to reveal fluid pathway extent, morphology and structural associations. With progressive uplift and cooling, brittle deformation inherited the mylonitic shear zone network at Grimsel Pass, preconditioning fault geometry into segmented ductile shear zone reactivations and inter-shear zone linkages. We discriminate two types of ‘pipe’ like, vertically oriented pathways: up-flow (1) within major fault linkages and (2) along spatially restricted segments of former ductile shear zones reactivated by brittle deformation. In both cases, low-permeability mylonitic shear zones which were not reactivated provide important hydraulic seals. These observations show that fluid flow along fault planes is not spatially continuous, but rather highly channelised into sub-vertical flow domains, with important implications for the exploration and exploitation of geothermal energy.

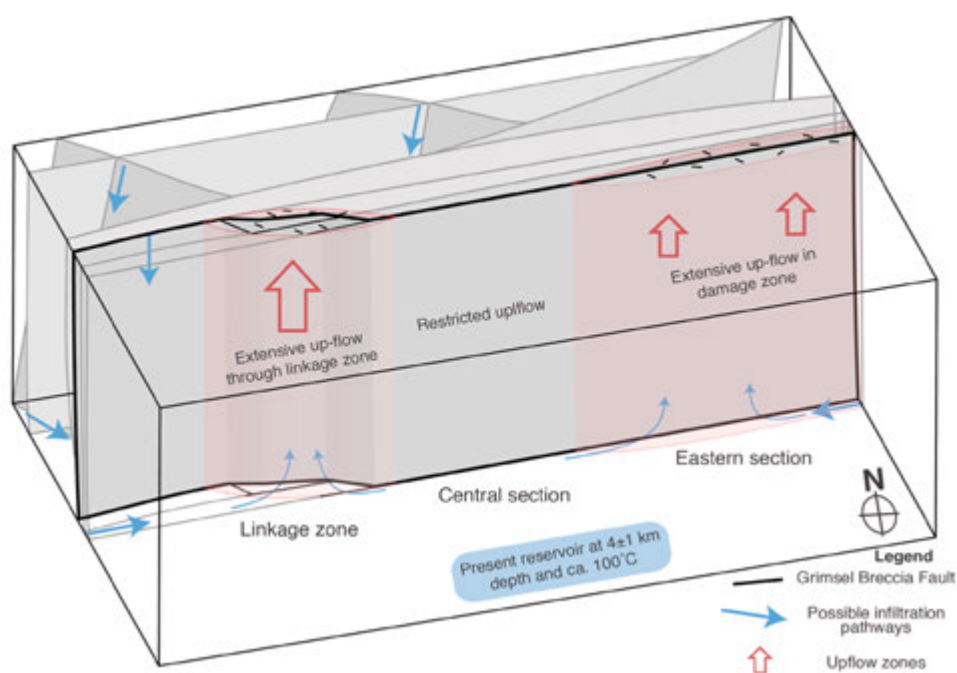


Figure 1. Simplified 3D model of the Grimsel Breccia Fault within a network of Alpine shear zones, with upflow zones and possible infiltration pathways indicated.

1.2

The accretion of foreland basin deposits and its effect on early orogenic processes: insights from the north-central European Alps, Switzerland

Armin Dielforder¹, Alfons Berger¹, Marco Herwegh¹

¹ *Institute of Geological Sciences, University of Bern, Baltzerstrasse 1+3, CH-3012 Bern (armin.dielforder@geo.unibe.ch)*

The north-central European Alps in Switzerland provide unique insights into the tectonic evolution of the orogenic front since the closure of the North Penninic ocean and the impinging of the European passive margin on the subduction zone. The evolution can be divided into four major tectonic phases partly overlapping in space and time. (1) The initiation of the North Alpine Foreland Basin and the subsequent accretion of its early sedimentary infill (the so-called Infrahelvetetic flysch units, IFUs) to the advancing 'Penninic accretionary wedge'. (2) Basal accretion of the Helvetic nappes and thrusting of the nappes along major out-of-sequence thrusts (e.g. Glarus thrust) on top of the IFUs. (3) The shearing off and underplating of the Aar massif along a crustal detachment and (4) the consequent exhumation of the wedge. Interestingly, during the first two phases of the evolution the basal detachment was situated within the sedimentary units above the crystalline European basement (i.e. within the sedimentary basement cover or the accreted flysch units), while with the incipient underplating of the Aar massif the detachment relocated in the European basement, probably along the boundary between the upper and lower continental crust. Although such a down cutting of the detachment into lower structural levels is a common process observed in orogens worldwide, the underlying processes are poorly constrained and remain debated (e.g. van den Beukel, 1992; Seno, 2008).

In our contribution, we discuss how the accretion of the Infrahelvetetic flysch units influenced the tectonic evolution of the orogenic front during out-of-sequence thrusting (OOS-thrusting) and the relocation of detachment into the crystalline basement. First, we present structural observations from the IFUs demonstrating that the sediments were accreted in a unlithified stage and experienced the diagenetic dehydration syntectonically. We argue, that the IFUs provided therefore an effective 'fluid reservoir' keeping the pore fluid in the wedge and along the basal detachment at high values. In a second step, we show that such high pore fluid pressures are actually required for the observed style of OOS-thrusting and result in a tectonic setting that is similar to low-stress subduction zones. Finally, we propose that OOS-thrusting effectively reduced the pore fluid pressure within the system causing an increase in the average shear stress on the basal detachment. We argue that the strengthening of the detachment resulted in the broad locking of the fault and caused a relocation of the deformation to the base of the upper continental crust, where ductile shearing at lower mean shear stresses was possible.

In summary, our study suggest that the prograde evolution of the orogenic front was controlled by the accretion of unlithified foreland basin deposits that promoted high pore fluid pressures and low shear stresses in the upper ~20 km of the wedge, mimicking the setting of low stress subduction zones. At later stages, however, decreasing pore fluid pressures resulted in a strengthening of the basal detachment and promoted the relocation of deformation into the crystalline basement, resulting in a tectonic setting that is commonly considered as 'collisional'.

REFERENCES

- Seno, T. 2008: Conditions for crustal block to be sheared off from the subducted continental lithosphere: What is an essential factor to cause features associated with collision? *Journal of Geophysical Research*, 113, B04414.
- van den Beukel, J. 1992: Some thermomechanical aspects of the subduction of continental lithosphere. *Tectonics*, 11, 316–329.

1.3

Neotectonic Fault Structures, Sedimentary Infill and Bedrock Topography of Lake Thun

Stefano C. Fabbri¹, Marco Herwegh¹, Fritz Schlunegger¹, Stefan Volken², Andreas Möri², Christian Hübscher³, Benedikt J. Weiss³, Cédric Schmelzbach⁴, Heinrich Horstmeyer⁴, Flavio S. Anselmetti⁵

¹ *Institute of Geological Sciences, University of Bern, Baltzerstr. 1+3, CH-3012 Bern (stefano.fabbri@geo.unibe.ch)*

² *Bundesamt für Landestopografie swisstopo, Seftigenstr. 264, CH-3084 Wabern*

³ *Institute of Geophysics, University of Hamburg, Bundesstr. 55, D-20146 Hamburg*

⁴ *Institute of Geophysics, Dept. of Earth Sciences, ETH Zürich, CH-8092 Zürich*

⁵ *Institute of Geological Sciences and Oeschger Centre of Climate Change Research, University of Bern, Baltzerstr. 1+3, CH-3012 Bern*

Perialpine Lake Thun is surrounded by steep mountains with impressive topography and constrained by a basin extending orthogonally to the general strike direction of the Alpine nappe front. The northeastern shoreline is predominantly shaped by the Drusberg-nappe and the Subalpine Molasse fronts, which are in stark contrast to the southwestern shore built by the structurally higher units of the Klippen- and Niesen- nappes. This pattern suggests a major fault along the lake axis and high tectonic activity of the region from Eocene times throughout the Late Miocene (Pfiffner, 2011). The area is dominated today by a strike-slip stress regime with a slight normal faulting component (Kastrup et al., 2004).

Strong historic earthquakes (i.e. intensities $I_0 \geq V$) are well documented in the area by the earthquake catalogue of Switzerland ECOS-09 (e.g. Frutigen, 1729 AD, $M_w=5.2$, $I_0=VI$). Large subaquatic, earthquake-triggered mass movements were recognized to occur frequently in Swiss Lakes (Strasser et al., 2013). Some of these represent the occasional occurrence of even stronger earth-quakes (i.e. $M_w \sim 6.5$) in the Alpine region, which are expected to produce noticeable surface ruptures. Since erosional surface processes complicate the recognition of earthquake-caused topographic offsets, the high preservation potential of a lakefloor and its subsurface is the ideal environment to identify such geomorphologic features recorded in lacustrine sediments.

As part of a multi-disciplinary study that combines geophysical, geological and field methods, all aiming to find potentially active fault structures in the area between Interlaken and Bern, we conducted a multi-channel reflection seismic survey on Lake Thun in March 2015. We used a two-chamber Mini GI Airgun (15/15 in³) in combination with a streamer of 100 m length and 24 channels as acquisition tools and recorded 42 lines with a total length of 183.5 km. Previous seismic surveys on Lake Thun (e.g. Finck et al., 1984) used Airguns and a multi-channel setup as well, though they did not achieve the same resolution as the single-channel Pinger (3.5 kHz) seismic campaign carried out in 2007 (Wirth et al., 2011). The setup used in this survey overcomes the drawbacks of limited resolution and penetration depth, using a state-of-the art airgun. The following processing steps were applied to the data: frequency filtering, muting, velocity analysis, multiple suppression, stacking and post-stack FX-deconvolution, migration and time to depth conversion.

The seismic data set clearly reveals prominent reflections and characteristic seismic facies delineating three main stratigraphic sequences starting with the glacio-lacustrine deposits (Late Glacial to Holocene), underlain by glacial deposits, which in turn overlay bedrock. Total thickness of the Quaternary sedimentary infill amounts to 300 m at the deepest point of the basin.

First neotectonic analysis identified a few sets of normal and reverse faults in the northwestern part of the basin within the glacio-lacustrine deposits that may point to a transpressional strike-slip regime. This zone appears on multiple profiles and lines up with prominent lake floor features and geomorphologic patterns in the surrounding landscape, making it a potential candidate for a fault that is active in the Quaternary period.

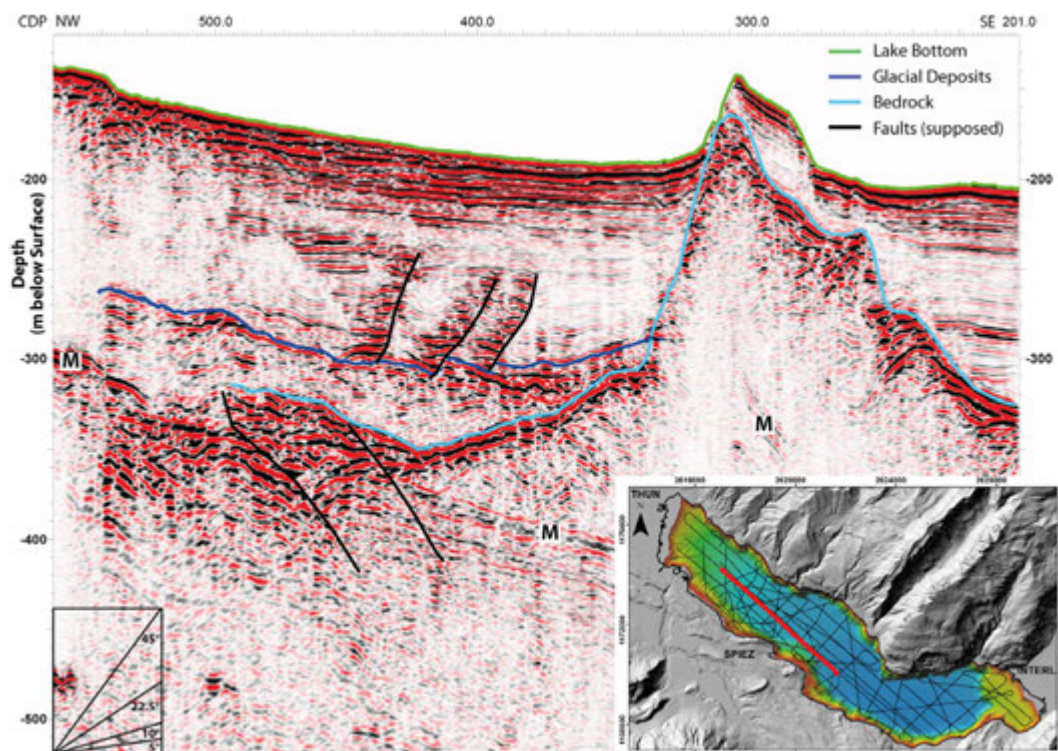


Figure 1: Processed seismic section with preliminary interpretation of glacio-lacustrine sediments, glacial deposits and bedrock horizon. Three similarly oriented fault structures may be part of a larger fault zone recorded on several lines. See inset for location of the line. M: Remnants of surface multiples. CDP spacing: 2m.

REFERENCES

- Finckh, P., Kelts, K., and Lambert, A., 1984: Seismic Stratigraphy and Bedrock Forms in Perialpine Lakes, Geological Society of America Bulletin, 95, p.1118-1128.
- Kastrup, U., Zoback, M. L., Deichmann, N., Evans, K. F., Giardini, D., and Michael, A. J., 2004: Stress field variations in the Swiss Alps and the northern Alpine foreland derived from inversion of fault plane solutions, Journal of Geophysical Research-Solid Earth, 109, p.1-22.
- Pfiffner, O. A., 2011: Structural Map of the Helvetic Zone of the Swiss Alps, including Vorarlberg (Austria) and Haute Savoie (France), Swiss Geological Survey, 1-128.
- Strasser, M., Monecke, K., Schnellmann, M., and Anselmetti, F. S., 2013: Lake sediments as natural seismographs: A compiled record of Late Quaternary earthquakes in Central Switzerland and its implication for Alpine deformation, Sedimentology, 60, p.319-341.
- Wirth, S. B., Girardclos, S., Rellstab, C., and Anselmetti, F. S., 2011: The sedimentary response to a pioneer geo-engineering project: Tracking the Kander River deviation in the sediments of Lake Thun (Switzerland), Sedimentology, 58, p.1737-1761.

1.4

3D fold growth in transpression

(Paul Niggli Medal Lecture)

Marcel Frehner¹

¹ Geological Institute, ETH Zurich, Sonneggstrasse 5, CH-8092 Zurich (marcel.frehner@erdw.ethz.ch)

Geological folds in transpression are inherently 3D structures; hence their growth and rotation behavior is studied using 3D numerical finite-element simulations (Figure 1). Upright single-layer buckle folds in Newtonian materials are considered, which grow from an initial point-like perturbation due to a combination of in-plane shortening and shearing (i.e., transpression with convergence angle α). The resulting fold growth exhibits three components (Figure 2):

Fold amplification (vertical): Growth from a fold shape with low limb-dip angle to a shape with larger limb-dip angle.

Fold elongation (parallel to fold axis): Growth from a dome-shaped (3D) structure to a more cylindrical (2D) structure.

Sequential fold growth (perpendicular to axial plane): Growth of new anti- and synforms adjacent to the initial isolated fold.

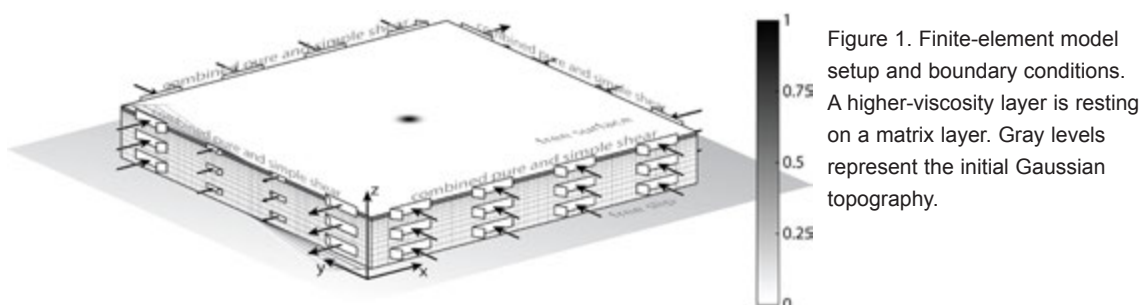


Figure 1. Finite-element model setup and boundary conditions. A higher-viscosity layer is resting on a matrix layer. Gray levels represent the initial Gaussian topography.

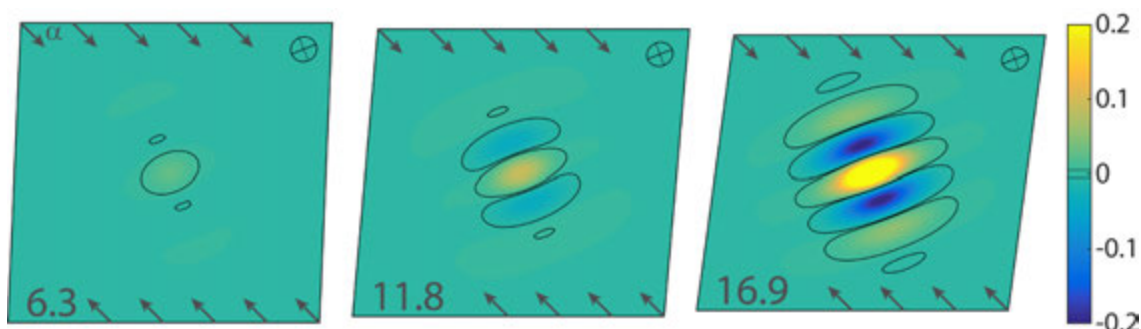


Figure 2. Top view of example numerical simulation with convergence angle $\alpha=45^\circ$. Background strain, ϵ_{bg} (given in %) is increasing from left to right. Colors represent the vertical fold amplitude; black contour lines mark half the initial value ($A_0/2$) defining the individual sequential folds. Each upper-right corner shows the horizontal strain ellipse with its major and minor axes.

Generally, the numerical simulations show that the fold growth rates are smaller for shearing-dominated than for shortening-dominated transpression. In spite of the growth rate, the folding behavior is very similar for the different convergence angles and similar to the previously studied pure-shear case (Frehner, 2014). In particular, the two lateral directions always exhibit similar growth rates implying that the bulk fold structure always occupies a roughly circular area.

Fold axes are always parallel to the major horizontal principal strain axis (λ_{max} , i.e., long axis of the horizontal finite strain ellipse, Figure 2 & 4), which is initially also parallel to the major horizontal instantaneous stretching axis (ISA_{max}). After initiation, the fold axis rotates with λ_{max} (Figure 2 & 4). Sequential folds appearing later do not initiate parallel to ISA_{max} , but parallel to λ_{max} , i.e. parallel to the already existing folds, and also rotate with λ_{max} . Therefore, fold axes are not passive material lines and hinge migration takes place as a consequence.

The numerical results are used to explain the fold axis rotation data of the transpressional analog models of Leever et al. (2011). The model fits the data very well confirming the fold axis rotation with λ_{max} .

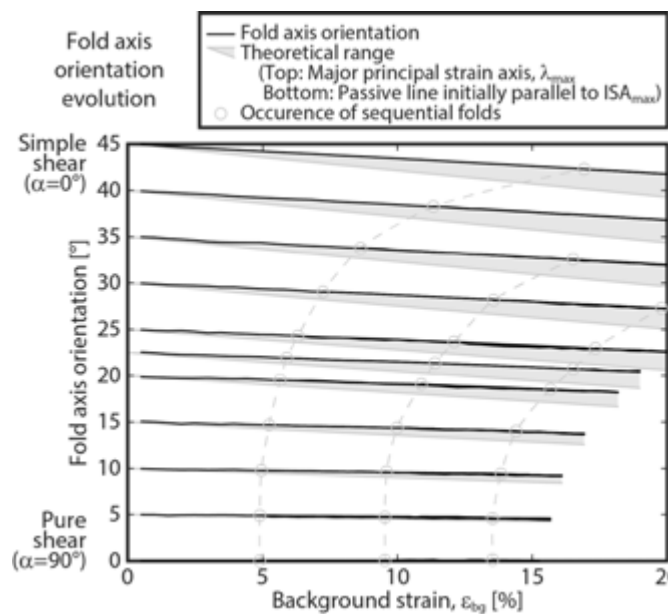


Figure 4. Evolution of fold axis orientation in top view of all individual sequential folds (individual anti- and synforms; black lines) with increasing background strain, ϵ_{bg} , and for different convergence angles (from $\alpha=0^\circ$, simple shear to $\alpha=90^\circ$, pure shear). Gray areas: theoretical range of fold axis orientation (Fossen et al., 2013).

ACKNOWLEDGEMENTS

I thank the Paul Niggli Foundation and the Swiss Society of Mineralogy and Petrology for awarding me with this medal. As this is the medal lecture, I will allow myself to begin the presentation with a short overview of my past research, for which I receive the Paul Niggli Medal.

REFERENCES

- Fossen, H., Teyssier, C. & Whitney, D.L. 2013: Transtensional folding, *Journal of Structural Geology*, 56, 89–102.
- Frehner, M. 2014: 3D fold growth rates, *Terra Nova*, 26, 417–424.
- Leever, K.A., Gabrielsen, R.H., Faleide, J.I. & Braathen, A. 2011: A transpressional origin for the West Spitsbergen fold-and-thrust belt: Insight from analog modeling, *Tectonics*, 30, TC2014.

1.5

Strain rate and stress field of Switzerland

Nicolas Houlié^{1,2}, Jochen Woessner, J.³, Markus Rothacher, M.² and Domenico Giardini ¹

¹ *ETH, Institute of Seismology and Geodynamics, NO F63, Sonneggstrasse 5, CH-8092 Zurich, Switzerland;
Phone: +41 44 633 71 26, Fax: +41 44 633 10 66; Email: nhoulie@ethz.ch*

² *ETH, Institute of Geodesy and Photogrammetry, Wolfgang-Pauli-Str. 15, CH-8093 Zurich, Switzerland*

³ *Swiss Seismological Service, ETH Zürich, Sonneggstrasse 5, Zürich, Switzerland*

In this study we test whether the surface deformation and the seismic activity are in agreement in terms of seismic moment release and stress/strain orientations within the territory of Switzerland. We find that for most of the country, the stress released ($\sim 2.0 \cdot 10^{11}$ Nm/yr) is consistent with the lithosphere deformation ($< 5 \cdot 10^{-8}$ /yr) constrained using the Global Positioning System (GPS). First, south of the Alpine front, we note that surface strain rates displays few agreement with long-term (and deep) deformation of the upper mantle. In this area, we propose that shear strain is being distributed in the upper crust as a result of the clockwise rotation of the Adria plate. Second, for three regions (Basel, Swiss Jura and Ticino), we find that seismic current activity and surface deformation not to be in agreement. In the Basel area, deep seismicity exists while surface deformation is absent. This situation contrasts to what is found in the Ticino and the Swiss Jura, where seismic activity is close to absent but surface deformation is detected ($\sim 2 \cdot 10^{-8}$ /yr). While the surface deformation and seismic activity is inconsistent for the Ticino, we find them to comply in the Valais region. While for the latter, $M_w \geq 6$ events are historically documented, the Ticino faces the potential of damaging earthquakes every hundred to few hundred years, on average.

REFERENCES

Houlié, N., Woessner, J., Giardini, D. and Rothacher, M., Strain rate and stress field of Switzerland, submitted

1.6

Structural controls, metal distribution and fluid characteristics of the giant Tertiary Kadjaran porphyry Cu-Mo deposit, Tethys metallogenic belt, Armenia, Lesser Caucasus

Samvel Hovakimyan^{1,2}, Robert Moritz¹, Rodrik Tayan², Marianna Harutyunyan² & Hervé Rezeau¹

¹ *Earth and Environmental Sciences, University of Geneva, Rue des Maraîchers 13, CH-1205 Genève, Switzerland (samvel.hovak@gmail.com)*

² *Institute of Geological Sciences of the Armenian National Academy of Sciences, 0019 Yerevan, Republic of Armenia*

The Cenozoic evolution of the Tethyan metallogenic belt within the Armenian segment generated the Meghri composite pluton and associated porphyry Cu-Mo and epithermal Au-polymetallic deposits and prospects of the region, including the giant world class Kadjaran porphyry Cu-Mo deposit (2244 Mt reserves, 0.3% Cu, 0.05% Mo and 0.02 g/t Au).

The Kadjaran deposit is hosted by a monzonite intrusion dated at 31.8 Ma (Moritz et al., 2015) belonging to the Meghri pluton. The western part of the deposit is limited by the north-west-oriented Tashtun fault, which traces the contact between the host monzonite and a younger porphyritic granite. The dykes within the deposit are mainly of porphyritic granodioritic composition. They are east-west oriented, and are interpreted to be genetically related to porphyry granitoids of Lower Miocene age (22 Ma) (Tayan, 1984; Moritz et al., 2015). The economic ores are located within the hanging wall, that is on the eastern side of the Tashtun fault. Cu-Mo ore stockwork is recognized along a more than 3.5 km-long and about 2 km-wide corridor.

Beside the Tashtun fault, an important ore-controlling role is the east-west- oriented Voghji fault, which is located along the northern part of the Kadjaran deposit. These east-west-oriented fracture zones are present in the open pit and east-west-oriented porphyritic granodiorite dikes and veins of different mineralization stages are associated with these zones.

Detailed structural mapping and interpretation of stereonet compiling ore-bearing fractures within the stockwork and vein zones allow us to define the main ore-controlling structures and main orientations of veins of the different mineralization stages of the Kadjaran deposit. The Kadjaran deposit is structurally controlled by a steeply dipping (65-85°) orthogonal system of east-west-, north-south and northeast-oriented (45-65°) fractures. The major ore-bearing faults of the deposit host a stockwork mineralization, with veins ranging in thickness from a few mm up to 5 cm. They can attain a length of up to a few tens of meters. They are predominantly shallow-dipping (25-40°), rarely up to 60°, they form parallel to sub-parallel oriented systems of veinlets.

Based on the 3D geological – structural block model of the Kadjaran deposit, based on exploration borehole Mo and Cu concentrations, we were able to define the distribution of these metals and their relationship with the main structures. The ore-enriched areas are zones sub-parallel to the east-west-oriented fractures. In particular, they are located in areas where they crosscut steeply-dipping (70-85°) east-west-, north-south- and northeast-oriented fractures.

On-going fluid inclusion studies are being carried out on quartz samples from the different mineralization stages. Five types of fluid inclusions were distinguished according to their nature, bubble size, and daughter mineral content: vapor-rich (VR), aqueous-carbonic (Ac), brine (B1), polyphase brine (B2) and liquid-rich (LR) inclusions (Fig.1).

Cathodoluminescence (SEM-CL) images reveal four generations of quartz. Molybdenite and chalcopyrite are associated with two different dark luminescent quartz generations, which contain typical brine, aqueous-carbonic and vapour-rich H₂O fluid inclusions, with some of them coexisting locally as boiling assemblages.

Microthermometric studies of fluid inclusions reveal abrupt changes between the early quartz-molybdenite, quartz-chalcopyrite (Th_{total} between 360° and 425°C) and the late quartz- chalcopyrite, quartz-galena-sphalerite vein stages (Th_{total} 300-250°C), which may reflect transition from a porphyry to an epithermal environment in the Kadjaran deposit (Fig.1). This interpretation is supported by field observations, with late vuggy silica and advanced argillic alteration in the central and eastern parts of the deposit. The presence of enargite and tennantite-tetrahedrite in the late paragenesis also supports a high- to intermediate-sulfidation epithermal environment.

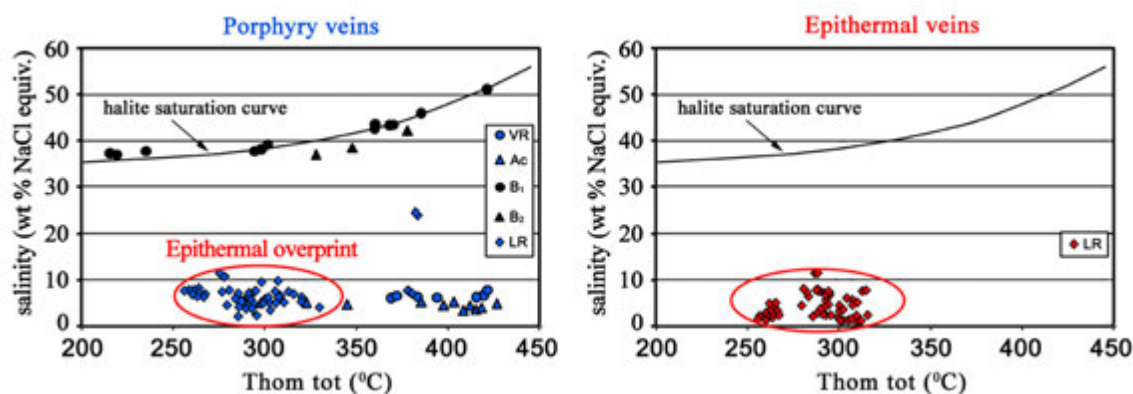


Figure 1. Summary plots of the microthermometric data of all fluid inclusion types of the porphyry and epithermal veins.

REFERENCES

- Moritz, R., Rezeau, H., Ovtcharova, M., Hovakimyan, S., Chiaradia, M., Tayan, R., Melkonyan, R., Ramazanov, V., Ulianov, A., Putlitz, B. 2015: Tethyan subduction to post-subduction magmatic evolution and pulsed porphyry Cu-Mo deposit emplacement in the southernmost Lesser Caucasus. In: Anne-Sylvie André-Mayer et al. (eds), Mineral resources in a sustainable world, 13th SGA Biennial Meeting, 24- 27 August 2015, France, Nancy v.1, p.145-148.
- Tayan, R. 1984: Features of development of fault structures of the Kajaran ore field. Proceedings of the Academy of Sciences of the Armenian SSR, Earth Sciences, V3, p.21-29. (in Russian with English abstract).

1.7

Late Miocene to Quaternary volcanism in NW Iran Azerbaijan: new geochemical and geochronological data

Anna Katharina Lechmann¹, Jean-Pierre Burg¹, Mohammad Faridi²

¹ *Geological Institute, ETH Zurich, Sonneggstrasse 5, CH-8092 Zurich (anna.lechmann@erdw.ethz.ch, jean-pierre.burg@erdw.ethz.ch)*

² *Geological Survey of Iran, Northwestern Regional Office, IR-5133-4359 Tabriz (mfaridi@gsi.ir)*

The Mesozoic to Present geology of Iran has been shaped by the northward subduction of the Neo-Tethys Ocean during convergence and subsequent collision between Arabia and Eurasia, leading to the generation of magmatic arcs and seeding the conditions for the formation of the Turkish-Iranian Plateau. Over this Plateau, Miocene to Quaternary magmatic rocks cover vast areas. Processes, such as lithospheric delamination or slab break-off, which led to this widespread magmatism are still debated.

We present major and trace element analyses together with LA-ICP-MS U-Pb zircon ages of domes and lavas from NW Iran Azerbaijan, with the goal to shed light on the generation and evolution of these recent magmatic rocks and compare them with previously published information. We focused on morphologically prominent domes scattered over the region. The sampled domes, dominantly dacitic to rhyolitic in composition, and the lavas, showing a wide range from basaltic to dacitic and few alkaline compositions, have tholeiitic to calc-alkaline and shoshonitic chemical features. REE patterns are steep and flatten towards the HREE. Plots of primitive mantle normalized trace elements systematically show a negative Nb-Ta anomaly indicating a subduction-modified component in the mantle source and/or crustal contamination.

U-Pb zircon ages on two tuffs and 8 dacites yield two distinct age distributions for both domes and lavas: (1) late Miocene (12.15– 5.62 Ma) and (2) early Pliocene – late Pleistocene (3.78 – 2.18 Ma). Ascribing these two age clusters to trace element compositions reveals that REE patterns became more depleted from late Miocene to late Pleistocene. Isotope compositions will help specifying the nature of the magma source and which processes were more efficient. On a plot of Rb/Sr vs Ba/Rb the samples follow a low Rb/Sr trend typical for an amphibole-bearing mantle source. Coeval lavas in neighbouring regions (e.g. Ararat) show similar major and trace element compositions and the wide compositional variability points to a heterogeneous mantle metasomatized by subduction-derived fluids. This mantle is identified as amphibole-bearing source becoming progressively depleted in trace elements during partial melting.

This work is supported by SNF Research Grant (project 200021_153124/1).

1.8

The Maggia-Sambuco nappe : stratigraphy, correlations and tectonic consequences (Central Alps)

Henri Masson¹, Albrecht Steck¹

¹ *Institut des Sciences de la Terre, Geopolis, Université de Lausanne, CH-1015 Lausanne (henri.masson@unil.ch)*

The Maggia nappe is one of the most puzzling tectonic objects in the Alps, at the center of the Central Alps. Well-known by the works of several pioneers of modern Alpine structural geology, this large, mainly gneissic body nevertheless remains highly enigmatic. The lack of connections and of obvious affinity with any of the surrounding units, and the complexity of its internal geometry, are the main causes of hot controversies with far-reaching consequences. In the past the Maggia has often been considered as tectonically equivalent to the Grand St-Bernard nappe or, in paleogeographical terms, to the Briançonnais domain. More recently its coherence has been disputed and it has been suggested that its N lobe (the Sambuco “spoon”) and its central part (the Maggia *s.str.* “stem”) belong to two distinct nappes of different origin that would be separated by a plate limit (Berger et al. 2007). Here we focus on the stratigraphic analysis of the sedimentary cover of the Sambuco element, defined as the Cristallina zone (Steck et al. 2013). Until now its stratigraphy was nearly completely unknown and even the limits of the nappe were uncertain.

Two types of stratigraphic columns are observed: (1) A “normal” type, that we interpret as a complete stratigraphic series of Triassic to early Mid-Jurassic age. (2) An “incomplete” type, characterized by large stratigraphic gaps, sharp sedimentary unconformities and the local presence of younger rocks.

The complete column starts with thin layers of quartzite and dolomite, ascribed by all authors to the Triassic. The important point is that this Triassic is definitely of Helvetic type and shows no affinity with the Briançonnais Triassic nor with its N extensions such as the “dolomie bicolore” of the Adula (Galster et al. 2012).

Above it comes a thick formation of dark-coloured quartzitic micaschists, rich in garnet, with a few thin intercalations of orange limestone. It forms most of what has been mapped until now in this zone as “Bündnerschiefer”. We name it the Naret Formation. It shows remarkable similarities with the “untere und mittlere Granatschiefer” (Liszkay 1965) or with the “basale Stgair-Serie” (Baumer et al. 1961, Frey 1967) of the Gotthard sedimentary cover. We propose a latest Triassic (Rhaetian) to earliest Liassic age.

The Naret Formation is surmounted by a uniform alternation of thin layers of calcareous sandstones and quartzic limestones, more calcareous at the base, called here the Massari Formation. It looks similar to the Lower Liassic of several Helvetic units, e.g. in the Morcles and Wildhorn nappes. It passes upwards to layers of white quartzite, sometimes with garnet, staurolite and kyanite. We name this characteristic intercalation the Val Sabbia Formation. It can be correlated with the thick quartzite of late Early Liassic (Lotharingian) age, so conspicuous in a large part of the Helvetic domain. It is followed by a thin band of poorly outcropping, brownish calcschist (Middle Liassic?), then by a thick, very uniform formation of black, garnet-rich micaschist which most probably represents the black shale formation of Late Liassic to Early Dogger (Aalenian) age that is nearly omnipresent in the Helvetic domain, e.g. the Coroi Formation of the Gotthard cover.

This whole sequence, interpreted as a complete series of Triassic to Mid-Jurassic age and of Helvetic affinity, is well developed around the Sambuco basement along its NW and N borders, where it is overlain by the Lebendun thrust. But elsewhere the Cristallina sequence can present a very different aspect, forming narrow bands, tightly pinched into the Sambuco basement, mainly made of calcitic, often conglomeratic marbles. Various types of marbles and breccias are so intimately associated that for practical reasons we group them under the name of Lago Scuro Formation. They have been ascribed by all authors to the Triassic, which is impossible for several reasons. The base of the Lago Scuro Formation is deeply erosive and cuts unconformably the Liassic and Triassic formations, reaching frequently the Paleozoic basement. We interpret the Lago Scuro Formation as the Late Dogger to Malm filling of narrow (half-) grabens generated by very active normal faulting, subsequently strongly deformed by Alpine tectonics. The combination of violent paleofault activity with submarine erosion by channelled debris flows at the foot of the fault scarps peeled the older sediments down to the basement.

Bussien et al. (2011) demonstrated the similarity in petrography and age of the Cocco (Maggia stem) and Matorello (Sambuco spoon) granites, a hint that the stem and the spoon, even if cartographically separated (Keller et al. 1980), belong to the same large tectonic unit (the Maggia *s.l.* nappe). Extreme deformation of the Mesozoic sediments on both sides of the stem (Pertusio on the E and Someo *s.str.* on the W; Preiswerk 1912) makes a confirmation by stratigraphic analysis of the sedimentary covers difficult, but preliminary results are compatible with this conclusion.

Conclusions:

1. During the Jurassic the facies of Helvetic type extended much farther S into the pile of the Penninic nappes than supposed until now.
2. In the Cristallina zone the post-Early Dogger sediments are only preserved where the Coroi Formation was scraped off by erosion. Usually these younger rocks have been *décollé* during Alpine orogeny and transported out of the study area on a sole of Coroi shales. Thus the Early Dogger black shales confirm once more their role of main *décollement* horizon in the Helvetic (*s.l.*) domain. A nice counter-example is the neighbouring Antigorio nappe where the absence of black shales (because of Dogger uplift and emersion) ensured the cohesion of the whole stratigraphic column during Alpine tectonics (Matasci et al. 2011).
3. In a broader geodynamical context, the domain of the Maggia-Sambuco nappe, with its spectacular paleofaults, appears as the “necking zone” that makes the transition from the proximal to the distal European continental margin.

1.9

Boudinage and folding as the same energy bifurcation of elasto-visco-plastic rocks

Peters Max¹, Herwegh Marco¹, Poulet Thomas^{2,3}, Regenauer-Lieb Klaus² & Veveakis Manolis^{2,3}

¹ *Institute of Geological Sciences, University of Bern, Switzerland*

² *School of Petroleum Engineering, University of New South Wales, Australia*

³ *CSIRO, North Ryde, NSW Australia*

In classical mechanics literature, boudinage and folding of real elasto-visco-plastic rocks are regarded as a geometric problem. This means that an initially present imperfection, which has an infinitesimal small amplitude, grows within either a linear viscous or incompressible power-law material, and ultimately leads to localization. The heterogeneity and anisotropy of polymineralic rocks in nature often justify this assumption. One drawback of this approach, for instance, is that boudinage and folding develop for different material parameters and/or power-law exponents, although they aim at a uniform description of the onset of localization. In the past, this problem has led to a discussion about the applicability of classical approaches to localized structures in nature (Hobbs et al., 2010 and references therein). Here, we are therefore concerned with an alternative, more generic localization theory, i.e. strain localization out of steady state in a homogeneous material at a critical material parameter and/or deformation rate.

We first discuss the validity of the material bifurcation theory for the onset of *dynamic* localization in ductile rocks (Regenauer-Lieb and Yuen, 2004) to geological applications, as recently applied in pinch-and-swell structures (Peters et al., 2015). In such a framework, instability arises out of the constitutive description. Strain localization is then studied out of homogeneous state for a critical set of parameters, i.e. the critical amount of shear heating and the critical layer width (Gruntfest, 1963). The resulting elasto-visco-plastic system of equations is solved in a 3-layer pure shear box setting, for constant velocity conditions, with the open-source finite element software package *REDBACK*¹.

We show by our numerical experiments that folding develops for the same material parameters and power-law exponent as boudinage, by simply inverting the sign of displacement. Boudinage and folding instabilities occur when the mechanical work, which is translated into heat, overcomes the diffusive capacity of the system. Both instabilities develop for the exact same dissipation number. Thus, folding and boudinage can consistently be treated as the same material failure mode due to fundamental energy bifurcations triggered by dissipative work out of homogeneous state. In future, our study will allow structural geologists to study localization phenomena of rate-and temperature-sensitive materials in terms of material parameters and critical deformation conditions.

REFERENCES

- Gruntfest, I.J. (1963). Transactions of the Society of Rheology, 7.
 Hobbs, B.E., Regenauer-Lieb, K. and Ord, A. (2010). Journal of Structural Geology, 32.
 Peters, M., Veveakis, M., Poulet, T., Karrech, A., Herwegh, M. and Regenauer-Lieb, K. (2015). Journal of Structural Geology, 78.
 Regenauer-Lieb, K. and Yuen, D. (2004). Physics of the Earth and Planetary Interiors, 142.

1) <http://github.com/pou036/redback.git>

1.10

A Nagssugtoqidian (W Greenland) crustal profile

Kai Sørensen¹, John A. Korstgård² & William E. Glassley³ ²¹ Retired, Geological Survey of Denmark and Greenland (kai.sorensen@hotmail.com)² Department of Geoscience, University of Aarhus, DK 8000 Århus C, Denmark³ University of California, Davis, California 95616, U.S.A.

The Nagssugtoqidian mobile belt of west Greenland illustrates some remarkable features: the wholesale deformation and metamorphism of a regional dyke swarm (the Kangamiut dykes) and the occurrence of three major shear zones traceable from coast to the Inland Ice: from N to S they are 1) the Nordre Strømfjord shear zone (NSSZ), 2) the Nordre Isortoq Zone, and 3) the Ikertog Zone. Pioneering work was done by Hans Ramberg (1949) on the Kangamiut dykes and Arthur Escher (referenced in Escher et al., 1976) on the structural segmentation. Most early workers (but not Ramberg) assumed the Nagssugtoqidian to consist of reworked Archean gneisses, but later isotopic work demonstrated the occurrence of (early Proterozoic) juvenile metasediments and igneous rocks (most prominent: Arfersiorfik Quartz Diorite) leading Kalsbeek et al (1987) to suggest the Nagssugtoqidian to be a result of collisional tectonics. Despite the extensive work done in the orogen no proper and properly scaled model of the Nagssugtoqidian crust exists. We have lately found evidence for HP and UHP metamorphism (Glassley et al., 2014) in the northernmost part of the Nordre Strømfjord shear zone which we accordingly interpret as the Nagssugtoqidian suture

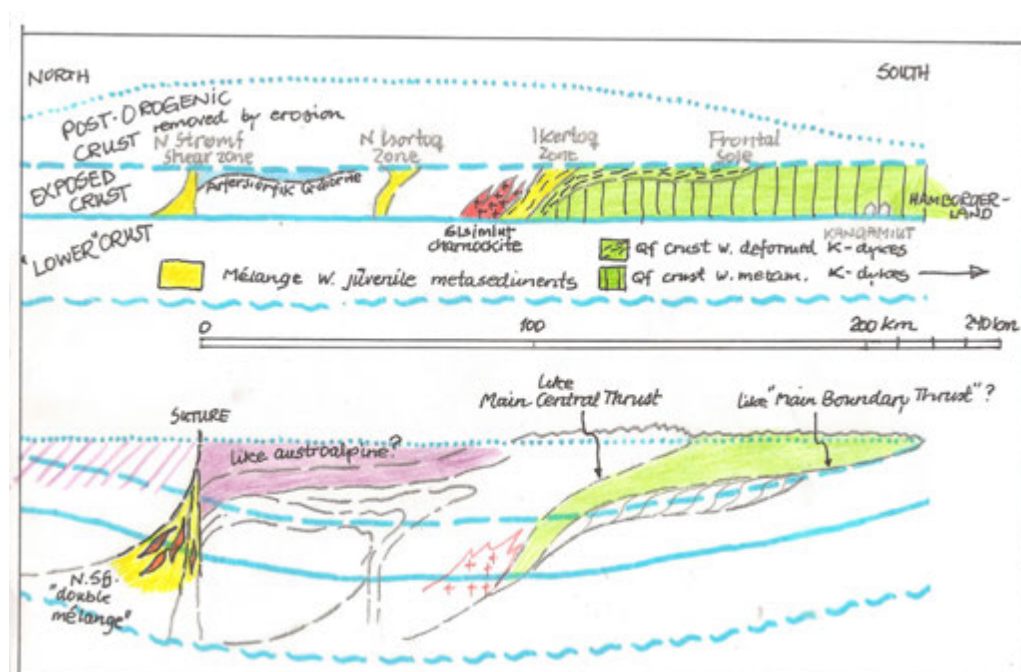


Figure 1. Crustal Profile through the nagssugtoqidian. Colored band above: the depth interval accessible to direct observation. Below: Speculative synorogenic crustal profile. Further explanation: see text. The profiles reflect work in progress and that the Nordre Isortoq Zone is only poorly known. No vertical exaggeration.

The gravity and geology suggest that in general the deepest crustal levels are exposed along the coast and the most shallow levels along the Inland Ice. In the uppermost part of Fig. 1 this width of exposed crust carries coloring depicting the three major shear zones, the Arfersiorfik Quartz Diorite, the Sisimiut charnockite and the foreland region with deformed and undeformed but metamorphosed Kangamiut dykes. Significant metamorphism of the dykes can be traced as far south as to Hamburger Land. Present day crust varies in thickness between 48 to 35 km: between the broken blue line and wavy line in Fig. 1.

Our interpretation of the synorogenic crust – the orogenic wedge, with the dotted upper surface of upper part of figure horizontalized – appears as the lower part of Fig. 1, where we freely allude to Alpine and Himalayan analogies. Obs! the width of the orogen as measured from the NSSZ to Hamburger Land is similar to that seen within the Himalayas (Tsangpo suture to the Siwaliks on the order of 250 km).

Rock assemblages in the three major shear zone can be termed lithospheric melanges (sensu Trommsdorff, 1990), and at least the northern part of the NSSZ as a double melange: the matrix of the lithospheric melange being in itself an ophiolitic melange (sensu Gansser, 1974). Estimating the thickness of crust removed from metamorphic PT estimates suggest the amount removed as that between the broken blue and the dotted blue in the upper part of figure 1. It appears that the distinct segmentation of the presently exposed Nagssugtoqidian reflects a number of thrust ramps which may have developed as parts of asynchronous foreland propagating thrusts. The involvement of one or two microcontinents cannot be excluded.

REFERENCES

- Gansser, A. 1974: The ophiolitic melange, a world wide problem on Tethyan examples. *Eclog. Helv.* 67, 479-507.
- Glassley, W.E., Korstgård, J.A., Sørensen, K. & Platou, S.W., 2014: A new UHP metamorphic complex in the 1.8 Ga Nagssugtoqidian Orogen of West Greenland. *American Mineralogist* 99, 1315-1334
- Escher, A., Sørensen, K. & Zeck, H.P. 1976: Nagssugtoqidian mobile belt of West Greenland. In Escher, A. & Watt, W.S. (eds.) *Geology of Greenland*, 77-95. GGU Copenhagen.
- Kalsbeek, F., Pidgeon, R.T. & Taylor, P.N. 1987: Nagssugtoqidian mobile belt of Western Greenland: cryptic suture between two Archean continents – chemical and isotopic evidence. *Earth Planet. Sci. Lett.*, 985, 354-385
- Ramberg, H., 1949: On the petrogenesis of the gneiss complexes between Sukkertoppen and Christianshaab, West Greenland. *Meddr. Dansk Geol. Forening* 11, 312-327.
- Trommsdorff, V. 1990: Metamorphism and tectonics in the Central Alps: the Alpine lithospheric melange of Cima Lunga and Adula. *Mem. Soc. Geol. It.* 45, 39-49.

1.11

Effects of transtension and inherited structures on continental rift interaction in 4D analogue models

Frank Zwaan¹, Guido Schreurs

¹ *Institute of Geological Sciences, University of Bern, Baltzerstrasse 1 + 3, CH-3012 Bern (frank.zwaan@geo.unibe.ch)*

INTRODUCTION

The interaction of individual rift segments determines the evolution of a rift system and subsequent continent break-up. Inherited heterogeneities control where initial rifts will form and since these are often not properly aligned, rift segments form separately and need to interact. Another important factor affecting rift-segment interaction is the obliquity of plate divergence (transtension), which also promotes continent break-up (Brune et al., 2012).

Both analogue and numerical techniques have been used to model rift interaction (e.g. Acocella et al., 1999; Allken et al., 2012) but transtension has never been applied. Here we present a first-order analogue study that elaborates upon earlier studies by assessing the effects of (1) transtension, (2) rift offset and (3) presence and geometry of additional inherited weak zones that link rift segments. An improved analogue set-up allows more freedom in inherited structure geometry. Model analysis with X-Ray Computer Tomography (CT) techniques reveals internal structures in 3D and with time (4D).

RESULTS

Our experiments yield the following results:

- Increasing the degree of transtension (decreasing angle α , see Fig. 1a) controls the general rift structures. Wide rifts form in orthogonal divergence settings, narrower rifts with oblique internal structures occur under transtensional conditions and narrow strike-slip dominated systems develop towards the strike-slip domain;
- Rift interaction through transfer zones (hard linkage) is generally promoted by 1) decreasing rift offset and 2) increasing the degree of transtension. However, initial rift linkage might involve the formation of accommodation zones (soft linkage) and associated relay ramps due to the interplay of divergence direction and rift offset;
- Rift-linking weak zones have little effect on rift interaction, unless they are oriented ca. perpendicular to the divergence direction;
- Since the orthogonal divergence models resemble natural examples (Fig. 1b), our transtension models might predict what structures can be expected in natural transtension settings.

OUTLOOK

Work in progress involves the influence of more complex inherited structure geometry and of dextral and sinistral transtension. Future work will test the effects of changing divergence rates along strike (scissorlike divergence).

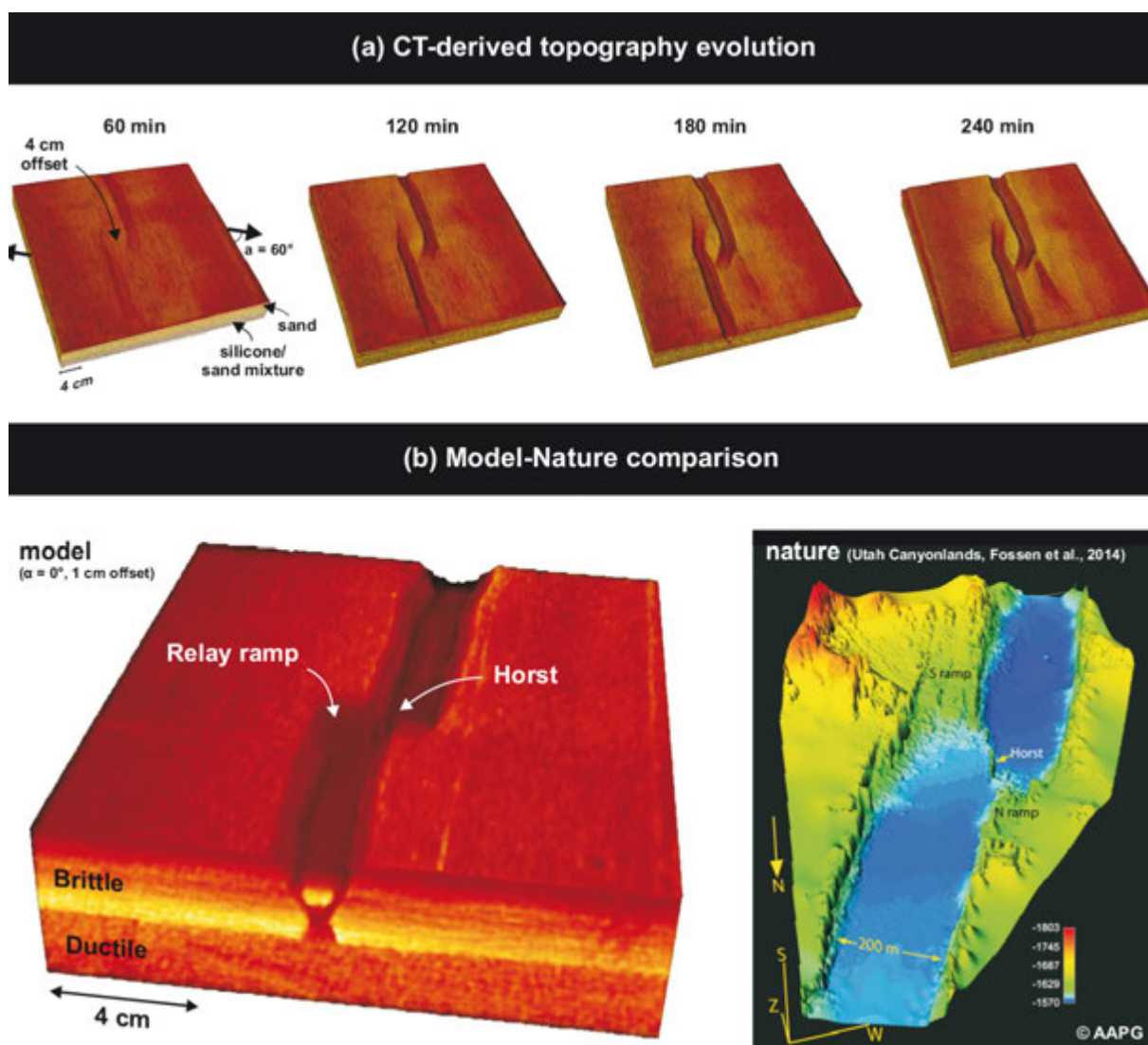


Figure 1. a) CT-derived model topography evolution. b) Model-nature comparison: to the left CT-derived model topography that resembles the Devils Lane stepover (Canyonlands, Utah) to the right. Modified after Fossen et al. (2010) and © AAPG.

REFERENCES

- Acocella, V., Faccenna, C., Funiciello, R. & Rossetti, F. 1999: Sand-box modelling of basement-controlled transfer zones in extensional domains. *Terra Nova* 11, 49-156.
- Allken, V., Huismans, R. S. & Thieulot, C. 2012: Factor controlling the mode of rift interaction in brittle-ductile coupled systems: A 3D numerical study. *Geochemistry, Geophysics, Geosystems* 13, Q05010.
- Brune, S., Popov, A. A. & Sobolev, S. V. 2012: Modeling suggests that oblique extension facilitates rifting and continental break-up. *Journal of Geophysical Research* 117, B08492.
- Fossen, H., Schultz, R. A., Rundhovde, E., Rotevatn, A. & Buckley, S. J. 2010: Fault linkage and graben stepovers in the Canyonlands (Utah) and the North Sea Viking Graben, with implications for hydrocarbon migration and accumulation. *AAPG Bulletin* 94, 597-613.

P 1.1

Focal Mechanism Analysis of Seismic Events from Microseismic Monitoring in Mont Terri Rock Laboratory, St-Ursanne (JU) : A Workflow

Martinus Abednego¹, Patrick Blascheck², Jon Mosar¹, Christophe Nussbaum³, Manfred Joswig², Paul Bossart³

¹ *Earth Sciences, Department of Geosciences, University of Fribourg, Chemin du Musée 6, CH-1700 Fribourg (martinussatiapurwadi.abednego@unifr.ch)*

² *Institut für Geophysik, Universität Stuttgart, Azenbergstr. 16, 70174 Stuttgart, Deutschland*

³ *Mont Terri Project, Federal Office of Topography swisstopo, Fabrique de Chaux, CH -2882 St-Ursanne*

Since April 2014, two mini-array seismographs (Seismic Navigating System / SNS) [Joswig, 2008] were installed in the Mont Terri underground rock laboratory to monitor seismic activity in the vicinity of the laboratory in St-Ursanne (JU). Two additional SNS were installed respectively on July and September 2015 at the surface near the area of the rock laboratory. Seismic events were detected and catalogued remotely by the Geophysics Institute of Stuttgart University from the seismic records of the SNSs and the permanent seismographs of the Swiss Seismological Service (SED) using NanoSeismicSuite detection and location methodology [Sick et al., 2012]. This monitoring allows us to catalogue microseismicity ($M_L \approx -2.0$ to 2.0) which is used for geological and tectonic analysis to characterize seismogenic tectonic faults in the vicinity of the rock laboratory.

During the excavation of the rock laboratory, orientations of existing faults and striae were measured, documented, and mapped [Nussbaum et al., 2011]. On the basis of these measurements, groups of fault orientations and sense of slips were determined. These groups derive 7 focal mechanisms which are 1 group of SSE-dipping, 3 groups of SW-dipping, 2 groups of NNE-trending, and 1 group of Sub-Horizontal. Each focal mechanisms produces specific synthetic waveform at each seismographs near the laboratory.

Due to the low energy content of the microseismic events, focal mechanism determination through first motion analysis [Reasenber & Oppenheimer, 1985] is not applicable. Therefore, this scientific poster presents a workflow to attribute the known focal mechanism near the laboratory to the seismic events catalogued by correlating the synthetic and the recorded seismograms.

REFERENCES

- Joswig, M. 2008: Nanoseismic monitoring fills the gap between microseismic networks and passive seismic, *First Break*, 26, 121-128.
- Nussbaum, C., Bossart, P., Amann, F. & Aubourg, C. 2011: Analysis of tectonic structures and excavation induced fractures in the Opalinus Clay, Mont Terri underground rock laboratory (Switzerland), *Swiss Journal of Geosciences*, SP Birkhäuser Verlag Basel, 104, 187-210.
- Reasenber, P. & Oppenheimer, D. 1985: FPFIT, FPLOT, and FPPAGE: FORTRAN computer programs for calculating and displaying earthquake fault plane solutions, U. S. Geological Survey, U.S. Dept. of the Interior, Geological Survey : [Books and Open-File Reports Section, distributor].
- Sick, B., Walter, M. & Joswig, M. 2012: Visual Event Screening of Continuous Seismic Data by Supersonograms, *Pure and Applied Geophysics*, SP Birkhäuser Verlag Basel, 1-11.

P 1.2

Analysis of earthquakes focal zones in relation to tectonic structures of the Greater Caucasus (Azerbaijan)

Fuad Aliyev¹, Talat Kangarli¹ & Jon Mosar²

¹ Institute Geology and Geophysics of Azerbaijan, Azerbaijan National Academy of Sciences, H. Javid av. 119, AZ-1143 Baku, Azerbaijan

² Department of Geosciences, University of Fribourg, Ch. Du Musée 6, 1700 Fribourg (jon.mosar@unifr.ch)

As part of the Alpine-Himalayan orogenic belt the Caucasus is located between the converging European (Scythian) and Arabian plates. The northward directed collision of the Arabian plate induces continued shortening in the larger Caucasus region. This deformation is expressed by an intense and important seismicity in the whole area.

Important and destructive historical and recent earthquakes have occurred on the southern slopes of the Greater Caucasus in Azerbaijan and Georgia. More recently in Azerbaijan the instrumental registration has made it possible to record ever weaker earthquakes. Since 2002 digital seismic stations allow for a more detailed analysis. Hereafter, we discuss the spatial distribution and tectonic significance of these earthquakes in the region of Azerbaijan.

Several main tectonic zones can broadly be distinguished in Azerbaijan: in the offshore domain the South Caspian Sea forms an initiating N-directed subduction zone beneath the Absheron Ridge at the southern edge of the Middle Caspian Sea. To the south the Lesser Caucasus forms the transition zone to the Arabian plate. To the north the Greater Caucasus forms an important doubly vergent orogenic wedge with important S-directed thrusting. The Kura Basin, between the Lesser and Greater Caucasus, forms a deep flexural foreland basin to the Greater Caucasus.

Based on the analysis of the some 22638 digitally recorded earthquakes we can discriminate different tectonic regimes with distinct characteristics. Thus the 3D and 2D spatial analyses reveals some major clusters in the foothills of the Greater Caucasus, in the transition zone towards the Caspian Sea and in the Caspian Sea. The analysis of focal mechanisms shows a similar distinction with reverse faulting, strike-slip and normal faulting. The analysis of the cumulative frequency of the earthquakes yields the b-factor. This b-values varies with distinct tectonic regimes and in our analysis we can discriminate 3 different b-values: 0.81 associated with thrusting, 0.9 associated with strike-slip, and 1.1 correlated with normal faulting.

All three approaches concur to discriminate several different tectonic regimes: a) thrusting/reverse faulting associated with the thrust tectonics of the Greater Caucasus; b) strike-slip faulting associated with the complex N-S oriented transition zone from the Kura Basin/Greater Caucasus to the very deep S Caspian Sea, floored by oceanic crust, and c) normal faulting associated with the upper parts of the beginning subduction zone of the S Caspian Sea towards the N under the Absheron Ridge.

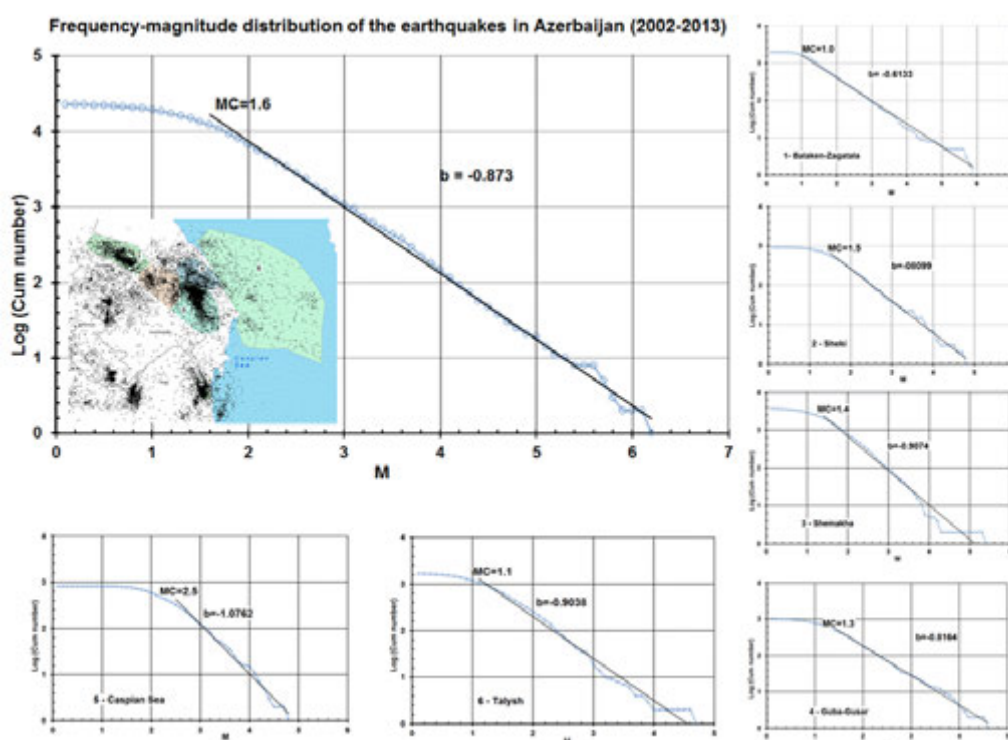


Figure 1. Frequency-magnitude distribution of the earthquakes in Azerbaijan for all earthquakes and for different zones (map in inset). MC = magnitude of completion; b = b-value (slope of curve).

P 1.3

Rearward landsliding in sensitive clays: February 2011 massive failures at the Çöllolar coalfield, eastern Turkey

Naki Akçar¹, Vural Yavuz², Susan Ivy-Ochs³, Franziska Nyffenegger^{1,4}, Ola Fredin^{5,6}, Fritz Schlunegger¹

¹ *Institute of Geological Sciences, University of Bern, Baltzerstrasse 1-3, CH-3012 Bern, (akcar@geo.unibe.ch)*

² *Faculty of Mines, Istanbul Technical University, TR-80626 Maslak, Istanbul*

³ *Laboratory of Ion Beam Physics (LIP), ETH Zurich, Otto-Stern-Weg 5, CH-8093 Zurich*

⁴ *Institut Siedlungsentwicklung und Infrastruktur, Berner Fachhochschule, Pestalozzistrasse 20, CH-3401 Burgdorf*

⁵ *Geological Survey of Norway (NGU), P.O. box 6315 Sluppen, NO-7491 Trondheim*

⁶ *Norwegian University of Science and Technology (NTNU), NO-7491 Trondheim*

The Elbistan basin is an intramontane basin, which is located in the eastern Turkey and bound by the Taurus and Antitaurus Mountains. The basin covers an area of 900 km² at a mean elevation of about 1200 m. The basement rock in this field is karstic limestone, which is overlain by a thick layer of clay (>100 m), followed by 20-50 m thick Lignite series that is overlain by the 20-50 m thick Gytja sequence. These deposits are overlain by Quaternary deposits, comprising the top surfaces of the terraces of the Hurman River, which drains the surface and ground water from the surrounding hills to the northeast towards the center of the Elbistan basin.

The Çöllolar open pit mine, situated in the northwestern sector of the Elbistan basin, contains 90 km² of mineable coal which has been excavated since 2008. In February 2011, two landslides in which 10 workers were killed, occurred in this field. Of the two landslides, the 2nd and largest which covers an area of ca. 2.3 km², was caused by the collapse of the northeastern wall of the open-pit mine. The failure was made of successive rearward collapses with the debris flowing into the open-pit. In this study, we focus on the geologic factors that led to instability and the trigger of the landslides. To reveal these factors, we employ sedimentological and geotechnical analysis of deposits, with a special emphasis on the Pliocene lacustrine carbonaceous sediments and the sensitivity of the overlying Quaternary clays.

First results from the fieldwork and the mineralogical composition and physical properties of the collected samples indicate that the landslide was caused by the liquefaction of one of the layers within the thick sequence of this part of the Elbistan basin based on the flow style of the movement and nature of the failure. In brief, we conclude that massive failures at the Çöllolar coalfield are unique examples of sensitive clay landslides occurred in a subtropical arid region beyond the extent of Quaternary glaciations.

P 1.4

Lateral change in subduction polarity: Insight from 3D thermo-mechanical numerical modeling

Stephane Beaussier¹, Taras Gerya², Jean-Pierre Burg¹

¹ *Geological Institute, ETH Zurich, Sonneggstrasse 5, CH-8092 Zurich
(stephane.beaussier@erdw.ethz.ch, jean-pierre.burg@erdw.ethz.ch)*

² *Institute of Geophysics, ETH Zurich, Sonneggstrasse 5, CH-8092 Zurich (taras.gerya@erdw.ethz.ch)*

Many orogenies display along-strike variations in their orogenic wedge geometry. For instance, the Alps is an example of lateral changes in the subducting lithosphere polarity. High resolution tomography has shown that the southeast dipping European lithosphere is separated from the northeast dipping Adriatic lithosphere by a narrow transition zone at about the “Judicarian” line (Kissling et al. 2006). The formation of such 3D variations remains conjectural.

Previous study from Luth et al. (2013), used analogue modeling to investigate the lateral coupling between two domains of opposing subduction polarity. Yet, its initial setting imposes the lateral polarity change. Conversely, we investigate the conditions that can spontaneously induce such lithospheric structures, and intend to identify the main parameters controlling it.

Using the 3D thermo-mechanical code, I3ELVIS (Gerya and Yuen 2007) we modeled a Wilson cycle starting from a heterogeneous continental lithosphere in an extensional setting resulting in continental breakup and oceanic spreading. At a later stage, divergence is gradually reversed to convergence, which induce subduction of the oceanic lithosphere formed during oceanic spreading. In this model, all lateral and longitudinal structures of the lithospheres are generated self-consistently, and are consequences of the initial continental structure, tectono-magmatic inheritance, and material rheology.

Our first results indicate that lateral changes of subduction polarity are controlled by the angle between the plate suture and the shortening direction and enable by rheological weakening of incipient subduction interface due to hydration. The geometry of the transition zone between domains with different subduction polarity seems to be mainly controlled by rheological parameters defining brittle/plastic yielding conditions for the lithosphere.

REFERENCES

- Gerya, T. V., and D. A. Yuen. 2007: “Robust Characteristics Method for Modelling Multiphase Visco-Elasto-Plastic Thermo-Mechanical Problems, *Physics of the Earth and Planetary Interiors*, 163 (1-4), 83–105.
- Kissling, E., S. M. Schmid, R. Lippitsch, J. Ansorge, and B. Fugenschuh. 2006: *Lithosphere Structure and Tectonic Evolution of the Alpine Arc: New Evidence from High-Resolution Teleseismic Tomography*, Geological Society, London, *Memoirs*, 32 (1), 129–45.
- Luth, S, E. Willingshofer, D. Sokoutis, and S. Cloetingh. 2013: Does Subduction Polarity Changes below the Alps? *Inferences from Analogue Modelling*, *Tectonophysics*, 582, 140–61.

P 1.5

The Nidar Ophiolite and its surrounding units in the Indus Suture Zone (NW Himalaya, India): new field data and interpretations

Nicolas Buchs¹ & Jean-Luc Epard¹

¹ *Institut des sciences de la Terre (ISTE), University of Lausanne, Géopolis, CH-1015 Lausanne (Nicolas.Buchs@unil.ch)*

The Nidar Ophiolite is located between the North Himalayan nappes and the Indus Suture Zone in NW Himalaya in eastern Ladakh (India). Based mainly on geochemical argument, this ophiolite is classically interpreted as a relic of an intra-oceanic arc (Mahéo et al. 2000; Mahéo et al. 2004), which developed at around 140 Ma, prior to the collision between the Indian and Eurasian plates (Ahmad et al. 2008).

From top to bottom, this ophiolite is composed of various sedimentary rocks (radiolarites, polygenic conglomerates and carbonates), volcanic rocks (pillow lavas, basaltic to andesitic in composition), gabbros (Fe- and layered gabbros, pegmatites and minor troctolites), serpentinites, dunites, pyroxenites and peridotites (mainly harzburgites). The Nidar Ophiolite underwent an anchizonal metamorphism with preservation of primaries structures (layering) and volcanic textures (pillow lavas). This study is mainly focused on new field observations across the ophiolite and the surrounding units. A new detailed geologic map of the ophiolite between the Nidar village and Kyun Tso area is presented.

The upper part of the ophiolitic complex is an alternation of volcanic and sedimentary rocks (500-1000 m thick) and the lower part consists of large outcrops of gabbros (3000m thick). These mafic rocks are separated from the serpentinitized ultramafic rocks by a 200m thick ophiolitic breccia and continental Indus Molasse slices. The Nidar Ophiolite is made up of the classical rock type succession (ultramafites, gabbros, pillow basalts, radiolarites), but the internal structure is far more complex than previously suggested. New field data (geologic and structural maps, lithologic sections, etc.) coupled with new geochemical analysis will help to constrain the geodynamic context and deformation history

REFERENCES

- Ahmad, T., Tanaka, T., Sachan, H., K., Asahara, Y., Islam, R. & Khanna, P., P. 2008: Geochemical and isotopic constraints on the age and origin of the Nidar Ophiolitic Complex, Ladakh, India: Implications for the Neo-Tethyan subduction along the Indus suture zone. *Tectonophysics* 451 (1–4): 206/24.
- Mahéo, G., Bertrand, H., Guillot, S., Mascle, G., Pêcher, A., Picard, C. & De Sigoyer, J. 2000: Témoins d'un arc immature téthysien dans les ophiolites du Sud Ladakh (NW Himalaya, Inde). *Comptes Rendus de l'Académie des Sciences - Series IIA - Earth and Planetary Science* 330 (4): 289/95.
- Mahéo, G., Bertrand, H., Guillot, S., Villa, I., M., Keller, F. & Capiez, P. 2004: The South Ladakh ophiolites (NW Himalaya, India): an intra-oceanic tholeiitic arc origin with implication for the closure of the Neo-Tethys. *Chemical Geology* 203 (3–4): 273/303.

P 1.6

Duration of inverted metamorphic sequence formation across the Himalayan Main Central Thrust (MCT), Sikkim

Stefania Cioldi¹, Evangelos Moulas¹, Lucie Tajcmanová¹ & Jean-Pierre Burg¹

¹ *ETH Zurich, Department of Earth Sciences, Sonneggstrasse 5, 8092 Zurich, Switzerland*

The Himalayan orogenic belt has been a fascinating field of geological studies for more than 150 years. Since then advances in the application of analytical methods allowed collecting a wealth of data and clarifying concepts on orogenic processes. Nevertheless, many issues are still debated so that the Himalayas remain an attractive and inspiring subject of research.

The aim of this study is to investigate the tectonic setting and the timescale of inverted isograds related to crustal-scale thrusting at the Main Central Thrust (MCT) in the Sikkim region, Northeast India. Several models considering petrochronology, geothermobarometry and structure geology have been proposed to explain the inverted metamorphic gradient without reaching a common agreement. We aim to contribute to the understanding of links between the mechanical and thermal evolution of the MCT and elucidate the nature and origin of orogenic heat using garnet geospeedometry.

Garnets provide a sensitive record of metamorphic conditions and are potential chronometers. Their compositional zoning is used as a gauge for rate estimates of element diffusion within the mineral.

Our inverse-fitting numerical model considering FRactionation and Diffusion in GarnEt (FRIDGE) calculates garnet composition profiles by introducing both P-T-t paths and bulk-rock composition for a specific sample. P-T conditions were estimated by convectional geothermobarometry supported by phase equilibria modelling and measured garnet chemical compositions.

Simulations were then compared with measured profiles. Modelling diffusion and fractionation chemical zoning profiles in garnet for the four major elements Fe, Mg, Mn and Ca allows estimating the duration of peak metamorphic conditions for each samples. Results placed in their structural context help determining the mechanical and thermal processes causing the inverted isograds.

An overview of the regional geological setting, methods used in this project, SHRIMP U-Pb geochronological data and preliminary FRIDGE results are presented.

P 1.7

Multi-layer lithospheric extension: implications for Mesozoic rifting in the Alps

Thibault Duretz¹, Geoffroy Mohn², Filippo Schenker³, Stefan M. Schmalholz¹

¹ *Institute of Earth Sciences, University of Lausanne, Géopolis, CH-1015 Lausanne (thibault.duretz@unil.ch)*

² *Université de Cergy-Pontoise, 33 boulevard du Port, F-95011 Cergy-Pontoise*

³ *SUPSI, University of Applied Sciences and Arts of Southern Switzerland, Via Trevano, CH-6952 Canobbio*

The Alpine belt have undergone a polyphase geological history spanning the Devonian-Carboniferous Variscan orogeny, the Permian post-Variscan extension, the Mesozoic rifting and ultimately the Late Cretaceous to Tertiary Alpine orogeny. In particular, Permian post-orogenic processes are responsible for strongly pre-structuring the continental crust/lithosphere prior to the Mesozoic rifting. This event was characterized by the emplacement of acid and mafic intrusions at all crustal levels and is associated to high-temperature metamorphism. Therefore, before Mesozoic rifting the continental crust was likely considerable mechanically heterogeneous due to a variety of different rock types and the dependence of mechanical strength on temperature. These pre-rift mechanical heterogeneities and the thermal inheritance likely played a key role for the development of the Liguro-Piemontese and Valaisan domains.

We investigate the role of pre-rift inheritance on the development of rifted margins using two-dimensional thermo-mechanical models of lithospheric extension. In the model we represent the pre-rift mechanical heterogeneities with a mechanical layering. We study the control of mechanical layering on the extension of the continental lithosphere. The mechanical layering causes a multi-stage depth-dependent extension. In the first rifting phase, lithospheric deformation is decoupled: while the crust undergoes thinning by brittle (frictional-plastic) faults, the lithospheric mantle accommodates extension by symmetric ductile necking. In a second rifting phase, deformation in the crust and lithospheric mantle is coupled and marks the beginning of an asymmetric extension stage. Low angle extensional shear zones develop across the lithosphere and exhume subcontinental mantle. Furthermore, crustal allochthons and adjacent basins develop coevally.

We describe the kinematic and geometrical features as well as the thermal evolution predicted by the numerical models. We discuss the implication of these first-order features in the context of the Alpine geological history.

P 1.8

Multi-layer extension: implications for the development of ductile shear zones

Thibault Duretz¹, Stefan M. Schmalholz¹

¹ *Institute of Earth Sciences, University of Lausanne, Géopolis, CH-1015 Lausanne (thibault.duretz@unil.ch)*

The mechanisms that control the formation of ductile shear zones are still debated. We investigate the formation of ductile shear zones in sedimentary and metamorphic rocks. Such rocks are often characterised by lithological layering whereby layers have different mechanical strength. Using two-dimensional numerical simulations, we investigate the ductile deformation of multi-layers during layer-parallel extension.

Two distinct modes of deformation are identified depending on the rheology of the layers. With power-law viscous layers and linear viscous interlayers, the extension is accommodated by independent continuous boudinage (necking) of the competent layers. For multi-layers consisting of both power law layers and interlayers, the deformation is accommodated by two successive mechanisms. In the first stage the competent layers undergo necking and in a second stage a localized shear zone develops across the layers. The deformation style thus switches from distributed and symmetric multi-layer necking to localised and asymmetric shearing. The shear zone leads to a vertical off-set, which can reach several times the layer thickness.

Shear localisation takes place although the rheology is strain rate hardening (power-law stress exponent > 1) and in the absence of material softening and/or energy feedback mechanism (e.g. shear heating). It is induced by structural softening as the development of a shear zone decreases the bulk strength and hence the work required to deform the multi-layer. We show that shear zones can form in multi-layers if the interlayer thickness is approximately equal to or less than the layer thickness. Only three layers can be sufficient to trigger shear localization.

P 1.9

Geological Structure of Georgia and Geodynamic Evolution of the Caucasus

Irakli Gamkrelidze¹, Kakhaber Koiava¹ & Jon Mosar²

¹ *Ivane Javakhishvili State University, Alexandre Janelidze Institute of Geology, A. Politkovskaia str. 5, GEO-0186 Tbilisi, (gamkrelidzei@yahoo.com)*

² *Département de Géosciences - Sciences de la Terre, Université de Fribourg, Chemin du Musée 6, CH-1700 Fribourg, (mosar@unifr.ch)*

The territory of Georgia is a component of Caucasian segment of the Mediterranean (Alpine-Himalayan) collisional orogenic belt. The Greater Caucasian, Black Sea-Central Transcaucasian, Baiburt-Sevanian and Iran Afghanistan accretionary terranes are identified within the Caucasus, and in geological past represented island arcs or microcontinents (Fig.1) The territory of Georgia covers the S part of the Greater Caucasian terrane, Black Sea – Central Transcaucasian terrane and northern part of the Baiburt-Sevanian terrane (Gamkrelidze, 1986; Gamkrelidze & Shengelia, 2005). The territory is built up of Neoproterozoic and Paleozoic metamorphic complexes (migmatites, gneisses, granite-gneisses, metabasites, metaophiolites) and Mesozoic and Cenozoic sedimentary, submarine and subaerial volcanic rocks and of intrusives of various age and composition. These rocks have quite various character within the different terranes and subterrane of Georgia (Gamkrelidze, 1997; Gamkrelidze et al., 2015).

The Earth's crust of Georgia contains tectonic structures of different age, type, scale and genesis, and complex tectonic nappes are found both in the pre-Alpine crystalline basement and in the sedimentary cover (Gamkrelidze, 1991; Gamkrelidze & Shengelia, 2005). Late Alpine southward-directed nappes are established on the southern slope of the Greater Caucasus. They are formed as a result of northward advance and underthrusting of the rigid Transcaucasian massif beneath the Greater Caucasian folded system mainly during the pre-Late Pliocene time (Rodanian phase).

On the basis of paleomagnetic and traditional geological data as well as the newest plate tectonic reconstructions it can be shown that the earliest period of evolution of the Caucasus and adjacent areas was linked to the evolution of the Proto-Paleotethys ocean, along with the active margins during the Neoproterozoic and Paleozoic time generate supra-subduction regional metamorphism and granitoid magmatism, connected with Grenville, Baikalian (Cadomian), Caledonian and Variscan orogenies. Since the Triassic, in the rear of gradually closing Paleotethys, the Mesotethys (Neotethys) oceanic basin and later (starting from the end of the Middle Jurassic) the Lesser Caucasian branch (bay) of the Neotethys developed.

During the Mesozoic and Cenozoic time the northern active margin saw the formation of the Greater Caucasian marginal sea, the Transcaucasian island arc, the Adjara-Trialetian intraarc rift and the Lesser Caucasian island arc. Each of these realms has its specific accumulation of sedimentary and supra-subduction effusive and intrusive rocks associated to succession of several pre-orogenic, early orogenic and late orogenic (collisional) folding phases. The latter started in the Late Miocene and is characterized by an important compression of the region, linked to the advance of the Arabian plate to the north. GPS data and rates of contemporary vertical uplift of the Greater and Lesser Caucasus indicate the continuation of collisional process at present too.

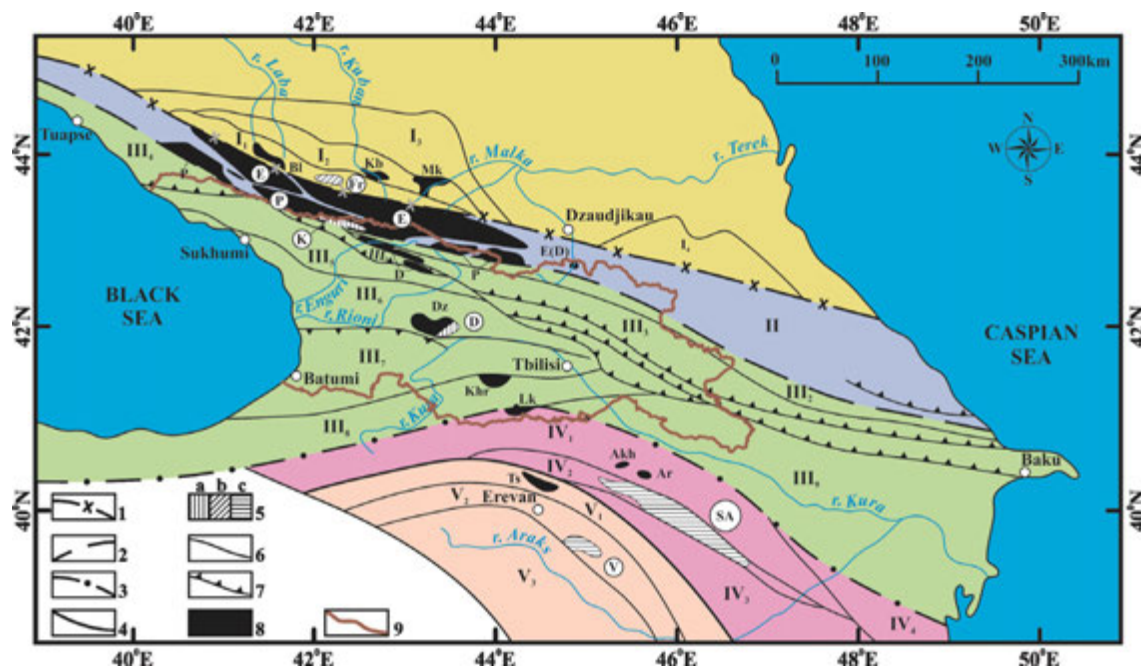


Figure 1. Tectonic subdivision of the Caucasus on the basis of terrane analysis (Gamkrelidze & Shengelia, 2005).

I - Part of Scythian platform involved in Neogene time into rising of the Greater Caucasus; I_1 - Forerange zone, I_2 - Laba-Malka (Bechasin) zone, I_3 - zone of North Caucasian monocline, I_4 - Daghestan Limestone zone. Accretionary terranes and subterrane: II - Greater Caucasian terrane; III - Black Sea-Central Transcaucasian terrane. Subterrane: III_1 - Chkalta-Laila, III_2 - Kazbegi-Tphan, III_3 - Mestia-Dibrar, III_4 - Novorosiisk-Lasarevskoe, III_5 - Gagra-Java, III_6 - Dzirula, III_7 - Adjara-Trialeti, III_8 - Artvin-Bolnisi, III_9 - Middle and Lower Kura; IV - Baiburt-Sevanian terrane. Subterrane: IV_1 - Somkhito-Karabakh, IV_2 - Sevan-Akera, IV_3 - Kafan, IV_4 - Talysh; V - Yran-Afghanian terrane. Subterrane: V_1 - Miskhan-Zangezur, V_2 - Erevan-Ordubad, V_3 - Araks. 1 - borders of terranes-ophiolite sutures (here and there presumable) marking the location of small and large oceanic basins: 1 - of Early?-Middle Paleozoic age, 2 - of Neoproterozoic-paleozoic age, 3 - of Neoproterozoic-Early Mesozoic age, 4 - of Mesozoic age; 5 - ophiolite terranes (obducted plates): 5_a - of Neoproterozoic-Paleozoic? age 5_b - of Paleozoic age, 5_c - of Mesozoic age; 6 - borders of subterrane (deep faults or regional thrusts); 7 - detached cover nappes of Alpine age; 8 - exposures of pre-Alpine crystalline basement: GC - Greater Caucasian, D - of Dizi series of Southern slope of the Greater Caucasus, Dz - Dzirula, Khr - Khrami, Lk - Loki, Akh - Akhum, Ar - Asrikchai, Ts - Tsakhkunyats; 9 - boundary of the territory of Georgia.

REFERENCES

- Gamkrelidze, I.P. 1986: Geodynamic evolution of the Caucasus and adjacent areas in Alpine time. *Tectonophysics*. 127, 261-277.
- Gamkrelidze, I.P. 1991: Tectonic nappes and horizontal layering of the Earth's crust in the Mediterranean belt (Carpathian, Balkanides Caucasus). *Tectonophysics*. 196, 385-396.
- Gamkrelidze, I.P. 1997: Georgia. In: *Encyclopedia of European and Asian regional geology*. Chapman and Hall, London, 256-261.
- Gamkrelidze, I.P. & Shengelia, D.M. 2005: Precambrian-Paleozoic regional metamorphism, granitoid magmatism and geodynamics of the Caucasus. *Scientific World*, Moscow, (in Russian).
- Gamkrelidze, I.P., Gamkrelidze, M., Loladze, M. & Tsamalashvili, T. 2015: New tectonic map of Georgia (Explanatory Note). *Bull. Acad. Sci. Georgia*, 9, #1, 110-116.

P 1.10

Structural and metamorphic subdivision of the central Sesia Zone (Aosta Valley, Italy)

Francesco Giuntoli¹, Paola Manzotti^{1,2}, Martin Engi¹ & Michel Ballèvre²

¹ *Institut für Geologie, University of Bern, Baltzerstrasse 1+3, CH-3012 Bern, Switzerland (francesco.giuntoli@geo.unibe.ch)*

² *Université de Rennes, Géosciences Rennes, UMR-CNRS 6118, University of Rennes1, Rennes Cedex, France*

The Sesia Zone in the Western Alps is a continental terrane derived from the NW-Adriatic margin and polydeformed at HP conditions during Alpine convergence. Subdivisions of the Sesia Zone classically have been based on the dominant lithotypes: Eclogitic Micaschist Complex (EMC), Seconda Zona Diorito-Kinzigitica (2DK), and Gneiss Minuti Complex (GMC). However, recent work (Regis et al. 2014) on what was considered a single internal unit revealed that the EMC comprises two or more tectonic slices that experienced substantially different PTdt-evolutions.

The juxtaposition of the different complexes has long been debated: Williams & Compagnoni (1983) proposed that the main contact in the Sesia Zone is a thrust juxtaposing EMC and GMC. This contact reflects a metamorphic jump from >1.5 GPa, 550 °C and jadeite+quartz bearing rocks (EMC) to 1.5-1.3 GPa - 500-550 °C and plagioclase-bearing rocks (GMC). For Spalla et al. (1991) the main difference between EMC and GMC is the amount of strain experienced at greenschist facies conditions. They specified that there are neither lithological nor metamorphic differences between the two complexes, being units formed at eclogitic conditions, both in the stability field of Jd+Qz.

Zucali & Spalla, 2011 used the distinction of the Sesia Zone into an Upper element and a Lower element (as already proposed by Dal Piaz et al., 1972), and the latter was subdivided into EMC, where the dominant Alpine imprint is at eclogite facies conditions, and GMC, where Alpine greenschist facies conditions dominate.

In view of these debates, detailed regional petrographic and structural mapping (1:3k to 1:10k) was undertaken and combined with extensive sampling and petrochronological analysis. Results lead us to propose a detailed map for the Sesia Zone in the Aosta Valley between Val del Lys and Val d'Ayas.

A set of field criteria was developed and applied, aiming to recognize and delimit the first order tectonic units in this complex structural and metamorphic context. The approach rests on three types of criteria used in the field: (1) Discontinuously visible metasedimentary trails considered to be monocyclic (from Permo-Mesozoic protoliths, mostly carbonates); (2) mappable high-strain zones; and (3) visible differences in metamorphic imprint. Note that these key features were used in combination, i.e. not one criterion alone; this allows us to delimit the position of the main units in a detailed map, in which the essence of previous maps has been integrated as well.

We propose an Internal Complex that includes micaschists associated with mafic rocks and orthogneiss. The main foliation is always eclogitic, dipping moderately NW. It can be further subdivided into three eclogitic sheets, each 0.5–3 km thick, separated by (most likely monometamorphic) sediments, <10–50 m thick. These contain calcschist, siliceous marble and impure quartzite in the case of Col Fenêtre, and siliceous dolomite marble E of Mont Prial. Local greenschist facies overprint is strong close to the tectonic contact against the neighbouring complex, typically producing a mylonitic foliation.

The External Complex comprises mostly orthogneiss with minor paragneiss. Several discontinuous lenses of overprinted pre-Alpine amphibolite-granulite occur, representing the 2DK; these are often aligned with greenschist facies shear zones within orthogneiss. Combining these features, three main tectonic sheets are delimited in the External Complex, with the main foliation being of greenschist facies and dipping moderately SE.

A hectometric shear zone (Barmet SZ) is identified between the Internal and the External complexes. It is made up of wedge-shaped bands of meta-granite and meta-diorite with few mafic boudins and lenses of paragneiss, bounded by thin bands of siliceous dolomite marble. The main mylonitic foliation dips SE and is of greenschist facies, but omphacite, glaucophane, and garnet occur as relics in an older foliation that formed prior to juxtaposition. Towards the SW, the width of the Barmet SZ diminishes from 500 m to a few meters.

The juxtaposition between the Internal Complex and the External Complex is a major tectonic contact reflecting greenschist facies condition. The main eclogitic foliation of the Internal Complex is cut at 40-50° by the greenschist mylonitic foliation of the Barmet SZ.

REFERENCES

- Dal Piaz, G.V., Hunziker, J.C., Martinotti, G., 1972. La Zona Sesia e Lanzo e l'evoluzione tettonico-metamorfica delle Alpi nordoccidentali interne. *Memorie della Società Geologica Italiana* 11, 433-460.
- Regis, D., Rubatto, D., Darling, J., Cenko-Tok, B., Zucali, M., Engi, M., 2014. Multiple metamorphic stages within an eclogite-facies terrane (Sesia Zone, Western Alps) revealed by Th-U-Pb petrochronology. *Journal of Petrology*, 55, 1429-1456.
- Spalla, M. I., Lardeaux, J. M., Dal Piaz, G. V., & Gosso, G., 1991. Métamorphisme et tectonique à la marge externe de la Zone Sesia-Lanzo (Alpes occidentales). *Memorie di Scienze Geologiche*, 43, 361-369.
- Williams, P. F., & Compagnoni, R. (1983). Deformation and metamorphism in the Bard area of the Sesia Lanzo Zone, Western Alps, during subduction and uplift. *Journal of Metamorphic Geology*, 1, 117-140.
- Zucali, M. & Spalla, M. I., 2011. Prograde lawsonite during the flow of continental crust in the Alpine subduction: Strain vs. metamorphism partitioning, a field-analysis approach to infer tectonometamorphic evolutions (Sesia-Lanzo Zone, Western Italian Alps). *Journal of Structural Geology*, 33, 381-398.

P 1.11

Evidence for Liassic to Dogger syndedimentary normal faulting in the Western Swiss Molasse Basin based on seismic interpretation

GRUBER Marius¹, SOMMARUGA Anna¹, MOSAR Jon¹

¹ University of Fribourg, Department of Geosciences, Earth Sciences, Chemin du Musée 6, CH-1700 Fribourg, Switzerland (marius.gruber@unifr.ch, anna.sommaruga@unifr.ch, jon.mosar@unifr.ch)

In Liassic to Dogger times, the South-European realm is in an overall extensional stress regime associated with the opening of the central Atlantic and the Alpine Tethys basin. This leads to syndedimentary normal faulting and enhanced subsidence (e.g. Wetzel et al. 1993, eastern Jura Mountains; Mettraux & Mosar 1989, Briançonnais domain; Birkhäuser et al. 2001, Molasse basin).

This study is part of a regional scale structural analysis of the Western Molasse basin in the Canton of Fribourg. It focusses on a new structural interpretation of eleven 2D-seismic lines near the Romanens-1 well North to the frontal Subalpine Molasse thrust. The area is located in the SE part of the Swabian Basin, N of the Alemannic High.

The Romanens area is structured by different tectonic elements: [i] a NE-SW trending, SE dipping syndedimentary normal fault system confined to the Mesozoic units, [ii] a N-S trending subvertical strike-slip fault system crosscutting the Mesozoic and the Cenozoic units, [iii] a NE-SW trending, SE dipping thrust fault system in the Cenozoic units (Subalpine Molasse) and [iiii] a low-angle décollement level dipping to the SE and parallel to the dip of the Base Mesozoic horizon in Middle Triassic units (top mechanical basement *s.l.*).

This study places special emphasis on the NE-SW trending syndedimentary normal fault system in Mesozoic units. Former seismic interpretations already highlighted the existence of normal faults in the Romanens area (Sommaruga et al. 2012, Meier 2010) but their lateral extent remained unknown and no syndedimentary component was observed.

The normal fault system is characterized by 3 soft linked fault zones of 6-9 km length each, forming a half-graben and downthrowing the SE hangingwall by about 250m in the central part of each fault zone. Displacement dies out towards the fault tips and is relayed from one fault to the other. Thickness variations are observed on the hangingwall side in Liassic and Dogger units showing a thickening towards the fault plane while on the footwall side, these units show a thinning towards the fault plane. This configuration suggests a syndepositional NW-SE extensional event in Liassic to Dogger times which can be correlated with the rifting phase of the Tethys ocean formation (Stampfli & Hochard 2009). Upper Jurassic to Lower Cretaceous units do not show significant thickness variations.

Mesozoic and Cenozoic units are detached during the Miocene time along a décollement level located in Middle Triassic evaporites and transported towards the NW, leading to the formation of duplex- and fishtail-structures within the Muschelkalk unit and a detachment fold in the overlying units. A recent interpretation of one seismic line in the Romanens area suggests that these fishtail-structures crosscut the Mesozoic and Cenozoic units (Mosar et al. 2014). Further investigation will focus on the influence of inherited normal faults (in the Mesozoic layers and at the Base Mesozoic horizon) on the development of inversion structures (fishtails in this case) and on the lateral extent of these structures. Studies further to the NE at the edge of the Permo-Carboniferous trough of N Switzerland have revealed the importance of this genetic link.

REFERENCES

- Birkhäuser, Ph., Roth, Ph., Meier, B. & Naef, H. 2001. 3D- Seismik: Räumliche Erkundung der mesozoischen Sedimentschichten im Zürcher Weinland, Nagra NTB 00-03, 158 S.
- Meier B. 2010. Ergänzende Interpretation reflexionsseismischer Linien zwischen dem östlichen und westlichen Molassebecken. Nagra Arbeitsbericht NAB 10-40, 48 S.
- Mettraux & Mosar 1989. Tectonique alpine et paléotectonique liasique dans les Préalpes Médiannes en rive gauche du Rhône, *Eclogae geol. Helv.* 82/2, S. 517-540.
- Mosar J., Abednego M., Gruber M. & Sommaruga A. 2014. Tectonics between the Préalpes Klippen and the swiss western Molasse Basin in the Bulle region (Fribourg). Poster SGM 2014, Switzerland.
- Sommaruga A., Eichenberger U. & Marillier F. (2012). Seismic Atlas of the Swiss Molasse Basin, *Beiträge zur Geologie der Schweiz – Geophysik*, v. 44, 88 p.
- Stampfli, G.M. & Hochard, C. 2009. Plate tectonics of the Alpine realm, Geological Society, London, Special Publications v. 327, p. 89-111.
- Wetzel, A., Vincenzo, A. & Gonzalez, R. 1993. Sedimentation und Tektonik im Ostjura: Bericht über die Exkursion der Schweizerischen Geologischen Gesellschaft am 29.9.1992, *Eclogae geol. Helv.* 86/1, S. 313-332.

P 1.12

Deformation of an experimental drainage network in oblique collision

Laure Guerit¹, Stéphane Dominguez², Jacques Malavieille² & Sébastien Castelltort¹¹ *Earth Surface Dynamics, University of Geneva, Rue des Maraichers 13, CH-1205 Genève, Switzerland*² *Géosciences Montpellier, University of Montpellier II, 34000 Montpellier, France*

In oblique collision settings, parallel and perpendicular components of the relative plate motion can be partitioned into different structures of deformation and may be localized close to the plate boundary, or distributed on a wider region. In the Southern Alps of New Zealand, it has been proposed that one-third of the regional convergence is distributed in a broad area along the Southern Alps orogenic wedge. To better document and understand the regional dynamics of such systems, reliable markers of the horizontal tectonic motion over geological time scales are needed. River networks are able to record a large amount of distributed strain and they can thus be used to reconstruct the mode and rate of distribution away from major active structures.

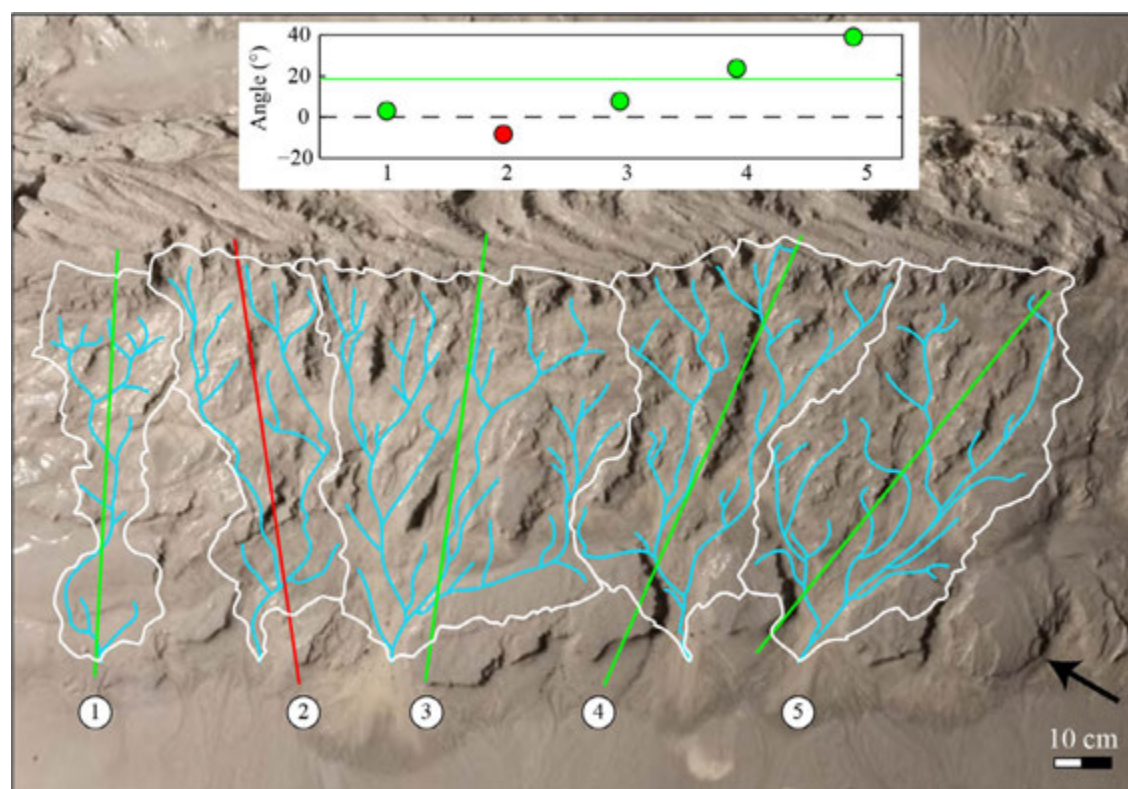


Figure 1. Orientation of the main drainage basins at the end of the experiment: on average, they are rotated clockwise.

To explore the controls on river resilience to deformation, we develop an experimental model to investigate river pattern evolution over a doubly-vergent orogenic wedge growing in a context of oblique convergence. We use a rainfall system to activate erosion, sediment transport and river development on the model surface. At the end of the experiment, the drainage network is statistically rotated clockwise, confirming that rivers can record the distribution of motion along the wedge.

Image analysis of channel time-space evolution shows how the fault-parallel and fault-perpendicular components of motion decrease toward the fault and impose rotation to the main trunk valleys. However, rivers do not record the whole imposed rotation rate, which suggest that the natural lateral channel dynamics can alter the capacity of rivers to act as passive markers of deformation.

P 1.13

Numerical investigation of the transition between folding and thrusting: applications to the Swiss Jura and Canadian Foothills foreland fold-and-thrust belts

Florian Humair¹, Arthur Bauville^{1, 2}, Jean-Luc Epard¹, & Stefan Schmalholz¹

¹ *University of Lausanne, Institute of Earth Sciences, Lausanne, Switzerland (florian.humair@unil.ch)*

² *Institute of Geosciences, Johannes Gutenberg University Mainz, D-55128 Mainz, Germany*

In order to investigate the development of thrust-related anticlines affecting a sedimentary rock sequence over weak detachment layer, we examine the mechanics of thrust (or ramp) formed as a consequence of detachment folding using 2D numerical simulations. In particular, we analyse the transition between two end-member styles of deformation: (1) detachment folding and (2) thrust ramps with related anticlines. Initial models' configuration consists of two plastic materials: a thin weak basal layer overlaid by several kilometers of stronger sediment. The weak layer is thicker on one side of the model than on the other and folding is initiated at the center, where the jump occurs. A series of models systematically illustrates the effects of 1) the initial geometrical perturbation (sediment-detachment thickness ratio, hinterland-foreland detachment thickness ratio, height of the step), 2) the rheological properties of the detachment (frictional vs. viscous) and 3) the erosion on the structural evolution of the overlaying sedimentary sequence.

The different models are compared to natural examples from the Jura Mountains and the Foothills of the Canadian Rockies fold-and-thrust belts, classically interpreted as thin-skinned belts where folds develop over weak detachment horizons. These belts are characterized by asymmetric thrust related anticlines which are displaying steep to overturned forelimbs as well as curved and steep backlimbs along with the presence of back-thrusts (hinterland-verging).

Preliminary results highlight that the development of thrusts at the base of anticlines is related to an initial stage of low-amplitude symmetric buckling. In turn, folding of the strong layer further amplifies in response to the propagation of the previously formed thrusts. Back-thrusts are initiated during the first increments of deformation and progressively stop accommodating deformation in favor of foreland-vergent thrust where the detachment layer is thinner. The foreland vergent thrust can then passively transport the anticline.

The resulting geometry of the folded sediment sequence appears to be influenced by both the sediment-detachment thickness ratio and the hinterland-foreland detachment thickness ratio. However, the main factor controlling the fold style is the height of the initial perturbation (step), i.e. low step favour symmetric folding while high step favor the development of foreland vergent thrust folds.

First order geometry and kinematics of modeled folds and thrusts agree with field observations and cross-sections from the Jura and the Foothills of the Canadian Rockies (from literature and constructed). In a second step, we compared strain ellipses and principal stress orientation from the models with fracture distributions from natural examples. Finally, we mapped the distribution of fracturing in the model through time in order to constrain the evolution and distribution of deformation mechanism.

P 1.14**Formation of necking zones during lithospheric rifting**

Jaquet, Yoann; Schmalholz, Stefan; Duretz, Thibault

Institute of Earth Sciences, University of Lausanne, CH-1015 Lausanne, (yoann.jaquet@unil.ch)

Although numerous models of rift formation have been proposed, the formation of necking zones and rifted margins remains unclear. However these structures are commonly observed in both fossil and present-day passive margins. It is thus of primary interest to understand the mechanisms that control the formation of necking zones. In this study, we use a combination of 1-D necking analysis, 2-D power law viscous flow models and viscoelastoplastic thermo-mechanically coupled models to investigate how necking zones evolve and what controls their dimensions. We use the 1-D necking analysis to extract the effective rheological parameters for a lithosphere undergoing necking phase. We employ these effective rheological parameters in the 2-D power law models of lithosphere extension and study the geometry of the resulting necking zones. These results are compared with those obtained using 2-D viscoelastoplastic thermo-mechanical models. Our results of systematic analysis indicate a constant necking width of ~50 km which is not dependent on the shortening strain rate used. This result is in good agreement with field observation of the Alpine Tethys from *Beltrando et al. 2014* and *Mohn et al. 2014*.

REFERENCES

- Beltrando, M., Manatschal, G., Mohn, G., Dal Piaz, G.V., Vitale Brovarone, A., Masini, E. (2014), Recognizing remnants of magma-poor rifted margins in high-pressure orogenic belts: The alpine case study, *Earth Science Reviews* 131, 88-115, doi: 10.1016/j.earscirev.2014.01.001
- Mohn, G., Manatschal, G., Beltrando, M., Hauptert, I. (2014), The role of rift-inherited hyper-extension in Alpine-type orogens, *Terra Nova* 26, 347-353, doi: 10.1111/ter.12104

P 1.15**Mapping the subsurface with seismic and GPS data**Krisztina Kelevitz^{1,2}, Nicolas Houlié^{1,2}, Domenico Giardini¹ & Markus Rothacher²¹ *Institute of Geophysics, ETH Zurich, Switzerland*² *Geodesy and Geodynamics Lab, ETH Zurich, Switzerland*

Acquiring more data has always been necessary to increase our knowledge of the interior structure of the Earth: to enhance models, explore new areas, and increase the resolution. Introducing a new type of data can give a new insight and a different perspective of the already explored territories.

We propose to use GPS waveforms as well as seismic waveforms when modeling the interior structure of the Earth. GPS receivers record a measurement of the displacement occurring at the ground due to the earthquake. GPS observations do not clip at large ground motions, therefore capable of recording an earthquake of any magnitude at any distance from the epicenter when the ground motion exceeds the nominal GPS noise level (2 mm) (Houlié et al., 2011).

We present the first results of mapping the subsurface with a dataset that is a combination of broadband seismometer and GPS observations. We show comparison of subsurface models from the Japan area.

REFERENCES

- Houlié, N., Occhipinti, G., Blanchard, T., Shapiro, N., Lognonne, P., and Murakami, M. (2011). New approach to detect seismic surface waves in 1Hz-sampled GPS time series. *Sci Rep*, 1:44.

P 1.16

Rheology during high temperature granular flow - inferences from microstructures

Rüdiger Kilian¹, Luiz Fernando Grafulha Morales², Max Peters³

¹ *Institute of Geology and Paleontology, University of Basel (ruediger.kilian@unibas.ch)*

² *Helmholtz Centre, GFZ Potsdam, Germany*

³ *Institute of Geological Sciences, University Bern, Switzerland*

Polymineralic rocks in high strain zones in nature often show microstructures, which are interpreted to form during diffusion creep (s.l.). Accordingly, these zones are interpreted to behave in a linear-viscous manner. Such microstructures are anti-correlated phase distributions, small grain sizes or equiaxed grain shape. The absence of a crystallographic preferred orientation (CPO), attributed to rigid body rotation of individual grains at flow stresses too low to allow crystal plasticity, is also taken as an indication of diffusion creep. However, the interplay of processes leading to e.g. an anti-correlated phase distribution or the presence of a CPO in polymineralic rocks are entirely clear.

We will present an example of an ultramylonitic shear zone formed during upper amphibolite facies conditions in which a granulite facies protolith is transformed to a fine-grained mixture of quartz (50%), biotite (20%), white mica (20%), oligoclase (7%) and ilmenite/rutile, all with grain sizes < 10 µm diameter. Different phases occupy specific fabric positions.

Biotite stacks and plagioclase grow in extensional sites between quartz grains. Concurrently, biotite is replaced by white mica which defines the foliation, accompanied by growth of garnet rims and dissolution of plagioclase in compressional sites. Quartz grains form columnar structures forming an angle of 30-60° with the foliation, inclined towards the inferred shortening direction. The specific position of phases present strain-insensitive fabric elements. The microstructural positions of the phases can be related to the kinematics in granular flow accompanied by incongruent dissolution, and precipitation. The alignment of quartz grains into columnar aggregates subparallel to the inferred shortening direction can be compared to jamming during the dynamic formation of force chains during flow of granular media. However, quartz possess a weak CPO. It can be shown that the CPO is distinct from random, that it is not inherited from the protolith and that it developed during flow of the ultramylonite. Subgrains and newly recrystallized quartz grains form synkinematically, mostly by subgrain rotation recrystallization and only minor grain boundary migration - quartz grain boundaries are readily pinned by non-quartz phases. It is suggested that in the columnar quartz aggregates, differential stresses become sufficiently high to allow for crystal plastic yielding and that dislocation creep acts as an accommodating mechanism during granular flow. Accordingly, this ultramylonite may possess a non-linear rheology and deform at much higher flow stresses or strain rates, even if microstructures are typical for a diffusion creep (s.l.) mechanism.

P 1.17

Cenozoic volcanoclastic signatures in sandstones of the Central and Southern Alps: their age, derivation and geodynamic significance - A project layout

Lu Gang¹, Wilfried Winkler¹, Sean Willett¹, Albrecht von Quadt², Maria Giuditta Fellin¹, Meinert Rahn³, Peter Brack²

¹ *Department of Earth Sciences, Geological Institute, ETH Zürich, Sonneggstrasse 5, 8092 Zürich, Switzerland (gang.lu@erdw.ethz.ch)*

² *Department of Earth Sciences, Sonneggstrasse 5, 8092 Zürich, Switzerland*

³ *Swiss Federal Nuclear Safety Inspectorate ENSI, Industriestrasse 19, 5200 Brugg, Switzerland*

Tertiary syn-tectonic volcanic products sparsely occur in the Alpine orogen. They are located in three basinal settings: (1) the Northern Alpine early foreland basin (Late Eocene? to Oligocene Taveyannaz and Champsaur Fms.; e.g. Rahn et al. 1995), (2) the Southern Alps foreland basin (Oligocene-Miocene Como Formation and Gonfolite Lombarda Group, e.g. Malusa et al. 2011), and (3) Middle to Late Eocene South Alpine turbiditic sandstones intercalated within deep-water successions of the Trento area (e.g. Sciunnach and Borsato 1994). The chronostratigraphic range of the formations

correlates with the Cenozoic intense Alpine collision, however, the derivation and geodynamic significance of the volcanic material is poorly defined. It is likely that the Eocene-Oligocene volcanoclastic material was supplied from volcanic bodies related to the Adamello (42-33 Ma) and Bergell (32-30 Ma) intrusions as well as eruptions along the palaeo-Insubric/Giudicarie lines. Volcanic dykes cross-cutting sediments of the northern foreland suggest that volcanic sources could have also occurred along the Penninic orogenic front in the Oligocene (e.g. Pfiffner 2014).

The present project investigates the volcanoclastic deposits to evaluate their temporal and genetic relationship with the hypothetical magmatic provinces. Beside standard provenance analysis methods (e.g. detrital sandstone modes), the project mainly proposes a detailed analysis of detrital zircon grains in the various formations. We combine (1) single detrital zircon grain U/Pb laser ablation ICP-MS dating, (2) trace element analysis of detrital zircons (essentially using P, Y, Th, U, Nb, Ta, REE and Hf concentrations) indicating the magmatic environment in which the zircons crystallised, and (3) $^{176}\text{Hf}/^{177}\text{Hf}$ isotope ratios to reveal their origin from either mantle or crust (crustal contamination as a result of single- or polyphase recycling).

Detrital zircon age populations are expected to provide an improved geochronologic estimate of the extent of the late Alpine volcanic activity. Comparisons of geochemical signatures of the detrital zircons and their magmatic sources will allow evaluating their contribution in space and time.

Preliminary results show detrital zircon ages with three major age populations: Pan-African/Cadomian (Ediacaran–Ordovician), Variscan (Middle Devonian–Carboniferous), post-Variscan (Permian). These populations are a common feature of various Alpine flysch formations (e.g. Beltrán et al. 2013). Cenozoic detrital zircons in the range from 29.97 ± 0.67 Ma to 36.31 ± 0.67 Ma are present in a minority of the investigated samples (Fig. 1). The younger ages overlap with the age range of the Bergell intrusion, the older ones with the Adamello intrusion.

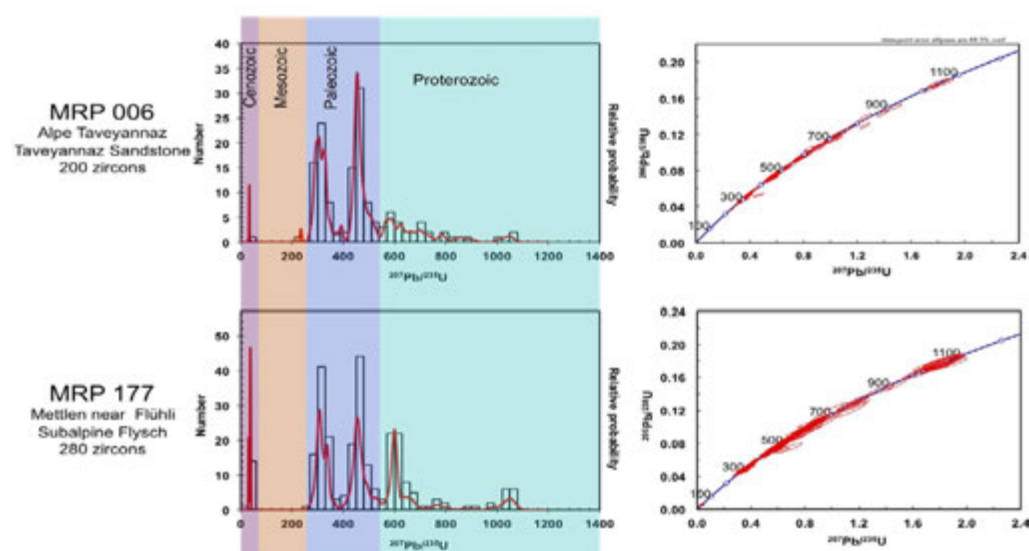


Figure 1. Detrital zircon U–Pb ages of Taveyannaz sandstones shown by histograms, relative probability and concordia diagrams

ACKNOWLEDEMENTS

The support of LG by a Chinese Scholarship (CSC) is appreciated.

REFERENCES

- Beltrán-Triviño A, Winkler W. & von Quadt A. 2013: Tracing Alpine sediment sources through laser ablation U–Pb dating and Hf-isotopes of detrital zircons. *Sedimentology* 60, 197–224
- Malusà, M.G., Villa, I.M., Vezzoli, G. & Garzanti, E. 2011. Detrital geo-chronology of unroofing magmatic complexes and the slow erosion of Oligocene volcanoes in the Alps. *Earth and Planetary Science Letters* 301(1-2), 324–336.
- Pfiffner, A. 2014: *Geology of the Alps*. Haupt, Bern, 376 p.
- Rahn, M.K., Stern, W.B., & Frey, M. 1995. The origin of the Taveyannaz sandstone: arguments from whole-rock and clinopyroxene composition. *Schweiz. Mineral. Petrogr. Mitt.* 75, 213-224.
- Sciunnach D. & Borsato A. 1994. Plagioclase-arenites in the Molveno Lake area (Trento): record of an Eocene volcanic arc. *Studi Trent. Sci. Nat.*, 69, 81- 92.

P 1.18

Tectonics of northern Switzerland's Permo-Carboniferous Trough as inferable from revised and densified 2D-seismic reflection data

Madritsch, Herfried¹, Henry Naef², Stefan Heuberger³ & Beat Meier³

¹ *Nagra, Hardstrasse 73, CH5430 Wettingen (herfried.madritsch@nagra.ch)*

² *geosfer AG, Teufener Strasse 3, CH-9000 St. Gallen (henry.naef@geosfer.ch)*

³ *Proseis AG, Schaffhauserstrasse 418, CH-8050 Zürich (beat.p.meier@proseis.ch)*

The Permo-Carboniferous Trough of northern Switzerland has inspired tectonic interpretations ever since its identification during Nagra's subsurface exploration for a potential nuclear waste repository in the mid 80ies (e.g. Laubscher 1986; Diebold et al. 1991; Marchant et al. 2000). These interpretations largely rely on 2D seismic reflection data widely available across the region. Only recently this dataset has been fully reprocessed and significantly densified requiring a critical revision of the numerous existing and often opposing interpretations. For this purpose the entire seismic data set was re-interpreted on behalf of Nagra, also taking into account a new Bouguer anomaly (Green et al. 2013). As a result, a tectonic map of the Permo-Carboniferous Trough was developed (Naef & Madritsch 2014).

The study revealed that despite significantly improved seismic data quality and interpretability in the area of Northern Switzerland the tectonic interpretation of the Permo-Carboniferous Trough remains ambiguous and largely conceptual. Seismic imaging of the basement appears to be strongly influenced by the structural conditions of the sedimentary cover and its associated seismic reflection behavior. Moreover the seismic facies of crystalline basement units and Late Paleozoic sediments is not clearly distinguishable in many cases. However, due to the recent substantial densification of the 2D seismic grid in key areas and additional interpretation support provided by the Bouguer anomaly maps the overall robustness of the troughs structural interpretations could be improved. Some new aspects concerning the possible kinematics of trough formation and indications confirming the troughs important role as important precursor structure during later, post-Paleozoic tectonic events are highlighted below.

In the area of northern Switzerland the ENE-WSW striking Permo-Carboniferous Trough reveals a clear half graben geometry. The orientation of this half graben changes laterally across a WNW-ESE striking transfer fault. Overall the western part of the investigated trough section appears to be characterized by pull apart tectonics. Post-Paleozoic extension reactivation of some major trough bounding faults is witnessed by the development of monoclines in the above lying Mesozoic and Cenozoic sediments. Differential subsidence most likely related to this extensional reactivation of the trough appears to have onset already in Mesozoic times as is indicated by thickness variations of the Mesozoic sedimentary strata. Evidence for substantial inversion of the trough, reported from more westerly sections of the trough near Basel (e.g. Ustaszewski & Schmid 2007) could not be identified in northern Switzerland. A mild transpressive reactivation however cannot be fully excluded either.

REFERENCES

- Diebold, P. et al. 1991: Zur Tektonik der zentralen Nordschweiz. Interpretation aufgrund regionaler Seismik, Oberflächengeologie und Tiefbohrungen. Geol. Ber. Landeshydrol. u. -geol. 14 (auch: Nagra Tech. Ber. NTB 90-04).
- Green A.G., et al. 2013: Gravity data in Northern Switzerland and Southern Germany. Nagra Arbeitsber. NAB 13-40.
- Laubscher, H. 1986: The eastern Jura – Relations between thin-skinned and basement tectonics, local and regional. Geol. Rundschau 75/3, 535-553, Stuttgart.
- Marchant, D. et al. 2005: Paleotectonic evolution of the Zürcher Weinland (northern Switzerland), based on 2D and 3D seismic data. Eclogae geol. Helv. 98/3, 345-362.
- Naef, H. & Madritsch, H. 2014: Aktualisierung der tektonischen Karte des Nordschweizer Permokarbondrogs. Nagra Arbeitsber. NAB 14-17.
- Ustaszewski, K. & Schmid, S.M. 2007: Latest Pliocene to recent thick-skinned tectonics at the Upper Rhine Graben – Jura Mountains junction. Swiss J. Geosci. 100, 293-312.

P 1.19**Shallow interplate seismicity vs. intraplate Wadati-Benioff zone intermediate-depth seismicity: Insights from a structural analysis of Alpine high-pressure ophiolite-hosted pseudotachylytes (Corsica, France)**Rémi Magott¹, Olivier Fabbri¹ & Marc Fournier²¹ *Laboratoire Chrono-environnement UMR CNRS 6249, Univ. Bourgogne Franche-Comté, F-25000 Besançon (remi.magott@univ-fcomte.fr)*² *Sorbonne Universités, UPMC Univ. Paris 06, UMR 7193, ISTEP, F-75005 Paris, France*

Most pseudotachylyte veins in the Cima di Gratera ophiolitic thrust sheet, Alpine Corsica, were formed under blueschist to eclogite metamorphic facies conditions, corresponding to lithostatic pressures at 50~90 km depths (Austrheim & Andersen, 2004; Andersen & Austrheim, 2006; Andersen et al., 2014; Deseta et al., 2014). Peridotite-hosted pseudotachylyte veins are clustered in fault zones located either immediately beneath the paleo-Moho tectonic contact with overlying oceanic crust gabbros or at short (< 1 km) distance from it. They can thus be considered as the result of seismic ruptures in the upper seismic zone of a Cretaceous east-dipping Wadati-Benioff zone. Pseudotachylyte vein-bearing fault zones are either parallel to the contact or make an angle of about 55° to it. Shear criteria associated with vein formation indicate top-to-the-west or top-to-the-northwest shear senses. Such shear senses agree with focal mechanisms of intermediate depth Wadati-Benioff upper seismic zones (downdip 'compression', Igarashi et al., 2001). Gabbro-hosted pseudotachylyte veins are of two types: post-mylonitization veins contemporaneous with the peridotite-hosted veins, and pre-mylonitization veins formed earlier along the oceanic crust-oceanic mantle (Moho surface). The possibility that the pre-mylonitization veins were formed at shallow depths (close to the trench), as suggested for the 2004 Sumatra megathrust earthquake (Singh et al., 2008), is discussed.

REFERENCES

- Andersen, T., Austrheim, H., 2006. Fossil earthquakes recorded by pseudotachylytes in mantle peridotite from the Alpine subduction complex of Corsica. *Earth and Planetary Science Letters* 242, 58-72.
- Andersen, T.B., Austrheim, H., Deseta, N., Silkose, P., Ashwal, L.D., 2014. Large subduction earthquakes along the fossil Moho in Alpine Corsica. *Geology* 42, 395-398.
- Austrheim, H., Andersen, T.L., 2004. Pseudotachylytes from Corsica: fossil earthquakes from subduction complex. *Terra Nova* 16, 193-197.
- Igarashi, T., Matsuzawa, T., Umino, N., Hasegawa, A., 2003. Spatial distribution of focal mechanisms for interplate and intraplate earthquakes associated with the subducting Pacific plate beneath the northeastern Japan arc- A triple-planed deep seismic zone. *Journal of Geophysical Research* 106, 2177-2191.
- Singh, S.C. et al., 2008. Seismic evidence for broken oceanic crust in the 2004 Sumatra earthquake epicentral region. *Nature Geoscience*, doi:10.1038/ngeo336.

P 1.20

Phanerozoic surface history of southern Peninsular India from apatite (U-Th-Sm)/He dataSanjay Kumar Mandal¹, Maria Giuditta Fellin², Jean-Pierre Burg¹, and Colin Maden²¹ *Geological Institute, ETH Zürich, Sonneggstrasse 5, 8092 Zürich, Switzerland*² *Institute of Geochemistry and Petrology, ETH Zürich, Clausiusstrasse 25, 8092 Zürich, Switzerland*

Quantifying bedrock cooling histories is crucial for understanding the long-term landform evolution across the passive margin and their control onto the sediment routing system over the overwhelming part of the continental surface. To constrain the lower-temperature cooling histories and their relationship to the Phanerozoic tectonic events of the southern Peninsular India, we present new apatite (U-Th-Sm)/He analyses of 39 Precambrian basement samples. The new AHe ages range from 38.1 ± 6.8 to 364.2 ± 44.6 Ma, are younger in the Palghat Gap region and older in the inland Deccan Plateau. Thermal modeling based on apatite (U-Th-Sm)/He data, indicate enhanced cooling and exhumation in the interior of the Deccan Plateau by Permian-Triassic times, followed by a gradual cooling up to the present. This discrete episode of cooling was associated with continental extension that preceded the Early Jurassic breakup of Gondwana. Bedrock cooling and exhumation on the southeastern and southern limits of the Deccan Plateau was likely accomplished by Late Cretaceous drainage reorganization. The old (>200 Ma) AHe age distributions over the >2600 m high Nilgiri Plateau reflect very low erosion/exhumation rates during the last ~ 200 Ma and adds to examples of long-lived post-orogenic topography. The relatively younger AHe ages from the ~ 30 km wide low topographic region within the Western Ghat Mountains attest for intense Late Tertiary erosion likely facilitated by erodible lithological backbone of the Neoproterozoic shear zone. AHe ages across the western coastal plain challenges the widely held notion of ~ 3 km of post breakup erosional rebound of the margin. Rather the new AHe data are more compatible with no more than 1-1.5 km of crustal unroofing along the coastal strip.

P 1.21

Tectonics in the Greater Caucasus: a N-S section along the Georgian Military Road - Georgia

Jeremiah Mauvilly², Kakhaber Koiava¹, Irakli Gamkrelidze¹ & Jon Mosar²

¹ *Ivane Javakhishvili State University, Alexandre Janelidze Institute of Geology, A. Politkovskaia str. 5, GEO-0186 Tbilisi, (gamkrelidzei@yahoo.com)*

² *Département de Géosciences - Sciences de la Terre, Université de Fribourg, Chemin du Musée 6, CH-1700 Fribourg, (mosar@unifr.ch)*

For over 200 years the Georgian Military Road crosses the central Greater Caucasus and connects the cities of Tbilisi to the south in Georgia and Vladikavkaz to the north in Russia. Along this road it is possible to have an insight into the different tectonic units of the Greater Caucasus from the pre-Mesozoic Crystalline Basement in the Main Range to the Tertiary Molasse type sediments in the foreland basin Molasse subzone and the recent volcanic extrusives.

The Greater Caucasus is Europe's highest mountain belt and stretches from the Caspian Sea to the East to the Black Sea to the West. The present-day orogen has evolved from of a backarc-type continental rift basin into a doubly vergent intracontinental orogenic wedge during the Alpine collisional event due to the S-N convergence of the Arabian and the European (Scythian) plates. No subduction zone under the Greater Caucasus and no remnants of Jurassic oceanic floor are known. Thus the Greater Caucasus has its origin in an extensively stretched and heavily intruded crust during early Jurassic (numerous sills can be observed and locally pillow lavas are known) that has subsequently been inverted. Unlike the Greater Caucasus, both the S Caspian Sea and the E Black Sea show incipient subductions of oceanic lithosphere towards the north. To the north and the south the orogen is bordered by deep flexural Molasse type basins. The main orogenic transport direction (pro-wedge) is to the the S. North-directed thrusting is unevenly spread on the northern flanks of the orogen and best developed in the eastern part (Dagestan). The imbrication of different tectonic nappes generated a post-Sarmatian uplift of some 4 km and has been accompanied since the Late Miocene by important volcanic activity (Mt Elbrus 5641m, Mt. Kazbek 4047m).

Our poster shows preliminary results from a structural investigation along the Military Road N-S profile. We highlight the differences in structural style between the tectonic nappes from S to N. The Kartli Molassic Subzone forms the foreland basin to the S and is mostly made of Tertiary series and shows imbricated fault-bend fold structures. The Mestia-Tiane Zone on the southern slopes is predominantly developed in Cretaceous series and is made of a succession of tectonic imbricates with large coaxial folds separated by major thrust zones. The Kazbegi-Lagodekhi Zone forms the first major topographic summits and is developed mostly in Jurassic limestone series. Its structural style is dominated by large en echelon arranged folds and thrusts. In the core of the mountain range we have the Main Range Zone with Lower Jurassic series and pre-Mesozoic basement as well as Jurassic intrusives. The Main Range Zone is the most intensely deformed part of the mountain range and is separated from the Kazbegi-Lagodekhi Zone by the Main Caucasus Thrust (MCT). This major thrust zone stretches across the whole orogenic belt. Further to the N across the political border into Russia, we have the Northern slopes made of Jurassic and Cretaceous north-dipping series that are subdivided into several structural units separated by thrusts possibly steeply dipping to the S. The northernmost zone is formed by the flexural Tertiary Terek Basin.

We characterise the general structural style and type of deformation in the different units and document the expression of the major thrust zones that separate the different units.

P 1.22

Fault anatomy of the La Sarraz strike-slip fault system

Nicole Schmitt¹, Renata Grassi¹, Stephen A. Miller², Lea Perrochet¹, Benoît Valley² & Jon Mosar¹

¹ *Département de Géosciences - Sciences de la Terre, Université de Fribourg, Chemin du Musée 6, CH-1700 Fribourg, (jon.mosar@unifr.ch)*

² *Center for Hydrogeology and Geothermics, University of Neuchâtel, Rue Emile-Argand 11, CH -2000 Neuchâtel*

The understanding of the distance to failure (criticality) of the faults in the Alpine foreland is of strategic importance for the development the geothermal resources in Switzerland. Fault evolution involves highly coupled processes leading to a complex anatomy of fault zones. In turn, this complex anatomy will have a leading impact on current fault properties, behavior and stability. Our study is part of a larger joint venture between sisstopo, the Department of Geosciences of the University of Fribourg and the Center for Hydrogeology and Geothermics of the University of Neuchâtel. The project is dedicated to the Stress State, Fault Criticality and Fluids; Bearing on resource development in Switzerland. The main focus of the project is the investigation of an outstanding natural laboratory situated along the La Sarraz fault system in the Molasse basin at the edge of the Jura mountains. This NW-SE oriented right-lateral fault system shows spectacular outcrops in quarries in the Éclépens region (Fig. 1; Mormont quarry of LafargeHolcim). This fault is linked in a conjugate fault setup to the N-S trending sinistral Pontarlier strike-slip fault zone. In an initial phase, our project focusses on a detailed description of the fault anatomy, the overall fault characteristics and an analysis of the observed faults and associated striation.

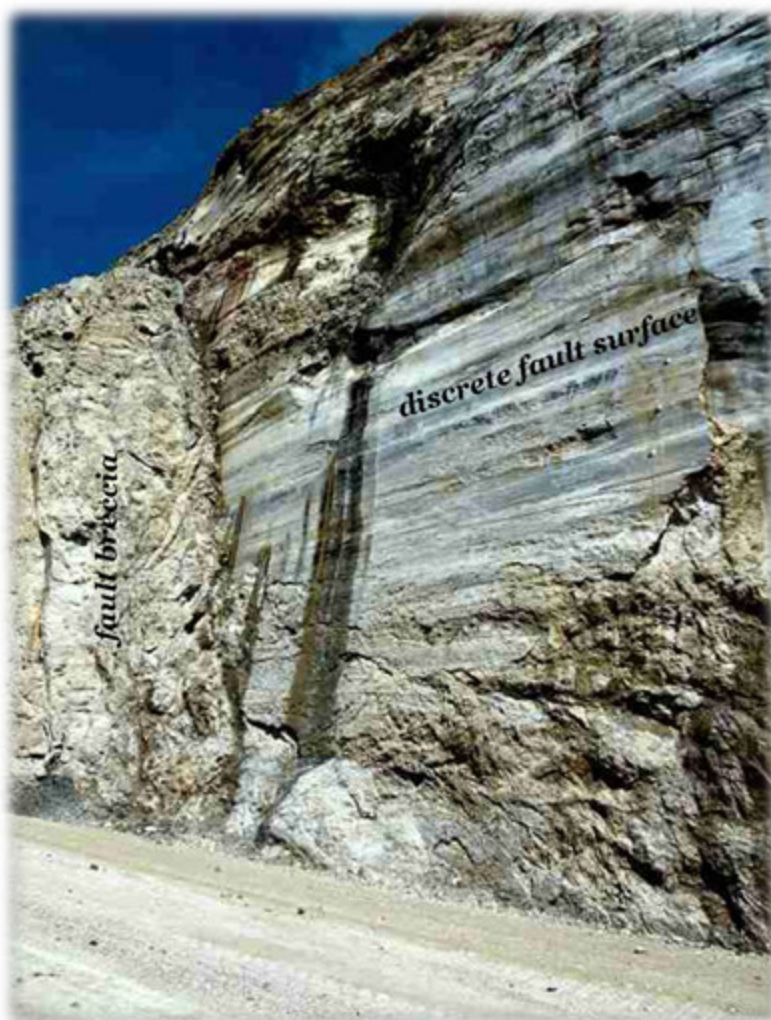


Figure 1. NW (left) – SE (right) oriented section of the La Sarraz fault system outcropping in the La Sarraz-Eclépens quarry. Ondulating distinct fault planes with strongly marked striations and fault damage zone are visible on this picture. Fault has dextral offset.

Our poster shows preliminary results from a fault/striation analysis and a detailed regional mapping of the NW-SE oriented La Sarraz Fault system. The fault is made of two branches isolating limestone series of Cretaceous age that form a topographically elongated ridge. Overall this fault system acts as a Riedel shear system. Towards the Mormont quarry to the E the northern branch evolves into a complex termination with multiple smaller faults, whereas the southern branch crosses the flat alluvial plain to the east of the quarry to cut into the Molasse series to the E (Cridec quarry). The Mormont quarry* itself is located between the two main branches and shows a major fault plane (Fig. 1) oriented almost W-E with a dextral movement. In addition to the large active Mormont quarry several abandoned quarries and good outcrops made it possible to sample abundant information on the faults and striation. This in turn made it possible to determine a local stress field and have insight into the geometrical complexity of the major discrete faults analysed. The major quarry fault show a set of several major decametric-scale discrete undulated fault planes separating zones with fault breccia. Associated are right-lateral faults with an angle of 15° left and right. In addition we can observe several associated fault sets with ENE-WSW; NW-SE and NNE-SSW orientations. The determined stress field in all investigated sites shows a strike-slip regime with a subhorizontal SE-NW compression, subhorizontal NE-SW extension and a vertical intermediate axis.

* The Eclépens site of LafargeHolcim is warmly thanked for giving access to their quarry.

P 1.23

Extreme surface uplift rates revealed by late quaternary marine terraces in the Iranian Makran

Raphaël Normand¹, Guy Simpson¹ & Abbas Bahroudi²

¹ *Section des sciences de la Terre et de l'environnement, University of Geneva, Rue des Maraichers 13, CH-1205 Genève. (Raphael.Normand@unige.ch)*

² *Exploration department, School of Mining Engineering, University of Tehran, Northern Kargar avn, P.O. Box 11365-4563, Tehran.*

We have studied and dated a sequence of uplifted marine terraces exposed along the coastal margin of the Makran subduction zone in southern Iran. The terraces contain abundant marine shell material that we have dated using the ¹⁴C technique. Most of the studied terraces have ages between 29200 and 47000 yrs. B.P.. The highest terrace culminates at 220m a.s.l. and has an age of ca. 32000 yrs.B.P.. Considering that the terrace formed at a time when the sea level was considerably lower than today (probably ca. -80m), we estimate an average surface uplift rate close to 9 mm/yr during the late Quaternary. This rate exceeds most subduction zone uplift rates by a factor of at least three. Although the reason why the Makran experiences anomalously high surface uplift rates is presently unknown, our results highlight that major permanent deformation accumulates within the overthrust plate through time, even far inland from the plate boundary (which is currently ca. 150km further seaward). This deformation is not easily explained by classic elastic rebound theory, which predicts that interseismic and coseismic deformation of the crust over one seismic cycle are equal in magnitude but opposite in sign, so that they completely cancel. We speculate that although elastic rebound theory may reasonably apply for strike slip zones, the situation is probably considerably more complicated at dip-slip dominated plate boundaries (such as the Makran) due to gravity.

P 1.24

Stresses and pressures at the quartz-coesite transition in deformation experiments

Bettina Richter¹, Holger Stünitz² & Renée Heilbronner¹

¹ *Geologisch-Paläontologisches Institut, University of Basel, Bernoullistrasse 32, CH-4056 Basel (bettina.richter@unibas.ch)*

² *Department of Geology, Tromsø University, Dramsveien 201, N-9037 Tromsø*

Experiments on quartz gouge were performed in a Griggs-type deformation apparatus at displacement rates of $\sim 1.3 \times 10^{-5}$ mms⁻¹ or $\sim 1.3 \times 10^{-4}$ mms⁻¹, at $P_c = 1.0$ GPa or 1.5 GPa and $T = 600^\circ\text{C}$ to 800°C . The starting material is a natural hydrothermally grown quartz single crystal that was crushed to a powder with grain size $d < 100 \mu\text{m}$.

Coesite is found if the maximum principle stress (σ_1) is in the coesite stability field. In general the confining pressure (P_c) and the mean stress (P_m) of these samples are below the quartz-coesite phase transition. Coesite is not found if σ_1 is below the quartz-coesite phase transition. At $T = 600^\circ\text{C}$, σ_1 is always in the coesite stability field. But coesite is only present in the high strain experiment, indicating slow transformation kinetics.

In one sample we observed that σ_1 crosses the quartz-coesite transition during the loading part and after progressive weakening crosses the transition back into the quartz stability field. The microstructure of this sample shows the formation of coesite and the reverse transformation from coesite to quartz.

The coesite growth penetrates the sample and coesite grows around and in between larger quartz clasts. At high stresses, where P_m is also above the quartz-coesite phase transition, coesite often forms radiating aggregates. At lower stresses, where only σ_1 lies in the stability field of coesite, and at low strain the coesite grains have a preferred orientation of the b-axes (sub-) parallel to σ_1 . With increasing strain, the rigid coesite grains rotate and align with the preferred quartz fabric.

For coesite to be found, it is sufficient that σ_1 reaches values above the transformation pressure. If σ_1 drops back into the quartz stability field during an experiment, a back-reaction from coesite to quartz is observed. It appears therefore that the pressure that defines the quartz-coesite phase transition is not P_c or P_m , but σ_1 .

P 1.25**Preliminary results of the Swiss National Map, sheet Osogna (no. 1293,1:25'000)**

Filippo Luca Schenker¹, Christian Ambrosi¹, Cristian Scapozza¹, Claudio Castelletti¹ & Matteo Maino²

¹ *Institute of Earth Sciences, University of Applied Sciences and Arts of Southern Switzerland (SUPSI), Via Trevano, CH-6952 Canobbio (filippo.schenker@supsi.ch)*

² *Dipartimento di Scienze della Terra e dell'Ambiente, University of Pavia, via Ferrata 1, I-07100 Pavia*

We present preliminary results of the geological map of the Osogna sheet, (Swiss National Map no. 1293,1:25'000). The area extends S-N from Claro to Biasca and W-E from Lavertezzo to the Pizzo di Claro, respectively. From bottom-to-top, the mapped area includes the subpenninic gneissic nappes of the Leventina, Simano, Adula/Cima-Lunga and Maggia. These nappes derive from the same post-Variscan gneissic crust complicating their lithological distinction. In particular, the boundary between the Leventina and the Simano gneisses is not clear. Generally, the boundary was traced within leucogneisses by joining quartzite, amphibolite or paragneiss lenses. Nevertheless, we could not find any quartzite and the amphibolite and paragneisses lenses are vertically distributed in the tectonostratigraphy and do not form a single folded horizon. Furthermore, no significant strain gradient related to top-to-the-foreland shearing has been observed between these two units, also when paragneisses and amphibolites were present. Therefore, we present evidence that the top-to-the-foreland deformation between the Leventina and the Simano units was more distributed than commonly assumed, questioning the allochthonous character of the Simano unit.

P 1.26

Parasitic folds with wrong vergence: How asymmetries can be inherited

Timothy Schmid¹, Marcel Frehner¹

¹ Geological Institute, ETH Zurich, Sonneggstrasse 5, CH-8092 Zurich
(schmidt@student.ethz.ch)

An S-shaped asymmetric parasitic fold develops on the right limb of a larger upright antiform (Ramsay & Huber, 1989). Here, the opposite asymmetry is investigated by conducting two-dimensional numerical simulations of multilayer folding. The finite-element method is employed to model compression and folding of a multilayer stack with linear viscous rheology (Figure 1).

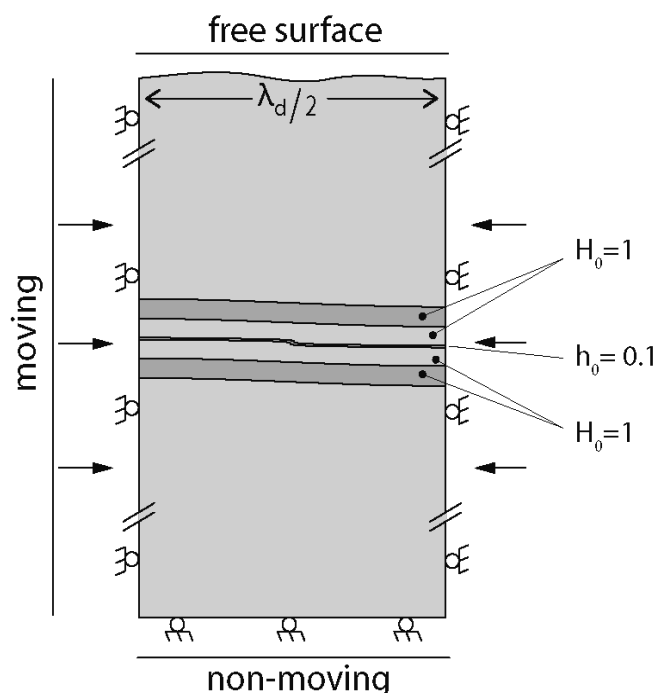


Figure 1. 2D model box with a free-slip boundary condition at the bottom and on the left and right side. On the top, the model is bounded by a free surface and the model is shortened horizontally. A thin layer containing a pre-existing asymmetry is surrounded by a matrix embedded between two thick layers. The thick-layer system has a different dominant wavelength than the thin layer. To obtain new asymmetries on the thin layer during compression, a random perturbation is added to the thin layer.

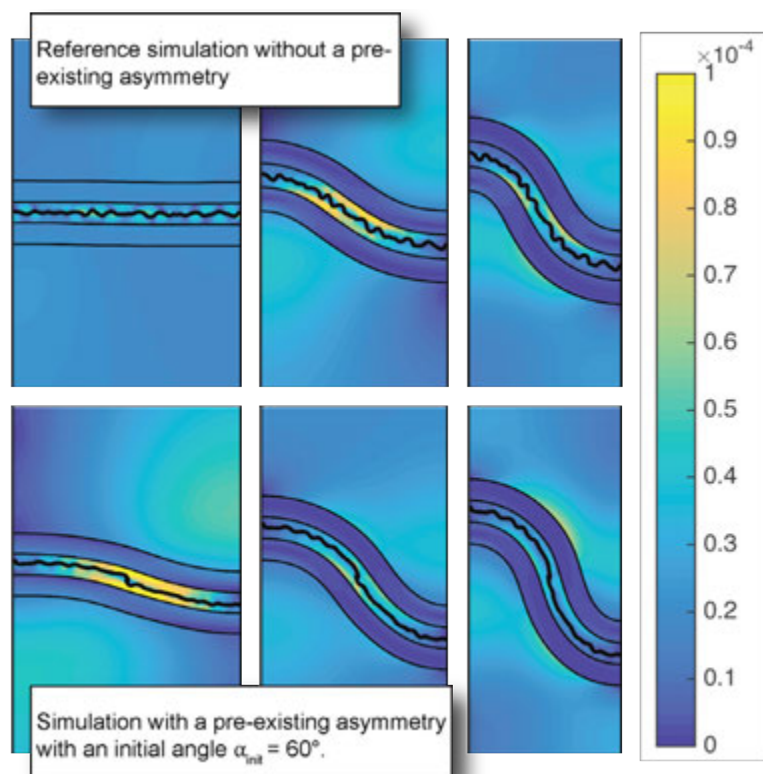
The simulations investigating the behavior of the pre-existing asymmetry during compression are divided into three settings:

1. Investigation of the initial angle of the pre-existing asymmetry and its influence on the development of new asymmetries.
2. Behavior of the multilayer system during folding, if the horizontal position of the pre-existing asymmetry varies.
3. Influence of the large scale initial amplitude on buckling and shearing of parasitic folds.

The simulations with varying initial angle of the pre-existing asymmetry show retaining asymmetries during the compression, especially for overturned asymmetries. Horizontally shifting the pre-existing asymmetry suggests that the horizontal position disturbs the sinusoidal development of the thick layer during folding.

Pre-existing asymmetries are most pronounced with a small initial perturbation of the thick layer. In addition, newly formed asymmetries show similar traits. The influence of the initial perturbation of the thick layer on thin layers is already investigated in Frehner (2006) but without pre-existing asymmetries.

The geometry of the thin layer, particularly the horizontal position of the pre-existing asymmetry, has an unforeseen effect on the amplification of the thick layer during folding. Further, the random perturbation causes small differences in the thin layer position that causes results that differ remarkably from each other.



REFERENCES

- Frehner, M. & Schmalholz, S.M., 2006: Numerical simulations of parasitic folding in multilayers. *Journal of Structural Geology*, 28, 1647–1657
- Ramsay, J.G. & Huber, M.I., 1989: *The techniques of modern structural geology, Vol.1: Strain analysis*, 4th edition, Academic Press, London, ISBN 0-12-576921-0

P 1.27

Thermal localization in a heterogeneous lithosphere

Marcel Thielmann¹

¹ Bayerisches Geoinstitut, Universität Bayreuth, Universitätsstraße 30, 95447 Bayreuth (thielmann.marcel@gmail.com)

Localization of ductile deformation in the lithosphere is one of the prerequisites for the formation of shear zones and the initiation of subduction. A recent study (Thielmann and Kaus, 2012) has shown that shear heating is a viable mechanism to create lithospheric-scale shear zones. It was also shown that during lithosphere compression, folding precedes and significantly influences shear zone formation. In that study a homogeneous lithosphere was used, in reality however, the lithosphere is highly heterogeneous.

Here I therefore investigate the effect of heterogeneities on the deformation behaviour of a compressed lithosphere using 2D numerical models. The lithosphere is approximated as a layer where heterogeneity fields are prescribed by translating 2D Gaussian random rough surfaces with different correlation lengths to material properties. The governing equations of mass, momentum and energy are solved in 2D using the finite element package MILAMIN_VEP (e.g. Kaus, 2010).

Results show that a very heterogeneous stress field develops under compression where regions of high stresses consequently experience more shear heating. This has a significant impact on the timing of the onset of localization (if it occurs). Furthermore, the anisotropy of the heterogeneity as well as their correlation length has a non-negligible effect.

REFERENCES

- Kaus, B. J. P. 2010, Factors that control the angle of shear bands in geodynamic numerical models of brittle deformation, *Tectonophysics*, 484, 36–47.
- Thielmann, M., and B. J. P. Kaus 2012, Shear heating induced lithospheric-scale localization: Does it result in subduction? *Earth and Planetary Science Letters*, 359-360, 1–13, doi:10.1016/j.epsl.2012.10.002.

P 1.28

3D fold geometry at Panixer pass

Pascal von Däniken¹, Marcel Frehner¹

¹ Geological Institute, ETH Zurich, Sonneggstrasse 5, CH-8092 Zurich
(pascalvd@student.ethz.ch)

At the Panixer Pass in the eastern Swiss Alps the Panixer Pass Transverse Fold is oriented approximately perpendicular to most alpine structures. It represents a plunging fold with Verrucano in its core, which is cut by the Glarus Thrust; hence Verrucano can be found below the Glarus Thrust (Figure 1). The structural buildup of the Infrahelvetetic Complex changes considerably across the Panixer Pass Transverse Fold.

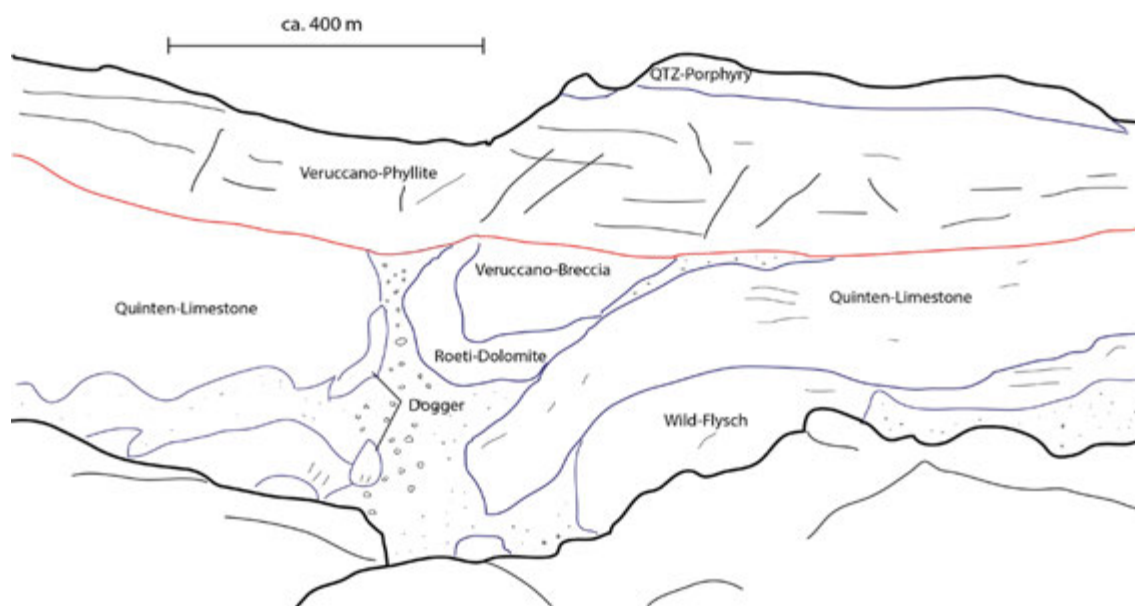


Figure 1. Sketch (after photograph) of the Panixer Pass Transverse Fold, seen from NW.

This Panixer Pass Transverse Fold has been known for a long time and multiple theories on its evolution have been published (Oberholzer, 1933; Wyssling, 1950). However, none of those is satisfying, especially under modern structural geological and tectonic viewpoints. The main aim of this study is to get a better insight into the Panixer Pass Transverse Fold by field mapping and structural analysis in combination with producing a 3D structural model using the GeoModeller software. To produce the 3D model, geologic contact data and orientation data gathered in the field were used in combination with interpreted data in the form of cross-sections.

A 3D structural model was created (Figure 2) that honors the observed surface geology and the expected subsurface geometry. It is in good agreement with earlier cross-sections (Wyssling 1950; Pfiffner 1978). Additionally, idealistic foliation planes were added to the 3D model. The aim is to compare the foliation orientation to the 3D geology and to illustrate the difference of foliation orientation below and above the Glarus Thrust.

Based on the observed structures in the mapping area, a series of deformation events was worked out. Generally, the result relates well to the deformational phases defined by Milnes & Pfiffner (1977). Some differences may be due to the difference in scale of the studies.

The results show that the Panixer Pass Transverse Fold formed simultaneously with the thrusting in the Infrahelvetetic Complex. A combination of lateral ramp and strike-slip fault is presented as interpretation of the Panixer Pass Transverse Fold. Due to heterogeneity in the Verrucano trough, a lateral ramp developed, which caused the difference in the structural style on either sides of the transverse fold. A sequence of block diagrams was created to illustrate the deformation events.

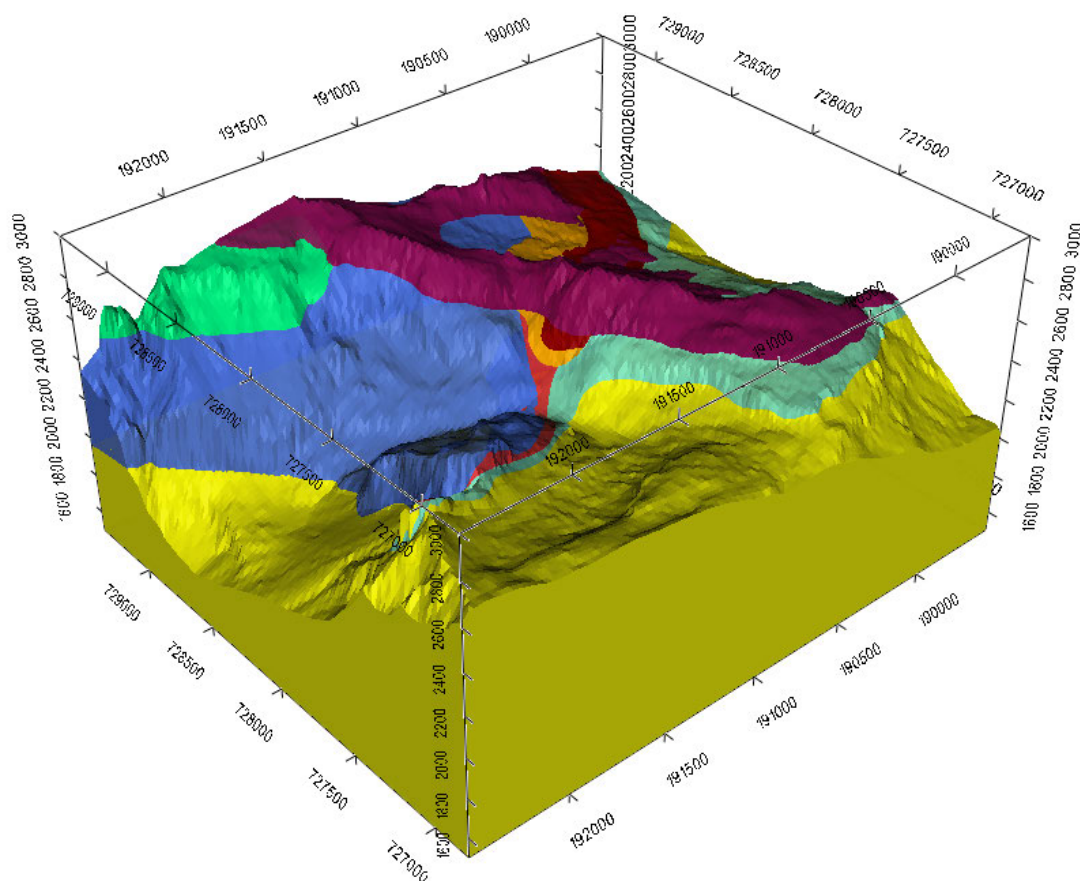


Figure 2. 3D structural model of the Panixer pass area, seen from NW. The box is 1500 m high.

REFERENCES

- Milnes, A. G. & Pfiffner, O. A. 1977: Structural development of the infrahelvetetic complex, eastern Switzerland. *Eclogae Geologicae Helveticae*, 70, 83–95.
- Oberholzer J. 1933: *Geologie der Glarneralpen*, Bern: Francke.
- Pfiffner, O. A. 1978. Der Falten- und Kleindeckenbau im Infrahelvetikum der Ostschweiz. *Eclogae Geologicae Helveticae*, 71, 61–84.
- Wyssling, L. E. 1950: *Zur Geologie der Vorabgruppe*. Ph. D. dissertation, ETH Zurich.

P 1.29**Inverted localization of deformation in the “dry” middle crust across the Woodroffe Thrust, Central Australia**

Sebastian Wex¹, Neil Mancktelow¹, Friedrich Hawemann¹, Alfredo Camacho² & Giorgio Pennacchioni³

¹ *Department of Earth Sciences, ETH Zurich, Sonneggstrasse 5, CH-8092 Zurich*

² *Department of Geological Sciences, University of Manitoba, 125 Dysart Rd, Winnipeg, Manitoba, R3T 2N2 Canada*

³ *Department of Geosciences, University of Padua, Via Gradenigo 6, 35131 Padua*

Young orogens, such as the Alps, mainly expose the upper part of the continental crust and it is not possible to follow large-scale thrusts to great depth in order to study their changing rheological behaviour. This knowledge, however, is crucial for determining the overall kinematic and dynamic response during collision, as middle to lower crustal rocks represent the major part of the total crustal section. Information from deeper parts of the continental crust can only be obtained directly by investigating regions where these levels are now exhumed.

The Musgrave Ranges region in Central Australia is a very well exposed, semi-desert area, in which numerous large-scale shear zones developed during the intracratonic Petermann Orogeny around 550 Ma. The most prominent structure is the ~600 km long E-W trending Woodroffe Thrust, which placed ~1.2 Ga granulites onto similarly-aged granitoids and amphibolite-granulite facies gneisses along a south-dipping thrust plane with a top-to-north shear sense. Ductile deformation related to this thrusting was mainly accommodated in a continuous sequence of protomylonites, mylonites, ultramylonites and sheared pseudotachylytes, which preferentially localized in the footwall rather than in the hanging wall. On a regional scale, conditions are generally “dry”, as indicated by: 1) lack of syn-tectonic quartz veins; 2) the fine dynamically recrystallized grain size of quartz (av. 30 µm) and feldspar (<10 µm); 3) dominantly porosity-free quartz grain boundaries; 4) metastable plagioclase in the presence of K-feldspar, which rarely shows any significant sericitization; and 5) breakdown of plagioclase to kyanite + garnet, rather than to kyanite + clinozoisite.

Thorium concentrations estimated from airborne surveys show a pronounced contrast between higher values in the footwall and lower values in the hanging wall. This clear distinction between hanging wall and footwall units is an inherited feature due to 1) partial melting and associated depletion in incompatible thorium during the earlier ~1.2 Ga granulite facies metamorphism and 2) the fact that the footwall predominately consists of granitoids rather than granulites. However, the spatial resolution is currently insufficient to precisely determine the original boundary between the two compositionally similar protoliths within the thrust zone. Measuring the thorium concentration in felsic assemblages across the Woodroffe Thrust, using gamma spectrometry, allowed a precise quantification of the extent to which the hanging wall was cannibalized into the Woodroffe Thrust mylonites.

The preferential concentration of mylonites in the footwall of a thrust is unusual and cannot be explained by geothermobarometry, which yields uniform P/T estimates of ~650°C and 1.2 GPa in the hanging wall and lower P/T conditions of ~600°C and 0.8 GPa for the immediately underlying footwall. Pseudotachylytes, which have been identified as the preferred nucleation sites for shearing under “dry” mid-crustal conditions, are present on both sides. The most likely explanation for the inverted localization of deformation across the Woodroffe Thrust is either 1) the observed greater abundance of hydrous minerals in the footwall and potentially also in the pseudotachylytes developed from them or 2) externally derived fluids, introduced on a very local scale. Field and microscopic observations suggest that externally introduced fluids are scarce and, where present, possibly rich in CO₂, as indicated by the crystallization of calcite in otherwise completely non-carbonaceous rocks. On the other hand, the higher abundance of hydrous minerals in the footwall could more easily localize deformation and recrystallization. We favor a combination of model 1) and 2) based on the close correlation between the variable extent of hanging wall cannibalization and regional trends in: 1) the variation of plagioclase breakdown reactions; 2) the abundance of fine-grained calcite; and 3) the variation in the size and abundance of micro-scale etch pits on recrystallized quartz grains (“fossil” porosity acting as a proxy for free fluid activity during deformation). However, a process explaining the associated minor cannibalization of the lowermost hanging wall is still lacking.

P 1.30

About the Autochthony of Constantinois Neritic Shelf (NE Algeria)

El Hadj Youcef Brahim¹, Mohamed Chadi², Rami Djeflal³

¹ Department of Earth Science and universe , University of Batna ,Laboratory of Geology and Environment, Constantine –Algeria (wahidyb@yahoo.fr)

² Normal Superior School, Laboratory of Geology and Environment, Constantine-Algeria

³ Department of eEarth Science and Universe , University of Batna.

The synthesis of stratigraphic and structural data of Constantinois limestone massifs has allowed the refining of the southern Tellian series at nummilites stratigraphy and proposing a structural model. The most significant sites and less disturbed by tectonics, are the Texas syncline and southern flank of Guerioun massif, exactly at the Djebel Ras Rihane.

Also, at the level of Texas syncline, and surmounting the hard ground which ended the Aptian neritic limestone, the marly levels had provided Cenomanian microfauna: *Favusella washitensis*, *Rotalipora appenninica*, *R. cushmani*, *R. brotzeni*, *Hedbergella* sp., and *Praeglobotruncana stephani*.

On the southern reverse of Djebel Ras Rihane, at the level of Chaabet Ras Chiboub notch, we can observe, on the hard ground that terminates the Aptian neritic limestones, a clayey Cenomanian over one hundred meters of thickness. The samples from these clays have provided many *Hedbergella*, *Rotalipora brotzeni*, *R. cushmani*, *R. globotruncanoides* and *Praeglobotruncana* gr. *Stephani*.

The top of these clays has provided Coniacian foraminifera and revamped Cenomanian *rotalipora*. The study of the stratigraphic series of s neritic massifs allowed the refining of our predecessor's results. Also the yellow marls stratigraphically surmounting the terminal Aptian- basal Albian through a hard ground, represents the Cenomanian-Turonian.

Microscopic analysis of samples from this hard ground highlights sedimentological phenomena that attest the emersion of Constantinois platform during the terminal Aptian- basal Albian.

In the Constantinois limestone massifs, "the southern Tellian units at Nummilites " represent the normal marly cover of neritic limestones.

2. Mineralogy, Petrology, Geochemistry

Sébastien Pilet, Bernard Grobéty, Eric Reusser

Swiss Society of Mineralogy and Petrology (SSMP)

TALKS:

- 2.1 Balashova A., Mattsson H.B., Hirt A.M., Almqvist B.S.G.: The evolution of the Oldoinyo Lengai volcano and the origin of the Lake Natron Footprint Tuff (northern Tanzania)
- 2.2 Bellver-Baca M.T., Chiaradia M.: RAFC processes and temporal factors favouring porphyry mineralisation in high Sr/Y magmas
- 2.3 Bergemann C., Gnos E., Berger A., Whitehouse M., Walter F., Bojar H.-P.: Hydrothermal monazite records Eo-Alpine retrograde evolution in the Eastern Alps
- 2.4 Burn M.: Implications of allanite – monazite – zircon age data for Permian magmatism in the Southern Alps
- 2.5 Davies J.H.F.L., Schaltegger U., Baresel B., Bouvier A.-S., Baumgartner L.P.: Identifying and understanding Pb loss in baddeleyite
- 2.6 Dolejs D., Spillar V.: Creating a pluton, from crystal nucleus to the entire intrusion
- 2.7 Ellis B., Szymanowski D., Troch J., Bachmann O., Wotzlaw J.F., Guillong M., Bindeman I., Schmitt A.: Post-caldera volcanism at the Heise volcanic field: implications for petrogenetic models
- 2.8 Giuntoli F., Lanari P., Kunz B., Burn M., Engi M.: Garnet growth and resorption as a tracer of Alpine HP-rehydration of Permian granulite: a case study in the Sesia Zone (NW Alps)
- 2.9 Hartung E., Caricchi L., Floess D., Wallis S., Harayama, S.: Takidani Granodiorite: Insights into a young magma chamber
- 2.10 Kunz B.E., Regis D., Manzotti P., von Niederhäusern B., Burn M., Giuntoli F., Engi M.: Pre-Alpine and pre-rifting crustal evolution of continental fragments in the Western Alps
- 2.11 Lavoie J., Moritz R., Popkhadze N., Spangenberg J., Ulyanov A., Chiaradia M.: The Late Cretaceous Beqtakari prospect: evidence for subaerial epithermal mineralization in the Bolnisi mining district, Georgia, Lesser Caucasus
- 2.12 Manzini M., Bouvier A.-S., Baumgartner L., Rose-Koga E., Schiano P., Shimizu N.: Oxygen isotopes variation in melt inclusions from MORB samples
- 2.13 Martenot F., Bouvier A.S., Baumgartner L., Caricchi L., Schaltegger U.: Apatite volatile and trace element variations: a new tool to study geochemical and petrogenetic processes in the calc-alkaline Adamello batholith
- 2.14 Mullis J., Felix H., Proce M., Wolf M., Vennemann T., Franz L., de Capitani C., Antognini M., Bucher K.: Fluid evolutions and their significance in the Lötschberg and Gotthard base tunnels, Switzerland
- 2.15 Rezeau H., Moritz R., Wotzlaw J.-F., Tayan R., Ulyanov A., Stern R.A.: Batholith construction over 30 million years in the Lesser Caucasus: temporal and geochemical constraints
- 2.16 Roggero D., Pilet S., Müntener O.: Geochemical and petrological evidence for a link between the Cenozoic calc-alkaline and alkaline volcanism in north-western Sardinia, Italy
- 2.17 Siron G., Baumgartner L., Bodner R.: What does chlorine content in biotite say about the metamorphic fluids: Case studies from the Torres del Paine and Western Adamello contact aureoles
- 2.18 Stern W.B.: Phosphate: a neglected clue to technology and systematics of ancient glass
- 2.19 Tajčmanová L., Moulas, E., Vrijmoed J., Podladchikov Y.: Can grain-scale pressure variations provide direct constraints on rheology?
- 2.20 Zhong X., Vrijmoed J., Tajčmanová L., Moulas E.: On coupling of viscous relaxation and chemical diffusion under grain scale pressure variation

POSTERS:

- P 2.1 Arbiol C., Kouzmanov K., Dini A., Wälle M.: Major and trace element geochemistry of a distal Fe skarn – Torre di Rio, Elba Island (Italy): Insights from hedenbergite, epidote and ilvaite LA-ICP-MS analyses
- P 2.2 Rottier B., Kouzmanov K., Bouvier A.-S., Wälle M., Fontboté L.: Shallow porphyry stockwork veining at Cerro de Pasco: constraints from fluid inclusions, in-situ oxygen isotope and trace element analysis by SIMS and LA-ICP-MS
- P 2.3 Bovay T., Kouzmanov K., Dini A., Wälle M., Vassileva R., Gerdjikov I.: Distal johannsenite-hedenbergite skarns at Madan, Bulgaria and their link to Pb-Zn mineralization: constraints from trace element analyses in skarn silicates
- P 2.4 Casanova V., Kouzmanov K., Bouvier A.-S., Fontboté L., Baumgartner L.: Tracing hydrothermal fluid evolution in the epithermal deposit of Colquijirca: insights from in-situ oxygen and trace element analyses in quartz
- P 2.5 Chatzipanagiotou Ch.: Genetic relationships between spatially associated arsenide and sulphide magmatic ores from the Carratraca Ultramafic Massif (Málaga, south Spain)
- P 2.6 Fekete S., Weis P., Driesner T., Heinrich C.A., Baumgartner L., Bouvier A.-S.: High resolution, in situ ^{18}O analyses of quartz from the Yankee Lode tin deposit (Mole Granite, Australia)
- P 2.7 Karadima N., Kouzmanov K., Dini A., Wälle M., Spangenberg J., Poté J.: Sulfur isotopes and trace element analyses of ore and gangue minerals from the Rio Marina Fe-deposit, Elba Island: implications for formation mechanism and fluid sources
- P 2.8 Botter C., Grobéty B.: SEM/EDS and TEM/EDS analyses of volcanic particles sampled above the surface of the Erta'Ale lava lake, Danakil depression, Ethiopia, using a remotely-controlled self-closing sampler
- P 2.9 Malvoisin B., Mazzini A., Miller S.A.: Temperature record in clasts expelled from the LUSI mud eruption (Indonesia): evidence for large scale hydrothermal activity
- P 2.10 Régnier A., Caricchi L., Londoño J.M., Mendez R.A.: Petrological evolution and pre-eruptive conditions of a highly explosive volcano showing signs of unrest: Cerro Machin, Colombia (Master project)
- P 2.11 Ricchi E., Caricchi L., Bindeman I., Wotzlaw J.: The generation and architecture of crustal rhyolitic reservoirs: insights from the Kilgore Tuff eruption
- P 2.12 Scignari M., Pioli L., Caricchi L., Andronico D.: Driving mechanisms of 1651 and 2002 eruptions at Etna volcano (Italy)
- P 2.13 Tamagnone Cosmelli E.: Petrography and geochemistry of Cusín and Cubilche volcanic complexes (Interandean Valley, Ecuador)
- P 2.14 Wanke M., Ellis B.S., Bachmann O., Guillong M., Clynne M.A.: Plutonic xenoliths from Mount St. Helens – a window into the magma plumbing system
- P 2.15 Didier A., Putlitz B., Baumgartner L., Bouvier A.-S.: New calibration for $\delta^{18}\text{O}$ analysis of monazite by SIMS
- P 2.16 Schaltegger U., Wotzlaw J.-F., Ovtcharova M., Schoene B., Davies J.H.F.L., Baresel B.: Limits of precision and reproducibility in high-precision isotope-dilution U/Pb geochronology

- P 2.17 Schmid R., De Capitani C., Franz L., Rahn M.: Semi-quantitative Raman spectroscopy on fluor-hydroxyapatite serial solid solutions
- P 2.18 Seitz S., Putlitz B., Baumgartner L., Escrig S., Meibom A., Bouvier A-S., Vennemann T.: NanoSIMS study on quartz phenocrysts
- P 2.19 Ulianov A., Müntener O., Schaltegger U., Bussy F.: Detection in LA-ICPMS: Construction and performance evaluation of decision rules
- P 2.20 Naumenko-Dèzes M.O., Bouman C., Nägler Th.F., Mezger K., Villa I.M.: High accuracy analysis of the whole range of Ca natural isotopes by TIMS
- P 2.21 Bach N., Kouzmanov K., Caricchi L., Dini A., Wälle M.: Compositional variations of peritectic garnet in peraluminous leucogranite sills from Elba Island (Italy): Implications for crustal melt generation processes
- P 2.22 d'Abzac F.-X., Davies J., Schaltegger U.: The Silicon isotope composition of zircons: a tracer for magma evolution ?
- P 2.23 Sliwinski J., Zimmerer M., Guillong M., Bachmann O., Lipman P.: Zircon U-Pb Age Distributions in Cogenetic Crystal-Rich Dacitic and Crystal-Poor Rhyolitic Members of Zoned Ignimbrites in the Southern Rocky Mountains by Chemical Abrasion Inductively-Coupled-Plasma Mass Spectrometry (CA-LA-ICP-MS)
- P 2.24 Hirsiger C., Bussy F., Epard J.-L., Masson H., Steck A., Ulianov A.: The Lower Permian Alpigia magmatic complex and its country rock (Upper Maggia Valley, Central Alps): petrology, geochronology and structural position
- P 2.25 Proce M., Mullis J., Franz L., Antognini M.: Fluid investigation on T-max and retrograde inclusions in quartz from the Southern part of the Gotthard base tunnel, Central Alps
- P 2.26 Wolf M., Mullis J., Pettke T., Franz L., Vennemann T.: Retrograde fluid-geochemical evolution and mass transfer: an example from the Gotthard Base Tunnel
- P 2.27 Pazhakhzadeh L., Ebrahimi Nasrabadi Kh., GHaemi F., Darvishi khatooni J.: The genesis of fluorite in the Koh-sefid region of Sarakhs, Iran
- P 2.28 Dörner E.L., Leander F., Rüdiger K.: Petrographic and microtectonic investigation of the metamorphic rocks of the Wehratal
- P 2.29 Kuster A., Franz L., Wetzel A.: Investigations of gravels from the Klemmbach based on sedimentological and petrographic methods
- P 2.30 Lafay R., Baumgartner L.-P., Schwartz S.S., Montes-Hernandez G., Vennemann T.: The Ophicalcites of the Chenaillet Complex, (Western Alps, France): a fossil hydrothermal system?
- P 2.31 Luisier C., Baumgartner L., Putlitz B., Vennemann T., Schmalholz S.: The Origin of Whiteschist in the Monte Rosa Nappe (Western Alps)
- P 2.32 Süssenberger A. & Schmidt S.Th.: Clay minerals as geo-thermometer under low grade metamorphic conditions: a comparative study based on chemistry/crystallinity variations of illite and chlorite and Raman spectroscopy on carbonaceous material
- P 2.33 Pandey O.P., Mezger K., Upadhyay D., Villa I.M.: Evolution of Earth's Archean crust: insights into Singhbhum craton, eastern India
- P 2.34 El Korh A., Deloule E., Luais B., Boiron M.C., Vigier N., Bastian L.: Lithium behaviour and isotopic fractionation in high-pressure metabasites (Ile de Groix, France): a coupled LA-ICPMS, MC-ICPMS and SIMS study

2.1

The evolution of the Oldoinyo Lengai volcano and the origin of the Lake Natron Footprint Tuff (northern Tanzania)

Anna Balashova¹, Hannes B. Mattsson¹, Ann M. Hirt² & Bjarne S.G. Almqvist³

¹ *Institute of Geochemistry and Petrology, Department of Earth Sciences, Swiss Federal Institute of Technology (ETH Zürich), Sonneggstrasse 5, 8092 Zürich, Switzerland (anna.balashova@erdw.ethz.ch)*

² *Institute of Geophysics, Swiss Federal Institute of Technology (ETH Zürich) Sonneggstrasse 5, 8092 Zürich, Switzerland*

³ *Department of Earth Sciences, Geophysics, Uppsala University, Geocentrum, Villavägen 16, 752 36 Uppsala, Sweden*

During its evolution the Oldoinyo Lengai volcano (northern Tanzania) has erupted magmas with a compositional range from nephelinites to phonolites and carbonatites. Intrusive, metasomatic and cumulate enclaves are commonly found in all silicate products of the volcano. A new detailed geochemical and mineralogical study of 162 samples of fresh volcanic silicate material from debris avalanches and from the edifice of the volcano indicates that phonolites and (melilite)-combeite-wollastonite-nephelinites associated with carbonatites were generated via different evolutionary paths. A compilation of isotopic data from literature shows that these two suites originate from isotopically distinct parental melts. Temporally, the first stage of evolution included the phonolitic path, whereas the second, modern stage includes the production of combeite-wollastonite-bearing nephelinites, closely associated with the famous natrocarbonatites.

The modern stage (i.e., less than 10 ka) is characterised by the mildly explosive natrocarbonatitic activity, which is alternating with highly explosive, nephelinitic eruptions. Distal products of these nephelinitic eruptions cover a wide area around the volcano, however only the most recent eruptions have been documented. In this context, we paid special emphasis to the origin of the Lake Natron Footprint Tuff which has preserved hominid footprints (and receiving considerable interest within the anthropological community in recent years). The Footprint tuff is the most significant volcanoclastic horizon in the area around Oldoinyo Lengai. Based on the geochemical, mineralogical and magnetic data we collected from this site, we propose that the footprint-bearing horizon was deposited during one eruption of the Oldoinyo Lengai volcano (corresponding to the late nephelinitic stage of volcanism) and was slightly reworked by water. The material that comprises the upper horizon, which covers the footprints, consists of aeolian sediments from the Lake Natron – Engaruka Monogenetic Volcanic Field (i.e., melilititic in composition). Based on the petrology in combination with field observations and climatological data from the region we further conclude that the age of the Footprint tuff must be less than 11 ka, and thus approximately 110'000 years younger than previously suggested (Gibbons, 2011).

REFERENCES

Gibbons, A. 2011: Ancient footprints tell tales of travel, *Science* 332, 534-535

2.2

RAFC processes and temporal factors favouring porphyry mineralisation in high Sr/Y magmas

Bellver-Baca Maria Teresa¹, Chiaradia Massimo¹

¹ *Earth and Environmental Science Department, University of Geneva, Rue des Maraîchers 13, CH-1205 Geneva, Switzerland.*

Porphyry systems supply most of copper and an important part of gold to our economy (Sillitoe, 2010).

The relationship of giant porphyry systems with high Sr/Y magmas (also known as adakites or adakite-like magmas) has long been recognised (see summary of data in Loucks, 2014). Magmatic processes leading to high Sr/Y magmas are most likely formed during tectonic events leading to crustal thickening, favouring fractional crystallisation of amphibole and garnet (which fractionate Y), with subordinate plagioclase (which fractionate the Sr), since the latter is not stable at high pressure (e.g., Chiaradia, 2015). Those processes are reflected in most of the porphyry-associated magmatic suites which repetitively display progressively increasing Sr/Y values.

Magmatic processes leading to high Sr/Y last several million years, and the mineralisation occurs at the end of the magmatic cycles, coincident with the highest Sr/Y ratios (e.g. Yanacocha, Peru; El Teniente, Chile; Los Pelambres, Chile; Corocochuayco, Peru). However, when those magmatic cycles leading to high Sr/Y levels take place in a shorter time-scale (few ka), the systems are apparently barren (e.g. Chachimbiro, Ecuador). The current research involves the comparison of the long-lived (~4Ma) mineralised Yanacocha magmatic system with the short-lived (~0.4Ma) apparently barren Chachimbiro Volcanic Complex, with the aim of better understanding the changes which lead to magmatic fertilisation and the role time may have in magmatic specialisation.

REFERENCES

- Chiaradia, M. 2015: Crustal thickness control on Sr/Y signatures of recent arc magmas: an Earth scale perspective. *Scientific reports*. 5, 8115.
- Loucks, R.R. 2014: Distinctive composition of copper-ore-forming arc magmas. *Australian Journal of Earth Sciences: An International Geoscience Journal of the Geological Society of Australia*, v. 61 (1), p. 5–16
- Sillitoe, R. H. 2010: Porphyry Copper Systems. *Society of Economic Geologists Economic Geology*, v. 105, pp. 3–41

2.3

Hydrothermal monazite records Eo-Alpine retrograde evolution in the Eastern Alps

Christian Bergemann¹, Edwin Gnos², Alfons Berger³, Martin Whitehouse⁴, Franz Walter⁵, Hans-Peter Bojar⁶

¹ University of Geneva, Geneva, Switzerland (christian.bergemann@unige.ch)

² Natural History Museum of Geneva, Geneva, Switzerland

³ University of Bern, Bern, Switzerland

⁴ Swedish Museum of Natural History, Stockholm, Sweden

⁵ University of Graz, Graz, Austria

⁶ Universalmuseum Joanneum, Graz, Austria

High precision SIMS isotope dating, yielding ^{232}Th - ^{208}Pb monazite crystallization ages, provide insights into multiple phases of brittle deformation in the Eastern Alps. Nappe stacking occurred before and during regional metamorphism during the Eo-Alpine collision in the Cretaceous. This was followed by an transtensional phase (e.g. Dallmeyer et al., 1996) associated with the formation of the Gosau sedimentary basins still preserved in central Eastern Alps and the Northern Calcareous Alps. All three analyzed cleft monazites were sampled in cavities mineralized with dolomite±calcite±quartz and are located in a zone of brittle faults near the southern border of the Greywacke zone. Two of the sampled cleft sites are in direct proximity of the Palten-Liesing fault with the third sample site being close to the Salzach-Ennstal-Mariazell-Puchberg (SEMP) fault zone. The Neogene brittle tectonic activity of these fault zones (Wölfler et al., 2011), however, was not recorded within the monazite crystals. Only the Eo-Alpine evolution is preserved, with the older ages coinciding with cooling and continued nappe stacking in the area. Monazite crystallization was renewed at a time of transtensional movements linked with sedimentation of the Cretaceous Gosau Group and continued over several Ma.

The ^{232}Th - ^{208}Pb crystallization ages of the hydrothermal monazites span a time of ~20 Ma from around 90 to 70 Ma distributed in two age groups. The spatial distribution of age spots in combination with chemical zoning suggest a stepwise growth likely associated with subsequent partial replacement due to dissolution-reprecipitation processes.

REFERENCES

- Dallmeyer, R.D., Neubauer, F., & Handler, R. 1996: Tectonothermal evolution of the internal Alps and Carpathians: evidence from $^{40}\text{Ar}/^{39}\text{Ar}$ mineral and whole-rock data, *Eclogae Geologicae Helvetiae*, 89, 203-227.
- Wölfler, A., Kurz, W., Fritz, H., & Stüwe, K. 2011: Lateral extrusion in the Eastern Alps revisited: Refining the model by thermochronological, sedimentary, and seismic data, *Tectonics*, 30, TC4006.

2.4

Implications of allanite – monazite – zircon age data for Permian magmatism in the Southern Alps

Marco Burn¹

¹ *Institut für Geologie, Universität Bern, Baltzerstrasse 1+3, 3012 Bern (marco.burn@geo.unibe.ch)*

Permian alkaline magmatism in the Southern Alps is thought to be a result of the delamination of the Variscan orogen. Decompression in the Mantle lead to Mantle melts that rose to the depth of their neutral buoyancy and started to produce a MASH (melting-assimilation-storage-homogenization) zone. MASH-processes from time to time lead to positively buoyant melts that propagated into the upper crust and produced shallow magmatic intrusions and volcanic complexes. The duration of this magmatism in the Southern Alps is well constrained to a 10-15 m.y. time window (e.g. Schaltegger and Brack, 2007), based principally on zircon geochronology.

In this contribution we present data from one single granodioritic stock of the Cima d'Asta magmatic body. The relative crystallization history of the major and minor phases was established by detailed petrographic observations using textural analysis, micro-mapping and geochemical modelling. Biotite is the first major mineral to crystallize in the melt, followed by plagioclase, K-feldspar and quartz. Apatite is found as inclusions in zircon and biotite and is therefore probably the first mineral to crystallize in the melt. Crystallization of zircon and monazite from melt are closely linked to the crystallization of biotite. Monazite is later resorbed in the magma and overgrown by a first generation of allanite, which is in textural equilibrium with quartz and K-spar. A second growth stage of allanite is of notably different composition (e.g. higher Th-concentrations) due to incorporation of the incompatible trace elements of the last remaining melt. Late stage hydrothermal alteration is recorded in several mineral phases of the granodioritic stock. Allanite shows alteration domains concentrated on the interface of the compositional change recorded in the two magmatic growth stages. A second generation of monazite is associated with the hydrothermal alteration of these allanites.

LA-ICP-MS age-dating of the several growth stages of the datable minerals reveals an inconsistency between magmatic monazite (282.3 ± 2.1 Ma) and zircon (282.8 ± 2.3 Ma) ages to the younger magmatic allanite age (275.0 ± 1.7 Ma). The petrographic observations of the sample indicate allanite to be the representative geochronometer for the final crystallization of the shallow intrusion. Magmatic zircon and monazite ages appear to represent an earlier part of the history of the magmatic evolution, possibly still in the MASH-zone. Late hydrothermal alteration recorded in the second growth stage of monazite is constrained to 267.1 ± 4.7 Ma using a Tera-Wasserburg intercept age.

REFERENCES

Schaltegger, U., and Brack, P., 2007: Crustal-scale magmatic systems during intracontinental strike-slip tectonics: U, Pb and Hf isotopic constraints from Permian magmatic rocks of the Southern Alps: *International Journal of Earth Sciences*, v. 96, no. 6, p. 1131-1151.

2.5

Identifying and understanding Pb loss in baddeleyite

Joshua H.F.L. Davies¹, Urs Schaltegger¹, Björn Baresel¹, Anne-Sophie Bouvier² & Lukas P. Baumgartner²

¹ *Université de Genève, 13 Rue des Maraîchers, 1205 Genève, Switzerland. Joshua.davies@unige.ch*

² *Swiss SIMS, Université de Lausanne, Géopolis, Lausanne CH-1015, Switzerland*

Baddeleyite (ZrO₂) is a trace phase in mafic rocks that is commonly used for U-Pb geochronology, especially in Precambrian samples. Baddeleyite U-Pb ages often plot close to concordia and appear to be less susceptible to Pb loss than zircon with the same age and uranium content. So far, only a few dating studies focusing on baddeleyite have been conducted at very high temporal resolution (e.g. Rioux et al., 2010; Sell et al., 2014) and in these studies, small degrees of Pb loss appear to be an almost ubiquitous problem.

Pb loss in zircon is well known to correlate with oxygen isotope disturbance, where fluid interaction with metamict zircon facilitates recrystallization and Pb loss (Valley et al., 1994; Davies et al., 2015). Areas of zircon crystals that have suffered Pb loss can be selectively removed from crystals using a pre-treatment known as chemical abrasion before analysis. Attempts to apply the chemical abrasion techniques to baddeleyite have been unsuccessful (Rioux et al., 2010) and there is currently no way to identify or deal with Pb loss for baddeleyite.

Here we present new data that suggests that Pb loss in baddeleyite occurs through a different process to zircon. Using Raman, electron microprobe, oxygen isotopes (SIMS), electron imaging and U-Pb TIMS data we show that highly metamict baddeleyite recrystallizes from a monoclinic to a metastable tetragonal phase at a nano-scale. We suggest that this recrystallization is a solid-state process rather than fluid mediated and that re-crystallization in this manner facilitates Pb loss, especially in the outer rims of baddeleyite crystals or along cracks. With our new understanding of the physical process of Pb loss in baddeleyite, we suggest new ways to identify and deal with Pb loss in the future.

REFERENCES

- Davies, J.H.F.L., Stern, R.A., Heaman, L.M., Rojas, X. and Walton, E. 2015: *American Mineralogist* 100, 1952-1966.
- Rioux, M., Bowring, S.A., Dudas, F., and Hanson, R. 2010: *Contributions to Mineralogy and Petrology* 160, 777-801.
- Sell, B., Ovtcharova, M., Geux, J., Bartolini, A., Jourdan, F., Spangenberg, J.E., Vincente, J-C. and Schaltegger, U. 2014: *Earth and Planetary Science Letters* 408, 48-56.
- Valley, J.W., Chiarenzelli, J.R. and McLelland, J.M. 1994: *Chemical Geology* 234, 105-126.

2.6

Creating a pluton, from crystal nucleus to the entire intrusion

David Dolejš¹, Václav Špillar¹

¹ *Institute of Petrology and Structural Geology, Charles University, Albertov 6, CZ-12843 Praha 2
(david.dolejs@natur.cuni.cz)*

Magma differentiation by crystal fractionation represents one of the fundamental mechanisms producing chemical diversity of the Earth's oceanic and continental crust, and of all igneous bodies. The processes, which involve crystal nucleation and growth, crystal-melt mechanical interactions, dictate rheology of the evolving magma suspension and define appearance of the resulting igneous texture, but are not accessible to direct observation and thus remain only poorly known. We developed a set of high-resolution simulation algorithms, which predict the formation of igneous texture and the mechanical interactions and rheological feedback in cooling magma bodies. These models allow us to evaluate the role of crystal nucleation and growth kinetics, as well as the rheological and mechanical consequences of solidification, and lead to a new genetic typology of plutonic bodies.

Crystal nucleation and growth in a static three-dimensional regime using constant, linearly increasing, exponential, and Gaussian functions for the rates of nucleation and growth yield equigranular to seriate textures. The simulated crystal size distributions of all textures are nearly linear to concave-down (previously interpreted as formed by equilibration coarsening), and identical distribution patterns can result from multiple non-unique combinations of nucleation and growth rates. Textures resulting from random homogeneous nucleation have clustering index substantially lower than previously predicted. Additional simulations with progressively increasing amount of heterogeneous nuclei during crystallization, cause initially equigranular textures to evolve to porphyritic, bimodal and spherulitic types. The corresponding crystal size distributions become concave-up curved, the clustering index progressively decreases, and the grain contact relationships record increased clustering. Such crystal size distributions previously interpreted as resulting from multistage crystallization, mixing of crystal populations, grain agglomeration, or size-dependent growth are now predicted, consistently with other textural parameters, to form by heterogeneous crystal nucleation. In representative volcanic and plutonic rocks, including cumulate rocks, 60 to 99 % of all nuclei are heterogeneous.

Rheological properties, internal dynamics, and life time span of igneous bodies have profound implications on solidification regime of intrusive bodies in the lithosphere. We use one-dimensional model of cooling and crystallization of a horizontal melt sheet (laccolith or a single intrusive pulse) to fully couple: (i) cooling by both conductive and convective heat transfer, (ii) crystallization approximated by binary eutectic behaviour via Gibbs energy of crystallization as a driving force of crystal nucleation and growth, and (iii) feedback between effective magma viscosity and gravitational settling of crystals in the magma.

The model thus integrates progressive texture formation in a crystal mush in dynamically forming solidification fronts and convection domains. Exploration of the parameter space (melt viscosity, pluton thickness, and time) predicts significant variations in the style of magma chamber evolution and solidification. Small magma chambers crystallize by two opposite and gradually progressing solidification fronts; large magma chambers containing high-viscosity magmas crystallize gradually and uniformly by rapidly proceeding crystal interlocking whereas those filled with low-viscosity magmas form an asymmetric footwall solidification front underlying the convecting crystal mush. In the melt viscosity-pluton thickness space, our simulations predict several pluton types, which provide basis for genetic typology of intrusive bodies: (i) vigorously convecting suspensions with one-sided (footwall) crystallization front, which predominantly forms by crystal accumulation – characteristic of low-viscosity and thick intrusions; (ii) convecting suspensions, which evolve into a stationary regime, where crystallization front may be one-sided (low-viscosity melts) or symmetric (high-viscosity melts and thin intrusions); (iii) stationary suspensions, which solidify by symmetric crystallization fronts with homogeneous crystal content and texture evolution – characteristic of high-viscosity melts and thin tabular bodies. These coupled thermal, mechanical and kinetic models serve to develop a genetic classification of intrusive bodies, including a total of eight subtypes, which is further linked to textural appearance and structural diversity of intrusive unit, and should facilitate interpretation of internal dynamics in natural magma chambers.

2.7

Post-caldera volcanism at the Heise volcanic field: implications for petrogenetic models

Ben Ellis¹, Dawid Szymanowski¹, Juliana Troch¹, Olivier Bachmann¹, Jörn-Frederik Wotzlaw¹, Marcel Guillong¹, Ilya Bindeman², Axel Schmitt³

¹ *Institute of Geochemistry and Petrology, ETH Zurich, NM Clausiusstrasse 32, CH-8092 Zurich (ben.ellis@erdw.ethz.ch)*

² *Department of Geological Sciences, University of Oregon, Eugene, Oregon 97403, USA*

³ *Department of Earth and Space Sciences, University of California–Los Angeles, Los Angeles, California 90095, USA*

The Heise volcanic field, located in the eastern Snake River Plain (USA) represents the immediate precursor to the currently active Yellowstone volcanic system. In keeping with the rest of the province, the silicic volcanism from the Heise volcanic field is recorded in distal ignimbrites on the margins of the plain and widely dispersed tephra layers. The largest ignimbrites of the Heise volcanic field (the Blacktail and Kilgore tuffs) are comparable in volume to the ‘super-eruptions’ from the Yellowstone field. Previous work (e.g. Bindeman et al. 2007; Watts et al. 2011; Wotzlaw et al. 2014) have used the systematic changes in O isotopic composition of the rhyolites to develop the ‘cannibalisation model’ of petrogenesis for the low- $\delta^{18}\text{O}$ rhyolites whereby hydrothermally altered precursor volcanics are down-dropped by caldera collapse and assimilation to provide the low- $\delta^{18}\text{O}$ signature. The calderas themselves are obscured by the later eruptions of basaltic lavas and so little is known about the nature of these structures and the post-caldera record of volcanism. Fortunately geothermal investigations near Sugar City, Idaho, have provided a drillcore penetrating more than a kilometre of rhyolite within the centre of the plain, which we utilise here.

By combining a wide array of parameters (e.g. major and trace elements in pyroxenes, feldspar, glasses, Pb isotopes in sanidine and glasses, O isotopes in pyroxene, quartz and sanidine, U/Pb ages via SIMS and ID-TIMS) and comparing the drillcore rhyolite with that exposed on the surface it is clear that the two records are entirely independent. Rhyolite from the drillcore is not found on the margins of the plain, nor are the regionally extensive ignimbrites found within the drillcore.

Given that outcrops of Kilgore Tuff surround the Sugar City drillcore, the absence of Kilgore Tuff within the core requires explanation. Indeed at the Heise cliff section (some 20 km due south) the Kilgore Tuff is found at an elevation of >1,800 m while at the base of the drill core (800 m) it has not yet been reached. This cannot be explained by Basin and Range faulting which runs broadly NNE-SSW and is does not disrupt the young volcanics by this magnitude. We interpret this >1 km of displacement to represent crossing of a caldera margin located between Sugar City and the Heise cliffs.

Thus, we propose that the Sugar City drillcore represents an intracaldera succession and indeed our geochronology indicates that this succession entirely post-dates the Kilgore Tuff (4.4876 ± 0.0023 , Wotzlaw et al. 2014).

Notably, within the deeper portions of the Sugar City drillcore the rhyolites are hydrothermally altered and low $\delta^{18}\text{O}$ (from conventional bulk analyses). SIMS U/Pb geochronology constrains the eruption ages of these hydrothermally altered rhyolites to be ‘Heise-related’ so the subsequent alteration and burial of these rocks provides strong support for the ‘cannibalisation model’ at Heise. Further, the unaltered post-Kilgore rhyolites show an increasing magmatic $\delta^{18}\text{O}$ (from laser fluorination) consistent with a ‘recovery’ stage as proposed for the Yellowstone magmatic system.

REFERENCES

- Bindeman, I.N., Watts, K.E., Schmitt, A.K., Morgan, L.A., & Shanks, P.W. 2007: Voluminous low- $\delta^{18}\text{O}$ magmas in the late Miocene Heise volcanic field, Idaho: implications for the fate of Yellowstone hotspot calderas, *Geology* 35, 1019-1022
- Watts, K.E., Bindeman, I.N., Schmitt, A.K., 2011: Large-volume rhyolite genesis in caldera complexes of the Snake River Plain: Insights from the Kilgore Tuff of the Heise volcanic field, Idaho, with comparison to Yellowstone and Bruneau-Jarbridge rhyolites, *Journal of Petrology*, 52, 857-890
- Wotzlaw, J.-F., Bindeman, I. N., Watts, K. E., Schmitt, A. K., Caricchi, L. and Schaltegger, U. 2014: Linking rapid magma reservoir assembly and eruption trigger mechanisms at evolved Yellowstone-type supervolcanoes, *Geology*, 42, 807-810.

2.8

Garnet growth and resorption as a tracer of Alpine HP-rehydration of Permian granulite: a case study in the Sesia Zone (NW Alps)

Francesco Giuntoli¹, Pierre Lanari¹, Barbara Kunz¹, Marco Burn¹, Martin Engi¹

¹ *Institut für Geologie, University of Bern, Baltzerstrasse 1+3, CH-3012 Bern, Switzerland (francesco.giuntoli@geo.unibe.ch)*

The extent to which granulites are transformed to eclogites is thought to impose critical limits on the subduction of continental crust. Although it is seldom possible to document such densification processes in detail, the transformation is believed to depend on fluid availability and deformation.

Remarkably complex garnet porphyroblasts are widespread in eclogite facies micaschists in central parts of the Sesia Zone (Western Italian Alps). They occur in polydeformed micaschist with assemblages involving phengite + quartz + epidote + rutile ± paragonite, Na-amphibole, Na-pyroxene, chloritoid. Detailed study of textural and compositional types reveals a rich inventory of growth and partial resorption zones in garnet. These reflect several stages in the polycyclic metamorphic evolution. A most critical observation is that relic garnet cores indicate growth at ~800°C and ~0.75 GPa. These occur repeatedly in eastern parts of the Internal Complex (mapped by Giuntoli et al.; this conference) and are derived from granulite facies metapelites of Permian age. These dry protoliths thus must have been extensively hydrated during Cretaceous subduction, and garnet records the conditions of these processes.

In sample A two types of garnet crystals are found: mm-size porphyroclasts and smaller atoll garnets, some 100 µm in diameter. X-ray maps of porphyroclasts show complex zoning in garnet: a late Paleozoic HT-LP porphyroclastic core is overgrown by several layers of HP-LT Alpine garnet, these show evidence of growth at the expense of earlier garnet generations. Textures indicate three stages of resorption, with garnet cores being fractured and then sealed by garnet veins, rimmed by multiple Alpine overgrowth rims with lobate edges.

Garnet rim1 forms peninsular and embayed structures at the expense of core garnet. Rim2 surrounds rim1, both internally and externally, and seems to have grown mainly at the expense of the core. Rim3 grew mainly at the expense of earlier Alpine rims. In the same sample atoll garnet occurs, filled with quartz and rarely phengite, and the same Alpine overgrowth zones are observed.

In sample B garnet crystals show similar late Paleozoic HT-LP porphyroclastic fractured cores, but the first rim appears to be pre-Alpine. Then follow two Alpine generations, the first of which grew at the expense of pre-Alpine garnet. The two pre-Alpine generations show fractures, which were sealed by garnet of a composition similar to the Alpine rims. Modeling garnet growth zones is challenging, as each growth step demands an estimate of the effective bulk composition that varied locally (in time and space).

For the two samples, modelled using the XRF analysis of the bulk sample, the core of garnet is found to have formed at 800°C, 0.75 GPa, in accordance with the literature (e.g. Lardeaux & Spalla 1991).

Based on effective bulk compositions, the successive Alpine rims of sample A are found to reflect an increase from ~650°C, 1.5 GPa for rim1 to ~670°C, 1.7-2.0 GPa for rim2 and rim3. Allanite crystals contain inclusions of Alpine garnet, phengite and rutile; *in situ* geochronology (U-Th-Pb by LA-ICP-MS) on allanite yields a (minimum) age of ~69 Ma for the main growth of Alpine garnet rims. Zircon in these eclogitic micaschists shows partial resorption and new growth at 68-57 Ma as well as 310-250 Ma; garnet and zircon show a similar behaviour.

Sample B shows a pre-Alpine amphibolitic rim stable at ~630°C, 0.55 GPa; again similar condition are described in literature (e.g. Lardeaux & Spalla 1991). The two Alpine rims are stable at ~630°C, 1.6 GPa. Phengite and paragonite are intergrown with allanite and occur as inclusions in the fracture-affected portions of garnet; *in situ* geochronology on allanite yields ~74 Ma. This age is interpreted to mark the main crystallization of phengite and paragonite in the sample, coeval with fluid-influx and related deformation. Zircon in this sample shows a Permian rim but it does not show Alpine overgrowth.

The oxygen isotopic composition of quartz from different structural domains was analyzed by SIMS (Cameca-1280). In the two samples analyzed, each growth domain shows uniform $\delta^{18}\text{O}$ values (± 0.1 ‰), but variations overall show a range from ca. 13.5 to 15.1 ‰. Differences correlate with the petrographically identified growth generations. Detailed profiles across quartz grains indicate no major diffusion effects. Late quartz (e.g. in cores of atoll garnet) indicate a systematic trend towards $\delta^{18}\text{O}$ ~14.5 ‰ (from higher $\delta^{18}\text{O}$ in sample A, and from lower $\delta^{18}\text{O}$ in sample B). These trends suggest growth from a reactive hydrous fluid that circulated in the Sesia subduction channel, converting pelitic granulites back to micaschists at eclogite facies conditions. Fluid-influx in these samples clearly predates the deformation and blueschist-facies hydration

reported from Sesia Zone mylonites by Konrad-Schmolke et al. (2011).

In summary, the textures and mineral compositions clearly reflect reactive interaction of major amounts of hydrous fluids with dry protoliths at eclogite facies conditions. The protoliths are comparable to the metapelites with Permian intrusives found in the Ivrea Zone today, supporting the long held notion of an origin of the Sesia Zone at the NW-Adriatic margin.

REFERENCES

- Konrad-Schmolke, M., O'Brien, P.J., Zack, T. (2011). Fluid migration above a subducted slab – Constraints on amount, pathways and major element mobility from partially overprinted eclogite-facies rocks (Sesia Zone, Western Alps). *J. Petrol.* 52, 457-486
- Lardeaux, J. M. & Spalla, M. I. (1991). From granulites to eclogites in the Sesia zone (Italian Western Alps): A record of the opening and closure of the Piedmont ocean. *Journal of Metamorphic Geology*, 9, 35–59.

2.9

Takidani Granodiorite: Insights into a young magma chamber

Eva Hartung¹, Luca Caricchi¹, David Floess¹, Simon Wallis², Satoru Harayama³

¹ Department of Earth and Environmental Sciences, University of Geneva, Geneva, Switzerland (eva.hartung@unige.ch)

² Department of Earth and Planetary Sciences, Nagoya University, Nagoya, Japan

³ Geology Department, Shinshu University, Matsumoto, Japan

We are presenting new petrological data from one of the youngest exposed magma chambers in the world, the Takidani Granodiorite (Japan). This pluton has been suggested as a source for large volume ignimbrites ($> 300\text{km}^3$)². Takidani Granodiorite ($0.8 - 1.9\text{ Ma}$)^{2,7} is located within the active Norikura Volcanic Chain in the Northern Japan Alps and has been previously linked to large andesitic (1.76 Ma)⁴ and rhyolitic eruptions (1.75 Ma)⁴. The pluton is vertically zoned and consists of granites ($67 - 68\text{ wt.}\% \text{SiO}_2$) in the lower section and granodiorites ($65 - 66\text{ wt.}\% \text{SiO}_2$) in the middle section. The upper section is a chemically more evolved fine to coarse-grained porphyritic unit ($67 - 71\text{ wt.}\% \text{SiO}_2$). The porphyritic texture indicates rapid crystallisation, which could be the result of the late intrusion of this unit at the roof of the magmatic system.

However, no sharp contact is found between the underlying granodiorite and the porphyritic unit. Instead gradual changes of texture, major and trace element chemistry, and magnetic susceptibility are observed. This suggests that melt was either extracted from the granodiorite or that the granodiorite interacted with the porphyritic unit while both were in a molten or partially molten stage.

Electron microprobe analyses of plagioclases show three main crystal populations (Type I, II and III) with distinct anorthite and Fe contents. Type I plagioclase (An_{30-40}) occurs within the granodiorite and porphyritic unit, but is most abundant in the porphyritic unit. Type II plagioclase (An_{40-45}) is common in both, the granodiorite and the porphyritic unit. Type III plagioclase (An_{45-50}) is predominantly present in the granite. Few Type III crystals, however, are found within the granodiorite and the porphyritic unit. All plagioclase populations share a common rim (An_{20}) across the different units.

Two populations of amphiboles are identified and barometric calculations provide pressure estimates between 1.2 and 2 kbar for one population and 3 to 4 kbar for the other. Biotite compositions are relatively homogeneous across the different units with some differences in the granite unit.

Storage and crystallisation conditions of Takidani Granodiorite are derived from crystallisation experiments^{1,3}, barometry, thermobarometry⁶ and hygrometry⁵ and indicate that magmas was ultimately stored at 1.2 to 2 kbar, 850 to 875°C, and contained 4 to 5 wt.% H_2O . The appearance of biotite may indicate the presence of sulphur ($>0.1\text{ wt.}\%$)¹.

Overall, bulk rock and mineral chemistry suggest that the different units of Takidani Granodiorite were emplaced and cooled at the same or similar magmatic conditions. Mixing plagioclase populations as well as a gradual change in bulk rock geochemistry suggest that the porphyritic unit could have segregated from the granodiorite. We are currently working on the volcanic products putatively associated with the Takidani pluton, to determine whether the porphyritic unit was actually the source of large eruptions that produced more than 300km^3 of volcanoclastic deposits.

REFERENCES

- [1] Costa, F. 2004: Petrological and Experimental Constraints on the Pre-eruption Conditions of Holocene Dacite from Volcan San Pedro (36 S, Chilean Andes) and the Importance of Sulphur in Silicic Subduction-related Magmas, *Journal of Petrology*, 45(4), 855–881
- [2] Harayama, S. 1992: Geology Youngest exposed granitoid pluton on Earth : Cooling and rapid uplift of the Pliocene-Quaternary Takidani Granodiorite in the Japan Alps, central Japan, *Geology*, 20(July), 657–660.
- [3] Holtz, F., Sato, H., Lewis, J., Behrens, H. & Nakada, S. 2005: Experimental petrology of the 1991-1995 Unzen dacite, Japan. Part I: Phase relations, phase composition and pre-eruptive conditions, *Journal of Petrology*, 46(2), 319–337.
- [4] Kimura, J.-I. & Nagahashi, Y. 2007: Origin of a voluminous iron-enriched high-K rhyolite magma erupted in the North Japan Alps at 1.75 Ma: Evidence for upper crustal melting. *Journal of Volcanology and Geothermal Research*, 167(1-4), 81–99.
- [5] Lange, R. A., Frey, H. M. & Hektor, J. 2009: A thermodynamic model for the plagioclase-liquid hygrometer/thermometer, *American Mineralogist*, 94(4), 494–506.
- [6] Putirka, K. D. (2005). Igneous thermometers and barometers based on plagioclase + liquid equilibria: Tests of some existing models and new calibrations. *American Mineralogist*, 90(2-3), 336–346.
- [7] Sano, Y., Tsutsumi, Y., Terada, K. & Kaneoka, I. 2002: Ion microprobe U-Pb dating of Quaternary zircon: implication for magma cooling and residence time, *Journal of Volcanology and Geothermal Research*, 117, 285–296.

2.10

Pre-Alpine and pre-rifting crustal evolution of continental fragments in the Western Alps

Barbara E. Kunz¹, Daniele Regis¹, Paola Manzotti¹, Brigitte von Niederhäusern¹, Marco Burn¹, Francesco Giuntoli¹ & Martin Engi¹

¹ *Institute of Geological Sciences, University of Bern, Baltzerstrasse 1+3, CH-3012 Bern, Switzerland
(barbara.kunz@geo.unibe.ch)*

Adria-derived slices of continental crust are widely distributed across the Western Alps. However, their original relation within the Adriatic margin prior to rifting, subduction and exhumation is mostly unknown. Variable Alpine overprint makes correlation difficult, and in many cases only few mineral relics or pseudomorphs retain evidence of pre-Alpine history. Zircon, due to its robustness and variety of stored information, represents an ideal archive.

Comparing and linking slices of crust to their pre-Alpine/rifting position requires knowledge of the zircon characteristics in the source region, i.e. the Adriatic margin. Therefore we analysed clastic metasediments from the Ivrea Zone and established four types of core-rim relationships, a sequence of up to four metamorphic overgrowth rims and their geochemical characteristics (U-Pb ages, Th/U ratios and Ti-in-Zrn temperatures). We also studied clastic metasediments in Adria-derived slices of continental crust of the Western Alps (IIDK, EMS, Valpelline and Emilius klippe). A mostly weak Alpine overprint in the IIDK and Valpelline slices allows recognition of numerous similarities (zircon, mineral assemblage, *P-T* conditions) with the Kinzigite Formation in the Ivrea Zone. However, strongly overprinted slices, such as most parts of the EMS and Emilius klippe, are less straightforward to link to a counterpart in the present Southern Alps (Adriatic margin). By applying our approach based on combined zircon characteristics, we were able to relate even strongly overprinted samples from the EMS and the Emilius klippe to samples from the Ivrea Zone.

The approach used in this study combines textures of zircon growth and resorption with age data and trace element characteristics. Comparisons based on such records provide a tool for robust correlations across tectonic fragments. In the present case, the evolution of lower continental fragments in the Western Alps were shown to be very similar – up to the onset of Permian rifting – as in the Ivrea Zone.

2.11

The Late Cretaceous Beqtakari prospect : evidence for subaerial epithermal mineralization in the Bolnisi mining district, Georgia, Lesser Caucasus.

Jonathan Lavoie¹, Robert Moritz¹, Nino Popkhadze², Jorge Spangenberg², Alexey Ulyanov², Massimo Chiaradia¹

¹ *Department of Earth Sciences, University of Geneva, Rue des Maraîchers 13, CH-1205 Genève*

² *Janelidze Institute of Geology & Ivane Javakishvili Tbilisi State University 1 Chavchavadze Avenue, 0179 Tbilisi, Georgia*

³ *Institute of Earth Surface Dynamics, University of Lausanne, Bâtiment Géopolis CH-1022 Chavannes-près-Renens (lavoie.jonathan.8@gmail.com)*

The Beqtakari epithermal prospect is an Au-Ag-Zn-Pb±Cu project that sits in the Artvin-Bolnisi tectonic unit along the Somkheto-Karabakh island arc (SKIA), it stretches from southern Armenia to Georgia. The volcanism associated to this island arc is the result of subduction of the Neotethys Ocean verging northeast below the Eurasian margin. The Late Cretaceous volcanism in the Bolnisi mining district is characterized by an emerging island arc of bimodal mafic-felsic composition with igneous activity expressed as lava, dome, pyroclastic flow, hyaloclastite and volcano-sedimentary sequences emplaced in transitional marine to subaerial environment. The most important deposit in the district is the nearby controversial transitional Madneuli Cu-(Au) mine, hosted in the Mashavera Formation, considered as a shallow submarine volcanic-hosted massive sulfide separated in two ore bodies: massive sulfide with a stratiform shape overlying a deeper stockwork (Gialli 2013, Popkhadze et al. 2014).

Located stratigraphically just above the Mashavera formation, the Tandzia formation is composed of mafic lava and breccia, which is just below the host rocks of the Beqtakari prospect, the Gasandami Formation. The host rocks in Beqtakari are characterized by a devitrified pyroclastic flow composed of pumice and ash with lithic clasts from bloc to lapilli size fragments that underwent hydrothermal alteration and welding. This unit played an important role in the mineralization due to its permeability. The latest volcanic event consists of a rhyodacitic dome, lava and dikes that cross-cut the mineralization. This latter unit was subject to whole-rock geochemistry and isotope analyses along with other late Cretaceous volcanic rock formations in the district and the basement. Their signatures have enrichment in LILE and a weak depletion in incompatible HFSE, implying a subduction-related signature. The heavy REE are depleted with respect to MORB for the older Mashavera felsic rocks and the successive formation are getting more enriched relative to the precedent event up to the Gasandami formation. This depleted character is in accordance with a positive epsilon value of $^{144}\text{Nd}_{t=0}$ implying little to no crustal contamination and magma depleted source.

The hydrothermal footprint at Beqtakari goes from propylitic alteration distally toward an inner progressive contact with the argillic alteration that is in sharp contact with a silicified zone, which is controlled by an inferred fault. The range of temperature obtained from illite crystallinity is between 250 to 150°C, which is consistent with the hydrothermal temperature in epithermal systems. A metal zonation is observed at Beqtakari where the pervasive silicification is Au-rich and a hydrothermal breccia at depth hosts the Au-polymetallic mineralization. Based upon descriptions of seventeen sections of drillholes, this polymetallic hydrothermal breccia shows a moderate dip toward northeast with a tabular shape and abundant jigsaw fit texture and overprinting of the argillic alteration over silicic. The ore mineralogy is Fe-poor sphalerite, chalcopyrite, galena, pyrite, tennantite ± tetrahedrite ± marcasite and arsenian pyrite. The $\delta^{34}\text{S}$ values show that the sulfate composition was not much influenced by Cretaceous marine seawater, supporting a subaerial environment. Secondary fluid inclusions assemblages of H_2O -NaCl in transparent sphalerite from the Au-polymetallic zone allowed to determine two assemblages that yield homogenization temperatures and salinities of $232 \pm 18^\circ\text{C}$ with $3.6 \pm 0.4\%$ NaCl for Fia (I) and $272 \pm 13^\circ\text{C}$ with $3.6 \pm 0.1\%$ NaCl for Fia (I)_{sub-type}. Based on petrographic observations, microprobe analyses of sphalerite of the same mineralization stage, the fluid inclusion study, and mineral associations and textures, we suggest an intermediate sulfidation epithermal character for the Beqtakari prospect during the Au-polymetallic stage.

After comparing all the characteristics from both the Madneuli deposit and the Beqtakari prospect, the geodynamic environment of the Bolnisi mining district shows a typical transition between shallow marine high-sulfidation VMS toward subaerial environment epithermal deposits at Beqtakari.

REFERENCES

- Gialli, S., 2013. The Controversial Polymetallic Madneuli Deposit, Bolnisi District, Georgia: Hydrothermal Alteration and Ore Mineralogy. Unpublished MSc Thesis, University of Geneva, Switzerland 149p.
- Popkhadze, N., Moritz, R., Gugushvili, V., 2014. Architecture of Upper Cretaceous Rhyodacitic Hyaloclastite at the polymetallic Madneuli deposit, Lesser Caucasus, Georgia. *Cent. Eur. J. Geosci.* 6, 308-329.

2.12

Oxygen isotopes variation in melt inclusions from MORB samples

Mélina Manzini¹, Anne-Sophie Bouvier¹, Lukas Baumgartner¹, Estelle Rose-Koga², Pierre Schiano², Nobumichi Shimizu³

¹ *Institute of Earth Sciences, University of Lausanne, CH-1005 Lausanne, (melina.manzini@unil.ch)*

² *Laboratoire Magmas et Volcans, Université Blaise Pascal, CNRS, F-63000 Clermont-Ferrand*

³ *Department of Geology and Geophysics, Woods Hole Oceanographic Institution, USA-MA02543 Woods Hole*

Melt inclusions (MI) hosted in high-Mg olivine are thought to retain the magma composition, unaffected by late processes. It has already been shown that MI have larger variations in major, trace and isotopic composition than matrix glasses or bulk rocks. Several processes could explain this larger scatter, making conclusion unclear. In order to better constrain the small-scale variability of MORB melt-inclusions, we analysed MI's from two Mid-Atlantic Ridge MORB samples. The major and trace elements compositions of MI from this region have been found to reflect source heterogeneity as well as melting processes (Laubier et al., 2012). $\delta^{18}\text{O}$, volatiles and trace elements in MI were analysed using the CAMECA IMS 1280-HR of the SwissSIMS at Lausanne. Different glass standards with composition ranging from basaltic to rhyolitic have been used to calibrate the instrumental mass fractionation. Two international basaltic standards (BHVO and BCR) have been used as running standards, to check instrument stability. The $\delta^{18}\text{O}$ reproducibility on standard glasses was 0.2-0.3‰ (2SD). $\delta^{18}\text{O}$ in MI display a large range (up to 2.5‰) within each sample, whereas the published bulk average $\delta^{18}\text{O}$ for Atlantic MORB glasses is $+5.5 \pm 0.3\text{‰}$ (Eiler et al., 2000). Trace elements coupled with $\delta^{18}\text{O}$ indicate that neither fractional crystallization nor partial melting could account for the large $\delta^{18}\text{O}$ scatter observed. The absence of relation between mobile elements (Cl, Ba, Sr) and $\delta^{18}\text{O}$ suggest that the observed variation could not be explained by fluid(s) contribution. First estimation of diffusion effect on $\delta^{18}\text{O}$ seems to indicate that diffusion alone could not explain the oxygen isotope range. Apart from diffusion, $\delta^{18}\text{O}$ variations could be explained by source heterogeneities and/or other small-scale magmatic processes (e.g., assimilation of oceanic crust altered at different T°) during MORB genesis.

REFERENCES

- Bouvier A.-S., Métrich N., Deloule E. 2008: Slab-derived fluids in the magma source of St. Vincent (Lesser Antilles arc): Volatile and light element imprints, *Journal of Petrology* 43, 1427-1448.
- Gurenko A. A., Chaussidon M. 2002: Oxygen isotope variations in primitive tholeiites of Iceland: evidence from a SIMS study of glass inclusions, olivine phenocrysts and pillow rim glasses, *Earth and Planetary Science Letters* 205, 63-79.
- Hartley M.E., Thordarson T., Fitton J.G., EIMF, 2013: Oxygen isotopes in melt inclusions and glasses from the Askja volcanic system, North Iceland, *Geochimica et Cosmochimica Acta* 123, 55-73.
- Laubier M., Gale A., Langmuir C. H. 2012: Melting and crustal processes at the FAMOUS segment (Mid-Atlantic ridge): New insights from olivine-hosted melt inclusions from multiple samples, *Journal of Petrology* 53, 665-698.
- Eiler J.M., Schiano P., Kitchen N., Stolper E.M. 2000: Oxygen-isotope evidence for recycled crust in the sources of mid-ocean-ridge basalts, *Letters to Nature* 403, 530-534.

2.13

Apatite volatile and trace element variations : a new tool to study geochemical and petrogenetic processes in the calc-alkaline Adamello batholith

Florian Martenot¹, Anne-Sophie Bouvier², Lukas Baumgartner², Luca Caricchi¹, Urs Schaltegger¹

¹ *Section des Sciences de la Terre et de l'Environnement, University of Geneva, Rue des Maraîchers 13, CH-1205 Genève*

² *Swiss SIMS, University of Lausanne, Bâtiment Géopolis UNIL-Mouline, CH-1015 Lausanne*

Apatite is the most abundant phosphate in igneous rocks and an important host for volatiles (OH, F, Cl) and rare earth elements (REE). Volatile and trace element concentration variations in apatite can provide great potential for unraveling complex histories of igneous rocks. In order to further develop the potential of apatite as a tool to study geochemical and petrogenetic processes, apatite grains from different units of the Adamello batholith (N. Italy) were analysed.

The calc-alkaline Adamello batholith is composed of several superunits dated from 43 to 33 Ma with rock compositions ranging from granodiorite to gabbro. The intricate emplacement history of this plutonic complex is well constrained through a number of studies conducted over several decades.

Apatite crystals were extracted from representative samples of each superunit from the Adamello batholith. The major and trace element as well as the volatile composition of the grains was obtained through electron microprobe and laser-ablation ICP-MS analyses. In order to increase the precision of measured volatile concentrations in the samples, SIMS analyses were also conducted following the internal self-calibration method introduced by Boyce et al. 2012.

Apatite volatile concentrations between different samples vary from F-rich to OH-rich, with a constant depletion in Cl. At the grain scale, volatile zoning was observed, indicating temporal equilibrium of the apatite crystals with different melt batches of different volatile concentrations. Apparently diffusion was slow enough so that some volatile zoning was maintained. These compositional heterogeneities are attributed to differences in the type of crustal material assimilated by the magma and/or interaction with fluids of different origin and salinity.

Important variations of apatite REE patterns between the different superunits and significant differences in REE concentrations within some of the samples are also observed. In order to interpret these variations, a partition coefficient based numerical model using a Monte Carlo approach was developed. Considering fractional crystallization as the major petrogenetic process, the model recalculates the mineral assemblage and liquid proportions in equilibrium with the crystallizing apatite required to produce the observed REE patterns. Comparing these recalculated proportions to experimentally reproduced granitoid mineral assemblages allows a statistically robust estimate of P and T apatite crystallization conditions.

The results suggest that apatite grains were crystallizing deeper in the final stage of the pluton formation. Crystallization temperature variations also diminishes toward the younger superunits supporting the hypothesis of a thermally mature magmatic system in agreement with previous studies on the Adamello batholith.

2.14

Fluid evolutions and their significance in the Lötschberg and Gotthard base tunnels, Switzerland

Mullis Josef¹, Felix Hélène¹, Proce Medea¹, Wolf Mathias¹, Vennemann Torsten², Franz Leander¹, de Capitani Christian¹, Antognini Marco³ & Bucher Kurt⁴

¹ *Institute of Mineralogy and Petrography, University of Basel, Bernoullistrasse 30, CH-4056 Basel (josef.mullis@unibas.ch)*

² *Institute of Earth Sciences, University of Lausanne, Geopolis UNIL, CH-1015 Lausanne*

³ *Museo cantonale di storia naturale, Viale Cattaneo 4, CH-6901 Lugano*

⁴ *Institute of Mineralogy and Geochemistry, Albert-Ludwig University, Albertstrasse 23b, G-79104 Freiburg*

The present study is focused on the significance of paleofluids conserved in quartz crystals from Alpine fissures from the Lötschberg and Gotthard base tunnels. They contain maximum temperature and retrograde fluids. Some of them are compared with recent waters (Bergwasser) collected in the Northern part of the Gotthard tunnel (Seelig & Bucher 2010; Bucher 2011).

On the base of careful inclusion petrography, fluid evolution and mineral precipitation could be correlated with episodic tectonic events that occurred during late stages of collision and uplift. Several objectives are envisaged:

1. The dominance of fluid systems, close to temperature maximum conditions within the rock units
2. The pressure-temperature evolution close to temperature maximum conditions of the earliest fluid inclusion population along the base tunnels
3. Retrograde fluid evolution with their corresponding mineral parageneses due to Alpine tectonic events
4. Fluid migration triggered by Alpine tectonic events
5. Salinity behaviour of paleofluids up to recent waters.

Preliminary interpretation

1. In the Lötschberg base tunnel the dominant fluid systems contain light petroleum and methane in the North, followed by water-rich fluids and finally by some CO₂ bearing fluids in the autochthonous cover of the Southern Aare massif. Fluids in the Gotthard base tunnel are H₂O-rich in the North and CO₂-enriched in the South.
2. Pressure and temperature evolve in the Lötschberg base tunnel from ≤200 °C and <1.5 kbar in the North to ≥300 °C and ~3 kbar in the South. In contrast, fluid pressure in the Southern Gotthard base tunnel evolves, at an assumed temperature of 400 °C, from ≤1 kbar close to Bodio to >>3 kbar in the Southern Gotthard massif. As fluid pressures in the Lötschberg base tunnel reflect more or less the overburden during fluid trapping, the increase in fluid pressure in the Tessin area from South to North is interpreted to refer to increasing fluid saturation of rocks from South to North (Proce et al., this postsession).
3. Due to episodic tectonic events, several paleofluid populations and at least 3 mineral assemblages formed (Mullis 2011). One mineral assemblage within the Central Aare granite (Alpine fissure 42 W) is characterized by precipitation of anhydrite, baryte and pyrite, showing δ³⁴S of anhydrite of 25.6 ‰ (Wolf et al., this postsession).
4. Elevated salinities in the Southern Gotthard base tunnel close to Bodio are indicative for evaporitic rocks situated below the Leventina gneiss (Hiss 1975; Mullis et al. 1994). Sulphur in minerals like anhydrite, barite and pyrite within the Central Aare granite of the Northern Gotthard base tunnel is interpreted to originate from overlying Triassic evaporites.
5. Salinity of the trapped fluids evolved in the North of the Gotthard base tunnel from ~10 wt. % in the earliest fluid inclusion population to ≤2 wt. % NaCl equivalents in the youngest detected fluid inclusion population, and finally to bulk salinities between 0.27 to 0.035 wt. % in the recent waters (Seelig & Bucher 2010; Bucher 2011). Salinity decrease within paleofluids during retrograde conditions is well known (Mullis et al. 1994). It can be interpreted as dilution of salt-enriched metamorphic fluids through infiltration of meteoric water.

REFERENCES

- Bucher, K. 2011: Bergwässer. In: NEAT-Mineralien, Kristallschätze tief im Berg (Eds. P. Amacher und T. Schüpbach) 176-193. Verlag: GEO-Uri GmbH, Amsteg.
- Hiss, B. 1975: Metamorpher Anhydrit im Leventina Gneiss, Schweizerische mineralogische und petrographische Mitteilungen 55, 217-225.
- Mullis, J. 2011: Entstehung alpiner Zerrklüfte und Kluftminerale im Gotthard-Basistunnel, Abschnitt Amsteg-Sedrun und im

- Zugangs- und Kabelstollen von Amsteg. In: NEAT-Mineralien, Kristallschätze tief im Berg (Eds. P. Amacher und T. Schüpbach) 194-229. Verlag: GEO-Uri GmbH, Amsteg.
- Mullis, J., Dubessy, J., Poty, B. & O'Neil, J. 1994: Fluid regimes during late stages of a continental collision: Physical, chemical, and stable isotope measurements of fluid inclusions in fissure quartz from a geotraverse through the Central Alps, Switzerland. *Geochim. Cosmochim. Acta*, 58, 2239-2267.
- Seelig, U. & Bucher, K. 2010: Halogens in water from the crystalline basement of the Gotthard rail base tunnel (Central Alps). *Geochimica et Cosmochimica Acta* 74, 2581-2595.

2.15

Batholith construction over 30 million years in the Lesser Caucasus: temporal and geochemical constraints

Hervé Rezeau¹, Robert Moritz¹, Jörn-Frederik Wotzlaw², Rodrik Tayan³, Alexey Ulianov⁴ & Richard A. Stern⁵

¹ *Earth and environmental sciences, University of Geneva, Rue de Maraichers 13, CH-1205 Geneva (herve.rezeau@unige.ch)*

² *Institute of Geochemistry and Petrology, ETH Zurich, Clausiusstrasse 25, 8092 Zurich, Switzerland*

³ *Institute of Geological Sciences, National Academy of Sciences of Armenia, Yerevan 0019, Armenia*

⁴ *Institute of Earth Sciences (ISTE), University of Lausanne, Geopolis, 1015 Lausanne,*

⁵ *Department of Earth and Atmospheric Sciences, University of Alberta, Edmonton, Alberta, T6G2E3, Canada*

The Lesser Caucasus is a key area to understand the metallogenic and geodynamic link between the western and eastern domains of the Tethys belt. The southern part of the Lesser Caucasus records long lasting geological and metallogenic evolution from the Jurassic to the Cenozoic (Moritz et al., 2013). The Meghri-Ordubad composite pluton is located on the territories of southern Armenia, Nakhichevan, and northernmost Iran. The composite pluton illustrates a stationary Eocene to Miocene magmatic system that is temporarily and spatially associated with porphyry Cu-Mo deposits over an area of 1400 km².

Based on laser ablation ICP-MS zircon U-Pb dating on thirty samples, three successive magmatic episodes have been distinguished:

- (1) a Mid-Eocene gabbro - diorite - quartz diorite magmatic suite dated between 45.9 Ma and 43.0 Ma, associated with coeval north-north-east trending basaltic-andesitic dikes,
- (2) an Upper Eocene-Lower Oligocene gabbro - monzogabbro - monzodiorite - syenodiorite - quartz monzonite magmatic suite dated between 37.7 Ma and 28.2 Ma, contemporaneous with north-north-east trending trachyandesitic and syenitic dikes emplacement, and
- (3) an Upper Oligocene-Lower Miocene trachybasaltic mafic dike swarm yielding ages between 26.7 Ma and 24.3 Ma, followed by felsic granodioritic to granitic intrusions between 22.7 Ma and 22.2 Ma, which are coeval with east-west trending granodioritic dikes dated between 22.3 Ma and 21.2 Ma.

Based on Re-Os molybdenite dating (Moritz et al., 2013), two distinct ore forming episodes are recognized during the Eocene with the formation of porphyry Cu-Mo deposits (Agarak at 44.2 Ma; Hanqasar at 43.1 Ma; Aygedzor at 42.6 Ma), and the Late Oligocene with the formation of porphyry Mo-Cu deposits (the giant Kadjaran between 27.2 Ma and 26.4 Ma).

Within this geochronological framework, we illustrate important geochemical changes from the calc-alkaline mid-Eocene magmatic suite to an alkaline-shoshonitic signature in the Upper Eocene-Lower Oligocene suite and a transition from alkaline dikes to calc-alkaline granodiorites in the Upper Oligocene-Lower Miocene suite. These major element characteristics together with systematic variations in LREE/HREE and/or MREE/HREE ratios suggest an evolution from subduction-related calc-alkaline magmatism to post-subduction collisional alkaline magmatism over time.

The Hf isotopic composition of U-Pb dated zircons isotopic compositions become systematically more juvenile from the mid-Eocene to Lower Miocene magmatic episodes. These trends either reflect a decrease in crustal contamination through time or a change in the crustal contaminant to cannibalization of young juvenile intrusions. The oxygen isotopic composition of representative samples slightly increase from 5 to 6 ‰ indicating a mantle-like source from the mid-Eocene to Lower Miocene.

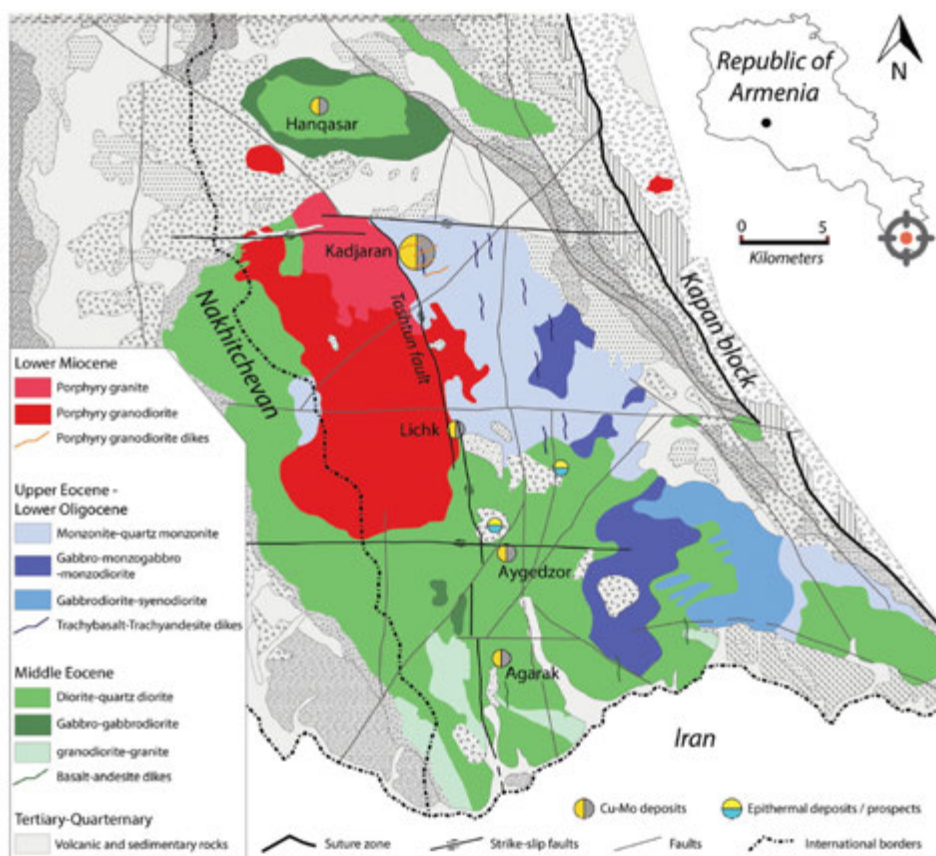


Figure 1. Geological map of the composite Meghri-Ordubad pluton. Modified after Karamyan et al. (1974).

REFERENCES

- Karamyan K, Guyumjyan H, Djrbashyan R, and Tayan R, (1974) The Geological map of the Zangezur ore region, Scale 1:50 000. Institute of Geological Science of the Armenian National Academy of Sciences (in Russian).
- Moritz R., M., J., Ovtcharova, M., Spikings, R., Selby, D., Melkonyan R., Hovakimyan, S., Tayan R., Ulianov, A., & Ramazanov, V. (2013) Jurassic to Tertiary metallogenic evolution of the southernmost Lesser Caucasus, Tethys belt.: In : Erik Jonsson et al. (eds), Mineral deposit research for a high-tech world, 12th SGA Biennial Meeting, 12-15 August 2013, Sweden, Uppsala 3:1447-1450.

2.16

Geochemical and petrological evidence for a link between the Cenozoic calc-alkaline and alkaline volcanism in north-western Sardinia, Italy

Davide Roggero¹, Sébastien Pilet¹ & Othmar Müntener¹

¹ *Institute of Earth Sciences, University of Lausanne, 1015 Lausanne, Switzerland (davide.roggero@unil.ch)*

Arc and intraplate magmatism are two types of volcanic activities that produce geochemically different magmatic rocks. Since they are generally present in distinct localities, their origins are explained by distinct petrological processes. However, there are multiple magmatic arcs where alkaline intraplate-type magmas are observed. The island of Sardinia, central Mediterranean, is one of these areas. During the Miocene-Oligocene, Sardinia was center of a calc-alkaline volcanism associated to the subduction of Ionian plate. The tectonic regime in Sardinia changed during the Pliocene-Pleistocene with the shift of the subduction zone to the southeast below Sicily-Calabria. This tectonic change is associated in Sardinia with the emission of alkaline lavas characterized by geochemical signature mostly similar to OIB.

Trace elements composition and radiogenic isotopes ratios of basalts/andesites support the idea that the mantle source of calc-alkaline lavas represents a depleted peridotite enriched by fluids and/or melts from the dehydration of the subducting Ionian plate. In addition, fractional crystallization at crustal level is critical to explain the range of lava composition, from basalt to dacite, observed in this calc-alkaline sequence. At the opposite, alkaline lavas are characterized by major, trace elements and isotopes composition comparable to oceanic island and continental basalts. The EM1 isotopic signature recorded by these alkaline lavas support the hypothesis of a deep source and has been used to demonstrate the existence of a Mediterranean mantle plume. An alternative suggests that this EM1 signature could be related to the melting of metasomatized lithospheric mantle, metasomatism linked to the delamination and melting of lower crust during ancient orogenesis. However, the main problem of these latter models is that the alkaline magmatism origin is completely decoupled with the previous calc-alkaline magmatic activity during the Oligo-Miocene. Here, we propose an alternative petrogenetic model where the evolution of the calc-alkaline magmatic system creates the future source for the alkaline volcanism in Sardinia.

Based on the fractional crystallization sequence recorded in Sardinia, crystallization experiments in calc-alkaline systems and melting experiments on amphibole-rich veins, we assume that olivine-pyroxene, garnet-pyroxene and amphibole-pyroxene lithologies could be formed beneath the Sardinian arc during the Oligo-Miocene subduction-related volcanism. Subsequently, the density contrast between the ultramafic cumulates and lithospheric mantle would induce delamination of these cumulates. Progressive heating of these cumulates included in hotter lithospheric mantle produces the partial melting of the low-solidus amphibole-rich cumulates, and generation of melts with comparable trace elements content to the most primitive Plio-Pleistocene alkaline lavas.

Our study suggests a potential petrogenetic link between the generation of calc-alkaline and alkaline magmas in Sardinia. In this hypothesis, the alkaline magmas represent melting of high pressure amphibole cumulates produced during the fractional crystallization of calc-alkaline magmas at the base of the crust.

REFERENCES

- Bell, K., Lavecchia, G. & Rosatelli, G. 2013: Cenozoic Italian magmatism - Isotope constraints for possible plume-related activity, *Journal of South American Earth Sciences*, 41, 22-40.
- Lustrino, M. 2005: How the delamination and the detachment of lower continental crust can influence basaltic magmatism, *Earth Science Reviews*, 72, 21-38.
- Pilet, S., Baker, M. B. & Stolper, E. M. 2008: Metasomatized Lithosphere and the Origin of Alkaline Lavas, *Science*, 320, 916-919.

2.17

What does chlorine content in biotite say about the metamorphic fluids: Case studies from the Torres del Paine and Western Adamello contact aureoles.

Guillaume Siron¹, Lukas Baumgartner¹ & Robert Bodner¹

¹ *University of Lausanne, Institute of Earth Sciences, CH1015 Lausanne, Switzerland*

Chloride is often the dominant anion in geothermal fluids. Cl concentrations determine the solubility of major rock-forming elements and by inference their mobility. The mobility in turn influences mineral textures and mineral equilibration. The OH⁻-Cl⁻ exchange between biotite and fluid, together with fluid-speciation calculations, can be used to estimate chlorine compositions¹ of fluids and element mobility. What we test here is, if Cl concentrations reflect prograde, peak or retrograde fluid composition.

We studied Cl contents in biotites from meta-pelites using electron microprobe (the detection limit is about 40ppm) and investigated two very different contact aureoles: the shallow crustal Torres del Paine (TP) aureole (3 km; 750 bar) in Patagonia and the mid-crustal Western Adamello (WA) aureole (10 km; 2.5 kbar²) in the Italian Alps. Rocks selected show only minor retrograde alteration of the peak mineral assemblage.

The TP granites intruded into Cretaceous turbidites. The Cl content in biotite is nearly constant at about 150ppm across the entire contact aureole. Only some samples close to the contact show higher concentrations of 1500-2000ppm. Note, that in these samples some retrograde biotites – based on structural criteria – are found, and they are Cl-poor (100-200ppm).

The WA tonalite intruded into a pre-Permian basement with a Permotriassic cover². Cl in biotite is quite constant at 200ppm, and biotite inclusions – found in andalusite or garnet – have the same Cl-concentration as matrix biotites.

These results are surprising, since they indicate that – when speciation of chlorine is taken into account – Cl concentration of the fluid increase with metamorphic grade, due to increasing association of Cl. The increase would also have to occur in such a way, that Cl in biotite does not change – an unlikely proposition. In addition, this would be in conflict with simple Rayleigh fractionation models, which predict that Cl should decrease quickly during dehydration due to the preference of Cl for the fluid phase.

Similarity, since the Cl in matrix and in inclusions are the same, it is unlikely that Cl in biotite represent a retrograde overprint. We suggest that biotite sequesters Cl upon crystallization, and diffusion (subsequently) is too slow to establish Cl-biotite-fluid equilibrium on the scale of a biotite grain. The predicted zoning requires better analytics. Initial test with the SIMS suggests that we can measure Cl, F and OH with the required higher analytical precision.

REFERENCES

- ¹Zhu, C. & Sverjensky, D.A. 1991: Partitioning of F-Cl-OH Between Minerals and Hydrothermal Fluids. *Geochimica et Cosmochimica Acta*, 55, 1837-1858.
- ²Floess, D. & Baumgartner, L. 2013: Formation of garnet clusters during polyphase metamorphism. *Terra Nova*, 25, 144-150.

2.18

Phosphate: a neglected clue to technology and systematics of ancient glass

Willem B. Stern¹

¹ *Institute for Mineralogy and Petrography, Basel University*

Phosphate is a hitherto widely ignored or neglected clue to technology and systematics of ancient alkali-calcium hollow- and flat glass.

Since 35 centuries man-made alkali-calcium glass has been used as a base-material for producing glass objects. By blending as educts finely ground quartz sand acting as a network former and alkali carbonate as a network modifier/flux a silicate glass is obtained at melting temperatures between 800° and 1500°C according to mixing ratio and flux composition, figures 1, 2.

Alkali carbonates like soda/trona or potash/kalicinite are instable under wet surface conditions, and hence rare in nature. The occurrence of trona in evaporites of the near East and Egypt is probably the reason why Na-Ca glass was invented in these regions, and was manufactured there for a long time span. Between the 9th and 19th century however, a potassium-based glass-making technology was dominant in Central Europe, where the ash of beech-wood logs (*fagus sylvatica*) contributed the network modifier instead of unavailable soda.

Phosphate is with 900 g/t a trace element in the earth crust, and in geogene minerals like quartz, calcite or trona/soda from evaporitic deposits, but it is together with K₂O an essential biogene main component of native ashes from terrestrial plants, which were used as educts for making K-Ca glass. Phosphate is together with Na₂O a biogene main component also in native halophyte ash and was used *possibly* in Roman time as an educt for making Na-glass, fig. 2. When biogene native ashes of plants or vertebrates are processed by washing, a man-made, P-depleted alkali carbonate may result, suitable as educt for producing glass.

2002 an archaeometrical cooperation started between the Bern Archeological Service and the Basel Geochemical Labs in connection with the excavation of a preindustrial glass hut operating 1699 till 1714 near Court (Jura Bernois).

Over 340 specimens have been analysed for chemical main components and trace elements, including 182 glass fragments. A main question of the archaeologists was whether the shards excavated near the kiln were [A] cullet collected elsewhere for recycling, or else [B] débris of the production site itself. The question was unexpectedly easy to answer, i.e. option [B].

Most glass fragments consisted of phosphate-rich forest glass, displaying a yellowish-greenish tinge. But 25% were colourless, and virtually free of phosphate and colouring iron oxides, fig. 1 binary diagrams (left). They were probably produced with local eocene Hupper earths as a network former, and potash extract from native local beech- or pine as a network modifier/flux without addition of a stabiliser, Stern and Gerber 2004, 2009, Gerber and Stern 2012, Stern 2009.

One may ask whether Sodium-Calcium glass of Roman time was produced with phosphate free soda/trona from evaporitic deposits (e.g. Wadi Natrun in Egypt) or else with native or processed halophyte ash from desertic areas, fig.2. The answer is not yet clear, and more research needs to be done by applying the phosphate criterion.

Alkali-Calcium glass, educts and products, composition and melting behaviour

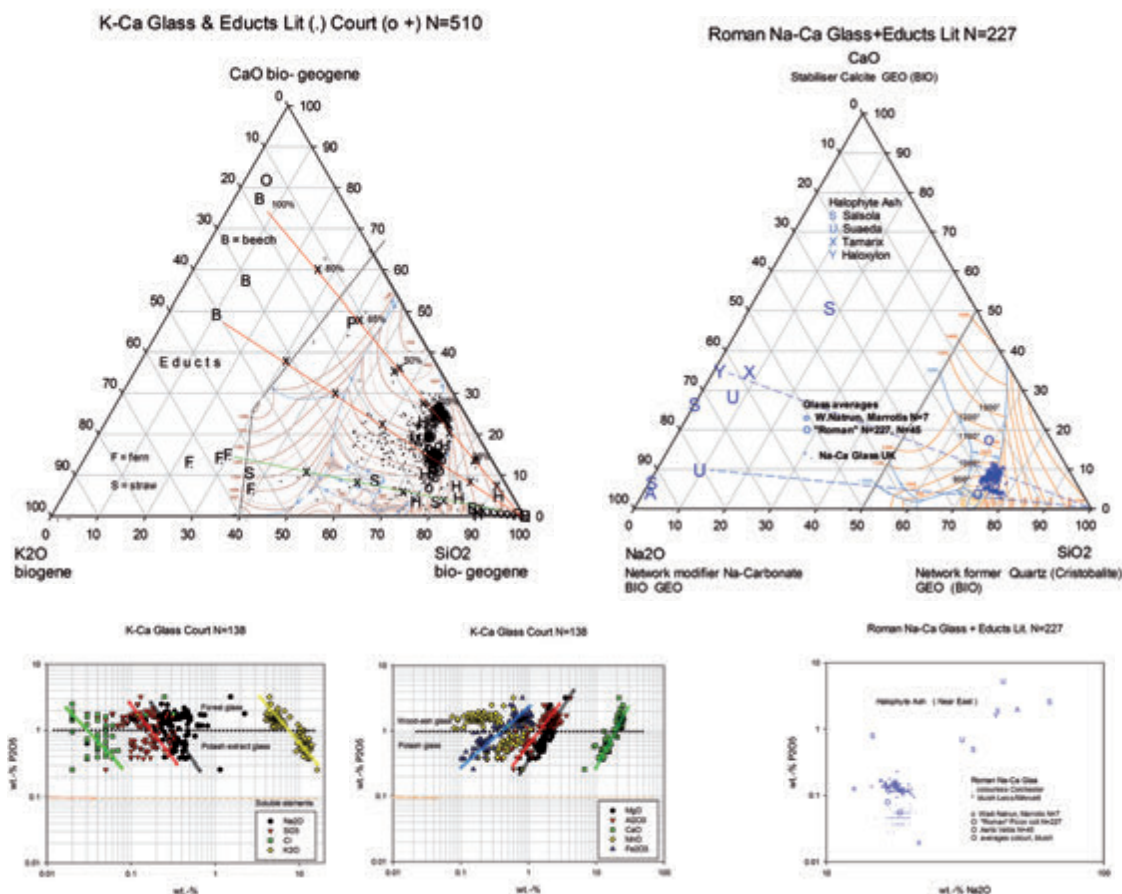


Figure 1a-c (left). Preindustrial K-Ca glass from Court. Educts coded in capitals, products as symbols (P-rich forest glass = +, P-depleted potash glass = o). The ternary and binary diagrams are widely self-explanatory
 Figure 2 a,b (right). Roman Na-Ca glass from different sources, ref. Stern 2015

REFERENCES

- Gerber, Y. & Stern, W.B., 2012: Archäometrische Analyse der Gläser, in: Chr. Gerber, editor, Court, Pâturage de l'Envers. Une verrerie forestière jurassienne du début du 18e siècle, 2, 95-162, 261-277
- Stern, W.B. & Gerber, Y., 2004: Potassium-Calcium Glass: New Data and Experiments. *Archaeometry*, 46, 137-156
- Stern, W.B., & Gerber, 2009: Ancient Potassium-Calcium Glass and its Raw Materials (Wood-Ash, Fern-Ash, Potash) in Central Europe. *Mitteilungen der Naturforschende Gesellschaft beider Basel*, 11, 107-122
- Stern, W.B., 2010: Stroh als Quelle erneuerbarer Energie. *Swiss Bulletin for Applied Geology*, 15, 95-103
- Stern, W.B., 2015: Phosphate in historical Glass and Theophilus Presbyter's Glass Making Recipe, Basel, ISBN 978-3-033-05193-5

2.19

Can grain-scale pressure variations provide direct constraints on rheology?

Lucie Tajčmanová¹, Evangelos Moulas¹, Johannes Vrijmoed¹ & Yuri Podladchikov²

¹ *Department of Earth Sciences, ETH Zurich, Sonneggstrasse 5, CH-8092 Zurich (lucie.tajcmanova@erdw.ethz.ch)*

² *Institute of Earth Sciences, University of Lausanne, CH-1015 Lausanne*

Recent analytical and theoretical advances imply that petrographic observations should be reconsidered in the light of pressure variations. On one hand, this opens new horizons in metamorphic petrology. On the other hand, it can bring some uncertainties into the currently common assumptions, such as pressure to depth conversion. In fact, if all observations are treated only by conventional methods based on the constant pressure assumption, the interpretations may not represent the appropriate mechanism explaining the microstructure. Considering pressure variations as the other possible interpretation, an alternative model for the development of petrographic observations can be inferred. However, interpreting observed variations in metamorphic grades due as a pressure variation in the same depth are not suitable for pressure-to-depth conversion. Ignoring such pressure variations in petrological analysis can lead to errors in depth estimates that are comparable to the typical thickness of the whole continental crust. Interestingly, microstructures reflecting pressure variations might provide important indications on differential stress and strength variations in a rock. Therefore, here we show how the pressure variation can be used to constrain rheology properties directly from natural microstructures. We document that observations, such as UHP microstructures, would not lose their importance but might play a different role in geodynamic reconstructions.

2.20

On coupling of viscous relaxation and chemical diffusion under grain scale pressure variation

Xin Zhong¹, Johannes Vrijmoed¹, Lucie Tajcmanova¹, & Evangelos Moulas¹

¹ *Department of Earth Sciences, ETH Zurich, Sonneggstrasse 5, CH-8092. (xin.zhong@erdw.ethz.ch)*

Compositional zoning in metamorphic minerals have been generally recognized as an important geological feature to decipher the metamorphic history. The observed chemical zoning of, e.g. garnet, is commonly interpreted as disequilibrium between the fractionated inner core and the surrounding matrix. However, chemically zoned minerals were also observed in high grade rocks ($T > 800^\circ$) where the duration of metamorphic processes was independently dated to take several Ma. This implies that temperature may not be the only factor, and grain scale pressure variation was proposed to be a complementary factor that may significantly contribute to the formation and preservation of chemical zoning in high temperature metamorphic minerals [Tajcmanová 2013, 2015]. To investigate such coupled process, classical irreversible thermodynamics is used to model viscous relaxation coupled with chemical diffusion. The numerical approach is applied to the chemically zoned plagioclase rim described by [Tajcmanová 2013]. The diffusion process operating during the plagioclase rim formation can lead to a development of a pressure gradient. Such a pressure gradient if maintained during ongoing viscous relaxation can lead to the preservation of the observed chemical zonation in minerals.

A dimensionless number, Deborah number, is defined as the ratio between the Maxwell viscoelastic relaxation time and the characteristic diffusion time. It characterizes the relative influence between the maintenance of grain scale pressure variation and chemical diffusion. Thus this number is important for the coupling of the two processes. Two extreme mechanism regimes are shown, namely the mechanically-controlled regime (high Deborah number) and diffusion-controlled regime (low Deborah number). In the mechanically-controlled regime, the grain scale pressure variation and so thus the chemical zonation can be maintained due to slow viscous relaxation. Furthermore, by utilizing experimental flow law and diffusion coefficient, Deborah number is estimated at a variety of physical conditions, such as temperature, grain size, strain rate and stress. The goal is to understand the dominant mechanism in the coupling process in different metamorphic environment.

REFERENCES

- Tajcmanova, L., Y. Podladchikov, R. Powell, E. Moulas, J.C. Vrijmoed, and J.A.D. Connolly, 2013: Grain-scale pressure variations and chemical equilibrium in high-grade metamorphic rocks. *Journal of Metamorphic Geology*, 32(2):195-207.
- Tajcmanova, L., J.C. Vrijmoed, and E. Moulas, 2015: Grain-scale pressure variations in metamorphic rocks: implications for the interpretation of petrographic observations. *Lithos*, 216-217:338-351.

P 2.1

Major and trace element geochemistry of a distal Fe skarn - Torre di Rio, Elba Island (Italy): Insights from hedenbergite, epidote and ilvaite LA-ICP-MS analyses.

Carlos Arbiol¹, Kalin Kouzmanov¹, Andrea Dini², Markus Wälle³

¹ *Department of Earth Sciences, Section of Earth and Environmental Sciences, University of Geneva, Rue de Maraîchaire 13, CH-1205 Genève. (carlos.arbiol@etu.unige.ch)*

² *CNR, Istituto di Geoscienze e Georisorse, Pisa, Italy*

³ *Institute of Geochemistry and Petrology, ETH Zürich, 8092 Zürich, Switzerland*

Distal skarns are calc-silicate rocks formed by the interaction between magmatic fluids and carbonate hosts without direct link with a causative intrusion. In the present study we use trace element patterns in main skarn silicates from a classical type locality in Tuscany to trace the genetic link with the Miocene magmas. The Torre di Rio distal Fe skarn is located south of the Rio Marina village, Elba Island (Italy). It is hosted by calc-schists belonging to the Acquadolce Unit (Bortolotti et al., 2001), with a strong foliation dipping to the NW that is preserved in most parts of the skarn. The skarn body presents a spectacular mineral zonation, with hedenbergite, ilvaite and epidote domains. While hedenbergite and ilvaite zones are developed in carbonate-dominated host (marbles and calc-schists), the epidote zone is formed by selective replacement of silicate rocks (mica-schists).

Clinopyroxene forms up to 40 cm in diameter spherical aggregates from fibrous crystals in the main pyroxene zone, mixed patchy texture with epidote at the transition to the epidote zone, and layered "zebra-like" texture together with ilvaite, towards the contact with the ilvaite zone. The clinopyroxene occurring in the skarn has an Fe-rich composition corresponding to the hedenbergite end-member. Slight compositional variation is recorded at the crystal tips, where Mg is fully replaced by Fe and, therefore, clinopyroxene becomes even more hedenbergitic in composition. Trace element composition of hedenbergite does not show important variations along single crystals. Copper, Cr and Rb are below their limit of detection by LA-ICP-MS, while Zn content is up to 60 ppm. Nickel (up to 40 ppm) and Co (up to 12 ppm) seem to be enriched in the crystal cores, while being below detection at the rim. Anomalous B and Sn contents (100s ppm) are also observed. REE_{total} content is as low as 2-4 ppm. REE pattern of hedenbergite is characterized by low LREEs and high HREEs, and important variations have been observed only for some heavy REEs.

Ilvaite is a hydrated sorosilicate ($\text{CaFe}^{+3}(\text{Fe}^{+2})_2\text{O}(\text{Si}_2\text{O}_7)(\text{OH})$) mainly constituted by Fe (39%), Ca (10%) and Si (13%), with minor amounts of Mn, Al and Mg.

The first LA-ICP-MS analyses of ilvaite reveal anomalous contents on different trace elements. Boron content in ilvaite is up to 170 ppm, Zn up to 70 ppm, Ga up to 40 ppm, Ge up to 60 ppm, As up to 300 ppm, Sn up to 0.45% and REE_{total} up to 400 ppm. On the contrary, Ni and Cu are below detection limit, while Th and U present concentrations of <1 ppm. The REE pattern of ilvaite is similar to the one of hedenbergite.

Epidote has a complex patchy zoning revealed by BSE imaging, mainly produced by Fe-Al substitution. Trace element geochemistry of epidote is characterized by high Sn (up to 990 ppm) and Ga (up to 130 ppm) content and low Pb (up to 6 ppm). Cobalt, Ni, Cu and Zn are at or below their limit of detection by LA-ICP-MS, while Th and U contents are <1 ppm. Furthermore, REE contents are usually <100 ppm, but some analysis show REE_{total} contents up to 690 ppm. The REE pattern of epidote differs significantly from those of hedenbergite and ilvaite – with enrichment of LREEs and depletion of HREEs. In some cases negative Eu anomaly has been observed.

The significant B and Sn anomaly detected in the skarn minerals at Torre di Rio is a common characteristic of the magmatic rocks occurring on Elba Island (but also along the Tuscan Magmatic Province) and the Fe-ores of Rio Marina. The magmatic rocks (granites, rhyolites and pegmatites) have a B content ranging from 20 to 1500 ppm, with tourmaline occurring as a common mineral (Dini et al., 2005). It is, therefore, believed that part of this magmatic boron was introduced into the hydrothermal system and incorporated into the skarn minerals. On the other hand, Fe-ores (hematite) from the Rio Marina deposit (1km north of the Torre di Rio skarn) are significantly enriched in Sn (190-8400 ppm), but also in W (87-4950 ppm) as reported by Benvenuti et al. (2013).

This characteristic geochemical signature of the rocks in Elba Island, and in the Tuscan Magmatic Province, is a direct evidence of the complex tectonic, magmatic and hydrothermal evolution of the region.

REFERENCES

Benvenuti, M., Dini, A., D'Orazio, M., Chiarantini, L., Corretti, A., & Costagliola, P. 2013: The tungsten and tin signature of iron ores from Elba Island (Italy): A tool for provenance studies of iron production in the Mediterranean region,

Archaeometry, 55, 479-506.

Bortolotti, V., Fazzuoli, M., Pandeli, E., Principi, G., Babbini, A., & Corti, S. 2001: Geology of central and eastern Elba Island, Italy, *Ofioliti*, 26 (2a), 97-150.

Dini, A., Gianelli, G., Puxeddu, M., & Ruggieri, G. 2005: Origin and evolution of Pliocene-Pleistocene granites from Larderello geothermal field (Tuscan Magmatic Province, Italy), *Lithos*, 81, 1-31.

P 2.2

Shallow porphyry stockwork veining at Cerro de Pasco: constraints from fluid inclusions, in-situ oxygen isotope and trace element analysis by SIMS and LA-ICP-MS

Bertrand Rottier¹, Kalin Kouzmanov¹, Anne-sophie Bouvier², Lukas P. Baumgartner², Markus Wälle³ and Lluís Fontboté¹

¹ *Earth and Environmental Sciences, University of Geneva, 1205 Geneva, Switzerland (Bertrand.Rottier@unige.ch)*

² *Institute of Mineralogy and Geochemistry, University of Lausanne, 1015 Lausanne, Switzerland*

³ *Institute of Geochemistry and Petrology, ETH Zürich, 8092 Zürich, Switzerland*

The Miocene epithermal base metal deposit of Cerro de Pasco in central Peru located along the eastern margin of a large diatreme-dome complex (Baumgartner et al., 2008) is the second largest known epithermal base metal ("Cordilleran") deposit after Butte in Montana, USA. Recently, multiple porphyry events at Cerro de Pasco have been reported (Rottier et al., 2014). Two types of porphyry mineralization have been found: (i) magmatic and hornfels clasts with typical A- and B-type quartz-molybdenite veins incorporated in the diatreme-breccia and also in E-W trending quartz-monzonite porphyry dykes; and (ii) a porphyritic andesitic plug crosscut by a stockwork of quartz-magnetite-chalcopryrite-pyrite veins, cropping out in the central part of the diatreme. This contribution is focused on results obtained on the second type of porphyry mineralization.

The andesitic plug crops out at the same elevation as the epithermal mineralization in the district. No important erosion pre- or post-dating the epithermal stage of ore formation has been recognized at Cerro de Pasco. The plug is affected by pervasive chlorite-epidote-magnetite alteration spatially associated with a network of up to 2 cm-thick quartz-magnetite-chalcopryrite-pyrite porphyry style veinlets (Fig. 1A). Microscopic observations reveal high chalcopryrite/pyrite ratios in the veins, with up to 5% chalcopryrite in some samples, both sulfides being affected by supergene oxidation. Quartz veins are banded in places (Fig. 1B) and SEM-CL imaging reveals two different quartz generations: 1) high-luminescence euhedral and in places fine-grained sulfide-free quartz (Qz1); 2) late low-luminescence euhedral quartz (Qz2) crosscutting and overgrowing Qz1 and commonly intergrown with sulfides (Fig. 1C).

Qz1 presents assemblages of vapor inclusions and hydrous salt melt inclusions (HSMI). The HSMIs contain several transparent crystals (halite, sylvite, anhydrite, and an unknown phase), hematite flakes, unknown opaque phase, and vapor bubbles; no liquid is optically distinguishable (Fig. 1D). Final halite melting occurs between 580° and 600°C corresponding to a salinity of >70% NaCl eq. (Stern et al., 1988). The total homogenization temperature (Th) is > 600°C. The association of vapor inclusions and HSMIs indicates pressure of entrapment of < 1kbar (Dreisner and Heinrich 2007). Qz1 has a high Ti content (100 to 356 ppm; based on 18 LA-ICP-MS analyses and 6 SIMS analyses) indicating a high formation temperature (>600°C based on Ti-in-quartz geothermometer; Huang and Audétat, 2012). Qz2 is spatially associated with sulfides and hosts only L-V inclusions with Th from 270° to 330°C and salinity from 0.2 to 25 wt% NaCl. This large range of salinity might result from a late stage mixing of a low-salinity fluid with some residual hydrous salt melt. The Ti content of Qz2 is low, from 2.4 to 7.6 ppm (SIMS analyses n=5). In-situ SIMS oxygen isotope analyses on the two quartz generations provide distinctly different results: $\delta^{18}\text{O}_{\text{Qz1}} = 10.2\text{‰}$ (n=31, $2\sigma=0.5$) and $\delta^{18}\text{O}_{\text{Qz2}} = 13.1\text{‰}$ (n=9, $2\sigma=0.9$). The calculated $\delta^{18}\text{O}$ of water in equilibrium with quartz yields for Qz1 $\delta^{18}\text{O}_{\text{fluid}} = 8.9\text{‰}$ at 650°C and for Qz2 $\delta^{18}\text{O}_{\text{fluid}} = 7.2\text{‰}$ at 330°C (Matsuhisa et al., 1979). These values indicate a strong magmatic signature of the fluid. The difference of 1.9 ‰ between the two quartz generations could be due to a minor meteoric water input (<10%) or to a change of $\delta^{18}\text{O}$ of the magmatic fluid with time.

Our results indicate a two step-formation of the banded porphyry quartz veins. Hot hydrous silica-rich andesitic magma is emplaced in a shallow subvolcanic environment leading to direct exsolution of vapor and a hydrous salt melt. Qz1 precipitated from such fluids at high temperature (>600°C). The formation Qz2 and the sulfides at lower temperature (270-330°C) could result from (i) input of a second predominantly magmatic lower-temperature fluid resulting in cooling of the system, or (ii) incursion of meteoric water (partly equilibrated) that mix with magmatic fluids

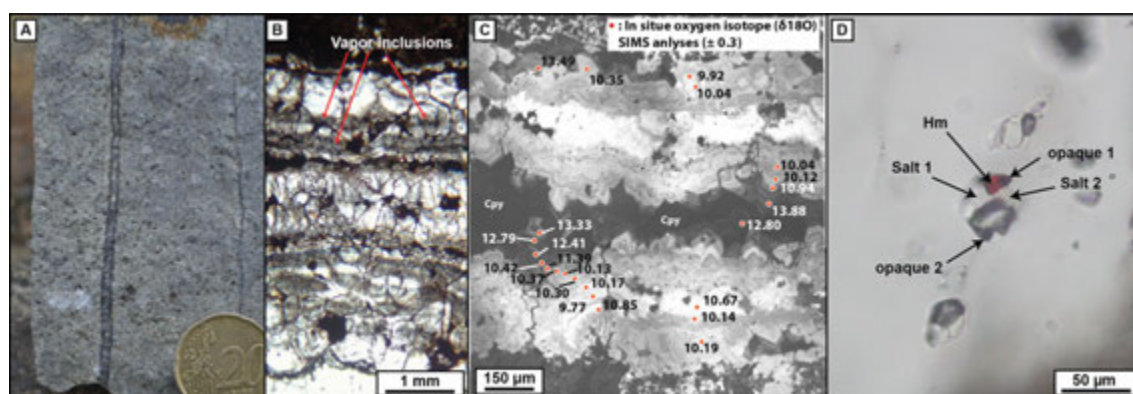


Figure 1. A) Banded vein crosscutting the andesite plug; B) Transmitted light photography of a banded vein; C) SEM-CL image of a banded vein with results from SIMS oxygen isotope analysis; D) HSMIs inclusions in Qz1.

REFERENCES

- Baumgartner, R., Fontboté, L., & Vennemann T. 2008: Mineral zoning and geochemistry of epithermal polymetallic Zn-Pb-Ag-Cu-Bi mineralization at Cerro de Pasco, Peru, *Economic Geology*, 103, 493-537.
- Driesner, T., & Heinrich C.A. 2007: The system H₂O-NaCl. Part I: Correlation formulae for phase relations in temperature-pressure-composition space from 0 to 1000 °C, 0 to 5000 bar, and 0 to 1 XNaCl, *Geochimica et Cosmochimica Acta*, 71, 4880-4901.
- Huang, R. & Audétat A. 2012: The titanium-in-quartz (TitaniQ) thermobarometer: A critical examination and re-calibration, *Geochimica et Cosmochimica Acta*, 84, 75-89.
- Matsuhisa, Y., Goldsmith, J.R. & Clayton R.N. 1979: Oxygen isotopic fractionation in the system quartz-albite-anorthite-water, *Geochimica et Cosmochimica Acta*, 43, 1131-1140.
- Rottier, B., Kouzmanov, K., Casanova, V., Bendezú, R., Cuéllar, D., Fontboté L. 2014: First evidence of multiple porphyry events in the Cerro de Pasco polymetallic district, central Peru. 12th Swiss Geoscience Meeting, Fribourg 2014, 87-88.
- Sterner, S.M., Hall, D.L. & Bodnar R.J. 1988: Synthetic fluid inclusions. V. Solubility relations in the system NaCl-KCl-H₂O under vapor-saturated conditions, *Geochimica et Cosmochimica Acta*, 52, 989-1005.

P 2.3

Distal johannsenite-hedenbergite skarns at Madan, Bulgaria and their link to Pb-Zn mineralization: constraints from trace element analyses in skarn silicates

Thomas Bovay¹, Kalin Kouzmanov¹, Andrea Dini², Markus Wälle³, Rossitsa Vassileva⁴, Ianko Gerdjikov⁵

¹ *Section of Earth and Environmental Sciences, University of Geneva, Geneva, Switzerland (thomas.bovay@etu.unige.ch)*

² *CNR, Istituto di Geoscienze e Georisorse, Pisa, Italy*

³ *Institute of Geochemistry and Petrology, ETH Zürich, Zürich, Switzerland*

⁴ *Geological Institute, Bulgarian Academy of Sciences, Sofia, Bulgaria*

⁵ *Faculty of Geology and Geography, Sofia University, Sofia, Bulgaria*

Madan ore field represents one of the most significant manifestations of vein-type Pb- Zn mineralization in Europe. The ore field occupies the southwestern part of the Central Rhodopean polymetallic district in south Bulgaria. The mineralization is controlled by six large, up to 10-15 km long, NNW-SSE trending subvertical major fault zones and is mainly hosted by the Madan allochthon unit, which overlies tectonically the Arda unit. The Madan unit consists of alternation of gneisses, schists, amphibolites and marbles. Marbles are the main host for large replacement Pb-Zn metasomatic ore bodies (Ivanov et al. 2000). Rhyolitic dikes pre-dating the polymetallic mineralization intruded group of non-mineralized faults with WNW-ESE direction in the northern part of the ore field (Ivanov et al. 2000; Marchev et al. 2005; Vassileva et al. 2009; Kaiser-Rohrmeier et al. 2013).

The aim of this study is to establish a genetic model for the distal skarn formation and its role in the subsequent polymetallic mineralization. This work focuses on three deposits from the Madan ore field, namely (from north to south): Kroushev Dol, Petrovitsa, and Gjudjurska. The deposits are characterized by the occurrence of distal johannsenite-hedenbergite skarn bodies, formed by the interaction of hydrothermal fluids with marbles along lithological contacts and faults. Simultaneously to the early clinopyroxene formation within the marble, a syngenetic hydrothermal alteration dominated by epidote ± titanite affected the gneiss in contact with the marble horizons.

Electron microprobe analyses on clinopyroxenes yield dominantly johannsenite compositions, typical of distal Zn skarns (Meinert et al., 2005). LA-ICP-MS analyses reveal anomalously high Zn concentrations in the clinopyroxenes – as much as 250 ppm, while Cu and Pb rarely exceed 1 ppm. Optical cathodoluminescence followed by selective carbonate dissolution and textural SEM study along the skarn front show the presence of a few-mm to a centimeter-thick layer dominantly made of recrystallized fine-grained Mn-rich calcite. At the boundary between the skarn association and the marble the bladed shape of the pyroxene turns into a hairy-like texture made by an intergrowth of pyroxene and amphiboles, as confirmed by Raman microspectroscopy. BSE imaging on samples from Kroushev Dol shows sharp changes of the clinopyroxene blade close to the contact with the marble consisting of significant change in chemical composition and growth direction of the crystal. These features are indicative of a complex late-stage skarn formation with multiple dissolution-replacement reactions.

Neoformed titanites appear to be an important part of the skarn assemblage affecting the gneiss, along the contact with marbles, forming euhedral crystals elongated in the foliation plan of the host. Euhedral titanites from the Petrovitsa and Gjudjurska deposits display constant major element composition in the core and Nb-rich rim as confirmed by LA-ICP-MS analyses. Common sector zoning, as illustrated by BSE images, is due to zonal distribution of trace elements. REE spectra of titanite are consistent within single samples; however titanites from different lithologies display rather significant differences in light and/or heavy REE patterns, thus indicating that the environment of skarn formation, the skarn mineral paragenesis and the composition of the protolith strongly influence the partitioning of various elements between the different calc-silicates.

REFERENCES

- Ivanov Z et al. (2000) Guide to Excursions, ABCD-GEODE 2000 Workshop, Borovets: 6-20.
 Kaiser-Rohrmeier M et al. (2013) *Economic Geology* 108: 691-718.
 Marchev et al. (2005) *Ore Geology Reviews* 27: 53-89.
 Meinert et al. (2005) *Economic Geology* 100th Anniversary Volume: 299-336
 Vassileva R et al. (2009) *Geochemistry, Mineralogy and Petrology* 47: 31-49.

P 2.4

Tracing hydrothermal fluid evolution in the epithermal deposit of Colquijirca: insights from in-situ oxygen and trace element analyses in quartz

Vincent Casanova¹, Kalin Kouzmanov¹, Anne-Sophie Bouvier², Lluís Fontboté¹ & Lukas Baumgartner²

¹ *Section of Earth and environmental sciences, University of Geneva, Rue des Maraichers 13, CH-1205 Genève (vincent.casanova@unige.ch)*

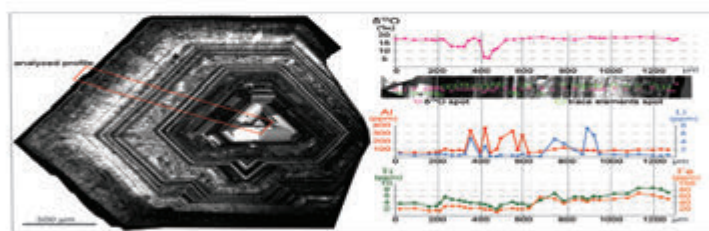
² *SwissSIMS, Institute of Earth sciences, University of Lausanne, bâtiment Géopolis, CH-1015 Lausanne*

Previous studies on porphyry-related epithermal polymetallic (Cordilleran) deposits suggest that fluid mixing between low to moderately saline magmatic fluids and low-salinity meteoric waters plays an important role in ore precipitation (Catchpole et al., 2015, Deen et al., 1994, Rusk et al. 2008). Colquijirca is one of the major porphyry-related epithermal deposits of the Miocene Polymetallic Belt in central Peru (Bendezú and Fontboté, 2009). It is an 8 km long mineralized corridor replacing carbonates at shallow depth exhibiting well-defined metal and alteration zoning. Previous work using bulk technique for O-H isotope analyses of alunite, kaolinite, dickite, and quartz evidenced mixing between magmatic and meteoric fluids during mineralization (Bendezú, 2007).

At Colquijirca, quartz is present throughout the paragenetic sequence. It can therefore be used as a proxy for O isotopic variations of the mineralizing fluid in space and time. In this study, we use secondary ion mass spectrometry (SIMS) to study in-situ O isotopes and trace element variations from different quartz growthbands to track fluid mixings at different stages of mineralization.

Doubly polished 500 µm quartz chips cut perpendicular to the c-axis have been mounted in indium together with quartz standards. Point analyses of O isotopes (¹⁶O, ¹⁸O) and trace elements (Li, Al, Ti, Fe) have been acquired, using a Cameca® IMS 1280-HR at the SwissSIMS lab, along profiles across different growth zones in quartz previously identified by scanning electron microscopy-cathodoluminescence (SEM-CL) imaging. Spatial resolution is typically around 15-20 µm for O isotopes and 20 µm for trace elements. The 2σ standards reproducibility error achieved for δ¹⁸O is ≤0.32 ‰. The internal error, higher than the standard reproducibility, for all 4 analyzed trace elements range between 5 % and 22 %.

δ¹⁸O isotopic signatures obtained in quartz from the main ore stage vary between 2.8 ‰ and 18.8 ‰ with up to 15.8 ‰ variation within a single crystal. No systematic variations according to the stages nor geographic position have been recognized. Despite important variations, most of the data range between 15.8 ‰ and 18.8 ‰. The lowermost values are found in bands rarely exceeding 100 µm in thickness and representing less than 20 % of the crystal (Fig. 1). The variations between the lowermost values and the values around 15.8 ‰ and 18.8 ‰ are generally sharp on a 20 µm scale. Only few trace element analyses have been performed to date. Aluminum and Li present sharp and important variations within a single crystal. Iron and Ti have smoother variation curves and a positive correlation (Fig. 1). The lowest δ¹⁸O values are lower than those obtained in a previous study, all stages included (10.2 ‰, Bendezú, 2007). Trace element content does not clearly correlate with δ¹⁸O nor with the oscillatory-zoning observed on CL-images. Fluid inclusion microthermometry suggests temperatures around 250°C during the main ore stage. Assuming that precipitation occurred at equilibrium we can calculate the δ¹⁸O of the mineralizing fluid (Matsuhisa et al., 1979). The system is dominated by a fluid with values of δ¹⁸O around 9 ‰ to 10 ‰ with episodic incursions of fluids with δ¹⁸O as low as -7 ‰, most probably of dominantly meteoric origin.



A

B

Figure 1. **A:** SEM-CL image of a quartz crystal from the main ore stage cut perpendicular to its *c*-axis **B:** $\delta^{18}\text{O}$ (pink spots) and Al, Li, Ti, and Fe (green spots) content variations across a selected profile. Uncertainties are smaller or similar to point size.

REFERENCES

- Bendezú, R., 2007: Shallow polymetallic and precious metal mineralization associated with a Miocene diatreme-dome complex: the Colquijirca district in the peruvian andes, *Terre& Environnement*, 64, 221p.
- Bendezú, R., & Fontboté, L., 2009: Cordilleran epithermal Cu-Zn-Pb-(Au-Ag) Mineralization in the Colquijirca district, Central Peru: deposit-scale mineralogical patterns. *Economic Geology*, 104, 905-944.
- Catchpole, H., Kouzmanov, K., Putlitz, B., Fontboté, L., & Seo, J.H., 2015: Zoned base metal mineralization in a porphyry system: Origin and evolution of mineralizing fluids in the Morococha district, Peru. *Economic Geology*, 110, 39-71.
- Deen, J.A., Rye, R.O., Munoz, J.L., & Drexler, J.W., 1994: The magmatic hydrothermal system at Julcani, Peru - Evidence from fluid inclusions and hydrogen and oxygen isotopes. *Economic Geology*, 89, 1924-1938.
- Matsuhisa, Y., Goldsmith, R.N., & Clayton, R.N., 1979 : Oxygen isotopic fractionation in the system quartz–albite–anorthite–water. *Geochimica Cosmochimica Acta*, 42, 1131–1140.
- Rusk, B.G., Reed, M.H., & Dilles, J.H., 2008: Fluid inclusion evidence for magmatic-hydrothermal fluid evolution in the porphyry copper-molybdenum deposit at Butte, Montana. *Economic Geology*, 103, 307–334.

P 2.5

Genetic relationships between spatially associated arsenide and sulphide magmatic ores from the Carratraca Ultramafic Massif (Málaga, south Spain)

Christos Chatzipanagiotou¹, Fernando Gervilla² & Lluís Fontboté¹

¹ *Department of Earth Sciences, University of Geneva, Rue de Maraichers 13, CH-1205 Geneva, Switzerland (Christos.Chatzipanagiotou@etu.unige.ch)*

² *Departamento de Mineralogía y Petrología, Facultad de Ciencias, Universidad de Granada 18002 Granada, Spain*

The Carratraca massif is one of the several Iherzolite massifs outcropping in the Serranía de Ronda area, which is located in the westernmost part of the internal zones of the Betico–Rifean Cordillera, part of the Mediterranean Alpine Belt. These massifs are portions of upper mantle emplaced at high temperature in the continental crust and display a top to bottom zoning. They are zoned in three tectono–metamorphic domains i) garnet mylonites to spinel tectonites, ii) granular peridotites and iii) plagioclase tectonites. Between the spinel tectonites (old protolith) and granular peridotites exists a narrow boundary characterised as a recrystallisation/coarsening front and corresponds to a combination of partial melting during lithosphere thinning and fast dynamic cooling (Lenoir et al., 2001). Three ore types occur in these massifs: chromite–Ni arsenide (Cr–Ni) ores, sulphides–graphite (S–G) ores, and chromite (Cr) ores. Only Cr–Ni ores were mined in the past for nickel.

The studied mines are the i) San Agustín (Cr–Ni ores) and ii) El Gallego (S–G ores). The main ore minerals at San Agustín are chromite and nickeline with minor rammelsbergite, gersdorffite, rutile, and some accessory sperrylite and gold, associated with cordierite, ± plagioclase. This type of ore display orthomagmatic textures and, in places, high temperature plastic deformation. The mineralisation occurs as small veins that cross-cut the foliation of the host peridotites, and have been formed by the crystallisation of chromite-carrying immiscible arsenide melt rich in noble metals (Gervilla et al., 1996). At El Gallego (S–G ore) the main mineralogical assemblage is pyrrhotite, petlandite, chalcopyrite, cubanite, chromite, rutile, graphite and minor cobaltite–gersdorffite, nickeline and bismuthotellurides, associated with phlogopite. The mineralisation occurs as veins, partly displaying a stockwork-like pattern, and occur along a fault zone. The San Agustín mine is hosted by spinel tectonites whereas El Gallego mine is located upward in the mantle section and is hosted by garnet mylonites. Previous studies suggest that S–G ores formed later than Cr–Ni ores from residual sulphide liquids segregated after crystallisation of Cr–Ni ores.

In order to calculate the bulk content of major and trace elements, and noble metals, six selected samples were analysed by ICP-MS. The PGEs and Au patterns normalised to chondritic values (Fig. 1) reveal high content of noble metals in the samples. In particular, three samples display a positive anomaly in Pt in agreement with the presence of micron-sized grains of sperrylite (PtAs₂) (Fig. 1), and some alloys consisted mainly of Au (up to 60% wt) and Cu (32% wt), and some Pt (4% wt), Ni (3% wt) in the ore assemblage. This is in contrast to previous results in some samples from the same type of ores which showed negative Pt anomalies and no PGM grains (Fig. 1).

In addition, the As shows a positive correlation with the PGEs content in the samples, in contrast with other semi-metals (Bi, Te) that reveal a negative correlation. However, it's worth to note that the Pt-richest sample (containing 7677 ppb Pt) shows the lowest As content (453 ppm As), but it shows the highest amount of Bi (7.6 ppm) plus Te (9 ppm). This is in accordance with the presence of many micro-grains of bismuthotellurides in this sample. The previous statements suggest that either Pt became concentrated by other semi-metals (e.g. Bi and Te), or segregated earlier from the As-saturated melt in the form of sperrylite, as Helmy's et al. (2013) experimental results show.

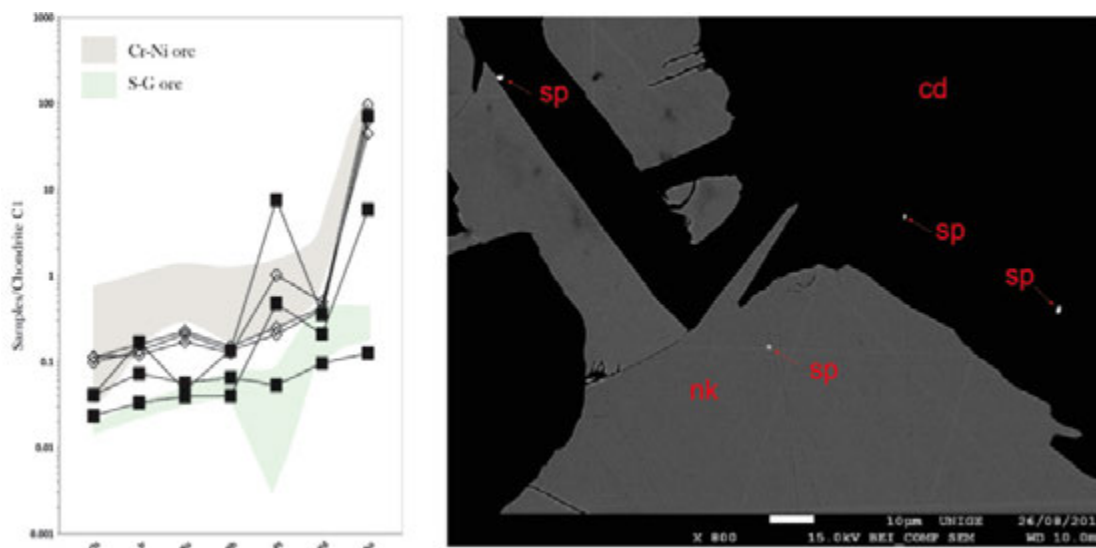


Figure 1. Left image: Chondrite – normalised (Naldrett & Duke 1980) patterns of the samples from San Agustín (open diamonds) and El Gallego (black squares). Data for the Cr-Ni ores and S-G ores from Gervilla et al., 1996. Right image: SEM image of platinum mineral (nk: nickeline, sp: sperrylite, cd: cordierite)

REFERENCES

- Gervilla F., Leblanc M., Torres-Ruiz J., & Hach-Alí P. 1996: Immiscibility between arsenide and sulfide melts: a mechanism for the concentration of noble metals. *The Canadian Mineralogist*, 34, 485-502
- Helmy H.M., Ballhaus C., Fonseca R.O.C. & Nagel T.J. 2013: Fractionation of platinum, palladium, nickel, and copper in sulfide-arsenide systems at magmatic temperature. *Contributions to Mineralogy and Petrology* 166 (6), 1725-1737.
- Lenoir X., Garrido C., Bodinier J-L., Dautria J-M., & Gervilla F. 2001: The recrystallization front of the Ronda peridotite: Evidence for melting and thermal erosion of subcontinental lithospheric mantle beneath the Alboran basin. *Journal of Petrology*, 42, 141-158
- Naldrett A., & Duke J.M. 1980: Pt metals in magmatic sulfide ores. *Science*, 208, 1417-1424

P 2.6

High resolution, in situ ^{18}O analyses of quartz from the Yankee Lode tin deposit (Mole Granite, Australia)

Szandra Fekete¹, Philipp Weis¹, Thomas Driesner¹, Christoph A. Heinrich¹, Lukas Baumgartner² & Anne-Sophie Bouvier²

¹ *Institut of Geochemistry and Petrology, ETH Zürich, Clausiusstrasse 25, CH-8092 (szandra.fekete@erdw.ethz.ch)*

² *Institut of Earth Sciences, Quartier UNIL-Mouline, Bâtiment Géopolis, CH-1015 Lausanne*

High resolution, in situ oxygen isotope measurements of quartz have the potential to detect changing fluid sources during the evolution of a hydrothermal system. We exploit this potential by analyzing euhedral growth zones of quartz in the tin-mineralized Yankee Lode (Mole Granite, Australia) deposit, for which there is strong fluid inclusion evidence of meteoric water incursion into the evolving mineralizing magmatic-hydrothermal system.

We use a well-characterized sample from the study of Audétat et al. (1998) who established a detailed sequence of fluid inclusion generations related to individual quartz growth zones. Microthermometry and LA-ICP MS trace element analyses of these fluid inclusions demonstrated the progressive dilution of hot magmatic water by meteoric fluids and the authors identified this as an efficient precipitation mechanism of cassiterite.

The aim of the present research is to test if the suggested model of mixing of magmatic and meteoric waters is also detectable by oxygen isotopes, using the high-resolution SwissSIMS for in situ analyses across a whole section of an euhedral quartz crystal from the innermost zone up to the rim. The detailed crystallization temperature evolution available from Audétat et al. (1998) allows accurate calculation of the fluid isotopic compositions during individual growth stages. This and an expected strong contrast between magmatic ($\delta^{18}\text{O} = 5\text{--}10\text{‰}$) and contemporaneous meteoric water at Yankee Lode (ca. -15‰ , Sun and Eadington, 1987) implies that this sample is an excellent candidate for testing the method.

Prior to ^{18}O measurements, SEM cathodoluminescence (CL) petrography was conducted to obtain precise textural control on individual growth zones. The growth zones can be grouped into four petrographically distinct growth stages (Q1-Q4). The in situ ^{18}O measurements were carried out in each growth stage as indicated by different CL intensities.

Growth temperatures were taken from fluid inclusions analyzed in previous studies (Audétat et al. 1998, Audétat, 1999). Calculated $\delta^{18}\text{O}$ values of the quartz- and/or cassiterite-precipitating fluid show significant variability through the studied section. The first and second quartz generations were precipitated from a magmatic-like fluid with $\delta^{18}\text{O}$ values of $\sim 8\text{--}10\text{‰}$. $\delta^{18}\text{O}$ values of Q3- and tourmaline-precipitating fluid shows a clear transition from magmatic values of $\sim 8\text{‰}$ to $\delta^{18}\text{O}$ values of $\sim -5\text{‰}$. The outermost quartz-chlorite-muscovite zone was precipitated from a fluid with a significant meteoric water component with a very light $\delta^{18}\text{O}$ value of ca. -15‰ which is consistent with values found by previous studies (Sun and Eadington, 1987) using conventional O-isotope analysis.

The occurrence of the first cassiterite minerals are linked to the Q2 generation, precipitating from a fluid with apparent magmatic signature. The main tin deposition event takes place during Q3 precipitation, which is in good agreement with intense meteoric water incursion (lighter $\delta^{18}\text{O}$ values, tourmaline). This apparent discrepancy can be explained by the presence of a fluid of meteoric origin that was isotopically equilibrated with the hot but already solidified granitic intrusion under rock-dominated conditions prior their transfer to the cold ore deposition site (Heinrich, 1990).

REFERENCES

- Audétat, A., Günther, D., Heinrich, C. A. 1998: Formation of a Magmatic-Hydrothermal Ore Deposit: Insights with LA-ICP-MS Analysis of Fluid Inclusions: *Science*, 279, 2091-2094.
- Audétat, A. 1999: The magmatic-hydrothermal evolution of the Sn/W-mineralized Mole Granite (Eastern Australia): PhD Thesis, 211.
- Heinrich, C.A. 1990: The Chemistry of Hydrothermal Tin(-Tungsten) Ore Deposition: *Economic Geology*, 85, 457-481.
- Sun, S. and Eadington, J. 1987: Oxygen Isotope Evidence for the Mixing of Magmatic and Meteoric Waters during Tin Mineralization in the Mole Granite, New South Wales, Australia: *Economic Geology*, 82, 43-52.

P 2.7

Sulfur isotopes and trace element analyses of ore and gangue minerals from the Rio Marina Fe-deposit, Elba Island: implications for formation mechanism and fluid sources.

Natalia Karadima¹, Kalin Kouzmanov¹, Andrea Dini², Markus Wälle³, Jorge Spangenberg⁴ & John Poté⁵

¹ Department of Earth Sciences, University of Geneva, Rue de Maraîchaire 13, CH-1205 Genève (Natalia-Konstantina.Karadima@etu.unige.ch)

² Istituto di Geoscienze e Georisorse, CNR, Pisa, Italy

³ Institute of Geochemistry and Petrology, ETH Zurich, 8092 Zurich, Switzerland

⁴ Institute of Earth Sciences, University of Lausanne, 1015 Lausanne, Switzerland

⁵ Institut F.-A. Forel, University of Geneva, 10 Route de Suisse, Versoix, Switzerland

Elba Island is located in the Northern Tyrrhenian Sea and is considered to be the innermost outcrop of the Northern Apennines Chain. Since Late Miocene it was affected by post-collisional extension and widespread magmatism of the Tuscan Magmatic Province (8.4-5.9 Ma) which resulted in the emplacement of two acidic plutons, Monte Capanne granitoid and Porto Azzuro monzogranite with ages 6.8Ma and 6-5.4Ma respectively (Bortolotti et al., 2001), and several dyke-laccolith complexes of variable composition. Iron-ore deposits associated with distal hedenbergite-ilvaite skarns are spatially related to the younger magmatic stage (~5.9 Ma, Lippolt et al., 1995) but never in direct contact with the intrusions.

This study is focused on the Rio Marina Fe-deposit which, is one of the six ore deposits on the island. It is located on the Eastern coast of Elba and is hosted in the "Verrucano Formation". Iron ore occurs as massive stratiform to pod-like hematite \pm pyrite bodies and/or vein type ore bodies that follow an overall N-S trend. The ore bodies are restricted mainly to the upper 150-250m of a Permo-Triassic schists and along their contact with the overlying Upper Triassic "Calcare Cavernoso", a marble sequence (Bodechtel, 1965). The host mica schists are strongly affected by complex hydrothermal events which make them appear locally as grey-yellowish to green or reddish-violet in color. The main mineral assemblage consists of hematite, adularia, quartz and chlorite, with minor sphalerite, chalcopyrite, galena, rutile, apatite and fluorite.

In order to decipher the complexity of hydrothermal events, sulfur isotope analyses were carried out in parallel to trace element study on the main ore and gangue minerals in the deposit. Sulfur isotope analyses on sulfides (pyrite, sphalerite and chalcopyrite) vary between $\delta^{34}\text{S}$ 9.4 and 4.2 ‰. Large single pyrite crystals (up to 6 cm in diameter) were cut perpendicular to the main crystal face and small samples were collected along core-to-rim profiles in order to study the evolution of trace element and isotopic signature of pyrite with time. Significant decrease in $\delta^{34}\text{S}$ was registered (up to 2.5 ‰), indicating changes in the source fluid signature (Fig. 1a). ICP-MS trace element analyses on the same pyrite aliquots show a clear correlation of specific trace elements (i.e. Co, Cu, Ni, Se) with the decreasing $\delta^{34}\text{S}$ (Fig. 1b), illustrating ore precipitation in an evolving hydrothermal system. Furthermore, electron microprobe and LA-ICP-MS analyses on both ore and gangue minerals reveal complex chemistry of the main hydrothermal products. Chlorite as the main alteration mineral shows an anomalous chemistry and optical properties.

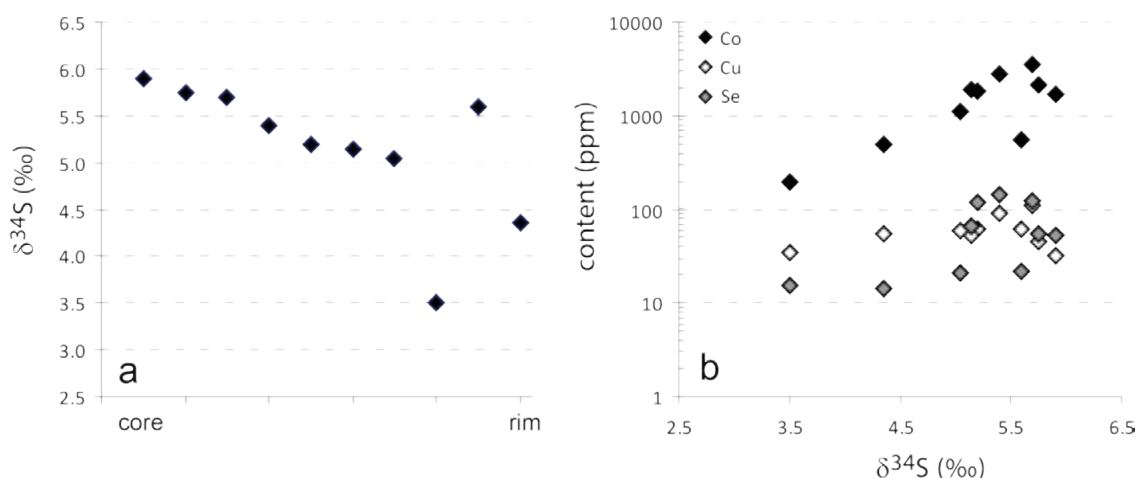


Figure 1. Sulfur isotopes (a) and ICP-MS trace element analyses (b) on a single pyrite crystal along a core-to-rim profile.

Our results illustrate the complex character of the hydrothermal system at Rio Marina where two or more fluid sources were involved in the iron ore-deposition post-dating skarn formation with no direct link with a causative magmatic body.

REFERENCES

- Bodechtel J., 1965: Zur Genese der Eisenerze der Toskana und der Insel Elba. Neues Jahrb. Min. Abhandl., 103:147-162
- Lippolt H.J., Wernicke R.S. & Bähr R. 1995: Paragenetic specularite and adularia (Elba Island): concordant (U+Th)-He and K-Ar ages. Earth Planet Sci. Lett. 132, 43-51
- Bortolotti V., Pandeli E. & Principi G. 2001: The Geology of Elba Island: an historical introduction. Ofioliti, 26 (2a), 79-96

P 2.8

SEM/EDS and TEM/EDS analyses of volcanic particles sampled above the surface of the Erta'Ale lava lake, Danakil depression, Ethiopia, using a remotely-controlled self-closing sampler

Cédric Botter¹, Bernard Grobéty¹

¹ *Département des Géosciences et FRIMAT, University of Fribourg, Chemin du musée 6, CH-1700 Fribourg*

Gas-to-particle conversion and coalescence of ultrafine aerosol particles are the processes generating nanometric solid secondary volcanic particles within high temperature magmatic emissions. Due to the poor accessibility of most of the degassing lava bodies found in open-vent settings, only particles formed by precipitation within liquid droplets are usually sampled in relatively aged plumes in which magmatic and atmospheric water condensates. The chemical and mineralogical compositions of such polyphasic and hydrated particles are not anymore the ones characterizing the first solids formed at the source.

In January 2015, the level of the permanent lava lake relative to the caldera floor of the Erta'Ale volcano was so high that it permitted the sampling of particles within high temperature magmatic emissions less than two meters above the lake surface. Pristine particles impacted onto different types of sampling substrates within a remotely-controlled self-closing cylinder preventing air and humidity to interact with the aerosol sample during recovery and cooling of the sampler. Manual single-particle analyses using SEM/EDS and TEM/EDS were performed on the samples to investigate the mineralogy, chemistry and morphology of the particles. The high temperature samples were compared with filter samples collected at the rim edge of the lake-hosting pit crater. Automated single-particle analyses using SEM/EDX were performed on the later.

Two different particle populations with different chemistry, mineralogy and particle size distribution occur on the sampling substrates. K and Na sulfate-composed particles having diameters of 100-300 nm of which a part is crystalline K sulfate and the other amorphous Cu-bearing K and Na sulfate are found within a very dense and regularly distributed population of 20-60 nm-sized, sulfur-dominated particles. Differences observed between the high temperature samples and the samples taken on the pit rim include the appearance of chloride and mixed sulfate-chloride particles on the later. Since the high temperature samples lack evidences of droplet impacts, the sulfate/sulfur phases identified in the particles are likely to be solids directly generated by gases within the still unaltered magmatic emissions.

P 2.9

Temperature record in clasts expelled from the LUSI mud eruption (Indonesia): evidence for large scale hydrothermal activity

Benjamin Malvoisin¹, Adriano Mazzini², Stephen A. Miller¹

¹ *Centre d'hydrogéologie et de Géothermie, rue Emile Argand 11, Neuchâtel, Switzerland*

² *The Centre for Earth Evolution and Dynamics, University of Oslo, Sem Sælandsvei 24, Blindern 0316 – Oslo, Norway.*

In May 2006, the LUSI mud eruption began in East Java (Indonesia) and led to the displacement of around 30,000 people. The eruption initiated nearly two days after a large earthquake that struck Java Island. The water and gas geochemistry indicate that Lusi is a sedimentary hosted hydrothermal system rooted at >4 km depth. To better understand the Lusi plumbing system and to constrain from which depth the solid fraction originates, we studied the temperature record of erupted clasts collected at the crater site. Three types of clasts were studied based on morphological and mineralogical basis. The first type is limestones mainly composed of Ca- and Fe-bearing carbonates. The clasts of the second type are light grey shales (LGS) containing carbonaceous matter, illite/smectite mixture, plagioclase and quartz. The third type is also a shale containing hydrocarbons and with a black colour (black shales, BS) and the additional presence of Na-rich plagioclase, biotite and chlorite. The presence of these latter minerals indicates hydrothermal activity at relatively high temperature. A better constraint on temperature was obtained by using both Raman spectroscopic carbonaceous material thermometry (RSCM) and chlorite geothermometry. Temperatures below 200°C were determined for the LGS with RSCM. These temperatures are in agreement with the geothermal gradient recorded from a neighbouring exploration borehole and suggest that these clasts likely originate from the Upper Kalibeng Fm located at ~1.5 km depth. For the BS, higher temperatures were measured with values between 250 and 300°C with RSCM and between 140°C and 270°C with chlorite geothermometry. Such high temperatures, the absence of pollen and microfossils, point to a deep origin of the BS shale coinciding with the lacustrine Ngimbang Fm. Ngimbang is the Eocene regional source rock located at ~4 km depth where temperatures ~200 °C are expected. These results confirm the scenario of large scale circulation of hydrothermal fluids beneath LUSI connected with the neighboring Arjuno-Welirang volcanic complex.

P 2.10

Petrological evolution and pre-eruptive conditions of a highly explosive volcano showing signs of unrest: Cerro Machin, Colombia (Master project)

Antoine Régnier¹, Luca Caricchi¹, John Makario Londoño² & Ricardo Arturo Mendez²

¹ Section of earth and environmental sciences, University of Geneva, Rue de Maraichers 13, CH-1205 Genève (ant_regnier@hotmail.com)

² Servicio Geológico Colombiano, Manizales, Colombia

The biggest eruption of Volcan Cerro Machin (VCM) in Colombia occurred ~3600 years before present (BP). With the reactivation of the magmatic system under the volcano it is fundamental to characterize the eruptions from a petrological point of view. Pumices from its pyroclastic flows are composed of plagioclase, unzoned and reversely zoned amphiboles, olivine and biotite, which show no disequilibrium textures. Comparison with experimental work on similar rock composition and geo-thermo-barometry provides pre-eruptive temperature of $820 \pm 20^\circ\text{C}$ and storage pressure of 2-3.5kbar at moderate oxygen fugacity (NNO+1.3 to NNO+1.6 \pm 0.2). Water content compared to experiments is about 6.6 \pm 0.5 wt%. Chemically zoned and unzoned amphiboles show an increase in Mg# in rims. The zoned group shows a decrease of REE concentration to the rim suggesting the potential supply of mafic melt in a dacitic magmatic reservoir. The second group show elevated REE content on the rim combined with high Mg#, which can be accounted for by the flushing of sulfur through the magmatic system in a last stage (Scaillet and Evans, 1999). Bulk rock compositions and petrographic assemblages from different eruptions (1200BP eruptions and actual dome) are similar to this study and are also analysed. Both eruptions have geochemical adakitic signatures and have high Sr isotopic ratio ($^{87}\text{Sr}/^{86}\text{Sr} \sim 0.70495$) controlled by continental crust or a sediment signature from the slab. With all these information, it is now easier to understand the behaviour of the volcano, and its potential evolution toward a future eruption.

REFERENCES

- Laeger, K., Halama, R., Hansteen, T., Savov, I. P., Murcia, H. F., Cortés, G. P., & Garbeschönberg, D. (2013). Crystallization conditions and petrogenesis of the lava dome from the ~900 years BP eruption of Cerro Machin Volcano, Colombia. *Journal of South American Earth Sciences*, 48, 193-208.
- Méndez, R. A. (2002). Evaluación de la amenaza volcánica potencial del Cerro Machin (departamento del Tolima, Colombia).
- Scaillet, B., & Evans, B. W. (1999). The 15 June 1991 eruption of Mount Pinatubo. Phase equilibria and Pre-eruption P-T-fO₂-fH₂O conditions of the dacite magma. *Journal of Petrology*, 40(3), 381-411.
- Thouret, J. C., Cantagrel, J.-M., Robin, C., Murcia, A., Salinas, R., Cepeda, H. Quaternary eruptive history and hazard-zone model at Nevado del Tolima and Cerro Machin volcanoes, *Journal of Volcanology and Geothermal research* 66 (1-4), p. 397-426

P 2.11

The generation and architecture of crustal rhyolitic reservoirs: insights from the Kilgore Tuff eruption

Emmanuelle Ricchi¹, Luca Caricchi¹, Ilya Bindeman² & Jörn Wotzlaw¹

¹ *Section of Earth and Environmental Sciences, University of Geneva, Rue de Maraichers 13, CH-1205 Genève (Emmanuelle.Ricchi@etu.unige.ch)*

² *Department of Geological Sciences, University of Oregon, Eugene, OR 97403-1272*

The Heise volcanic field is the most recent and complete cycle of volcanism preceding the still active Yellowstone volcanic field. Isotopic and geochronological studies of the Kilgore Tuff, the largest eruption produced by the Heise volcanic field, suggest that the assembly of separated reservoirs of eruptible magma preceded this super eruption (Watts et al., 2011, Wotzlaw et al., 2014). The buoyancy associated to this process may have been sufficient to trigger the eruption (Caricchi et al., 2014, Wotzlaw et al., 2014). Geophysical imaging of present day Yellowstone magmatic system also shows the existence of several isolated and potentially melt-rich regions within a highly crystallised magmatic mush (Miller and Smith, 1999). Additionally, recently, the presence of a basaltic lower-crustal magma body providing the link between this shallow mushy magma reservoir and the mantle plume has been revealed (Huang and al., 2015).

While recent studies suggest that the merging of multiple pockets of eruptible magma may be commonly preceding super-eruptions (Ellis et al., 2014; Wotzlaw et al., 2014), no detailed geochemical, petrographic and petrological work along the stratigraphy of the deposits of these large eruptions has been performed to bolster this interpretation. This, together with the possibility that the sequence of events that preceded the eruption of the Kilgore Tuff may be similar to those that will occur before a future Yellowstone super-eruption, are the main motivations of this study.

New geochemical data on the Kilgore Tuff were acquired along stratigraphic profiles. Whole-rock and high-spatial resolution analyses of matrix glass, feldspars, pyroxenes, zircons and melt inclusions were carried out for several stratigraphic layers of two Kilgore Tuff deposits on the south-east and north-west rim of the Heise caldera.

The analyses reveal that the deposit is heterogeneous along the stratigraphy with significant variations of glass matrix composition both in term of major and trace elements, as well as differences in mineral chemistry. These variations are not continuous from the base to the top of the deposits.

Pre-eruptive pressure, temperature and water content for the samples collected at various stratigraphic levels were estimated using rhyolite-MELTS simulations, two-feldspar thermometry, clinopyroxene-liquid thermobarometry, zircon saturation thermometry. The results suggests that the reservoir that fed the Kilgore Tuff eruption had a complex architecture with isolated melt-rich pockets dispersed at various depths and located at different distance from the caldera rims that were sampled discontinuously during the eruption.

REFERENCES

- Caricchi, L., Annen, C., Blundy, J., Simpson, G., Pinel, V., 2014, Frequency and magnitude of volcanic eruptions controlled by magma injection and buoyancy: *Nature Geoscience*, v.7, p.126-130, doi: 10.1038/ngeo2041.
- Ellis B.S., Bachmann O., Wolff J.A., 2014, Cumulate fragments in silicic ignimbrites: The case of the Snake River Plain, *Geology*, v.42, no.5, p.431-434, doi: 10.1130/G35399.1.
- Miller, D. S., and R. B. Smith (1999), P and S velocity structure of the Yellowstone volcanic field from local earthquake and controlled-source tomography, *J. Geophys. Res.*, 104(B7), 15105–15121, doi:10.1029/1998JB900095.
- Watts, K.E., Bindeman, I.N., Schmitt, A.K., 2011, Large-volume Rhyolite Genesis in Caldera Complexes of the Snake River Plain: Insights from the Kilgore Tuff of the Heise Volcanic Field, Idaho, with Comparison to Yellowstone and Bruneau Jarbidge Rhyolites: *Journal of Petrology*, v. 52, p. 857-890, doi:10.1093/petrology/egr005.
- Wotzlaw, J.F., Bindeman, I.N., Watts, K.E., Schmitt, A.K., Caricchi, L., Schaltegger, U., 2014, Linking rapid magma reservoir assembly and eruption trigger mechanisms at evolved Yellowstone-type supervolcanoes: *Geology*, doi:10.1130/G35979.1.
- Hsin-Hua Huang, Fan-Chi Lin, Brandon Schmandt, Jamie Farrell, Robert B. Smith, and Victor C. Tsai, 2015, The Yellowstone magmatic system from the mantle plume to the upper crust, *Science*, Vol. 348 no. 6236 pp. 758-759, DOI: 10.1126/science.aab1828.

P 2.12

Driving Mechanisms Of 1651 And 2002 Eruptions At Etna Volcano (Italy)

Milena Scignari¹, Laura Pioli¹, Luca Caricchi¹, Daniele Andronico²

¹ *Section of Earth and Environmental Sciences, University of Geneva, Geneva, Switzerland*

² *Istituto Nazionale di Geofisica e Vulcanologia (INGV), Sezione di Catania, Catania, Italy*

Mount Etna is a type case of open vent basaltic volcano. It shows a large range of eruptive styles as lava flows, Strombolian explosions, lava fountains, Subplinian and Plinian eruptions (Branca and Del Carlo, 2005), which are not usual for basaltic systems. Its frequent and sometimes violent volcanic activity poses a risk to the populated region of eastern Sicily. However, at the moment there is little understanding on the mechanisms driving explosivity and controlling eruptive styles. This issue poses strong limitations on the quantification of volcanic hazard at short and medium time scales.

To address this question we are comparing two different eruptions; one occurred in 1651 before the 1669 Montirossi eruption, which generated a large lava flow field and is characterized by large plagioclase phenocrysts and the 2002-3 eruption that was a spectacular explosive eruption accompanied by an effusive event. These two eruptions show distinct phenocryst assemblages (particularly plagioclase crystal content and size) and compositions and represent ideal end-members in the volcanic activity of Etna.

A detailed characterization of the physical properties of the lava and scoria of these two eruptions (e.g. density, vesicularity, grain size distribution and componentry) is compared with their geochemical and petrological properties (bulk and phenocryst composition, CSDs) to understand how conduit and magma chamber processes affected the eruptive dynamics. Moreover, a detailed sampling of the 2002-3 products will allow the comparison of lava and tephra erupted from the same fissural vents and will help to understand which properties in the plumbing system permits the manifestation of these two different eruptive styles.

Preliminary results for the 2002 tephra show homogeneous characteristics, unimodal grain size distribution, typical of a strombolian explosion, predominance of tachylite, and little lithic content, and allow the quantification of the textural differences between the studied eruptions. However, particles are often altered with a reddish or a yellowish alteration, the distinction between them is difficult.

REFERENCES

- Andronico, D., Branca, S., Calvari, S., Burton, M., Caltabiano, T., Corsaro, R., Del Carlo, P., Garfi, G., Lodato, L., Miraglia, L., Murè, F., Neri, M., Pecora, E., Pompilio, M., Salerno, G., Spampinato, L., 2005. A multi-disciplinary study of the 2002-03 Etna eruption: insights into a complex plumbing system. *Bull Volcano* (2005)67:314-330
- Branca, S., Del Carlo, P., 2005. Types of eruptions of Etna volcano AD 1670-2003: implications for short-term eruptive behavior. *Bull Volcano* (2005)67:732-742
- Fornaciai, A., Perinelli, C., Armienti, P., & Favalli, M. (2015). Crystal size distributions of plagioclase in lavas from the July–August 2001 Mount Etna eruption. *Bull Volcano* (2015)77, 70.
- Lanzafame, G., Mollo, S., Iezzi, G., Ferlito, C., Ventura, G., 2013. Unraveling the solidification path of a *pahoehoe* "cicirara" lava from Mount Etna volcano. *Bull Volcano* (2013)75:703

P 2.13

Petrography and geochemistry of Cusìn and Cubilche volcanic complexes (Interandean Valley, Ecuador)

Elisa Tamagnone Cosmelli¹ Massimo Chiaradia¹ Luca Caricchi¹

¹ Section of Earth and Environmental Sciences, University of Geneva, Rue de Maraichers 13, CH-1205 Genève

This study is part of a regional scale project focused on the across- and along-arc variability of the Ecuadorian magmatism. In particular, it is carried out in the frame of the well studied 50-km long NW-SE-trending transect comprising nine volcanoes (Pilavo, Yanaurcu, Chachimbiro, Chuicocha-Cotacachi, FuyaFuya, Imbabura, Mojanda and Cayambe) across the Andean Cordilleras in the North of Ecuador (0°-0°30"N) (e.g. Chiaradia et al., 2011; Béguelin et al., 2015; Samaniego et al., 2005; Robin et al., 2008; Bryant et al., 2006). The investigation of additional four volcanic edifices (Cusìn, Cubilche, Pangaladera volcanoes and Cunrru dome) carried out in this Master thesis aims to reconstruct geochemical changes of closely spaced volcanic edifices in this transect and to investigate the spatial and temporal variability of petrogenetic processes at adjacent volcanic edifices (< 7 Km). We carried out sampling and field observations on the four volcanoes, petrographic study on numerous thin sections, geochemical and isotopic analysis on the whole rocks (XRF, Laser Ablation ICPMS, radiogenic isotope of Pb, Nd and Sr), in situ mineral analysis (major elements microprobe analysis on plagioclase and pyroxene) and geochronology (⁴⁰Ar/³⁹Ar). The study of these volcanoes and of their xenoliths has also provided data that could improve the understanding of the lithological nature of the basement in the Interandean Valley (continental or oceanic crust?), which is poorly known because covered by Tertiary to Quaternary volcanic and volcanoclastic deposits.

Results of this study show that Cusìn magmatic rocks are more evolved, enriched in incompatible elements and isotopically more crustal than those of the other three volcanic edifices investigated. The more evolved isotopic signature suggests a more significant crustal assimilation in the magma reservoir of Cusìn or of a transition from less to more radiogenic basement rocks (transition from the oceanic to the continental basement). We have carried out Monte Carlo simulations of assimilation and crystal fractionation (ACF) processes using the REE geochemistry of the volcanic rocks and appropriate parent and assimilant reservoirs. REE spectra of Cusìn volcano need at least 30% of assimilation ($r = 0.3 = \text{mass of assimilated material} / \text{mass of the initial magma}$) of a mid-crust reservoir and $34 \pm 9\%$ of fractionation to be reproduced by the model. On the other hand REE spectra of Cubilche require near zero assimilation ($r = 0.05 \pm 0.04$) and a lower amount of crystal fractionation ($F = 18 \pm 4\%$). The new data acquired in this study have also allowed us to refine and increase the spatial resolution of geochemical and isotopic compositions for the NW-SE trending across-arc transect above mentioned. This now densely "populated" transect (13 volcanoes) displays regular increase in Sr isotopic ratio from the frontal arc towards the back-arc. In contrast major and trace elements do not always show systematic changes along the transect. We conclude that geochemical changes depend on peculiar localized magmatic evolutions of each single volcanic center whereas the systematic changes of radiogenic isotopes across the transect are related to the nature of the basement (oceanic towards the trench and continental towards the back-arc) and to the amount of assimilated material in the magma reservoirs.

REFERENCES

- Chiaradia, M., Müntener, O., Beate, B. 2011: Enriched basaltic andesites from mid-crustal fractional crystallization, recharge, and assimilation (Pilavo volcano, Western Cordillera of Ecuador). *Journal of Petrology*, 52, 1107-1141.
- Béguelin, P., Chiaradia M., Beate B., Spikings R. (2015). The Yanaurcu volcano (Western Cordillera , Ecuador): A fi eld , petrographic , geochemical , isotopic and geochronological study. *Lithos*, 218-219, 37-53
- Bryant, J. A., Yogodzinski, G. M., Hall, M. L., Lewicki, J. L. & Bailey, D. G. (2006). Geochemical constraints on the origin of volcanic rocks from the Andean Northern Volcanic Zone, Ecuador. *Journal of Petrology* 47,1147-1175.
- Robin C., Samaniego P., Le Pennec J.L., Mothes P., van der Plicht J. (2008). Late Holocene phases of dome growth and Plinian activity at Guagua Pichincha volcano (Ecuador). *Journal of volcanology and geothermal research*, 176, 7-15
- Samaniego, P., Martin, H., Monzier, M., Robin, C., Fornari, M., Eissen, J.-P., and Cotten, J., 2005, Temporal evolution of magmatism in the Northern volcanic zone of the Andes: The geology and petrology of Cayambe Vol- canic Complex (Ecuador): *Journal of Petrology*, v. 46, p. 2225–2252

P 2.14

Plutonic xenoliths from Mount St. Helens – a window into the magma plumbing system

Maren Wanke¹, Ben S. Ellis¹, Olivier Bachmann¹, Marcel Guillong¹, Michael A. Clynne²

¹ *Institute of Geochemistry and Petrology, Department of Earth Sciences, ETH Zürich, Clausiusstrasse 25, CH-8092 Zürich (maren.wanke@erdw.ethz.ch)*

² *U.S. Geological Survey, Volcano Science Center, 345 Middlefield Rd, Menlo Park, CA 94025, USA*

Mount St. Helens is an active stratovolcano in the southern Washington portion of the Cascade arc. It has erupted lavas carrying a variety of plutonic xenoliths, dominantly derived from the Tertiary crust beneath the volcano. However, two samples yielded zircon crystallization ages of 5-108 ka (n=29) and 45-486 ka (n=16), overlapping with zircon ages from the volcanic rocks (Claiborne 2010). These two samples are interpreted to represent crystal mush from the recent volcanic system. Ages as well as textural and mineralogical differences from crustal xenoliths (25.5 ± 0.08 Ma) were further used to distinguish five different types of “young” inclusions. These comprise xenoliths of gabbroic to dioritic ortho- (type 1), meso- (type 2), and ad-cumulates (type 3) in dacite domes of the Pine Creek eruptive period (~2900 BP) that are dominated by amphibole, plagioclase, occasional orthopyroxene and oxides (\pm apatite and zircon) with variable amounts of residual melt. The classification is based on textural characteristics, though, each type has distinctive mineral compositions. Type 4 inclusions are formed by crystal aggregates in Late Pine Creek andesites (~2600 BP) composed of pyroxene-plagioclase-oxide-bearing assemblages. A heterad-cumulate (type 5) found in 1980 dacite consists of olivine, plagioclase, ortho- and clinopyroxene (\pm oxides and apatite) with poikilitic overgrowth of amphibole. Textural relationships and mineral chemistry were combined with thermobarometers to identify the magmatic conditions during crystallization. Different types of cumulates were formed from basaltic andesitic to rhyolitic melts at mid to upper crustal pressures. Plagioclases and amphiboles in a type 3 cumulate gave crystallization temperatures and pressures around 780-885 °C and 1.2-3.5 kbar (Holland & Blundy 1994, Anderson & Smith 1995). Orthopyroxene-liquid thermobarometry on two other cumulate types resulted in 978-1003 °C at 1.9-4.2 kbar (type 1) and 1077-1086 °C at 3.8-5.5 kbar (type 5) (Putirka 2008). Three different pyroxene thermobarometers used on the gabbroic crystal aggregates (type 4) returned overlapping temperatures and pressures of 946-990 °C at 1.7-6.4 kbar, 985-1012 °C at 2.2-4.8 kbar, and 988-1036 °C at 1.5-5.8 kbar (the error is expected to be around 2.1-3.2 kbar and 41-56 °C, Putirka 2008). Mineral compositions in a gabbroic ad-cumulate (type 3) are similar to those in its dacitic host rock. Hence, such cumulates may have co-erupted with their extracted melt. However, the variability of cumulate types returning mid to upper crustal pressures indicates extensive fractionation of different types of magma at depths between 5 and 20 km confirming the inferred outline of the mid to upper crustal magma reservoir beneath Mount St. Helens (Pallister 1992). The variability of magmas is consistent with pervasive mixing expected in a relatively narrow “bottle-shaped” reservoir.

REFERENCES

- Anderson, J. L., and Smith, D. R., 1995: The effects of temperature and fO₂ on the Al-in-hornblende barometer. *American Mineralogist*, v. 80, p. 549-559.
- Claiborne, L. L., Miller, C. F., Flanagan, D. M., Clynne, M. A., and Wooden, J. L. 2010: Zircon reveals protracted magma storage and recycling beneath Mount St. Helens. *Geology*, v. 38, no. 11, p. 1011-1014.
- Holland, T., and Blundy, J. 1994: Non-ideal interactions in calcic amphiboles and their bearing on amphibole-plagioclase thermometry: Contributions to Mineralogy and Petrology, v. 116, p. 433-447.
- Pallister, J. S., Hoblitt, R. P., Crandell, D. R., and Mullineaux, D. R. 1992: Mount St. Helens a decade after the 1980 eruptions: magmatic models, chemical cycles, and a revised hazards assessment. *Bulletin of Volcanology*, v. 54, no. 2, p. 126-146.
- Putirka, K., 2008: Thermometers and Barometers for Volcanic Systems, in Putirka, K., and Tepley, F., eds., *Minerals, Inclusions and Volcanic Processes*, Volume 69. Reviews in Mineralogy and Geochemistry, Mineralogical Society of America, p. 61-120.

P 2.15

New calibration for $\delta^{18}\text{O}$ analysis of monazite by SIMS

Amélie Didier, Benita Putlitz, Lukas Baumgartner, Anne-Sophie Bouvier.

Institute of Earth Sciences, University of Lausanne, Quartier UNIL-Mouline, Bâtiment Geopolis, 1015 Lausanne, Switzerland (amelie.didier@unil.ch)

Monazite – an accessory mineral commonly used for dating of crustal rocks – is often sensitive to interactions with fluids, which can enhance its recrystallization. Monazite has been shown to record several episodes of fluid/rock interaction within a single grain. The coupled, in situ determination of age and oxygen isotope composition by SIMS is ideal to harness this potential. However, well characterized monazite standards for oxygen isotopes are scarce (Ayers et al., 2006; Breecker and Sharp, 2007; Rubatto et al., 2014). Several standards are needed, because the instrumental mass fractionation is up to 3 ‰ for $\delta^{18}\text{O}$ for different monazite chemical compositions.

Here we present chemical and isotopic compositions of several monazites with different ratio of monazite (YREEPO_4), brabantite ($\text{CaTh}(\text{PO}_4)_2$) and huttonite (ThSiO_4). We selected four monazites; their chemical composition reflects the range of chemical variations in most magmatic, metamorphic and hydrothermal monazites: MOACYR ($\text{Mnz}_{91}\text{Brab}_3\text{Hutt}_6$; Seydoux-Guillaume et al., 2002), MANANGOUTRY ($\text{Mnz}_{82}\text{Brab}_9\text{Hutt}_9$; Paquette et Tiepolo, 2007), and BASEL (Mnz_{99}) have homogeneous chemical and isotopic compositions (uncertainties 2SD ca. $\pm 0.3\text{--}0.4\text{‰}$); GENEVA ($\text{Mnz}_{88}\text{Brab}_3\text{Hutt}_9$) is less homogeneous (uncertainties 2SD ca. $\pm 0.5\text{--}0.6\text{‰}$) and is only partially suitable for standardisation, but is used here to check the influence of the chemical composition on the instrumental mass fractionation. True $\delta^{18}\text{O}$ of each monazite have been obtained by laser fluorination (LF) and is $1.45 \pm 0.10\text{‰}$ for MOACYR; $10.35 \pm 0.30\text{‰}$ for MANANGOUTRY; $8.40 \pm 0.20\text{‰}$ for BASEL and $9.57 \pm 0.20\text{‰}$ for GENEVA. The USGS 44069 monazite, already investigated by Rubatto et al., 2014 ($\delta^{18}\text{O} = 7.67 \pm 0.13\text{‰}$; $\text{Mnz}_{93}\text{Brab}_7$), has been added to this set of materials.

On the basis of these five monazites, a calibration curve can be established. Our data suggest, that the IMF ($= \delta^{18}\text{O}_{\text{SIMS}} - \delta^{18}\text{O}_{\text{LF}}$) is simply correlated with the YREEPO_4 content of monazite. These results seem to disagree with those of Breecker and Sharp (2007), who suggested that IMF is dependent on the Th content only.

MOACYR, MANANGOUTRY and BASEL are excellent standards for SIMS $\delta^{18}\text{O}$ analyses.

REFERENCES

- Ayers JC, Loflin M, Miller CF, Barton MD, Coath CD (2006) In situ oxygen isotope analysis of monazite as a monitor of fluid infiltration during contact metamorphism: Birch Creek Pluton aureole, White Mountains, eastern California. *Geology* 34:653-656.
- Breecker, D.O. and Sharp, Z.D. 2007, A monazite oxygen isotope thermometer, *American Mineralogist*, 92, 1561-1572.
- Paquette, J.-L., Tiepolo M. 2007, High resolution (5 μm) U-Th-Pb isotope dating of monazite with excimer laser ablation (ELA)-ICPMS, *Chemical Geology*, 240, 222-237.
- Seydoux-Guillaume, A.-M., Paquette, J.-L., Wiedenbeck, M., Montel, J.-M., Heinrich, W. 2002, Experimental resetting of the U-Th-Pb systems in monazite, *Chemical Geology*, 191, 165-181.
- Rubatto, D., Putlitz, B., Gauthiez-Putallaz, L., Crépeau, C., Buick, I.S., Zheng Y.-F. 2014, Measurement of in-situ oxygen isotope ratios in monazite by SHRIMP ion microprobe: Standards, protocols and implications, *Chemical Geology* 380, 84-96.

P 2.16

Limits of precision and reproducibility in high-precision isotope-dilution U/Pb geochronology

Urs Schaltegger¹, Jörn-Frederik Wotzlaw^{1,2}, Maria Ovtcharova¹, Blair Schoene^{1,3}, Joshua H.F.L. Davies¹ & Björn Baresel¹

¹ Department of Earth Sciences, University of Geneva, rue des Maraîchers 13, 1205 Geneva (urs.schaltegger@unige.ch)

² Geochemistry and Petrology, ETH Zürich,

³ Department of Geosciences, Princeton University, Guyot Hall, Princeton, USA

High-precision U-Pb geochronology using chemical abrasion isotope dilution thermal ionization mass spectrometry (CA-ID-TIMS) techniques requires the careful assessment of short- and long-term intralaboratory analytical reproducibility. The accuracy and reproducibility is monitored by repeated analyses of synthetic U-Pb solutions distributed through the EARTHTIME consortium (Condon et al., 2008), and of well-characterized and homogeneous natural zircon reference materials.

We here report U-Pb isotopic data for two synthetic and six natural reference materials analyzed at the University of Geneva Isotope Laboratory over a period of more than eight years. All analyses were performed employing a Thermo Scientific TRITON TIMS equipped with a MasCom secondary electron multiplier. We document how external variables (SEM changes, measurement strategies, different mass bias corrections linked to EARTHTIME ET535 and ET2535 tracers) influence both short- and long-term reproducibility. Our large high-precision data sets of synthetic reference solutions (2 sigma = 0.017 to 0.10% uncertainty on single analysis), as well as our data from natural zircon reference materials, display dispersion in excess of analytical uncertainty. This excess dispersion is similar over periods of several days to several years suggesting that the excess scatter results from some unaccounted for short-term rather than long-term fluctuation.

We further report new high-precision U-Pb dates for a series of international zircon reference materials (Temora, R33, Plesovice, GJ-1, AusZ2/5) relative to the EARTHTIME tracer solutions (Condon et al., 2015; McLean et al., 2015) providing a fully traceable set of reference values that take into account our intra-laboratory reproducibility.

With these data we can demonstrate subpermil precision and reproducibility on $^{206}\text{Pb}/^{238}\text{U}$ dates from the UNIGE laboratory, clearly better than the 0.1% uncertainty target on $^{206}\text{Pb}/^{238}\text{U}$ dates formulated by EARTHTIME about 10 years ago. We define our next target as being the 0.01% precision and reproducibility ("accuracy") level on $^{206}\text{Pb}/^{238}\text{U}$ dates for the entire history of the Earth between 4.6 Ga and 400 ka, which we anticipate to achieve during the next 10 years. Such precision and reproducibility is essential when correlating planetary biotic and abiotic events over time.

REFERENCES

- Condon, D.J., McLean, N.M., Schoene B., Bowring S., Parrish R. & Noble, S. 2008: Synthetic U-Pb 'standard' solutions for ID-TIMS geochronology, *Geochimica Cosmochimica Acta*, 72, A175.
- Condon, D.J., Schoene B., McLean, N.M., Bowring S. & Parrish R. 2015: Metrology and traceability of U-Pb isotope dilution geochronology (EARTHTIME Tracer Calibration Part I), *Geochimica Cosmochimica Acta*, 164, 464-480.
- McLean N.M., Condon, D.J., Schoene B. & Bowring S. 2015: Evaluating uncertainties in the calibration of isotopic reference materials and multi-element isotopic tracers (EARTHTIME Tracer Calibration Part II), *Geochimica Cosmochimica Acta*, 164, 481-501.

P 2.17

Semi-quantitative Raman spectroscopy on fluor-hydroxyapatite serial solid solutions

Ramon Schmid¹, Christian De Capitani¹, Leander Franz¹ & Meinert Rahn²

¹ Mineralogisch-Petrographisches Institut, Universität Basel, Bernoullistrasse 30, CH-4056 Basel
(ramon.schmid@stud.unibas.ch)

² Eidgenössisches Nuklearsicherheitsinspektorat ENSI, Industriestrasse 19, CH-5200 Brugg

Apatite, in a geological sense, naturally occurs as solid solution of the three endmembers hydroxyapatite (HAp), fluorapatite (FAP) and chlorapatite (ClAp) with the reduced general chemical formula A_5X_3Y , where A is mainly occupied with Ca^{2+} , X with PO_4^{3-} and Y with F^- , Cl^- or OH^- (Zattin et al. 2007). There are various possible substitutions on each position but this study is mainly concerned with calcium phosphate fluor-hydroxyapatites.

Depending on its chemical composition, apatite shows distinct fission track annealing. For F/Cl apatites, a correlation of these characteristics with etch pit diameters (Dpar) was found (Zattin et al. 2007). This led to the possibility to only measure Dpar to obtain the F/Cl ratio. While such a calibration for F/Cl is possible with quantitatively determined concentrations of the halogens by electron probe microanalysis, OH^- is not measurable. Hence, a non-destructive method to at least semi-quantitatively determine contents of OH^- is needed. That is where Raman spectroscopy is consulted. Since this is not a quantitative method a calibration by means of well characterized apatites had to be done.

Therefore, Raman active vibrational features of calcium phosphate fluor-hydroxyapatite serial solid solutions were investigated to identify quantifiable relations to their hydroxyl contents. In order to observe preferably pure samples all fluor-hydroxyapatite nanopowders were synthesised by wet chemical precipitation. Samples held F/ OH^- ratios varying from fluor to hydroxy endmember and were analysed with Raman spectroscopy. Specific Raman modes were evaluated by means of band intensity and shift. Semi-quantitative OH^- content correlation within the investigated system is best signified on the basis of normalised intensities of the OH stretch mode at 3572 cm^{-1} and presented results show a similar tendency as previous studies (O'Shea et al., 1974).

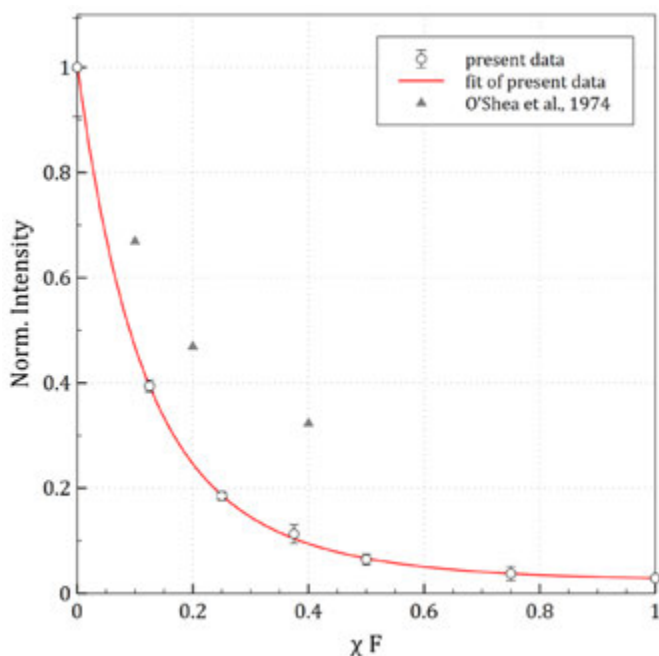


Figure 1. Doubly normalized intensity of OH stretch mode versus F content with 2σ standard deviation. By way of comparison with O'Shea et al. (1974) present normalized intensity was normalized against itself so that HAp (0% substitution) featured an intensity of 1.

REFERENCES

- O'Shea, D.C., Bartlett, M.L. & Young, R.A. 1974: Compositional analysis of apatites with laser-Raman spectroscopy: (OH, F, Cl) apatites, *Archives of Oral Biology*, 19, 995-1006.
- Zattin, M., Berasni, D. & Carter, A. 2007: Raman microspectroscopy: A non-destructive tool for routine calibration of apatite crystallographic structure for fission-track analyses, *Chemical Geology*, 240, 197-204.

P 2.18

NanoSIMS study on quartz phenocrysts

Susanne Seitz¹, Benita Putlitz¹, Lukas Baumgartner¹, Stephane Escrig², Anders Meibom², Anne-Sophie Bouvier¹, Torsten Vennemann³

¹ *Institute of Earth Sciences, University of Lausanne, CH-1015 Lausanne, (susanne.seitz@unil.ch)*

² *Laboratory of Biological Geochemistry, École Polytechnique Fédérale (EPFL), Lausanne, CH-1015, Lausanne*

³ *Institute of Earth Surface Dynamics, University of Lausanne, CH-1015 Lausanne*

The volcanic El Quemado Complex was deposited from the Middle to Late Jurassic during the breakup of Gondwana. This complex is part of a large silicic igneous province, which includes the Chon Aike Province in Southern Patagonia and related rocks from the Antarctic Peninsula (Pankhurst et al., 2000; Riley et al., 2001). The study area is located in vicinity of the Fitz Roy Plutonic Complex (Ramirez et al. 2012) near the village of Chaltén (Argentina). Here the El Quemado Complex consists of rhyolitic and dacitic ignimbrites, lava flows and domes. We studied quartz phenocrysts to provide new insights into the timescales of volcanic processes and magma sources.

Quantitative Ti-analyses was carried out at the SwissSIMS and we used the NanoSIMS (CASA, University of Lausanne) to acquire several high-resolution Ti-profiles (data are reported $^{48}\text{Ti}/^{29}\text{Si}$ ratio) across growth respectively resorption zones as identified by cathodoluminescence. Note, that all high-resolution (ca. 700 nm) NanoSIMS transects show sharp changes in the $^{48}\text{Ti}/^{29}\text{Si}$ ratio.

We noticed distinct differences between quartz phenocrysts from (a) rhyolite flows and (b) their volcanoclastic equivalents. The former (a) show classic oscillatory magmatic zoning and diffusion modeling of titanium in quartz reveals a surprisingly short time-scale for quartz crystallization of 3.4 ± 1.3 yr. This suggests crystal growth during non-interrupted (fast) magma ascent. Thus, the oscillatory zoning and the variation of the Ti concentration of these qtz-phenocrysts do not reflect T, P variations of the magmatic system, but rather local a_{Ti} changes around the growing crystal. Fast crystal growth rates relative to diffusion of Ti in rhyolitic melts result in disequilibrium growth, hence the oscillatory zoning rather represents growth kinetics and care must be taken when using Ti-in-quartz thermometry !

In contrast, quartz phenocrysts from (b) volcanoclastic rocks show complicated zoning often marked by events of resorption and re-growth, rather suggesting storage in a mush, with heating or pressure cycles before eruption. Diffusion modeling shows overgrowth rims formed 0.9 to 3.5 years before eruption.

Additional information comes from oxygen isotope analyses. The results of laser-fluorination analyses show high $\delta^{18}\text{O}$ -values (11-14‰) for both types of qtz-phenocrysts compatible with a crustal magma source for the El Quemado complex (see also Riley et al. 2001). SIMS analyses further reveal the absence of $\delta^{18}\text{O}$ -zoning and confirm that they indeed preserved their magmatic oxygen isotope signature and are not affected by late stage alteration.

REFERENCES

- Pankhurst, R.J., Riley, T.R., Fanning, C.M., and Kelley, S.P., 2000, Episodic silicic volcanism in Patagonia and the Antarctic Peninsula: chronology of magmatism associated with the break-up of Gondwana: *Journal of Petrology*, v. 41, no. 5, p. 605–625
- Ramírez de Arellano, C., Putlitz, B., Müntener, O., and Ovtcharova, M., 2012, High precision U/Pb zircon dating of the Chaltén Plutonic Complex (Cerro Fitz Roy, Patagonia) and its relationship to arc migration in the southernmost Andes: *Tectonics*, v. 31, no. 4
- Riley, T.R., Leat, P.T., Pankhurst, R.J., and Harris, C., 2001, Origins of large volume rhyolitic volcanism in the Antarctic Peninsula and Patagonia by crustal melting: *Journal of Petrology*, v. 42, no. 6, p. 1043–1065.

P 2.19

Detection in LA-ICPMS: Construction and performance evaluation of decision rules

Alex Ulianov¹, Othmar Müntener¹, Urs Schaltegger² & François Bussy¹

¹ *Institute of Earth Sciences, University of Lausanne, Géopolis, CH-1015 Lausanne (alexey.ulianov@unil.ch)*

² *Section of Earth and Environmental Sciences, University of Geneva, Rue de Maraichère 13, CH-1205 Genève*

Laser ablation inductively coupled plasma mass spectrometry (LA-ICPMS) is frequently employed for the analysis of minute isotope contents in the presence of a background noise. Distinguishing between the sample signal and the background noise at a given confidence level thus represents a routine challenge. For count numbers N_b and N_s collected during (equally long) background and sample measurements, respectively, the statistical significance of their net value, $N_s - N_b$, can be considered: how probable is it to obtain such value by subtracting two count number estimates coming from a common statistical distribution (i.e., when N_s and N_b represent measured estimates of the same mean activity)? If, based on the analysis of a model distribution of the net count numbers, we decide that this is probable, the signal is statistically indistinguishable from the background: the analysed isotope is not detected. If the corresponding (one-sided) probability is below some threshold, it is detected. The net signal value on the divide between the above alternatives, given in net counts or mass content units, is called critical level; optionally, it can be complemented by the computation of the detection limit; such values are often reported in the literature. Less discussed is the appropriateness of computational methods used to estimate these values. Troubles arise from attempts to apply Gaussian confidence intervals to small, discretely distributed count numbers contained in real LA-ICPMS acquisitions, and from a non-optimal estimation of the net count number standard deviation in some of the methods used for the computation of critical levels for paired measurements. Combined, these factors may result in uncontrolled, excessively high rates of false detections (background reported as detection of analyte in the sample). We provide a review of methods, otherwise called decision rules, available for the critical level estimation and discuss how to evaluate the performances of these rules to enable an educated computation of LA-ICPMS detection capabilities, including the case of small count numbers. For practical purposes, we especially recommend using decision rules based on the square root transform of the original count numbers. The corresponding critical level, in the intensity based notation, for any t_b/t_s ratio, at a frequently used k_α value of 1.645 (5% of false detections) is given as follows:

$$L_c = (I_s - I_b)_c = d \left(\frac{1}{t_b} - \frac{1}{t_s} \right) + 0.677 \left(\frac{1}{t_s} + \frac{1}{t_b} \right) + 1.645 \sqrt{(I_b t_b + d) \frac{1}{t_b} \left(\frac{1}{t_s} + \frac{1}{t_b} \right)}$$

where I_b and I_s , t_b and t_s denote background and signal intensities and total counting times, respectively. The value of d can be set to 3/8 or to 0.4, it does not seem that either of these values is clearly preferable. This recommendation agrees with earlier recommendations made in texts of radioactivity monitoring, where this formula is appreciated for its robust behaviour in a wide range of mean background count numbers and t_b/t_s ratios. It also agrees with recommendations given in texts of mathematical statistics and biometrics, where, in addition to the robust behaviour, it is approved for its relatively high power. A viable alternative to decision rules based on the square root transform is the mid- p adjusted version of the binomial decision rule. It is slightly more conservative and less powerful, however, and less computation friendly.

Using decision rules derived from the background standard deviation only, including rule

$$L_c = k_\alpha \sqrt{2N_b}$$

and its versions adapted for unequal background / signal counting times is not recommended, contrary to the current practice of LA-ICPMS. At small background count numbers typical of LA-ICPMS measurements, using these rules results in elevated, poorly controlled rate of false detections.

REFERENCES

- Altshuler, B., & Pasternack, B. 1963: Statistical measures of the lower limit of detection of a radioactivity counter. *Health Phys.*, 9, 293-298.
- Przyborowski, J. & Wilenski, H., 1940: Homogeneity of results in testing samples from Poisson series, *Biometrika*, 31, 313-323.

- Nicholson, W.L., 1966: Statistics of net-counting-rate estimation with dominant background corrections, *Nucleonics*, 24, 118-121.
- Strom, D.J. & MacLellan, J.A. 2001: Evaluation of eight decision rules for low-level radioactivity counting, *Health Phys.*, 81, 27-34.
- MARLAP Multi-Agency Radiological Laboratory Analytical Protocol Manual, vol. 19-20, version from July 2004, <http://www.epa.gov/>.
- Huffman, M.D., 1984: An improved approximate two-sample Poisson test, *Appl. Stat.*, 33, 224-226.
- Gu, K., Ng, H.K.T., Tang, M.L. & Schucany, W.R., 2008: Testing the ratio of two Poisson rates, *Biom. J.*, 50, 283-298.
- Ulianov, A., Müntener O. & Schaltegger, U. 2015: The ICPMS signal as a doubly stochastic Poisson process, *J. Anal. At. Spectrom.*, 30, 1297-1321.
- Longerich, H.P., Jackson S.E. & Günther, D. 1996: Laser ablation inductively coupled plasma mass spectrometric transient signal data acquisition and analyte concentration calculation, *J. Anal. At. Spectrom.*, 11, 899-904.
- Currie, L.A. 1995: Nomenclature in evaluation of analytical methods including detection and quantification capabilities (IUPAC recommendations 1995), *Pure Appl. Chem.*, 67, 1699-1723.

P 2.20

High accuracy analysis of the whole range of Ca natural isotopes by TIMS

Maria O. Naumenko-Dèzes¹, Claudia Bouman², Thomas F. Nägler¹, Klaus Mezger¹, Igor M. Villa^{1,3}

¹ *Institute für Geologie, Universität Bern, Baltzerstrasse 1+3, 3012 Bern, Switzerland*

² *Thermo Fisher Scientific, Hanna-Kunath-Strasse. 11, 28199 Bremen, Germany*

³ *Università di Milano Bicocca, Piazza della Scienza 4, 20126 Milano, Italy*

Calcium is the fifth most abundant element in the terrestrial planets. The abundance of Ca isotopes and their variations are important to quantify processes in astrophysics, biology and geology. Such a wide spread of possible applications requires a uniform base to make different studies comparable. In geological applications a substantial obstacle to data intercomparison is the usage of (a) different reference materials; (b) different Ca isotope ratios published by different authors; and (c) different mass-dependent fractionation correction laws. Our study compares two most widely used Ca reference materials SRM915a and b; provides an internal consistency check for the published Ca isotopic compositions (Russell et al., 1978; Jörg et al., 2012; Shen et al., 2002); and suggests an internally consistent instrumental fractionation correction.

For the present study the Ca isotope compositions of SRM 915a and SRM 915b were determined by measuring the whole range of Ca isotopes from mass 40 to 48 simultaneously in static mode using a multicollector configuration adapted specifically for this purpose on a Thermo Scientific Triton *Plus*TM thermal-ionization mass-spectrometer (TIMS). It is equipped with a specially developed extra large Faraday cup (L5) for the analysis of ⁴⁰Ca and a special Faraday cup (H4) with extended mass range for ⁴⁸Ca, allowing simultaneous measurement of masses 40 to 48 amu. The uncertainty is limited by choosing sample sizes <1 µg. With this setup the measurement uncertainties were 0.06 ‰ for ⁴⁰Ca/⁴⁴Ca.

This unique equipment allowed us to carry out an internal consistency check for published Ca isotopic compositions. It was performed using the ⁴⁰Ca/⁴⁴Ca ratio for SRM 915a corrected with the exponential law using fixed ratios (⁴²Ca/⁴⁴Ca, ⁴³Ca/⁴⁴Ca and ⁴⁸Ca/⁴⁴Ca) published by the respective authors. The results (fig. 1) show that the calculated ⁴⁰Ca/⁴⁴Ca ratios are identical amongst each other for the isotope composition of Russell et al (1978); they are consistent for the values from Jörg et al. (2012) at the 3 σ level and inconsistent amongst each other for the isotopic composition of Shen et al. (2009). This result supports usage of Ca ratios of Russell et al (1978) as a reference isotopic composition.

Application of different ratios for instrumental fractionation correction revealed the problem of incomplete fractionation correction with the exponential law, which becomes a problem when ratios with large mass difference are used for fractionation correction (e.g. ⁴⁸Ca/⁴⁴Ca to correct ⁴⁰Ca/⁴⁴Ca). For Nd isotopes Caro et al. (2003) suggested an additional correction term to the commonly used exponential correction law. The adaptation of this equation for Ca isotopes strongly reduces artifacts due to an incomplete fractionation correction.

With this improved exponential correction to the internally consistent ratios of Russell et al (1978), ⁴⁰Ca/⁴⁴Ca is 47.1649 ± 0.0047 of SRM 915a and 47.1613 ± 0.0028 for SRM 915b.

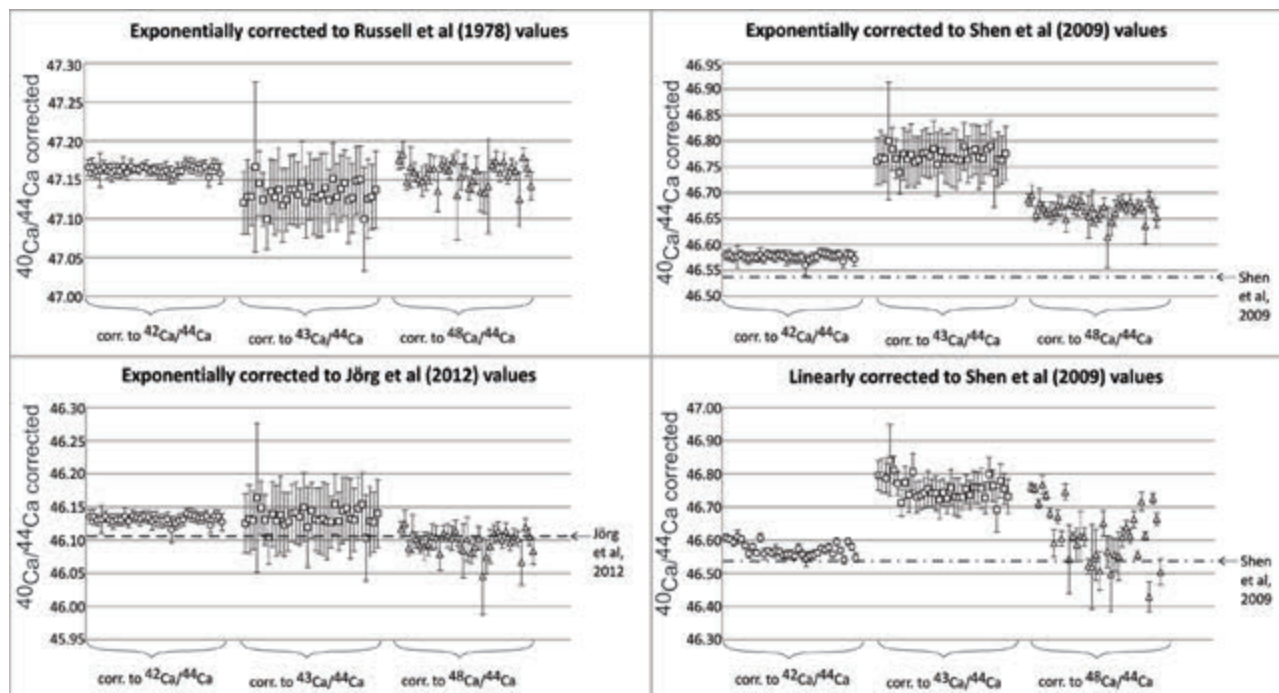


Figure 1. Comparison of the normalization protocols for 25 high intensity measurements of SRM 915a. The $^{40}\text{Ca}/^{44}\text{Ca}$ ratio was corrected with the exponential law applying three correction ratios $^{42}\text{Ca}/^{44}\text{Ca}$ (circles), $^{43}\text{Ca}/^{44}\text{Ca}$ (squares) and $^{48}\text{Ca}/^{44}\text{Ca}$ (triangles).

REFERENCES

- Caro G., Bourdon B., Birck J.-L., Moorbath S., 2003. ^{146}Sm - ^{142}Nd evidence from Isua metamorphosed sediments for early differentiation of the Earth's mantle, *Nature* 423, 428–432.
- Jörg, G., Amelin, Y., Kossert, K., Lierse v. Gostomski, C., 2012. Precise and direct determination of the half-life of ^{41}Ca . *Geochimica et Cosmochimica Acta* 88, 51–65.
- Russell W.A., Papanastassiou D.A., Tombrello T.A., 1978. Ca isotope fractionation on the earth and other solar system materials, *Geochim. Cosmochim. Acta* 42, 1075–1090.
- Shen J.J.-S., Lee D.-C., Liang W.-T., 2009. Absolute Ca isotopic measurements using an improved double spike technique, *Terr. Atmos. Ocean. Sci.* 20, 455–464.

P 2.21

Compositional variations of peritectic garnet in peraluminous leucogranite sills from Elba Island (Italy): Implications for crustal melt generation processes

Núria Bach¹, Kalin Kouzmanov¹, Luca Caricchi¹, Andrea Dini², Markus Wälle³

¹ Department of Earth Sciences, Section of Earth and Environmental Sciences, University of Geneva, Rue de Maraichers 13, CH-1205 Geneva, Switzerland (nbacholler@gmail.com)

² CNR, Istituto di Geoscienze e Georisorse, Pisa, Italy

³ Institute of Geochemistry and Petrology, ETH Zürich, CH-8092 Zürich, Switzerland

Recent geochemical and isotopic studies of late Miocene peraluminous granites from Elba Island (Italy), point out the prominent role of entrainment of peritectic phases during the formation of crustal melts in post-collisional orogenic settings (Farina *et al.*, 2012; 2014). In spite of the convincing evidence for entrainment, peritectic minerals have never been observed being easily dissolved and assimilated by the melts during the decompressional transfer from source to emplacement level (Clemens *et al.*, 2011 and references therein).

In this contribution we describe the first finding of peritectic garnet in peraluminous leucogranites associated with the Monte Capanne plutonic complex (7.4-6.9 Ma; Elba Island, Italy). The presence of garnets in these rocks indicates that they are produced by partial melting of metasediments at depth and not by fractionation of the monzogranitic pluton itself (Dini *et al.*, 2002).

The peraluminous garnet-bearing leucogranites associated with Monte Capanne are composed mainly by quartz, K-feldspar, plagioclase and garnet. These rocks are extremely acidic, with silica content reaching 75% and aluminium content of 15% approximately. The garnets present in this leucogranite are rounded, homogeneous in size (of about 200-300 µm), and are characterised by cores that are rich in inclusions. The inclusions are mainly of quartz, but K-feldspar, plagioclase, biotite and rarer titanite and ilmenite are also present. The garnets are typically almandine-rich (66-75%) with a spessartine component that ranges from 20 to 29 %. The other garnet end-members concentrations are low (below 2%). The content of almandine-spessartine along the crystals shows a patchy zonation, although in some grains there is a weak core-to-rim zonation with rich almandine rims and rich spessartine cores.

The P-T conditions were calculated using data from LA-ICP-MS analyses. The content of heavy REEs in the rims is higher than in the cores. The pressure was determined using the method proposed by Bea *et al.* (1997) using the equation: $P = 3.6 + 5.6 \cdot \text{Gd/Dy}$. Three different values were obtained from each garnet grain, two values from the rim and one from the core. The values range from 4.5 to 6.5 kbar, with a mean value of 5.6 kbar (for the cores). Zircon saturation thermometry gives temperature estimates of about 780°C (Watson and Harrison, 1983).

P-T conditions estimates from trace element distribution in the analysed garnets (ca. 4.5-6.5 kbar and 780°C) suggest that partial melting, dominated by muscovite breakdown, occurred in the lowermost portion of the Tuscan continental crust. The calculated P-T conditions are in agreement with a peritectic origin for the garnets. The garnet crystallization took place probably in a zone not far from the base of the Tuscan continental crust (~23km) due to muscovite dehydration (Fig. 1).

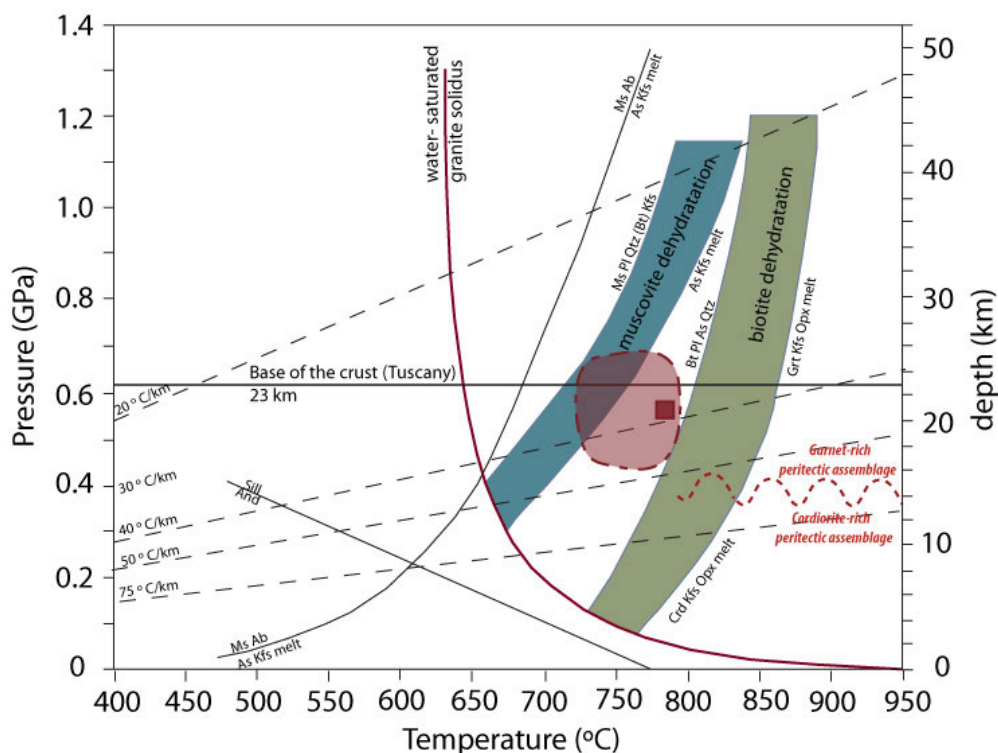


Figure 1. P-T diagram showing conditions for muscovite and biotite dehydration as well as crystallization conditions of the garnet-bearing leucogranite (in red). Modified from Dini *et al.* (2005).

REFERENCES

- Bea, F., Montero, P., Garuti, G., Zacharini, F., 1997. Pressure-Dependence of Rare Earth Element Distribution in Amphibolite- and Granulite- Grade Garnets. A LA-ICP-MS Study. *Geostandards and geoanalytical research* 21(2), 253-270.
- Clemens, J.D., Stevens, G., Farina, F., 2011. The enigmatic sources of I-type granites: the peritectic connexion. *Lithos* 126, 174–181.
- Dini, A., Innocenti, F., Rocchi, S., Tonarini, S., Westerman, D.S., 2002. The magmatic evolution of the late Miocene laccolith-pluton-dyke granitic complex of Elba Island, Italy. *Geol. Mag.* 139, 257–279.
- Dini, A., Gianelli, G., Puxeddu, M., Ruggieri, G., 2005. Origin and evolution of Pliocene-Plesitocene granites from the L'Arderello geothermal field (Tuscan Magmatic Province, Italy). *Lithos* 81, 1-31.
- Farina, F., Stevens, G., Dini, A., Rocchi, S., 2012. Peritectic phase entrainment and magma mixing in the late Miocene Elba Island laccolith-pluton-dyke complex (Italy). *Lithos* 153, 243–260.
- Farina, F., Dini, A., Rocchi, S., Stevens, G., 2014. Extreme mineral-scale Sr isotope heterogeneity in granites by disequilibrium melting of the crust. *Earth and Planetary Sciences Letters* 399, 103-115.
- Watson, E.B., Harrison, T.M., 1983. Zircon saturation revisited' temperature and composition effects in a variety of crustal magma types. *Earth and Planetary Science Letter* 64, 295-304.

P 2.22

The Silicon isotope composition of zircons: a tracer for magma evolution ?

François-Xavier d'Abzac¹, Joshua Davies¹ & Urs Schaltegger¹

¹ *Département des Sciences de la Terre, University of Geneva, Rue de Maraichers 13, CH-1205 Genève*

The Si isotopic composition of igneous rocks varies over ~0.4‰ in $\delta^{30}\text{Si}$ units (Savage et al. 2013) in the Earth's crust. Furthermore, the $\delta^{30}\text{Si}$ value increases with the degree of magmatic differentiation (Savage et al. 2011).

Recently, Zambardi et al. (2014) have confirmed this result by measuring Si isotopes in a single well defined magmatic series (Cedar Butte, ID, USA) for which they also showed a dependence of the $\delta^{30}\text{Si}$ on temperature. The same study argues that crystal fractionation appears not to be involved in Si isotopic fractionation at the scale of the whole rock. On the other hand, Trail & Savage (2015) demonstrate a resolvable isotopic fractionation between mantle-derived and continental zircon crystals. Moreover, the same study shows experimental resolvable equilibrium isotopic fractionation between quartz and zircon.

Our study is motivated by: (i) the potential of Si isotopes as markers of magma evolution in the mantle and in the continental crust, (ii) the knowledge of zircon mineral geochemistry and behaviour throughout magma evolution and (iii) the occurrence of mineral specific Si isotope fractionation to investigate its potential in zircons as a tracer of the evolution of the Earth's interior.

We are studying a comprehensive set of natural reference zircons of various ages and from various host rocks: Mudtank (Carbonatite, 570 Ma), Temora-2 (Gabbroic diorite, 416.8 Ma), Plešovice (Granulite, 337.2 Ma), R33 (Monzodiorite, 419.2 Ma), GJ-1 (Pegmatite, 600.6 Ma), Acasta (Tonalite Gneiss, 4.01 Ga), North Mountain Basalt (201.4 Ma), Fish Canyon Tuff (28.2 Ma).

Measurements have been conducted at the University of Geneva on a Thermo Scientific "Neptune Plus" MC-ICP-MS following the conventional sample preparation/isotope analysis method described in Zambardi & Poitrasson (2011).

Preliminary results on standards reference materials show an external reproducibility of the $\delta^{30}\text{Si} = 0.11\text{‰}$ (2SD), equivalent to the state of the art ~0.07 ‰ (2SE) reported by Zambardi & Poitrasson (2011). Reference natural whole rock samples BHVO-1 (Basalt, Hawaii, USA), AGV1 (Andesite, Oregon, USA), DRN (Diorite, France), GA (Granite, France), JA-2 (Andesite, Japan) and JP-1 (Peridotite, Japan) have been measured and reproduce the $\delta^{30}\text{Si}$ reference values within error.

REFERENCES

- Savage, P. S., R. B. Georg, H. M. Williams, K. W. Burton & A. N. Halliday. 2011: Silicon isotope fractionation during magmatic differentiation. *Geochimica et Cosmochimica Acta*, 75, 6124-6139.
- Savage, P. S., R. B. Georg, H. M. Williams & A. N. Halliday. 2013: The silicon isotope composition of the upper continental crust. *Geochimica et Cosmochimica Acta* 109, 384-399.
- Trail, D. & Savage P. S. 2015: Si isotopes in zircon from experiments, granites, and mantle-derived samples. *Goldschmidt Abstracts 2015*.
- Zambardi, T., C. C. Lundstrom, X. Li & M. McCurry, 2014: Fe and Si isotope variations at Cedar Butte volcano; insight into magmatic differentiation. *Earth and Planetary Science Letters* 405, 169-179.
- Zambardi, T. & F. Poitrasson, 2011: Precise Determination of Silicon Isotopes in Silicate Rock Reference Materials by MC-ICP-MS. *Geostandards and Geoanalytical Research* 35, 89-99.

P 2.23**Zircon U-Pb Age Distributions in Cogenetic Crystal-Rich Dacitic and Crystal-Poor Rhyolitic Members of Zoned Ignimbrites in the Southern Rocky Mountains by Chemical Abrasion Inductively-Coupled-Plasma Mass Spectrometry (CA-LA-ICP-MS)**

Jakub Sliwinski¹, Matt Zimmerer², Marcel Guillong¹, Olivier Bachmann¹, Peter Lipman³

¹ *Institute of Geochemistry and Petrology, ETH Zürich, Clausiusstrasse 25, 8092 Zürich, Switzerland*

² *New Mexico Bureau of Geology & Mineral Resources, 801 Leroy Place, Socorro NM 87801-4796*

³ *United States Geological Survey, Volcanic Hazards Program, Menlo Park, CA*

The San Juan locus of the Southern Rocky Mountain Volcanic Field (SRMVF) in SW Colorado represents an erosional remnant of a mid-Tertiary (~37-23 Ma) ignimbrite flare up that produced some of the most voluminous ignimbrites on Earth. A key feature of many SRMVF ignimbrites is compositional zonation, with many volcanic units comprising both dacitic and rhyolitic horizons. Geochemical, field and petrographic evidence suggests that dacites and rhyolites are cogenetic. Here, we report U-Pb zircon ages by chemical abrasion inductively-coupled-plasma mass spectrometry (CA-LA-ICPMS) for rhyolitic and dacitic components in four units: the Bonanza, Rat Creek, Carpenter Ridge and Nelson Mountain Tuffs. All units show zircon age spectra that are either within analytical uncertainty of Ar/Ar ages or are appreciably older, indicating prolonged magma residence times (~500 ka) prior to eruption. Anomalously young Pb-loss zones in zircon have been largely removed by chemical abrasion. Older, inherited zircons and zircon cores (60-2000 Ma) are rare in all samples, suggesting limited assimilation of upper crustal Precambrian country rock or complete resorption during recharge events and magma chamber growth.

P 2.24**The Lower Permian Alpigia magmatic complex and its country rock (Upper Maggia Valley, Central Alps): petrology, geochronology and structural position**

Caroline Hirsiger, François Bussy, Jean-Luc Epard, Henri Masson, Albrecht Steck & Alexey Ulianov

Institut des Sciences de la Terre (ISTE), Université de Lausanne, Géopolis, CH-1015 Lausanne (jean-luc.epard@unil.ch)

The Alpe d'Alpigia is located in the Upper Maggia valley (Ticino) west of the village of Fusio in the Lepontine dome of the Central Alps. It consists of a metamorphosed mafic to intermediate magmatic complex subdivided into a meso- to leucocratic "Alpigia Gneiss" and a darker gabbroic facies on the 1:25'000 geological map of Keller et al. (1980). This complex is intruding a series of banded amphibolites, as well as ortho- and paragneisses. The structural position of the Alpe d'Alpigia is disputed for many years (review in Steck et al. 2013), as it is located at the convergence point of four structural units: the Maggia, Sambuco, Simano and Antigorio nappes. No decisive field observation has been put forward so far to solve this dilemma. A potential approach is to date the Alpigia magmatic complex and to compare its age with that of magmatic events in the surrounding tectonic units. Although not decisive, this criterion added to existing stratigraphic and structural data could help solving the problem.

The Alpigia complex is a calc-alkaline magmatic series displaying a differentiation trend from cumulitic hornblendites to gabbros, gabbro-diorites, quartz-diorites, tonalites and leucogranites. Despite a relatively strong deformation, mingling features between mafic and intermediate to felsic facies are still visible, pointing to their (sub)contemporaneous emplacement. Zircons have been extracted and dated in situ with the U-Pb LA-ICPMS technique on the basis of cathodoluminescence imaging. A gabbro sample yielded a mean $^{206}\text{Pb}/^{238}\text{U}$ age of 292.8 ± 2.0 Ma (95% confidence level, based on 23 measurements), whereas a tonalite yielded an age of 293.9 ± 1.2 Ma (35 measurements) and a leucogranite an age of 288.7 ± 3.4 Ma (15 measurements). These three dates are almost overlapping within uncertainties and point to a magmatic event at ca. 292 Ma.

The mafic layers of the banded amphibolites intruded by the Alpigia magmatic complex display basaltic compositions with tholeiitic geochemical characteristics. The associated felsic layers consist of a quartz + plagioclase \pm amphibole \pm carbonates mineral assemblage. They are chemically very heterogeneous, ranging from 50 to 76 wt-% SiO_2 , and display unusual concave-shaped REE chondrite-normalized patterns with low to very low MREE values, but positive Eu anomalies. Further investigations are needed to decipher the origin of these felsic layers and to establish if they are contemporaneous with the basaltic horizons or not. Zircons were extracted from two different felsic samples. Cathodoluminescence imaging revealed complex internal structures with a homogeneous whitish external envelope suggesting metamorphic recrystallization. As a matter of fact, measured dates spread over a large range from ca. 480 down to 160 Ma. Both samples yielded a consistent subset of data allowing calculation of mean $^{206}\text{Pb}/^{238}\text{U}$ ages. The first sample yielded an age of 476.3 ± 5.2 Ma and the second sample an age of 464.5 ± 4.1 Ma. Although no field evidence has been found to establish the contemporaneity of the felsic and tholeiitic mafic layers, the latter are most probably no younger than Ordovician.

An augengneiss from the host rock of the Alpigia magmatic complex has also been dated. Gem-quality zircons yielded a mean $^{206}\text{Pb}/^{238}\text{U}$ age of 451.8 ± 2.8 Ma based on a coherent set of 19 measurements. Three inherited zircon cores gave ages of 553.8 ± 9.4 , 507.8 ± 7.6 and 492.4 ± 8.5 , respectively. This ca. 450 Ma magmatic age is typical of the so-called "older orthogneisses" found in most Alpine basement units.

The ca. 292 Ma age of the Alpigia calc-alkaline magmatism is very similar to that of the neighbouring Antigorio pluton, where Bergomi et al. (2007) dated a tonalite at 296 ± 2 Ma, granodiorites at 294 ± 5 and 290 ± 3 Ma, and a granite at 289 ± 4 Ma. Conversely, Bussien et al. (2011) obtained mean $^{206}\text{Pb}/^{238}\text{U}$ ages of 300 ± 5 Ma and 302 ± 8 Ma for the Matorello granodiorite in the Sambuco unit and 308 ± 7 Ma for the Cocco granodiorite in the Maggia unit. Thus, if the spatial distribution of late Variscan magmatic ages is used as a paleogeographic criterion, the Alpigia magmatic complex and its host rock should be linked to the Antigorio nappe rather than to the Sambuco-Maggia units, in line with the tectonic interpretations of Keller et al. (1980) and Steck et al. (2013).

REFERENCES

- Bergomi, M. A., Tunesi, A., Shi, Y.-R., Colombi, A. & Liu D.-Y. 2007: SHRIMP II U/Pb geochronological constraints of pre-Alpine magmatism in the Lower Penninic Units of the Ossola Valley (Western Alps, Italy), Geophysical Research Abstracts, 9, 07780, European Geosciences Union.
- Bussien, D., Bussy, F., Magna, T. & Masson, H. 2011: Timing of Paleozoic magmatism in the Maggia and Sambuco nappes and paleogeographic implications (central Lepontine Alps). Swiss Journal of Geosciences, 104, 129.

- Keller, F., Wenk, E., Bianconi, F. & Hasler, P. 1980: Blatt 1272 P. Campo Tencia. In Geologischer Atlas der Schweiz 1: 25,000, Atlasblatt, 73.
- Steck, A., Della Torre, F., Keller, F., Pfeifer, H. R., Hunziker, J. & Masson, H. 2013: Tectonics of the Lepontine Alps: ductile thrusting and folding in the deepest tectonic levels of the Central Alps. *Swiss Journal of Geosciences*, 206, 427–450.

P 2.25

Fluid investigation on T-max and retrograde inclusions in quartz from the Southern part of the Gotthard base tunnel, Central Alps

Proce Medea¹, Mullis Josef¹, Franz Leander¹ and Antognini Marco²

¹ *Institute of Mineralogy and Petrography, University of Basel, Bernoullistrasse 30, CH-4056 Basel
(medea.proce@gmail.com)*

² *Museo Cantonale di Storia Naturale, Viale Cattaneo 4, 6901 Lugano.*

The present study is focused on fluid inclusions in quartz, formed during maximum and decreasing temperature conditions.

The main topics investigated are:

1. the evolution of fluid composition from T-max to retrograde conditions
2. the evolution of fluid composition and pressure at 400 °C from Bodio to the North of the Piora valley
3. the evolution of fluids within metasedimentary rocks of the Piora valley and its migration toward the adjacent crystalline units
4. the difference between surface and NEAT base tunnel fluids.

Specific samples of Tessin habit quartz (THQ) from Alpine fissures and from quartz segregates (QS) of the Gotthard base tunnel (sampled by the museo cantonale di storia naturale of Lugano) were analysed. They originate from gneisses of the Southern Gotthard massif as well as from various gneisses of the Penninic Lucomagno and Leventina nappes (Bonanomi et al. 1992). THQ from Alpine fissures and QS were also collected in different lithologies at the surface of the Piora valley. Fluid inclusions were investigated by microthermometry and some of them also by Raman-Spectroscopy.

Fluid inclusions in QS are stretched or decrepitated, due to prograde heating, and are therefore not used for interpretation. In any case they contain the highest amount of CO₂. Tessin habit quartz (THQ), formed close to the T-max conditions contain CO₂-enriched fluids in \pm idiomorphic inclusions. Late retrograde H₂O-enriched fluid inclusions are common in both, QS and THQ.

Results:

1. The evolution from the earliest (T-max) to younger (retrograde) fluid inclusion populations in THQ displays a characteristic decrease in CO₂ content, from ≥ 73 to ≤ 5 % CO₂ at pressures from ~ 3 to ≤ 2 kbar.
2. CO₂ within T-max and retrograde fluid inclusion populations is often contaminated by other volatiles like N₂, CH₄, H₂S and CO.
3. T-max fluids in the base tunnel show an increase in CO₂ as well as an increase in fluid pressure from South (Leventina nappe) to North (Southern Gotthard massif).
4. A decrease in CO₂ content from the Piora valley toward the Lucomagno nappe in the South and the Gotthard massif in the North is noticed.
5. One sample collected in the dolomite from Pizzo Colombe contains 4.9 mole % NaCl equivalents, a very saline aqueous fluid with a significant content of H₂S (2.0 mole %), whereas the CO₂ content is relatively low (12.1 mole %).
6. The difference in fluid pressure between the samples from the base tunnel and the Piora valley situated some 1900 m above is 0.4-0.5 kbar. In addition Piora samples display elevated quantities of additional volatiles dissolved in CO₂.

Discussion and conclusions:

1. The sources of CO₂ are metasedimentary rocks of the Piora valley and metasediments situated below the Leventina nappe. This is supported by fluid inclusions from the vicinity, containing high CO₂ contents. CO₂ was predominantly produced by decarbonation of metasedimentary rocks and oxidation of graphitic material (Mullis et al., 1994).
2. Fluid pressure increase from South to North in the base tunnel suggests that temperatures were higher and rocks much drier in the South than in the North. Thus the amount of expected metasediments below the Leventina and Lucomagno nappe must be smaller in the South than in the North.
3. The difference of 0.4-0.5 kbar in fluid pressure between the earliest fluid inclusion populations in the Gotthard base tunnel and the Piora valley refers to an overburden of 1.6 to 1.9 km in the Piora valley. This indicates that rocks were more or less saturated with fluids during inclusion formation in the Northern part of the Ticino area.
4. The decrease of CO₂ during retrograde conditions within a given locality is probably controlled by infiltration of meteoric water and carbonate precipitation, which remains to be proved by stable isotope investigations.
5. Fluid migration from the Piora valley toward the Lucomagno nappe in the South and the crystalline Gotthard massif

in the North is controlled by the dominance of metasedimentary rocks present in the Piora valley.

6. High saline fluid with a remarkable content of H_2S and a relatively low CO_2 content from Pizzo Colombe originates from the Piora dolomite host rock and is explained by the salting-out effect.
7. CO_2 contaminated by other volatiles like CH_4 , N_2 , H_2S , CO in the base tunnel is interpreted to originate from evaporates situated below the Lucomagno and Leventina nappes (Hiss 1975).
8. As volatile contaminated CO_2 occurs at T-max as well as in retrograde inclusion populations, sulfate reduction must have occurred at T-max conditions or even during prograde conditions.

REFERENCES

- Bonanomi, Y., Dietler, T. & Etter, U. 1992: Querschnitt zwischen dem südlichsten Aar-Massiv und der Lucomagno-Decke im Bereich des Gotthard-Basistunnel, *Eclogae Geologica Helvetica* 85/1, 257-266.
- Hiss, B. 1975: Metamorpher Anhydrit im Leventina Gneiss. *Schweizerische mineralogische und petrographische Mitteilungen* 55, 217-225.
- Mullis, J., Dubessy, J., Poty, B. & O'Neil, J. 1994: Fluid regimes during late stages of a continental collision: Physical, chemical, and stable isotope measurements of fluid inclusions in fissure quartz from a geotransverse through the Central Alps, Switzerland, *Geochimica et Cosmochimica Acta* 58, 2239-2267.

P 2.26

Retrograde fluid-geochemical evolution and mass transfer: an example from the Gotthard Base Tunnel.

Mathias Wolf¹, Josef Mullis¹, Thomas Pettke², Leander Franz¹ & Torsten Vennemann³

¹ Mineralogisch-Petrographisches Institut, University of Basel, Bernoullistrasse 30, CH-4056 Basel
(mathias.wolf@stud.unibas.ch)

² Institute of Geological Sciences, University of Bern, Baltzerstrasse 1+3, CH-3012 Bern

³ Institute of Earth Sciences, University of Lausanne, Geopolis building, CH-1015 Lausanne

In this study, the influence and evolution of the fluid phase on mass transfer and mineral precipitation within the Alpine fissure W42 in the Gotthard Base Tunnel has been investigated. The occurrence of remarkable amounts of relatively late precipitated anhydrite in this fissure is a feature that has been reported only once for an Alpine fissure (Preiswerk 1913). The lack of sulphur within the host rock (Central Aare Granite) raises the question about the origin of the sulphur and thus the source of the fluid. To answer that question, microthermometric and LA-ICP-MS measurements were done on aqueous fluid inclusions as well as measurements of the isotopic composition of the sulphur bearing phases.

$\delta^{34}\text{S}$ -values between +20 ‰ and +25 ‰ for anhydrite, baryte and pyrite suggest a volcanic and/or sedimentary (i.e. evaporitic) origin for the sulphur (Thode 1970). Because of the lack of larger amounts of sulphur within the surrounding rocks, a mass transfer over a remarkable distance is indicated for the time of sulphate and sulphide precipitation. The fluid inclusions that formed during that stage of fissure evolution document an intense tectonic activity and show a first increase in bulk salinity up to ~9.5 wt.% NaCl-equivalent (Fig. 1, populations 4a & 4b). The elemental concentration data achieved by LA-ICP-MS are in agreement with this evolution and show an increased solubility of K-feldspar and plagioclase during that time, along with elevated concentrations of B, As, Ba, and Rb. Together, these elemental characteristics are consistent with a shale-type sedimentary source. The latest analysed fluid inclusions show a second increase in bulk salinity (Fig. 1, population 8), mainly due to an increase in calcium content. This late increase in salinity is thought to be due to the retrograde fluid flow that is closely related to zeolite precipitation towards the end of fissure evolution.

The Alpine fissure W42 is part of a hydrological system within the Aar massif that was controlled by tectonic activity. Increased sulphate and calcium concentrations in recent waters (Seelig & Bucher 2010) are thought to be a result of interaction of meteoric water with minerals within the rocks and fissures. The precipitation of these minerals, particularly anhydrite, is the result of a medium to large scale mass transfer that was triggered by tectonic activity.

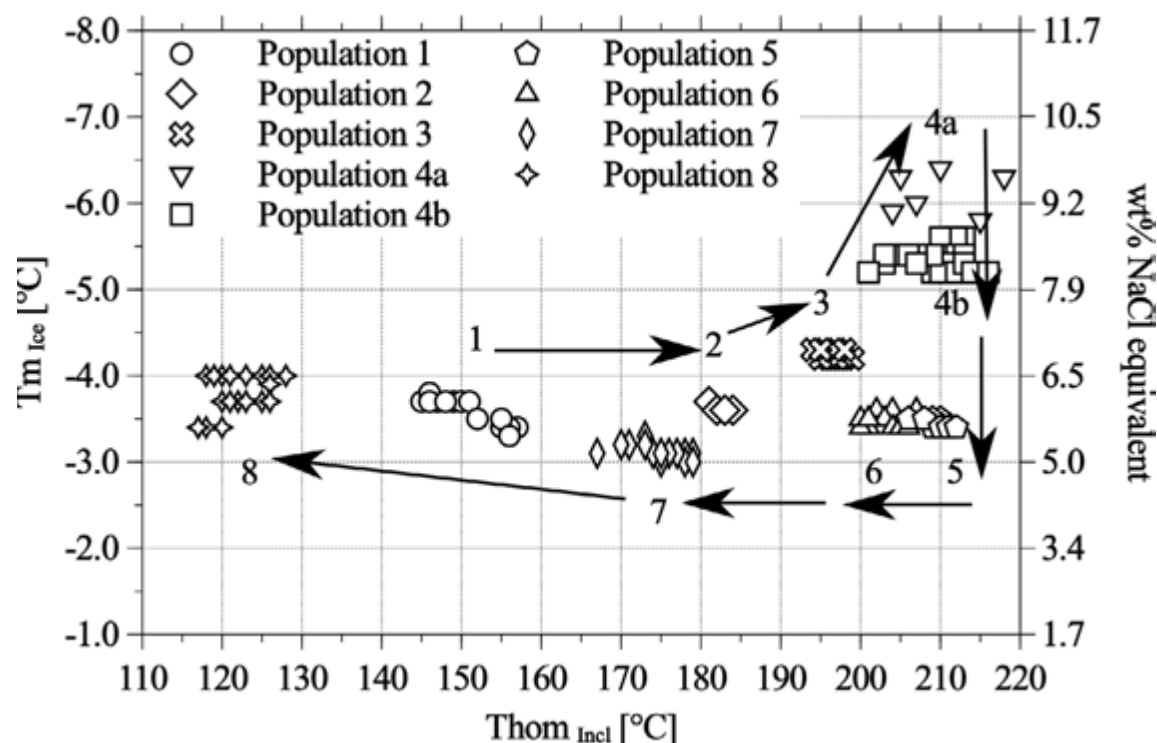


Figure 1. $Thom$ vs. T_{m_ice} for 8 fluid inclusion populations. All populations were found in quartz, except population 4a that was found in anhydrite.

REFERENCES

- Preiswerk, H. 1913: Die metamorphen Triasgesteine im Simplontunnel. In: Verhandlungen der Naturforschenden Gesellschaft in Basel. Vol. XXIV, 1-31.
- Seelig, U. & Bucher, K. 2010: Halogens in water from the crystalline basement of the Gotthard rail base tunnel (central Alps). *Geochimica et Cosmochimica Acta* 74, 2581-2595.
- Thode, H. G. 1970: Sulfur isotope geochemistry and fractionation between coexisting sulfide minerals. In: Geological Society of America Special Paper 3, 133-144.

P 2.27

The genesis of fluorite in the Koh-sefid region of Sarakhs, Iran

Leila Pazhakhzadeh¹, Khosro Ebrahimi nasrabadi², Farzin GHaemi² & Javad Darvishi khatooni³

¹ *Ferdowsi university of Mashhad (L_Pazhakhzadeh@yahoo.com)*

² *Geology department, Ferdowsi university of Mashhad*

³ *Geological survey of Iran*

Kuh Sefid Flourite mine is placed 110 km far from south east of mashhad and is close to kuh sefid village. The closest towns to the mentioned mine, are Sarakhs and torbat-jam that established in 110 km of north east and 65 km of south east with regard to the mine position, respectively. Geological and stony units include the region related to Sazand Kashafrud with the age of beneath til upward Jurasik and primarily contain the combination of sand, shell, marl, limestone and in some regions made up of konglomera. In the initial inspections of this mine, blocks of detrital stones of lime, marl and siliceous can be seen, so that the mineral substance has filled up the available spaces between detrital pieces and mineralization has occurred there.

Faults with protraction of north west-south east can be seen in mine in such a way that the most of fluorite mineralization which is accompanied with some minerals such as siliceous and calcite have been occurred in protraction of these fragments. In terms of construction geology, the mentioned stony units in the region have created alternative rounded and synclinal shapes in such a manner that the mine is placed in the middle of these synclinal shapes. Fluorite veins in this synclinal shape are difference in diameter of 2 up to 2.5 m and length of 50 m (Rajabzadeh, 2007).

Hydrothermal solutions with maximum temperature of 181°C and minimum temperature of 125°C and average temperature of 152°C in protraction of faults, cracks and fragments, have created mineral substance. Existence of some pieces of stones such as Basalt and porphyry stones like Tuff and also low-depth penetrative stones with Andesitic combination near Kuh Sefid mine in the distance of 5 km from south of mine and with regard to geological evidences, petrography, mineralization and homogenous temperature of fluids inclusion, it can be concluded the mine is a Fluorite mine which belongs to Epithermal family.

REFERENCES

Rajabzadeh, M. A. 2007: A fluid inclusion study of a large MVT barite-fluorite deposit: Koshmicheh, central Iran, Iranian Journal of Science & Technology 3.73-87.

P 2.28

Petrographic and microtectonic investigation of the metamorphic rocks of the Wehratal

Dörner Eva Lisa, Franz Leander & Kilian Rüdiger

Department Umweltwissenschaften, University of Basel, Bernoullistrasse 32, CH-4056 Basel (eva.doerner@unibas.ch)

The "Wiese-Wehratal-Diatexit"-Complex in southern Baden-Wuerttemberg, Germany is composed of migmatic para-/ orthogneisses and amphibolite lenses and is intruded by granitic bodies all of which are related to Variscan orogeny (e.g. Kalk et al., 2000).

The aim of this study is to investigate the link between peak metamorphic conditions of the Wiese-Wehratal-Complex and microstructures combining thermodynamic modeling by DOMINO-THERIAK (de Capitani & Petrakakis, 2010), winTWQ (Berman, 2007) and conventional geothermobarometry. A representative set of hand specimens has been analyzed by optical and electron microscopy as well as electron micro probe analysis.

The peak metamorphic assemblage of the leucocrate gneisses is garnet – sillimanite – biotite – plagioclase – orthoclase – quartz – ilmenite. Sillimanite is barely preserved, but muscovite pseudomorphs after sillimanite are recognized. Mafic gneisses are mainly composed of \pm amphibol – \pm biotite – plagioclase – orthoclase – quartz. Retrogression is indicated by flame perthite, perthite exsolutions, intense chloritization, sericitization, saussuritization and related to the Cenozoic hydrothermal overprint. Altered samples have been carefully omitted during analysis.

Garnet-biotite thermometry combined with GASP barometry yields PT conditions of 736-768 (± 30) °C and 0.75-0.76 (± 0.1) GPa. The winTWQ-Programm yields PT conditions of 790-810 °C and 0.57-0.71 GPa. The modeled equilibrium assemblage using the thermodynamic data of Holland & Powell (1998) lies within the range from 698-843 °C at 0.64-0.70 GPa. Amphibolites give PT conditions of 793-824 (± 50) °C and 0.68 (± 0.15) GPa using conventional geothermometer and geobarometer (Colombi, 1988; Bhadra & Bhattacharya, 2007).

In leucocrate gneisses the main foliation (319/47) is defined by a compositional layering consisting of garnet, biotite and sillimanite rich layers alternating with quartz and feldspar rich layers all of which represent the peak assemblage. Quartz shows lobate grain boundaries, left-over grains and window structures indicative of grain boundary migration recrystallization. At a small scale, lobes are rearranged into low index planes. Quartz shows chessboard subgrain patterns as well as melt pockets with concave boundaries containing kfs.

A particular prominent microstructure in qtz-plg-kfs layers is a highly regular lobate phase boundary, which represents 52% of all boundaries. Phase boundary migration occurred most commonly between kfs and qtz (61%), qtz and plg (29%), kfs and plg (10%). Lobes are between 8-300 μ m broad and migrate in both directions. Unlike kfs cores, kfs lobes do not show perthite exsolution lamellae.

It is suggested that the layering results from synkinematic melt segregation. The phase boundary migration found in those layers is interpreted to develop synkinematically. The formation and the implication of the peculiar phase boundary structure will be discussed.

REFERENCES

- Berman, R. G. (2007). winTWQ (version 2.3): a software package for performing internally-consistent thermobarometric calculations. (G. S. Canada, Ed.) Geological Survey of Canada, p. 41 Seiten.
- Bhadra, S., & Bhattacharya, A. (2007, April). The barometer tremolite + tschermakite + 2 albite = 2 pargasite + 8 quartz: Constraints from experimental data at unit silica activity, with application to garnet-free natural assemblages. *American Mineralogist*, 92(4), pp. 491-502.
- Colombi, A. (1988). Métamorphisme et géochimie des roches mafiques des Alpes ouest-centrales.
- de Capitani, C., & Petrakakis, K. (2010). The computation of equilibrium assemblage diagrams with Theriak/Domino software. *American Mineralogist*, 95: 1006-1016.
- Holland, T., & Powell, R. (1998). An internally consistent thermodynamic data set for phases of petrological interest. *J. metamorphic Geol.*, 16, pp. 309-343.

P 2.29

Investigations of gravels from the Klemmbach based on sedimentological and petrographic methods

Andrea Kuster¹, Leander Franz¹ & Andreas Wetzel²

¹ *Institut für Mineralogie und Petrographie, University of Basel, Bernoullistrasse 32, CH-4056 Basel (andrea.kuster@stud.unibas.ch)*

² *Geologisch-Paläontologisches Institut, University of Basel, Bernoullistrasse 32, CH-4056 Basel*

In the framework of an extensive study of the University of Basel, gravel lithologies of the Rhine River and its tributaries are examined. The investigations of the gravels are based on petrographic and sedimentological methods and should provide information on the transport processes and the origin of the various gravels.

The Klemmbach is one of the tributaries of the Rhine River. It is a small river in the surrounding area of the town of Badenweiler in the southern part of the Black Forest, Germany. The river has a total length of 20.1 km, runs from east to west and ends in the Rhine River.

The Black Forest formed during Prevariscan and Variscan orogenic processes (Geyer & Gwinner, 1991). There are four different units, which differ with respect to metamorphic processes and sedimentation. These are from the north to the south: Baden-Baden Zone, Central Black Forest Gneiss Complex, Badenweiler-Lenzkirch Zone, and Southern Black Forest Gneiss Complex (Echtler & Chauvet, 1991/1992). For this study, the Badenweiler-Lenzkirch Zone is very important, because the Klemmbach mainly flows through this zone.

Samples were taken at 7 different sites along the Klemmbach, which flows through numerous different geological units. Consequently, the gravels comprise a large variety of different rocks. Most pebbles are of igneous origin, whereas pebbles of metamorphic, sedimentary and hydrothermal origin are only present in small quantities. Petrographic studies reveal a dominance of volcanic pebbles, which originate from the Badenweiler-Lenzkirch Zone. These rocks have an Upper Devonian to Lower Carboniferous age. Furthermore, different types of granite pebbles were found at each sampling site at the Klemmbach. The medium-grained, undeformed and deformed granites were probably part of the Malsburg Granite from the Southern Black Forest Gneiss Complex. Granite pebbles with granophyric textures and fine-grained, hydrothermally overprinted granite pebbles probably originate from dykes. Coarse-grained granite pebbles might have been supplied from the Central Black Forest Gneiss Complex or from the Southern Black Forest Gneiss Complex. Pebbles of metamorphic origin comprise orthogneisses, amphibole gneisses and amphibolites. These rocks may be derived from the Central Black Forest Gneiss Complex, north of the thrust-fault boundary of the Badenweiler-Lenzkirch Zone. All sedimentary rocks were part of the Badenweiler-Lenzkirch Zone and mainly consist of different types of greywacke, which often contain volcanic components. At the westernmost sampling site in the town of Badenweiler, Hauptrogenstein Formation, Bajocian to Bathonian in age, were found. Even though sedimentary rocks crop out in this area while the Klemmbach traverses the Rhinegraben boundary fault blocks, they only occur in small numbers.

A compelling feature in all collected rocks is their distinct secondary hydrothermal alteration. Brockamp et al. (2014) showed that especially the Upper Visean greywackes and magmatic rocks from the Badenweiler-Lenzkirch Zone experienced a polyphase hydrothermal overprint, which is evident by strong sericitization and illitization of feldspars and chloritization of biotite. These features are particularly well developed in greywackes and volcanic rocks (Figs.1 and 2) and to a minor extent in plutonic and metamorphic rocks.

The sedimentological studies did not show the expected trend of a decreasing nominal diameter. The textural maturity, which has been determined by using sphericity and roundness, does not show an increase with distance from the source area. Possibly maturity values were affected by statistical artefacts, because a too low number of pebbles of sedimentary, metamorphic and hydrothermal rocks were sampled. Furthermore, large parts of the Black Forest were heavily influenced by the last glaciation 130'000-10'000 years ago. Very likely, glacial processes transferred subrounded or even rounded gravel to the Badenweiler-Lenzkirch Zone.

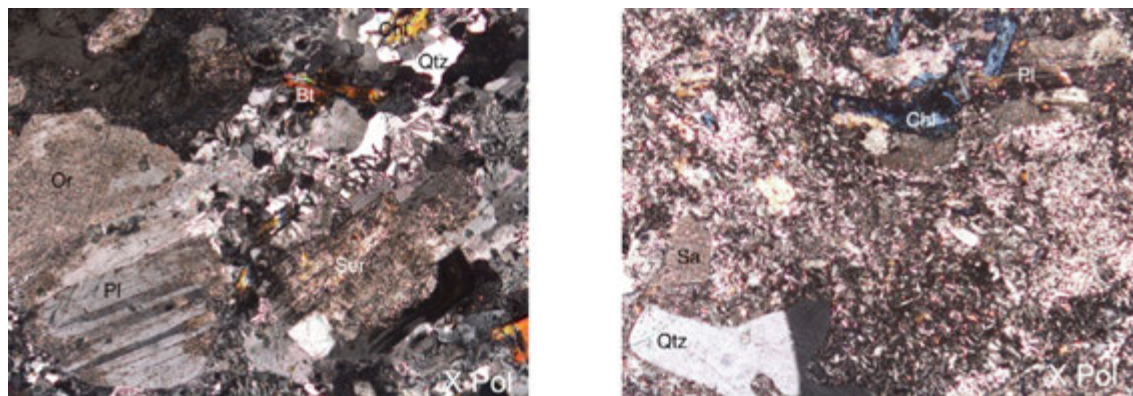


Figure 1 (left): Granophyric granite with sericitization and illitization of plagioclase (Pl) and orthoclase (Or); width of the photo 2.5 mm.

Figure 2 (right): dacite with illitization of sanidine (Sa) and chloritization of biotite (Chl); width of the photo 2.5 mm.

REFERENCES

- Brockamp, O., Schlegel, A. & Wemmer K. 2014: Complex hydrothermal alteration and illite K-Ar ages in Upper Visean molasse sediments and magmatic rocks of the Variscan Badenweiler-Lenzkirch suture zone, Black Forest, Germany, *Int J Earth Science*, 683-702
- Echtler, H. & Chauvet, A. 1991/1992: Carboniferous convergence and subsequent crustal extension in the southern Schwarzwald (SW Germany) - *Geodynamica acta* 5.
- Geyer, O. & Gwinner, M. 1991: *Geologie von Baden-Württemberg*. Stuttgart, E. Schweizerbart'sche Verlagshandlung, 19-22

P 2.30

The Ophicalcites of the Chenaillet Complex, (Western Alps, France): a fossil hydrothermal system?

Romain Lafay¹, Lukas P. Baumgartner¹, Stephane Schwartz², German Montes-Hernandez³ Torsten Vennemann¹

¹ *Institute of Earth Sciences, University of Lausanne, Géopolis, 1015 Lausanne, Switzerland (romain.lafay@unil.ch)*

² *Univ. Grenoble Alpes, ISTerre, F-38041 Grenoble, France*

³ *CNRS, ISTerre, F-38041 Grenoble, France*

A detailed isotopic, petrologic, and geochemical study of the Chenaillet ophicarbonates (western Alps) has been started to study the sequence of fluid-rock interactions responsible for these ophicarbonates. While there is little doubt that they represent parts of an oceanic core-complex like serpentinites and ophicarbonates (Lemoine et al., 1987; Manatschal et al., 2011), a detailed study, notably on their stable isotope compositions, is missing. Preliminary studies suggest an oceanic alteration of these ultramafic rocks within a hydrothermal system.

At the study location, ophicalcite bodies are mainly breccia composed of serpentinite clasts embedded in a fine, carbonaceous matrix. Three events of carbonation occurred. During the first generation, local carbonation of possibly olivine occurred inside the serpentine mesh. Associated with these replacements is a network of micrometric to centimetric calcite veins (pre- or syn- clast formation). The second event is marked by micritic carbonate (<300 µm) formation, filling the space between the clasts. No traces of fossil fragments have been found. Chrysotile and sulfide co-precipitate with the micritic calcite. Finally, a new generation of calcite veins crosscut the entire ophicalcite. Some minor dolomite formed along serpentinite-calcite interfaces.

The $\delta^{13}\text{C}$ (VPDB) values for all different carbonates have a range between -0.6 ‰ and 0.4 ‰, and $\delta^{18}\text{O}$ (VSMOW) values have a range between 12 ‰ and 14.5 ‰ in the clasts, the micrites average at 11.6 ± 0.5 ‰, and the third generation calcite veins have values between 12.5 and 15.5 ‰. The results suggest a relatively high temperature for carbonate precipitation, (i.e. at least 120 °C assuming a $\delta^{18}\text{O}$ value of seawater) which confirms previous studies of the micritic calcite (Lemoine et al., 1983). Differences in values might also reflect changes of seawater/rock interaction for the different carbonation stages. We also noted important differences in concentrations for minor elements (especially Sr, Fe, and Mn) between different carbonate generations.

These data support a model of a slow-spreading ocean floor. Past studies of hydrothermal activity on the ocean floor document important hydrothermal activity near extensional faults of oceanic core complexes. For Chenaillet, the (Früh-Green et al., 2003) ultramafic rocks were exhumed and massive carbonate deposits have been formed, related to white smokers. The Chenaillet ophicarbonates appear to have recorded oceanic serpentinitization at depth followed by multistep carbonatization during cooling along detachment faults. Extensional tectonic activity might be involved for the serpentinite breccia formation. Subsequently, calcite crystallization cemented the ultramafic debris in a hot hydrothermal context, possibly in a framework comparable to present-day Lost City or Rainbow hydrothermal fields.

REFERENCES

- Lemoine, M., Bourbon, M., de Graciansky, P.-C., Letolle, R., 1983. Isotopes du carbone et de l'oxygène de calcaires associés à des ophiolites (Alpes occidentales, Corse, Apennin): indices possibles d'un hydrothermalisme océanique téthysien. - *Rev Géogr Phys Géol Dyn* 24, 305–314.
- Lemoine, M., Tricart, P., Boillot, G., 1987. Ultramafic and gabbroic ocean floor of the Ligurian Tethys (Alps, Corsica, Apennines): In search of a genetic model. *Geology* 15, 622–625.
- Manatschal, G., Sauter, D., Karpoff, A.M., Masini, E., Mohn, G., Lagabrielle, Y., 2011. The Chenaillet Ophiolite in the French/Italian Alps: An ancient analogue for an oceanic core complex? *Lithos* 124, 169–184.

P 2.31

The Origin of Whiteschist in the Monte Rosa Nappe (Western Alps)

Cindy Luisier¹, Lukas Baumgartner¹, Benita Putlitz¹, Torsten Vennemann² & Stefan Schmalholz¹

¹ *Institut des Sciences de la Terre, Université de Lausanne (cindy.luisier@unil.ch)*

² *Institut des Dynamiques de la Surface Terrestre, Université de Lausanne*

The origin of whiteschist in the Monte Rosa Nappe, Western Alps, has been discussed since their discovery by Bearth (1952). They are commonly found in the metagranites of the internal crystalline massifs (Monte Rosa, Gran Paradiso and Dora Maira). Ferrando (2012) argued for a metasomatic alteration of crustal rocks by mantle fluids. We present new field, petrologic and geochemical data suggesting that a late magmatic hydrothermal fluid is responsible for the metasomatism, in agreement with the proposition of Pawlig et al. (2001) and Darbellay (2006).

The Monte Rosa whiteschists consists of talc-chloritoid-phengite and locally garnet – kyanite bearing assemblages exposed as 10-50 m bodies in the alpine metagranites. The well-exposed transition between the unaltered granites and the whiteschists allows for a detailed examination of the alteration halo. Structural observations show the morphology of the whiteschists bodies: they are not genetically linked to shear zones, and are crosscut by all schistosity generations. Granite quartz grains are incorporated into the external parts of the whiteschist, confirming a granite protolith, as well as a static formation of the alteration zones characteristic for late hydrothermal alteration of shallow granites after emplacement. The relative enrichment in magnesium and depletion in calcium and sodium of the whiteschist compared to the granites from which they derived indicate high fluid fluxes.

To determine the origin of the fluids, we measured the oxygen and hydrogen isotopic composition of the granites and whiteschist along a profile. Carbon and oxygen isotopic compositions of carbonate-bearing whiteschists and associated carbonate veins were determined as well. The oxygen isotopic composition of fluids in equilibrium with whiteschists corresponds to either fluids coming from serpentinite dehydration (Dessimoz, 2006) or late magmatic hydrothermal fluids. Hydrogen whole rock isotopic compositions fit near surface water compositions and carbon isotopic compositions are compatible with juvenile fluids. Model ages given by Sr isotopes in whiteschists are 100 to 190 Ma (Pawlig, 2001) and indicate a two-stage evolution.

Combined with whole rock compositions, the new data suggest that the whiteschist geochemical composition is related to a late magmatic hydrothermal fluid event in the Permian, whereas the mineralogy is the high-pressure metamorphic product of a previously established alteration assemblage of chlorite, sericite, and quartz.

REFERENCES

- Bearth, P. 1952: Beitr. Geol. Karte Schwiez NF 96, 94 p.
 Darbellay, B. 2006: Master thesis, University of Lausanne (Switzerland)
 Dessimoz, M. 2006: Master thesis, University of Lausanne (Switzerland)
 Ferrando, S. 2012: Terra Nova, 24, 423–436
 Pawlig, S. 2001: PhD thesis, University of Mainz (Germany)
 Pawlig, S. et al. 2001: SMPM 81,329-346

P 2.32

Clay minerals as geo-thermometer under low grade metamorphic conditions: a comparative study based on chemistry/crystallinity variations of illite and chlorite and Raman spectroscopy on carbonaceous material.

Annette Süssenberger¹ & Susanne Theodora Schmidt¹

¹ *Section des sciences de la Terre et de l'environnement, University of Geneva, Rue de Maraîchaire 13, CH-1205 Genève*

Clay minerals in metapelitic rocks are facies determining minerals. Their variation in composition and degree of ordering are used as potential indicator for diagenesis and burial up to sub-greenschist facies conditions. Determining the temperature of low grade metamorphic events using clay minerals is often not straightforward due to uncertainties of calibration methods used for different geo-thermometers as well as the coexistence of various generations of clay minerals in the same rock sample. This study aims to correlate and compare temperature estimations obtained from Kübler (KI) and Árkai (AI) indices, chlorite and illite chemistry as well as carbonaceous material.

The investigated study area is located east of the Patagonian Cordillera and is part of the Patagonian fold-and-thrust belt which forms the western part of the Magellanes retro-arc basin (Chile, 51°S). In this basin structure a >4000 m thick marine sequence of turbidites, sandstones and shales was deposited during the Late Cretaceous (Turonian-Campanian). A compressional deformation along the foreland basin margin resulted in an intense folding and thrust faulting of the Upper Cretaceous Punta Barrosa and the lowermost Cerro Toro Formation. Further east, the Upper Cerro Toro and overlying basin formations are lacking this metamorphic overprint. Folding and thrust faulting of the sedimentary sequence are supposed to have occurred before the Middle Miocene plutonic phase of the Torres del Paine intrusion.

Preliminary results of this study defined the onset of deformation around 60 Ma with later reactivation in the westernmost part (ca. 46 Ma, K/Ar on synkinematically formed illites). Illite dominates in the matrix, is aligned along cleavage planes and consists for the majority of the samples of the 1M polytype. Illite and chlorite crystallinity values are in good agreement and depict epizonal to diagenetic conditions with anchizonal conditions for most of the samples. Epizonal values are observed in spots of localized deformation and in contact to the Miocene Torres del Paine intrusive complex or the Jurassic (?) porphyry complex, respectively. Chlorite appears either as biotite replacement or as matrix filling mineral. The analysed chlorites display trioctahedral clinochlore, chamosite or pennantite compositions.

The formation of high temperature chlorites in the range of 330-360°C with Si/Al ratios of around 0.9 are observed in the metamorphic contact aureole as a result of thermal overprint during the magmatic emplacement. With increasing distance to the contact metamorphic aureole the Si/Al ratio is increasing whereas the XFe ratio is decreasing, indicating progressive smectite interlayering and confirming the regional anchizonal conditions observed with KI and AI and chlorite temperatures of about 220-240°C. Carbonaceous material generally occurs as diffuse matrix spots or as elongated streaks and is showing temperatures which are in good agreement with chlorite temperatures as well as KI and AI values.

P 3.33

Evolution of Earth's Archean crust: insights into Singhbhum craton, eastern India

Om Prakash Pandey¹, Klaus Mezger¹, Dewashish Upadhyay² & Igor M Villa¹

¹ *Institute of Geological Sciences, University of Bern, Baltzerstrasse 1+3, CH-3012 Bern* (om.pandey@geo.unibe.ch)

² *Department of Geology and Geophysics, Indian Institute of Technology, Kharagpur, India*

Records of the evolutionary history of the Earth are mainly preserved in the continental crust. But, the formation of the continental crust and its evolution with time is still highly debated among geoscientific community globally (e.g., Dhuime et al. 2015).

One of the principal problems in understanding Precambrian geological processes is that only a tiny fraction of the old (> 3.6 Ga) continental crust is preserved today. These include the purported 4.3 Gyr old Nuvvuagittuq greenstone belt (O'Neil et al. 2008) and the 4.0 Ga Acasta gneisses in the Canadian Shield, Archean terranes (3.8-3.6 Ga) in Greenland, ca. 4.4 Ga components in the Yilgarn craton and Hadean zircon from Jack Hills in the Australian shield (Wilde et al. 2001) and some occurrences in the South African and Brazilian Shields. A major pulse of continental crust formation seems to have been initiated at ca. 3.5 Ga and by the end of the Archean about 70% of the present day continental crust has formed in about 20% of Earth's history.

In this context, the Singhbhum craton in central peninsular India assumes significance as it formed right at the start of this major crust formation episode. The craton is one of the oldest cratonic nuclei and exposes a diverse geological association of Paleo-Archean to Meso-Archean mafic to felsic igneous and minor sedimentary rocks that are extremely well preserved and pristine and thus ideally suited for understanding Archean crust-mantle evolution. The Singhbhum craton is surrounded by the North Singhbhum Mobile belt (NSMB) to the North, the Eastern Ghats Belt to the southeast and the Bastar craton to the southwest (Saha 1994). The major crustal units of the craton are the supracrustal rocks of the Older Metamorphic Group (OMG), TTGs of the Older Metamorphic Tonalite Gneisses (OMTG), and Singhbhum Granite (SG) and Banded Iron Formations (BIF). The Paleo- to Meso-Archean crust of the Singhbhum craton evolved in polycyclic events within a narrow time interval between 3.46 and 3.32 Ga but preserve some relics of ca. 3.6 Ga old materials (Upadhyay et al. 2014).

Lead isotopes from leached K-feldspar grains from different felsic igneous rocks reveal a homogenous mantle source attesting to the pristine character of the rocks. The isotope characteristics are consistent with derivation of crustal material from a pristine and undepleted mantle source. These characteristics indicate that strong depletion of the mantle source prior to this major crust formation episode was minor and there existed only small regions of enriched continental crust prior to 3.5 Ga or it was well mixed back into the mantle during the Early Archean.

REFERENCES

- Dhuime, B., Wuestefeld, A., and Hawkesworth, C.J. 2015: Emergence of modern continental crust about 3 billion years ago, *Nature Geosciences*, 8, 552-555.
- O'Neil, J., Carlson, R.W., Francis, D., Stevenson, R.K. 2008: Neodymium-142 Evidence for Hadean Mafic Crust, *Science*, 321, 1828-1831.
- Saha, A.K., 1994: Crustal evolution of Singhbhum-North Orissa, eastern India, *Geological Society of India*, 27, 1-341.
- Upadhyay, D., Chattopadhyay, S., Kooijman, E., Mezger, K., Berndt, J. 2014: Magmatic and metamorphic history of Paleoarcheantonite-trondhjemite-granodiorite (TTG) suite from the Singhbhum craton, eastern India, *Precambrian Research*, 252, 180-190.
- Wilde, S.A., Valley, J.W., Peck, W.H., and Graham, C.M. 2001: Evidence from detrital zircons for the existence of continental crust and oceans on the Earth 4.4 Gyr ago, *Nature*, 409, 175-178.

P 2.34

Lithium behaviour and isotopic fractionation in high-pressure metabasites (Ile de Groix, France): a coupled LA-ICPMS, MC-ICPMS and SIMS study

Affé El Korh¹, Etienne Deloule¹, Béatrice Luais¹, Marie-Christine Boiron², Nathalie Vigier³, Luc Bastian³

¹ CRPG-CNRS, Université de Lorraine, UMR 7358, BP 20, F-54501 Vandoeuvre-lès-Nancy Cedex, France (elkorh@crpg.cnrs-nancy.fr)

² GeoRessources, Université de Lorraine, CNRS, UMR 7359, BP 70239, F-54506 Vandoeuvre-lès-Nancy, France

³ Laboratoire d'Océanographie de Villefranche-sur-Mer, UMR 7093, 181 chemin du Lazaret, F-06230 Villefranche-sur-Mer, France

Lithium is an alkaline fluid mobile light element that can be used as a tracer of fluid-mediated mass transfers between oceanic crust and mantle in subduction zones. The two lithium isotopes (⁶Li and ⁷Li) can fractionate during fluid-rock interactions related to subduction zone metamorphism (e.g. Zack et al., 2003; Marschall et al., 2007). During hydrothermal alteration Li and $\delta^7\text{Li}$ increase in the oceanic basaltic crust and pelitic sediments compared to fresh MORBs and mantle (Decitre et al., 2002; Woodland et al., 2002; Tomascak et al., 2008). Isotopically heavy Li-rich fluids may be released during all stages of devolatilisation in subduction zones, particularly at the blueschist to eclogite facies transtion. However, the mode of Li mobilisation and isotope fractionation through the different stages of HP metamorphism is still in debate (e.g. Zack et al., 2003; Marschall et al., 2007; Halama et al., 2011). Li abundances and isotopic composition were measured in a suite of metabasites of blueschist, eclogite and retrograde greenschist facies from the Ile de Groix, a Variscan HP terrane (peak P–T conditions: 1.6–2.5 GPa; 500–600°C; El Korh et al., 2009).

Li concentrations were determined by AA Spectrometry ($\pm 2\text{--}10\%$; 1σ) for whole rocks, and by LA-ICPMS ($\pm 2\text{--}12\%$; 1σ) for minerals. Li concentrations in metabasites (16–124 ppm) are significantly higher than in fresh MORB (≤ 8 ppm). Even if they cover a large range of values, the Li concentrations do not vary according to the metamorphic facies. Main Li-hosting minerals are: 1) glaucophane (48–319 ppm) and omphacite (27–145 ppm) in blueschists and eclogites; 2) chlorite (13–182 ppm) and albite (41–212 ppm) in retrograde greenschists (see also El Korh et al., 2009).

Li isotopes in whole rocks ($\delta^7\text{Li}_{\text{L-SVEC}} \pm 0.1\text{--}0.6\%$; 2σ SE) were measured using a NeptunePlus MC-ICPMS (ThermoFisher Scientific) after sample dissolution and Li separation by ion exchange chromatography (Vigier et al., 2008). The metabasite $\delta^7\text{Li}$ values decrease from blueschists (+4.1 to -0.6 ‰) to eclogites (-2.5 to -4.8 ‰), while the $\delta^7\text{Li}$ values in retrograde greenschists cover the same range as in high-pressure rocks (+3.6 to -4.5‰). These values are generally lower than those of fresh MORB ($+3.4 \pm 1.4\%$, 2σ ; Tomascak et al., 2008) and of heavy-Li low-T altered oceanic crust. (-1.7 to +7.9 ‰; Chan et al., 2002).

Li isotopes in glaucophane, omphacite and barroisite from blueschists and eclogites were measured in situ by SIMS using a Cameca ims1280-HR (external 2σ SE $\pm 1.5\%$). The $\delta^7\text{Li}$ values of glaucophane (-4.4 to +11.4 ‰ in blueschists; -9.9 to +2.4 ‰ in eclogites) and omphacite (-21.5 to +4.9 ‰ in eclogites) are scattered within each sample, and vary on average from one sample to the other. However, the absence of core-to-rim zonation and the absence of correlation between the Li contents and Li isotopic compositions indicates that no late Li diffusion along grain boundaries occurred.

The high whole rock Li abundances compared to fresh MORB results from pre-HP low-T hydrothermal processes. Besides, the low $\delta^7\text{Li}$ values of metabasites whole rocks and minerals compared to fresh and altered MORB argues for kinetic Li fractionation related to metasomatic processes during subduction, as observed in orogenic eclogites (e.g. Marschall et al., 2007; Halama et al., 2011). The $\delta^7\text{Li}$ whole rock–mean glaucophane correlation indicates that glaucophane grew in isotopic equilibrium with its host rock under HP conditions. Consequently, low $\delta^7\text{Li}$ fractionation results from early pre-HP metasomatism, which may have occurred at lower P–T conditions in the subduction zone.

In eclogites, omphacite plots along the whole rock–mean glaucophane correlation line, also indicating equilibrium with its host rock. For only one sample, omphacite has a low $\delta^7\text{Li}$ compared to the whole rock and glaucophane, suggesting that this sample underwent metasomatic processes under eclogite facies P–T conditions. Retrograde barroisite formed along omphacite rims have a mean $\delta^7\text{Li}$ value similar to that of omphacite, but exhibit a large spread of $\delta^7\text{Li}$ values, suggesting localised Li fractionation during early retrogression. Greenschists have whole rock Li abundance and $\delta^7\text{Li}$ values within the same range as blueschists and eclogites. Therefore, the increase of the $\delta^7\text{Li}$ values toward positive values in the most retrogressed samples highlight a Li mineral/fluid isotopic exchange during rehydration reactions.

Our results emphasise the advantages of combining bulk and in-situ analyses to better understanding the Li behaviour during subduction and exhumation. They point out that Li is relatively well preserved during the HP-LT metamorphic processes, as it is incorporated in several different phases.

REFERENCES

- Decitre, S., Deloule, E., Reisberg, L., James, R. & Mevel, C., 2002: *Geochemistry Geophysics Geosystems* 3, 10.1029/2001GC000178.
- Chan, L.H., Alt, J.C. & Teagle, D.A.H., 2002: *Earth and Planetary Science Letters* 201, 187–201.
- El Korh, A., Schmidt S. Th., Ulianov, A. & Potel, S., 2009: *Journal of Petrology* 50, 1107–1148.
- Halama, R., John, T., Harms, P., Hauff, F. & Schenk, V., 2011: *Chemical Geology* 281, 151–166.
- Marschall, H.R., Pogge von Strandmann, P.A.E., Seitz, H.-M., Elliott, T. & Niu, Y., 2007: *Earth and Planetary Science Letters* 262, 563–580.
- Tomascak, P.B., Langmuir, C.H., Le Roux, P.J. & Shirey, S.B., 2008: *Geochimica et Cosmochimica Acta* 72, 1626–1637.
- Vigier, N., Decarreau, A., Millot, R., Carignan, J., Petit, S., France-Lanord, C., 2008: *Geochimica et Cosmochimica Acta*, 72, 780–792.
- Zack, T., Tomascak, P.B., Rudnick, R.L., Dalpe, C. & McDonough, W.F., 2003: *Earth and Planetary Science Letters* 208, 279–290.

3. Gemmology

Michael S. Krzemnicki, Laurent E. Cartier

*Swiss Gemmological Society (SGG),
Swiss Society of Mineralogy and Petrography (SSMP)*

TALKS:

- 3.1 Balmer W., Krzemnicki M.S.: Be-detection by FTIR on corundum: a preliminary report
- 3.2 Cartier L.E., Meyer J.B., Krzemnicki M.S.: Origin and species determination of organic gems: DNA fingerprinting as a novel method in gemmology
- 3.3 Dzikowski T.J., Cempírek J., Groat L.A., Dipple G.M., Giuliani G.: Origin of gem corundum in calcite marble: The Revelstoke occurrence in the Canadian Cordillera of British Columbia
- 3.4 Elmaleh E., Schmidt S.T., Karampelas S., Galster F.: Characterization of sapphires from Madagascar, Sri Lanka, Tanzania and Burma
- 3.5 Hänni H.A.: Microscopic study of inclusions in gemstones
- 3.6 Hanser C.: Spectroscopic study of Co-bearing spinel from Luc Yen (Vietnam)
- 3.7 Kiefert L., Schollenbruch K., Xu W.: Natural green amber from Ethiopia
- 3.8 Krzemnicki M.S., Revol V., Hanser C., Cartier L.E., Hänni H.A.: X-ray phase contrast and X-ray scattering images of pearls
- 3.9 Zhou W., Dzikowski T.: Species identification and treatment detection in dark coloured pearls

3.1

Be-detection by FTIR on corundum: a preliminary report

Walter A. Balmer^{1,2}, Michael S. Krzemnicki²

¹ Department of Geology, Faculty of Science, Chulalongkorn University, Bangkok 10330 University, Bangkok 10330, Thailand (w.balmer@quicknet.ch)

² Swiss Gemmological Institute SSEF, Aeschengraben 26, 4051 Basel, Switzerland

In mid-2001 Be-diffusion for corundum was first reported, when suddenly an unusually large number of Padparadscha coloured sapphires appeared in the market (Hänni & Pettke, 2002). Ever since, gemmological laboratories were confronted with the challenging task of detecting Be in corundum. Be however is a very light element and therefore not detectable by conventional ED-XRF trace-element analysis. New analytical methods had to be found in order to detect Be in gemstones, which potentially had been diffusion treated. Soon LA-ICP-MS (Guillong & Günther, 2002; Abduriyim & Kitawaki, 2006) and LIBS (Krzemnicki et al., 2004; Krzemnicki et al., 2007) were introduced to the field of gemmology. Although these methods are highly sensitive and Be can be detected efficiently, they were also very sophisticated and costly. Many laboratories with smaller budgets and less specialised personnel were therefore left with no solution in the detection of Be-treatments in general and corundum in particular.

In order to investigate the potential of FTIR as a possible analytical method for Be-detection in gemmology, three samples of colourless sapphires created by three different producers of synthetic corundum were investigated before and after Be-diffusion treatment (brownish colour after treatment). The Be-diffusion treatment was carried out by local burners in Chantaburi, Thailand, along with a batch of commercially treated corundum, processed at the same time.

Besides known artefacts related to atmospheric CO₂, H₂O, and grease no other signals were recorded for the examined synthetic corundum samples before treatment. Subsequent to Be-diffusion treatment two new features were observed in all three samples instead: a distinct band at 3053 cm⁻¹ and a less pronounced band at 2490 cm⁻¹.

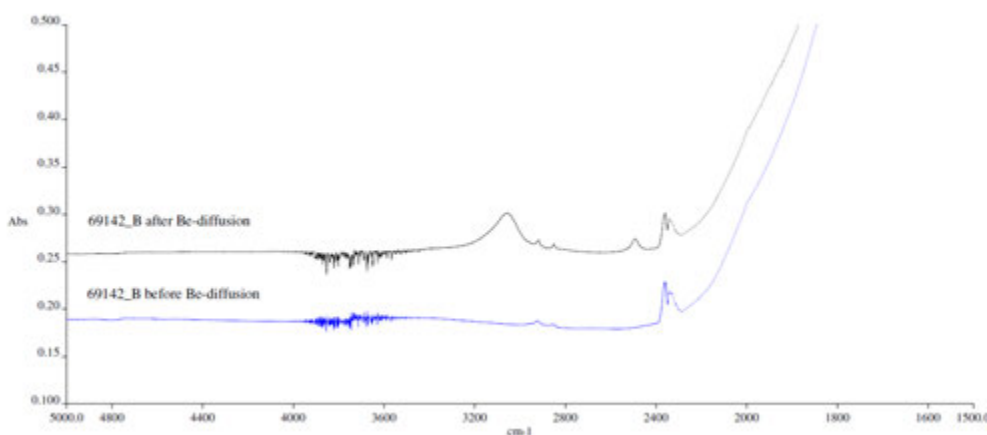


Figure 1. Synthetic sapphire before (blue trace) and after Be-diffusion treatment (black trace) revealing a distinct absorption band at 3053cm⁻¹ and a less pronounced band at 2490cm⁻¹.

The band at 3053 cm⁻¹ seems to be the same band as observed by Kitawaki & Abduriyim (2008) at 3068 cm⁻¹ and is located in an IR-range where bands related to diasporite (Farmer, 1974; Downs, 2006), dolomite (Downs, 2006), and an “unknown” band (Smith & van der Bogert, 2006) had been described before. The band at 2490cm⁻¹ however lays in an IR-range where no common artefacts nor signals of inclusions in corundum are known so far (Balmer, 2011).

Due to the fact that the described bands were occurring in all three investigated synthetic corundum samples only after Be-diffusion, we assume that the presence of these two bands at 3053 cm⁻¹ and 2490cm⁻¹ are possibly indicative for the detection of a Be-diffusion treatment in corundum. Cross-checking with a number of commercially available yellow Be-diffusion treated sapphires (analysed by LAICPMS) from different sources has shown, that they all show the same bands after treatment. Although further testing on a larger sampling and other corundum colours (before and after Be-diffusion) have to be collected, it has been possible to demonstrate that FTIR has the potential to be used as an alternative and less costly analytical method for Be-detection in corundum in the future.

REFERENCES

- Abduriyim, A., Kitawaki, H. 2006: Application of laser ablation – inductively coupled plasma – mass spectrometry (LA-ICP-MS) to gemology, *Gems & Gemology*, 42(2), 98-118.
- Balmer, W.A. 2011: Petrology, Geochemistry, and Gemmological Characteristics of Marble-Hosted Ruby Deposits of the Morogoro Region, Tanzania, unpublished Ph.D. thesis, Department of Geology, Faculty of Science, Chulalongkorn University, Bangkok, Thailand, 185pp.
- Farmer, V.C. 1974: The infrared spectra of minerals, Mineralogical Society Monograph, 4, Mineral Society, London, 539pp.
- Guillong, M., Günther, D. 2001: Quasi 'non-destructive' laser ablation-inductively coupled plasma-mass spectrometry fingerprinting of sapphires, *Spectrochimica Acta Part B*, 56, 1219-1231.
- Hänni, H.A., Pettke, T. 2002: Eine neue Diffusionsbehandlung liefert orangefarbene und gelbe Sapphire, *Zeitschrift Deutsche Gemmologische Gesellschaft*, 51(4), 137-512.
- Kitawaki, H., Abduriyim, A. 2008: Identification of Be-diffusion treated corundum, *Gemmology*, 9, 24-27.
- Krzemnicki, M.S., Hänni, H.A., Walters, R.A. 2004: A new method for detecting Be diffusion-treated sapphires: Laser induced breakdown spectroscopy (LIBS), *Gems & Gemology*, 40(4), 314-322.
- Krzemnicki, M.S., Pettke, T., Hänni, H.A., 2007: Perspectives of LIBS in gemstone testing .Analysis of light elements such as beryllium, boron, lithium, Poster Publication, GIT2007, Bangkok, Thailand.
- Downs, R.T., 2006: The RRUFF Project: an integrated study of the chemistry, crystallography, Raman and infrared spectroscopy of minerals. Program and Abstracts of the 19th General Meeting of the International Mineralogical Association in Kobe, Japan. www.rruff.info
- Smith, C.P., van der Bogert, C. 2006: Infrared Spectra of Gem Corundum, Proceedings of the GIA Gemological Research Conference, *Gems & Gemology*, 42(3), 92-93.

3.2

Origin and species determination of organic gems: DNA fingerprinting as a novel method in gemmology

Laurent E. Cartier^{1,2} Joana B. Meyer³, Michael S. Krzemnicki¹

¹ *Swiss Gemmological Institute SSEF, Aeschengraben 26, 4051 Basel, Switzerland (laurent.cartier@ssef.ch)*

² *Institute of Earth Sciences, Faculty of Geosciences, University of Lausanne, Lausanne, 1015, Switzerland*

³ *Swiss Federal Institute for Forest, Snow and Landscape Research WSL, Zürcherstrasse 111, Birmensdorf, 8903 Switzerland*

Organic gems such as pearls are some of the oldest gems collected and used in jewelry by mankind. Although not geological in origin, organic gem materials such as corals, ivory and pearls are products of biomineralization processes.

Organic gems such as pearls usually contain minute amounts of organic matter bound by a mineral matrix. This organic matter may contain small amounts of DNA that can be extracted and analyzed using novel extraction and fingerprinting techniques. This method was developed and published in 2013 using different types of pearls and oyster species (Meyer et al., 2013). This method has been further refined so that the pearl does not need to be destroyed (i.e. quasi non-destructive) and the amount of required material has been considerably reduced.

This innovation offers a number of testing and marketing opportunities within the billion US\$ international pearl industry. DNA fingerprinting can offer conclusive identification of the oyster species to which a pearl corresponds. Furthermore, the method has the potential to reveal the geographic origin of a pearl –which is an important factor for the valuation of pearls– based on more specific fingerprinting.

Although this method has only been applied to pearls thus far, it is currently being tested for precious coral and ivory. Past destructive research on ivory samples showed that it is possible to determine the regional origin of an ivory sample based on extracted DNA (Wasser et al., 2004). Furthermore, this method can be applied to other gem-relevant materials such as giant clam shells and (precious) corals. The novelty of this method is its quasi non-destructive nature, which makes it highly interesting for the jewelry industry. This research is also very relevant to the work of international customs within the context of organic gems protected by the Convention on International Trade in Endangered Species of Wild Fauna and Flora (CITES).

This method can increase transparency (through origin and species determination) and prevent fraud by identifying protected species for other organic gems. DNA fingerprinting as a tool in gemmology illustrates the importance of collaborating with researchers from other fields in order to develop new gemstone testing techniques for the 21st century.

REFERENCES

- Meyer, J.B., Cartier, L.E., Pinto-Figueroa, E.A., Krzemnicki, M.S., Hänni, H.A., and McDonald, B.A., 2013. DNA fingerprinting of pearls to determine their origins. *PLOS ONE*, 8(10), e75606.
- Wasser, S.K., Shedlock, A.M., Comstock, K., Ostrander, E.A., Mutayoba, B., and Stephens, M., 2004. Assigning African elephant DNA to geographic region of origin: Applications to the ivory trade. *PNAS*, 101(41), 14847–52.

3.3

Origin of gem corundum in calcite marble: The Revelstoke occurrence in the Canadian Cordillera of British Columbia

Tashia J. Dzikowski ^a, Jan Cempírek ^b, Lee A. Groat ^c, Gregory M. Dipple ^c, Gaston Giuliani ^d

^a SSEF Swiss Gemmological Institute, Aeschengraben 26, CH-4051 Basel

^b Department of Geological Sciences, Masaryk University, Kotlarska 2, 65937 Brno, Czech Republic

^c Department of Earth, Ocean and Atmospheric Sciences, University of British Columbia, 2207 Main Mall, Vancouver, BC V6T1Z4, Canada

^d IRD et CRPG/CNRS, Centre de Recherches Pétrographiques et Géochimiques, 15 rue Notre Dame des Pauvres, Vandoeuvre-lès-Nancy 54501, France

The calcite marble-hosted gem corundum (ruby, sapphire) occurrence near Revelstoke, British Columbia, Canada, occurs in the Monashee Complex of the Omineca Belt of the Canadian Cordillera. Corundum occurs in thin, folded and stretched layers with green muscovite + Ba-bearing K-feldspar + anorthite ($An_{0.85-1}$) ± phlogopite ± Na- poor scapolite. Other silicate layers within the marble are composed of: (1) diopside + tremolite ± quartz and (2) garnet ($Alm_{0.7-0.5}Grs_{0.2-0.4}$) + Na-rich scapolite + diopside + tremolite + Na,K-amphiboles. Non-silicate layers in the marble are either magnetite- or graphite-bearing.

Predominantly pink (locally red or purple) opaque to transparent corundum crystals have elevated Cr_2O_3 (≤ 0.21 wt.%) and variable amounts of TiO_2 ; rare blue rims on the corundum crystals contain higher amounts of TiO_2 (≤ 0.53 wt.%) and Fe_2O_3 (≤ 0.07 wt.%). The associated micas have elevated Cr, V, Ti, and Ba contents. Petrography of the silicate layers show that corundum formed from muscovite at the peak of metamorphism (~650–700 °C at 8.5–9 kbar). Because the marble is almost pure calcite (dolomite is very rare), the corundum was preserved because it did not react with dolomite to spinel + calcite during decompression. The scapolite-bearing assemblages formed during or after decompression of the rock at ~650 °C and 4–6 kbar. Gem-quality corundum crystals formed especially on borders of the mica-feldspar layers in an assemblage with calcite.

Whole rock geochemistry data show that the corundum-bearing silicate (mica-feldspar) layers formed by mechanical mixing of carbonate with the host gneiss protolith; the bulk composition of the silicate layers was modified by Si and Fe depletion during prograde metamorphism. High element mobility is supported by the homogenization of $\delta^{18}O$ and $\delta^{13}C$ values in carbonates and silicates for the marble and silicate layers. The silicate layers and the gneiss contain elevated contents of Cr and V due to the volcanoclastic component of their protolith.

3.4

Characterization of sapphires from Madagascar, Sri Lanka, Tanzania and Burma

Emilie Elmaleh¹, Susanne Theodora Schmidt¹, Stefanos Karampelas², Federico Galster³

¹ *Section of Earth and Environmental Sciences, University of Geneva, Switzerland*

² *Gübelin Gem Lab, Lucerne, Switzerland*

³ *Faculty of Geosciences and Environment, University of Lausanne, Switzerland*

A suite of 136 light blue to dark blue, whitish to greenish sapphires of the Gübelin Gem collection was examined from Madagascar (mines of Andranondambo, Andilamena and Ilakaka), Tanzania (Songa), Sri Lanka (Elahera, Ratnapura and Balangoda) and Burma (Mogok) using a combination of classical gemmology, UV-VIS-NIR, FTIR, and RAMAN spectroscopy, EDXRF and LA-ICP-MS trace element analysis. In addition, zircon, apatite and rutile inclusions were identified and U-Pb dating on zircon inclusions was carried out.

Three physico-chemical parameters are particularly important for determining a sapphire and its possible origin of formation and mining district provenance:

- 1) The presence of characteristic inclusions such as kaolinite, boehmite, calcite, apatite, rutile, and zircon, as well as fluid inclusions, spinell and graphite,
- 2) the intensity and/or absence of certain absorption bands of the UV-Vis-NIR spectra and
- 3) the chemical trace element composition, especially the elements Fe, Ti, Cr, V and Ga.

Out of the suite of 136 samples, 17 gems contained zircon inclusions with a size < 150 µm suitable for U-Pb dating by ICP-MS. Zircon inclusions were examined using cathodoluminescence (CL) to reveal information about the external morphology and the internal textures.

Zircon xenocrysts occur as cores in many zircon grains of which some show a typical magmatic growth zoning. They are normally mantled by newly grown zircon rims..

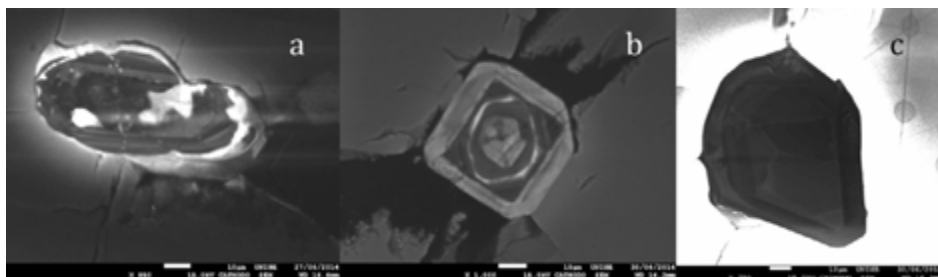


Figure 1 CL-images of zircon inclusions: (a) Andilamena mine (Saman039a), Madagascar; (c) Ilakaka mine (FSMA121), Madagascar; (c) Balangoda mine (SASL01), Sri Lanka

Zircons from the Andilamena and Ilakaka mine from Madagascar (Fig. 1a&b) show the oldest age with an U-Pb age of 1580 ± 300 Ma and 1470 ± 550 Ma, respectively which is older than the host rock (<600 Ma). All these ages are considered as mixed ages of an earlier magmatic core and later overgrowth(s). Samples from Ratnapura and Balangoda (Sri Lanka) were dated at 560 ± 8 Ma and 550 ± 7 Ma (U-Pb age) which is accordance with the host rock age. Zircons from Mogok (Burma) show the youngest U-Pb age of 67 ± 5 Ma. This age is older than expected as the host rock is 30 Ma old. However, the external morphology of these zircons is possibly of detrital origin, and they were likely to be incorporated during the crystallisation of the sapphire.

3.5

Microscopic study of inclusions in gemstones

Henry A. Hänni

Swiss Gemmological Institute SSEF, Aeschengraben 26, CH – 4002 Basel

Introduction

The identification of gemstones is classically done using optical mineralogy, UV-VIS spectroscopy, FTIR-, Raman spectroscopy to identify the mineral species and varieties. An important difference to pure mineralogical identification is that gemstones must be analysed destruction free. The natural or synthetic origin as well as the possible presence of an enhancement of the appearance are important issues. In addition, origin determination has become extremely important, so that chemical tests are increasingly important.

Traditionally, gemstones are investigated with binocular microscopes with low magnifications from 10x – 60x. While direct transmission of light is common in mineralogy, gemstones are usually inspected in dark field illumination. The features looked for are included minerals, healed fissures, fluid inclusions and growth characteristics. In some special cases immersion in higher refractive liquids is necessary, mainly to study growth development and colour zoning.

The diagnostic value of inclusion pictures has been demonstrated by founders of the science of gemmology from the 1930s onwards. The Swiss pioneer in inclusion study was Eduard J. Gübelin (1913 – 2005). He published three volumes of “Photoatlas of inclusions in Gemstones”, together with John I. Koivula. The present presentation should show a few diagnostic inclusion pictures taken from faceted gemstones that were submitted for identification and test reports to the Swiss Gemmological Institute SSEF during the last 30 years.

Natural gemstones

Natural gemstones can contain inclusions typical for the variety or even for the geological source and these can be indicators for a gemstone's origin. Protogenetic rutile crystals or syngenetic rutile precipitations are typical for corundum (ruby and sapphire). While apatite, zircon and rutile are common for many origins, mica, pargasite (Fig. 1) or pyrochlore are more helpful for origin determination.

In emeralds two- and three-phase inclusions are frequent, as well as carbonates, mica, apatite and other solid phases.

Treated gemstones

Fissure filling is very wide spread for lower qualities of gemstones, it has been performed with oils in older times, today low viscose lead glass is widely used. When higher temperatures are applied, heat treatment with assistance of borates leads to partial healing i.e. re-crystallisation of fissures. Glassy residues are then observed. At high temperatures the diffusion of chromophore trace elements, mainly Ti in sapphires is performed in order to increase the blue colour, due to $\text{Fe}^{2+}/\text{Ti}^{4+}$ pairs. Diffusion from outside is shallow for Ti, but deeper for Be, the latter providing a yellow colour. With emeralds and tourmalines that have fine fissures, and porous stones such as turquoise and some jadeites, impregnation with oils and resins is quite common. Such treatments may be suspected, but identification is more conclusive with FTIR or Raman spectroscopy.

Synthetic material

The more valuable gemstones like ruby, emerald, alexandrite and spinel have been copied i.e. synthesised through a variety of techniques. From melt drop Verneuil process to flux growth and hydrothermal growth, all techniques can have characteristic internal features indicating they are man made products. And again microscopy may be the short cut method for identification.

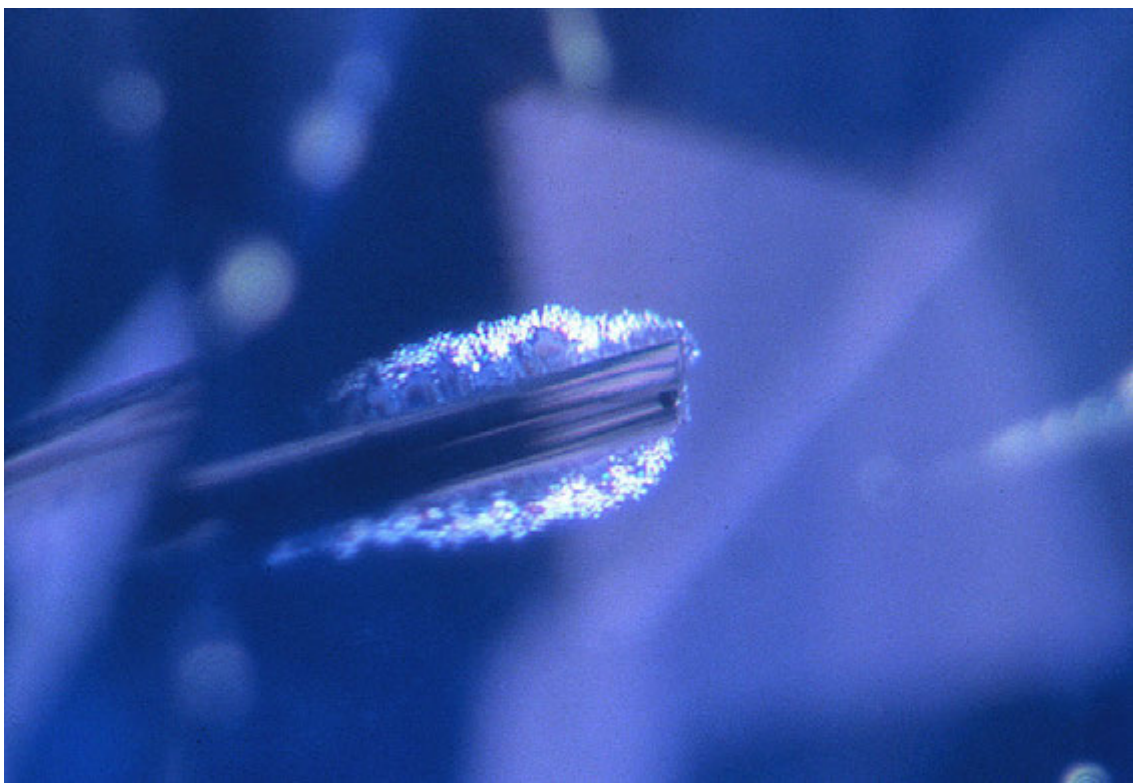


Figure 1. A pargasite needle in a sapphire from Kashmir, characteristic guest mineral for this deposit. Photo H.A. Hänni, SSEF.

REFERENCES

Gübelin, E.J. & Koivula, J.I. (2004): Photoatlas of Inclusions in Gemstones, Opinio, ISBN/EAN978-3-03999-041-2

3.6

Spectroscopic study of Co-bearing spinel from Luc Yen (Vietnam)

Carina Hanser^{1 2}

¹ *Institute of Earth and Environmental Sciences, Mineralogy-Petrology-Geochemistry, University of Freiburg, Albertstr. 23b, D-79104 Freiburg (carina.hanser@googlemail.com)*

² *Swiss Gemmological Institute SSEF, Aeschengraben 26, 4051 Basel*

Over the past few years spinels have increased in popularity and thus in their relevance for the gem industry. These gemstones are classically known for their red to pink colour caused by chromium. However, blue cobalt-containing spinels from the Luc Yen region in Vietnam have more recently reached the market. These spinels from Luc Yen often show a slight alexandrite effect by changing their colour to a more purple tone under a tungsten light source (incandescent light). Although the Raman spectra only show differences between natural and synthetic cobalt spinels, the absorption trends in UV-Vis spectroscopy and the photoluminescence spectra also vary within the group of natural spinels. The different behaviour of both natural subgroups, the colour-changing spinels and those of invariant colour, is due to their diverse trace element chemistry – notably cobalt and iron - detected by LA-ICP-MS.

3.7

Natural green amber from Ethiopia

Lore Kiefert¹, Klaus Schollenbruch², Wenxin Xu²

¹ *Gubelin Gem Lab Ltd., Maihofstrasse 102, CH-6006 Luzern (lore.kiefert@gubelingemlab.com)*

² *Gubelin Gem Lab Ltd., Maihofstrasse 102, CH-6006 Luzern*

The discovery of Ethiopian amber is relatively new (Schmidt et al., 2010), and previous literature does not give an exact location. Also, the described amber appears to be mostly yellowish brown in colour.

On a recent visit to Ethiopia, one of the authors (LK) was presented with several pieces of green amber (Figure 1 left), which sometimes resembled the appearance of green autoclaved amber as seen in the mid- to late 2000's (Abduriyim et al., 2009). However, the colour of some of these was distinctly different, and some of the pieces contained plant matter and even insects (Figures 1& 2).



Figures 1 & 2. Insects in green amber from Ethiopia

The amber deposits are located approximately 150 km north-northwest of Addis Ababa, near the town of Alem Ketema (Figure 2). According to the local geologist, Dr. Begosew Abate, who studied the area where the green amber is found, it occurs within Mesozoic sedimentary rocks just under the contact with the oldest Cenozoic volcanic rocks, in which opal bearing layers are found (Abate, pers. comm. 2014).

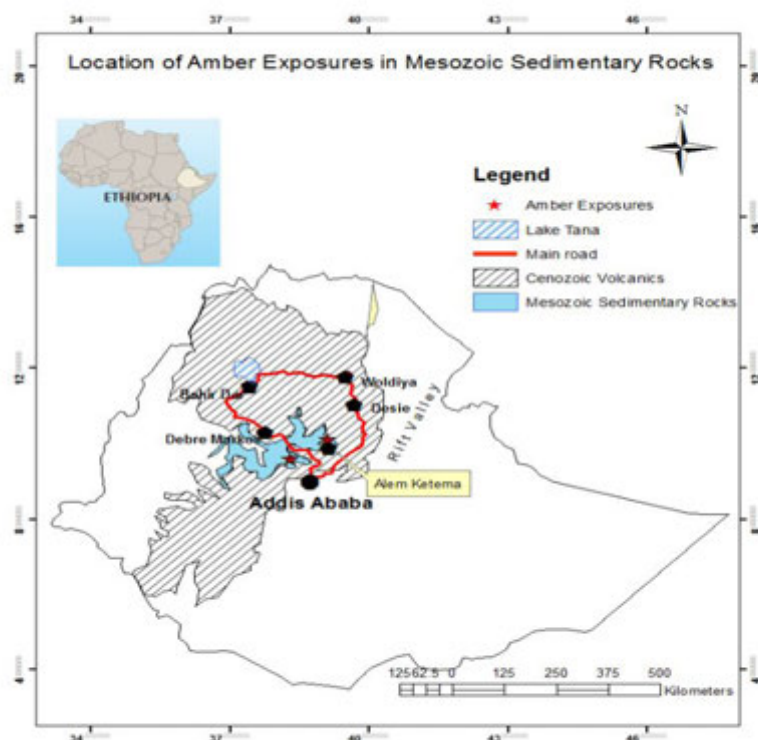


Figure 2. Location of amber deposits in Ethiopia. The green amber is found near Alem Ketema. Map: Begosew Abate.

The amber deposits are hosted within cretaceous age sandy limestones and exposed at different localities within the canyons cut by major tributaries of the Blue Nile river such as Jema, Wonchit and Muger. Amber occurs in at least three colors, i.e., green, blue green, yellowish and reddish. Ethiopian Amber is new to the market but it is attracting more and more people in recent days.

The presentation will focus on the properties of green amber from Ethiopia, showing inclusion photos and FTIR spectra that may also be used to distinguish it from its treated counterpart.

ACKNOWLEDGEMENTS

The authors wish to thank Tewodros Sintayehu of Orbit Ethiopia plc for the supply of the amber pieces, as well as Dr. Begosew Abate of Orbit Ethiopia plc for geological information of this amber.

REFERENCES:

- Abduriyim, A., Kimura, H., Yokoyama, Y., Nakazono, H., Wakatsuki, M., Shimizu, T., Tansho, M. & Ohki, S. 2009: Characterization of "Green Amber" With Infrared and Nuclear Magnetic Resonance Spectroscopy, *Gems & Gemology*, 45, 3, 158-177.
- Schmidt, A.R., Perrichot, V., Svojtka, M., Anderson, K.B., Belete, K.H., Bussert, R., Dörfelt, H., Jancke, S., Mohr, B., Mohrmann, E., Nascimbene, P.C., Nel, A., Nel, P., Ragazzi, E., Roghi, G., Saupe, E.E., Schmidt, K., Schneider, H., Selden, P.A. & Vavra, N. 2010. Cretaceous African life captured in amber. *Proc. Nat. Academy Sci. USA*, 107, 16, 7329-7334.

3.8

X-ray Phase Contrast and X-ray Scattering Images of Pearls

Michael S. Krzemnicki¹, Vincent Revol², Carina Hanser³, Laurent Cartier¹, Henry A. Hänni¹

¹ Swiss Gemmological Institute SSEF; Aeschengraben 26, CH-4051 Basel (michael.krzemnicki@ssef.ch)

² CSEM Centre Suisse d'Electronique et Microtechnique SA, CH-6055 Alpach

³ Institut für Geo- und Umweltwissenschaften, Albert-Ludwigs Universität, D-79104 Freiburg i. Br.

The separation of natural pearls from cultured pearls is relevant to the multi billion pearl and jewellery trade. It is mainly based on the analysis and observation of the internal structures of pearls, traditionally done by X-ray radiography (Anderson 1931, Strack 2006, Sturman 2009). Slight variations in X-ray absorption (attenuation) within a pearl are then linked to the presence, concentration, and orientation of organic matter or voids within the calcium carbonate pearl matrix. In recent years, X-ray microtomography (Xray- μ CT) has strongly contributed to a better understanding of the spatial distribution of such internal features (Wehrmeister et al. 2008, Krzemnicki et al. 2010). With this study we were able for the first time to simultaneously register conventional X-ray absorption, X-ray phase contrast, and X-ray scattering (darkfield) images of numerous natural and cultured pearl samples from various pearl oyster and mussel species.

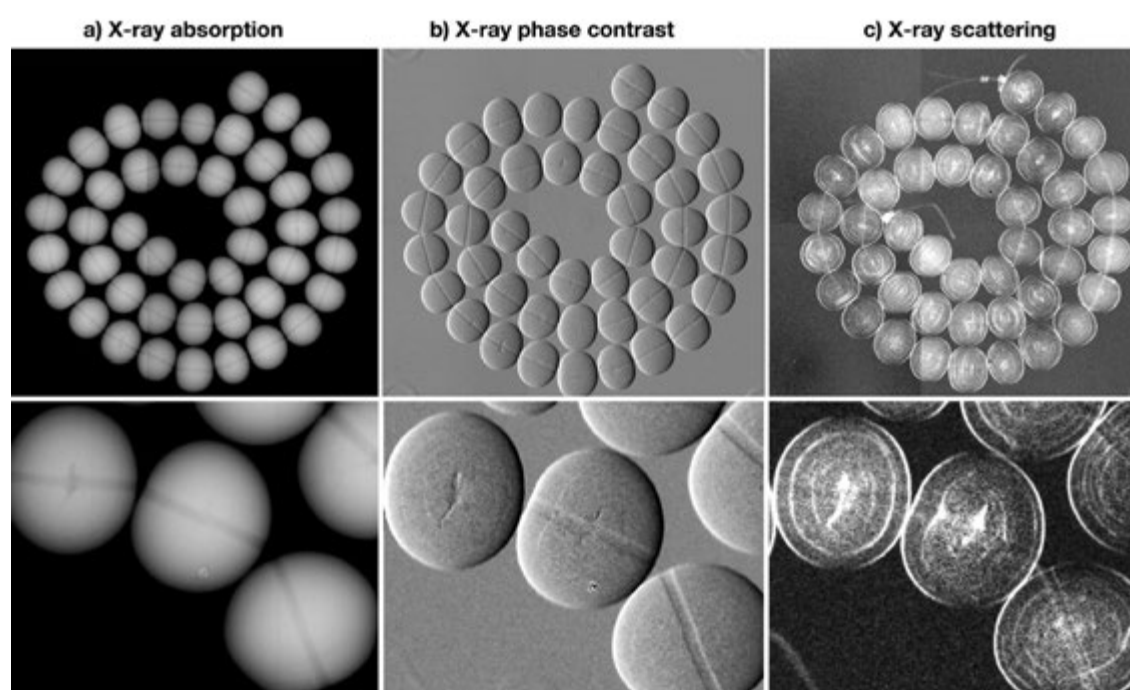


Figure 1: Comparison of a) X-ray absorption (attenuation), b) X-ray phase contrast, and c) X-ray scattering images of a strand of 44 beadless freshwater cultured pearls from China (*Hyriopsis cumingii*).

By using an experiment setup at the CSEM (Revol et al., 2011), the most promising results were obtained from X-ray scattering (Figure 1c). As presented here for a strand of beadless freshwater cultured pearls, it revealed not only their multi-layered onion-like growth structure, but also in great detail the complex geometry of their characteristic central void structure.

Our preliminary results show that both, X-ray phase contrast and X-ray scattering are adding valuable information to conventional X-ray absorption (radiography) when analysing the internal structures of pearls.

REFERENCES

- Anderson, B. W. 1931: The use of X-rays in the study of pearls. *British Journal of Radiology*, 5, 57-64.
- Krzemnicki, M.S., Friess, S.D., Chalus, P., Hänni, H.A., & Karampelas, S. 2010: X-ray computed microtomography: Distinguishing natural pearls from beaded and non-beaded cultured pearls. *Gems & Gemology*, 46 (2), 128–134.
- Revol, V., Jerjen, I., Kottler, C., Schütz, P., Kaufmann, R., Lüthi, T., Sennhauser, U., Straumann, U., & Urban, C. 2011: Sub-pixel porosity revealed by X-ray scatter dark field imaging. *Journal of Applied Physics*, 110, 4, doi: 10.1063/1.3624592

Strack, E. 2006: Pearls. Rühle-Diebener Verlag, 707 pp. ISBN: 978-3981084801

Sturman, N. 2009: The microradiographic structures of non-bead cultured pearls. www.giathai.net/pdf/The_Microradiographic_structures_in_NBCP.pdf (accessed: April 2015)

Wehrmeister, U., Goetz, H., Jacob, D.E., Soldati, A.L., Xu, W., Duschner, H., & Hofmeister, W. 2008: Visualization of the internal structure of freshwater cultured pearls by computerized X-ray microtomography. *Journal of Gemmology*, 32 (1–2), 15–21.

3.9

Species identification and treatment detection in dark coloured pearls

Wei Zhou¹, Tashia Dzikowski¹

¹ SSEF Swiss Gemmological Institute, Aeschengraben 26, CH-4051 Basel (wei.zhou@SSEF.ch)

In the jewellery market, dark-coloured pearls vary in colour range from grey to brown and black, with blue, green or purple orient considered highly desirable (George 1971). These naturally coloured dark pearls may belong to several different saltwater pearl oyster species but have very similar appearances. *Pinctada margaritifera*, *Pteria sterna* (Kiefert et al. 2004), *Pteria penguin* (*P. penguin*) and also black pearls from Abalone are common types found in the trade. Meanwhile, some light coloured pearls can be also treated to obtain dark coloured pearls (Komatsu & Akamatsu 1978). Gemmological observation and examination along with UV-VIS spectrometry, Raman spectrometry and energy dispersive X-ray fluorescence (ED-XRF) are useful methods to distinguish pearl species mostly based on differences of their colour pigments (Britton 1983, Iwahashi & Akamatsu 1994, Karampelas 2011). Identification of treated dark pearls is also possible using these techniques.

Figure 1 shows the UV-Vis reflectance spectra of studied pearl samples from different oyster species (*P. margaritifera*, *P. sterna*, *P. penguin*) and a silver (Ag) treated dark pearl. In figure 2, typical Raman spectra of natural-coloured pearl species from *P. margaritifera*, *P. sterna* and *P. penguin* are presented. The spectra (Fig. 2) were recorded using an argon-ion laser (514nm). Energy dispersive X-ray fluorescence analyses of Abalone pearls reveal, that they contain iodine (I) as minor constituent, in contrast to the other investigated species. In the case of silver-treated pearls of artificial dark colour a distinct Ag concentration can also be detected using ED-XRF.

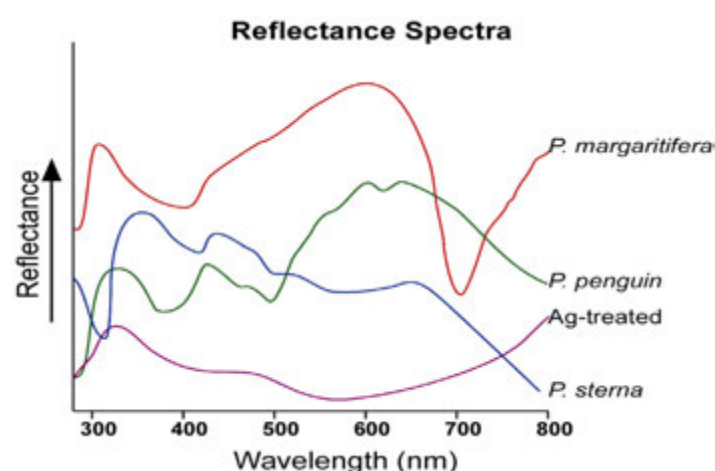


Figure 1. UV-Vis reflectance spectra of pearls from *P. margaritifera*, *P. penguin*, *P. sterna* and a silver (Ag)-treated pearl.

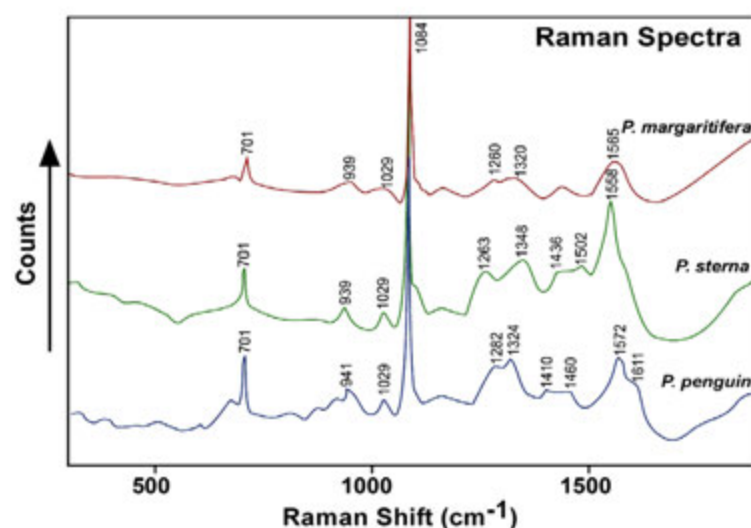


Figure 2. Raman spectra of a black pearl from *P. margaritifera*, a dark grayish brown natural pearl from *P. sterna* and a brown pearl from *P. penguin*.

In summary, UV-Vis spectroscopy offers the possibility to distinguish *P. margaritifera* pearls from other dark coloured species (based on their absorption band at approximately 700nm) (Huang 2006, Karampelas et al. 2011) and to detect Ag-treated pearls. Raman spectroscopy then provides further option to distinguish *P. margaritifera*, *P. sterna* and *P. penguin* pearls based on their specific Raman shift peak positions. Finally, the ED-XRF reveals the chemical composition of Abalone pearls and Ag-treated pearls, which have distinct iodine (I) and silver (Ag) content, respectively.

REFERENCES

- Britton, G. 1983: The Biochemistry of Natural Pigments. Cambridge University Press, Cambridge.
- George C. D. 1971: The black pearls. History and development. Lapidary Journal, 25, 136-147.
- Huang Y.L. 2006: Visible absorption spectrum representation of Tahitian black pearls and treated pearls. Journal Gems and Gemmology, 8, 1, 5-8.
- Iwahashi Y., Akamatsu S. 1994: Porphyrin pigment in black-lip pearls and its application to pearl identification. Fisheries Science, 60, 1, 69-71.
- Karampelas S., Fritsch E., Gauthier J-P., Hainschwang T. 2011: UV-VIS-NIR reflectance spectroscopy of natural-color saltwater cultured pearls from *Pinctada margaritifera*. Gems & Gemology, 47, 1, 31-35.
- Kiefert, L., McLaurin Moreno, D., Arizmendi, E., Hänni, H.A., and Elen, S. 2004: Cultured Pearls From The Gulf of California, Mexico, Gems & Gemology, 40, 26-38.
- Komatsu H., Akamatsu S. 1978: Differentiation of black pearls. Gems & Gemology, 16, 1, 7-15.

4. Palaeontology

Christian Klug, Torsten Scheyer, Lionel Cavin

*Schweizerische Paläontologische Gesellschaft,
Kommission des Schweizerischen Paläontologischen Abhandlungen (KSPA)*

TALKS:

- 4.1 Aguirre-Fernández G., Jost J.: Re-evaluation of the fossil cetaceans from Switzerland
- 4.2 Costeur L., Mennecart B., Schmutz S., Métais G.: *Palaeomeryx* (Mammalia, Artiodactyla) and the giraffes, data from the ear region
- 4.3 Foth C., Hedrick B.P., Ezcurra M.D.: Ontogenetic variation and heterochronic processes in the cranial evolution of early saurischians
- 4.4 Frey L., Rücklin M., Kindlimann R., Klug C.: Alpha diversity and palaeoecology of a Late Devonian Fossilagerstätte from Morocco and its exceptionally preserved fish fauna
- 4.5 Joyce W.G., Rabi M.: A Revised Global Biogeography of Turtles
- 4.6 Klug C., Frey L., Rücklin M.: A Famennian Fossilagerstätte in the eastern Anti-Atlas of Morocco: its fauna and taphonomy
- 4.7 Leder R.M.: Morphometric analysis of teeth of fossil and recent carcharhinid selachians
- 4.8 Martini P., Costeur L., Schmid P., Jagher R., Le Tensorer J.-M.: The diversity of Pleistocene Camelidae in El Kowm, Syria: craniodental remains
- 4.9 Marty D., Stevens K.A., Ernst S., Paratte G., Lovis C., Cattin M., Hug W.A., Meyer C.A.: Processing and analysis with 'Cadence Toolset' of Late Jurassic dinosaur track data systematically acquired during ten years of excavations prior to construction of Highway A16, NW Switzerland
- 4.10 Mennecart B., Costeur L.: A new approach to determine the phylogenetic relevance of the bony labyrinth: the case of the Cervid lineage
- 4.11 Meyer C.A., Wetzel A.: The Late Triassic bonebed of Niederschönthal (Norian, Knollenmergel, Füllinsdorf BL) – Amanz Gressly's dinosaur locality revisited
- 4.12 Meyer, C.A., Thüring, S., Wizevich, M., Thüring, B., Marty, D.: The Norian and Rhaetian dinosaur tracks of eastern Switzerland in the light of sequence stratigraphy
- 4.13 Peybernes C., Chablais J., Martini R.: Evolution and paleobiogeography of reef biota in the Panthalassa domain during the Late Triassic: insights from reef limestone of the Sambosan Accretionary Complex, Japan
- 4.14 Schaefer K., Hug W.A., Billon-Bruyat J.-P.: Catalogues of the palaeontological heritage from the A16 – Transjurane highway (Canton of Jura): example of the Mesozoic marine crocodilians
- 4.15 Tajika A., Klug C.: Intraspecific variation of volumetric growth trajectories in nautilids and ammonites

POSTERS:

- P 4.1 Eva A. Bischof: Fossil echinoids of the St. Ursanne Formation in the Swiss Jura Mountains
- P 4.2 Menecart B., Pirkenseer C.M.: Study of the microfauna from the Falun (Langhian, France): preliminary data on the Ostracoda
- P 4.3 Scherz K.: The morphology of the petrosal bone of cats (Felidae) and its phylogeny and paleoecological implications

4.1

Re-evaluation of the fossil cetaceans from Switzerland

Gabriel Aguirre-Fernández¹ & Jürg Jost²

¹ Paläontologisches Institut und Museum, Universität Zürich, Karl-Schmid-Strasse 4, 8006 Zürich
(gabriel.aguirre@pim.uzh.ch)

² Bärenhubelstrasse 10, CH-4800 Zofingen

Fossil cetaceans (whales and dolphins) from Switzerland and other paratethyan localities (e.g. Austria, Hungary and Slovakia) are poorly understood, yet their fossil record is relevant to large-scale hypotheses on the evolution of cetaceans. It has been proposed that a marked pulse in cetacean radiation during the Late Miocene was driven by abiotic factors, including the closure of the Tethys (Steeman et al., 2009). To single out the independent roles this and other drivers is necessary to focus on finer-scale studies covering different geographic locations. Regionally, reappraisals have been published for cetacean fauna of the Mediterranean (e.g. Bianucci and Landini, 2002) and the North Sea (e.g. Lambert, 2008). Here, we build on Pilleri's (1986) effort to describe the fossil cetacean fauna of Switzerland, which is now outdated.

The taxonomy of the Swiss cetaceans is particularly challenging: only isolated remains of fossil rostra, mandibles, teeth, earbones, and vertebrae have been found. So far, we have restudied and identified material in four collections, with many smaller collections still to be visited. Our preliminary results indicate an absence of delphinids (*contra* Pilleri, 1986) and a fauna mainly composed of physeteroids (today represented by sperm whales) and a diverse range of platanistoids (today represented by the Ganges river dolphin), including the families Squalodontidae and Platanistidae.

The fossils in the J. Jost and B. Lüdi collections are precisely dated. Most cetaceans are from the Safenwil-Muschelsandstein (Luzern Formation, ca. 19 Ma) and the Staffelbach-Grobsandstein (St. Gallen Formation, ca. 18 Ma). The fossil sharks and rays from the Safenwil-Muschelsandstein indicate a shallow water setting, while the Staffelbach-Grobsandstein fossils indicate deeper water.

The taxonomy of Swiss physeteroideans was reanalyzed by direct comparison of the holotypes at the Royal Belgian Institute of Natural Sciences in Brussels: *Eudelphis mortezelensis*, *Placoziphius duboisi*, *Orycterocetus crocodilinus*, and *Physeterula dubusi*). Taxonomic adjustments are a sign of the health of the science of taxonomy (Pyle and Michel, 2008), and this ultimately permeates on all research with taxonomic content, including the widely-used Paleobiology Database.

REFERENCES

- Bianucci, G. & Landini W. 2002: Change in diversity, ecological significance and biogeographical relationships of the Mediterranean Miocene toothed whale fauna. *Geobios*, 24, 19-28.
- Lambert, O. 2008: Sperm whales from the Miocene of the North Sea: a re-appraisal. *Bulletin de L'Institut Royal des Sciences Naturelles de Belgique, Sciences de la Terre*, 78, 277-316.
- Pilleri, G. 1986: The Denticeti of the Western Paratethys (Upper Marine Molasse of Switzerland). *Investigations on Cetacea*, 19, 11-114.
- Pyle, R. L. & Michel E. 2008: ZooBank: Developing a nomenclatural tool for unifying 250 years of biological information. *Zootaxa*, 1950, 39-50.
- Steeman, M. E., Hebsgaard M. B., Fordyce R. E., Ho S. Y. W., Rabosky D. L., Nielsen R., Rahbek C., Glenner H., Sorensen M. V. & Willerslev E. 2009: Radiation of extant cetaceans driven by restructuring of the oceans. *Systematic Biology*, 58, 1-13.

4.2

***Palaeomeryx* (Mammalia, Artiodactyla) and the giraffes, data from the ear region**

Loïc Costeur¹, Bastien Mennecart¹, Sylvia Schmutz¹, Grégoire Métais²

¹ Natural History Museum, Basel, Augustinergasse 2, CH-4001 Basel, Switzerland (loic.costeur@bs.ch)

² UMR 7207 CNRS-MNHN-UPMC, 75005 Paris, France

Palaeomeryx is an okapi to deer-like animal that was abundant throughout Europe in the Early to early Late Miocene. Very few complete skulls (Duranthon et al., 1995, Rössner, 2010) and no complete or partial skeleton of the European Palaeomerycidae are known. Qiu et al. (1985) described a complete skeleton of a Chinese *Palaeomeryx* but the bad preservation on a slab prevented any in depth-analysis. Its peculiar morphology and the presence of cranial appendages that look like the giraffid ossicones have long been a matter of debate. *Palaeomeryx* and the other representatives of its family (e.g., *Ampelomeryx*, *Germanomeryx*) were supposedly considered sister taxa to Giraffidae (Ginsburg, 1985). A sister group relationship to Cervidae has been proposed for *Palaeomeryx* (Janis & Scott, 1987) and is now mostly accepted. Very few isolated ossicones were found and only the preservation of complete skulls of *Ampelomeryx* from the Early Miocene of Spain and France (Duranthon et al., 1995) revealed how these appendages were positioned on the skull. This led to propose affinities of the Palaeomerycidae to the North American Dromomerycidae, sometimes included as Dromomerycinae in the Palaeomerycidae family (Prothero, 2007). *Palaeomeryx* and its relatives are thus mostly known through isolated tooth material, or more or less complete jaws. This taxon gave its name to the *Palaeomeryx*-fold, a structure of the lower molars that is common to many primitive members of Ruminantia.

Here we investigate the petrosal bone and the bony labyrinth of *Palaeomeryx* and compare it to both living giraffids: the giraffe (*Giraffa camelopardalis*) and the okapi (*Okapia johnstoni*). Four isolated petrosal bones of *Palaeomeryx kaupi* from the French Early Miocene MN4 locality Artenay, one skull fragment of *Palaeomeryx eminens* from the German Middle Miocene MN7/8 locality Steinheim were CT-scanned and the inner ear was segmented and reconstructed. A juvenile and an adult giraffe petrosal bones together with an adult okapi petrosal bone were CT-scanned and reconstructed too. A work in progress on the bony labyrinth in the deer lineage since the Early Miocene provides the comparative basis for plesiomorphic and derived states in stem Cervidae and Cervidae.

Although the giraffe and the okapi petrosal bones look different, they are close to one another, e.g., they both have a double transpromontorial sulcus on the promontorium, a similar subarcuate fossa or a blunt anterior process of the tegmen tympani. *Palaeomeryx* has a different petrosal bone with a single transpromontorial sulcus, a relatively smaller tegmen tympani or a larger fossa for the tensor tympani muscle, like in the white-tailed deer *Odocoileus*. The bony labyrinth of *Palaeomeryx* is fairly different from that of *Giraffa* or *Okapia*. While both extant genera share a quickly diverging vestibular aqueduct, or a flattened cochlea, *Palaeomeryx* shows a straight vestibular aqueduct, running parallel to the common crus (a very much deer-like condition), a rather massive cochlea mimicking the plesiomorphic condition in the deer lineage, or a lateral canal branching within the posterior ampulla, much like in deer but also reminiscent of the condition seen in the okapi. The giraffe has a different branching pattern, higher than the ampulla and closer to the vestibule.

Our data on the ear region cannot firmly indicate if the hypothesis of affinities of *Palaeomeryx* to deer is more supported than that to giraffes. Data on Miocene giraffes are still lacking and a complete understanding of plesiomorphic characters in the ear region of pecoran ruminants is not yet fully achieved.

REFERENCES

- Duranthon, F., Moya-Sola, S., Astibia H., & Köhler M. 1995: *Ampelomeryx ginsburgi* nov. gen., nov. sp. (Artiodactyla, Cervoidea) et la famille des Palaeomerycidae. Comptes Rendus de l'Académie des Sciences, 321, 339-346.
- Ginsburg L. 1985 : Systématique et evolution du genre *Palaeomeryx* (Artiodactyla, Giraffoidea) en Europe. Comptes Rendus de l'Académie des Sciences, 301, 1075-1078.
- Janis C.M., Scott K.M. 1987: The interrelationships of higher ruminant families with special emphasis on the members of the Cervoidea. American Museum Novitates, 2893, 1-85.
- Prothero D.R. 2007: Family Palaeomerycidae. In Prothero D.R. & Foss, S.E. The Evolution of Artiodactyls. The John Hopkins University Press, pp. 241-248.
- Qiu, Z.-X., Jan D., Jia H., & Sun B. 1985: Preliminary observations on the newly found skeletons of *Palaeomeryx* from Shanwang, Shandong. Vertebrata Palasiatica, 23, 173-195.
- Rössner G.E. 2010: Systematics and palaeoecology of Ruminantia (Artiodactyla, Mammalia) from the Miocene of Sandelzhausen (southern Germany, Northern Alpine Foreland Basin). Paläontologische Zeitschrift, 84, 123-162.

4.3

Ontogenetic variation and heterochronic processes in the cranial evolution of early saurischians

Christian Foth¹, Brandon P. Hedrick², Martín D. Ezcurra³

¹ Department of Geosciences, University of Fribourg/Freiburg, Chemin du Musée 6, 1700 Fribourg, Switzerland;

² Department of Earth and Environmental Science, University of Pennsylvania, 251 Hayden Hall, 240 S 33rd Street, Philadelphia, PA 19104, USA;

³ Sección Paleontología de Vertebrados, Museo Argentino de Ciencias Naturales "Bernardino Rivadavia", Buenos Aires C1405DJR, Argentina

Heterochrony describes phenotypic changes in evolution due to shifts in the timing or rate of developmental processes in an organism relative to its ancestor. Two primary processes are recognized: paedomorphosis and peramorphosis.

Paedomorphosis occurs when the later ontogenetic stages of an organism retain characteristics from earlier ontogenetic stages of its ancestor, whereas a peramorphic organism is ontogenetically more developed than the later ontogenetic stages of its ancestor (Klingenberg 1998).

Within dinosaurs, non-avian saurischian skulls underwent at least 165 million years of evolution and shapes varied from elongated skulls, such as in the theropod *Coelophysis*, to short and box-shaped skulls, such as in the sauropod *Camarasaurus* (Weishampel *et al.* 2004).

A number of factors have long been considered to drive skull shape, including phylogeny, dietary preferences and functional constraints (e.g. Witzel & Preuschoft 2005, Foth *et al.* 2013). However, heterochrony is increasingly being recognized as a major factor in dinosaur evolution (e.g. Bhullar *et al.* 2012).

In order to quantitatively analyse the impact of heterochrony on saurischian skull shape, we analysed five ontogenetic trajectories (*Massospondylus*, *Coelophysis*, a megalosaurid taxon, *Allosaurus* and *Tarbosaurus*) using 2D geometric morphometrics in a phylogenetic framework consisting of 35 saurischian species. In this framework we evaluated how heterochrony affected skull shape through both ontogenetic and phylogenetic trajectories using principal component analyses and multivariate regressions.

The ontogenetic trajectories sampled show great variation in length and direction, but follow some very general trends (Fig 1a). General peramorphic skulls include more elongate and slender snouts, elongate antorbital fenestrae, oval orbits, dorsoventrally shallower post-rostral regions, and more massive maxillae, jugals, and postorbitals. Paedomorphic skulls show the opposite features.

We found that the hypothetical ancestor of Saurischia led to basal Sauropodomorpha mainly through paedomorphosis in terms of skull shape, while this trend was reversed in basal sauropods due to strong modifications of the snout. In contrast, early theropod evolution was characterized mainly through peramorphosis. Within theropods paedomorphic events occurred two times independently, in basal ceratosaurs and Avetheropoda. The latter event indicates that the paedomorphic trend previously found in advanced coelurosaurs (Bhullar *et al.* 2012) may extend back to the early evolution of Avetheropoda.

Within Avetheropoda, the skull evolution of the large-bodied theropods *Allosaurus* and *Tarbosaurus* was influenced by peramorphosis. Therefore, not only are changes in saurischian skull shape complex due to the large number of factors that affect skull shape, but heterochrony itself is complex, with a number of reversals throughout non-avian saurischian evolution (Fig. 1b).

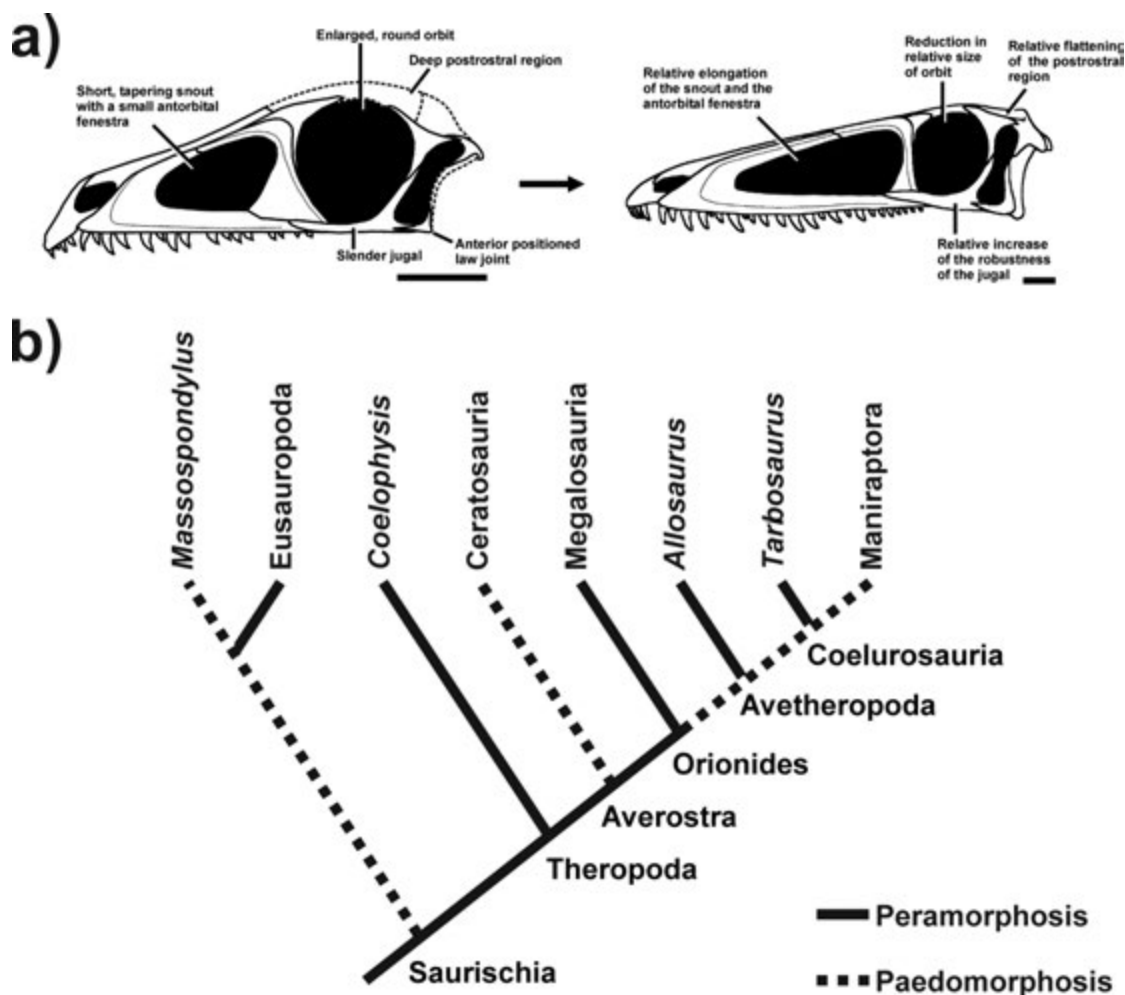


Figure 1 a) Generalized ontogenetic patterns in saurischian skulls exemplified for the basal theropod *Coelophysis* (modified after Foth et al. in review). b) Simplified phylogeny of Saurischia showing the main heterochronic trends of the skull. Peramorphosis is shown by solid lines and pedomorphosis by dashed lines.

Bullet list: Dinosauria, Saurischia, Sauropodomorpha, Theropoda, skull shape, ontogeny, heterochrony, evolution, geometric morphometrics

REFERENCES

- Bhullar B-A, Marugán-Lobón J, Racimo F, Bever GS, Rowe TB, Norell MA, Abzhanov A. 2012. Birds have pedomorphic dinosaur skulls. *Nature* 487, 223–226.
- Foth, C., Rauhut, O. W. M. 2013. Macroevolutionary and morphofunctional patterns in theropod skulls: a morphometric approach. *Acta Palaeontol. Pol.* 58, 1–16.
- Foth, C., Hedrick, B. P. & Ezcurra M. D. In review. Cranial ontogenetic variation in early saurischians and the role of heterochrony in the diversification of predatory dinosaurs. *PeerJ*.
- Klingenberg, C.P. 1998. Heterochrony and allometry: the analysis of evolutionary change in ontogeny. *Biol. Rev.* 73, 79–123.
- Weishampel, D. B., Dodson, P. & Osmólska, H. 2004. *The Dinosauria*. Berkeley, University of California Press.
- Witzel, U. & Preuschoft, H. 2005. Finite-element model construction for the virtual synthesis of the skulls in vertebrates: case study of *Diplodocus*. *Anat. Rec.* 283A, 391–401.

4.4

Alpha diversity and palaeoecology of a Late Devonian Fossilagerstätte from Morocco and its exceptionally preserved fish fauna

Linda Frey¹, Martin Rücklin², René Kindlimann¹ & Christian Klug¹

¹ *Paläontologisches Institut und Museum, University of Zürich, Karl Schmid-Strasse 4, CH-8006 Zürich
(linda.frey@pim.uzh.ch)*

² *Naturalis Biodiversity Center, Postbus 9517, NL-2300 RA Leiden*

A Late Devonian Fossilagerstätte with exceptionally preserved fish skeletons, mainly of chondrichthyans, placoderms, and rare sarcopterygians, is known for more than half a century from the eastern Anti-Atlas of Morocco. Although the according localities and parts of their fish contents are long known, some faunal elements have only been found recently. For the first time, we found nearly completely articulated shark specimens including skeletal elements and possibly soft tissue remains as well as abundant phyllocarid crustaceans. In order to reconstruct the preferred habitats and the depositional environment of these fishes, we examine the accompanying fauna for alpha diversity. The excellent exposures of Late Devonian to Early Carboniferous sediments and their faunal associations are rich in invertebrates and allow studying changes in alpha diversity and faunal composition.

We collected several faunas containing invertebrates and vertebrates of early Famennian to early Tournaisian age along two sections in the Maïder region (eastern Anti-Atlas). The specimens of each fauna were determined as far as possible and their frequencies were counted in order to observe changes in diversity. Moreover, the different taxa were grouped to ecological categories of tiering, motility and feeding behavior to describe the ecological diversity within the habitat of the fishes.

Preliminary analyses of the data show a fluctuating species richness through the studied sections. The layers containing the fish remains have a very low diversity in invertebrates with nearly missing benthos and are clearly dominated by phyllocarids. The low number of taxa, in combination with the occurrence of phyllocarids and fishes in iron-rich nodules and the occurrence of small siderite nodules represent a sea floor sediment deposited under low oxygen conditions, thus yielding a possible explanation for the exceptional preservation. Apparently, nearly perfect environmental conditions prevailed in several phases of the Famennian allowing the preservation of these gnathostome fishes.

4.5

A Revised Global Biogeography of Turtles

Walter G. Joyce¹, Márton Rabi²

¹ *Department of Geosciences, University of Fribourg, Chemin du Musée 6, 1700 Fribourg, Switzerland
(walter.joyce@unifr.ch)*

² *Department of Geosciences, University of Tübingen, Hölderlinstr. 12, 72074 Tübingen, Germany*

Over the course of the last decades, much effort has gone into unraveling the biogeographic history of turtles, but while much progress has been achieved in resolving post-Jurassic dispersal events, traditional phylogenetic hypotheses have yielded incongruous results in regards to the early history of the group.

Methods.

We re-evaluate the fossil record of turtles in context of recent phylogenetic analyses and fossil finds, including the extensive record of fragmentary but diagnostic remains. However, given that near-coastal and marine turtles readily disperse across aquatic barriers, a broad set of neritic to pelagic groups were disregarded from consideration. Given that significant disagreement still exists among current phylogenetic hypotheses, much effort was placed in tracing unambiguously monophyletic groups through the fossil record. We nevertheless employed molecular backbone constraints, given that the molecular phylogenies are more consistent with the fossil record than current, morphological phylogenies.

Results.

Among derived, aquatic turtles, we recognize four clades that can be traced back to four discrete biogeographic centers: Paracryptodira in North America and Europe, Pan-Cryptodira in Asia, Pan-Pelomedusoides in northern Gondwanan landmasses and Pan-Chelidae in southern Gondwanan landmasses. This pattern is partially mirrored by three clades of primarily terrestrial, basal turtles: Solemydidae in North American and Europe, Sichuanchelyidae in Asia, and Meiolaniformes sensu stricto in southern Gondwanan landmasses. Although the exact interrelationships of these clades remain unclear, most can be traced back to the Middle Jurassic.

Discussion.

The conclusion that the two primary lineages of pleurodires and paracryptodires can be traced back to mutually exclusive land masses is not novel, but the realization that the early history of pan-cryptodires is restricted to Asia has not been realized previously, because traditional phylogenies implied an early, global presence of pan-cryptodires. The timing of the origin of the three primary clades of derived turtles (i.e., Pan-Pleurodira, Pan-Cryptodira, and Paracryptodira) correlates with the opening of the central Atlantic and the formation of the Turgai Strait in the Middle Jurassic, somewhat later than predicted by molecular calibration studies. The primary diversity of extant turtles therefore appears to have been driven by vicariance. A similar hypothesis could also be formulated for the three clades of basal turtles that survive at least into the Late Cretaceous, but given that their combined monophyly remains uncertain, it is unclear if their diversity was also driven by vicariance, or if they emulate a vicariance-like pattern. Although most groups remained within their primary geographic range throughout their evolutionary history, the dominant vicariance signal was thoroughly obfuscated by rich dispersal from littoral to marine turtles and crown cryptodires.

4.6

A Famennian Fossilagerstätte in the eastern Anti-Atlas of Morocco: its fauna and taphonomy

Christiann Klug¹, Linda Frey¹ & Martin Rücklin²

¹ *Paläontologisches Institut und Museum, Karl Schmid-Strasse 4, CH-8006 Zürich (chkflug@pim.uzh.ch)*

² *Naturalis Biodiversity Center, Postbus 9517, NL-2300 RA Leiden*

Nearly 80 years ago, French palaeontologists discovered Devonian fish remains in the Moroccan desert. Mainly placoderm skulls and shoulder girdles, acanthodian fin spines, sarcopterygian remains and locally abundant isolated shark teeth and fin spines have been recorded from the Tafilalt and Maïder regions. Although nearly the entire Devonian succession yields vertebrate remains, greater abundance and sometimes articulated specimens occur mainly in Frasnian and Famennian sediments.

The Famennian Fossilagerstätten of the eastern Anti-Atlas yielded morphologically complete placoderm and chondrichthyan skeletons in recent years. 3D-preserved skulls of chondrichthyans and onychodontid sarcopterygians offer the possibility to unveil aspects of their internal morphology using CT technology. In these cases, the skulls are embedded in the thickest parts of iron rich nodules. The concretions wedge out and the postcranial skeleton is often not contained or incomplete. Since the nodules are embedded in deeply weathered claystones, the postcranial skeletons are usually heavily fragmented and nearly impossible to extract and prepare. Sometimes parts of the dermal scales and body outline are preserved, documenting the overall morphology of the fishes.

Remarkably, these vertebrate fossils are associated with the oldest documented cases of pseudoplanktonic crinoids, *Moroccocrinus* and *Mrakibocrinus*, which lived attached to drift wood. Additionally, a layer with phyllocarid crustaceans, sometimes with appendages, underpins the identification as Konservatagerstätte, remotely reminiscent of the Jurassic Holzmaden Posidonia Slate or the Devonian Hunsrück Slate. Vertebrates and phyllocarids occur in flat highly ferruginous nodules containing iron oxides and hydroxides. These are most likely products of a deep weathering of pyrite. Fresh samples extracted from below the weathered zone contain pyritic ammonoids, confirming this hypothesis and suggesting sedimentation in oxygen depleted conditions.

4.7

Morphometric analysis of teeth of fossil and recent carcharhinid selachians

Dr. Ronny Maik Leder¹

¹ *Florida Museum of Natural History, University of Florida, 1659 Museum Road PO Box 117800, Gainesville, FL 32611-7800, USA (leder.ronnymaik@flmnh.ufl.edu)*

The morphological variability of dental structures of carcharhinid sharks within and between the different specimens is insufficiently investigated. Without knowledge of the species specific parameter exact taxonomic classification of fossil sharks based on their teeth is nearly impossible.

A comprehensive analysis of dental structures of recent carcharhinid sharks for species specific attributes was used to transfer the results to their next fossil relatives. Special attention was directed to morphological comparison between fossil teeth from West Atlantic and Central Asian origin.

Against existing methods a morphometric analysis model was developed that avoids manual data collection by reducing the shape data with a matrix of different transcription methods like distance transformation. The new method of automatic algorithmic morphometry (AAM) defined the crucial species specific attribute complexes by analysing more than 3000 single teeth from 120 individuals of 41 species of recent carcharhinids and transferred the data into a new developed analysis program along with a special database.

The individual study of every single specimen in terms of ontogenetic, sexual respectively mono- / digynath heterodonty as well as intra- and interspecific variance in tooth morphology proofed the fact that identifying carcharhinid sharks just by means of tooth morphological attributes is possible and that these attributes are qualified for systematic purposes. The success of the systematic classification is highly depending on the tooth position and the investigated species. The heterodonty influence on the taxonomic significance is occasionally tremendous which strongly reduces the unambiguity of the classification.

An enormous bandwidth in morphological overlap and interpenetration within the several species as well as across species and genus level is existing. Within the comprehensive study using just single teeth of fossil or recent origin it is sometimes impossible to clarify if there is just an innerspecific variance or already a species specific difference.

From the results of the morphometric analysis and the transfer of the data to the fossil record resulted the necessity to evaluate fossil teeth of carcharhinid sharks not just with the existing descriptive methods of taxonomy but also to use more aspects of functional morphology. Therefore six functional morphologic groups were defined for the first time whereby ecological conclusions are possible.

REFERENCES

Leder, R., M. 2014: Morphometrische Analyse der Kieferbezahnung fossiler wie rezenter carcharhinider Selachier, Leipzig, Univ. Diss. 2014, 399 S. 111 graph. Darst., +1 CDROM

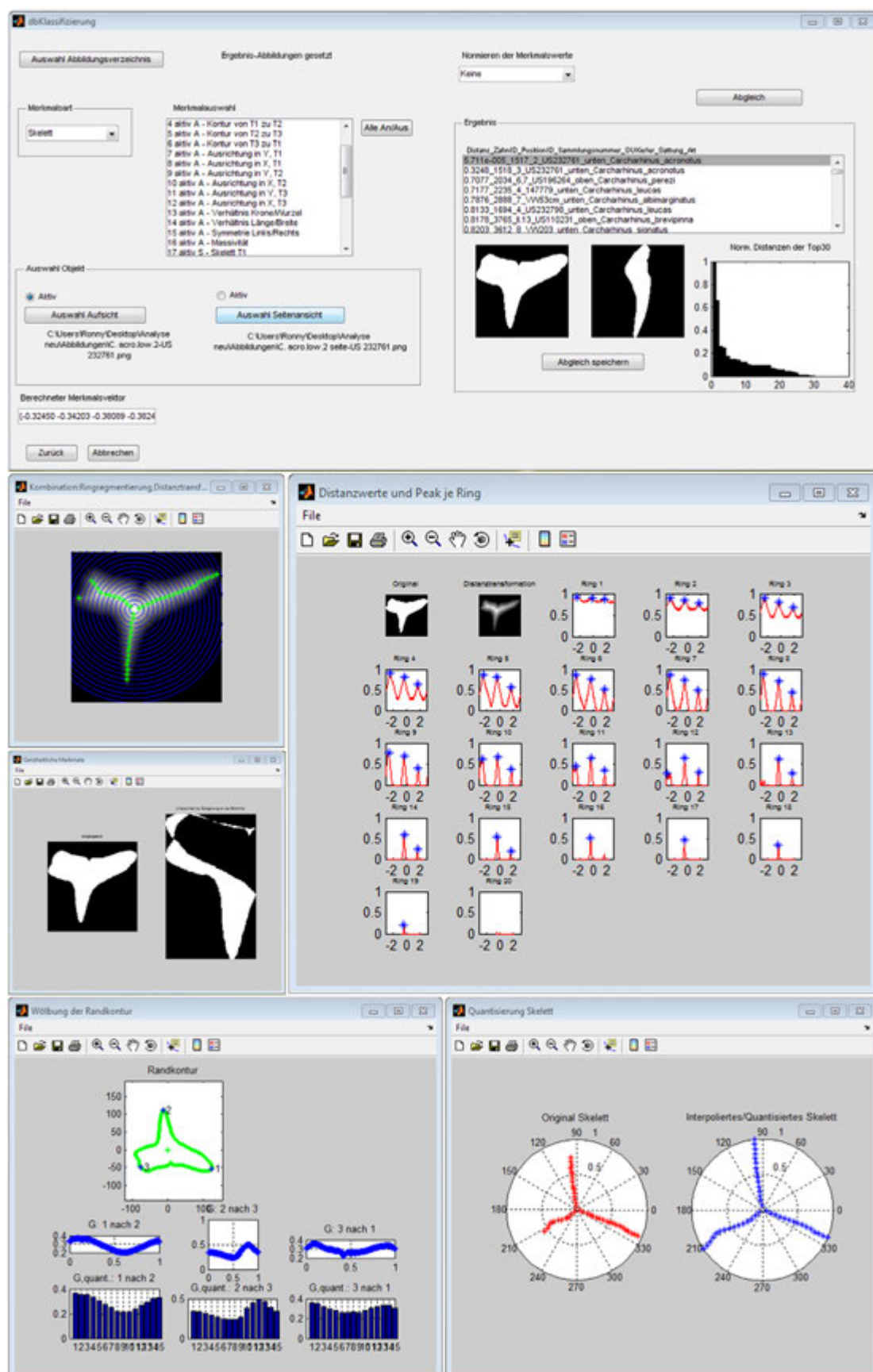


Figure 1. classification mask of the morphometric analysis program (AAM) with the transcription components of the data reduction. Leder 2014

4.8

The diversity of Pleistocene Camelidae in El Kowm, Syria: craniodental remains

Pietro Martini^{1,2}, Loïc Costeur², Peter Schmid^{1,3}, Reto Jagher¹, Jean-Marie Le Tensorer¹

¹ Institut für Prähistorische und Naturwissenschaftliche Archäologie, University of Basel, Spalenring 145, CH-4055 Basel (pietro.martini@unibas.ch)

² Naturhistorisches Museum Basel, Augustinergasse 2, CH-4001 Basel

³ Evolutionary Science Institute, University of the Witwatersrand, Private Bag 3, Wits 2050, South Africa

Family Camelidae (Artiodactyla, Mammalia) includes some very important domestic animals from the Old World and South America, such as Bactrian camel, dromedary, llama and alpaca. However, the origins of the family and most of its fossil species were found in North America. The first camels are known from the middle Eocene (Uintan NALMA, ~45 Ma) (Honey et al. 1998), while their maximal diversity was reached in the Miocene, when at least 13 genera and 20 species lived at the same time (Semprebon and Rivals 2010). Camelids colonized Eurasia and South America at the end of the Miocene, and went extinct in North America at the end of the Pleistocene.

The first camelids known in the Old World are recorded in the late Turolian (MN13, Messinian, ~6 Ma) (Van der Made et al. 2002) and are included in *Paracamelus*. Early species were much larger than modern camels; later species survived in the Black Sea region until the early Pleistocene (~2 Ma). This genus is considered paraphyletic (Geraads 2014) and was ancestral to the modern forms. Four fossil species of *Camelus* have been described: *C. grattardi* GERAADS 2014 (Ethiopia, 2.2 Ma), *C. sivalensis* FALCONER & CAUTLEY 1836 (Indian subcontinent, 2 Ma), *C. thomasi* POMEL 1983 (Algeria and Morocco, middle Pleistocene) and *C. knoblochi* NEHRING 1901 (Russia and central Asia, middle-late Pleistocene).

Although the North American fossil record is well studied, the diversity and evolution of camelids in the Old World is poorly known, with few species accurately described and unclear phylogenetic relationships. In particular, there is no founded hypothesis about the ancestry or the domestication of the two recent camel species (*Camelus bactrianus* and *C. dromedarius*).

There are few Old World sites with abundant camel fossils that may help clarify this issue. One of them is the El Kowm Basin, Central Syria. The composed stratigraphic sequence from the several sites in this region spans from the Early Pleistocene (1.8 Ma) to the Late Pleistocene (50 Ka), and is very rich in archaeological and paleontological remains (Le Tensorer et al. 2011). The fauna is dominated by Camelidae, Equidae, Rhinocerotidae and Bovidae (gazelles, larger antelopes and buffaloes) with scarce remains of Carnivora, Suidae, Elephantidae, Struthionidae, Testudinidae. This composition suggests the same arid steppe environment as existing today. The fauna includes the same major taxa throughout the sequence, but the species represented varied over time.

Paleontological studies of the El Kowm collection are underway. Here we present provisional result, with a focus on the cranial and mandibular remains of camelids. In this study we include samples from the three sites of the El Kowm Basin that were excavated by the University of Basel: Nadaouiye Aïn Askar, Hummal and Aïn al Fil. Together, they cover most of the temporal sequence known from the region.

The mandibular material can be divided into two well-defined, very different morphological groups. The first is a sample of 9 specimens from the Mousterian cultural levels in Hummal, which are archaeologically firmly dated to the Late Pleistocene (130-50 Ka). The second is a single specimen from the Upper Acheulean levels of Nadaouiye Aïn Askar, which are dated to the Middle Pleistocene (520-320 Ka). There is only one fairly complete cranium, also from Nadaouiye. Both the cranium and the two forms of mandibula are unlike any known form and likely represent new species. Additional fragmentary material from these and from other layers suggests an even greater morphological diversity.

The cranial and postcranial material studied so far indicates that a minimum of five camel species differing in size and morphology lived in the El Kowm area over the last 1.8 Ma. This number is already greater than the total of fossil *Camelus* species known to date. However, the actual diversity of camelids in El Kowm was likely even higher: there are non-diagnostic specimens that cannot be assigned to the well-known forms, and most of the material is unstudied yet. Therefore, this region provides a unique opportunity to study the evolution of these charismatic animals.

REFERENCES

Geraads, D. 2014. *Camelus grattardi*, sp. nov., a new camel from the Shungura Formation, Omo Valley, Ethiopia, and the relationships of African fossil Camelidae (Mammalia). *Journal of Vertebrate Paleontology* 34:1481-1485.

- Honey, J. J., J. A. Harrison, D. R. Prothero, and M. S. Stevens. 1998. Camelidae. Pp. 439-462 in *Evolution of Tertiary Mammals of North America: Terrestrial Carnivores, Ungulates, and Ungulatelike Mammals* (C. M. Janis, K. Scott and L. L. Jacobs, eds.). Cambridge University Press, Cambridge.
- Le Tensorer, J.-M., V. von Falkenstein, H. Le Tensorer, and S. Muhesen. 2011. Hummal: A very long Paleolithic sequence in the steppe of Central Syria - Considerations on Lower Paleolithic and the beginning of Middle Paleolithic in The Lower and Middle Palaeolithic in the Middle East and Neighbouring Regions (J. M. Le Tensorer, R. Jagher and M. Otte, eds.). *Etudes et Recherches Archéologiques de l'Université de Liège (ERAUL)*, Liège.
- Semprebon, G. M., and F. Rivals. 2010. Trends in the paleodietary habits of fossil camels from the Tertiary and Quaternary of North America. *Palaeogeography, Palaeoclimatology, Palaeoecology* 295:131-145.
- Van der Made, J., J. Morales, S. Sen, and F. Aslan. 2002. The first camel from the Upper Miocene of Turkey and the dispersal of the camels into the Old World. *Comptes Rendus Palevol* 1:117-122.

4.9

Processing and analysis with 'Cadence Toolset' of Late Jurassic dinosaur track data systematically acquired during ten years of excavations prior to construction of Highway A16, NW Switzerland

Daniel Marty^{1,1}, Kent A. Stevens², Scott Ernst¹, Géraldine Paratte¹, Christel Lovis¹, Marielle Cattin¹, Wolfgang A. Hug¹ and Christian A. Meyer³

¹ Office de la Culture, Paléontologie A16, 2900 Porrentruy 2, Switzerland,
e-mail: daniel.marty@jura.ch, martydaniel@hotmail.com ('corresponding author')

² Department of Computer and Information Science, University of Oregon, OR 97403, USA

³ Naturhistorisches Museum Basel, Augustinergasse 2, 4001 Basel, Switzerland

Excavations along Highway A16 by the Palaeontology A16 from 2002-2011 recorded 59 ichnoassemblages (>17,000 m²) comprising nearly 14,000 tracks (including 254 sauropod and 409 tridactyl trackways), providing systematic documentation (field measurements, sitemaps, (ortho)photographs, 3D-laser scans), plus the preservation of 700 track-bearing slabs and 200 casts with a total surface of >700-800 m².

The track data are currently in the processing (standardisation, cross-checking) and analysis phase (2012-2018), whereas vectorising of sitemaps (global track positions) and assembling of trackway parameter measurements (relative track positions) in a data base are important tasks, constituting the two major, non-relational data sets.

Since 2012 an ichnological data base and software toolset called 'Cadence' has been developed and used to extract and integrate information from the sitemaps with the trackway parameter measurements to create an extensive trackway data base for statistical data-mining and analyses. 'Cadence' introduces to ichnology the explicit association of uncertainty estimates with all quantitative data, entered through an interactive 3D-graphical interface.

Uncertainty estimation helps control the propagation of error within computations, and permits sophisticated, multivariate statistical analyses between and within individual trackways based on the internal integrity of relative and global measurements. 'Cadence' permits exploration of potential relationships with a minimum of a priori conventional assumptions about the trackmakers (such as of hip height, gleno-acetabular distance, gauge, gait), and may provide more defensible conclusions about trackmaker size, identity, locomotion, and even social behaviour and interactions.

This approach builds from a purely geometrical description of the data by avoiding pitfalls such as the subjective interpretation of a smooth 'trackway path' and by introducing 'curvature', a geometrical curved trackway path that will necessarily be described in terms of uncertainty and with minimal biological interpretation.

The Cadence Toolset is applicable to other data sets in the animal kingdom and collaborations (e.g., of 3D-track morphometric variation, substrate properties and mechanics).

4.10

A new approach to determine the phylogenetic relevance of the bony labyrinth: the case of the Cervid lineage

Bastien Mennecart¹ & Loïc Costeur¹

¹ Natural History Museum, Basel, Augustinergasse 2, CH-4001 Basel, Switzerland (mennecartbastien@gmail.com)

In the last decade, studies based on inner ear morphology flourished thanks to easier access to computer tomography. This structure is deeply associated to the locomotor system and proved to be a source of relevant phylogenetic information. Inner ears in Mesozoic mammals, marsupials, xenarthrans, elephants, primates, or rodents are currently under study, while that of ruminants, (one of the most diversified group of living large mammals) remains understudied (Costeur 2014). These analyses usually present classical descriptions, but morphometrics and geometric morphometrics have started to be employed. Unfortunately, the use of geometric morphometrics provides a phenotypic tree and these studies often fail to account for intraspecific variability. Moreover, many discrete morphological characters cannot be taken into account in such analyses.

Here we propose to test the phylogenetic relevance of the inner ear morphology based on comparisons of this structure in extinct and extant Cervidae. Stem antlered Cervidae such as *Procervulus* and *Lagomeryx* are known as far back as 18 Ma. The relationships within the living deer are stable and the phylogenetic trees resulting from molecular data (mitochondrial and nuclear) are similar. However, no phylogeny based on morphological characters alone reflects the molecular-based results. Moreover, controversial results on divergence time between the groups have been proposed, mainly because of the lack of consensus on the relationships among the fossil cervids. For example, the emblematic *Megaloceros* is part of the basal radiation of *Cervus* according to molecular data, of the *Dama* radiation in combined analyses (molecular and morphological), or even closely related to the “basal Cervini” *Eucladoceros* when morphological characteristics are taken into account (e.g. Lister *et al.* 2005).

Using a superimposition process (“Landmarks” software), direct comparison between selected inner ears was made. We observed the bony labyrinth of 21 cervid species, including all living tribes and several taxa from key periods: the Early Miocene (origin of stem deer), the Middle Miocene (possible crown deer) and the Plio-Pleistocene (origin of today’s disparity). Intraspecific variability was characterized. Between two specimens (*Capreolus capreolus*, extant) and six specimens (*Procervulus praelucidens*, Early Miocene), the differences between juveniles and adults, or intraspecific variability are observed.

Similarly to what is observed among the Tragulidae ruminants (Costeur and Mennecart, in prep), no large intraspecific differences are observed. The size of the semicircular canals and the angle between the canals may vary a little, such as the size of the endolymphatic sac. The total cochlea length can also vary by as most as half a turn. However, these differences are smaller than the interspecific variability. Stem deer can easily be distinguished in having the plesiomorphic characters of a large first cochlear turn, a vestibular aqueduct that is aligned with the common crus. The distinction between the living Capreolinae and Cervinae can be made on the basis of the insertion of the lateral semicircular canal into the posterior ampula. Cervinae retain the primitive aspect having a high insertion, while in the Capreolinae, the connexion is lateral. This Capreolinae apomorphic state demonstrates that *Croizetoceros pyreanicus* is the oldest indubitable Capreolinae (6 Ma), even if Late Miocene species have been tentatively attributed to this subfamily (Croitor & Stefaniak 2009). The differences between the various tribes and subtribes can be done based on the shape and position of the endolymphatic sac. Looking at the inner ear morphology, *Megaloceros* clearly differs from *Eucladoceros* in having a triangular endolymphatic sac, starting below the end of the common crus, much like in *Dama*. On the contrary, *Eucladoceros* possesses a very elongated endolymphatic sac starting above the common crus. This may be the apomorphy of the *Cervus-Rusa* lineage that would include “*Cervus*” *ruscinensis* as the oldest known representative, dating back to 5 Ma. The general morphological similarities between *Megaloceros* and *Eucladoceros* observed in previous phylogenetic analyses are probably linked to symplesiomorphic characteristics and common evolutionary trends in gigantic size and heavy antlers such as proposed by Vislobokova (2013).

REFERENCES

- Costeur L. 2014: The petrosal bone and inner ear of *Micromeryx flourensianus* (Artiodactyla, Moschidae) and inferred potential for ruminant phylogenetics. *Zitteliana Reihe B*, 32, 1–16.
- Costeur L. & Mennecart B. in prep: Intraspecific variability of the inner ear structure within the lesser mouse-deer (*Tragulus kanchil*). *Journal of mammalian evolution*.
- Croitor R., Stefaniak K. 2009: Early Pliocene deer of Central and Eastern European regions and inferred phylogenetic relationships. *Paleontographica Abteilung A*, 287, 1–39.
- Lister A.M., Edwards C.J., Nock D.A.W., Bunce M., van Pijlen I.A., Bradley D.G., Thomas M.G., & Barnes I. 2005: The

- phylogenetic position of the “giant deer” *Megaloceros giganteus*. *Nature*, 438, 850–853.
- Vislobokova I.A. 2013: Morphology, Taxonomy, and Phylogeny of Megacerines (Megacerini, Cervidae, Artiodactyla). *Paleontological Journal*, 47(8), 833–950.

4.11

The Late Triassic bonebed of Niederschönthal (Norian, Knollenmergel, Füllinsdorf BL) – Amanz Gressly's dinosaur locality revisited

Christian A. Meyer¹, & Andreas Wetzel²

¹ Naturhistorisches Museum Basel, Augustinerstrasse 2, CH-4001 Basel, (christian.meyer@bs.ch)

² Geologisch-Paläontologisches Institut, Universität Basel, Bernoullistrasse 32, CH-4056 Basel

Since its initial discovery in 1856 the locality of the first Swiss dinosaur remains on the riverbank of the Ergolz (Niederschönthal, Füllinsdorf BL) has almost fallen into oblivion (Rütimeyer 1856). Apart from the description of the remains of *Plateosaurus* (Huene 1908 = *Gresslyosaurus*) discovered by the Swiss iconic geologist Amanz Gressly not much attention was given to this locality. In 1901 Karl Strübin excavated at the same locality without much success (Strübin 1901a,b). Later on, Tanner (1978) shortly described the section and the fossil remains that were collected at the locality during construction work. However, up to now neither the associated fossils nor the depositional environment have gained much attention. Similarly, at the famous *Plateosaurus* locality in Frick (AG) the faunal content was studied in some detail, but the environmental setting is just assumed. In 2009 the original locality was temporarily exposed again during the renovation of the small bridge over the river Ergolz and the section was revisited by C. Meyer.

Apart from the well known cranial and postcranial remains of *Plateosaurus*, in Niederschönthal the associated fauna and flora is poorly known compared to the coeval deposits of the Frick locality. Re-examination of the specimens collected by Gressly and others stored in the collection of the Natural History Museum Basel revealed the presence of a highly diverse fauna. Phytosaur remains (osteoderms, vertebrae, cranial fragments, long bones, ilia) constitute the dominant elements belonging to *Myriosuchus* Huene 1911. Large coniform coprolites, some with freshwater clams inside are also frequent. Plant remains as well as rounded pebbles of charcoal have been collected. Teeth of small theropods, a single plastron fragment of a ?terrestrial turtle and fish teeth are also present as well as remains of hybodontid sharks. The overall aspect of the fauna points to a terrestrial habitat having freshwater ponds and rivers. Postcranial material of *Plateosaurus* is also known from a locality further upstream (ARA Liestal; Museum.BL) that still awaits its description.

Whereas Tanner (1978) attributed a Rhaetian age to the bonebed and interpreted it as a lagoonal deposit in a marine environment, we suggest a Norian age and a somewhat different depositional setting. The sedimentary succession indicates an alluvial plain environment. Channels fill deposits with embedded caliche nodules and bones of varying state of preservation point to short-term high energy “pluvial” events that washed away soils and carcasses of terrestrial vertebrates from the catchment area. The top of these channels contain large fragments of wood that appear to be current aligned. The mud deposits most probably resulted from overbank sedimentation or sheetfloods. Intercalated fine sandstones with numerous thin-shelled pelecypods are seen as indication of a playa lake environment.

In contrast, the dinosaur beds of Frick contain many articulated skeletons of *Plateosaurus*. A complete skeleton of a small coelophysoid theropod with a sphenodontid in its stomach still awaits a formal description. Isolated theropod teeth of unknown affinity are frequent and a complete carapace of a turtle *Proganochelys* was found in a nearby locality. Previous studies suggest a miring of the prosauropods (Sander 1992) based on the taphonomy of the articulated skeletons. This might be the most plausible scenario for some beds although up to now sedimentological evidence is missing. However some bones in both localities (Frick, Niederschönthal) show deep cracks indicating intensive weathering during long time exposure on the sediment surface. The latter is also known from the famous *Plateosaurus* bone beds of Trossingen (Schoch & Seegis 2013).

The disparity in the faunal composition might either reflect a different taphonomic history or distinct habitats. In order to understand the sedimentary environment as well as the Late Triassic continental ecosystems of northern Switzerland a detailed sedimentological analysis of the dinosaur beds of Frick is in dire need.

REFERENCES

- Huene, F. 1908: Die Dinosaurier der europäischen Triasformation. Geol. Paläont. Abh. N.F. 10/1.
 Huene F. v. 1911: Die jungtriassische Wirbeltierfauna von Niederschönthal bei Basel. Centralblatt Mineral. Geol. Paläont. 13, 422-424.
 Schoch, R. & Seegis, D. 2014: Taphonomy, deposition and pedogenesis in the Upper Triassic dinosaur beds of Trossingen. Palaeobiodiversity and Paleoenvironments. DOI 10.1007/s12549-014-0166-8.
 Strübin, K. 1901a: Neue Aufschlüsse in den Keuper-Liasschichten von Niederschönthal (Basler Tafeljura). Eclogae geol. Helv. 7/2, 119-123.
 Strübin, K. 1901b: Neue Untersuchungen über Keuper und Lias bei Niederschönthal (Basler Tafeljura). Verh. Natf. Ges.

- Basel 13, 586-602.
- Rütimeyer, L. 1856: Fossile Reptilknochen aus dem Keuper (in der Nähe von Liestal). Verh. Schweiz. Natf. Gesellschaft 41, 62-64.
- Sander, P. M. 1992: The Norian *Plateosaurus* bonebeds of central Europe and their taphonomy. *Palaeogeography, Palaeoclimatology, Palaeoecology* 93:255-299.
- Tanner, K. M. 1978: Die Keuper-Lias Fundstelle von Niederschönthal, Kanton Baselland. Bull. Ver. Schweiz. Petroleum-Geol. & Ing. 44/106, 13-23.

Fig.1 Stratigraphy of Late Triassic sequence of the Ela Park

Figure 2. 3D contour model of a prosauropod manuspes couple (Uglix Plattenkalk Member, Hauptdolomit Group; Val Gravaratschas, Ela Park)

4.12

The Norian and Rhaetian dinosaur tracks of eastern Switzerland in the light of sequence stratigraphy

Meyer, Christian A.¹, Thüring, Silvan², Wizevich, Michael³, Thüring, Basil¹ & Marty, Daniel¹

¹ Naturhistorisches Museum Basel, Augustinerstrasse 2, CH-4001 Basel, (christian.meyer@bs.ch)

² Naturmuseum Solothurn, Klosterplatz 2, CH-4500 Solothurn, Switzerland

³ Department of Geological Sciences, Central Connecticut State University, USA;

Prosauropod and theropod footprints from the middle and upper part of the Hauptdolomit Group (HDG; Mid to Late Norian) from the Upper Austroalpine Ela Nappe in the Parc Ela nature park (Canton Graubünden; southeastern Switzerland) and the Swiss National Park (Engadin Dolomites) provide important information on the paleobiogeographic distribution of the early dinosaurs (Meyer et al. 2010). Up to now, seven levels with dinosaur tracks have been detected in a stratigraphic range spanning the Norian to Late Rhaetian (Fig 1; Meyer et al. 2013). The large theropod tracks from Parc Ela attributed to the ichnotaxon *Eubrontes* (UPM:Uglix Plattenkalk Member of the HDG Group) and those from the Swiss National Park (Diavel Formation) together with the record from the coeval Dolomia Principale of the Tre Cime di Lavaredo (Dolomites, Italy) are the oldest unequivocal evidence of very large theropod dinosaurs. Furthermore trampled surfaces in the upper part of the HDG (Fig.1, 1; Ela Park; Late Alaunian to Early Sevatian) at three different locations indicate the presence of large dinosaurs. At the boundary between the HDG and the Kössen Formation (Aelpliorn Member) a trackway with deep quadradactyl pes prints as well as tridactyl manus prints can be attributed to a facultative bipedal prosauropod (Fig.1, 3; Fig. 2) In the youngest part of the Kössen Formation (Fig 1, 7; Silvaplana Member) sauropod tracks are also present.

The UPM contains at least 3 different levels with tracks (Fig. 1,2-4) the lowermost is a laterally persistent surface that is heavily trampled, these are probably associated with a 4th order sequence boundary. The exact sequence stratigraphic position of the trackbearing levels in the Swiss National Park remains to be determined. The levels in the Diavel Formation are most likely time equivalent with the trampled levels in the middle part of the HDG of the Ela Park. It seems quite possible that the highest levels in the Murtèr Formation and Murteret Dolomite are coeval with those in the UPM. The uppermost track level in the UPM corresponds to the No2 third-order sequence boundary (Gianola & Jacquin, 1998; McCann 2008; Alaunian/Sevatian boundary). This stratigraphic unit is time equivalent with the Knollenmergel of the Keuper that has yielded numerous skeletons of the prosauropod *Plateosaurus*. The sauropod tracks in the Silvaplana Member appear to be situated close to the Rh 2 third-order sequence boundary at the end of a shallowing upward cycle.

The track levels that have been detected in the Dolomites seem to be slightly older than previously suggested by Belvedere et al. (2014). According to our own field observations, the tracks that have been found in the Tre Cime di Lavaredo (Capella Alpini, Cima Piccola, Cima Ovest) and the Averau area are most likely situated at the No1 third-order sequence boundary (Lacian/Alaunian boundary) and therefore older than those from the Swiss sites.

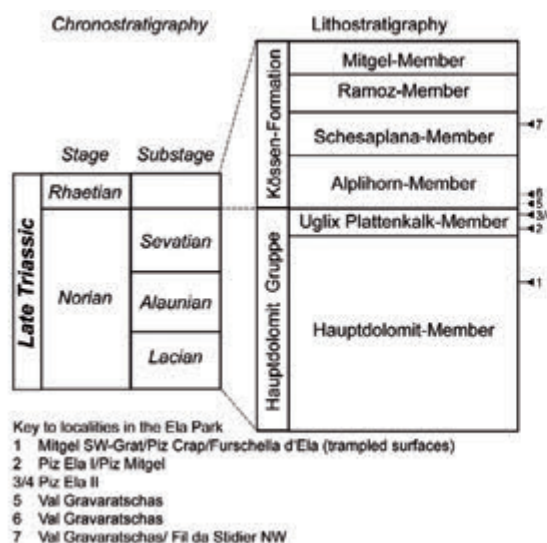


Fig.1 Stratigraphy of Late Triassic sequence of the Ela Park

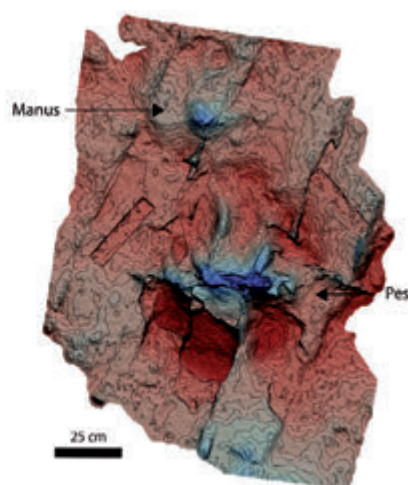


Figure 2. 3D contour model of a prosauropod manus and pes prints (Uglix Plattenkalk Member, Hauptdolomit Group; Val Gravaratschas, Ela Park)

REFERENCES

- Belvedere, M., Mietto, P. & Meyer, C.A. 2014: Timing and ichnotaxonomy of the oldest dinosaur tracks in the Dolomites and adjacent Switzerland. 12th Meeting of the European Association of Vertebrate Palaeontologists, Torino, Abstract Volume, p. 16.
- Furrer, H. & Lozza, H. 2008: Neue Funde von Dinosaurierfährten im Schweizerischen Nationalpark. *Cratschla* 1, 17–21.
- Gianolla, P. & Jacquin, T. 1998: Triassic sequence stratigraphic framework of Western European Basins. In: *Mesozoic and Cenozoic Sequence Stratigraphy of European Basins*, SEPM Special Publication 60, 643–650.
- McCann, T. 2008: *The Geology of Central Europe. Vol. 2: Mesozoic and Cenozoic*. The Geological Society, London
- Meyer, C.A., Thüring, B., Costeur, L. & Thüring, S. 2010: Tracking early dinosaurs – new discoveries from the Upper Austroalpine Nappes of Eastern Switzerland (Hauptdolomit, Norian). 8th Meeting of the European Association of Vertebrate Palaeontologists, Abstract Volume, Aix-en-Provence, p. 58.
- Meyer C.A., Marty, D., Thüring, B., Stecher, R. & Thüring, S. 2013: Dinosaurierspuren aus der Trias der Bergüner Stöcke (Parc Ela, Kanton Graubünden, SE-Schweiz). *Mitteilungen der Natforschenden Gesellschaft beider Basel* 14, 135–144.

4.13

Evolution and paleobiogeography of reef biota in the Panthalassa domain during the Late Triassic: insights from reef limestone of the Sambosan Accretionary Complex, Japan

Camille Peybernes¹, Jérôme Chablais², Rossana Martini¹

¹ *Department of Earth Sciences, University of Geneva, Rue des Maraîchers 13, CH-1205 Genève*

² *Geneva Petroleum Consultants International, CH-1211 Genève*

Paleoecology and paleobiogeography of Triassic reef biota are mainly based on the investigation of Tethyan and East Panthalassa reef localities. Conversely, western Panthalassa reef biota were poorly documented until recently. Therefore, reef limestone occurrences from the western Panthalassa domain are pivotal to understand the global Triassic reef evolution. In this contribution, we investigate Upper Triassic reef limestone from the Sambosan Accretionary Complex (Japan), aiming at improving our knowledge of the Upper Triassic reef ecosystem in the huge Panthalassa domain.

The Upper Triassic carbonates from the Sambosan Accretionary Complex record the evolution of diversified shallow water environments from the initiation of the carbonate platform during the Ladinian?-Carnian to its demise in the Rhaetian. Accordingly, the Sambosan limestone yield valuable insights regarding the reef recovery and development that took place during the Middle and Late Triassic. These profound environmental changes and biotic turn over are well-known in the Tethys but poorly documented in the Panthalassa.

Our results provide additional constrains for understanding the evolution and the biogeographic distribution of Upper Triassic reef biota. Quantitative microfacies analysis, combined with an integrated biostratigraphy (i.e., reef biota associations together with conodonts and foraminifer biostratigraphic markers), allow us to well characterize both Ladinian?-Carnian and Norian-Rhaetian reef bioconstructions in the Sambosan limestone. To quantitatively compare the Sambosan reef biota with their counterparts, we compiled the occurrences of 186 genera of calcareous sponges, microproblematica and foraminifers from 18 reef areas located in the Tethys and Panthalassa oceans. Multivariate statistics (cluster analyses and ANOSIM tests), based on this taxonomically homogenized dataset, strengthen the Tethyan affinity of the reef biota from the Sambosan Accretionary Complex.

This original study refines the biostratigraphic framework of the shallow water carbonates of the Sambosan Accretionary Complex, considered here as representative of West Panthalassa atoll-type environments. These findings highlight the long geological history of carbonate build-ups in the Panthalassa during the Late Triassic and emphasize the biogeographic connections with the Tethyan domain.

4.14

Catalogues of the palaeontological heritage from the A16 – Transjurane highway (Canton of Jura): example of the Mesozoic marine crocodilians

Schaefer Kévin, Hug Wolfgang Alexander, Billon-Bruyat Jean-Paul

Paléontologie A16, Section d'archéologie et paléontologie, Office de la culture, République et Canton du Jura, Hôtel des Halles, CP 64, 2900 Porrentruy 2 (kevin.schaefer@jura.ch)

After twelve years of intensive fieldwork and now sixteen years of scientific research, the Paléontologie A16 moves into its last three years of activity. Until 2018, and additionally to more than 60 scientific publications, nearly 150 conference presentations and 34 scientific collaborations with students on their way to access different academic degrees, the five remaining research groups will publish their scientific final reports.

One step towards the presentation of the large amount of data and the most important scientific results is the publication of an extensive documentation of the fossil collection, through a series of sixteen catalogues called "Catalogues du patrimoine paléontologique jurassien - A16". With this series of catalogues, the paleontological heritage of the Canton of Jura is made more attractive, for both scientists as well as for a more general public. This can contribute to future investigations such as comparisons with other collections, of contemporary age and from different European localities. Also, all catalogues show a methodological approach that could be applied to valorize other fossil collections.

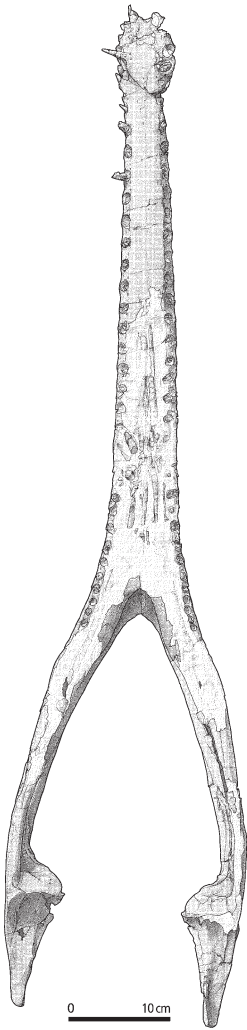
Here, we introduce this series with a catalogue dealing with the thalattosuchians (the Mesozoic marine crocodilians), from the Kimmeridgian of the region of Porrentruy (Schaefer 2012a, b; Schaefer & Billon-Bruyat 2014). This catalogue shows the most representative specimens of the collection, in order to indicate both the taxonomic diversity and the kind of preserved material. The standardized sheets are composed of scientific (systematics, anatomy, stratigraphy, locality) and technical (related illustrations, analyses, bibliography) information, and specimens' illustrations (photographs, drawings). Two families, four genera and five species are represented (the teleosaurids *Steneosaurus jugleri*, *S. cf. bouchardi*, *Machimosaurus hugii*, and the metriorhynchids *Metriorhynchus* sp., *Dakosaurus maximus*), by means of 36 specimens (including skeletons, isolated cranial and post-cranial elements). In conclusion, this catalogue gives a good and quick scientific overview of this crocodilian collection; it will be a helpful tool for future research, conservation, visits and exhibitions.

We gratefully acknowledge all implied experts, such as excavation teams, fossil preparators, illustrators, editors and scientists, which have been involved in the compilation of the document. Our special thanks also go to the Federal Roads Office (FEDRO) and the Canton of Jura (RCJU) for financing this work.

Teleosauridae, *Steneosaurus* cf. *bouchardi*
TCH006-1439



Détermination	
Famille: Teleosauridae	Anatomie: mandibule
Genre: <i>Steneosaurus</i>	Particularités: –
Espèce: cf. <i>bouchardi</i>	Détermination (nom / date): JPBB, KS / 2012
Stratigraphie	
Couche: 4500	Biostratigraphie: Eudoxus
Lithostratigraphie: Marnes à <i>virgula</i> inférieures	Chronostratigraphie: Kimméridgien supérieur
Formation: Reuchenette	
Site	
Nom: Courtedoux-Tchâfoué (CTD-TCH)	Coordonnées CH: 250421/568731
Unité: 56	Altitude absolue: 504,87m
Alignement (*N): –	
Figures	
Photos de studio	Photos de terrain
TCH006-1439_man_dor_E025_3703.jpg*	TCH006-1439_ens_3522.jpg*
TCH006-1439_man_gch_E025_3718.jpg*	TCH006-1439_ens_9591.jpg*
TCH006-1439_man_ven_E025_3699.jpg*	TCH006-1439_ens_9952.jpg*
	TCH006-1439_ens_20070914007-36.jpg*
Dessins scientifiques	Relevés de terrain
TCH006-1439_man_dor_E025_val.tif*	TCH006-r117 (1:10)
TCH006-1439_man_dor_E033_val.pdf	TCH006r.118 (1:1)
TCH006-1439_man_dor_E033_val.tif*	
Analyses	
Géochimie (δ ¹⁸ O phosphates)	
Bibliographie A16	
Schaefer K. 2012a: Variabilité de la morphologie dentaire des crocodiliens marins (Thalattosuchia) du Kimméridgien d'Ajoie (Jura, Suisse). Travail de Master non publié, Université de Fribourg, 111p.	
Schaefer K, Billon-Bruyat J.-P. 2014: The crocodilian <i>Steneosaurus</i> cf. <i>bouchardi</i> in the Kimmeridgian of Switzerland. Abstract, 12th Swiss Geoscience Meeting 2014, Fribourg, p. 135-136.	
Bibliographie utile	
Andrews C.W. (1913). A descriptive catalogue of the marine reptiles of the Oxford clay (Part II). British Museum (Natural History), 206 pp.	
Buffetaut E., Makinsky M. (1984). Un crâne de <i>Steneosaurus</i> (Crocodylia, Teleosauridae) dans le Kimméridgien de Villerville (Calvados). Bulletin trimestriel de la Société Géologique de Normandie et des Amis du Muséum du Havre 71, 19-24	



Excerpt from the catalogue: example of the mandible of *Steneosaurus* cf. *bouchardi* TCH006-1439 (Late Kimmeridgian, Courtedoux–Tchâfoué). On the left side: scientific and technical sheet. On the right side: scientific illustration of the specimen in dorsal view.

REFERENCES

Schaefer, K. 2012a: Variabilité de la morphologie dentaire des crocodiliens marins (Thalattosuchia) du Kimméridgien d'Ajoie (Jura, Suisse). Unpublished master thesis, University of Fribourg, 111 pp.

Schaefer, K. 2012b: Variability of the dental morphology in marine crocodilians (Thalattosuchia) from the Kimmeridgian of Ajoie (Jura, Switzerland). Abstract, 10th Swiss Geoscience Meeting 2012, Bern, 212–213.

Schaefer, K. & Billon-Bruyat, J.-P. 2014: The crocodilian *Steneosaurus* cf. *bouchardi* in the Kimmeridgian of Switzerland. Abstract, 12th Swiss Geoscience Meeting 2014, Fribourg, 135–136.

4.15

Intraspecific variation of volumetric growth trajectories in nautilids and ammonites

Amane Tajika & Christian Klug

Paläontologisches Institut und Museum, Universität Zürich, Karl-Schmid-Strasse 4 CH-8006 Zürich
(amane.tajika@pim.uzh.ch)

Ammonoids and nautilids are well-known, externally shelled cephalopods. While ammonoids went extinct at the end of the Cretaceous, nautilids survived. Because of their morphological similarity of the external shell, lots of palaeontologists have investigated Recent *Nautilus* as an actualistic example to better understand the obscure ammonoid palaeobiology. Despite all the research efforts to explore *Nautilus* ecology and anatomy, phragmocone (buoyancy apparatus) geometry and volume have not been sufficiently studied. However, ammonoids and nautilids are phylogenetically not the closest regardless of their similar external shells. Ammonoid phragmocones record both growth and palaeoecology. *Nautilus* phragmocones can be an important reference to palaeoecology of fossil nautilids since they have maintained nearly the same shell over a long period of time. Comparison of phragmocones of ammonoids and nautilids can provide important clues on differences in palaeoecology, which would have resulted in ammonoid extinction and nautilid survival at the end of the Cretaceous.

Only quite recently, empirical volume models of ammonoids have been reconstructed to calculate buoyancy (Lemanis et al., 2015; Naglik et al., 2015; Tajika et al., 2015). However, all these studies addressed only one specimen per species. These results may thus be biased due to intraspecific variation. Individuals may or may not represent be representative for the taxon. Here we present intraspecific variation of phragmocone chamber volumes in living *Nautilus pompilius* from the Philippines and of the Jurassic ammonite *Normannites* from Switzerland.

The reconstruction of the ammonite specimens was carried out using grinding tomography. The specimens were ground off and exposed surfaces were scanned in alternation with an increment of 0.06 mm, generating 422 images. Every 4th image was retraced in Adobe® Illustrator (Adobe Systems). Then the retraced image stacks were imported to VGstudiomax®2.1 (Volume Graphics) in which 3D models were constructed. By contrast, 30 *Nautilus* specimens (12 males, 9 females, 9 indeterminable) were reconstructed using Computed tomography. 30 specimens were scanned with a resolution in the range of 0.311 and 0.440 mm. Subsequently segmentation was conducted in Avizo®8.1 (FEI Visualization Sciences Group) and volumes of each chamber were extracted and measured in Meshlab (ISTL–CNR research center) and Matlab 8.5 (Math Works), respectively. The reconstructed two ammonites and a *Nautilus* are shown in Figure 1.

The volumetric growth trajectories of *Normannites* show a very similar trend during early to middle ontogeny. A considerable divergence occurred in late ontogeny, most-likely resulting in different buoyancy regulations. In the last several chambers, both specimens display a strong fluctuation of volumes. Growth trajectories from *Nautilus* showed a quite high variability, still following logistic curves. In *Nautilus*, chamber volumes were also reduced in latest ontogeny (only in the last chamber). Statistical tests suggest that the shells of the two sexes of *Nautilus* differ only slightly and that there is a strong overlap in morphology between the two sexes. Nevertheless, overall intraspecific variation of all specimens exceeds that of one sex only. Covariation between chamber widths and volumes in *Normannites* and *Nautilus* were assessed. The results suggest that *Normannites* are more flexible in shell construction. *Nautilus* appears to stick to a certain morphology, changing the shape much less than the Jurassic ammonite throughout ontogeny.

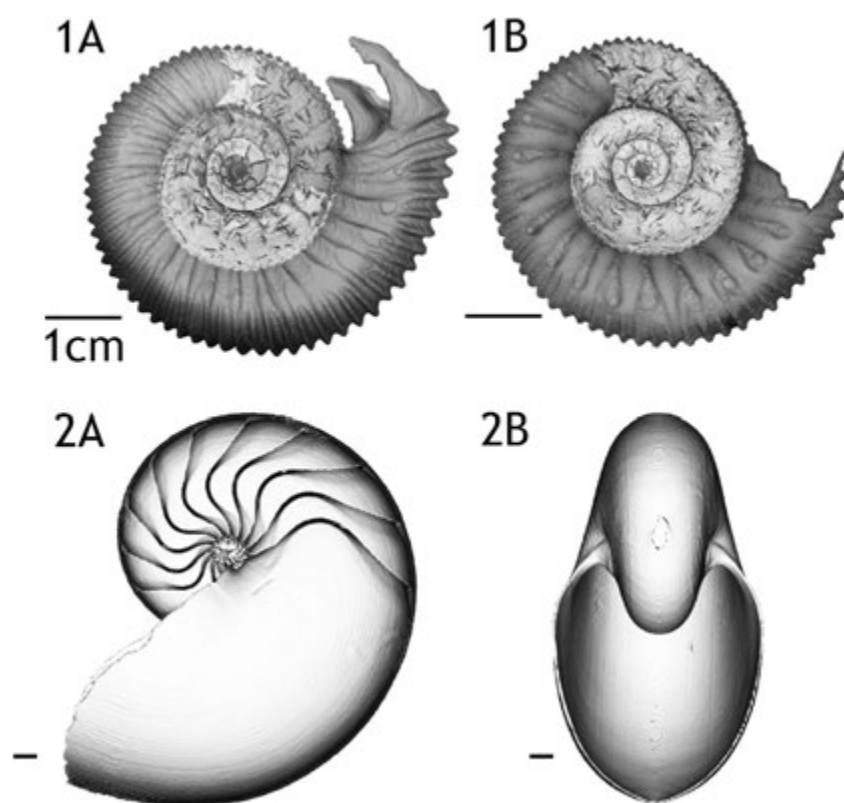


Figure 1. Reconstructed ammonites, *Normannites* and living *Nautilus*. (1A) *Normannites* Specimen 1; (1B) *Normannites* specimen 2; (1C) *Nautilus pompilius*.

REFERENCES

- Lemanis R, Zachow S, Fusseis F, Hoffmann R. 2015. A new approach using high-resolution computed tomography to test the buoyant properties of chambered cephalopod shells. *Paleobiology* 41(02):313–329.
- Naglik C, Rikhtegar F, Klug C. 2015. Buoyancy of some Palaeozoic ammonoids and their hydrostatic properties based on empirical 3D-models. *Lethaia*. DOI: 10.1111/let.12125.
- Tajika A, Naglik C, Morimoto N, Pascual-Cebrian E, Hennhöfer D, Klug C. 2015. Empirical 3D model of the conch of the Middle Jurassic ammonite microconch *Normannites*: its buoyancy, the physical effects of its mature modifications and speculations on their function. *Historical Biology* 27(2):181–191.

P 4.1

The Fossil Echinoids of the St. Ursanne Formation in the Swiss Jura Mountains

Eva A. Bischof

*Department of Geosciences, University of Fribourg, Chemin du Musée 6, 1700 Fribourg, Switzerland
(eva.bischof@unifr.ch)*

Since the beginning of the Triassic, echinoids play a prominent role in marine benthic communities (Kroh & Smith, 2010). Although echinoids reached their greatest level of diversity in shallow marine areas (Durham et al., 1966), they also populated the full spectrum of other marine habitats throughout their history, ranging from the poles to the equator and from the intertidal zone to the deep-sea. The echinoid skeleton is composed of a large number of individual elements with complex microarchitecture and therefore provides a rich basis for morphological studies. Given that the skeleton of echinoids is shaped by the environment (Sumrall & Brochu, 2008) and that they are common occurrences in the fossil record, echinoids can be considered to be facies fossils (Kroh & Smith, 2010) and the group therefore features prominently in evolutionary and paleobiological studies.

As part of my master's thesis, I am measuring nine lithostratigraphic profiles from the St. Ursanne Formation in the Swiss Jura Mountains and then correlating the carbonate microfacies of these localities with the fossil echinoids they contain. The latter step requires identifying more than 300 echinoid specimens to species level that were collected over the course of the last 200 years at these localities.

There are no previous studies for the St. Ursanne Formation that examined a possible correlation of echinoid taxa and their respective facies. This work is therefore expected to provide new insights into the sedimentology, lithostratigraphy and paleobiology of this formation.

REFERENCES

- Durham, J. W., Fell, H. B., Fischer, A. G., Kier, P. M., Melville, R. V., Pawson, D. L., Wagner, C. D. 1966: Treatise on Invertebrate Paleontology, Part U Echinodermata 3, Echinozoa-Echinoidea, The Geological Society of America.
- Kroh A., Smith, A. B. 2010: The phylogeny and classification of post-Palaeozoic echinoids. *Journal of Systematic Palaeontology*, 8, 147-212.
- Sumrall, C. D, Brochu, C. A. 2008: Viewing paleobiology through the lens of phylogeny. *Paleontological Society Papers* 14, 165-183.

P 4.2

Study of the microfauna from the Falun (Langhian, France): preliminary data on the Ostracoda

Bastien Mennecart¹ & Claudius M. Pirkenseer²

¹ *Natural History Museum, Basel, Augustinergasse 2, CH-4001 Basel, Switzerland (mennecartbastien@gmail.com)*

² *Université de Fribourg, Géologie, chemin du musée 6, CH-1700 Fribourg, Switzerland*

The « Falun » formation is a shelly sand, mainly Langhian in age (Middle Miocene). These deposits extend from the French Atlantic coastline, between Brittany and Vendée Regions to westwards to Orléans (Figure 1). It forms the ancient Ligerian Gulf along the current Loire river valley. Since the 18th century, the richness in fossils (e.g. the giant shark *Megaselachus megalodon*) permitted a systematic study of the area. A large diversity of marine invertebrates was described (e.g. more than 600 species of Mollusca). Between 1959 and 2000 more than 35 contributions on mammals were published by Léonard Ginsburg. However, until now, data on microfossils remains scarce. An overview of the regional ostracod fauna reported 53 species (Charrier & Carbonnel 1980), but those were not documented in detail. Benthic Foraminifera have been described for the area of Thenay (Margerel 2009).

Since 2007, the national inventory of geological heritage ("Inventaire National du Patrimoine Géologique") permits an overview of all the Falun localities (predominantly quarries). Prof. J.-J. Macaire and C. le Doussal (local advisor for Indre-et-Loire and Loire-et-Cher) and local authorities provided access to protected geological sites (regional natural geological reserve of Pontlevoy, geological reserve and protected area of Falun d'Amberre) and technical support. Falun deposits from Morvilliers (Chapelle-Saint-Martin-en-Plaine) are for the first time investigated since 50 years thanks to a backhoe. This area represents the most oriental extension of the formation (even if new marine vertebrate fossils are currently under study from the Ouzouer-le-Marché collections). Sediments from Villbarou, picked in a cellar, are also under study. The construction of a new road in falun deposits provided rich vertebrate remains at the industrial zone of Contres (Loir-et-Cher).

A comparison of the fossil record from 15 different localities and 20 different facies is in progress in the oriental part of the "Falun Sea". Initially a study on the ostracod assemblages will be carried out. A preliminary appraisal of several samples allowed the identification of at least 50 species, at least one possibly new. The presence of the genera *Aurila*, *Costa*, *Cytherelloidea*, *Cytheretta*, *Loxoconcha*, *Olimfalunia*, *Cytheridea* (amongst others) indicate shallow marine to nearshore environments, comparable to those reported from the Serravalian of the Aquitaine Basin (e.g. Ducasse & Cahuzac 1997). Even though the variability of the assemblages between the individual localities is rather low (except the species richness), we can observe large differences in the preservation and abundance of the material (from well preserved to eroded, perforated specimens), indicating differences in the environment and position of the Langhian coastline.

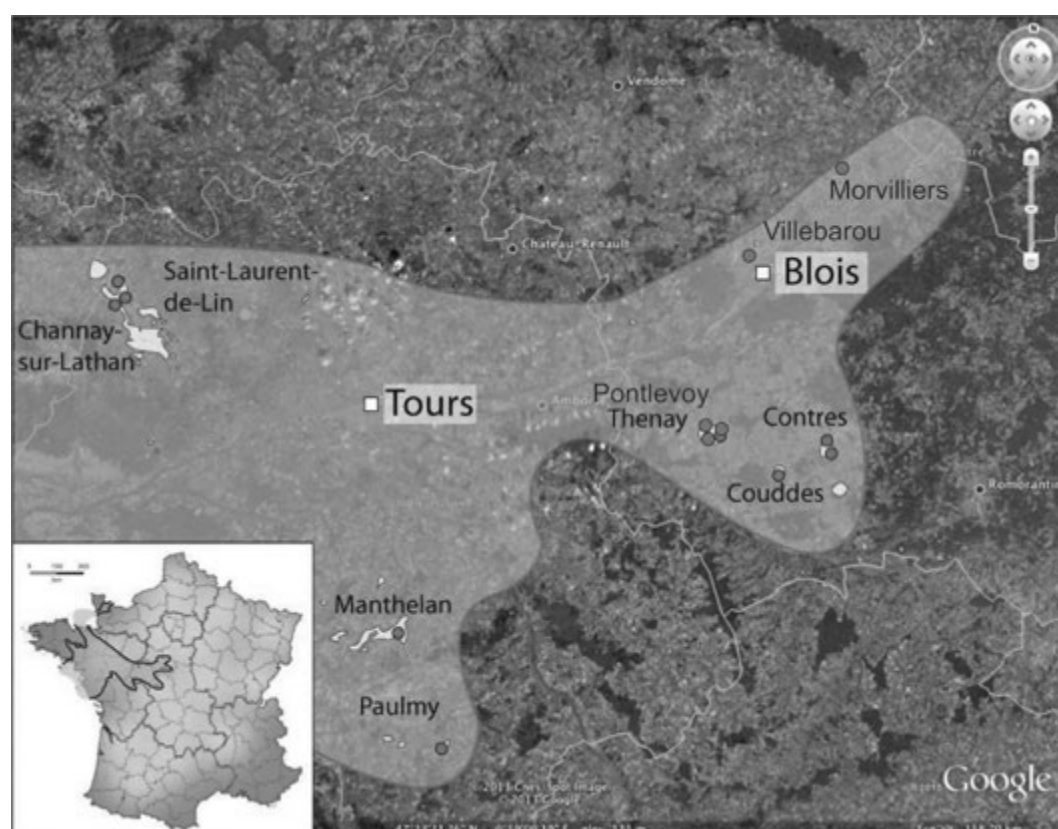


Figure 1. Map of the studied Falun localities (dark dots). The transparent white area represents the maximum extension of the Falun Sea surface. The Falun deposits currently known are indicated in light grey.

REFERENCES

- Charrier P., Carbonnel G. 1980: Les ostracodes néogènes du bassin de Savigné-sur-Lathan (Faluns de Touraine) I. Biostratigraphie et paléoécologie. *Géobios*, 13(6), 941-945.
- Ducasse O. & Cahuzac B. 1997: Les ostracodes indicateurs des paléoenvironnements au Miocène Moyen (Serravalien) en Aquitaine (sud-ouest de la France). *Revue de Micropaléontologie*, 40(2), 141-166.
- Margerel J.-P. 2009. Le foraminifères benthiques des Faluns du Miocène moyen du Blésois (Loir-et-Cher) et de Mirebeau (Vienne) dans le Centre-Ouest de la France. *Géodiversitas*, 31(3), 577-621.

P 4.3

The morphology of the petrosal bone of cats (Felidae) and its phylogeny and paleoecological implications

Karin Scherz

Department of Geosciences, University of Fribourg, Chemin du Musée 6, CH-1700 Freiburg (karin.scherz@unifr.ch)

The inner ear of mammals consists of the cochlea and the vestibular system, which are housed within the petrosal bone, that is often well preserved in the fossil record because of its compactness (Loïc 2014; Luo et al. 2010). Given that the petrosal surrounds the inner ear tightly, it forms a natural mold, which can be used to reconstruct this soft tissue structure in fossil taxa. However, traditional techniques demanded serially sectioning skulls to investigate the inner ear, thereby fully destroying the specimen.

X-ray computed tomography (CT) allows scanning the inside of a skull without damaging the specimen. This technique has therefore become prevalent in recent years, because it enables reconstructing the internal and external morphology of fossil and recent skulls (Luo and Ketten 1991). The petrosal has hereby revealed itself to be a structure of notable interest, as it preserves many morphological features of paleoecological and/or phylogenetic interest (Spaulding et al. 2009; Ciffeli 1982). Although much research had been dedicated to the cranial anatomy of cats (Felidae), only little is known about the morphology of their petrosals.

For my research, I am scanning and digitally reconstructing the petrosals of a broad sample of recent and fossil cats to explore its significance to the paleoecology and systematics of the group.

REFERENCES

- Ciffeli, R.L. 1982: The petrosal structure of *Hypsodus* with respect to that of some other ungulates, and its phylogenetic implications, *Journal of Paleontology*, 56, 795-805.
- Costeur, L. 2014: The petrosal bone and inner ear of *Micromeryx flourensianus* (Artiodactyla, Moschidae) and inferred potential for ruminant phylogenetics, *Zitteliana B*, 32, 1-16.
- Luo, Z. & Ketten D.R. 1991: CT scanning and computerized reconstruction of the inner ear of multituberculate mammals, *Journal of Vertebrate Paleontology*, 11, 220-228.
- Luo, Z., Ruf, I., Schultz, J.A. & Martin, T. 2010: Fossil evidence on evolution on the inner ear cochlea in Jurassic mammals, *Proceedings of the Royal Society B*, 278, 28-34.
- Spaulding, M., O'Leary, M.A. & Gatesy, J. 2009: Relationship of Cetacea (Artiodactyla) among mammals: increased taxon sampling alters interpretation of key fossils and character evolution, *PLoS ONE*, 4, e7062.

5. Stratigraphy

Alain Morard, Reto Burkhalter, Olivier Kempf, Ursula Menkveld-Gfeller

Swiss Committee for Stratigraphy (SKS/CSS)

Swiss Palaeontological Society (SPG/SPS)

TALKS:

- 5.1 Baresel B., Bucher H., Brosse M., Bagerphour B., Schaltegger U.: Ultra-high precision dating of mass extinction events: a combined zircon geochronology, apatite tephrochronology, and Bayesian age modelling approach of the Permian-Triassic boundary extinction
- 5.2 Chen C., Castelltort S., Guerit L., Paola C., Forman B.: Sedimentary signatures of the Paleocene-Eocene Thermal Maximum (PETM) in the South-Pyrenean foreland basin, Spain
- 5.3 Fantasia A., Föllmi K.B., Adatte T., Spangenberg J.E., Montero-Serrano J.-C.: The Early Toarcian Oceanic Anoxic Event: Insight from the Posidonia Shale across a Swiss transect
- 5.4 Jordan P., Bläsi H.R., Pietsch J., Deplazes G.: Subdivision of Late Triassic Klettgau-Formation of Northern Switzerland
- 5.5 Morard A., Baland P.: Transposition of the new harmonised lithostratigraphic master legend into the digital datasets of the Geological Atlas of Switzerland – concept and consequences
- 5.6 Pictet A., Delamette M., Matrion B., Mojon P.-O., Föllmi K.B., Adatte T., Spangenberg J.: The Perte-du-Rhône Formation, a new formation name for lowermost Aptian to lowermost Cenomanian marls and glauconitic sandstones of the Jura Mountains (France and Switzerland)
- 5.7 Pietsch J., Wetzel A., Jordan P.: A lithostratigraphic scheme for Schinznach Formation (Upper Muschelkalk of northern Switzerland)
- 5.8 Pirkenseer C., Rauber G.: Consolidation of lithostratigraphic units for the Cenozoic in the northern Jura
- 5.9 Schöllhorn I., Adatte T., Föllmi K. B.: Sedimentological, climatic and environmental changes during the Early Jurassic (Hettangian-Pliensbachian) on the northern Tethyan margin (Switzerland)

POSTERS:

- P 5.1 Abasaghi F., Darvishi Khatooni J.: Sequence stratigraphy of Sarvak formation in Kupal oil field, Iran
- P 5.2 Bieri L., Brack P., Bernasconi S.M.: A new tool applied to an old problem – correlation of Middle Triassic basin sediments using stable isotope stratigraphy
- P 5.3 Castellort S., Adatte T., Khozyem H., Thibault N., Brunet M.-F., Chiaradia M., Spangenberg J.: Stratigraphic framework and tectono-climatic implications of Upper Cretaceous to Neogene successions of the western Afghan-Tajik depression, Uzbekistan
- P 5.4 Honegger L., Castellort S., Clark J., Adatte T., Puigdefàbregas C., Dykstra M., Fildani A., Spangenberg J.: Continental-Marine correlations and climate signals in the Palaeogene foreland of the South Pyrenees
- P 5.5 Hunger G., Ventra D., Moscariello A., Veiga G.: Sedimentary responses to tectonic and climatic forcing: a high-resolution, integrated sedimentological-geochemical study in terrestrial foreland deposits (Mendoza, Argentina)
- P 5.6 Koiava K., Mosar J., Gavtadze T., Kvaliashvili L., Mauvilly J.: Late Triassic Calcareous Nannoplankton from Georgia and New Age of Moshevani Suite (Caucasus)
- P 5.7 Laziz O., Benabbas C., Boularak M.: Cretaceous environments and diagenetic events of neritic platform, Constantine mounts (North East of Algeria)
- P 5.8 Perret M., Segvic B., Castellort S., Clark J., Puigdefabregas C., Fildani A.: Propagation of detrital signals in the source-to-sink systems of the Tremp-Graus-Ainsa basins, Southern Pyrenean Foreland Basin, Spain
- P 5.9 Tahmasebi K., Darvishi Khatooni J., Mahari R.: Facies, Depositional Environment of Oligocene deposits in anarak area, Esfahan

5.1

Ultra-high precision dating of mass extinction events: a combined zircon geochronology, apatite tephrochronology, and Bayesian age modelling approach of the Permian-Triassic boundary extinction

Björn Baresel¹, Hugo Bucher², Morgane Brosse², Borhan Bagherpour² & Urs Schaltegger¹

¹ *Department of Earth Sciences, University of Geneva, Rue des Maraîchers 13, 1205 Geneva (bjorn.baresel@unige.ch)*

² *Paläontologisches Institut und Museum, University of Zürich, Karl-Schmid-Strasse 4, 8006 Zürich*

Chemical abrasion isotope dilution thermal ionization mass spectrometry (CA-ID-TIMS) U-Pb dating of single-zircon crystals is preferably applied to tephra beds intercalated in sedimentary sequences. By assuming that the zircon crystallization age closely approximate that of the volcanic eruption and ash deposition, U-Pb zircon geochronology is the preferred approach for dating mass extinction events (such as the Permian-Triassic boundary mass extinction) in the sedimentary record. As tephra from large volcanic eruptions is often transported over long distances, it additionally provide an invaluable tool for stratigraphic correlation across distant geologic sections. Therefore, the combination of high-precision zircon geochronology with apatite chemistry of the same tephra bed (so called apatite tephrochronology) provides a robust fingerprint of one particular volcanic eruption. In addition we provide coherent Bayesian model ages for the Permian-Triassic boundary (PTB) mass extinction, then compare it with PTB model ages at Meishan after Burgess et al. (2014).

We will present new high-precision U-Pb zircon dates for a series of volcanic ash beds in deep- and shallow-marine Permian-Triassic sections in the Nanpanjiang Basin, South China. In addition, apatite crystals out of the same ash beds were analysed focusing on their halogen (F, Cl) and trace-element (e.g. Fe, Mg, REE) chemistry. We also show that Bayesian age models produce reproducible results from different geologic sections. On the basis of these data, including litho- and biostratigraphic correlations, we can precisely and accurately constrain the Permian-Triassic boundary in an equatorial marine setting, and correlate tephra beds over different sections and facies in the Nanpanjiang Basin independently from litho-, bio- or chemostratigraphic criteria. The results evidence that data produced in laboratories associated to the global EARTHTIME consortium can provide age information at the 0.05% level of ²⁰⁶Pb/²³⁸U zircon dates.

REFERENCES

Burgess, S.D., Bowring, S., Shen, S.Z., 2014. High-precision timeline for Earth's most severe extinction. PNAS 111, 3316-3321.

5.2

Sedimentary signatures of the Paleocene-Eocene Thermal Maximum (PETM) in the South-Pyrenean foreland basin, Spain

Chen Chen¹, Sebastien Castellort¹, Laure Guerit¹, Chris Paola², Brady Forman³

¹ *Department of Earth Sciences, University of Geneva, Rue des Maraichers 13, CH-1206 Geneva, Switzerland (chen.chen@unige.ch)*

² *Department of Geology and Geophysics, and St. Anthony Falls Laboratory, University of Minnesota, Minneapolis, Minnesota 55414, USA*

³ *Department of Geology & Geophysics, Western Washington University, Bellingham, WA, USA*

Deciphering sedimentary signatures has prominent implication for paleogeographic reconstruction and interpreting the sedimentary record of Earth history: what can sediments and rocks tell us about the past?

The Paleocene-Eocene Thermal Maximum (PETM) is an extreme global warming event that occurred about 56 million years ago. Global temperatures are estimated to have increased by 5-8°, and it has been proposed to be a geologic analogue for anthropogenic climate change.

In the southern Spanish Pyrenees, based on outcrops and borehole information from the Tremp-Graus Basin, it is shown that a sea-level fall of at least 20 m occurred less than 75 kyr prior to the PETM. In the central part of the Tremp-Graus basin, the Paleocene to early Eocene record is shown by the Esplugafreda section. A paleo-incised valley carved into Esplugafreda formation and is interpreted as the unconformity boundary produced in response to the pre-PETM sea level fall. The valley filled by channel-like conglomeratic sandbodies at the bottom and finer reddish floodplain deposit in the rest of the section. The incised valley is capped by the Claret Conglomerate — an extensive sheet-like unit which ranges in thickness between 1m and 4m of and is generally interpreted as the river response to a dramatic climate change at the PETM because of its occurrence at or close to the PETM signal recorded in the stable isotope composition of paleosol nodules (Pujalte et al. 2014). The conglomerate unit ends abruptly and is overlaid by fine-grained yellowish soil which is mainly made up of silty mudstones with abundant small size carbonate nodules suggesting another shift in the hydrological cycle after the PETM. Sea level kept rising after the PETM and all of the section was inundated by the ocean in terms of Ilerdian of marine limestone on the top of the section.

Many studies (Schmitz & Pujalte 2003, 2007; Pujalte et al. 2014) suggested that grain size changes significantly across the based essentially on the observation of the coarse-grained Claret Conglomerate. We tested this assumption by performing a thorough field analysis of grain size within conglomerates in the formations below, at, and above the Claret conglomerate. Our results show that there is no significant grain size variation across the PETM.

To test our hypothesis, we performed several experiments of incised valley filling during a single base-level rise in the Saint Antony Falls Laboratory (SAFL, University of Minnesota). We systematically changed water discharge, sediment flux and the rate of base level rise rate to document the resulting effect on the stratigraphic signature preserved in the valley fill and compare it with the sedimentary record of the Esplugafreda section.

REFERENCES

- Schmitz, B. & Pujalte, V. 2007: Abrupt increase in seasonal extreme precipitation at the Paleocene-Eocene boundary. *Geology*, 35, 215–218.
- Simpson, G. & Castellort, S. 2012: Model shows that rivers transmit high-frequency climate cycles to the sedimentary record. *Geology*, 40, 1131–1134.
- Pujalte V, Schmitz B, Baceta J I. Sea-level changes across the Paleocene–Eocene interval in the Spanish Pyrenees, and their possible relationship with North Atlantic magmatism[J]. *Palaeogeography, Palaeoclimatology, Palaeoecology*, 2014, 393: 45-60.
- Schmitz B, Pujalte V. Sea-level, humidity, and land-erosion records across the initial Eocene thermal maximum from a continental-marine transect in northern Spain[J]. *Geology*, 2003, 31(8): 689-692.

5.3

The Early Toarcian Oceanic Anoxic Event: Insight from the Posidonia Shale across a Swiss transect

Fantasia Alicia¹, Föllmi Karl B.¹, Adatte Thierry¹, Spangenberg Jorge E.², Montero-Serrano Jean-Carlos ³

¹ *ISTE, University of Lausanne, 1015 Lausanne, Switzerland (alicia.fantasia@unil.ch)*

² *IDYST, University of Lausanne, 1015 Lausanne, Switzerland*

³ *ISMER, University of Rimouski, Quebec G5L 3A1, Canada*

The Early Toarcian was marked by an oceanic anoxic event (OAE; ~183 Ma, Early Jurassic), which was a global perturbation of paleoclimatic and paleoenvironmental conditions. Indeed, this episode records global warming, enhanced continental weathering, severe biotic crises, whereas extensive organic-rich sediments are noticeable for example in the Atlantic and in the Tethys. The T-OAE is associated with a negative carbon isotope excursion (CIE), recorded both in marine and terrestrial environments, which is commonly interpreted as due to the injection to the superficial reservoirs of isotopically-light carbon derived from the destabilization of methane hydrate in marine sediments and/or the thermal metamorphism of carbon-rich sediments (e.g. Hesselbo et al., 2000; Svensen et al., 2007). These perturbations were commonly related to a phase of intense volcanic activity due to the formation of the Karoo-Ferrar large igneous province in southern Gondwana.

Several studies of the T-OAE have been conducted on sediments in central and northwest Europe, but only few data are available concerning the Swiss sedimentary records. In the Early Jurassic, the northwestern Tethys Ocean predominantly consisted of shallow epicontinental sea with semi-restricted basins. In this ongoing project, we focus on sections corresponding to different paleogeographic domains: the Jura Mountains and the Briançonnais. Three sites were examined on the Jura Plateau (Rietheim, Gipf, Riniken NAGRA Borehole; canton Aargau) and one in the Préalpes Médiannes (Creux de l'Ours, canton Fribourg). The *H. exaratum* Subzone record black shales with high (up to 10 wt.%) total organic carbon (TOC) content consisting mainly of marine phytoplankton and algal material. High chemical weathering indexes ($\text{Ln}(\text{Al}_2\text{O}_3/\text{Na}_2\text{O})$ and CIA-K) during the T-OAE confirm an increase in continental weathering rates which is concomitant with kaolinite enrichments. This corroborates a more humid climate prevailing during this interval (e.g. Dera et al., 2011). The $\delta^{13}\text{C}_{\text{org}}$ and $\delta^{13}\text{C}_{\text{carb}}$ trends of the sections in the Jura Plateau confirm the erosion and/ or non-deposition (e.g. Kuhn & Etter, 1994; Röhl et al., 2001) of sediments dated as near the Pliensbachian-Toarcian boundary and from the *Harpoceras falciferum* Zone and our high-resolution geochemical approach highlight the influence of the paleogeographic and paleotopographic position of the studied sections.

REFERENCES

- Dera, G., Brigaud, B., Monna, F., Laffont, R., Pucéat, E., Deconinck, J.-F., Pellenard, P., Joachimski, M.M., Durlot, C., 2011. Climatic ups and downs in disturbed Jurassic world. *Geology* 39, 215–218.
- Hesselbo, S.P., Gröcke, D.R., Jenkyns, H.C., Bjerrum, C.J., Farrimond, P., Morgans Bell, H.S., Green, O.R., 2000. Massive dissociation of gas hydrate during a Jurassic oceanic anoxic event. *Nature* 406, 392–395.
- Kuhn, O., Etter, W., 1994. Der Posidonienschiefer der Nordschweiz: Lithostratigraphie, Biostratigraphie und Fazies. *Eclogae Geol. Helv.* 87, 113–138.
- Röhl, H.J., Schmid-Röhl, A., Oschmann, W., Frimmel, A., Schwark, L., 2001. The Posidonia Shale (Lower Toarcian) of SW-Germany: an oxygen-depleted ecosystem controlled by sea level and palaeoclimate. *Palaeogeogr. Palaeoclimatol. Palaeoecol.* 165, 27–52.
- Svensen, H., Planke, S., Chevallier, L., Mørch-Sørensen, A., Corfu, F., Jamveit, B., 2007. Hydrothermal venting of greenhouse gases triggering Early Jurassic global warming. *Earth Planet. Sci. Lett.* 256, 554–566.

5.4

Subdivision of Late Triassic Klettgau-Formation of Northern Switzerland

Peter Jordan¹, Hansruedi Bläsi², Johannes Pietsch¹ & Gaudenz Deplazes³

¹ *Geologisch-Paläontologisches Institut, University of Basel, Bernoullistrasse 32, CH-4056 Basel and Gruner Böhlinger AG, CH-4104 Oberwil (peter.jordan@gruner.ch)*

² *Institut für Geologie der Universität Bern, Baltzerstrasse 1+3, CH-3012 Bern*

³ *Nagra, Hardstrasse 73, CH-5430 Wettingen*

In the context of the harmonization of the Swiss stratigraphic scheme (HARMOS), the Triassic strata of Northern Switzerland have been recently subdivided into six formations (decision of the Swiss Stratigraphic Committee, 22. November 2014). In this study, a subdivision for the uppermost, the late-Triassic Klettgau-Formation, encompassing some 30 to 75 m of playa sediments with fluvial and marine intercalations, is proposed.

After considering different possibilities, including the adaption of the recently reviewed stratigraphic scheme of Southern Germany (Etzold & Schweizer 2005, Geyer & Gwinner 2011), a pragmatic approach has been preferred which is based mainly on the traditional Swiss subdivision. Decisive were outcrop studies and deep wells recorded traditional stratification, and the concept of mappable units established by the Swiss Geological Survey. The opportunity has been used to review and formally define the different members and their lateral variations. For that, type localities have been described and defined, some of them after specific excavations.

The base of the Klettgau-Formation, and of its lowermost Ergolz-Member is defined with the ending of the sulfate facies of underlying Bänkerjoch-Formation (the former "Gipskeuper").

The Ergolz-Member (formerly "Schilfsandstein" and "Untere Bunte Mergel") consists of variegated silty dolomitic marls with dolocretes and thin layers of fine grained sandstones deposited in a playa environment ("Überflutungs- oder Normalfazies", z.B. Etzold & Schweitzer, 2005). Locally, NNE-SSE-trending channels occur, probably following paleo-valleys ("Rinnen-Fazies", dito). The channels are deeply eroded in the underlying strata and filled by fine grained sand of Scandinavian origin.

The Gansingen-Member (formerly "Gansinger Dolomit s.l.") documents a marine transgression from SW. In North-western Switzerland it starts with partly porous dolomite with Carnian marine bivalves (Wildi 1976). In complete sections, the succession continues with an alternation of increasingly thinner dolomite beds with thin dolomitic marl interlayers. It ends with desiccation marks and a dramatic decrease of dolomite content (Peters 1964), marking the transition to terrestrial playa environment. Towards E (Weinland, Klettgau) and SE, the marine carbonates are replaced by litoral sabkha sediments, originally dolomitic sulfates, locally altered to dolomitic limestones (sulfate facies of Gansingen-Mb.). At several places, including the type locality, the Gansingen-Member has been eroded to great parts by Late Triassic erosion. Further E, a transition to coarse alluvial and fluvial sandstones of Vindelizian origin can be observed in the wells of the Seerücken area (Berlingen-Mb., new).

For practical reasons, the Gruhalde-Member (formerly "Obere Bunte Mergel" and "Knollenmergel") encompasses all playa sediments above the Gansingen-Member. Evidence in good outcrops in Switzerland and correlation with the well-established German stratigraphic scheme suggests that it consists of different sedimentary cycles separated by long time spans of no sedimentation and erosion. At the type locality, the lower part consists of variegated dolomitic marls including different desiccation horizons, sulfocretes and erosional channels. In the middle part, additionally, thin interlayers with coarse sand of Vindelizian origin can be observed, which may be correlated with the Seebi-Member of North-eastern Switzerland (see below). The upper part consists of mostly greenish-grey dolomitic marls, again, with channels fills. Evidence in Belchen section and Schafisheim well suggests that in North-western Switzerland the upper part is missed due to late Triassic erosion.

The Seebi-Member (formerly "Stubensandstein") includes layers of coarse grained alluvial and fluvial sandstones of Vindelician origin with calcite, siliceous or clay matrix. Locally, matrix fraction increases and becomes mostly dolomitic in the upper part (sandy dolomite facies of Seebi-Mb.). In the Klettgau area, dolocretes have formed in this upper part (dolomitic facies of Seebi-Mb.). The proposed definition of Seebi-Member demands a coarse grained sand layer of at least 1 m thickness. Consequently, Seebi-Member is restricted to North-eastern Switzerland with the middle part of Gruhalde-Member as its western equivalent (see above).

The Belchen-Member (formerly "Rhät-Sandstein") consists of partly fossiliferous coarse grained sands and greenish dark marls of estuarine to shallow marine origin. The sandstones are characterized by the bright saccharoid weathering. Due to late Triassic and early Jurassic erosion, Belchen-Member is restricted to North-western Switzerland and Lake Constance area.

In areas where the Belchen-Member is missing, the top of Klettgau-Formation is clearly defined by a change from continental to marine sediments of Early Jurassic Staffelegg-Formation. In North-western Switzerland, where Belchen-Member is overlain by sandy marine limestones of the Weissenstein-Member of Staffelegg-Formation, fixing the boundary is more sophisticated.

REFERENCES

- Etzold, A. & Schweitzer, V. 2005: Der Keuper in Baden-Württemberg. In: Deutsche Stratigraphische Kommission, 2005: Stratigraphie von Deutschland IV: Keuper. – Cour. Forsch.-Inst. Senckenberg, 253, 214 – 258.
- Geyer, O.F. & Gwinner, M.P. 2011: Die Geologie von Baden-Württemberg, 627 p., Schweizerbart, Stuttgart.
- Peters, Tj. 1964: Tonmineralogische Untersuchungen an einem Keuper-Lias-Profil im Schweizer Jura (Frick). Beiträge zur Geologie der Schweiz. Kleinere Mitteilungen, 32, 559 – 588.
- Wildi, W. 1976: Die Molluskenfauna des Gansinger Dolomites (Trias, Karnian, Mittlerer Keuper). Eclogae geol. Helv. 69/3, 671-684.

5.5

Transposition of the new harmonised lithostratigraphic master legend into the digital datasets of the Geological Atlas of Switzerland – concept and consequences.

Alain Morard¹, Pauline Baland¹

¹ Swiss Geological Survey (SGS), Federal Office of Topography swisstopo, Seftigenstrasse 264, CH-3084 Wabern (alain.morard@swisstopo.ch)

With the completion of the HARMOS project (Strasky et al. 2013), a standardised master legend is now available for the Geological Atlas of Switzerland 1:25000 (GA25). However, this harmonised lithostratigraphic scheme still has to be transposed into the individual digital datasets, together with a number of descriptive attributes (Data Model Geology). Geometrical modifications (where cartographic mismatches occur) will only be undertaken at a later point, when the dataset will be fully revised. The present contribution aims to explain how the new master legend will be implemented, before further revision work is undertaken. The most common configurations encountered will be discussed and illustrated, based on correlation tables established for the Jura domain between the old and new nomenclature.

When considering all mapped units in a GA25 dataset, four main recurring configurations can be recognised as concerns the more or less good concordance between the existing legend and the new lithostratigraphic scheme:

- 1) No geometrical change is necessary (only semantic modifications in certain circumstances, such as grouping smaller units together or updating the name).
- 2) Unit must be subdivided or a new formal group introduced. As an example, the Gorges de l'Orbe and Vallorbe Formations have not always been distinguished cartographically. Therefore, the boundary between the two units has to be newly traced where it is missing, or – if this proves to be impossible – a formal superordinate unit has to be introduced, so that each cartographic object gets a proper name and complete set of attributes (age, lithology, ...).
- 3) The existing boundary between two units must be redrawn, because alternate views have been developed through time and/or by different authors (e.g. the Upper Virgula Marls have sometimes been mapped together with the Reuchenette Formation instead of the Twannbach Formation, so that the boundary is slightly shifted from one place to the other).
- 4) Finally more complex configurations occur, in which a whole series of units must be revised. This is the case for the former «Sequanian facies», where both vertical and lateral subdivisions have been subsequently introduced.

In conclusion, in the transitional phase between the transposition of the harmonised lithostratigraphic master legend and the geometrical revision of the digital datasets, it is important that the remaining cartographic discrepancies be clearly documented, so that the end-user knows what is the validity and revision status of the different elements of the map he looks at. Therefore a specific attribute will be integrated to highlight in which cases the mapped objects are truly up-to-date and – if not – what kind of inconsistency still remains to be resolved. This attribute will also be of great help for the later revision process.

REFERENCES

- Strasky S., Morard A., Burkhalter R. & Möri, A. 2013 Harmonising the Swiss Lithostratigraphic Nomenclature. In: Rocha et al.: STRATI 2013 – First International Congress on Stratigraphy, Springer Verlag, 603-607
- Data Model Geology – Documentation and description in UML-Format and object browser. Swiss Geological Survey 2012. <http://www.geologieportal.ch/internet/geologieportal/en/home/knowledge/lookup/datamodel.html>

5.6

The Perte-du-Rhône Formation, a new formation name for lowermost Aptian to lowermost Cenomanian marls and glauconitic sandstones of the Jura Mountains (France and Switzerland)

Antoine Pictet ¹, Michel Delamette ², Bertrand Matrimon ³, Pierre-Olivier Mojon ⁴, Karl B. Föllmi ¹, Thierry Adatte ¹, Jorge Spangenberg ¹

¹ Institut des Sciences de la Terre, Université de Lausanne, 1015 Lausanne, Switzerland, antoine.pictet@unil.ch

³ 1 ter rue du Pont, 10450 Bréviandes (France) ; Biogéosciences, UMR 6282 CNRS, Université de Bourgogne, 6 boulevard Gabriel, 21000 Dijon, France

⁴ Rue du Centre 81, CH-2405 La Chaux-du-Milieu, Switzerland

During the late Early Cretaceous, following the deposition of the northern Tethyan Urgonian carbonate platform, major palaeoceanographic, climatic, and tectonic changes occurred, which resulted in changes in the carbonate factory, and repetitive drowning and emersion phases. The marls and sandstones overlaying the Urgonian carbonates are reported here to the newly created Perte-du-Rhône Formation, which gathers the Aptian, Albian, and earliest Cenomanian sediments in the Jura Mountains. They are known from a relatively small number of outcrop areas throughout the Jura range of France and western Switzerland.

The Perte-du-Rhône Formation is subdivided into two members, the marly Fulie Member at the base, and the sandy-glauconitic Mussel Member at the top. They deposited on the roof of the former innermost Urgonian platform when situated in the inner Jura range (Guillaume 1966), and on the "Pierre jaune de Neuchâtel" when situated on the outer tabular Jura, and finally on Jurassic layers in direction of the Paris Basin (Guillaume 1966). The Perte-du-Rhône Formation itself shows a gradation in age of the onset of sedimentation from the lowermost Aptian to the early Albian from the inner chain to the Burgundy threshold (tabular Jura), which was very probably emerged during the late Hauterivian to the latest Aptian. The most complete sections occur along main transtensive faults, such as as the Vuache (Charollais et al. 2013) and Pontarlier (Aubert 1959) faults, linked to the rotation of the Iberian micro-plate.

Both numerous ammonite findings (Renz & Jung 1978) as well as sequence stratigraphic correlations suggest a lowermost Aptian age for the drowning of the Urgonian platform with the installation of the Fulie Member, which ends in the early *P. melchioris* Zone. The Mussel Member was deposited from the late *P. melchioris* Zone to the lowermost Cenomanian. Six major phases of sea level fall are recorded through the Perte-du-Rhône Formation associated to one or several markers as important erosional hiatuses, iron shields, phosphatic conglomerates and negative carbon-isotope excursions, in the *D. oganlensis*, *D. furcata*, *P. melchioris*, *D. nodosocostatum*, *A. intermedius*, and *M. mantelli* Zones.

References:

- Aubert, D. 1959: Le décrochement de Pontarlier et l'orogénèse du Jura. Mém. Soc. Vaud. Sci. Nat. 12 (4), 93-152.
- Charollais, J., Wernli, R., Mastrangelo, B., Metzger, J., Busnardo, R., Clavel, B., Conrad, M., Davaud, E., Granier, B., Saint Martin, M. & Weidmann, M. 2013: Présentation d'une nouvelle carte géologique du Vuache et du Mont de Musièges (Haute-Savoie, France) : stratigraphie et tectonique. Arch. Sci. 66, 1–64.
- Frey, M. 1922: Die Asphaltlagerstätten im schweizerischen Juragebirge mit besonderer berücksichtigung des Val-de-Travers. Beitr. zur Geol. Der Schweiz, Geotech. série, IX Lief. : 36 pp.
- Guillaume, S. 1966: Le Crétacé du Jura français. Bulletin du Bureau de Recherches Géologiques et Minières, 1, 2, 3 et 6 : 297 p.
- Renz, O. & Jung, P. 1978: Aptian to Maastrichtian in the Swiss Jura Mountains. Eclogae geologicae Helvetiae, Basel, 71, 1–18.

5.7

A lithostratigraphic scheme for Schinznach Formation (Upper Muschelkalk of northern Switzerland)

Johannes Pietsch^{1,2}, Andreas Wetzel¹ & Peter Jordan²

¹ *Geologisch-Paläontologisches Institut, Universität Basel, Bernoullistrasse 32, CH-4056 Basel (johannes.pietsch@unibas.ch)*

² *Gruner Böhlinger AG, Mühlegasse 10, CH-4104 Oberwil*

Many different lithostratigraphic units are currently in use for the Upper Muschelkalk and the former Lower Keuper of northern Switzerland. They are mainly based on lithological characteristics or fossil content, such as Trochitenkalk, Coenothyrisbank or Mergelhorizont, or they were adopted from German units, for instance Grenzdolomit. In the context of the HARMOS project of Swiss Geological Survey to harmonize the Swiss stratigraphic scheme, the Upper Muschelkalk was redefined as Schinznach Formation (decision of the Swiss Stratigraphic Committee, 22. November 2014). The Schinznach Formation also includes the former lower Keuper ("Lettenkeuper").

A lithostratigraphic scheme for this formation considering valid "Guidelines for stratigraphic nomenclature" (Remane et al. 2005) is now proposed.

On the Maps of the Geologischer Atlas der Schweiz 1: 25000 traditionally two units of the Upper Muschelkalk "Trigonodus-Dolomit" and "Hauptmuschelkalk" are distinguished. Therefore a division of at least these two units or equivalent entities would be useful. A pragmatic approach is now proposed which is based mainly on the subdivision for northern Switzerland previously suggested by Merki (1961).

This scheme converts the frequently used main units into defined Members. In addition the rare and, therefore, important marker horizons and oolitic intervals are defined as beds. So the proposed subdivision of the Schinznach Formation contains four Members, two marker beds and three oolitic intervals, which are also defined as beds (Figure 1). The proposed boundaries are diachronous. This especially concerns the lower boundary of the Stamberg Member since this boundary is due to a diagenetic facies change.

Pietsch et al. (in prep.)	Geol. Atlas Schweiz 1:25000	Merki (1961)
Bänkerjoch Formation	Keuper	Hauptkeuper
<div style="display: flex;"> <div style="writing-mode: vertical-rl; transform: rotate(180deg);">Schinznach Formation</div> <div> <div>Asp Member</div> <div><i>Kaisten Bed</i></div> <div>Stamberg Member</div> <div><i>Eptingen Bed</i></div> <div>Liedertswil Member</div> <div><i>Dünnlengberg Bed</i></div> <div>Kienberg Member</div> <div><i>Salhöf Bed</i></div> <div><i>Fützen Bed</i></div> </div> </div>	<div>Trigonodus-Dolomit</div> <div>Hauptmuschelkalk</div>	<div>Lettenkohle</div> <div>Trigonodusdolomit</div> <div><i>Eptinger & Giebenacher Oolith</i></div> <div>Plattenkalk</div> <div><i>Mergelhorizont</i></div> <div>Ooberer Trochitenkalk</div> <div><i>Coenothyrisbank</i></div> <div>Unterer Trochitenkalk</div> <div><i>Basaloolith</i></div>
Zeglingen Formation	Anhydritgruppe	Anhydritdolomit

Figure 1. Lithostratigraphic units of the Upper Muschelkalk presently used and proposed units of the Schinznach Formation with beds (grey) and oolitic beds (dark grey), thickness not to scale

REFERENCES

- Merki, P. 1961: Der Obere Muschelkalk im östlichen Schweizer Jura, *Eclogae Geologicae Helvetiae*, 54, 137-219.
- Pietsch, J., Wetzel, A. & Jordan, P. in prep.: A new lithostratigraphic scheme for Schinznach Formation (Upper Muschelkalk of Northern Switzerland)
- Remane, J., Adatte, T., Berger, J., Burkhalter, R., Dall'Agnolo, S., Decrouez, D., Fischer, H., Funk, H., Furrer, H., Graf, H., Gouffon, Y., Heckendorn, W., Winkler, W. 2005: Guidelines for stratigraphic nomenclature, *Eclogae Geologicae Helvetiae*, 98, 385-405.

5.8

Consolidation of lithostratigraphic units for the Cenozoic in the northern Jura and southern Upper Rhine Graben (Switzerland)

Claudius Pirkenseer ¹ & Gaëtan Rauber ¹

¹ *Paléontologie A16, Office de la culture, rue de la Chaumont 13, CH-2900 Porrentruy*
(claudius.pirkenseer@jura.ch, gaetan.rauber@jura.ch)

During the last two decades the study of the Cenozoic deposits of the so-called “Jura-Molasse” re-intensified due to the construction of the highway A16, stimulating more complex interpretations of the palaeogeographic situation and lateral facies changes. Despite the detailed elaboration of summaries on the known lithostratigraphic units, no formal designation of formation names took place.

New stratigraphic data from the southern Upper Rhine Graben as well as the publication of a homogenized lithostratigraphy of the German Stratigraphic Commission need to be integrated to get a better overview of the larger stratigraphic context of the individual formations. The choice of type localities and names outside the immediate research area depends on information from the latter, since especially for the Oligocene the deposits of the Delémont, Ajoie and Laufen Basins represent condensed marginal extensions of formations closer to the depositional center of the southern Upper Rhine Graben. Since the evolution of tectonic events progressed in a comparatively similar fashion throughout the (southern) Upper Rhine Graben, supraregional lithostratigraphic units may be homogenized. An area with two different languages would greatly benefit from common formation names based on localities, and not as is the case up to now on predominantly descriptive terms that need to be translated (e.g., Marnes à Cyrènes, Cyrenenmergel, Cyrena Marls, Meeressand, Marnes à foraminifères).

Hence some supraregional stratigraphic names will be incorporated, new names proposed, historically well-established terms will be formalized, and some lithostratigraphic units will be consolidated (see table 1). Consequently the extreme diversity of local units at or below a possible member status named and defined differently for each Jura synclinal may be integrated in a formalized context.

As presented in the scheme some units will keep their historical name (e.g. Sidérolithique, Terre jaune), whereas others will be renamed (e.g. Steingang, conglomerates cotiers = Turckheim Fm), partly after well-described type localities in (e.g. Pulversheim Fm for Melettaschichten), and some will be combined and re-designated as members (e.g. Cyrenenmergel as member of the [new] Elsass Fm).

The new terminology is intended to be presented before the Swiss Stratigraphic Commission and to be summarized in a forthcoming publication.

Series	Group	Formation	Ref	Equivalent	Members	Ref	Equivalent	Setting
Miocene	OSM	Bois de Raube	SCS	official SCS	Montchaibeux		-	floodplain
	70MM	uncertain	SCS	official SCS	?Pécas		-	?marine
		Delémont	GREPPIN (1870)	ex Tullingen-Schichtlen (Subfm LGRB) et al. ex Calcaires delémontiens et al.	to be discussed	-	-	lacustrine
		Niederrödern	GRIMM (2005)	diverse, see ref	-	-	-	floodplain
Oligocene	Elsass	Elsass	-	ex Elsassier Molasse et al. ex Cyrenenmergel	Heidwiller	ROUSSE (2006)	ex partim Elsassier Molasse ex Molasse alsacienne continentale	river channel
					Reitzwiller		ex "baie à huîtres peu profonde" partim ex cyathula-Bank	della lagoon
					Birse		ex Molasse alsacienne marine partim ex Cyrenenmergel	deltatic
					Hagenbach		partim ex Cyrenenmergel	
		Pulversheim (DP202)	ROUSSE (2006)	ex Melettaschichten et al. Rosenberg Subfm (Mainz Basin)	to be discussed	-	?Rosenberg Subfm (Mainz Basin)	offshore marine
	Froidfontaine	Froidfontaine, Frauenweiler or Hochberg Wittenheim (DP212) Blauen	PHARISAT (1991) LGRB (2011) or GRIMM et al. (2011)	ex Fischschiefer et al. Frauenweiler Subfm (LGRB) Hochberg Subfm (Mainz Basin)	Prés Roses (exact attribution difficult)	LINIGER (1925)	partim ex cyathula-Bank	coastal marine to offshore
				ex Foraminiferenmergel et al. Wallau Subfm (Mainz Basin)				
				ex Meeressand et al. Alzey Fm (Mainz Basin)				
				ex Steingang, conglomerats colters				
		Turckheim	DURINGER (1988)		-	-	-	fan delta
		Terre jaune	GREPPIN (1870)	-	-	-	-	lacustrine
		none						
		none						
Eocene		Siderolithique	GREPPIN (1870) ROLLIER (1893)	numerous small local occurrences with different names and somewhat varying lithology	?Huppertsand ^f		-	terrestrial karstic

Table 1. Consolidated lithostratigraphic units of the northern Jura (Delémont, Ajoie and Laufen Basins, southern Upper Rhine Graben)

5.9

Sedimentological, climatic and environmental changes during the Early Jurassic (Hettangian-Pliensbachian) on the northern Tethyan margin (Switzerland)

Iris Schöllhorn¹, Thierry Adatte² & Karl Föllmi³

¹ Institut des Sciences de la Terre, University of Lausanne, Quartier UNIL-Mouline Bâtiment Géopolis, CH-1015 Lausanne (iris.schoellhorn@unil.ch)

² Institut des Sciences de la Terre, University of Lausanne, Quartier UNIL-Mouline Bâtiment Géopolis, CH-1015 Lausanne (thierry.adatte@unil.ch)

³ Institut des Sciences de la Terre, University of Lausanne, Quartier UNIL-Mouline Bâtiment Géopolis, CH-1015 Lausanne (karl.foellmi@unil.ch)

The Hettangian-Pliensbachian interval is marked by different phases of paleoenvironmental change, starting with the end-Triassic mass extinction event (ETME), c. 201.4 Ma ago (Schoene et al., 2010), which was marked by terrestrial ecosystem turnover, up to 50% loss in marine biodiversity (Raup et Seprosky, 1982) and large turnovers in global geochemical cycles (Hesselbo et al., 2002) linked to the onset of Central Atlantic Magmatic Province (CAMP) volcanism (Deenen et al., 2010). This time interval ends with a phase of major climate change near the Pliensbachian-Toarcian boundary, which is followed by the Early Toarcian oceanic anoxic episode (e.g., Suan et al., 2010). In this study, we examine the sedimentological, geochemical and environmental responses to these and intervening events on the northern Tethyan margin (Swiss Jura). With this purpose, a wide array of geochemical analyses (carbon- and oxygen-isotope, Rock-Eval, phosphorus content, mineralogy, trace and major element content and clay analyses) and sedimentary observations has been performed on one sections and two boreholes (Frick, Riniken and Kreuzlingen) forming a north-south/distal-proximal transect.

We observed two depositional systems: (1) the Schambelen Member (lower Hettangian) and the Frick Mb. (middle Upper Sinemurian), which are characterised by organic-rich shales intercalated by tempestites becoming more pronounced with the proximity of the continent; and (2) The Beggingen Member (Upper Hettangian to Lower Sinemurian) and the Grünschoz, Breitenmatt and Rietheim Members (upper Upper Sinemurian to Pliensbachian) are composed of carbonates marked by the presence of hiati, condensed beds, phosphate- and fossil-rich strata, and erosional features, which testify to a very dynamic environment characterised by overall low sediment-accumulation rates. With the exception of the Grünschoz Mb, the ratio kaolinite/(mica+smectite) measured in the clay fraction is lower in the condensed phosphate-rich beds than in the shales. Thus, the episodes of sedimentary condensation occurred during either drier climate or/and higher sea level. The related sea-level change could be linked to tectonically induced submarine relief prevailing in this region and/or global sea-level changes.

The geochemical analyses reveal also important environmental changes. Indeed, several carbon cycle perturbations occurred during this time interval:

- (a) Two negative carbon isotope excursions measured on the organic matter (CIEorg -2‰) are observed during the early Hettangian (Schambelen Mb.) accompanied by a change in organic matter (OM) composition, higher productivity (high hydroxyl indices) and anoxia (high trace element, pyrite and organic matter contents and the presence of pyrite framboids; cf. also Schwab and Spangenberg, 2006).
- (b) A -1‰ CIEorg is recorded near the Early-Late Hettangian boundary accompanied by the widespread onset of bioclastic limestone accumulation (Germany, Alps, Southern Alps, Carpathians -Van de Schootbrugge et al., 2008). The $\delta^{13}\text{C}$ decrease marks the stabilization of carbonate production and the decrease in export of excess carbon into organic reservoirs under reduced pCO_2atm . (Van de Schootbrugge et al., 2008).
- (c) The Early Sinemurian (Frick Mb.) is characterised by a +4‰ CIEorg in this sections. Nevertheless, the globality and causes of this CIE remain to be determined.
- (d) The Sinemurian-Pliensbachian boundary record a negative CIEorg (-3‰), followed by a positive CIE (+2‰) in the Early-Late Pliensbachian and a negative CIEorg (-1.5‰) during the Late Pliensbachian. These CIEs are also recorded in several other localities in carbonates, belemnites, wood and organic matter, and likely document global events. These CIEs are linked to OM preservation and/or productivity changes and/or ^{13}C -depleted carbon input(s).

REFERENCES

- Deenen, M. H. L., Rühl, M., Bonis, N. R., Krijgsman, W., Kürschner, W. M., Reitsma, M. & Van Bergen M. J. 2010 : A new chronology for the end-Triassic mass extinction, *Earth Planet*, 291, 113-125.
- Hesselbo, S. P., Robinson, S. A., Surlyk, F. & Piasecki, S. 2002 : Terrestrial and marine extinction at the Triassic-Jurassic boundary synchronized with major carbon-cycle perturbation: a link to initiation of massive volcanism?, *Geology*, 30:251–254.
- Raup, D. M. & Seproski J. J. 1982 : Mass Extinctions in the Marine Fossil Record. *Science*, 215, 1501-1503
- Schoene, B., Guex J., Bartolini A., U. Schaltegger & Blackburn T. J. 2010 : Correlating the end-Triassic mass extinction and flood basalt volcanism at the 100 ka level, *geology*, 38, 387-390.
- Schwab V.F. & Spangenberg J.E.** 2007 : Molecular and isotopic characterization of biomarkers in the Frick Swiss Jura sediments: A palaeoenvironmental reconstruction on the northern Tethys margin, *Organic Geochemistry*, 38, 419-439.
- Van de Schootbrugge, B., Payne, J. L., Tomasovych, A., Pross, J., Fiebig, J., Benbrahim, M., Föllmi, K. B. & Quan T. M. 2008 : Carbon cycle perturbation and stabilization in the wake of the Triassic-Jurassic boundary mass-extinction event, *Geochemistry Geophysics Geosystem*, 9, Q04028.

P 5.1

Sequence stratigraphy of Sarvak formation in Kupal oil field, Iran

Froogh Abasaghi¹, Javad Darvishi khatooni²¹ Ferdowsi university of Mashhad(Saghi0631@yahoo.com)² Geological survey of Iran

The purpose of this study is to interpret depositional environments, sequence stratigraphy, and evaluate diagenetic processes affected the Sarvak Formation in Kupal oil field. For this purpose, 351 thin sections from cores and cuttings from wells number 4, 20 and 48 have been studied. In addition, petrophysical logs, such as gamma, neutron, density, sonic, and charts of INPEFAGR were used. Environmental interpretation led to identification of 9 microfacies formed in the three facies belts including lagoons, shoal and open marine. Depositional environments are varying from inner ramp to outer ramp. In the area, Sarvak Formation formed in a homoclinal carbonate ramp without an effective barrier. Inner ramp environment was dominated by benthic foraminifers such as miliolids, nezzazata, textularia and alveolinids. In middle ramp, rudists and echinoderms were developed. In outer ramp, oligosteginids, planktonic foraminifers with transported materials from shallow parts were deposited. Analysis depositional of sequence stratigraphic led to identification of two sequences with sequence boundaries of Type 2. In the Kupal oil field, Sarvak Formation is overlain by Ilam Formation with erosional surface, therefore sequence bound between Sarvak and Ilam is SB1. The most important diagenetic processes identified include micritization, cementation, dissolution, replacement (dolomitization and hematization), neomorphism, physical and chemical compaction and biological disturbance that are operated in three stage including eogenesis, mesogenesis and telogenesis stages.

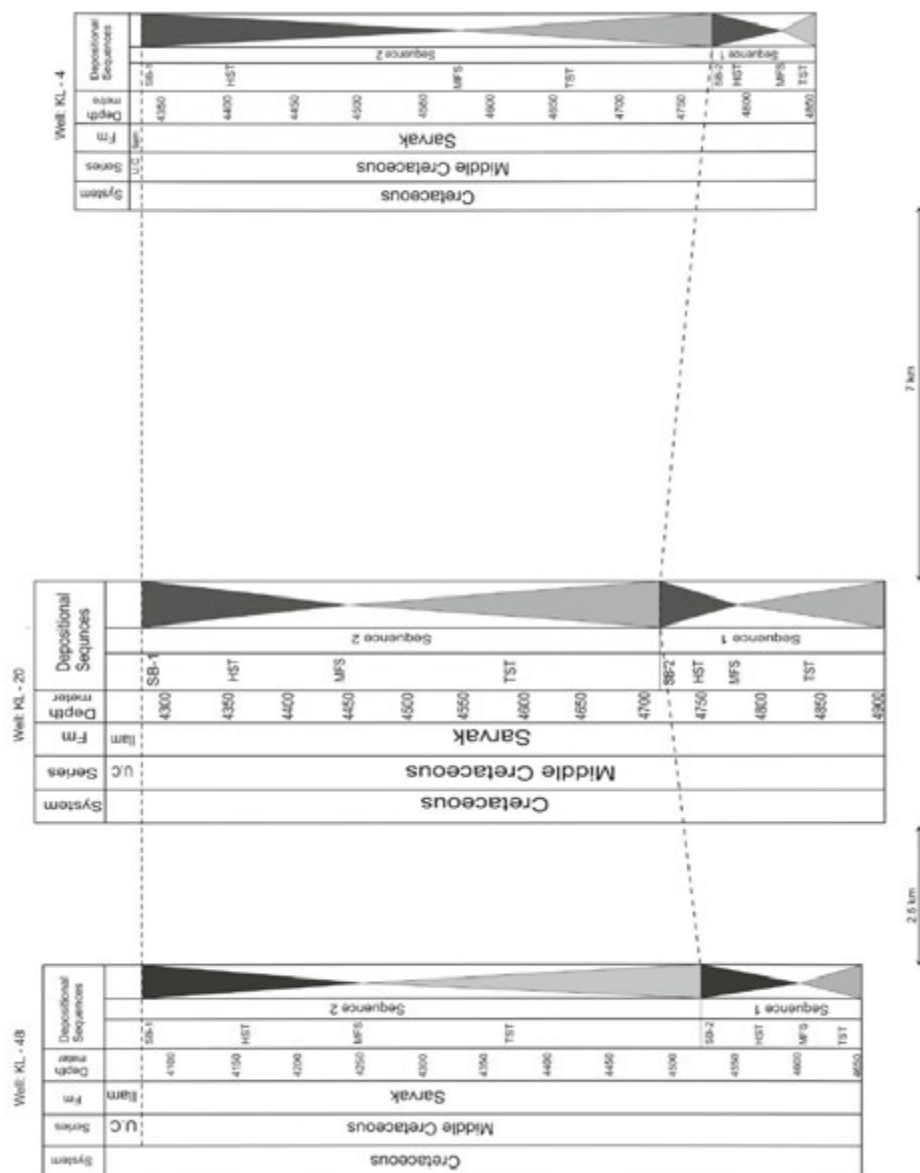


Figure 1. Sequence Stratigraphy compliances Sarvak formation in study In wells studied

REFERENCES

- Catuneanu O., 2006: Principles of sequence stratigraphy, Elsevier Publications, 375p.
- Schlager W., 2005: Carbonate Sdimentology and sequence stratigraphy, SEPM Concepts in Sedimentology and Paleontology Series 8, 200 p.

P 5.2

A new tool applied to an old problem – correlation of Middle Triassic basin sediments using stable isotope stratigraphy

Lisa Bieri¹, Peter Brack¹, Stefano M. Bernasconi¹

¹ *Department of Earth Sciences, ETH Zürich, Sonneggstrasse 5, 8092 Zürich (bieril@student.ethz.ch)*

The precise correlation of Middle Triassic sediment successions throughout Europe represents a over 100 year old problem in stratigraphy. Although ammonoids, conodonts, palynomorphs and other fossil groups and their associations provide important age constraints, the discontinuous occurrences of age-diagnostic fossils so far impeded a straightforward correlation of the sometimes highly variable Triassic successions. For Anisian sediments in the Southern Alps such correlations largely rely on the tracing of depositional sequences (e.g., Gianolla et al., 1998). However, in the heterogeneous stratigraphic successions the identification of correlatable sequences remains a challenge with further complications arising from synsedimentary tectonic activity. Therefore the confirmation of proposed correlations and much desired refinements need independent evidence. High-resolution chemostratigraphy and its correlation to local biostratigraphy represents a rather new approach for the characterization of Middle Triassic (Anisian) sediment successions with potential to help solving open stratigraphic problems.

We present a new continuous high-resolution stable isotope record obtained from bulk rock analysis of samples from South Alpine sedimentary successions of Anisian age. The $\delta^{13}\text{C}$ data of five sections covering a time interval of the Bithyan / Pelsonian to the Illyrian substages are correlated to the lithostratigraphy and biostratigraphy of the hemipelagic deposits of the Dont Fm in the Eastern Dolomites (e.g., Bechstädt and Brandner, 1970) and to Anisian successions around Recoaro in the central/southern portion of the Southern Alps (De Zanche and Mietto, 1981). Whereas the $\delta^{18}\text{O}$ results show evidence of diagenetic alteration, the $\delta^{13}\text{C}$ data are considered to reflect a primary marine signal. A positive excursion of +2 ‰ (CIE A) in supposedly lower Pelsonian sediments in the Eastern Dolomites can possibly be traced to a similar excursion in the record from Recoaro. Stratigraphic intervals immediately beneath or straddling the Pelsonian-Illyrian boundary are characterized by a distinct pattern, comprising a decrease of carbon isotope values of ~1 ‰ (CIE D), followed by an increase of 1-2 ‰ at the top of the Dont Fm (CIE E) and in the Recoaro Lst. (Figure 1).

These significant changes can be compared with new carbon isotope records from elsewhere in the Southern Alps (eastern Lombardy; Rebetez et al., in prep.) as well as from non-Alpine Middle Triassic sediments in the Germanic basin (Steudnitz, Germany; Lippmann et al., 2005).

The $\delta^{13}\text{C}$ record emerging from the South Alpine (i.e. Western Tethyan) and Germanic successions point to perturbations of the global carbon cycle of up to 3 ‰ during the Middle Triassic, i.e. in a range of global carbon variations similar to those in the Late Jurassic or Early Cretaceous (Weissert and Erba, 2004).

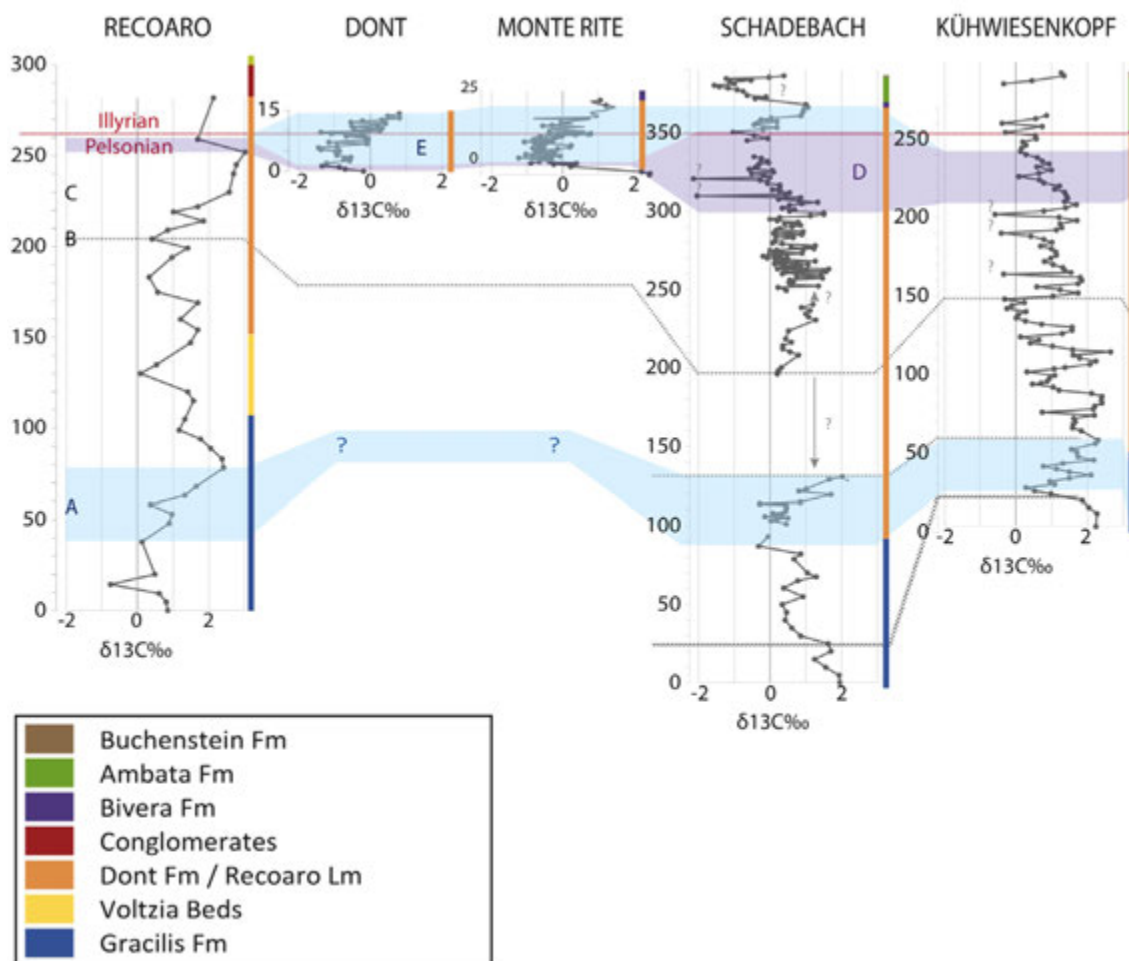


Figure 1. Middle Anisian C-isotope stratigraphy, correlated to bio- and lithostratigraphy. Light blue and purple bands mark significant changes in $\delta^{13}\text{C}$ -values (CIE A, D and E) at the different South Alpine locations (Recoaro and Eastern Dolomites: Dont, Monte Rite, Schadebach, Kühwiesenkopf).

REFERENCES

- Bechstädt, T., and Brandner, R., 1970, Das Anis zwischen St. Vigil und dem Höhlensteintal (Pragser-und Olang Dolomiten, Südtirol), Geologisches Institut der Universität.
- De Zanche, V. and Mietto, P., 1981, Review of the Triassic sequence of Recoaro (Italy) and related problems. Rend. Soc. Geol. It., v. 4, p. 25-28.
- Gianolla, P., 1998, Triassic sequence stratigraphy in the Southern Alps (Northern Italy): definition of sequences and basin evolution.
- Lippmann, R., Voigt, T., Baunack, C., Föhlisch, K. and Lützner, H., 2005, Geochemische Zyklen im Unteren Muschelkalk (Typus-Profil der Jena Formation, Steudnitz). Z. geol. Wiss, v. 33, no. 1, p. 27-50.
- Weissert, H., and Erba, E., 2004, Volcanism, CO₂ and palaeoclimate: a Late Jurassic–Early Cretaceous carbon and oxygen isotope record: Journal of the Geological Society, v. 161, no. 4, p. 695-702.

P 5.3

Stratigraphic framework and tectono-climatic implications of Upper Cretaceous to Neogene successions of the western Afghan-Tajik depression, Uzbekistan

Sébastien Castellort¹, Thierry Adatte², Hassan Khozyem³, Nicolas Thibault⁴, Marie-Françoise Brunet⁵, Massimo Chiaradia¹, Jorge Spangenberg⁶

¹ *Département des Sciences de la Terre, Université de Genève, Rue des Maraîchers 13, 1205 Genève, Switzerland*

² *ISTE, Geopolis, Université de Lausanne, 1015 Lausanne, Switzerland*

³ *Geology Department, Faculty of Sciences, Aswan University, 81528-Aswan, Egypt*

⁴ *Institute for Geosciences and Natural Resource Management, University of Copenhagen, Øster Voldgade 10, DK-1350 Københavns K., Denmark*

⁵ *Sorbonne Universités, UPMC Univ Paris 06, CNRS, Institut des Sciences de la Terre de Paris (iSTeP), 4 place Jussieu 75005 Paris, France*

⁶ *IDYST, Geopolis, Université de Lausanne, 1015 Lausanne, Switzerland*

The Tajik depression, in Afghanistan, Tajikistan and Uzbekistan is a sedimentary basin surrounded by the Tian Shan Mountains to the North, the Pamir Mountains to the East, and the Hindu-Kush to the South. It contains a thick record of Mesozoic to neogene sedimentary archives deposited in a critical epicontinental area at the transition between the western oceanic Tethys and para-Tethys domains and the eastern continental areas of Asia.

The stratigraphic record at this location holds important keys for understanding the interactions between global and secular climate signals due to the progressive closure of the Tethysian domain and rise of alpine reliefs as well as their effect on lithospheric vertical movements. Recently, several sections have been described in the eastern (1,2) and in the northern part of the area (3).

In this work, our aim is to describe the first order evolution of depositional environments and sequence stratigraphy of the successions of the western edge of this vast depression and to improve the stratigraphic framework constraining the timing of tectonic and climatic important events of the area. Preliminary results combining nannofossil biostratigraphy, strontium and carbon isotopes allow us to indentify a condensed interval around the Cenomanian-Turonian boundary and suggest a possible important hiatus in this period.

High-resolution continuous carbon isotope record through upper-paleocene to lower-eocene Suzak shale provides the first identification of the Paleocene-Eocene CIE in the area. Finally, ⁸⁷Sr/⁸⁶Sr strontium ages suggest that marine deposition persisted until after 34.35 Ma, i.e. after the end of the upper Eocene, and suggest that continentalisation in the area may be related with the Eocene-Oligocene sea-level fall, in a strongly diachronous but consistent fashion when considered with respect to evidences of continentalisation at 39Ma in the Eastern Tajik basin 3 and at 41-37Ma (4) in the Tarim basin.

Reconstruction of depositional environments indicates that the area behaved as a relatively stable shallow epicontinental platform continuously but very slowly subsiding and thus very sensitive to sea-level variations. As a result, the area was not prone to the development and preservation of thick black shale intervals during the cretaceous and PETM events.

REFERENCES

1. Bosboom, R. et al. timing, cause and impact of the late eocene stepwise sea retreat from the tarim basin (west china). *palaeogeography, palaeoclimatology, palaeoecology* 1–51 (2015). doi:10.1016/j.palaeo.2014.03.035
2. Bosboom, R. et al. Linking Tarim Basin sea retreat (west China) and Asian aridification in the late Eocene. *Basin Research* (2014). doi:10.1111/bre.12054
3. Carrapa, B. et al. Tectono-climatic implications of Eocene Paratethys regression in the Tajik basin of central Asia. *Earth and Planetary Science Letters* 424, 168–178 (2015).
4. Bosboom, R. et al. Late Eocene sea retreat from the Tarim Basin (west China) and concomitant Asian paleoenvironmental change. *Palaeogeography, Palaeoclimatology, Palaeoecology* 299, 385–398 (2011).

P 5.4

Continental-Marine correlations and climate signals in the Palaeogene foreland of the South Pyrenees

Louis Honegger¹, Sébastien Castellort¹, Julian Clark², Thierry Adatte³, Cai Puigdefàbregas⁴, Mason Dykstra², Andrea Fildani², Jorge Spangenberg⁴

¹ *Département des Sciences de la Terre, Université de Genève, Rue des Maraîchers 13, CH-1205 Genève (louis.honegger@etu.unige.ch, sebastien.castellort@unige.ch)*

² *Statoil, 6300 Bridge Point Parkway, Austin, TX, USA*

³ *Institut des Sciences de la Terre, Université de Lausanne, CH-1015 Lausanne*

⁴ *Institut de Ciències de la Terra (CSIC), Carrer Lluís Solé Sabaris, 08028 Barcelona, Spain*

⁵ *IDYST, Geopolis, Université de Lausanne, 1015 Lausanne, Switzerland*

Continental to marine correlations have always been a challenge regarding to sequence stratigraphy. The longstanding debate is about how surfaces and sedimentary packages translate from one environment to another and the various origins that have been put forward to explain them : eustatic sea level changes, sediment supply variations, subsidence pulses or tectonic variations.

In the deep water system of the lower-middle Eocene Ainsa basin, in the southern Pyrenees (Spain), as well as in its fluvial counterparts in the Tremp-Graus basin, stratigraphic cyclicity in the form of repetitive packages of sand and shale alternations of intermediate timescales (10^4 to 10^6 years) has long been recognized and has typically been imputed to eustatic changes, with a modulation by active tectonics. Most of the studies have so far focused either on the deep water system or on their fluvial counterparts without a detailed effort at the correlation between both.

Our objective is to evaluate the role of eustatic variations, that are well known to have taken place at these periods, in generating or modifying such cyclicities and to understand the link, at high resolution, between the continental and marine deposits. This is particularly important in order to understand how sea-level fluctuations are tied to depositional environments over multi-millennial times-scales and how the deep-sea sedimentary record can be used to reconstruct the Earth's history of surface response to climate change.

To address these issues, a mapping and multi-proxy approach was undertaken in the Tremp-Graus and Ainsa basins. We focus on the middle Eocene Castissent formation, a major fluvial excursion and its deep marine time-equivalent; the turbiditic sequence between the systems of Arro and Banastón. Through a study of carbon and oxygen stable isotopes, geochemistry of major and trace elements and strontium dating performed on four increasingly distal cross-sections, we attempt to trace environmental signals across the whole source-to-sink system. These analyses coupled with thorough physical mapping on the field allow us to discuss hypotheses of climatic and eustatic controls of cyclicity.

REFERENCES

- Marzo, M., Nijman, W., Puigdefàbregas, C., 1988. Architecture of the Castissent fluvial sheet sandstones, Eocene, South Pyrenees, Spain 719738. doi : 10.1111/j.1365-3091.1988.tb01247.x
- Mutti, E., Séguret, M., Sgavetti, M., 1988. Sedimentation and Deformation in the Tertiary Sequences of the Southern Pyrenees. AAPG Mediterranean Basins Conference (1988 : Nice, France), p169
- Payros, A., Tosquella, J., 2009. Filling the North European Early/Middle Eocene (Ypresian/Lutetian) boundary gap : insights from the Pyrenean continental to deep-marine record. *Palaeogeogr.* 280, 313332. doi:10.1016/j.palaeo.2009.06.018
- Shanley, K., McCabe, P., 1994. Perspectives on the sequence stratigraphy of continental strata. *Am. Assoc. Pet. Geol. Bull.* 78, 544568

P 5.5

Sedimentary responses to tectonic and climatic forcing: a high-resolution, integrated sedimentological-geochemical study in terrestrial foreland deposits (Mendoza, Argentina)

Hunger G.¹, Ventra D.¹, Moscariello A.¹, Veiga G.²

¹ *Earth and Environmental Sciences, University of Geneva, rue des Maraichers 13, 1205 Geneva, Switzerland.*

Contact: gabriel.hunger@unige.ch

² *Centro de Investigaciones Geológicas, Universidad Nacional de La Plata - CONICET, Argentina*

Numerous studies relate foreland-basin infill to allogenic forcing, but to date only a few have been able to clearly disentangle the relative roles of tectonics and climate on long-term deposition. Here we present preliminary observations on the continental sedimentology and stratigraphy of the Central Argentinian Foreland. The basin infill records local environmental changes from the late Oligocene to the Quaternary, during active Andean orogeny.

The Mariño Formation comprises a large part of the basin infill, dating from ~15.7 to 12.0 Ma and extending over almost 1100 m in stratigraphy. The basal part is characterized by the intercalation of aeolian and fluvial deposits, followed vertically by the stacking of fluvial deposits with highly differentiated facies associations and architectures. This stratigraphic picture developed during the uplift of the Principal Cordillera suggests the interaction of different allogenic controls in the region.

This project aims to provide a detailed reconstruction of paleoenvironmental dynamics and to unravel the relative roles of climate and tectonics through a high-resolution, integrated compositional and sedimentological analysis of the Mariño Formation. The main objectives are: to detect geochemical signatures of allogenic controls; to track changes in sediment provenance and relative information on magmatism and exhumation in the uplifting Andes; and to recognize the effects of different allogenic drives on sedimentary processes and local environmental changes.

Our approach consists of high-resolution mineralogical and petrographical study using both conventional approach and automated QEMSCAN technology, heavy-minerals analysis, geochemistry, radiogenic isotope analysis, U-Pb and fission-track dating of detrital zircons.

The exceptional lateral exposure and the possibility to develop stratigraphic correlations calibrated with quantitative analytical approaches will constrain the relative role of different allogenic processes and offer insights for understanding similar sedimentary complexes in the subsurface.

Exploration and extraction of energy resources is increasingly reliant in the detailed characterization of sedimentary reservoirs. Besides providing an extensive outcrop analogue for the characterization and prediction of subsurface reservoirs, this project represents an important, ground-based test of mineralogical and geochemical methods for reservoir correlation and evaluation.

P 5.6

Late Triassic Calcareous Nannoplankton from Georgia and New Age of Moshevani Suite (Caucasus)

Kakhaber Koiava¹, Jon Mosar², Tamar Gavatdze¹, Lia Kvaliashvili³ & Jeremiah Mauvilly²

¹ *Ivane Javakhishvili State University, Alexandre Janelidze Institute of Geology, A. Politkovskaia str. 5, GEO-0186 Tbilisi, (koiava_ka@yahoo.com)*

² *Département de Géosciences - Sciences de la Terre, Université de Fribourg, Chemin du Musée 6, CH-1700 Fribourg, (mosar@unifr.ch)*

³ *LTD "GeoEngService", Ambrolauri str. 5, GEO-0160 Tbilisi, (l.kvaliashvili@yahoo.com)*

The Locki massif located in the southernmost part of Georgia administratively belongs to Bolnisi and Dmanisi regions and orographically presents the eastern part of the South Georgian highlands. The southern of Locki massif forms the axial part of Somkheti Ridge along the Georgian-Armenian boundary. The massif presents a large E-W oriented anticline structure composed of pre-Jurassic basement outcropping in its central part and surrounded by a Mesozoic-Cenozoic sedimentary cover.

Strata of conglomerates and quartz sandstones, known as Moshevani suite (Zesashvili, 1955) can be found in the lower part of the Lower Jurassic sediments almost everywhere on the Locki massif. This suite transgressively overlies pre-Jurassic rocks and is conformably followed by overlying sediments. The age of quartz sandstones and conglomerate strata, located on Locki massif (Moshevani suite) has so far been given as Hettangian (lowermost Jurassic).

The studied section of the Moshevani suite is located at the western periphery of Locki massif, at a distance of 1 km to the N-E of village Gora, in the gorge of the river Gorastskali.

The samples from Gorastskali gorge section were investigated from a nannofloral viewpoint. To this date studies of the rock samples from this section have indicate the lacking of calcareous nannofossils. However, a new sampling and in depth investigation has documented a complex association of calcareous nannofossils including *Crucirhabdus minutus* JAFAR, 1983; *C. primulus* ROOD, HAY & BARNARD, 1973; *Prinsiosphaera triassica* JAFAR, 1983; *Tetralithus cassianus* JAFAR, 1983; *T. pseudotrifidus* JAFAR, 1983; *Hayococcus floralis* JAFAR, 1983; known from Norian-Rhaetian stage (Jafar, 1983; Bralower et al., 1991). Based on these new calcareous nannoplankton data, strata of conglomerates and quartz sandstones in the Gorastskali gorge section (Moshevan suite) have been shown to be of Late Triassic age (Koiava et al., 2013). The detailed bio-stratigraphic attribution places the age of conglomerates and quartz sandstones Norian-Rhaetian epoch.

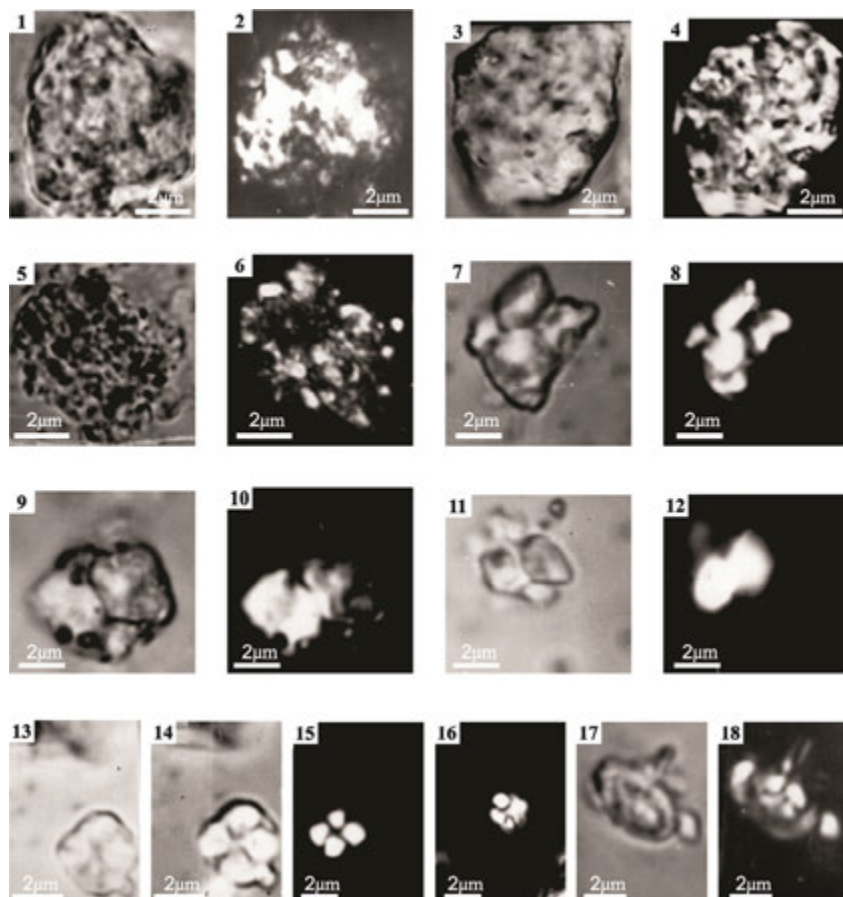


Plate 1. Upper Triassic calcareous nannofossils (All figures light micrographs magnified $\times 1\,200$). 1, 2 - *Prinsiosphaera triasica* JAFAR, 1983; 3, 4 - *Prinsiosphaera triasica* JAFAR, 1983; 5, 6 - *Prinsiosphaera triasica* JAFAR, 1983; 7, 8 - *Tetralithus pseudotrifidus* JAFAR, 1983; 9, 10 - *Tetralithus pseudotrifidus* JAFAR, 1983; 11, 12 - *Tetralithus cassianus* JAFAR, 1983; 13, 14 - *Hayococcus floralis* JAFAR, 1983; 15 - *Hayococcus floralis* JAFAR, 1983; 16 - *Crucirhabdus mintus* JAFAR, 1983; 17, 18 - *Crucirhabdus primulus* ROOD, HAY & BARNARD, 1973.

REFERENCES

- Bralower, T. J., Bown, P. R., & Siesser, W. G. 1991: Significance of Upper Triassic calcareous nannofossils from the Southern Hemisphere (ODP Leg 122, Wombat Plateau, N.W. Australia). *Marine Micropaleontology*, 17, 119-154.
- Jafar, A. S. 1983: Significance of Late Triassic calcareous Nannoplankton from Austrian and Southern Germany. *Neues Jahrbuch für Geologie und Paläeontologie*, 166, 218-259.
- Koiava, K., Gvartadze, T., Glonti (Bacho) V., Kvaliashvili, L. 2013: First Record on Lower Jurassic-Aalenian Calcareous Nannofossils of Georgia. The abstract volume of 5th International Scientific Conference of young scientists and students «Fundamental and applied geological science through the eyes of young scientists: achievements, prospects, problems and ways of their solutions», Baku, Azerbaijan, November 14-15, 171-172.
- Zesashvili, V. 1955: Geology of r. Poladauri basin. *Metsniereba*, Tbilisi, 1-190. (In Russian)

P 5.7

Cretaceous environments and diagenetic events of neritic platform, constantine mounts (north east of Algeria)

Ouided LAZIZ¹, Chaouki BENABBAS², moussa BOULARAK³

¹ *Environment- Geology Laboratory, Constantine University ,street 200 subdivision oued seguin Mila 43000 Algeria .
ouidedlaziz@gmail.com*

² *Environment- Geology Laboratory, Constantine University, new city constantine 25000 chaoukiben@hotmail.fr*

³ *Environment- Geology Laboratory, Constantine University, boussouf city 25000. boularak_moussa@yahoo.fr*

Carbonate mounds of Djebel Kellal -Constantine Rock, constitute one of the mid-Cretaceous outcrops (Cenomanian-Turonian) observed in the Constantine area. These geological deposits mainly neritic show rimmed shelf paleoenvironments. Cenomanian transgression, has recorded the installation of a reef building represented by bioclastic packstones, Rudists floatstone and echinoderms grainstones. During Turonian,, a moderate regression induced implementation proximal facies, starting with benthic foraminifera wackstones and ostracods(very protected environment) grainstones with large benthic foraminifera and oncoids(center very close to reef flat) and ends with dolomitic mudstones and calcispheres wackstones (supratidal-intertidal facies).

Burial neritic sediments and their uplift post diagenetic have generated textural and mineralogical changes, remarkable in the Cenomanian microfacies.

REFERENCES

- Aris Y., 1994 : Etude tectonique et micro tectonique des séries jurassiques à plio-quaternaires du Constantinois central (Algérie nord orientale) caractérisation des différentes phases de déformations. Doctorat d'université, Nancy I, 215p.
- Chadi M., 1991 : Etude géologique de monts de Ain M'lila (Algérie orientale). Thèse de Doctorat de l'Université de Nancy1, 191p
- Robaszynski F., 1994 : Le Cénomanien de la région de KalaatSénan (Tunisie centrale) litho-biostratigraphie et interprétation séquentielle 1994.revue paléobiologie .V12.pp351-505. Genève.

P 5.8

Propagation of detrital signals in the source-to-sink systems of the Tremp-Graus-Ainsa basins, Southern Pyrenean Foreland Basin, Spain

Marc Perret¹, Branimir Segvic¹, Sébastien Castelltort¹, Julian Clark², Cai Puigdefabregas³, Andrea Fildani²

¹ *Département des Sciences de la Terre, Université de Genève, Rue des Maraîchers 13, 1205 Genève, Switzerland*

² *Statoil, 6300 Bridge Point Parkway, Austin, TX, USA*

³ *Institut de Ciències de la Terra (CSIC), Carrer Lluís Solé Sabaris, 08028 Barcelona, Spain*

Late Cretaceous to Oligocene sedimentary fill of the Southern Pyrenean foreland basin consist of clastic and carbonate sediments deposited in an active tectonic system of piggyback foreland basin, which provides a record of the uplift, thrust movements, weathering and erosion of the growing mountain range. The very good outcrop conditions, continuity and stratigraphic framework of these well dated deposits make them an ideal laboratory to study how, in this tectonically active environment, and during a period of changing climates (paleogene-neogene), sediment pathways and provenance can be reconstructed. Previous research has identified several sources of sediment, as for instance southern and northern carbonate platforms acting as sources for shallow water carbonate clasts brought in the basin and an eastern-southeastern fluvial input for siliciclastic sediments (Dreyer et al., 1999; Fontana et al., 1989; Mutti, 1983; Payros et al., 2009). So far, most studies have focused separately either on the sandstone provenance in the fluvial-alluvial environment of the Tremp-Graus sub-basin, or on the deep-marine environment of the Ainsa sub-basin, without considering the whole source-to-sink relationship between these basins. There is therefore a lack of regional-scale sandstone provenance study that we offer to intend with a fast-forward method of petrographic evaluation of siliciclastic sediments.

In this study an analytical tool, QEMScan (Quantitative Evaluation of Materials by Scanning Electron Microscopy), is used as a new method for accurately quantifying petrography and provenance of the sediments and source rocks from the basement. The method uses polished thin sections. We double-check QEMSCAN results with classical optical microscopy and X-ray diffraction. It is our aim to provide insight into the sediment transport patterns and sediment source by observing several detrital signals such as mineralogical variability, heavy mineral ratios and clay minerals ratios and understand the source-to-sink relationship in this basin.

REFERENCES

- Dreyer, T., Corregidor, J., Arbues, P., Puigdefabregas, C., 1999. Architecture of the tectonically influenced Sobrarbe deltaic complex in the Ainsa Basin, northern Spain. *Sedimentary Geology* 127, 127–169.
- Fontana, D., Zuffa, G.G., Garzanti, E., 1989. The interaction of eustacy and tectonism from provenance studies of the Eocene Hecho Group Turbidite Complex (South-Central Pyrenees, Spain). *Basin Research* 2, 223–237.
- Mutti, E., 1983. The Hecho Eocene submarine fan system, south-central Pyrenees, Spain. *Geo-Marine Letters* 3, 199–202.
- Payros, A., Tosquella, J., Bernaola, G., Dinarès-Turell, J., Orue-Etxebarria, X., Pujalte, V., 2009. Filling the North European Early/Middle Eocene (Ypresian/Lutetian) boundary gap: Insights from the Pyrenean continental to deep-marine record. *Palaeogeography, Palaeoclimatology, Palaeoecology* 280, 313–332. doi:10.1016/j.palaeo.2009.06.018

P 5.9

Facies, Depositional Environment of Oligocene deposits in anarak area, Esfahan

Kobra Tahmasebi¹, Javad Darvishi khatooni² & Rahim Mahari³

¹ Islamic Azad University, Science and Research Branch, Tehran, Iran

² Geological survey of Iran

³ Department of Geology, Islamic Azad University, Tabriz, Iran

Lower Red Formation (Oligocene) consists mainly of clastic facies. The coveranextensive eara in North-East of Naein. Litology its often consisted sandstone,congolomerate,and mudstone,that some times consist interbeded of evaporatic and cabonatic minerals. Lower Red Formation (Oligocene) in Anarak region (South–East of Naein) consist of about 320 Meters of detrital and evaporatic facies.

This formation in Anarak area (North East Nain) is about 312 meter. that Consisting of clastic and evaporite facies. Lower Red Formation with unconformity bondry is On deposits of Eocene–ligocene. but in some cases, that these deposits are removed With an angular unconformity On older formations. are observed in this region. Quaternary sediments of the Lower Red Formation unconformably cover. The most important mineral deposits of lower red formation in Anarak is respectively, quartz, calcite, and albite. The petrographic studies, Units range than calcium carbonate rock fragments, feldspar and quartz formed. Major Diagenetic processes of Lower Red Formation in the study area Include cementation, compaction and fracture. The results of mineralogical studies were sediments Units formed from calcium carbonate rock fragments, feldspar and quartz. Accurate field and laboratory studies upon detrital layer of Lower Red Formation lead to break up four groups of facies, Facies group Braided rivers. It is involved deterital sediments of sandstone and congolomerate with sedimentary structures that shown BRAIDED RIVERES depositional invironmets. Facies group playa. Includes very fine mud deposits with chemical deposits that formed in PLAYA conditions.

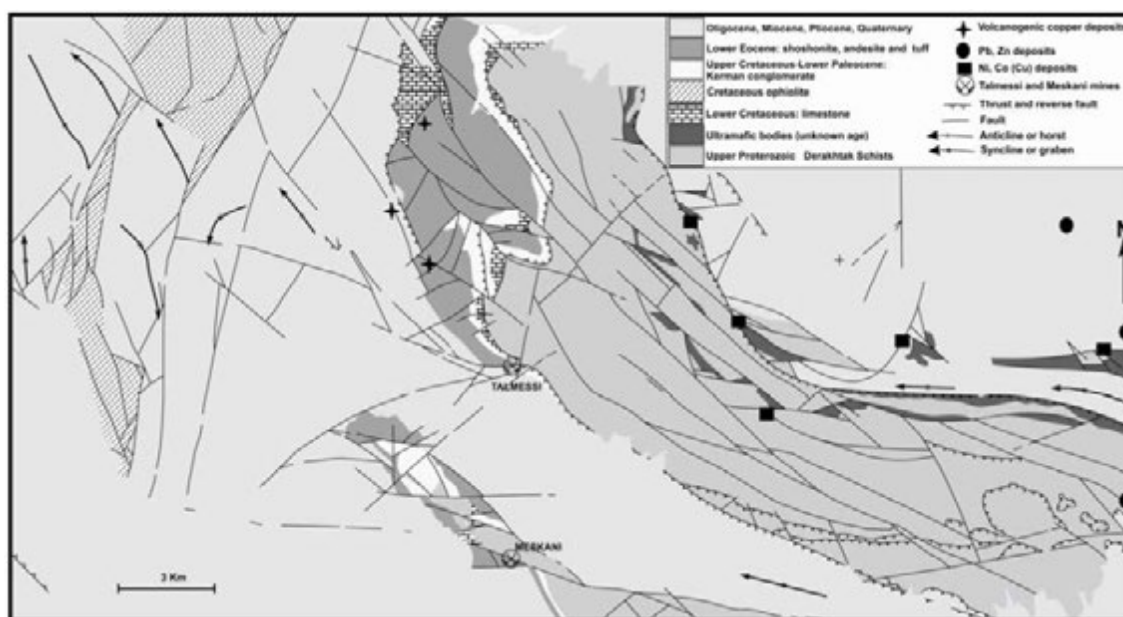


Figure 1. Geological map of Anarak and position of study area(Aghanabati, 2004)

REFERENCES

Aghanabati S. 2004: Iran's geology, mineral exploration Geological Survey of Iran Publishing, 586 pages

7. Geothermal Energy, CO₂ Sequestration and Shale Gas

Lyessé Laloui, Larryn Diamond, Paul Bossart

*Swiss Geothermal Society,
Swiss Association of Energy Geoscientists (SASEG)*

TALKS:

- 7.1 Aschwanden L., Adams A., Diamond L.W., Mazurek M.: Porosity and permeability of the Muschelkalk carbonate aquifer in the Swiss Molasse Basin and their relevance to geothermal energy and gas storage
- 7.2 Burri, P.: Unconventional hydrocarbons – opportunities and challenges (and the increasing role of geology)
- 7.3 Clerc N., Moscariello A., Renard P.: Structural Characterization of the Geneva Basin from 2D Seismic Reflection Data for Future Geothermal Resource Development
- 7.4 Deb R., Jenny P.: Numerical Modeling of Fluid Injection Induced Shear Failure in Fractured Reservoir
- 7.5 Li C., Laloui L.: Caprock and surface deformation induced by carbon dioxide injection
- 7.6 Makhnenko R., Mylnikov D., Laloui L.: Effect of liquid and supercritical CO₂ injection on petrophysical properties of rock
- 7.7 Manceau J.-C., Tremosa J., Lerouge C., Audigane P., Nussbaum C.: Well integrity evolution under chemical (CO₂), temperature and pressure stresses, Mont Terri underground rock laboratory
- 7.8 Nussbaum C., Valley B., Guglielmi Y.: In-situ clay faults slip hydro-mechanical characterization (FS experiment), Mont Terri underground rock laboratory
- 7.9 Obermann A., Kraft T., Wiemer S.: Potential of ambient seismic noise techniques to monitor injection induced subsurface changes at the St. Gallen geothermal site.
- 7.10 Rusillon E., Moscariello A.: The Kimmeridgian Reef Complex: a potential geothermal reservoir in the Greater Geneva Basin
- 7.11 Sutra, M., Spada, M., Burgherr, P.: Geothermal stimulation fluids: risky chemicals?
- 7.12 Valley B., Evans K. F.: Stress magnitudes estimate from borehole failure at the Basel EGS reservoir
- 7.13 Vilarrasa V., Bustarret G., Laloui L.: Early Low Permeability Fault Detection Method to Avoid Felt Induced Seismicity in Geologic Carbon Storage and Wastewater Disposal
- 7.14 Violay M., Madonna C., Burg J.-P.: Brittle versus ductile deformation as the main control of the deep fluid circulation in continental crust
- 7.15 Wanner C., Eichinger F., Jahrfield T., Diamond L.W.: Assessing the formation of large amounts of calcite scaling in geothermal wells in southern Germany
- 7.16 Zingg O., Meier P.: Developpement of a new EGS concept for Switzerland: the Haute-Sorne pilot project (JU)

POSTERS:

- P 7.1 Thien B., Kosakowski G., Kulik D.A.: Fluid-rock interactions in Icelandic hydrothermal systems
- P 7.2 Scott S., Driesner T., Weis P.: The Thermal Structure of High-Enthalpy Geothermal Systems
- P 7.3 Jansen G., Galvan B., Miller S.A.: Towards high resolution modeling of deep geothermal reservoirs on heterogeneous architectures
- P 7.4 Vogler D., Settgast R., Amann F., Bayer P., Elsworth D.: Experimental and Numerical Study of Permeability in Heterogeneous Fractures
- P 7.5 Ziegler M., Valley B., Evans K.F.: Fault orientations inferred from analysis of a microseismic cluster dataset of the Basel EGS reservoir agree well with borehole fracture data
- P 7.6 Preisig G., Negro F.: Enhancement of permeability in geothermal reservoirs: the example of the Salanfe lake – Val d'Illiez geothermal area
- P 7.7 Egli D., Herwegh M., Berger A., Belgrano T.: Structural observations from drill cores of the Grimsel hydrothermal breccia
- P 7.8 Moulas E., Madonna C.: Perm-Fit: a new program to estimate permeability at high P-T conditions
- P 7.9 Mauri G., Marguet L., Jansen G., Olivier R., Marti U., Baumberger R., Allenbach R., Kuhn P., Altwegg P., Miller S.A.: Gravity prospection in region of La Broye
- P 7.10 Adams A., Aschwanden L., Diamond L.W.: Porosity Enhancing Multi-event Dolomitization in the Upper Muschelkalk of the Swiss Molasse Basin: Implications for CO₂ Storage and Geothermal Energy
- P 7.11 Šegvić B., Moscariello A., Arbiol González C., Vacaturo G., Lehu R., D'Odorico A., Limeres A.C., Bernhardt C., Ancheta A., Morettini E.: Reservoir quality prediction based on clay minerals and zeolites distribution: new insights from the pyroclastic-rich Bajo Barreal Formation, Argentina
- P 7.12 Zanoni G., Šegvić B., Moscariello A., Tranchet L.: Reservoir geology, mineralogy and geochemistry of the Dentale and Gamba Formations (Early Cretaceous, Gabon): new insights both at regional and pore scale.
- P 7.13 Müller M.H., Epting J., Huggenberger P.: Combining approaches of monitoring and modelling groundwater temperatures to investigate the subsurface urban heat island of Basel, Switzerland
- P 7.14 Chenaker H., Houha B.: Hydrogeochemistry and Geothermometry of Thermal Groundwater of North-Eastern Algeria
- P 7.15 Do Couto D., Šegvić B., Moscariello A.: Petrography and geochemistry of the Lower Jurassic shale in the southwestern Molasse Basin
- P 7.16 Jaeggi D., Nussbaum C., Bossart P.: Overcoring of a CO₂ – injection borehole and sampling procedure

- P 7.17 Orellana F., Violay M.: Frictional properties of Opalinus Clay
- P 7.18 Schweinar K., Busch A., Bertier P., Stanjek H.: Pore space characteristics of Opalinus Clay – Insights from USANS/SANS experiments
- P 7.19 Alt-Epping P., Diamond L.W.: Coupled models of fluid-rock interaction induced by CO₂ injection into the U. Muschelkalk aquifer in N-Switzerland – code benchmarking and quantifying chemical trapping capacity
- P 7.20 Parmigiani A., Huber C., Bachmann O.: Lattice Boltzmann pore-scale calculations of buoyant non-wetting fluids in heterogeneous porous media
- P 7.21 Rinaldi A. P., Karvounis D., Urpi L., Dublanchet P.: Fluid flow and induced seismicity affected by asperities distribution during geothermal exploitation
- P 7.22 Urpi L., Rinaldi A.P.: Thermo-hydraulic-mechanical simulation of fluid-injection activity and associated fault reactivation with complex rheology.
- P 7.23 Räss L., Omlin S., Licul A., Podladchikov Y., Herman F.: Efficient development of memory bounded geo-applications to scale on modern supercomputers
- P 7.24 Poonoosamy J., Kosakowski G., Van Loon L.R., Mäder U.: A numerical and experimental reactive transport benchmark investigating the coupling between density driven flow, solute transport and chemical reactions
- P 7.25 Caspari E., Milani M., Rubino J.G., Müller T.M., Quintal B., Holliger K.: Numerical upscaling of seismic characteristics of fractured media
- P 7.26 Mallet C., Quintal B., Caspari E. & Holliger K.: Seismic energy dissipation due to wave-induced fluid flow in fractured network: comparison of laboratory data from creep tests with numerical simulations
- P 7.27 Shih P.-J. R., Frehner M.: Laboratory evidence for Krauklis wave resonance in fractures
- P 7.28 Chapman S., Tisato N., Quintal B., Holliger K.: Laboratory measurements of seismic attenuation of partially saturated Berea sandstone for a range of confining pressures

7.1

Porosity and permeability of the Muschelkalk carbonate aquifer in the Swiss Molasse Basin and their relevance to geothermal energy and gas storage

Lukas Aschwanden¹, Arthur Adams¹, Larry W. Diamond¹, Martin Mazurek¹

¹ *Institute of Geological Sciences, University of Bern, Baltzerstrasse 1+3, CH-3012 Bern (lukas.aschwanden@geo.unibe.ch)*

Deep saline aquifers are one of the options under consideration for geothermal energy production and gas storage in the Swiss Molasse Basin (SMB). Particularly the Middle Triassic carbonate rocks within the Middle Muschelkalk (Dolomit der Anhydritgruppe) and Upper Muschelkalk (Trigonodus-Dolomit, Hauptmuschelkalk) show encouraging aquifer properties along the northern margin of the SMB. However, the dimensions and distribution of porous and permeable zones within the aquifer are heterogeneous and there is a lack of understanding of how the aquifer properties evolve towards the south, at progressively greater depths in the basin. The present study aims at providing a conceptual model of the Muschelkalk that defines the magnitudes and the 3D distribution of porosity and permeability throughout the basin, thus supporting exploration for geothermal and gas-storage sites.

The model is being constructed from on-going investigations of drill cores and borehole log data from wells across the SMB. Drill cores and log data have been provided by Nagra and the Corporation for Swiss Petroleum (SEAG). The investigation of drill cores includes a variety of laboratory methods, such as visual logging of the geometry and frequency of macroscopic rock pores and fractures, identification of deposition environments (facies analysis) and measurements of porosity and permeability in bedding-parallel core plugs. Gamma-ray density is being determined along entire dry cores using a Multi-Sensor Core Logger (MSCL). The analyses permit both quantitative and conceptual understanding of the distribution and magnitudes of the aquifer properties, as well as of the processes that have created them.

The laboratory results show that the matrix porosity and permeability of the carbonates are determined by the combination of initial depositional environment (facies) and subsequent diagenetic processes: deposition of oolite shoals which created intergrain pore space; dolomitization which enhanced intercrystalline pore space; dissolution of bivalve shell fragments which formed moldic porosity; dissolution of anhydrite nodules which later dissolved to form cm-scale cavernous pores; pore clogging by mineral precipitation, and compaction and recrystallisation under high overburdens. As the extents of these processes are reflected in the density of the rock, their spatial variability can be examined in the MSCL log.

Robust correlations have been found between MSCL-density and plug porosity, and between plug porosity and plug permeability, allowing calculation of the distribution and average of these key properties. At the Schafisheim well, for example, the porosity calculated from the MSCL log (5.6%) fits well with that calculated from the borehole log (density porosity: 4.4%, sonic porosity 5.5% and neutron porosity: 4.1%). Furthermore, the MSCL-density logs show identical patterns to their corresponding borehole logs. Via these correlations, the permeability distribution can be reliably calculated from borehole logs.

Comparison of the new porosity and permeability data for wells across the SMB (Fig. 1) shows a rapid decrease in magnitudes within the first km below surface. Within the technically favoured depth range for geological storage of gas (800–2500 m) the average porosity and permeability fall from 13.8% to 4.2% and from $1.3 \times 10^{-16} \text{ m}^2$ to $1.7 \times 10^{-18} \text{ m}^2$, respectively. Below 2500 m depth, porosity and permeability maintain virtually constant values of 2–4% and 10^{-17} – 10^{-18} m^2 , respectively. Geothermal electricity production requires temperatures above approximately 120 °C, which corresponds to depths of above 3400 m (at a geothermal gradient of 35 °C/km). Thus, the target depth for geothermal electricity production falls within the porosity and permeability range of 2–4% and 10^{-17} – 10^{-18} m^2 , respectively.

The results for the available wells demonstrate that, in the absence of interconnected fracture networks, the porosity and permeability of the rock matrix in the Middle- and Upper Muschelkalk are too low for geothermal electricity production at depths greater than the 120 °C isotherm ($\geq 3000 \text{ m}$; Fig.1). Even for applications at shallower depths, such as the geological storage of gas or geothermal heat production, the matrix porosity and matrix permeability have only suboptimal magnitudes. Future work will be directed at characterizing the distribution of fracture networks in the SMB. In addition to structural studies, in-situ hydraulic tests will be an important means of quantifying the total permeability at the formation scale.

7.2

Unconventional hydrocarbons – opportunities and challenges and the increasing importance of the geologist

Peter Burri, SASEG

The discussion on unconventional hydrocarbons is mostly driven by emotional arguments and fundamental beliefs rather than scientific analysis and facts. Geoscientists have therefore a role to play to bring the debate back to a rational level.

Unconventional oil and gas are often seen as the product of new, not fully mastered, technologies where the challenge lies in “manufacturing-type”, repetitive operations. In fact the revolution has been triggered more by new geological insights into the functioning of hydrocarbon systems. Key elements of this new thinking are the creation of substantial new porosity in source rocks during thermal maturation, the capability of gas to move through nano-pores and the recognition that a very large part of the generated hydrocarbons are not expelled but remain in the source rock. It is only subsequently that the already long existing technologies, like horizontal drilling and hydraulic fracturing, were applied to exploit the new geological ideas.

The early boom in the US was indeed marked by an almost exclusive focus on drilling and stimulation; the result is that even today some 30% of the wells drilled are non-producers. The industry has now recognized that unconventional resources do not occur in blanket deposits that can be drilled anywhere but that the success of a play is highly dependent on sweet-spots, controlled by tectonic stress patterns, reservoir lithology, facies and geochemical factors – in short, by geology. This gives geoscientists again a decisive role in unconventional exploration.

In the early times of unconventional exploration the „gold-rush“ mentality in the US has led repeatedly to poor operations, resulting in technically and environmentally unacceptable accidents. What is, however, largely ignored in Europe is that - also due to public pressure - the industry has during the last decade developed best practices that allow safe and environmentally clean operations. The risk of these technologies is today not higher than that of any other well-run industrial activity. In Europe hydraulic fracturing and horizontal drilling have been applied thousand-fold in the last decades without any major safety or environmental problems. It is most remarkable that amongst the world's scientific institutions and organizations that have knowhow in the relevant disciplines (deep subsurface geology and geophysics, rockmechanics, drilling and subsurface engineering) not one has come to the conclusion that unconventional technologies like hydraulic fracturing should be forbidden. They all advocate establishing clear rules, standards and adequate controls. In Europe, institutions, opposed to a ban include all EU Academies of Science, the Geological Societies and Surveys and the relevant Research institutions like the BRGM or the German Bundesanstalt für Geologie und Rohstoffe. A ban of hydraulic fracturing would also be the end of all attempts to develop deep geothermal energy in Switzerland.

The huge increase in global gas resources over the past decade has led to a situation where the world's gas demand could be covered for 250 years or more at present consumption. This new supply situation provides the unique chance to rapidly substitute coal and partly oil with gas. Gas is by far the cleanest fossil fuel since it has only 50% of the CO₂ emissions of coal and – more importantly – produces virtually no other harmful by-products like sulphur or fine particle dust, the main cause of air pollution in large cities (a factor often forgotten in the CO₂ dominated discussion). Considering that fossil fuels cover 85% of global energy needs and that growth in renewables is unfortunately still very far away from only covering the annual growth of the global energy demand, such a switch to gas would be a major progress towards a cleaner environment.

Europe's energy demand is covered to 25% by gas. As long as we are so strongly dependent on gas, it makes eminent sense to produce as much of it here, domestically for reasons of supply security but even more so on environmental grounds:

- **We** determine and control the standards to assure a clean and safe production.
- We do not waste a substantial part of the energy to transport gas to Europe, often over thousands of kilometres.
- Methane emissions are virtually eliminated.
- We are politically and economically less vulnerable.

The exploration of hydrocarbons has, however, yet other benefits: the Swiss geoscientists should be most pleased with the acquisition of seismic and the drilling of deep exploration wells since these data constitute the main source of information for understanding the geology of the deep underground of Switzerland.

REFERENCES

- acatech (Editor) 2015: Hydraulic Fracturing: Eine Technologie in der Diskussion (acatech POSITION), München; Herbert Utz Verlag (English version in preparation).
- Burri P. 2014: Hydraulic Fracturing – Postscriptum. A geologist's attempt to summarize what we know and where we go. Swiss Bull. Angew. Geologie, Vol. 19/2, 143-150.
- EASAC (European Academies Science Advisory Council) 2014: Shale gas extraction: issues of particular relevance to the European Union. <http://www.easac.eu>
- Hartmann D. und Meylan B. 2014: Fracking in der Schweiz aus Sicht des Grund- und Trinkwasserschutzes. Swiss Bull. Angew. Geologie, Vol. 19/2, 109-113.
- Reichetseder, P. 2014: Clean Unconventional Gas Production: Myth or Reality? The Role of Well Integrity and Methane Emissions. Swiss Bull. angew. Geol., Vol. 19/2, 39-52.
- Reinicke, K. 2014: The Role of Hydraulic Fracturing for the Supply of Subsurface Energy. Swiss Bull. angew. Geol., Vol. 19/2, 5-17.

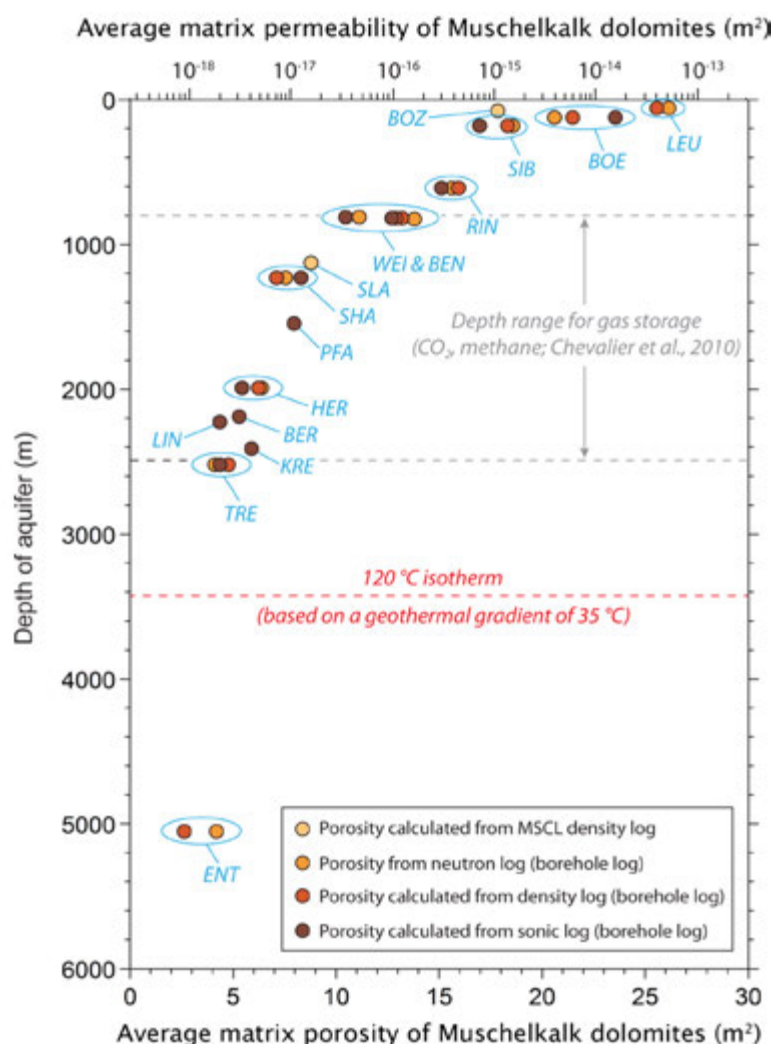


Fig. 1. Average matrix porosity and permeability of Muschelkalk dolomites based on core-plug analyses (i.e. disregarding connected fracture networks at the formation scale)

LEU: Leuggern
BOZ: Bözberg
BOE: Böttstein
SIB: Siblingen
RIN: Riniken, WEI: Weiach,
BEN: Benken
SLA: Schlattigen,
SHA: Schaffisheim, PFA: Pfaffnau
HER: Herdern
BER: Berlingen
LIN: Lindau
KRE: Kreuzlingen
TRE: Treykovagnes

7.3

Structural Characterization of the Geneva Basin from 2D Seismic Reflection Data for Future Geothermal Resource Development

Nicolas Clerc¹, Andrea Moscariello¹ & Philippe Renard²

¹ *Earth and Environmental Sciences, University of Geneva (nicolas.clerc@unige.ch)*

² *Center for Hydrogeology and Geothermics (CHYN), University of Neuchâtel*

The Greater Geneva Basin area covers the southwestern extremity of the North-Alpine foreland Molasse Basin. This transnational zone is tectonically restricted between the internal reliefs of the Jura arc Mountains to the northwest and the front of the Alpine thrusts to the southeast (Fig.1).

In this work, we investigate the structural framework and evolution of the basin through the characterization of fault-systems development from 2D seismic reflection data and geological surface observations. In collaboration with another PhD project aiming at characterizing reservoir facies and properties across the study area (see abstract by Rusillon and Moscariello at this conference), the ultimate goal is to build a consistent subsurface geological and structural framework of the subsurface in order to identify and understand better the distribution and characteristics of potential geothermal reservoirs. In this regard, these projects are developed in the context of the early phases of the «GEothermie 2020» program, jointly driven by the Geneva Industrial Services (SIG) and Geneva State authorities.

In the Geneva area, the overall shortening direction of the basin in response to the alpine compression is oriented NW-SE. This deformation is laterally accommodated by a series of major NW-SE trending sinistral strike-slip faults. However, as already suggested in the past by other authors, detail investigations reveal that the structural scheme of the Geneva basin is relatively more complex than usually simplified on regional-scale tectonic maps and studies: except for the major and well-known Vuache fault zone that can be observed as cross-cutting the entire basin, the Cruseilles, the Le Coin and the Arve fault zones (Fig. 1) appear to be made of smaller-scale fault segments (rather than continuous fault lines), which together absorb the overall deformation of the basin.

Investigations on the entire 2D seismic dataset over the Geneva area are being carried out to delineate the geometries (extensions, orientation) of these fault systems. However, in some parts, their 3D continuation and orientation are difficult to infer with good certainty from 2D seismic lines, leading to non-unique solutions. Correlations with surface observations and clear understanding of the cinematic relationships between these objects in the context of the structuration history of the basin helps to characterize better the structural framework of the Geneva Basin.

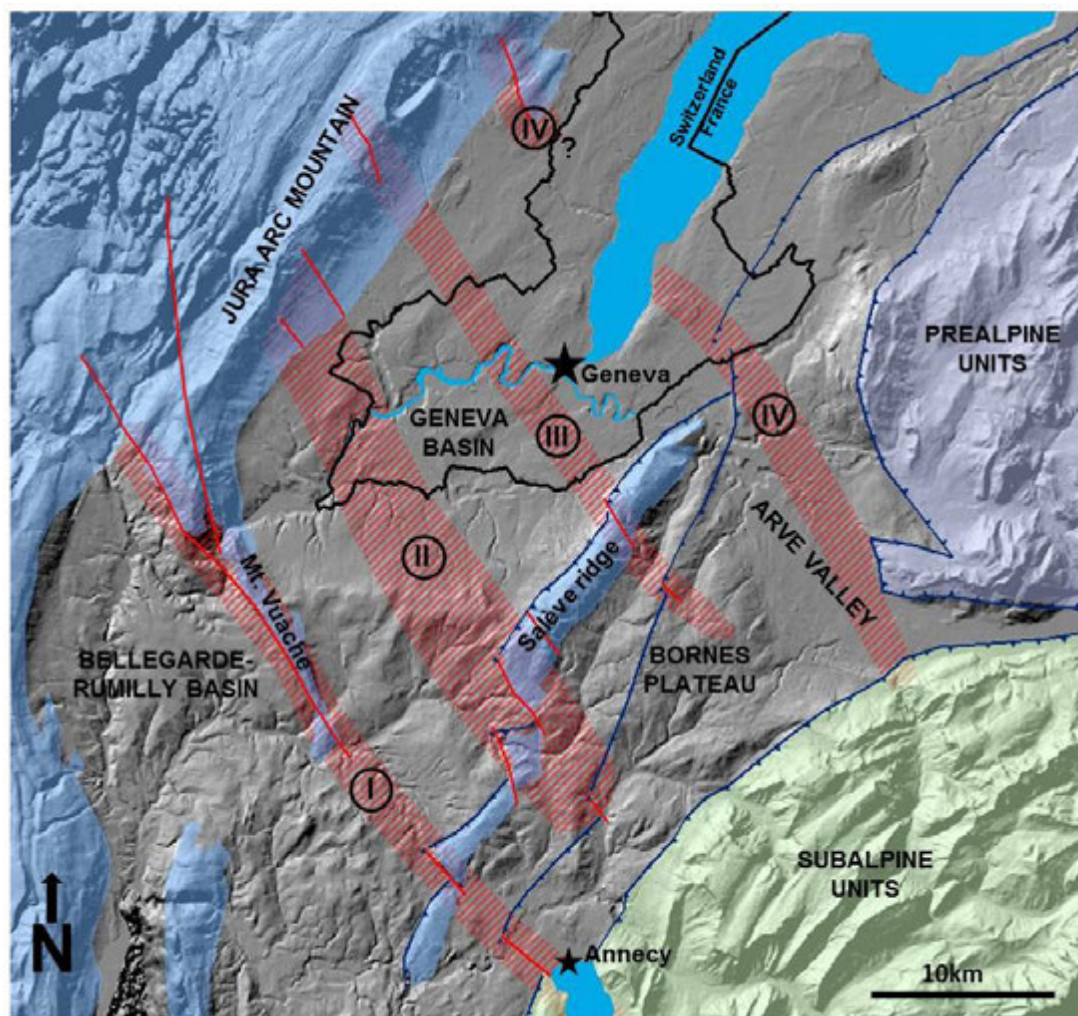


Figure 1. Area of study with indication of the main tectonic lineaments which are focus of the ongoing study: (I) Vuache fault zone; (II) Cruseilles fault zone; (III) Le Coin fault zone & (IV) Arve fault zone.

7.4

Numerical Modeling of Fluid Injection Induced Shear Failure in Fractured Reservoir

Rajdeep Deb, Patrick Jenny

Institute of Fluid Dynamics, ETH Zurich Sonneggstrasse 3, CH-8092 Zurich (debr@ethz.ch)

Numerical studies of enhanced geothermal systems (EGS) require efficient modeling and simulation of the coupled solid and fluid mechanics in the reservoirs. Geothermal systems are natural heat exchangers and the heat exchange between fluid and rock depends strongly on fracture network properties and fluid flow paths. Rock mechanics plays a key role in forming and creating new flow paths, and therefore a first objective is to obtain a physically accurate numerical modeling strategy to describe the geo-mechanics. Typical EGS reservoirs can be approximated by an elastic medium with a high fracture density. A number of properties such as fracture orientation with respect to the principal stress tensors, preferential fluid flow path, friction properties and fracture toughness etc. determine the different failure scenarios. Shear failure is one of the principal mean of achieving increased flow properties through the fracture network.

In order to properly describe the coupled fluid and solid mechanics problem in such systems, large fractures are generally represented as discrete manifolds embedded in the elastic domain, where the system cannot bear traction forces beyond a certain maximum limit. Failure occurs along the fracture manifolds, once the local shear force exceeds the local sustainable traction force. Then an irreversible rock displacement occurs along these manifolds, which is termed as slip. This slip is very important to determine the hydrodynamic flow radius in these fractures. Resolving the shear slip requires to have a domain discretization fully resolved around each fracture network while using traditional FEM or FVM approaches. But this is computationally expensive when the domain is filled with a lot of fractures. An alternative approach is to use special basis functions, which respect the discontinuity along the fractures. A method has been developed here, which resolves such discontinuities for any arbitrary fracture orientation in a finite volume discretization. The solution approach is grid convergent and independent of fracture degree of freedom locations with respect to the matrix domain grid points. We describe this approach as an extended finite volume method (XFVM). For illustration see Fig. 1. The method is coupled with a fluid flow solver, which is developed for flow along fractures surrounded by a porous matrix. The timescale of the shear slip is not resolved in the geo-mechanical problem, instead a new equilibrium equation is solved which describes shear slip along the fracture manifolds in such a way that a constitutive friction law relates the shear traction and compressive force along the fracture manifold. The slip solution triggers an increased flow radius along the fractures, which therefore increases the permeability of the fracture. The discretized mechanical equilibrium equation is solved using a fast multigrid method along with a local Gauss-Seidal pre-conditioner around the failed fracture segments.

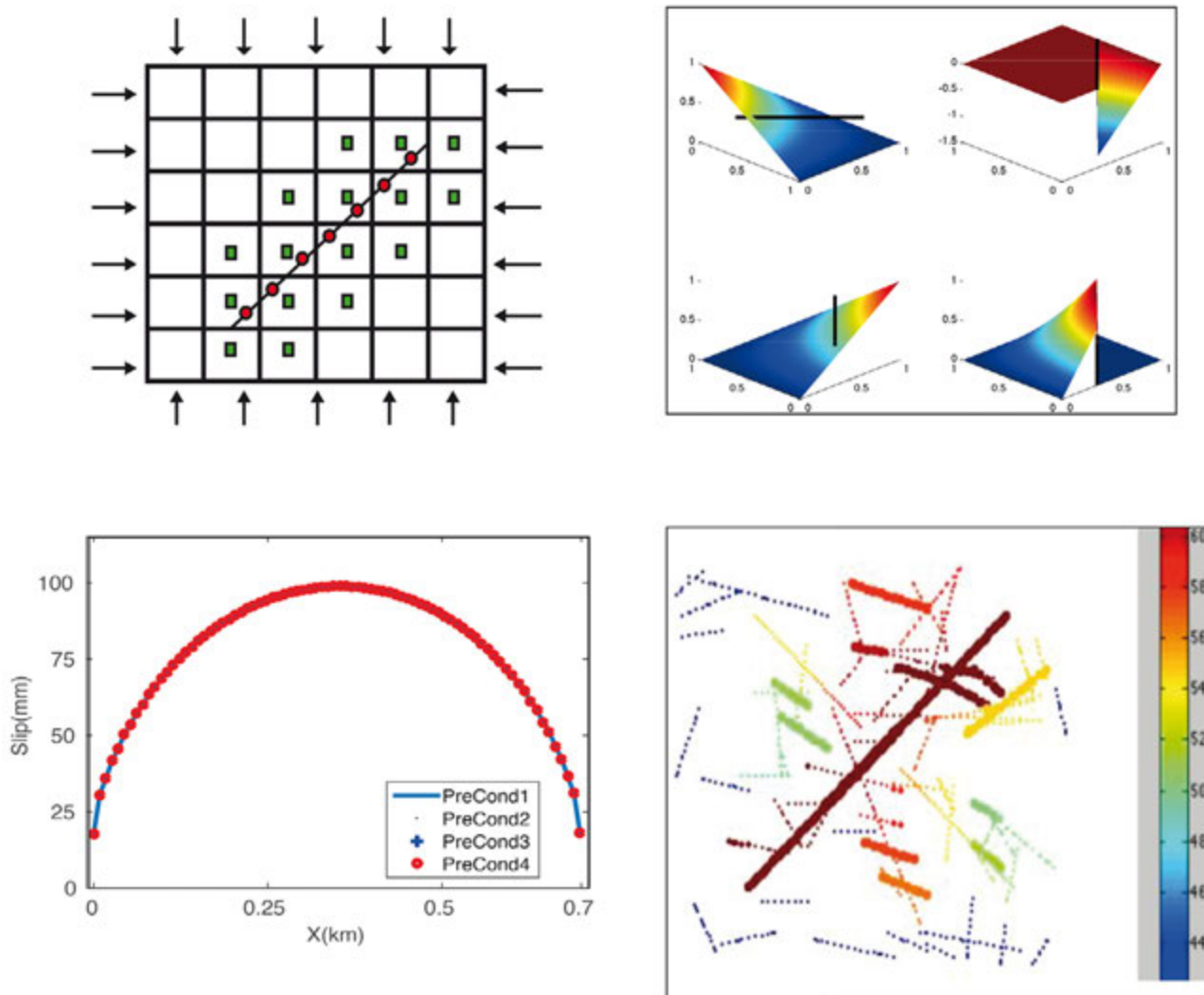


Figure 1. The figures respectively represent in clockwise order from top left, the discretization of the fractured domain, the discontinuity basis functions, the slip solution using different pre-conditioning for mechanical failure of large fractures and finally a snapshot of the pressure solution for a stochastic fracture network with thicker lines representing segments, which have already undergone shear failure and therefore have increased aperture.

REFERENCES

- Peng-Zhi, P., Rutqvist, J., Feng, X., Yan, F. & Jiang, Q. 2014: Rock Mechanics & Rock Engineering 47, 6, 2183-2198.
- Hajibeygi, H., Karvounis, D., & Jenny, P. 2011: A Hierarchical Fracture Model for the Iterative Multiscale Finite Volume Method Journal of Computational Physics 230, 8729-8743.
- McClure, M. & Horne, R 2012: Investigation of Injection Induced Seismicity Using a Coupled Fluid Flow and Rate/State Friction Model Geophysics 76, 6, 181-198.
- Deb, R., & Jenny, P. 2014: Modeling of Failure Along Predefined Planes in Fractured Reservoirs Proceedings, 39th Workshop on Geothermal Reservoir Engineering, Stanford University, Stanford, CA (2014).

7.5

Caprock and surface deformation induced by carbon dioxide injection

Chao Li¹ & Lyesse Laloui¹

¹ *Laboratory of Soil Mechanics - Chair "Gaz Naturel" Petrosvibri, Swiss Federal Institute of Technology of Lausanne, EPFL - ENAC – LMS Station 18 CH-1015 Lausanne (chao.li@epfl.ch)*

CO₂ storage in deep aquifer is considered as a compromising technology to reduce the impact of CO₂ on the greenhouse effect. Practically, large-volume (>1Mt/year) of CO₂ could be injected into a system which consists of a highly porous host aquifer covered by a very low permeable sealing caprock. High rate injection could result in an abrupt fluid pressures build-up, deforming the aquifer and compromising the integrity of caprock. The interaction between fluid flow and mechanical reaction of geomaterials gives rise to a complexly coupled system. It is crucial to understand such hydromechanical processes in order to secure the injection.

We investigate the geomechanical effects induced by CO₂ injection on the aquifer and the related interactions with the caprock. The proposed simulator incorporates real physical properties of supercritical CO₂ and elastic behaviour of involved geomaterials. A conceptual storage system is modelled to investigate the state of caprock deformation during the injection of CO₂, accounting changes in most influential hydro-mechanic properties. We benchmark the In-Salah CO₂ storage surface uplift measurement with the proposed model. A good agreement has been found between the measurement and the simulation, implying that it can be considered as a guide tool for assessing the CO₂ injection hydromechanical problems.

7.6

Effect of liquid and supercritical CO₂ injection on petrophysical properties of rock

Roman Makhnenko¹, Danila Mylnikov¹ & Lyesse Laloui¹

¹ Soil Mechanics Laboratory - Chair "Gaz Naturel" Petrosvibri, École Polytechnique Fédérale de Lausanne, EPFL ENAC IIC LMS, GC – Station 18, CH-1015 Lausanne (roman.makhnenko@epfl.ch)

Deep saline aquifers have the greatest potential for geological storage of CO₂ and due to their worldwide occurrence can play a major role in reduction of carbon dioxide emissions. CO₂ is usually injected in liquid state and, in sedimentary basins at depths below 800 meters, it transfers to the supercritical condition (scCO₂), which means that its temperature and pressure are above 31.1° C and 7.4 MPa. Carbon dioxide then can dissolve in the in-situ fluids and be trapped stratigraphically under the low permeable cap rock and in pore space of the storage formation, as well as by reacting with minerals that form it. Injected CO₂ changes the local effective stresses and temperatures and thus can significantly deform the aquifer and the surrounding media. Therefore, for the proper assessment of safe geologic storage, thermo-hydro-mechanical characterization of possible host and caprock material is needed.

Sandstone reservoirs, which mostly are high-permeable single-porosity systems, are usually considered as a host rock material. Berea sandstone - quartz-rich rock with 23% porosity and 60 mD permeability was fully saturated with water and its poroelastic parameters were measured. Then, liquid (20°C) and supercritical CO₂ (40°C) were injected at 10 MPa pressure and their relative permeability curves were obtained. Residual water saturation after CO₂ flow reached the steady-state condition was evaluated from measurements of Skempton's *B* coefficient, which reflects the compressibility of pore fluid. Relative permeability of liquid CO₂ was found to be 20% larger than the one at supercritical state and both of them are within the reported trends for high-permeable rocks. Thus far, it was found that CO₂ injection does not affect mechanical properties of the quartz-rich rock. However, this statement has to be tested for longer time periods and at elevated pressures.

Furthermore, Opalinus clay is considered to be a representative of the clay-rich caprock material for carbon dioxide storage. Analysis of the poromechanical behavior of the low-permeable shale is critical for anticipation and prevention of its failure and calculation of in-situ effective stresses, thus the preliminary characterization of the poroelastic effect was performed. Laboratory experiments indicated that the chemical effect of CO₂ dissolving in pore water of the caprock dominates at the early stages of injection and delays the mechanical effect of high pressure carbon dioxide desaturating the pores of shale and propagating through it. The chemical effect of high pressure CO₂ - pore fluid mixture on the mechanical properties of caprock is currently under consideration.

7.7

Well integrity evolution under chemical (CO₂), temperature and pressure stresses, Mont Terri underground rock laboratory

Manceau Jean-Charles¹, Tremosa Joachim¹, Lerouge Catherine¹, Audigane Pascal¹ & Nussbaum Christophe²

¹ BRGM, 3 avenue C. Guillemin 45060 Orléans Cedex 2 France (j.tremosa@brgm.fr)

² SWISSTOPO, Seftigenstrasse 264, 3084 Wabern, Switzerland

On a geological carbon dioxide storage site, wells (decommissioned or active) drilled through low-permeable caprock are potential connections between the CO₂ storage reservoir and overlying sensitive targets like aquifers. The integrity of wells over time is therefore essential for the fluids confinements (brine with or without dissolved CO₂ or buoyant gaseous CO₂). Well integrity can be defined as its capacity to maintain the isolation of fluids in the subsurface reservoirs. To ensure this isolation, the well casing and the caprock are bonded by a cement sheath; after abandonment, a cement plug is used to avoid upward migration within the casing. However, according to the literature wellbore integrity might be compromised by a) operational defects (during the drilling and cementing processes, during the operations where pressure and temperature changes can modify stress conditions, during the abandonment process) or b) chemical changes especially in the context of CO₂ storage where different chemical environments can be possibly found.

The evolution of the well integrity is therefore a complex combination of several physical processes (hydrological, thermal, mechanical and chemical at least) on the different materials and elements (formation, cement, casing, interfaces, annuli). The issue addressed in this study is the behaviour of the complete wellbore system in different conditions and especially under influence of CO₂.

An *in situ* experiment (Manceau et al., 2015) has been designed and run in the underground rock laboratory of Mont Terri (Saint-Ursanne, Switzerland) at an intermediate scale between the laboratory experiments (which offer the opportunity to assess specific phenomena over time) and field observations (which allow an assessment of the entire system in subsurface at a specific time). The experimental setup (Fig. 1) reproduces a small section of a wellbore in the Opalinus Clay of the underground rock laboratory (caprock-like formation) at scale 1:1 (5.5 " casing and Ø198 mm borehole), using carbon steel for the casing and class G cement. Below and above the well section, two different intervals have been designed for a continuous monitoring of the pressure and temperature conditions or for fluid injection and extraction (for fluid sampling for instance). Flow and reactive transport modelling as well as lab experiments are performed in parallel to enable a better interpretation and understanding of the observations.

During the successive stages of the *in situ* experiment, changes in temperature, in pressure and in chemical conditions (with or without CO₂) have been imposed in the system. The effective well permeability, which corresponds to the equivalent permeability of the cemented sheath that mimics the well hydraulic property, appears to be influenced significantly by the stresses that have been set. The effective well permeability has drastically decreased (about 3 orders of magnitude) after the temperature has been increased (Fig. 1). Similarly, it has been increased to more than 2 orders of magnitude after an instantaneous pressure increase at the well bottom (Fig. 1). The modeling of hydro-tests results, which suggests a pressure dependence of the well integrity, and the fluid chemical composition evolution suggest preferential flow pathways occurring at the interfaces between the caprock and the cement annulus. The replacement of the bottom interval water with pore water + dissolved CO₂ had lead to changes suggesting a carbonation at the Opalinus clay/cement annulus interface. Such a carbonation is suggested by the lower effect of pressure increase during the hydro-tests (Fig. 1) and by the differential evolutions of the non-reactive and the reactive tracers introduced with CO₂. Complementary analysis including the characterization of the wellbore materials overcored at the end of the experiment are on-going and will allow to quantify this carbonation.

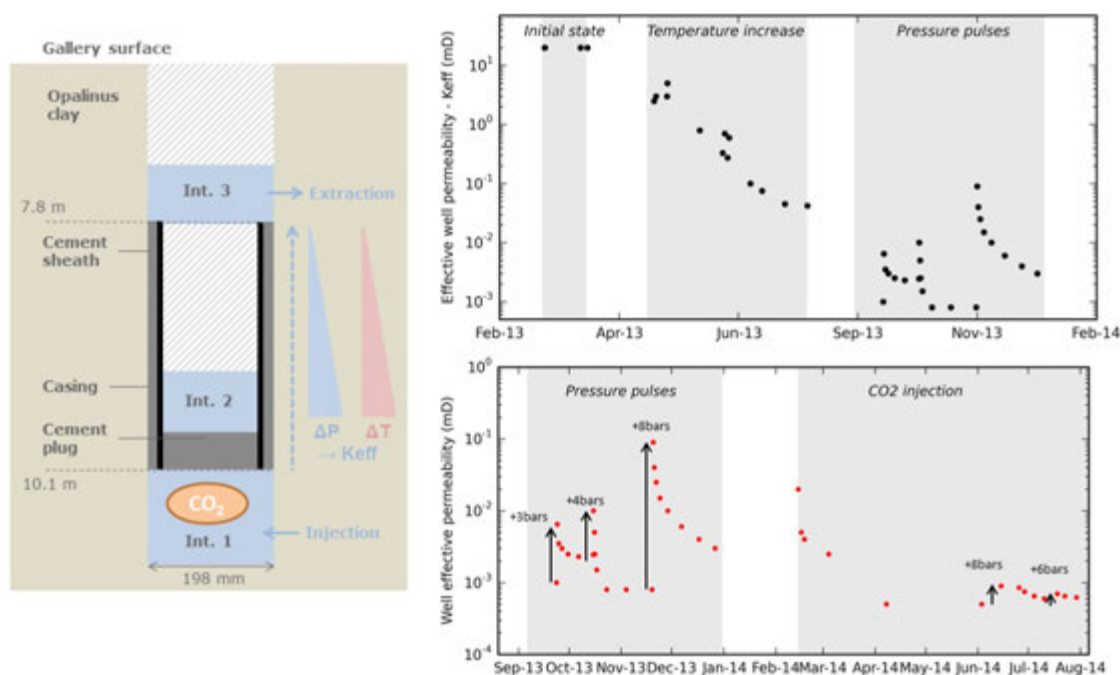


Figure 1. Concept of the *in situ* experiment (at the left); Evolution of the well effective permeability during the different periods of the experiment: initial state and under temperature, pressure and chemical (CO₂) stresses (at the right).

ACKNOLEGEMENTS

This work is performed as part of the EU-funded FP7 project ULTimateCO₂. The ULTimateCO₂ consortium would like to thank Swisstopo and Obayashi for funding a part of this experimentation.

REFERENCES

- Manceau, J.C., Tremosa, J., Audigane, P., Lerouge, C., Claret, F., Lettry, Y., Fierz, T. & Nussbaum, C. 2015: Well integrity assessment under temperature and pressure stresses by a 1:1 scale wellbore experiment, *Water Resources Research*, 51, doi:10.1002/2014WR016786.

7.8

In-situ clay faults slip hydro-mechanical characterization (FS experiment), Mont Terri underground rock laboratory

Christophe Nussbaum¹, Benoît Valley² & Yves Guglielmi³

¹ *swisstopo, Swiss Geological Survey, 3084 Wabern, Switzerland*

² *Center for Hydrogeology and Geothermics (CHYN), University of Neuchâtel, 2000 Neuchâtel (Switzerland)*

³ *CEREGE (UMR7330), Aix-Marseille University, CNRS-IRD, 13330 Marseille, France*

Little is known about the rock mechanical characteristics of pre-existing tectonic faults and their influence on rock mass properties and behavior in clay rocks. Underground research laboratories provide exceptional conditions to observe unaltered fault zones in claystones and to perform relatively well constrained experiments. They allowed exploring past movements of faults and paleofluids in three dimensions in unaltered conditions. This is particularly important for faults in clay formations which typically cannot be observed at the Earth's surface because of the strong weathering. Here we show how an experiment conducted in the Mont Terri underground rock laboratory may help at understanding (i) the conditions for slip activation and stability of pre-existing faults in low permeability clay formations, (ii) the evolution of the coupling between fault slip, pore pressure and fluids migration. Results obtained by the FS experiment are crucial in defining mechanisms of natural and induced earthquakes, their precursors and risk assessment but also the loss of integrity of natural low permeability barriers.

Recent data show that slow slip on faults may be a dominant deformation mechanism of claystones during hydraulic stimulation (Zoback et al., 2012). We argue that faults in clay rocks that are critically stressed, i.e. close to the rupture limit can be reactivated due to moderate stress variations comparable to stress variations associated with shallow underground excavations. The conditions for slip activation on clay faults are poorly understood, the clay content being suspected to constrain the frictional properties and the type of seismicity that can be triggered. Furthermore, micrometer-to-millimeter scale reactivations may lead to large increase in permeability with factor of 10 or more without generating significant seismicity. This appears to be mainly related to complex multi-scale geological processes linked to fault history such as differential hardening, partial sealing, pressure solution and gouge development within the fault zones than to the regional state of stresses. These unique results are of great importance in evaluating fault seal integrity in oil and gas exploration, production or CO₂ storage, and underground excavations in close vicinity to fault zones.

The key idea of the FS experiment is to conduct localized pressurizations in a borehole drilled through the Main Fault intersecting the rock laboratory. Water is injected between two inflatable packers (straddle packer system) at increasing flow rates in order to progressively decrease the effective stress until fault destabilization occurs. Experiment goes on while monitoring injection flow rate, pore pressure, fault slip and normal displacement evolution from the stable to the unstable fault states. Monitoring is performed at 500 Hz frequency with a new device called the HPPP probe (Guglielmi et al., 2013, 2015).

A first test was conducted in June 2015 at a depth of 47.20m from the gallery floor, clearly outside the influence of the excavation damage zone (Fig.1). The injection interval was located 2.5 m below the lower boundary of the Main Fault in order to perform a leak-off test. During this first test we produced a slip of 171µm for a slip rate of 1.2 to 4 µm/s and a dilatancy of 38µm on subhorizontal secondary faults included in the injection interval. We measured a strong increase in flowrate after 6300 seconds injection and the movement almost stopped when the flowrate increased. Likely, a high permeable fault (probably the Main Fault) has prevented further hydroshearing along the subhorizontal secondary faults. A series of new injections at different sections within the Main Fault is planned for October 2015 with an additional HPPP probe.

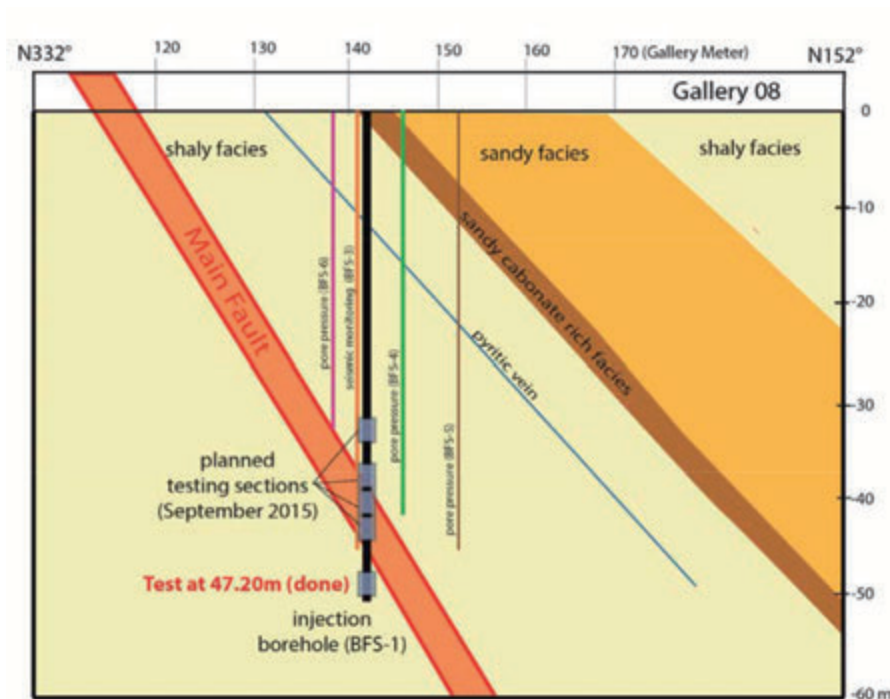


Figure 1. Concept of the FS experiment (vertical section). A series of injections is conducted without and outside the Main Fault using a HPPP probe.

ACKNOWLEDGMENTS

This work is funded by four Partners of the Mont Terri Consortium: swisstopo, ENSI, JAEA and US. DOE (though LBLN).

REFERENCES

- Guglielmi, Y., F. Cappa, H. Lançon, J.B. Janowczyk, J. Rutqvist, C.F. Tsang, and J.S.Y. Wang. 2013. ISRM Suggested Method for Step-Rate Injection Method for Fracture In-Situ Properties (SIMFIP): Using a 3-Components Borehole Deformation Sensor. *Rock Mech. Rock Eng.*, DOI 10.1007/s00603-013-0517-1.
- Guglielmi Y., Cappa F., Avouac J-Ph., Henry P. and Elsworth D. 2015.. Seismicity triggered by fluid injection–induced aseismic slip. *Science* 348, 1224 (2015); DOI: 10.1126/science.aab0476
- Zoback M., Kohli A., Das I. and McClure M. 2012. The importance of Slow Slip on Faults During Hydraulic Fracturing Stimulation of Shale Gas Reservoirs. *Society of Petroleum Engineer, SPE155476*, The Americas Unconventional Resources Conference, Pittsburgh, Pennsylvania, USA, 5-7 June 2012.

7.9

Potential of ambient seismic noise techniques to monitor injection induced subsurface changes at the St. Gallen geothermal site.

Anne Obermann¹, Toni Kraft¹, Stefan Wiemer¹

¹ *Schweizerischer Erdbebendienst (SED) ETH Zürich Sonneggstrasse 5, 8092 Zürich, Switzerland (luca.urpi@gmail.com)*

The failures of two recent deep geothermal energy projects in Switzerland (Basel, 2006; St. Gallen, 2013) have again highlighted that one of the key challenges for the successful development and operation of deep underground heat exchangers is to control the risk of inducing potentially hazardous seismic events. In St. Gallen, after an injection test and two acid injections that were accompanied by a small number of micro-earthquakes ($ML < 0.2$), operators were surprised by an uncontrolled gas release from the formation (gas kick). The “killing” procedures that had to be initiated following standard drilling procedures led to a $ML_{3.5}$ earthquake.

With ambient seismic noise cross correlations from nine stations, we observe a significant loss of waveform coherence that we can horizontally and vertically constrain to the injection location of the fluid. The loss of waveform coherence starts with the onset of the fluid injections 4 days prior to the gas kick. We interpret the loss of coherence as a local perturbation of the medium. We show how ambient seismic noise analysis can be used to assess the aseismic response of the subsurface to geomechanical well operations and how this method could have helped to recognize the unexpected reservoir dynamics at an earlier stage than the microseismic response alone, allowed.

7.10

The Kimmeridgian Reef Complex: a potential geothermal reservoir in the Greater Geneva Basin

Elme Rusillon¹ & Andrea Moscariello¹

¹ *Department of Earth Sciences, University of Geneva, 13 Rue de Maraichers, CH-1205 Genève*

Since 2013, the State of Geneva (Switzerland) has initiated a multistage program named GEothermie 2020, which aims at assessing and developing the deep geothermal energy resources of the trans-border (Swiss-French) Greater Geneva Basin. A review of the entire basin sequence ranging from Permo-Carboniferous to Lower Cretaceous units is carried out to target the potential reservoirs. Promising units were identified and are now thoroughly investigated for reservoir assessment.

The reservoir assessment comprises (1) a well log and detailed core petrophysical analyses, (2) a microfacies study using conventional petrography and automated QEMSCAN analyses and (3) a diagenetic study by optical cathodoluminescence. In parallel, a complementary PhD project investigates the structural framework of the basin (see abstract by Nicolas Clerc et al. in this conference) in order to identify faults and enhanced permeability zones resulting from fractures development and connectivity across the basin.

Measured porosity and permeability along with suitable depth and temperature suggest that the Kimmeridgian Reef Complex is the main reservoir target in the Greater Geneva Basin. Microfacies analyses on well samples and outcrop analogues show that the micro-porosity is the predominant intrinsic characteristic in this reservoir. Analogue geothermal reservoirs are already operational around the Munich area in the Malm of the Bavarian basin, where karstified and dolomitized sponge and coral reef system with intercalated lagoonal deposits offer a sustainable source of heat and electrical power (Lüschen et al. 2014; Weber et al. 2015). In the Geneva basin, similar facies are observed in the Kimmeridgian Reef Complex (Fookes 1995), although the diagenetic imprint is different and a significant lateral variability is observed.

All collected and measured sedimentological observations and petrophysical parameters are being integrated in a 3D subsurface model based on 2D seismic line interpretation. Reconstruction of depositional environment and diagenetic evolution through time in target reservoirs, coupled with seismic facies and structural analyses of the basin, are key

geological parameters for the successful development of geothermal energy in the Greater Geneva Basin.

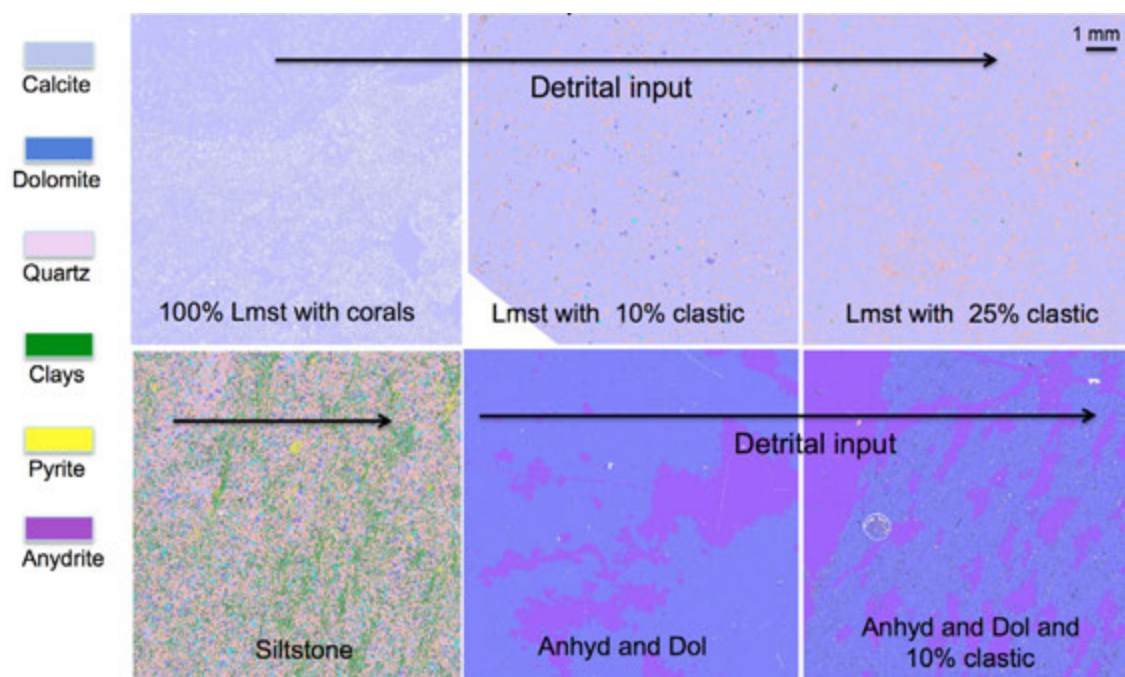


Fig. 1: High-resolution petrographical images obtained with QEMSCAN of carbonate, clastic, and dolomitic-anhydritic rocks. These images and quantitative compositional analysis are used in this study for both stratigraphic, sedimentological, paleoenvironmental and reservoir quality assessment interpretations.

REFERENCES

- Fookes E (1995) Development and Eustatic Control of an Upper Jurassic Reef Complex (St-Germain-de-Joux, Eastern France). *Facies* 33:129–150.
- Lüschen E, Wolfgramm M, Fritzer T, et al (2014) 3D seismic survey explores geothermal targets for reservoir characterization at Unterhaching, Munich, Germany. *Geothermics* 50:167–179.
- Weber J, Ganz B, Schellschmidt R, et al (2015) Geothermal Energy Use in Germany. *World Geothermal Congress*. pp 427–432.

7.11

Geothermal stimulation fluids: risky chemicals?

Emilie Sutra¹, Matteo Spada, Peter Burgherr

Laboratory for Energy Systems Analysis, Paul Scherrer Institut, CH-5232 Villigen PSI ¹emilie-marie.sutra@psi.ch

Expected to significantly contribute to the future supply of renewable energy and presenting wide potential resources, deep geothermal energy systems are not yet extensively established. As for any other energy technology, the extraction and exploitation of natural resources from the underground is never free of risk. To better constrain the associated risks with the deep geothermal energy, numerous studies have been carried out but were mainly focused on the induced seismicity risk.

Nevertheless, to be able to estimate how risky a technology can be, a comprehensive risk assessment should consider additional aspects. While the public concern about the hydraulic stimulation process keeps growing, the chemical stimulation (e.g., matrix acidizing) represents an alternative or complementary procedure to enhance the reservoir connectivity, which is nowadays commonly employed within the deep geothermal systems exploitation. Despite of it, the public detailed data disclosure of the composition of stimulation fluids, which represents key information, is still not a common habit in the geothermal community.

However, some partial disclosures are available in the literature mentioning the main components of the injected solutions, and in the best cases the concentrations and/or quantities used are also divulged. In addition, specific geothermal cases from Switzerland that were confidentially communicated are allowed to be used in this study, and include a complete detailed composition of the stimulation fluids.

In this study, we aim to assess the degree of risk associated with the hazardous substances employed during the chemical stimulation process for deep geothermal systems. After the collection of data from Switzerland and neighboring countries, an exposure and toxicity analysis is performed. To proceed, a probability assessment methodology is applied for the chemicals concentrations, enabling to determine the level of use that can be considered as risky for occupational human health and for the environment. In addition, correlated with these concentration levels, quantities of chemicals can be estimated to discuss implications in terms of safety measures and policy decisions.

7.12

Stress magnitudes estimate from borehole failure at the Basel EGS reservoir

Benoît Valley¹, Keith F. Evans²

¹ *Center for Hydrogeology and Geothermics, University of Neuchâtel, Emile Argand 11, CH-2000 Neuchâtel (benoit.valley@unine.ch)*

² *Institute for Geophysics, ETH Zürich, Sonneggstrasse 5, CH-8092 Zürich*

The in-situ state of stress plays a major role in determining the response of the rock mass to hydraulic stimulation injections, which are used to develop heat-exchangers in low-permeability EGS reservoirs. As such, stress and its heterogeneity must be specified in any geomechanical model of the stimulation process. This paper presents the results of an evaluation of stress magnitudes in the granitic EGS reservoir in Basel, Switzerland, that complements a previous analysis reported by Häring et al. (2008).

In Häring et al. (2008), the profile of minimum principal horizontal stress, Sh_{min} , was constrained by hydraulic tests, but the magnitude of the maximum horizontal principal stress, SH_{max} was uncertain. Here we derive estimates for SH_{max} by analysing breakout width data from an acoustic televiewer log run the 5 km deep borehole BS-1. Some 81% of the borehole below the granite top at 2.42 km is affected by breakouts (see Figure 1a and b), which is favourable for examining the depth trends of the estimates. A primary objective of the present analysis is to evaluate the impact of four different failure criteria on the SH_{max} magnitude estimates. The criteria where Rankine, Mohr-Coulomb, Mogi-Coulomb, and Hoek-Brown 3D. All were parametrized using strength data from a single multi-stage triaxial compressive test on a core plug taken from near the well bottom.

A numerical approach extending that proposed by Barton et al. (1988) was employed to derive SH_{max} magnitude from the estimated breakout widths. The analysis takes into account all stress components at the borehole wall including the remnant thermal stress arising from the cooling of the borehole wall by the drilling. Previous studies of breakout width have shown that small-scale fluctuations are associated with fractures, which reflect variations in strength or stress, or both. At larger scales, breakout width tends to decrease with depth (see Figure 1c). Assuming there is no significant systematic change in the strength characteristics of the rock along the length of the hole, for which there is no evidence, the large-scale trend has the consequence of implying a small gradient of the SH_{max} profile. This result is independent of the failure criterion, and also of the profile of Sh_{min} used in the analysis.

The absolute values of SH_{max} depend largely upon the failure criterion used. Criteria that consider the strengthening effect of the intermediate stress (Mogi-Coulomb and Hoek-Brown 3D) yield profiles that violate frictional limits on the strength of the crust above 4 km (not shown on Fig. 1), whereas the profiles of the Mohr-Coulomb and Rankine criteria (Fig. 1d) do not (the latter two are essentially identical for the case where pore pressure and wellbore pressure are equal and in the range of Sh_{min} and SH_{max} relevant for our analyses). The Mohr-Coulomb/Rankine criteria profiles indicate a trend in SH_{max} from favouring strike-slip faulting above 4200 m to strike-slip/normal faulting below. This is reasonably consistent with focal mechanisms recorded during the reservoir stimulation which show a mix of strike-slip and normal faulting throughout the depth range considered (Kraft and Deichmann, 2014).

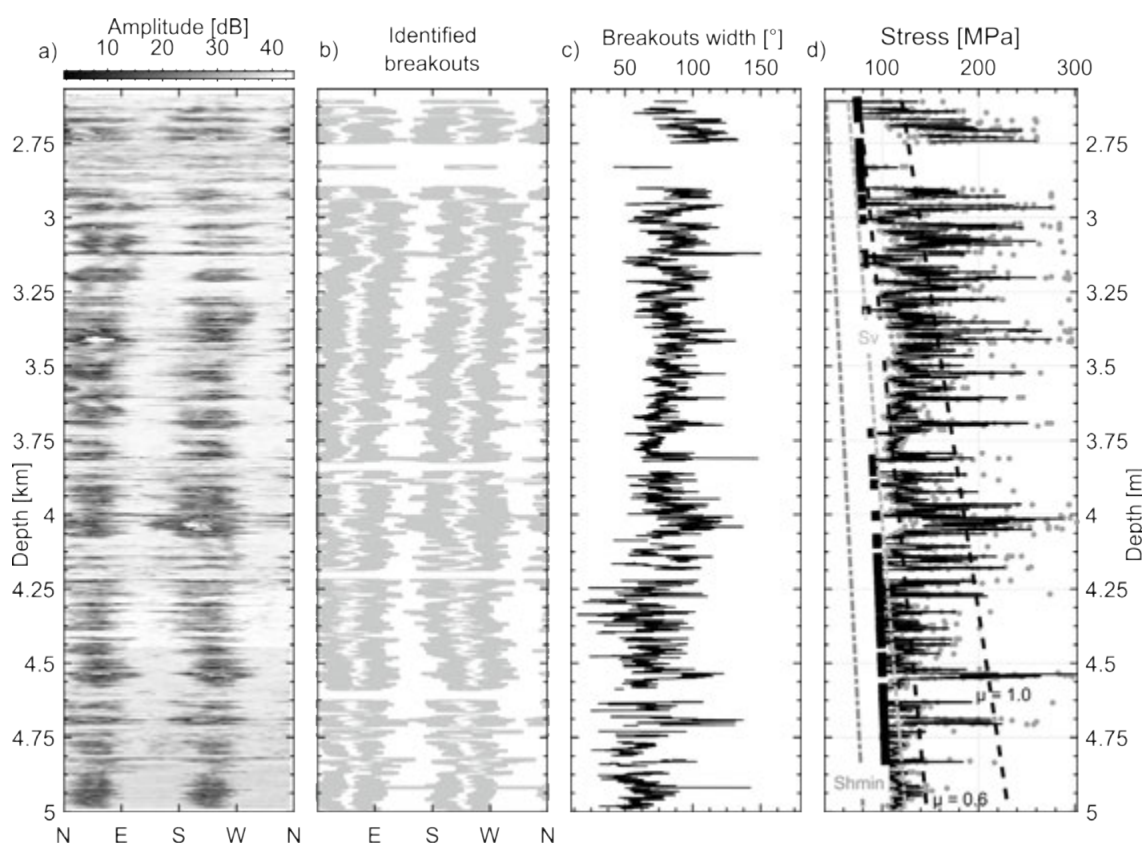


Figure 1. a) Unwrapped amplitude image from an acoustic televiewer run in the borehole BS-1 showing near-continuous breakouts traces. b) Sketch of identified borehole breakouts. White lines: breakout centres estimated visually as the deepest point of each breakout limbs. Light grey area: breakout span. c) Breakout width profile from averaging the width of both limbs. d) Maximum horizontal stress estimation using breakout width and a Mohr-Coulomb failure criteria.

REFERENCES

- Barton, C. A., Zoback, M. D., & Burns, K. L. 1988: In-situ stress orientation and magnitude at the Fenton geothermal site, New Mexico, determined from wellbore breakouts. *Geophysical Research Letters*, 15(5), 467–470.
- Haring, M., Schanz, U., Ladner, F., & Dyer, B. 2008: Characterisation of the Basel 1 enhanced geothermal system. *Geothermics*, 37(5), 469–495. doi:10.1016/j.geothermics.2008.06.002
- Kraft, T., & Deichmann, N. 2014: High-precision relocation and focal mechanism of the injection induced seismicity at the Basel EGS. *Geothermics*, 52, 59–73. doi:10.1016/j.geothermics.2014.05.014

7.13

Early Low Permeability Fault Detection Method to Avoid Felt Induced Seismicity in Geologic Carbon Storage and Wastewater Disposal

Victor Vilarrasa¹, Gil Bustarret¹ & Lyesse Laloui¹

¹ *Soil Mechanics Laboratory, Swiss Federal Institute of Technology in Lausanne, Route Cantonale, CH-1015 Lausanne (victor.vilarrasariano@epfl.ch)*

Fluid injection related to wastewater injection, geothermal energy and oil and gas production has significantly increased in the last years. Furthermore, huge amount of carbon dioxide (CO₂) will have to be stored in deep saline formations to mitigate climate change. These injection operations cause a pressure buildup and temperature decrease around the injection well, reducing the effective stresses (Vilarrasa and Laloui, 2015). This reduction brings the stress state closer to failure conditions, which may yield shear slip of pre-existing fractures or faults, induce seismicity. If this induced seismicity is felt on the ground surface, public acceptance can be negatively affected and may end up with the closure of the injection project, as occurred at Basel (Bachmann et al., 2012).

To avoid inducing felt seismic events, a good pressure management is essential. To assist pressure management, we propose a methodology to identify and locate low permeability faults that have remained undetected by geophysical methods due to their small offset. Such low permeability faults may generate an additional overpressure within the injection formation that could reactivate faults. By using diagnostic plots, changes in the trend of the overpressure can be detected with enough anticipation so that the injection operator can adopt the proper mitigation measures to keep overpressure below the maximum sustainable injection pressure. Thus, induced seismicity could be minimized and large events avoided.

We formulate the problem in terms of dimensionless variables. Thus, our methodology can be applied to all injection sites, regardless of their properties and geometrical distribution. We have successfully applied our methodology to water and CO₂ injection through a horizontal well in a confined aquifer that has a fault parallel to the well. We have found that in order to observe an additional overpressure with respect to the overpressure induced in an infinite homogeneous aquifer, the fault permeability should be at least three orders of magnitude lower than that of the aquifer. The divergence time between the overpressure of an aquifer with a fault and an aquifer without any fault is identified much before in the pressure derivative than in the pressure measurements. Thus, the use of diagnostic plots allows anticipating to additional overpressure that could induce felt seismic events.

REFERENCES

- Bachmann, C.E., Wiemer, S., Goertz-Allmann, B.P. & Woessner, J. 2012: Influence of pore-pressure on the event-size distribution of induced earthquakes. *Geophysical Research Letters*, 39(9), doi: 10.1029/2012GL051480.
- Vilarrasa, V. & Laloui, L. 2015: Potential fracture propagation into the caprock induced by cold CO₂ injection in normal faulting stress regimes. *Journal of Geomechanics for the Energy and the Environment*, 2, 22-31.

7.14

Brittle versus ductile deformation as the main control of the deep fluid circulation in continental crust

Marie Violay¹, Claudio Madonna² & Jean-Pierre Burg²

¹ EPFL ENAC, LEMR, Station 18, CH-1015 Lausanne (marie.violay@epfl.ch)

² Geologisches Institut, ETH Zurich, Sonneggstrasse CH-8092 Zurich

The Japan Beyond-Brittle Project (JBBP) and the Taupo Volcanic Zone-Deep geothermal drilling project in New Zealand (TVZ-DGDP) proposed a new concept of engineered geothermal development where reservoirs are created in ductile rocks. This system has a number of advantages including (1) a simpler design and control of the reservoir owing to homogeneous rock properties and stress states beyond the brittle ductile transition, (2) less probability for induced earthquakes. However, it is at present unknown what and how porosity and permeability can be engineered in such environments.

It has been proposed that the magmatic chamber is surrounded by a hot and ductile carapace through which heat transfer is conductive because the plastic behaviour of the rock will close possible fluid pathways. Further outward, as temperature declines, the rock will encounter the brittle-ductile transition with a concomitant increase in porosity and permeability. The thickness of the conduction-dominated, ductile boundary zone between the magmatic chamber and the convecting geothermal fluid directly determines the rate of heat transfer.

To examine the brittle to ductile transition in the context of the Japanese crust, we conducted deformation experiments on very-fine-grain granite in conventional servocontrolled, gas-medium triaxial apparatus (from Paterson instrument). Temperature ranged from 600°C to 1100°C and effective confining pressure from 100 to 150 MPa. Dilatancy was measured during deformation. The method consisted in monitoring the volume of pore fluid that flows into or out of the sample at constant pore pressure. Permeability was measured under static conditions by transient pressure pulse method. Mechanical and micro-structural observations at experimental constant strain rate of 10^{-5} s^{-1} indicated that the granite was brittle and dilatant up to 900 °C. At higher temperatures the deformation mode becomes macroscopically ductile, i.e., deformation is distributed throughout the sample and no localized shear rupture plane develops. These observations have important implications for deep geothermal power in Japan.

7.15

Assessing the formation of large amounts of calcite scaling in geothermal wells in southern Germany

Christoph Wanner¹, Florian Eichinger², Thomas Jahrfeld³, Larry W. Diamond¹

¹ *Institute of Geological Sciences, University of Bern, Baltzerstrasse 1+3, CH-3012 Bern (wanner@geo.unibe.ch)*

² *Hydroisotop GmbH, Woelkestr. 9, D-85301 Schweitenkirchen, Germany*

³ *renerco plan consult, Herzog-Heinrich Str. 13, D-80336 München, Germany*

The carbonate-dominated Malm aquifer in the Bavarian Molasse Basin is being widely exploited and explored for geothermal energy. Owing to karstification, the fracture spacing and permeability is high enough for continuous water extraction. Therefore, some 40 wells have been drilled in the greater Munich area over the last 10 years. Typical flow rates are between 30 and 130 L/s and the production temperatures reach up to 150 °C. Despite these favorable reservoir conditions, the use of many of the wells for heat and power production is highly challenging. The main difficulty, especially in the deep (>3000 m) boreholes with temperatures >120°C, is that substantial amounts of calcite scaling are hindering the proper operation of the pumps within the wells and of the heat exchangers at the surface.

We have conducted a detailed investigation of calcite scalings formed along the casing at one particular geothermal well over a period of ca. 3 months. The thickness of the scalings could be measured as a function of depth because a total of 68 new casing tubes were installed prior to this production period and because the tubes were taken out to replace the pump at the end of the period. Interestingly, the scaling was thinner where the casing tubes were initially coated with a plastic film, which was the case for about 40% of the tubes. Mineralogical and chemical analyses revealed that the scalings from the coated tubes were almost pure calcite whereas corrosion products such as pyrrhotite were identified in scalings from the uncoated tubes in addition to the dominant calcite. Moreover, methane gas and petroleum inclusions were identified in calcite crystals from both types of casing tubes.

To assess key processes controlling scaling formation a series of reactive transport model simulations were performed using the code TOUGHREACT V3. The simulations were run for a 800 m long domain corresponding to the part of the well located above the pump. A parabolic velocity distribution was defined using a 2D radial mesh to simulate the effect of a decreasing fluid upflow velocity towards the casing. Simulation results show that (i) enhanced corrosion of the casing, (ii) low pH values of the reservoir fluid as well as (iii) high pumping rates may all have contributed to the observed scaling formation. However, the degree of calcite supersaturation caused by corrosion and depressurization during fluid upflow is limited. Additional processes such as stripping of CO₂ into the identified methane-rich gas phase may thus have been a major control on scaling formation. Partial CO₂ exsolution is a likely driver for scaling formation because it immediately causes substantial supersaturation with respect to calcite.

7.16

Developpement of a new EGS concept for Switzerland: the Haute-Sorne pilot project (JU)

Olivier Zingg¹, Peter Meier¹

¹ Geo-Energie Suisse AG, Reitergasse 11, CH-8004 Zürich (o.zingg@geo-energie.ch)

The Basel Deep Heat Mining project was the first attempt to produce electricity using EGS technology in Switzerland (Häring et al. 2008). It was stopped in 2006 after an earthquake of magnitude $M_L = 3.4$ occurred during the stimulation of the crystalline basement. At that time, the Basel project had produced a unique dataset of seismic and hydraulic data which lead to a better understanding of stimulation process. Based on that knowledge, Geo-Energie Suisse developed a new reservoir stimulation concept which minimises seismic risk and at the same time enhances well productivity.

In contrast to a massive stimulation in a vertical borehole (Basel), Geo-Energie Suisse uses a multi-stage hydraulic stimulation in highly deviated wells in combination with open-hole packer technology. In addition, a complete logging and testing program is foreseen to calibrate and update risk models before proceeding with the main stimulation of the reservoir. The first seismic risk study combining deterministic and probabilistic models has been carried out following methodologies developed for previous EGS projects and by the Swiss Seismological Service (Baisch et al. 2009; Gischig et al. 2013; Mignan et al. 2015).

The Haute-Sorne EGS pilot project in Canton Jura aims at proving the technical feasibility of the concept and producing up to 5 MW electricity by 2020.

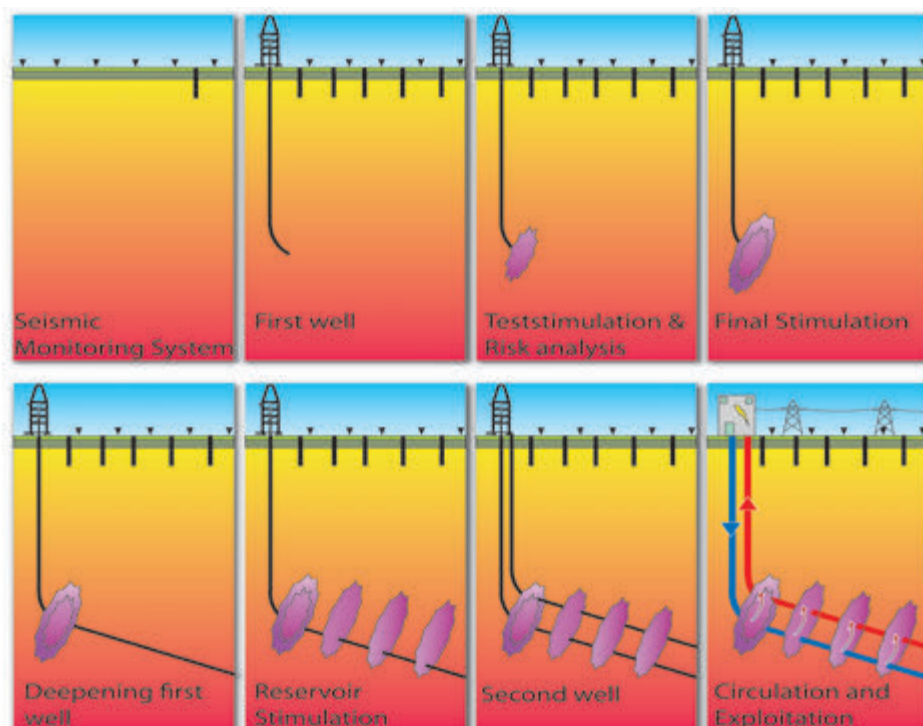


Figure 1. Conceptual design of the Haute-Sorne EGS pilot project

REFERENCES

- Baisch, S., Carbon, D., Dannwolf, U., Delacou, B., Devaux, M., Dunand, F., Jung, R., Koller, M., Martin, C., Sartori, M., Secanell, R., and R. Vörös, 2009. Deep Heat Mining Basel - Seismic Risk Analysis. SERIANEX study prepared for the Departement für Wirtschaft, Soziales und Umwelt des Kantons Basel-Stadt, Amt für Umwelt und Energie, <http://www.wsu.bs.ch/geothermie>, 553 pages
- Gischig, V. S., Wiemer S. (2013). A stochastic model for induced seismicity based on non-linear pressure diffusion and irreversible permeability enhancement. *Geophysical Journal International*, doi:10.1093/gji/ggt164
- Häring, M.O., U. Schanz, F. Ladner, Dyer B.C. (2008), Characterisation of the Basel 1 enhanced geothermal system. *Geothermics* 37, 469–495.
- Mignan, A. Landtwing, D., Kästli, P. Mena, B. Wiemer, S., 2015. Induced seismicity risk analysis of the 2006 Basel, Switzerland, enhanced Geothermal System project: Influence of uncertainties on risk mitigation, *Geothermics* 53 (2015), 133 -146

P 7.1

Fluid-rock interactions in Icelandic hydrothermal systems

Bruno Thien¹, Georg Kosakowski², & Dmitrii A. Kulik³

Laboratory for Waste Management (LES), Nuclear Energy and Safety Research Department, Paul Scherrer Institut, CH-5232 Villigen

¹ *bruno.thien@psi.ch*

² *georg.kosakowski@psi.ch*

³ *dmitrii.kulik@psi.ch*

Fluid circulation in natural or enhanced hydrothermal systems tends to alter the reservoir rocks. The resulting porosity and permeability changes are likely to influence the fluid circulation and the solute transport, which may affect the long-term performance of geothermal power generation.

Field observations suggest that active and fossil volcanic hydrothermal systems in Iceland reside in an intercalation of two different basaltic rock formations:

- (1) Volcanoclastites. They consist in tiny glassy fragments and breccia material. They exhibit high porosity and high permeability, and appear as completely altered in outcrops of the fossil high-temperature hydrothermal areas. In young surface formations, they are generally slightly weathered.
- (2) Lava flows. They consist in basaltic (minor rhyolitic) rocks crossed by fractures. They exhibit low-to-moderate porosity, which is generally poorly connected, resulting in low permeability. In fossil high temperature hydrothermal systems, the lavas appear not altered to moderately altered, except in a rim of maximum several centimeters thick around certain fractures.

With help of reactive transport models, using GEM-Selektor ([http:// gems.web.psi.ch](http://gems.web.psi.ch)) and OpenGeoSys-GEM codes, we investigated the causes for such contrasts in hydrothermal alteration patterns by studying the mineralogical evolution upon water-rock interaction.

In Thien et al. (2015) we postulate that the initial porosity of primary minerals and volume-porosity changes due to their transformation into secondary minerals are key factors to explain the different alteration extents observed in field studies. In addition, we found that the reactive surface area of the protolith, governed by fracture distribution and mineral grain sizes, is just as much an essential parameter. By constraining reaction kinetics we constrain the time necessary to obtain the observed alteration features to be between a few hours and a few years. The concepts developed in this study can be directly applied to various water-rock interaction systems, including those of interest for CO₂ sequestration.

REFERENCE

Thien, BMJ., Kosakowski, G. & Kulik D.A., 2015: Differential alteration of basaltic lava flows and hyaloclastites in Icelandic hydrothermal systems. *Geothermal Energy* 3:11.

P 7.2

The Thermal Structure of High-Enthalpy Geothermal Systems

Samuel Scott¹, Thomas Driesner¹, Philipp Weis²

¹ Institut für Geochemie und Petrologie, ETH Zürich, Clausiusstrasse 52, CH-8052 Zurich (samuel.scott@erdw.ethz.ch)

² GFZ German Research Centre for Geosciences, Telegrafenberg, DE-14473 Potsdam

Most of the electricity harnessed from geothermal heat is generated from high-enthalpy geothermal systems associated with subsurface magmatic intrusions driving active groundwater convection (White, 1961). Geologic conditions such as rock permeability and intrusion emplacement depth influence the thermal structure and the ability of the system to advect heat (Hayba and Ingebritsen, 1997). Major characteristics such as the subsurface temperature distribution, the depth of boiling zones, and the location of surface expressions change over time as the upper crust is heated and the intrusive heat source is cooled.

In this study, we use the Complex Systems Modeling Platform (CSMP++) to model porous media fluid flow around cooling magmatic intrusions (Weis et al., 2014). The key geologic factors investigated in our simulations include the host rock permeability, the initial geometry and depth of the intrusion, and the rock brittle-ductile transition temperature (Scott et al., 2015).

Host rock permeability strongly influences the deep thermal structure of geothermal systems. Systems with a permeability of 10^{-14} m^2 ('high' permeability) generally consist of dominantly liquid at depths $>1 \text{ km}$, whereas systems with a permeability of 10^{-15} m^2 ('intermediate') may develop extensive deep vapor-rich boiling or supercritical zones. Greater intrusion depth reduces the tendency to form deep boiling zones, as intermediate permeability systems driven by an intrusion emplaced at 2 km feature boiling from the intrusion to the surface while a equivalent system driven by an intrusion at do not develop boiling zones below $\sim 1.5 \text{ km}$ depth.

While a brittle-ductile transition temperature $>450^\circ\text{C}$ allows the advection of supercritical water near the intrusion, the extent and temperature of supercritical water reservoirs depends greatly on host rock permeability. In high permeability host rocks (Fig. 1a), efficient recharge of relatively cool ($\sim 200^\circ\text{C}$) liquid to the sides and top of the intrusion limits the development of supercritical conditions to a thin permeable zone around the intrusion at temperatures near $>375^\circ\text{C}$. Liquid saturation in such systems generally exceeds 0.7, but can be much lower within the upper 500 m of the surface. In intermediate permeability systems (Fig. 1b), recharge is more stagnant and extensive supercritical zones at temperatures $>400^\circ\text{C}$ develop. Liquid saturation in the core of the upflow is near 0.3-0.5, implying that the liquid phase is nearly immobile in such systems and mass and heat transport is dominantly controlled by vapor fluxes.

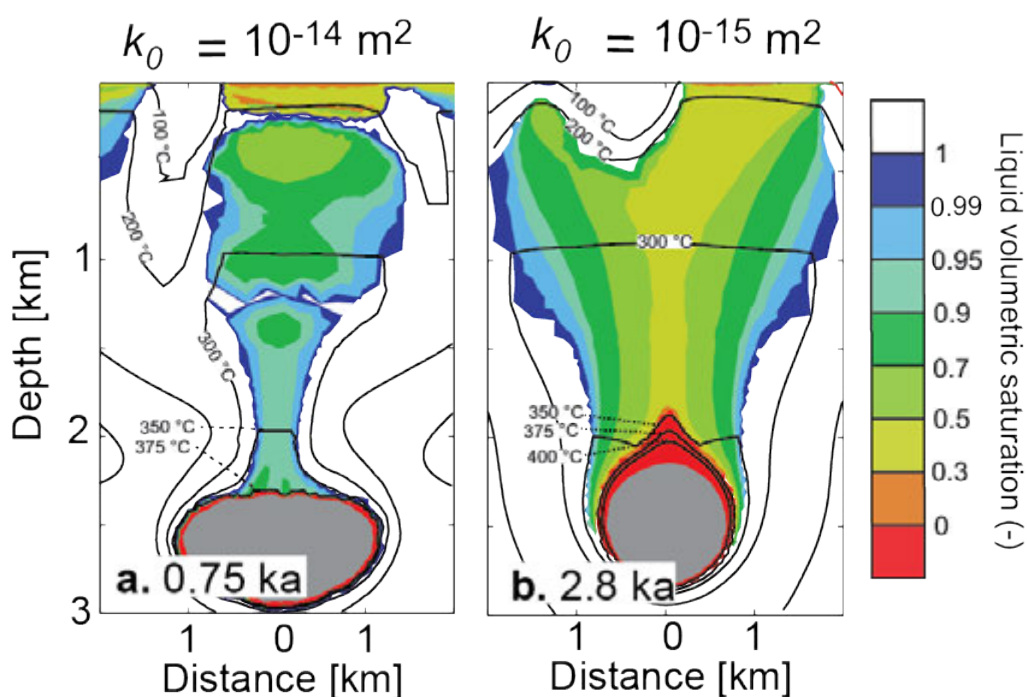


Figure 1. Characteristics of deep boiling and supercritical zones depend strongly on host rock permeability, as shown by the temperature distribution (black lines) and liquid saturation (colors) for two simulations with host rock permeability of **a.** 10^{-14} m^2 or **b.** 10^{-15} m^2 . For both simulations, the intrusion is emplaced with an upper depth initially at 2 km and the brittle-ductile transition temperature of the rock is 450°C .

REFERENCES

- Hayba, D.O., Ingebritsen, S.E., 1997. Multiphase groundwater flow near cooling plutons. *Journal of Geophysical Research*, 102, 12235. doi:10.1029/97JB00552
- Scott, S., Driesner, T., & Weis, P. 2015: Geologic controls on supercritical resources above magmatic intrusions. *Nature Communications*, 6, 7837, doi:10.1038/ncomms8837
- Weis, P., Driesner, T., Coumou, D., & Geiger, S. 2014: Hydrothermal, multiphase convection of H₂O-NaCl fluids from ambient to magmatic temperatures: a new numerical scheme and benchmarks for code comparison. *Geofluids*, 14, 347–371.
- White, D. 1957. Thermal waters of volcanic origin. *Geological Society of America Bulletin*, 68, 1637–1658.

P 7.3

Towards high resolution modeling of deep geothermal reservoirs on heterogeneous architectures

Gunnar Jansen¹, Boris Galvan¹, Stephen A. Miller¹

¹ Centre for Hydrogeology and Geothermics, University of Neuchâtel, Rue Emile-Argand 11, CH-2000 Neuchâtel (gunnar.jansen@unine.ch)

In geothermal reservoirs numerous processes occur simultaneously. Many of these processes are still under active research. Numerical models of deep geothermal reservoirs try to understand the system as a whole including coupled and non-linear processes. In addition to the complex multiphysics model a high spatial and temporal resolution is desired to further understand the stimulation process of reservoirs for deep heat mining including its permeability evolution.

These requirements can not be fulfilled by traditional sequential modeling software. A high degree of parallelization is needed to achieve this in a reasonable time frame. Modern high performance architectures increasingly build on the use of accelerators (e.g. the graphics processing unit GPU) as power consumption of new large pure processor based clusters is growing exponentially. Developing efficient code for these new heterogeneous systems can be challenging.

We implement a modern finite element code to meet the requirements by state-of-the-art models. The aim is to provide the means to exploit recent hardware innovation while maintaining portability and an adequate level of user adaptability. To this end we use scientific libraries such as finite element library *deal.II*, PETSc's scalable non-linear solvers and the mesh distribution provided by *p4est*. We will present our recent work on adaptive mesh refinement on parallel distributed domains in the context of deep reservoir simulations. We will further present some preliminary studies. This includes solutions for uncoupled processes as well as fully coupled non-linear solutions of processes such as fluid flow and mechanical deformation in the elastic and plastic regimes.

REFERENCES

- Bangert, W., Hartmann, R. & Kanschä 2007: *deal.II* – a general-purpose object-oriented finite element library, ACM Transaction on Mathematical Software, 33
- Burstedde, C, Wolcox, L, & Ghattas, O. 2011: *p4est*: Scalable Algorithms for Parallel Adaptive Mesh Refinement on Forests of Octrees, SIAM Journal on Scientific Computing, 33
- Balay, S. et al. 2015: PETSc Web Page, <http://mcs.anl.gov/petsc>

P 7.4

Experimental and Numerical Study of Permeability in Heterogeneous Fractures

Daniel Vogler¹, Randolph Settgast², Florian Amann¹, Peter Bayer¹ & Derek Elsworth³

¹ *Department of Earth Sciences, ETH Zurich, Zurich, Switzerland (daniel.vogler@erdw.ethz.ch)*

² *Lawrence Livermore National Laboratory, Livermore, USA*

³ *Department of Energy and Mineral Engineering, Pennsylvania State University, State College, USA*

Anthropogenic perturbations in a rock mass at great depth cause a complex thermal-hydro-mechanical (THM) response. This is of particular relevance when dealing with enhanced geothermal systems (EGS) and unconventional oil and gas recovery utilizing hydraulic fracturing. Studying the key THM coupled processes associated with specific reservoir characteristics in an EGS are of foremost relevance to establish a heat exchanger able to achieve the target production rate.

Many reservoirs are naturally low permeable, and the target permeability can only be achieved through the creation of new fractures or inelastic and dilatant shearing of pre-existing discontinuities. The latter process, which is considered to irreversibly increase the apertures of pre-existing discontinuities, has been shown to be especially important for EGS. Common constitutive equations linking the change in hydraulic aperture and the change in mechanical aperture are based on the basic formulation of the cubic law, which linearly relates the flow rate in a fracture to the pressure gradient. However, HM-coupled laboratory investigations demonstrate, that the relation between the mechanical and the hydraulic aperture as assumed in the cubic law, is not valid when dealing with very small initial apertures, which are likely to occur at great depth.

In a current study, we investigate pre-existing natural fractures in granite in hydro-mechanically coupled laboratory experiments. The samples were cyclically loaded with normal stresses between \$1\$ and \$68\$ MPa while maintaining constant fluid flow rates through the fractures. This experiment was performed for mated and displaced fracture surfaces. Results allow comparison of hydraulic and mechanical apertures in natural fractures. Laser scans of fracture surfaces taken before and after experiments are used to study the influence of topology changes on joint normal stiffness, aperture fields and fluid flow. Numerical simulations of the fracture aperture fields are compared to the experimental results.

P 7.5

Fault orientations inferred from analysis of a microseismic cluster dataset of the Basel EGS reservoir agree well with borehole fracture data

Martin Ziegler¹, Benoît Valley², Keith F. Evans³

¹ Department of Earth Sciences, ETH Zurich, Sonneggstrasse 5, CH-8092 Zurich (martin.ziegler@erdw.ethz.ch)

² Centre for Hydrogeology and Geothermics (CHYN), Université de Neuchâtel, Emile-Argand 11, CH-2000 Neuchâtel (benoit.valley@unine.ch)

³ Department of Earth Sciences, ETH Zurich, Sonneggstrasse 5, CH-8092 Zurich (keith.evans@erdw.ethz.ch)

Electricity production from petrothermal systems requires the circulation of fluids through rock masses that are sufficiently hot and thus, in areas with normal geothermal gradient like the Swiss foreland, involves drilling to depths often ranging between about 4 and 5 km below ground (e.g., Kohl et al., 2005). As a consequence, characterisation of the reservoir rock mass is often limited to observations and tests made in a small number of boreholes, sometimes in a single well like in the *Deep Heat Mining* project in Basel, Switzerland. Rock mass characterisation along the 5 km deep Basel-1 well included temperature profile, identification of permeable structures, state of stress and rock mechanical properties, lithology, and occurrence and properties of natural fractures (e.g., Ziegler et al., 2015). In order to build a structural model that can be used as input for numerical models aimed at predicting reservoir injection and production behaviour, knowledge of permeable fractures (e.g., brittle faults) that populate the reservoir away from the well is essential. Such information can partially be inferred from microseismic data obtained during stimulation operations. Previous studies by Asanuma et al. (2007), Dyer et al. (2010), Deichmann et al. (2014), and Kraft and Deichmann (2014), among others, investigated the waveform similarity of seismic events. Events with high seismic waveform similarity were grouped into clusters and interpreted to have originated from slip of patches of a common fault or fault zone. Improved techniques to pick P- and S-wave arrival times and master-event relocation led to substantial reduction of the relative location errors of the events in a cluster.

In this study we investigated the orientations of faults, inferred from the microseismic cluster dataset from Kraft and Deichmann (2014). This dataset includes 370 small clusters that have a median extent in x, y, and z directions of about 7 m, 9 m, and 12 m, and depth greater than 3.6 km bgs. We used principal component analyses to extract fault orientations for each cluster under the assumption that the events in a cluster have occurred on a single planar fault patch of negligible width. The uncertainty in the fault orientation estimates was assessed using Monte-Carlo-type simulations where the locations of the events within each cluster were varied within their individual location error ellipsoids. We then compared the orientations of inferred *well-constrained* faults (14 faults with orientation uncertainty characterised by one standard deviation (SD) <15°) and *moderately constrained* faults (36 faults; 15° < SD < 22.5°) with borehole fracture data. Our analysis shows considerable agreement in the strike directions (NNW to NW) of microseismically inferred faults (Figure 1a) and zones of high fracture frequency previously identified from image logs run in the Basel-1 well (Figure 1b). Some discrepancies were also evident: fault planes from seismic event clusters cover a very narrow range of orientations and are essentially vertical, with a slight tendency towards NE dipping; in contrast, fracture zones from fracture analyses at the well show a much larger orientation dispersion and have more SW dipping structures. However, only a small number of clusters (14%) yielded relatively robust fault orientations, most likely because the events in the clusters were not sufficiently widely dispersed. Thus, many failure planes activated within the reservoir were not identified in the analysis, either because the orientation of the fault patch could not be usefully constrained, or because the events were not a member of a cluster. Planes that slip aseismically will also remain undetected. These limitations will lead to a biased reservoir structural model. Thus, we are currently working on microseismic clusters of larger sizes (e.g., identified by Dyer et al., 2010) and on integration of the various Basel microseismic imaging datasets.

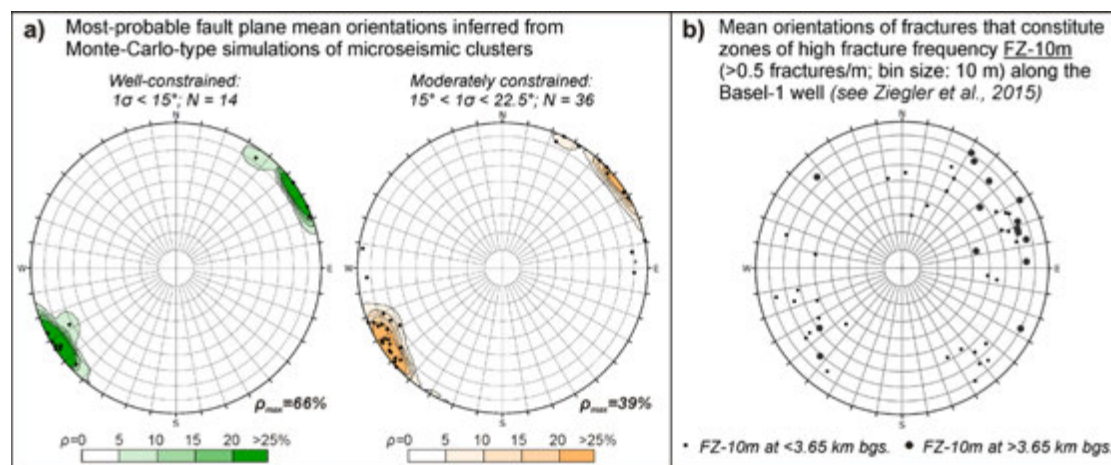


Figure 1. Comparison of a) poles to fault planes identified from microseismic clusters, with b) poles of fracture sets that constitute assumed planar fracture zones identified along the Basel-1 well. Note that the subvertical trajectory of the Basel-1 borehole leads to a bias in intersecting subvertical fractures, i.e., these are underrepresented in b). Lower hemisphere, equal area projections.

REFERENCES

- Asanuma, H., Kumano, Y., Hotta, A., Schanz, U., Niitsuma, H., & Häring, M. 2007: Analysis of microseismic events from a stimulation at Basel, Switzerland. *Trans. Geoth. Resour. Council*, 31, 265-269.
- Deichmann, N., Kraft, T. & Evans, K. F. 2014: Identification of faults activated during the stimulation of the Basel geothermal project from cluster analysis and focal mechanisms of the larger magnitude events. *Geothermics*, 52, 84-97.
- Dyer, B. C., Schanz, U., Spillmann, T., Ladner, F. & Häring, M. O. 2010: Application of microseismic multiplet analysis to the Basel geothermal reservoir stimulation events. *Geophysical Prospecting*, 58, 791-807.
- Kohl, T., Signorelli, S., Engelhardt, I., Andenmatten, N., Berthoud, C., Sellami, S. & Rybach, L. 2005: Development of a regional geothermal resource atlas. *J. Geophys. Eng.*, 2, 372-385.
- Kraft, T. & Deichmann, N. 2014: High-precision relocation and focal mechanism of the injection-induced seismicity at the Basel EGS. *Geothermics*, 52, 59-73.
- Ziegler, M., Valley, B. & Evans, K. F. 2015: Characterisation of natural fractures and fracture zones of the Basel EGS reservoir inferred from geophysical logging of the Basel-1 well. *Proc. World Geoth. Congr.*, 2015, Melbourne (Australia).

P 7.6

Enhancement of permeability in geothermal reservoirs: the example of the Salanfe lake – Val d'Illiez geothermal area

Giona Preisig^{1,2} & François Negro³

¹ EOAS – Geological Engineering, The University of British Columbia, 2207 Main Mall, V6T 1Z4 Vancouver BC, Canada (gpreisig@eos.ubc.ca)

² Swiss Geological Survey - swisstopo, Seftigenstrasse 264, CH-3084 Wabern bei Bern

³ Centre for Hydrogeology and Geothermics, University of Neuchâtel, Emile-Argand 11, CH-2000 Neuchâtel

Extraction of deep groundwater for accessing geothermal heat is an innovative method in the field of renewable energies. In engineered geothermal systems (EGS), targeting depths >3 km, the circulation and extraction of water is promoted by means of a doublets of wells and a stimulated reservoir. In geothermal projects of medium temperature, natural groundwater is extracted from deep aquifer systems located at depths from 1 to 3 km. Both cases are often characterized by a very low permeability of the reservoir, which limits the capacity to produce cost-efficient flow rates. This is principally because of mechanical, i.e. increasing stress with depth, and chemical, i.e. clogging of fractures by mineral filling, processes. Thus, reservoir stimulation by means of hydraulic shearing events is a critical method for the geothermics industry. To ensure permanent fracture permeability, hydraulic shearing aims to activate in shear natural pre-existing fractures favorably oriented, i.e. having an angle ranging between 15-45° with the maximum principal stress σ_1 , by means of injecting a fluid pressure lower than the minimum principal stress σ_3 . However, it is still unclear (i) how much the reservoir permeability is enhanced during hydroshear slip events and (ii) what is the resulting reservoir geometry.

The Salanfe lake – Val d'Illiez geothermal area (Valais, Switzerland) is an interesting field case for addressing these questions. In this work, we have analyzed the seismic events in the Salanfe lake – Val d'Illiez area between 1953 – 2000 (data from the Earthquake catalog, Fäh et al. 2011). First, all the recorded seismic events with moment magnitudes having an impact on shear dilation and fracture permeability, i.e. $M_w > 0$, have been plotted as a function of time and superimposed on the seasonal fluctuation of water levels in the Salanfe dam lake. At least 8 clouds of seismic events can be linked to the seasonal fluctuation of water levels in the lake. For these clouds, the time lag between maximum water level and the occurrence of the seismic event with higher moment magnitude, has increased over the years, suggesting a gain in reservoir volume and permeability. Second, shallow events (depth <5 km) for the period 1980-2000, have been superimposed on the fracturation map of Pantet (2004). Although the position of seismic events may imply important errors, two major deep flow paths can be interpreted. These have an orientation which is in agreement with the strike of the major fractured zones (N300°) highlighted in Pantet (2004), which are furthermore favourably oriented for hydroshear reactivation (Figure 1). One of the two major flow paths has been accidentally created in 1953 via the reactivation of a pre-existing shear zone. This zone has subsequently been stimulated several times with the fluctuation of water levels in the Salanfe lake, especially in 1996. In this year, the second major flow path has been created through the reactivation of another pre-existing shear zone. These observations are promising within the framework of efficient stimulation of geothermal reservoirs by means of multi-stage hydro-shearing injections.

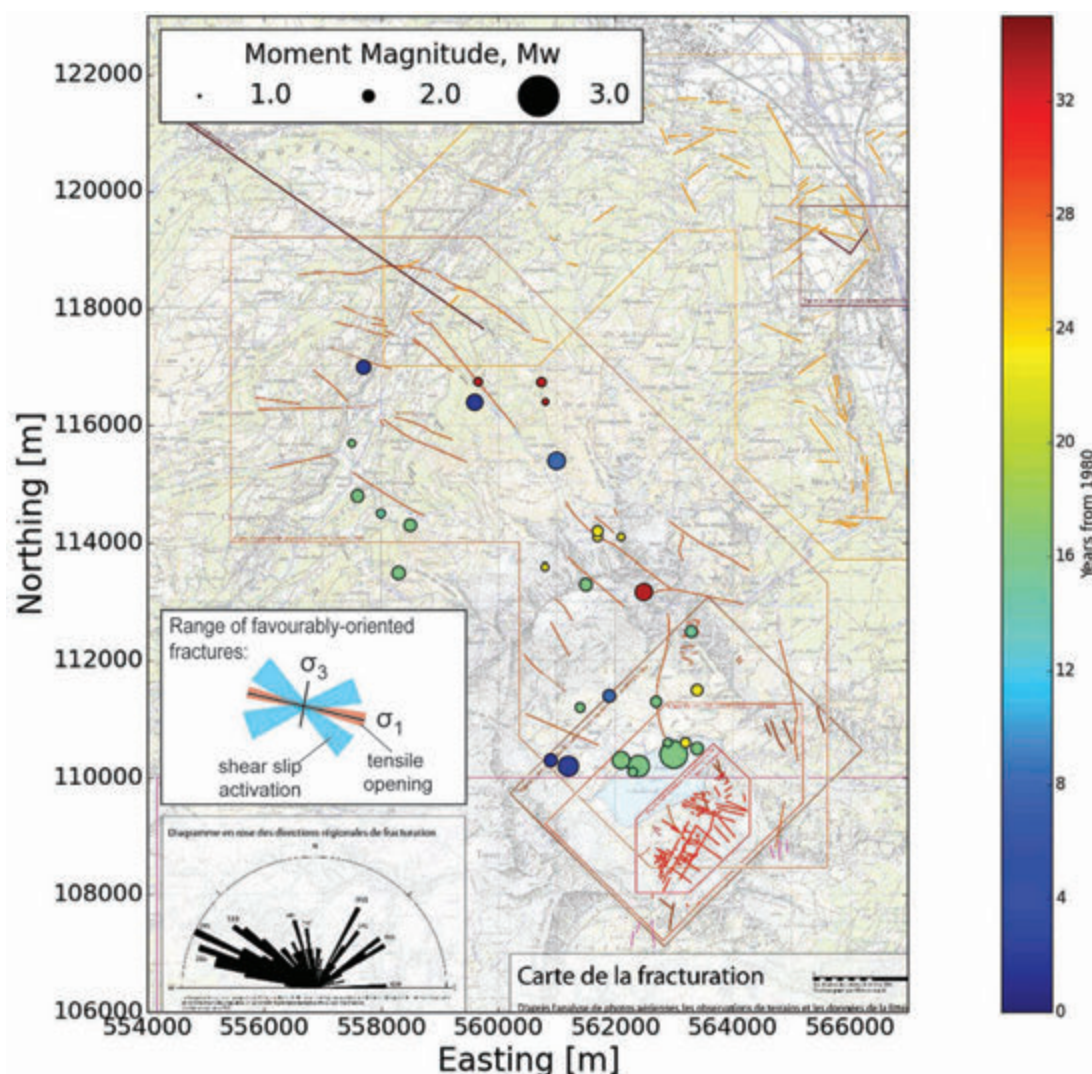


Figure 1. Seismic events associated to hydraulic shearing of fractures constituting the geothermal reservoir located between the Salanfe Lake and the Val d'Illiez (VS). Reactivation of fractures through hydroshear slip events is related to the water level in the Salanfe Lake (fracturation map from Pantet 2004).

REFERENCES

- Pantet, A. 2004: Etude structurale et hydrogéologique de la région de Salanfe et du massif des Dents du Midi (Valais, Suisse), Master's thesis, University of Lausanne, Lausanne, Switzerland.
- Fäh, D., Giardini, D., Kästli, P., Deichmann, N., Gisler, M., Schwarz-Zanetti, G., Alvarez-Rubio, S., Sellami, S., Edwards, B., Allmann, B., Bethmann, F., Wössner, J., Gassner-Stamm, G., Fritsche, S., Eberhard, D. 2011. ECOS-09 Earthquake Catalogue of Switzerland Release 2011 Report and Database. Public catalogue, 17. 4. 2011. Swiss Seismological Service ETH Zurich.

P 7.7

Structural observations from drill cores of the Grimsel hydrothermal breccia

Daniel Egli¹, Marco Herwegh¹, Alfons Berger¹, Tom Belgrano¹

¹ *Institut für Geologie, Universität Bern, Baltzerstr. 1 + 3, 3012 Bern (daniel.egli@geo.unibe.ch)*

Naturally porous and permeable rock masses constitute an attractive alternative to hydraulically enhanced geothermal systems, which in the past have caused significant artificial seismicity. However, the knowledge about such natural systems is still insufficient due to the inaccessibility of the deep of the northern Alpine foreland. This gap is meant to be bridged on the basis of an analogue study on an active hydrothermal breccia in the crystalline basement of the Aar massif. Detailed geological, geophysical and hydrological analyses on drill cores, the drill hole, as well as on surface exposures should improve the knowledge of natural hydrothermal systems as a potentially exploitable energy source. To that end, a cored drillhole through a known active hydrothermal breccia on the Grimsel Pass (Stalder 1964, Hoffmann 2004) has been performed during summer 2015. This active hydrothermal system in basement rocks of the Aar massif represents an analogue for potential geothermal reservoirs in the deep crystalline subsurface of the northern Alpine foreland as well as for other hydrothermal springs in the Aar and Aiguille Rouge massifs (e.g. Brigerbad, Leukerbad, Lavey les Bains). This study presents first observations and preliminary results on the micro- to mesoscale structures from drill cores of the Grimsel hydrothermal field describing the ductile and brittle deformation (shear zones, fractures, joints). Their spatial distribution around the central breccia zone as well as their continuity and permeability provide additional constraints on the water flow paths in such hydrothermal systems and further advance the understanding of their structural evolution.

REFERENCES

- Hoffmann, B.A., Helfer, M., Diamond, L.W., Villa, I.M., Frei, R. & Eikenberg, J. 2004: Topography-driven hydrothermal breccia mineralization of Pliocene age at Grimsel Pass, Aar massif, Central Swiss Alps. *Schweiz. Mineral. Petrogr. Mitt.*, 84, 271–302
- Stalder, H.A. 1964: Petrographische und mineralogische Untersuchungen im Grimselgebiet. *Schweiz. Mineral. Petrogr. Mitt.*, 44, 187–398.

P7.8

Perm-Fit: a new program to estimate permeability at high P-T conditions

Evangelos Moulas¹ & Claudio Madonna¹

¹ *Department of Earth Sciences – ETH Zürich, Sonneggstrasse 5, 8092, Zurich CH*

Several geological processes are controlled by porous fluid flow. The circulation of porous fluids influences many physical phenomena and in turn it depends on the rock permeability. The permeability of rocks is a physical property that needs to be measured since it depends on many factors such as secondary porosity (fractures etc).

We present a numerical approach to estimate permeability using the transient step method (Brace et al., 1968). When a non-reacting, compressible fluid is considered in a relative incompressible solid matrix, the only unknown parameter in the equations of porous flow is the permeability. Porosity is assumed to be known and the physical properties of the fluid (compressibility, density, viscosity) are taken from the NIST database. Forward numerical calculations for different values of permeability are used and the results are compared to experimental measurements. The extracted permeability value is the one that minimizes the misfit between experimental and numerical results. The uncertainty on the value of permeability is estimated using a Monte Carlo Bootstrap method.

REFERENCES

- Brace, W.F., Walsh J.B., & Frangos, W.T. 1968: Permeability of Granite under High Pressure, *Journal of Geophysical Research*, 73, 6, 2225-2236

P 7.9

Gravity prospection in region of La Broye

Guillaume Mauri¹, Laurent Marguet¹, Gunnar Jansen¹, Raymond Olivier², Urs Marti³, Roland Baumberger⁴, Robin Allenbach⁴, Pascal Kuhn⁴, Pierrick Altwegg⁵, Stephen A. Miller¹

¹ *Centre d'Hydrogéologie et de Géothermie, Université de Neuchâtel, Rue Emile-Argand 11, CH-2000 Neuchâtel (guillaume.mauri@unine.ch)*

² *Université de Lausanne, Institut des sciences de la Terre, Bâtiment Geopolis, UNIL-Mouline, CH-1015 Lausanne*

³ *Swisstopo, Geodetic developments and contracts, Seftigenstrasse 264, CH-3084 Wabern*

⁴ *Swisstopo, Geological Survey, Geological Data Process, Seftigenstrasse 264, CH-3084 Wabern*

⁵ *MIRARCO, Laurentian University, 935 Ramsey Lake Road, Sudbury, P3E 2C6, Ontario, CANADA*

The aim of the study is to bring new insight on the gravity variations in the region of La Broye. Recent gravity work on the western molasse bassin suggested that the region of La Broye was possibly on the rim of a large Permo-carboniferous sediment structure, but more information is required to properly define it. (Altwegg, 2015).

In the winter and spring of 2015, 100 km² were surveyed using a CG-5 gravimeter in the La Broye region to increase the measurement spatial density of gravity variations. A total of 824 new gravity stations were surveyed, and which includes 70 locations also measured in previous studies. The data set surveyed in 2015 is organised as follows:

- one profile, 22-km long and 100m sampling step (220 stations), and following the seismic line #14 (Sommaruga et al., 2012).
- a spatial survey with 4 to 6 gravity stations by square kilometer (604 stations).

In addition, gravity data sets from the 1983-gravity atlas (Klingele & Olivier, 1980; Olivier, 1983), as well as data from two M.Sc. work of the University of Lausanne (Lapaire, 2000; Clavier, 2001) were used in addition to our own measurements. Previous studies reported 1031 stations, which were scattered over an area of 30 km by 31km.

To reduce uncertainty when merging data sets, and to reduce uncertainty on each gravity data set, all data sets from previous surveys were re-processed using the Corr-Topo software (Altwegg, 2015) and the 2m digital elevation model from Swisstopo (Swisstopo, 2010). A regional gravity trend was calculated from the Bouguer values from all gravity data through a bilinear regression. The calculated regional trend was then subtracted from the new Bouguer anomaly map to obtain a residual gravity map for the region of La Broye.

Additionally, in order to remove gravity variations due to the surrounding Lakes of Neuchâtel and Murten, the gravity effect of each lake was calculated using both high resolution bathymetry data from the work of Reusch et al. (2015) and bathymetry data from the 1:25000 map from Swisstopo (Swisstopo, 2005; Swisstopo & SITN, 2010).

Gravity effects of potential underground structures were computed and synthetised into a sensitivity study to assess any potential effect on measured gravity variation. The sensitivity study was performed using the GINGER software (Altwegg et al., 2015).

A sensitivity study was also performed using a 2D approach to assess the gravity effects of a) the geological formation of either Tertiary or Quaternary ages and b) the possibility of a hypothetical deep formation of Permo-carboniferous sediment beneath the profile following the seismic line #14. The study was done using GINGER software.

The 2D structure of geological formation is based on the geological interpretation of Seismic line #14, such as presented in the Seismic Atlas (Sommaruga et al., 2012).

Finally, based on the result from the 2D sensitivity study, the choice was made to calculate the gravity response of the 3D geological model of Swisstopo for the area. Density values of each formation used for the model are based on previous studies on rock density (Wagner et al., 1999; Altwegg et al., 2013) and gravity studies (CREGE, 2012; Altwegg, 2015). The results of this forward gravity modelling have been compared to the residual gravity map to assess the possibility of the extent of a local deep formation of Permo-carboniferous sediment.

REFERENCES

- Altwegg, P., Marguet, L., Negro, F., Scheidt Schmitt, N. & Vuataz, F.-D. 2013: Inventaire géothermique et structural du Canton de Neuchâtel: IGS-NE (Rapport final). CREGE, Neuchâtel.
- Altwegg, P., Renard, P., Schill, E. & Radogna, P.-V. 2015: GInGER (GravImetry forGeothermal ExploRation): a new tool for geothermal exploration using grav-ity and 3D modelling software. In: Proc. World Geothermal Congress 2015, Melbourne, Australia, p. 7.

- Altwegg, P. 2015: Gravimetry for Geothermal Exploration, Methodology, computer programs and two cases studies in the Swiss Molasse Basin, Ph.Thesis, University of Neuchâtel, Neuchâtel, p. 274.
- Clavien, D. 2001: Modélisation gravimétrique de la région de Fétigny (Fr), Institut de Géophysique de l'Université de Lausanne (IGL-UNIL).
- CREGE – Laboratoire de Géothermie. 2012: Programme GeoNE - Développement de la géothermie profonde dans le canton de Neuchâtel. Rapport final de la Phase 1. Rapport CREGE 12-02 pour le Service de l'énergie et de l'environnement et pour le Service de l'économie, Neuchâtel 350pp.
- Klinge, E. & Olivier, R. 1980: La nouvelle carte gravimétrique de la Suisse (anomalie de Bouguer), Geophysique 20, Commission Swiss de Géophysique.
- Lapaire, F. 2000: Etude gravimétrique de la morphologie du fond molassique de la vallée de la Basse-Broye entre Payerne et Avenches, Institut de Géophysique de l'Université de Lausanne (IGL-UNIL)
- Olivier, R. 1983: L'Atlas Gravimétrique du Plateau Suisse, partie Ouest. Bull. Inst. Geophys. Univ. Lausanne, n°5, 49p., format A3.
- Reusch, A., Loher, M., Bouffard, D., Moernaut, J., Hellmich, F., Anselmetti, F. S., Bernasconi, S. M., Hilbe, M., Kopf A., Lilley, M. D., Meinecke, G., & Strasser, M. 2015: Giant lacustrine pockmarks with subaqueous groundwater discharge and subsurface sediment mobilization. Geophys. Res. Lett., 42, 3465–3473. doi: 10.1002/2015GL064179.
- Sommaruga, A., Eichenberger, U., Marillier, F. & Kissling, E., 2012. Seismic Atlas of the Swiss Molasse Basin, Matér. Géol. Suisse Géophysique. Swiss Geophysical Commission.
- Swisstopo, 2010. SwissALTI3D, 2m DEM
- Swisstopo & SITN, 2010. Carte bathymétrie de Neuchâtel, 1:25'000
- Swisstopo, 2005. Carte nationale de la Suisse, 1:25'000, carte 1165
- Wagner, J.-J., Gong, G., Sartori, M. & Jordi, St. (1999), Physical properties of rocks from the Swiss Alps and nearby areas, Geophysique 33, Commission Swiss de Géophysique.

P 7.10

Porosity Enhancing Multi-event Dolomitization in the Upper Muschelkalk of the Swiss Molasse Basin: Implications for CO₂ Storage and Geothermal Energy

Arthur Adams¹, Lukas Aschwanden¹, Larry Diamond¹

¹ *Institute of Geological Sciences, Baltzerstrasse 1+3, 3012 Bern, Switzerland (arthur.adams@geo.unibe.ch)*

The Upper Muschelkalk (Anisian/Ladinian) is an extensive deep saline aquifer in the Molasse Basin of northern Switzerland, which is under investigation for its potential for geothermal energy production and for industrial CO₂ storage. It is subdivided into a lower limestone unit (Hauptmuschelkalk) and a fully dolomitized formation (Trigonodus Dolomit). Both units represent a gently inclined carbonate ramp at the south-eastern extent of the Upper Muschelkalk Sea of the German basin. Despite ubiquitous mudstones composing the aquifer, reservoir characteristics such as matrix porosity and permeability are heterogeneously distributed within the basin. This is in part due to the depositional environment, diagenesis, burial depth and dolomitization history. Therefore, by constraining the dolomitization history alongside facies distributions we hope to extrapolate reservoir characteristics across the entire basin.

Since the geochemical signature of dolomite is representative of its formation conditions, this study focused on analyzing the trace element geochemistry and chemical properties of the dolomites and their precipitating fluids. Drill cores and log data have been obtained from the Corporation for Swiss Petroleum (SEAG) and Nagra. Multiple dolomite generations were distinguished by cathodoluminescence, microprobe analysis, stable isotope analysis, UV fluorescence and petrographical observations. Initial geochemical analysis indicates wide differences in porosity, petrography, Fe contents, Mg/Ca ratios and δ¹⁸O values.

Most of the Upper Muschelkalk consists of micritic limestone mudstones with porosity ranges from 1 – 10 %. However, the fully dolomitized Trigonodus Dolomit has average porosity values double and triple those of the calcitic mudstones. The occurrence of high porosity, microcrystalline, sucrosic dolomite beds in the Upper Muschelkalk also significantly raise porosities in both units. These beds may compose up to over 10 % of the entire unit and are therefore volumetrically significant.

The results reveal four distinct, porosity enhancing and decreasing, dolomite phases in the Upper Muschelkalk. (1) Most of the dolomite is early, extensive, and porosity-increasing dolomitization which, occurred in lagoonal facies. Porosity for this phase ranges from 10 – 30 %. (2) A late stage sucrosic dolomite found as localized beds which, increase porosity by up to 15 %. (3) A further extensive late stage dolomitization in the Hauptmuschelkalk associated with stylolitization. (4) Overdolomitization, which is unique to the lagoonal facies and occludes minor amounts of dolomitization.

Sucrosic dolomites in the basin have not yet been studied nor characterized, despite their abundant porosity increasing properties. Ongoing research will reveal whether their dolomitization pathways are interconnected throughout the basin, or rather represent localized hydrological events.

P 7.11

Reservoir quality prediction based on clay minerals and zeolites distribution: new insights from the pyroclastic-rich Bajo Barreal Formation, Argentina

Branimir Šegvić¹, Andrea Moscariello¹, Carlos Arbiol González¹, Griselda Vocaturo², Remi Lehu², Alejandro D'Odorico², Ana Cecilia Limeres², Carolina Bernhardt², Aniela Ancheta², Elena Morettini²

¹ *Department of Earth Sciences, University of Geneva, Rue de Maraichers 13, 1205 Geneva, Switzerland*

² *YPF, Dirección Exploración Upstream, Macacha Guemes 515 - CP 1106, Buenos Aires, Argentina*

The Golfo San Jorge area in central Argentina represents an intraplate basin consisting of several sedimentary formations, the oldest being of Jurassic age. The Cretaceous fluvio-lacustrine Bajo Barreal Formation, known for its large hydrocarbon accumulations, makes the upper portion of the basin fill and consists of an upper and lower stratigraphical Members laying above a well known regional tuffaceous marker. The Lower Member consists of floodplain mudstones with isolated channels and has an upward increase of sandstone content; the Upper Member is composed by grey and purple mudstones with thicker channel sand bodies. Both stratigraphical units are characterised by the presence of acid volcanoclastics and tuffaceous material mixed with siliciclastic sediments. Previous studies on the Bajo Barreal Formation suggest an active sedimentary input from contemporaneous volcanoclastic material derived from both direct fall-outs or rain-off processes. This material can make up to 15% of host rocks forming a so-called pseudomatrix produced by the disintegration of tuff and pyroclastic material. In this contribution we present the preliminary results on the reservoir petrography and mineralogy focusing on the characterisation of its volcanic component and related neoformed mineralization especially considering the clay and zeolite pore infill. The methodological approach include QEMSCAN®, SEM-EDS, and XRD studies on bulk samples and their clay fraction.

Our data from 5 wells show the reservoir rocks to be mainly formed by mudstones to fine- to medium grained sandstones (Figure 1.). Their mineralogy comprises quartz and feldspars, whilst volcanic component occasionally makes up to 50 % of the sample, resulting in form of very fine-grained tuff or volcanoclastics particles up to 2 mm in size. Their composition is presumably acidic, as indicated by the variety of albite, andesine, and quartz of poor grain homogeneity and unusual shapes detected with the QEMSCAN®. Corroborating the presence of volcanic material, XRD whole-rock data indicate high contents of amorphous matter (i.e. 25-35 °2θ bulging) and much lower contents of crystalline feldspar than initially suggested by QEMSCAN® data.

Alkali-rich volcanic component is readily altered to the range of secondary assemblages consisting primarily of clay minerals-like mixed-layered illite-smectite (I-S), chlorite, and kaolinite as well as zeolites stemming from the group of true zeolites (heulandite, clinoptilolite, or laumontite). Mixed-layered I-S is rich in dioctahedral smectite component (60-90% Sm) and it is mostly formed after tuffaceous hypohyaline matrix. Chlorite, on the other hand, stands out after volcanoclastics thus indicating a possible difference in volcanism. Kaolinite is replacing feldspars. The micro-textural context of zeolites is at the moment unknown due to their "exotic" chemistry that hampered their proper QEMSCAN® classification. Clay content can make up to 15% of analysed rocks, whereas XRD Rietveld analyses quantify zeolites in amounts not exceeding 5%.

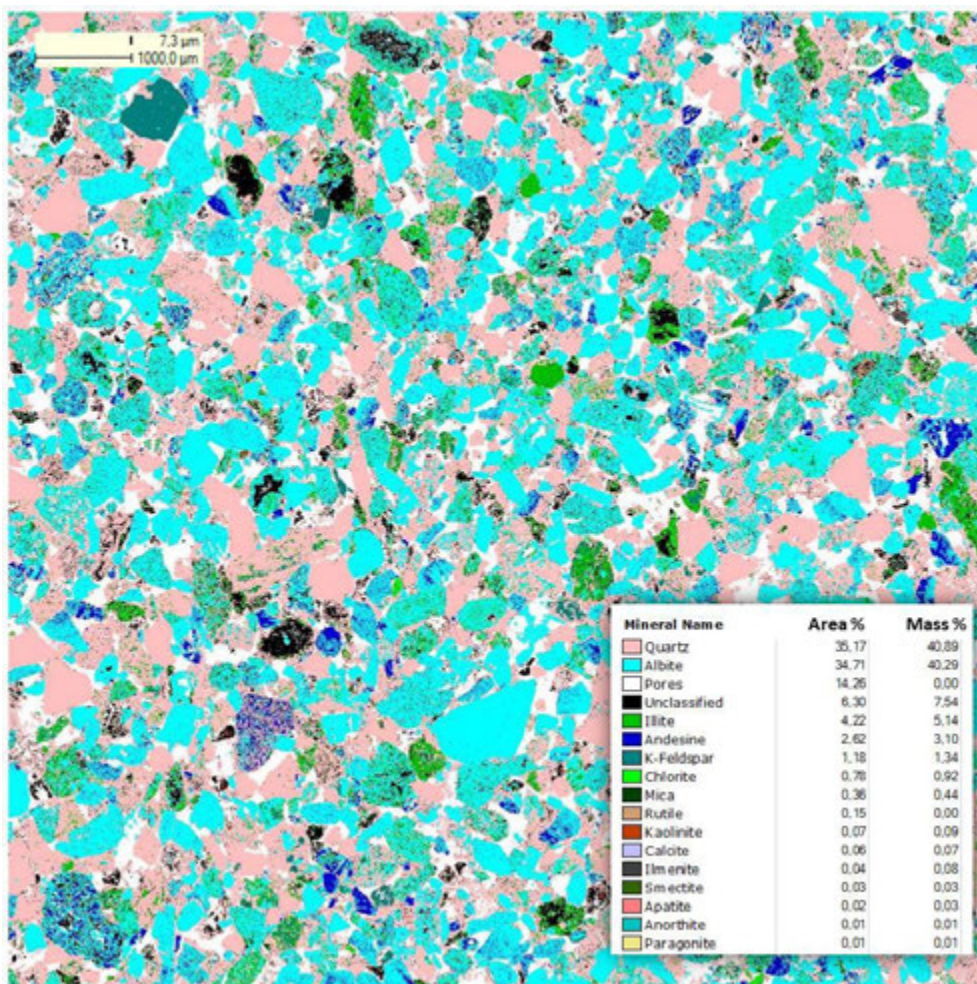


Figure 1. QEMSCAN® image showing a typical composition of fine-grained sandstone rich in volcanic material being altered to clay assemblages dominated by illite-smectite

Vertical current depth distribution of clays and zeolites is particularly interesting as I-S seems not to be present at depths shallower than 800 m, and deeper than 1400 m. Zeolites are reported in higher amounts at shallower depths than 800 m whilst at 1400 m and deeper chlorite is a dominant clay phase. For kaolinite no distribution pattern could have been elucidated. While a clear diagenetic sequence is still to be established, a clear trend in porosity values has been identified by a negative correlation with I-S abundances being significantly reduced at horizons with maximal content of this interlayered smectite-rich mineral. The identification and quantification of zeolites rich intervals has also an impact on porosity calculation from density-based wire-line log and allow a re-assessment of the stratigraphic distribution of reservoir properties. Ultimately, the results of this study will be used to define better the exploitation practices (e.g. EOR techniques) and thus increase reservoir productivity.

P 7.12

Reservoir geology, mineralogy and geochemistry of the Dentale and Gamba Formations (Early Cretaceous, Gabon): new insights both at regional and pore scale.

Giovanni Zanoni¹, Branimir Šegvić¹, Andrea Moscariello¹, Luc Tranchet²

¹ *Department of Earth Sciences, University of Geneva, Rue de Maraichers 13, 1205 Geneva, Switzerland*

² *Addax Petroleum Ltd, Route de Malagnou 101, 1224 Chêne-Bougeries, Switzerland*

The Gabon coastal region located along the equatorial West African continental margin, hosts several sedimentary basins with well-developed and prolific petroleum systems whose two key elements (source and reservoir) developed before the widespread deposition of mid Cretaceous salt following the opening of the south Atlantic.

A detailed knowledge on the reservoirs, their genesis, composition and distribution is therefore often lacking due to the difficulty to image the pre-salt stratigraphical sequence.

In this study, we focus on the Early Cretaceous Dentale and Gamba Formations in the onshore part of the South-Gabon sub-basin formed during the syn-rift and transition to post-rift time respectively. The two formations are separated by a 3 million year unconformity, both consisting of siliciclastic rocks thought to be accumulated in fluvial and lacustrine environments. The exceptional access to core material from these two reservoirs allowed us to provide unprecedented information on their mineralogy, geochemistry and thus origin and post-depositional diagenetic processes. The study included (1) QEMSCAN® petrographical analyses; (2) XRD study on whole rock and clay fraction, (3) ICP-MS whole-rock geochemistry, (4) SEM-EDS study on pore-filling mineralization, (5) stable isotope (C and O) and (6) cathodoluminescence investigations.

The whole-rock geochemical characteristics show clear distinctions between the two formations thus allowing for a new chemostratigraphical subdivision of these two sandy reservoirs which may be used for regional correlation. The clear geochemical differentiation between the two units also accounts for a different provenance and it is interpreted as a proxy for a different development/extension of catchment basin where the clastic sediments were sourced from. Ultimately this geochemical signature may also reflect the overall time represented by each stratigraphical unit.

The combined QEMSCAN® and XRD analyses on clay fraction within the Gamba Formation allowed the detection with high-level of certainty of the berthierine, a clay mineral that can be formed in fresh-water/brackish conditions confirming the hypothesis of transitional lacustrine/protected lagoonal systems formed at this transitional phase period. This is consistent with the mixed fresh water/marine $\delta^{13}\text{C}$ isotopic signatures on a carbonate level that we interpret as lacustrine in origin, and later dolomitised by marine carbonate cement during the subsequent mid-Aptian marine flooding.

The analyses on pore-filling clays indicate a mostly interlayered illite-smectite (I-S) and chlorite-smectite (C-S) mineral association. They are interpreted as the product of progressive evolution from the dioctahedral (I-S) and trioctahedral (C-S) smectitic precursors during burial of the host-rock. Speciation of diagenetically altered clay minerals with regard to both host rock formations provide us with new insights on a somewhat differing diagenetic history of the two reservoirs which we interpret as possibly controlled by the occurrence of coeval volcanoclastic material mixed with the clastic sediments derived from an external source. If this hypothesis is confirmed, this will be the first account of active volcanism recorded during Aptian times in the eastern coast of South Atlantic.

Finally, the study on clay minerals allowed us to provide accurate description and quantification of pore filling minerals and was a new controlling factor for log calibration and had a direct impact on porosity calculation.

Overall the findings provide new insights and ideas at regional and reservoir scale that will assist the future exploration and development of hydrocarbons in these two 'mature' reservoirs formations.

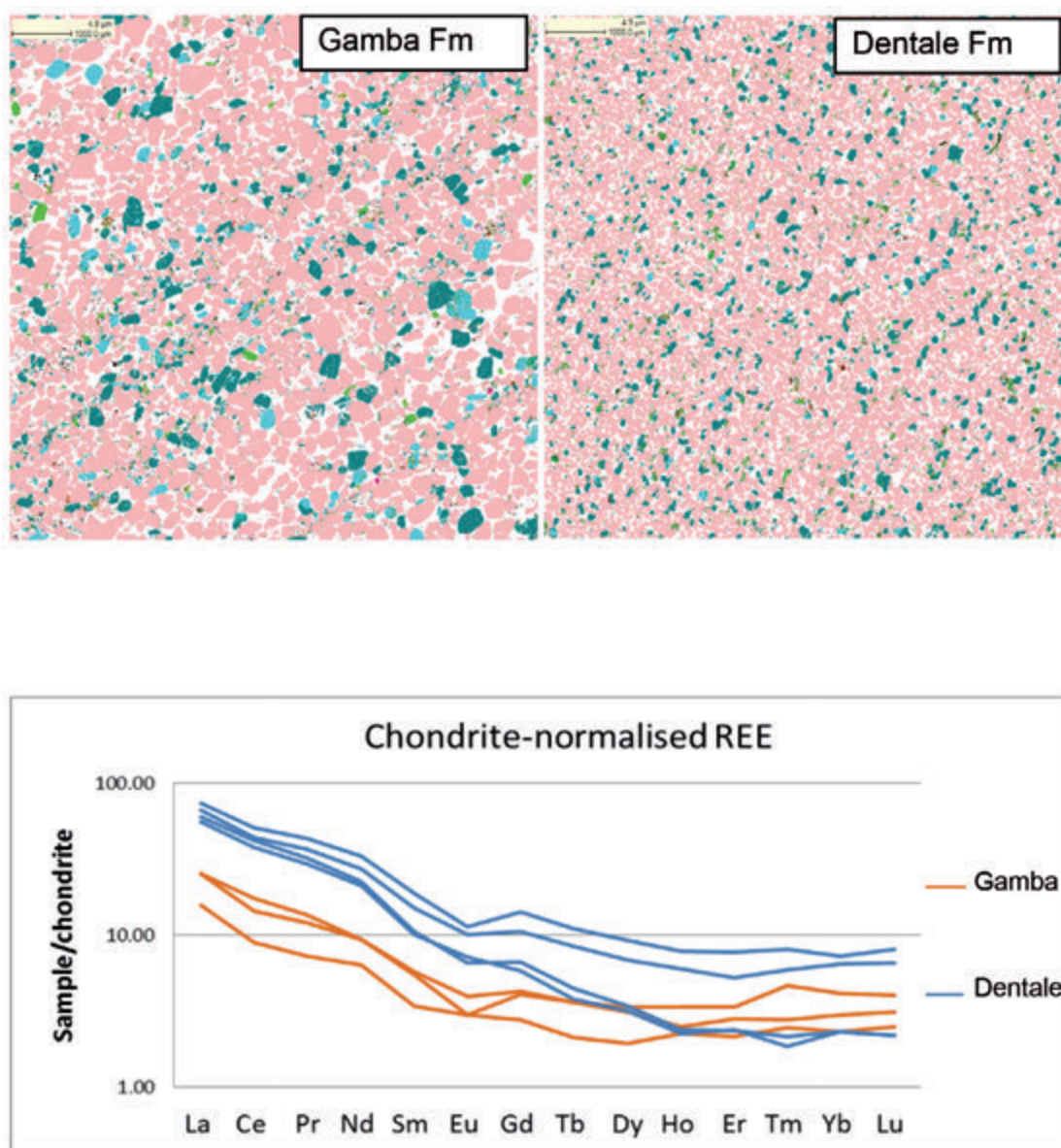


Figure 1. QEMSCAN® images showing a typical composition of fine-grained sandstone from the Gamba and Dentale Formations with a chondrite-normalized rare-earth element patterns for clay-rich samples of the same formations. The Gamba sandstone (subarkose) has generally higher K-feldspar content compared to the Dentale sandstone (quartzarenites). Legend of QEMSCAN® images: pink: quartz; green: k-feldspar; light blue: albite; light green: detrital chlorite.

P 7.13

Combining approaches of monitoring and modelling groundwater temperatures to investigate the subsurface urban heat island of Basel, Switzerland

Matthias H. Mueller¹, Jannis Epting¹, Peter Huggenberger¹

¹ *Applied & Environmental Geology, University of Basel, Bernoullistrasse 32, CH-4056 Basel
(matthias.h.mueller@unibas.ch)*

The temperatures of the shallow subsurface in urban areas are affected by numerous natural factors and anthropogenic influences. The latter comprise the thermal influence of tunnels, buildings in the subsurface, open and closed-loop geothermal systems, sealed surfaces, and infrastructure installations (e.g. district heating networks) (e.g. Epting et al. 2013, Benz et al. 2015). Groundwater in unconsolidated, highly permeable sediments plays an important role for advective heat transport, and therefore for the spatial (re)distribution of energy in the subsurface (e.g. Lo Russo & Taddia 2010). The effect of the current increase of groundwater temperatures, which can be observed in many urban areas (e.g. Zhu et al. 2010), on future thermal management of groundwater is not known yet. Therefore, adequate management strategies, which are based on monitoring and modelling tools, are required for urban groundwater bodies.

The groundwater and shallow subsurface temperatures in the urban area of Basel City are currently investigated. The use of conventional groundwater observation wells to investigate the influence of thermal groundwater use as well as deep and shallow building structures on groundwater temperatures is restricted since these wells rarely are located appropriately downstream of the thermal impact. Furthermore, conductive heat transport within conventional wells might bias the monitored temperature data. Therefore, besides conventional groundwater observation wells a series of multilevel temperature wells at specific locations and 3D numerical groundwater flow and heat transport models are used to assess thermal groundwater regimes in urban areas.

First results reveal that mean annual groundwater temperatures in urban areas range from about 11 to 17 °C (Figure 1). On average, they are 3.0 K higher compared to the mean annual air temperature, and 1.4 K higher compared to the mean annual groundwater temperatures in non-urban areas (open space, non-sealed areas), which range from 10 to 14 °C (Figure 1). The temperatures measured with the multilevel wells, which also measure temperatures in the unsaturated zone, range from 2 to 30 °C in 0.5 m depth below the asphalt. The soil temperatures measured at a meteorological station (MeteoSwiss 2015) in a non-urban area outside the city range from 2 to 23 °C in 0.5 m depth below the surface. This corroborates the importance of the influence of sealed surfaces for the elevated groundwater temperatures in urban areas. The subsurface temperature of a multilevel temperature well in 19.5 m below ground near a building (reaching the groundwater level) was seasonally varying around 15 ± 0.5 °C (mean \pm standard deviation). This suggests that heating periods in deep building structures can affect subsurface temperatures in urban areas.

The temporal temperature variations of some conventional observation wells could be simulated adequately within a sub-area of Basel, whereas at other locations no good match between observed and simulated temperatures could be acquired. These results indicate that the complex flow and thermal boundary conditions in some areas of the modelled sub-area are not yet entirely understood. However, the mean simulated annual groundwater temperatures in the observation wells, ranging from about 12.5 to 18.5 °C, correspond to the measured range of annual mean groundwater temperatures. This allows time integrated calculation of heat balances across model boundaries and defined cross-sections. The model is further used to conduct simulation tests, using different boundary conditions for the heat input on the top boundary and additional subsurface structures (e.g. sewage system networks) reaching the groundwater level. Further work will include the evaluation of the level of detail which is needed for the implementation of sealed or open surfaces and subsurface structures reaching the groundwater levels in the model.

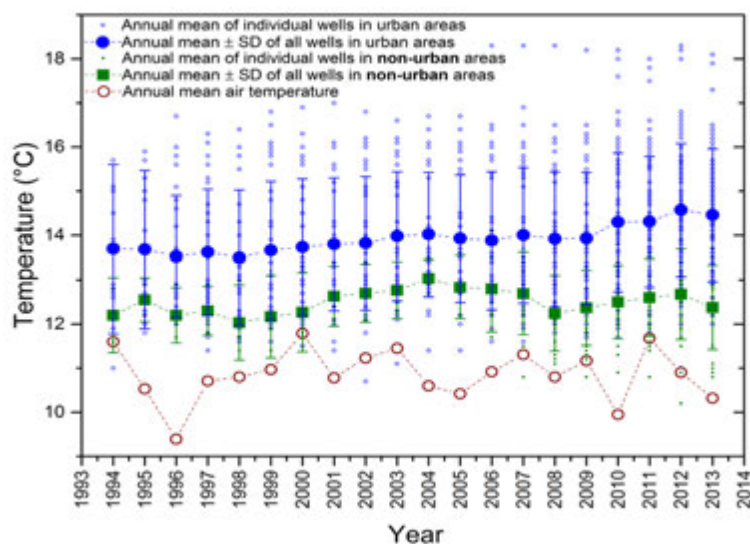


Figure 1. Annual mean groundwater temperatures in urban areas (blue symbols) and non-urban areas (green symbols) and mean annual air temperatures (red brown). Data provided by the Cantonal Environmental Agency Basel City (AUE BS), the local drinking water suppliers (IWB) and the Federal Office of Meteorology and Climatology MeteoSwiss.

REFERENCES

- Benz, S. A., Bayer, P., Menberg, K., Jung, S. & Blum, P. 2015: Spatial resolution of anthropogenic heat fluxes into urban aquifers, *Science of The Total Environment*, 524–525, 427-439.
- Epting, J., Händel, F. & Huggenberger, P. 2013: Thermal management of an unconsolidated shallow urban groundwater body, *Hydrol. Earth Syst. Sci.*, 17, 1851-1869.
- Lo Russo, S. & Taddia, G. 2010: Advective Heat Transport in an Unconfined Aquifer Induced by the Field Injection of an Open-Loop Groundwater Heat Pump, *American Journal of Environmental Sciences*, 6, 253-259.
- MeteoSwiss 2015: IDAweb The data portal of MeteoSwiss for research and teaching, Federal Office of Meteorology and Climatology, available at: meteoschweiz.admin.ch/web/en/services/data_portal/idaweb.html, access: 1 May 2015.
- Zhu, K., Blum, P., Ferguson, G., Balke, K.-D. & Bayer, P. 2010: The geothermal potential of urban heat islands, *Environmental Research Letters*, 5, 044002.

P 7.14

Hydrogeochemistry and Geothermometry of Thermal Groundwater of North-Eastern Algeria

Hichem CHENAKER¹, Belgacem HOUHA¹

¹ *Laboratory of LaSPI2A, Department of Sciences & Technology, University Abbas Laghrour, Khenchela, Algeria.*

This paper deals with the results of a hydrochemical and geothermal studies of the thermal waters in the northeastern of Algeria, eleven samples were taken in November 2012 and April 2014. The physicochemical parameters (temperature, pH, and electric conductivity) were measured in-situ, the temperature of the thermal water samples varied from 38 to 96°C, The pH value of these springs is slightly acidic to neutral, with high electrical conductivities about 4500µS/Cm.

Chemical and isotopic contents were employed in the investigation on the origin and evolution of thermal water and the evaluation of reservoir temperature in the geothermal systems. The water chemistry revealed two major hydrochemical facies namely sodium chloride (Na-Cl) and sodium sulfate (Na-SO₄). The mineral composition of the thermal waters reflects the geological formations found at the depth of origin and chemical changes samples were highly influenced by water-rock interaction.

The reservoir temperature estimation agrees qualitatively with results from cationic or silica geothermometers. The silica geothermometers seem to be the only one, which displays calculated temperatures in reasonable agreement with known local geothermal gradients or bottom-hole temperatures.

The thermal waters from the study area are depleted in ¹⁸O and ²H and fall on the Global Meteoric Water Line (GMWL) and Local Meteoric Water Line for northeastern Algeria, show that most thermal waters fit along the meteoric water line, with some exceptions due to Mediterranean precipitation, possible water-rock isotopic exchange or mixing with connate waters.

Keywords: Hydrochemical, isotopes, thermal waters, geothermometers, Algeria

P 7.15

Petrography and geochemistry of the Lower Jurassic shale in the southwestern Molasse Basin

Damien Do Couto¹, Branimir Segvic¹ & Andrea Moscariello¹

¹ *Department of Earth Sciences, University of Geneva, 13 Rue de Maraîchers, CH-1205 Geneva*

The Posidonia shales of Toarcian age (Lower Jurassic) are considered a potential effective seal for underground storage of CO₂ (Nagra, 2008; Chevallier et al., 2010) in the Molasse Basin. They have also been considered as a potential source rocks given their high content in organic matter (Leu and Gautschi, 2014). However, recent studies on shale gas development in North America indicate an increase in brittleness with increased content in TOC (Perez, 2014) rising some questions on the effectiveness and seal integrity potential of shale rocks with high content in total organic carbon. Our overall study aims at characterizing the petrography and the geochemistry of the Lower Jurassic shales in several wells (Figure 1) in order to define their texture and composition and estimate both their potential seal effectiveness and their source rock potential. In this paper we present the preliminary results of our investigations on the petrography and geochemistry from samples collected from several wells in the southwestern part of Switzerland where the subsurface data (2D seismic profiles and borehole data, Sommaruga et al., 2012) seem to indicate an increased thickness in Jurassic shales if compared to the northeastern part of the Swiss Plateau.

Tens of samples made of cuttings, core fragments and plugs have been gathered from several wells in the southwestern Molasse Basin (Figure 1). In most of these wells, digital well log data are available and help the interpretation of the shale content. This is the case for the Humilly-2 well in the center of the studied area where the Lower Jurassic shales from the Pliensbachian to the Toarcian reach up to 178 m. Each samples (selected according to their lithology and geophysical characteristics) were investigated by integrated semi-automated mineralogical analysis (QEMSCAN) coupled with X-ray diffraction on bulk rock and clay fraction and ICP-MS analyses and Rock-Eval.

In the Posidonia shales of the Humilly-2 well the clay assemblage consists of Illite, Illite-Smectite and Kaolinite. Major and minor elements in the Lower Jurassic shale show a significant increase in phosphate which corresponds to a coeval increase of uranium. While most of the Lower Jurassic shales hold a rather low amount of organic matter (<0.7%), an interval of about 12m in the Toarcian show high organic content up to 4% TOC.

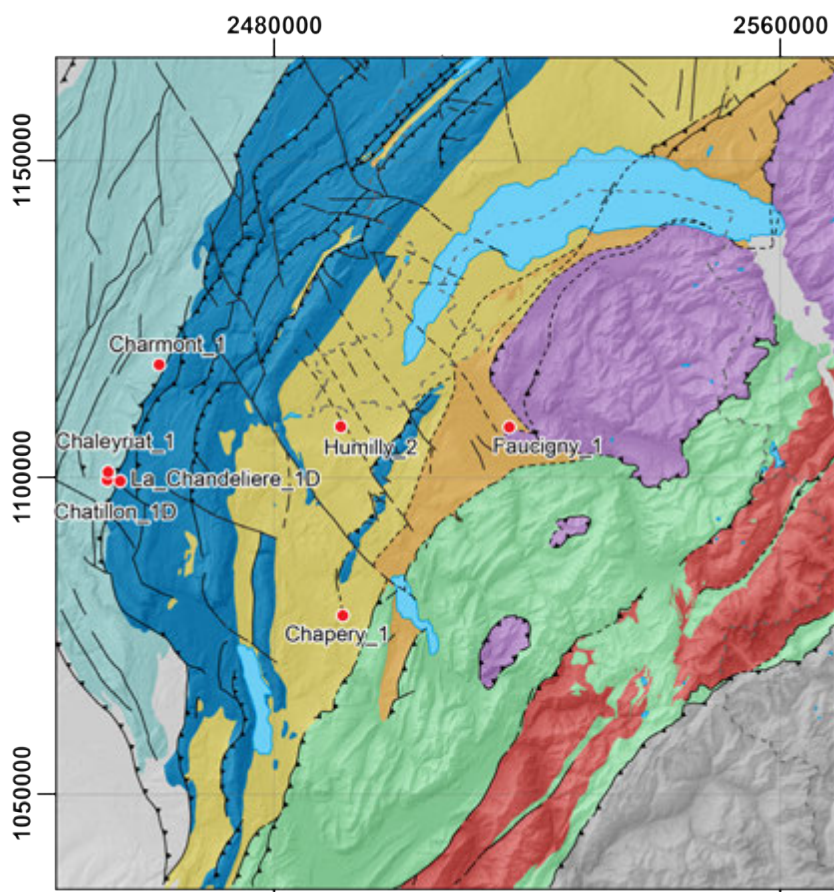


Figure 1. Geological map of the southwestern termination of the Molasse Basin. All the wells displayed in red have been sampled and analysed.

REFERENCES

- Chevalier, G., Diamond, L., & Leu, W., 2010 : Potential for deep geological sequestration of CO₂ in Switzerland: a first appraisal. *Swiss J. Geosci.*, 103, 427-455.
- Leu, W. & Gautschi, A., 2014: Shale gas potential of the Opalinus Clay and Posidonia Shale in Switzerland – A first assessment. *Swiss Bull. angew. Geol.*, 19/2, 95-107.
- Nagra 2008: Vorschlag geologischer Standortgebiete für das SMA- und das HAA-Lager. Darlegung der Anforderungen, des Vorgehens und der Ergebnisse. Nagra Technical Report NTB 08-03, Nagra, Wettingen, Switzerland.
- Sommaruga, A., Eichenberger, U. & Marillier, F. 2012: Seismic Atlas of the Swiss Molasse Basin. *Beitr. z. Geol. der Schweiz - Geophysik*, 44, 90 p.
- Perez R. 2014 Seismic Brittleness Index Volume Estimation from Well Logs in Unconventional Reservoirs., AAPG Annual Convention and Exhibition, Houston, Texas, April 6 -9, 2014 Search and Discovery Article #80381

P 7.16

Overcoring of a CO₂ – injection borehole and sampling procedure

David Jaeggi, Christophe Nussbaum, Paul Bossart

swisstopo, Mont Terri Project, Rue de la gare 63, CH-2882 St. Ursanne (david.jaeggi@swisstopo.ch)

For the CS (Near well sealing integrity for CO₂ storage) experiment a special overcoring technique was developed and applied, since the design required the lifting of the entire downhole system in one single piece of 5 m length. Overcoring of downhole installations such as sensors, testing probes or even complex downhole systems, e.g. custom-made packer systems is a widely used technique in drilling industry. In the Aalenian/Toarcian Opalinus Clay of the Mont Terri rock laboratory numerous experiments consisting of downhole installations in boreholes have been dismantled using the overcoring drilling technique (e.g. Bossart, 2000; Lahaye, 2005; Jaeggi & Wymann, 2014) over the last 20 years. Within the framework of the Mont Terri Project further overcoring experience could be gained by numerous campaigns encompassing the extraction of resin impregnated fractures (e.g. Bossart et al., 2002; Jaeggi et al., 2010).

A typical experiment at Mont Terri rock laboratory which requires the overcoring drilling technique for dismantling is conducted in 7 steps: i) Drilling of a small diameter pilot borehole (typically 76 mm diameter and depth of 10 -15 m), ii). Installation of a multipackersystem consisting of hydraulic packers, mechanical packers, e.g. grout packers, stainless steel rods, sintered filters in the interval, lines of stainless steel or polyamide, pressure and temperature sensors, iii). Monitoring period of several years, iv). Disconnection of the surface equipment and de-installation of the downhole system, v). Stabilization of the open borehole with resin, including break points for later core handling, vi). Overcoring of the stabilized core with a diameter of 250 to 350 mm, vii). Sampling by cutting discs, small-diameter sub coring and conditioning of samples.

The pilot borehole BCS-5 of the CS experiment exhibited a large diameter of 200 mm. The initial plan was to overcore the system with 350 mm single core barrel from 7 to 12 m depth. The lifting of the 5 m long piece was planned with custom-made sandwich tubes and a 4 m long axial counter drill into the ceiling due to insufficient height of the gallery. A lost grout packer during the lifting process made a change of the strategy necessary. In order to sample a part of the bottom cement, a 15 m long inclined borehole was drilled dipping -45° from the side. There was no success which led to the final strategy to recover the stuck grout packer first with a 500 mm overcore and subsequent overcoring of the downhole equipment with 350 mm.

Several lessons were learned from this recent overcoring which show, that the design of future large diameter downhole installations has to be adapted. Flexible systems are required, which enable the simple extraction of the cemented target intervals for sampling, encompassing modular systems which can easily be extracted from the surface by the drilling team and weak materials which can be removed with standard drill bits if necessary. Furthermore the diameter of the pilot borehole should be kept as small as possible and open intervals should be stabilized with resin prior to overcoring. For getting cement-clay interfaces of boreholes which have been subjected to heating and cooling cycles, sample extraction should be done with inclined boreholes, using the collar drilling technique. A sound planning of an overcoring procedure starts already in the very beginning with the design of the downhole system, where besides the scientists and engineers as well the future drilling company should be involved for getting the optimal solution.



Figure 1. Overcoring of the CS experiment at Mont Terri rock laboratory.

ACKNOWLEDGMENTS

This work is performed as part of the EU-funded FP7 project ULTimateCO₂. The ULTimateCO₂ consortium would like to thank swisstopo and Obayashi for funding a part of this experimentation.

REFERENCES

- Bossart, P. 2000: DI (diffusion experiment) Overcoring of borehole BDI-1. Lessons learned and recommendations, Mont Terri Technical Note TN2000-30.
- Bossart, P., Meier, P.M., Moeri, A., Trick, T. & Mayor, J.-C. 2002: Geological and hydraulic characterisation of the excavation disturbed zone in the Opalinus Clay of the Mont Terri Rock Laboratory, *Engineering Geology*, 66, 19-38.
- Jaeggi, D., Nussbaum, C., Moeri, A., Shao, H. & Müller, H. 2010: WS-H Experiment: Overcoring and structural analyses of the resin impregnated BHG-B11 overcore under plane and UV light, Mont Terri Technical Note, TN2010-32.
- Jaeggi, D. & Wymann, L. 2014: DR-A Experiment: Structural analyses and sampling of the BDR-A3 overcore, Mont Terri Technical Note, TN2014-16.
- Lahaye, F. 2005: EZ-A Experiment: Stress measurements campaign by overcoring in the Mont Terri Laboratory using CSIRO cells, Mont Terri Technical Note TN2004-86.

P 7.17

Frictional properties of Opalinus clay

Felipe Orellana¹ & Marie Violay¹

¹ *Laboratory of Experimental Rock Mechanics (LEMR), Swiss Institute of Technology Lausanne (EPFL), EPFL ENAC IIC LEMR, Station 18, CH-1015 Lausanne (felipe.orellana@epfl.ch)*

Opalinus Clay formation (OPA) is an indurated shale under study in the context of geological deep disposal of nuclear waste in Switzerland. We will study the frictional properties of fault zones in OPA to evaluate the long-term safety performance of the repository. A better understanding of fault stability and possible related leakages are the main goals.

In this project, we will focus on the effect of pore fluid pressure and micro-structural texture on the frictional properties of OPA. Series of friction experiments at different slip velocities and normal stress, on solid and granular material will be carried out. We have considered dry, fluid-saturated, and fluid reactive environments for the planned tests.

The main objective is to study the mechanisms involved during deformation and fracture permeability change. Using a bi-axial and a rotary shear apparatus, the systematic study of experimental faults should allow us to identify the couplings between hydraulic and mechanical properties, but also alteration reactions occurring during deformation.

Systematic investigations with different techniques have been carried out, and are planned to characterize OPA faulting zone. Among the techniques, we have studied the microstructure through X-Ray powder diffraction, Atomic Force Microscopy (AFM), SEM images and others. Petro-physical properties have been measured such as porosity (Mercury Intrusion Porosimetry and permeability (transient state method).

First results on the characterization of the faulting zone properties are presented.

P 7.18

Pore space characteristics of Opalinus Clay – Insights from USANS/SANS experiments

Kevin Schweinar¹, Andreas Busch², Pieter Bertier¹, Helge Stanjek¹

¹ *Clay and Interface Mineralogy, RWTH Aachen University, Bunsenstr. 8, D-52072 Aachen (kevin.schweinar@rwth-aachen.de)*

² *Shell Global Solutions International, Kessler Park 1, NL-2288 GS Rijswijk*

A comprehensive understanding of the porosity and pore size distribution (PSD) of mudrocks is crucial, not only to estimate the rock's ability to store oil or natural gas, but also to elucidate transport processes in sealing formations for disposal of nuclear waste or storage of carbon dioxide.

This contribution will present the outcome of the characterisation of pore structures of mudrocks using the results from (ultra) small angle neutron scattering ((U)SANS) experiments. Measurements have been performed on a set of Opalinus Clay samples, recovered from the shaly facies at the Mont Terri rock laboratory in St. Ursanne, Switzerland.

Conventional methods used to obtain information on pore structure characteristics of mudrocks are mainly based on fluid invasion techniques. Mercury injection porosimetry (MIP) is useful for characterising meso- and macropores, whereas low pressure gas adsorption (LPA) yields information about meso- and micropores. The lower limit for the former is approximately 2nm and the latter has an upper limit of ~300 nm (Clarkson et al. 2013). Total porosity values can be

measured by means of He pycnometry or water porosimetry (principle of Archimedes) which allows access to pores of atomic size.

In comparison, (U)SANS measurements allow the investigation of a wide pore size range (several Å – 6 µm, Fig. 1). This non-destructive method which does not require complicated sample preparation provides a total porosity, an internal surface area and PSD which can be compared with MIP and LPA data (Bertier et al., in press). Compared to fluid invasion techniques, the estimated porosity by (U)SANS can be slightly higher due to the fact that these measurements also account for closed porosity (Radlinski et al. 2004).

Calculated (U)SANS total porosities from this study show a good agreement with those measured by He pycnometry and water porosimetry as well as a fair accordance with N₂ adsorption data and further data published in literature (Pearson, 2003). Calculated PSD reflect the trends shown by PSD calculated from N₂ adsorption isotherms, however on a larger pore size range.

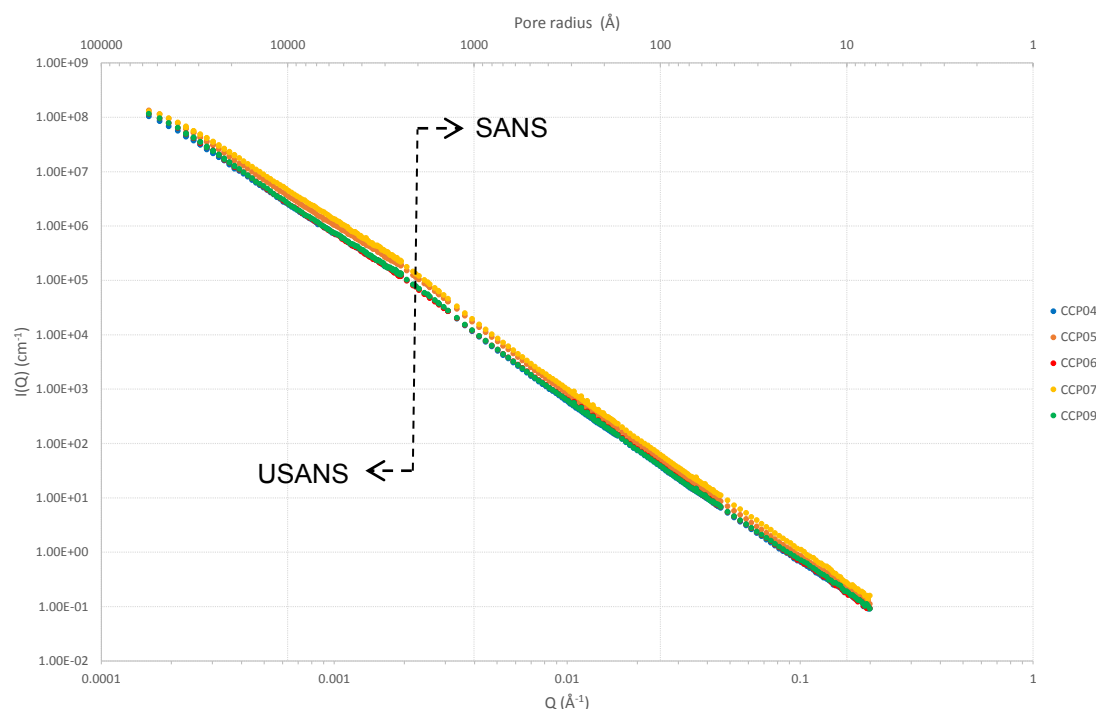


Figure 1. Combined USANS and SANS raw data of 5 Opalinus Clay samples illustrating accessible pore size range.

REFERENCES

- Bertier, P., Schweinar, K., Stanjek, H., Ghanizadeh, A., Clarkson, R.C., Busch, A., Kampman, N., Prinz, D., Amann-Hildenbrand, A., Krooss, B.M. in press: On the use and abuse of N₂ physisorption for the characterization of pore structure of shales. *Clays and Clay Minerals*.
- Clarkson, C.R., Solano, N., Bustin, R.M., Bustin, A.M., Chalmers, G.R., He, L., Melnichenko, Y.B., Radlinski, A.P., Blach, T.P. 2013: Pore structure characterization of North American shale gas reservoirs using USANS/SANS, gas adsorption, and mercury intrusion. *Fuel*, 103, 606-616.
- Radlinski, A.P., Mastalerz, M., Hinde, A.L., Hainbuchner, M., Rauch, H., Baron, M., Lin, J.S., Fan, L., Thiagarajan, P. 2004: Application of SAXS and SANS in evaluation of porosity, pore size distribution and surface area of coal. *International Journal of Coal Geology*, 59, 245-271.
- Pearson, F.J., Arcos, D., Bath, A., Boisson, J.-Y., Fernández, A.M., Gäbler, H.E., Gaucher, E., Gautschi, A., Griffault, L., Herán, P., Waber, H.N. 2003: Mont Terri Project – Geochemistry of Water in the Opalinus Clay Formation at the Mont Terri Rock Laboratory, *Berichte des BWG, Serie Geologie*, No. 5.

P 7.19

Coupled models of fluid-rock interaction induced by CO₂ injection into the U. Muschelkalk aquifer in N-Switzerland – code benchmarking and quantifying chemical trapping capacity

Peter Alt-Epping¹, & Larry W. Diamond

¹ *Institute of Geological Sciences, University of Bern, Baltzerstrasse 3, CH-3012 Bern (alt-epping@geo.unibe.ch)*

The Trigonodus Dolomite of the Upper Muschelkalk formation in the Swiss Molasse Basin constitutes a deep saline aquifer which owing to its elevated porosity and permeability has been considered a target for potential CO₂ injection (Chevalier et al., 2010) as well as for geothermal exploration. The variable results obtained by drilling into the Muschelkalk aquifer for geothermal exploitation, such as at Riehen, Schlattigen and Triemli, show that there is still a great deal of uncertainty regarding its hydro-geochemical characteristics. Numerical models are a useful tool to integrate and use this type of information to make quantitative predictions about the utilization potential and the hydro-geochemical implications following geothermal exploitation or CO₂ sequestration. For CO₂ sequestration, critical aquifer properties that need to be quantified are among others the storage capacity, injectivity and long-term isolation performance.

Numerical simulation of CO₂ injection and of the syn – and post-injection dynamics of the CO₂ plume is a challenging task owing to the complexity and coupled nature of the physical and chemical phenomena. During and shortly after injection, the immiscible CO₂ displaces the formation brine in a drainage-like process and migrates laterally and upward away from the injection wells, due to buoyancy forces. Once injection stops, CO₂ continues to migrate upward and displace water at the leading edge of the plume, while at the trailing edge water displaces CO₂ in an imbibition-like process. A trail of residual, immobile CO₂ is left behind the plume. The residual CO₂ and the CO₂ at the plume/brine interface slowly dissolves into the formation water, altering its chemical composition and density, while H₂O dissolves into the gas phase thus increasing the salinity of the brine. These changes in chemical composition of the brine along with perturbations of the pre-injection pressure and temperature conditions, induces disequilibrium reactions between the fluid and the rock. These may in turn affect the hydraulic properties of the rock and thus the injectivity and the migration of the plume via mineral dissolution-precipitation reactions.

We present a suite of reactive transport simulations that address different aspects of CO₂ injection into a carbonate aquifer patterned after the Upper Muschelkalk. The first set of simulations is used as a comparison between two reactive transport codes, PFLOTRAN and ToughReact. The aim of this comparison is to elucidate, track down and possibly remedy differences in the results that arise simply from the choice of codes. The comparison shows that for all computed CO₂ injection scenarios the results are similar even though PFLOTRAN uses a somewhat simpler approach for modeling H₂O-CO₂-NaCl systems. In our view the excellent computational performance of PFLOTRAN outweighs the inaccuracies arising from a simplified H₂O-CO₂-NaCl model, hence PFLOTRAN is our preferred code for simulating CO₂ injection scenarios.

A second set of simulations was aimed at elucidating the effect of high-resolution hydraulic and chemical heterogeneity on plume migration and CO₂ trapping (Figure 1A). Preliminary results show that the CO₂ plume moves preferentially along high permeability pathways. The dissolved and precipitated mineral volumes are too small to significantly affect the injectivity or the migration of the plume.

A third set of simulations explored the efficiency of chemical CO₂ trapping as a function of the aquifer permeability and the initial brine composition. The results show that the higher the permeability, the larger the spatial extent of the CO₂ plume and the larger the plume-brine contact area across which CO₂ dissolution occurs (Figure 1B). Thus, for homogenous permeability distribution, the CO₂ trapping efficiency is positively correlated with the aquifer permeability.

Whereas it is well known that a high salinity of the brine lowers the CO₂ solubility and hence the trapping capacity, little is known about the effect of the pre-injection pCO₂ on the CO₂ trapping capacity. In simulations we examined this effect for initial pCO_{2(g)} values ranging from 1e-3 to 0.1 bar. Results show that although there is a slight dependence of the CO₂ trapping capacity on the initial pCO_{2(g)}, the vastly higher CO₂ pressures attained during a typical injection project render this effect insignificant.

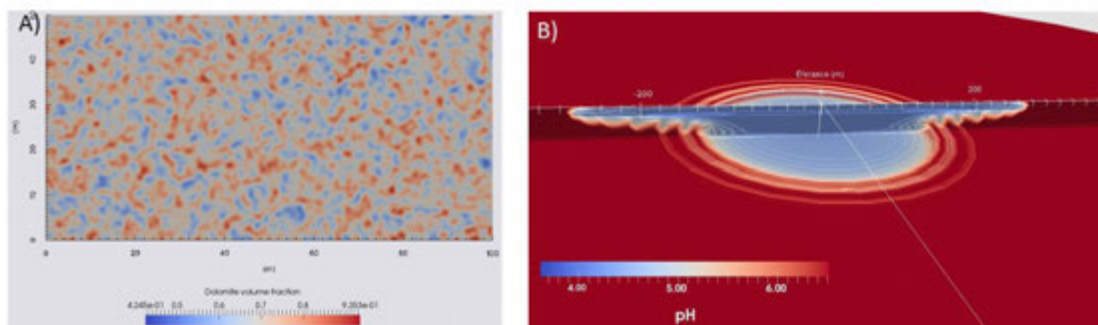


Figure 1: (A) Randomized dolomite distribution in the multi-mineral aquifer rock used to assess the impact of hydro-chemical heterogeneity on plume migration and CO₂ trapping; (B) Sections through a CO₂ plume (marked by a low pH) in a cylindrical domain with a homogeneous permeability of 1e-15 m² showing fingering due to subtle density changes upon CO₂ dissolution.

REFERENCES

Chevalier, G., Diamond, L. W. & Leu, W. 2010: Potential for deep geological sequestration of CO₂ in Switzerland: a first appraisal. *Swiss Journal of Geosciences* 103 (3)

P 7.20

Lattice Boltzmann pore-scale calculations of buoyant non-wetting fluids in heterogeneous porous media.

Andrea Parmigiani¹, Christian Huber² & Olivier Bachmann¹

¹ *Institute of Geochemistry and Petrology, ETHZ (andrea.parmigiani@erdw.ethz.ch)*

² *School of Earth and Atmospheric Sciences, GeorgiaTech US*

The lattice Boltzmann is a powerful numerical method for the modeling of immiscible fluids at the pore-scale. In this poster we report calculations for the buoyant migration of a non-wetting fluids in reactive and spatially heterogeneous porous media.

We present two pore-scale studies. In the first case, the migration of the non-wetting fluid is affected by the concurrent dissolution of the porous medium because of the reactivity of the buoyant invading fluid. In the second scenario a buoyant non-wetting fluid migrates across an heterogeneous medium, from a low to a high porosity layer. The two problems lead to similar outcomes: the migration of the buoyant non-wetting fluid is reduced at high porosity/permeability. These counter-intuitive results stem from the effect of solid confinement. High solid confinement (low porosity) stabilizes capillary fingering pathways and promotes efficient transport, while high porosity promotes the formation of an emulsion with discrete bubbles/slugs of non-wetting fluids.

P 7.21

Fluid flow and induced seismicity affected by asperities distribution during geothermal exploitation

Antonio Pio Rinaldi¹, Dimitrios Karvounis¹, Luca Urpi¹, Pierre Dublanchet¹

¹ *Schweizerischer Erdbebendienst (SED) ETH Zürich Sonneggstrasse 5, 8092 Zürich, Switzerland
(antoniopio.rinaldi@sed.ethz.ch, luca.urpi@sed.ethz.ch, karvounis@sed.ethz.ch)*

Many induced earthquake sequences could be seen as the rupture of brittle asperities along a fault zone, in response to fluid pressure changes generated by an injection at depth. Furthermore, the relocation of seismicity shows that these brittle patches only cluster on particular regions of the fault zone, which indicates that other portions of the fault are either creeping or not activated during the injection. This shearing behavior indicates heterogeneous permeability conditions within the fault zone.

Our goal is to explain some features often observed in deep geothermal system, where fault zone are stimulated to enhanced fluid circulation. For example at St. Gallen, the observed seismicity propagated at a rate of 1000 m/day toward SW in the initial phase, during which a magnitude 3.5 events occurred. In a second phase, seismicity was also observed to propagate toward NE along the fault zone.

Here, we first investigate the injection-induced seismic response of a heterogeneous fault plane featuring brittle asperities with low permeability embedded in higher permeability and ductile matrix. We first simulate the fluid flow and pressure evolution with a hydrogeological numerical simulator, which account for the heterogeneous permeability caused by the presence of a given distribution asperities. In order to get the seismicity associated with the simulated injection, we modeled in a second step the fault as a planar frictional interface, where brittle asperities are represented as unstable patches that can reactivate following a Mohr-Coulomb criterion. This coupled modeling approach allows to compute the seismicity generated by a localized fluid injection, and to investigate how a cloud of induced earthquakes propagates along a fault.

Furthermore, we investigate the effects of permeability changes due to seismic reactivation. The hydrogeological and first-order mechanical models are implicitly coupled to account for effects of shear displacement on the permeability changes. Such permeability changes, may cause at a later stage of post injection a change in seismicity propagation. Although simplified, our first-order analysis provides a reasonable explanation of the induced seismicity propagation during fault stimulation.

P 7.22

Thermo-hydraulic-mechanical simulation of fluid-injection activity and associated fault reactivation with complex rheology.

Luca Urpi¹, Antonio P. Rinaldi¹

¹ *Schweizerischer Erdbebendienst (SED), ETH Zürich, Sonneggstrasse 5, 8092 Zürich, Switzerland
(luca.urpi@sed.ethz.ch, antoniopio.rinaldi@sed.ethz.ch)*

Human activities such as carbon capture and storage, geothermal reservoir exploitation, unconventional hydrocarbon resources and waste water disposal requires injection of fluid into the underground.

A comprehensive review of cases of seismic events induced during fluid injection and of possible physical mechanisms (Ellsworth, 2009) points out the uncertainties in pinpointing the exact triggering process.

We propose here a deterministic forward approach to define a worst-case scenario, by evaluating the stress, temperature and pore pressure perturbations induced by fluid injection activity and their possible influence on reactivation of a nearby fault. The problem is here numerically addressed by means of a solver coupling a multiphase fluid flow code, addressing

the thermo-hydraulic components, with a geomechanical finite difference solver.

The fault is represented by means of interface elements and the fully dynamic simulation is computed for the rupture process.

Interface element obeys to a long-term frictional Mohr-Coulomb law, the quasi-static solution is evaluated for a locked fault. The quasi-static solution is evaluated for failure: if the failure criteria is satisfied the fault is set free to slip and the dynamic solution is calculated. Velocity- and strain-dependent frictional behavior of different patches of the fault influence the system evolution, resulting in larger or smaller slip length for the same injected volume. The signal recorded in the surface present different frequency content according to the rupture regime.

The fault is here approximated as a plane and therefore the kinematic properties of the fault (friction and its dependency on strain and/or velocity) will be defined as interface element properties. The single interface cannot be bended, but a bended fault can be represented by multiple interfaces not aligned, therefore the fault does not need to be necessarily a flat plane, although in the work presented here it is.

Pore pressure perturbation acts directly by reducing the normal effective stress, favouring unclamping of the fault, as well as increasing shear stresses, through the poroelastic stresses induced by increased pressure in the rock volume accomodating the injected fluid.

Temperature is acting both through its influence on water viscosity, as well as through its possible effect on constitutive fault parameters. Additionally, temperature perturbates the stress state due to rock mass cooling. The effect is similar to the poroelastic stress associated with fluid mass production, however the ratio of thermal to poroelastic stress can be quite large in deep fractured geothermal system (Segall, 1998).

We design a worst-case scenario and quantify the maximum slip that can be expected considering representative velocity-weakening and –strengthening behavior, therefore we analyzed the influence that can have on the storage a transition to velocity-weakening with depth. Fault rupture nucleated below the reservoir can propagate through the reservoir and reach the overlying cap-rock, promoting CO₂ leakage if the shearing deformation can enhance the permeability for the sealing material.

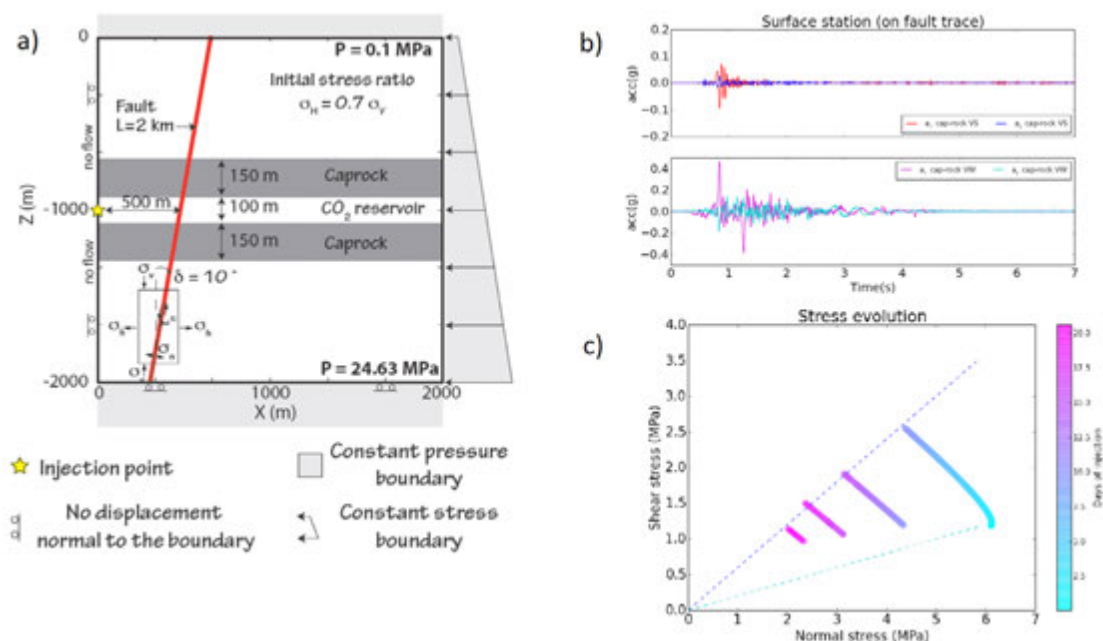


Figure 1. a) Model setup and boundary conditions. b) An example of the synthetic waveform generated by the rupture and recorded at the surface station. VS stands for velocity strengthening and VW for velocity weakening. c) Stress evolution on the nucleation point on the fault during high rate fluid injection. First event take place after 9 days, the second after 15 days.

REFERENCES:

- Ellsworth, W. L., 2009: Injection-induced Earthquakes, *Science*, 341, 1225942.
 Segall, P., & Fitzgerald S.D., 1998: A note on induced stress changes in hydrocarbon and geothermal reservoirs, *Tectonophysics*, 289, 117-128.

P 7.23

Efficient development of memory bounded geo-applications to scale on modern supercomputers

Ludovic Räss¹, Samuel Omlin¹, Aleksandar Licul², Yuri Podladchikov¹ and Frédéric Herman²

¹ *Institut des Sciences de la Terre (ISTE), University of Lausanne, Géopolis, Quartier Mouline, CH-1015 Lausanne (ludovic.raess@unil.ch)*

² *Institut des Dynamiques de la surface terrestre (IDYST), University of Lausanne, Géopolis, Quartier Mouline, CH-1015 Lausanne*

Numerical modeling is a key tool to investigate actual relevant topics in the area of geoscience. The current challenge is to solve problems that are multi-physics and for which the length scale and the place of occurrence might not be known in advance. Also, the spatial extend of the investigated domain might strongly vary in size, ranging from millimeters for reactive transport to kilometers for glacier erosion dynamics. An efficient way to proceed is to develop simple but robust algorithms that efficiently run and scale on modern supercomputers and permit therefore very high-resolution simulations.

We propose an efficient approach to solve memory bounded real-world applications on modern supercomputers architectures. We optimize the software to run on our newly acquired state-of-the-art GPU cluster *octopus*. Our approach shows promising preliminary results on important geodynamic and geomechanic problematics: we have developed a Stokes solver for glacier flow and a poromechanical solver with complex rheologies for nonlinear waves in stressed rocks.

We solve the system of partial differential equations on a Cartesian and regular grid and use an iterative finite difference scheme with preconditioning of the residuals. The MPI communication happens only locally (point-to-point); this method is known to scale linearly by construction. The *octopus* GPU cluster, which we use for the computations, has been designed to achieve maximal data transfer throughput at minimal hardware cost. It is composed of twenty compute nodes, each hosting four Nvidia Titan X GPU accelerators. These high-density nodes are interconnected with a parallel (dual-rail) FDR InfiniBand network.

Our efforts show promising preliminary results for the different physics investigated. The glacier flow solver achieves good accuracy in the relevant benchmarks and the coupled poromechanical solver permits to explain previously unresolvable focused fluid flow as a natural outcome of the porosity setup. In both cases, near peak memory bandwidth transfer is achieved. Our approach allows us to get the best out of the current hardware.

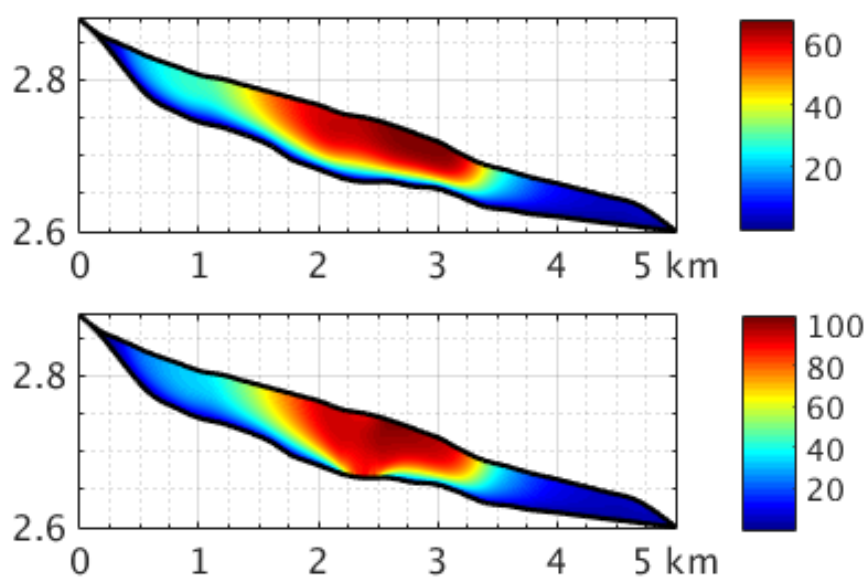


Figure 1. Simulation results for the Haut Glacier d'Arolla: L2-norm of the velocity [m/a]. (top) Case I without sliding zone. (bottom) Case II with sliding zone.

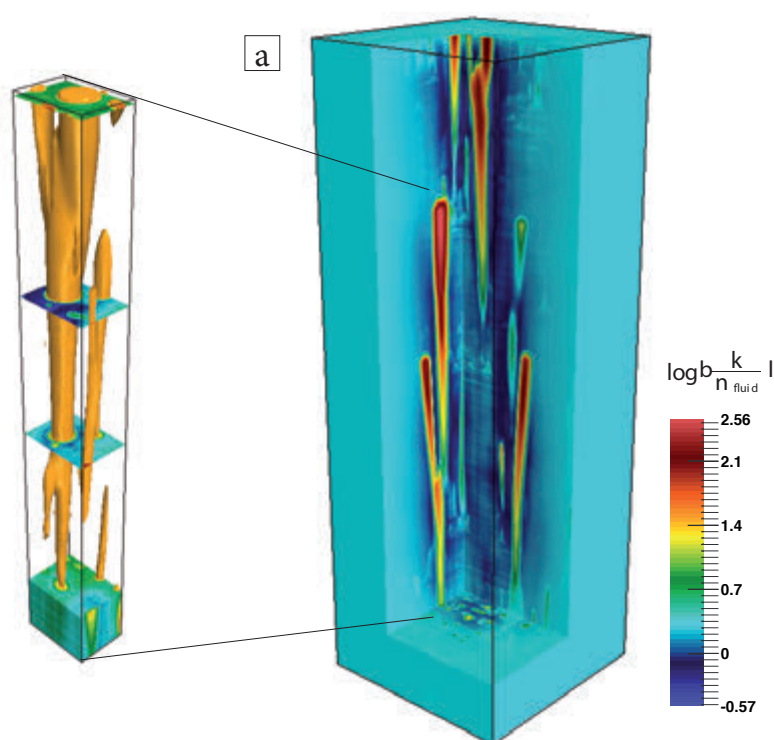


Figure 2. High permeability fluid pathway triggered as natural outcome from fluid flow coupled to poromechanic with time-dependent porosity. Log10 of normalized permeability over fluid viscosity is plotted.

P 7.24

A numerical and experimental reactive transport benchmark investigating the coupling between density driven flow, solute transport and chemical reactions

Poonoosamy Jenna¹, Georg Kosakowski¹, Luc R. Van Loon¹, Urs Mäder²

¹ Laboratory for Waste Management, Paul Scherrer Institut, CH-5232 Villigen PSI, Switzerland

² Rock Water Interaction, Institute of Geological Sciences, University of Bern, Baltzerstrasse 3, CH-3012 Bern, Switzerland

Reactive transport codes are increasingly used to predict the evolution of systems in the geological underground that are not easily experimentally accessible in space and time, for instance deep geological repositories for radioactive waste, CO₂ sequestration sites, or enhanced geothermal systems. Reactive transport models include complex couplings between chemical reactions, fluid and solute transport, and changes of material and fluid properties such as rock porosity and permeability. Although the numerical models are capable of investigating such systems, the application of these codes to real systems is hindered by the often unknown parametrization of material parameters (porosity, diffusivity, saturation, permeability, dissolution/precipitation kinetics and specific surface areas) that depend on sub-continuum chemical processes which induce changes in the pore space (precipitation/dissolution of mineral phases).

We designed a quasi 2D experimental reactive transport benchmark which aims to be reproducible, fast to conduct and with a simple chemical setup (Poonoosamy et al., 2015). The 2D setup is flexible enough to investigate several process couplings implemented in reactive transport codes: advective-diffusive transport of solutes, effect of liquid phase density on advective transport, and kinetically controlled dissolution/precipitation reactions causing porosity changes. In addition, the system allows to investigate the influence of microscopic (pore scale) processes on macroscopic (continuum scale) transport.

A quasi 2D Plexiglas tank of dimension $10 \times 10 \times 1$ cm was filled with a 0.01m thick reactive layer of celestite (SrSO_4), sandwiched between two layers of sand (Fig 1). Initially a liquid in equilibrium with SrSO_4 was injected until a stationary flow field was achieved. The placement of injection and extraction ports resulted in a highly asymmetric flow field. Chemical reactions and changes in the flow field were triggered by injection of a high density barium chloride solution causing initially an accumulation of the high density liquid at the bottom of the tank. Once the barium chloride reached the reactive layer, it enhanced the dissolution of celestite and barite (BaSO_4) was precipitated. Due to the higher molar volume of barite, its precipitation caused a porosity decrease and thus also a decrease in the permeability of the porous medium. The changes in the flow field in space and time were observed via injection of conservative tracers. The breakthrough of Cl^- and the change in Sr^{2+} and Br^{2+} concentration were measured in the effluents. In addition, an extensive post-mortem analysis of the reacted medium was conducted.

We used the OpenGeoSys-GEM simulator, which uses finite element solvers for fluid flow and mass transport, coupled with a Gibbs Energy Minimization (GEM) solver for chemical calculations (Kosakowski and Watanabe, 2014).

We could successfully model the flow (with and without fluid density effects) and the transport of conservative tracers with a (continuum scale) reactive transport model. The prediction of the reactive experiments initially failed. Only the inclusion of information from post-mortem analysis gave a satisfactory match for the case where the flow field changed due to dissolution/precipitation reactions. Currently the numerical calculations with OpenGeosys-GEM are compared with other reactive transport codes within the framework of the SeS benchmark project (Steefel et al., 2015). In addition we concentrate on the refinement of post-mortem analysis and the investigation of the dissolution/precipitation mechanisms on the pore scale. These results will be used to develop a pore scale reactive model that describes precipitation and dissolution of crystals at the pore scale for various transport and chemical conditions.

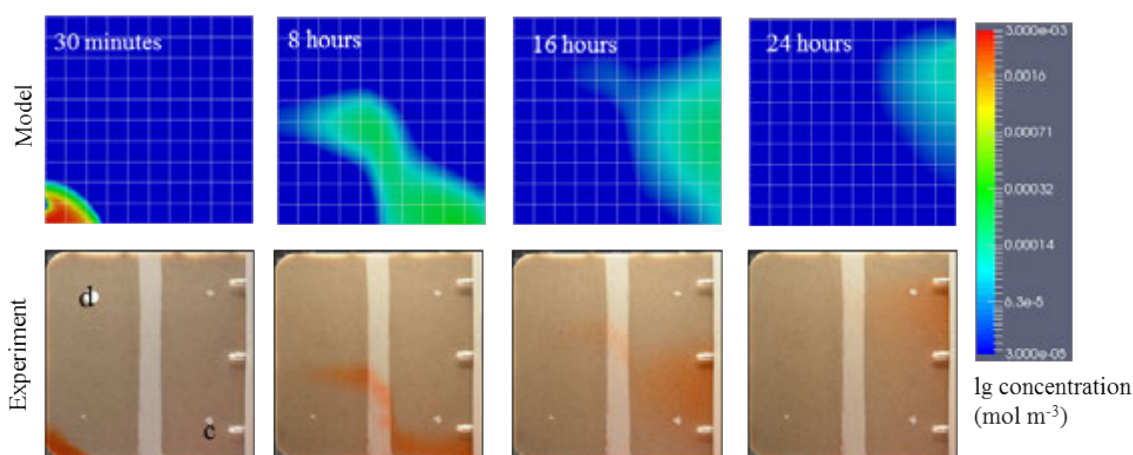


Figure 1. The temporal evolution of the tracer profiles of the model (top) and the experiment (bottom) during the injection of a concentrated barium chloride solution into the porous medium initially saturated with a liquid of lower density (water).

REFERENCES

- Kosakowski, G., & Watanabe, N. (2014). OpenGeoSys-Gem: A numerical tool for calculating geochemical and porosity changes in saturated and partially saturated media. *Physics and Chemistry of the Earth*, 70-71, 138-149.
- Poonoosamy, J., Kosakowski, G., Van Loon, L. R., & Mäder, U. (2015). Dissolution-precipitation processes in tank experiments for testing numerical models for reactive transport calculations: Experiment and modelling. *Journal of Contaminant Hydrology*, 177-178, 1-17.
- Steefel C. I., Appelo C. A. J., Arora C. A. J., Jacques D., Kalbacher T., Kolditz O., Lagneau V., Lichtner P. C., Mayer U. K., Meeussen J. C. L., Molins S., Moulton D., Shao H., Šimůnek J., Spycher N., Yabusaki S. B. & Yeh G. T. (2015) Reactive transport codes for subsurface environmental simulation, 19, 445-478.

P 7.25

Numerical upscaling of seismic characteristics of fractured media

Eva Caspari¹, Marco Milani¹, J. Germán Rubino¹, Tobias M. Müller², Beatriz Quintal¹ and Klaus Holliger¹

¹ *Institute of Earth Sciences, University of Lausanne, Quartier UNIL-Mouline, CH- 1015 Lausanne, Switzerland (Eva.Caspari@unil.ch)*

² *Energy Flagship, Commonwealth Scientific and Industrial Research Organization, 26 Dick Perry Ave, WA 6152 Kensington, Australia*

The seismic and hydraulic characterization of fractured rocks is still challenging, yet it has a number of important applications, such as, the sustainable use of groundwater, the optimized production of hydrocarbons and geothermal energy, and the safe storage of nuclear waste. While fractures and cracks tend to control the mechanical and hydraulic properties they can in general not be resolved directly, which makes it difficult to relate measured seismic attributes to the characteristics of the probed medium. In view of this, it is essential to understand how the effective properties of fracture rocks affect seismic observations.

Numerous effective medium theories were proposed to relate the effects of fractures to the overall elastic and hydraulic properties of the medium. Recent studies have shown that the attenuation and the velocity dispersion of seismic waves are sensitive to the elastic as well as the hydraulic properties of the probed medium and thus might provide critical insights into fracture characteristics. However, effective medium models tend to be based on analytical approaches and hence are inherently limited to simple geometries, low fracture densities, and/ or non-interacting fractures. These rather restrictive criteria are generally not fulfilled by actual fracture networks.

One way to overcome the inherent limitations of analytical models is through numerical upscaling procedures. In this study, we utilise a numerical approach based on the theory of quasi-static poroelasticity (Rubino et al. 2009, Quintal et al. 2011). A homogeneous oscillating displacement field is applied to a subvolume of a fractured porous medium. By spatial averaging of the resulting complex-valued stress and strain fields, the phase velocities and the attenuation as functions of frequency can be inferred. Since this approach is limited to a finite size of the investigated medium, the considered subvolume has to be at least the size of a representative elementary volume (REV) for the upscaled medium properties to be representative of the effective behaviour of the underlying heterogeneous medium. The adequate definition of an REV for a given upscaling problem is therefore of critical importance.

Hill's (1963) classical approach for elastic composites defines an REV as a sub volume which is (i) independent of the applied boundary conditions and (ii) structurally representative of the entire medium. The first aspect was studied in detail by Milani et al. (2014) for periodically fractured porous media. In this work, we extend this analysis to media containing randomly distributed horizontal and vertical fractures. The question then arises if the considered subvolumes represent the overall statistical properties of the underlying heterogeneous fractured media. To address the problem, we adapt a combined statistical and numerical approach proposed for elastic composite media (Kanit et al. 2003). Our results indicate that the overall statistical properties of the considered fracture distributions can be described with reasonable accuracy for computationally feasible REV sizes.

REFERENCES

- Hill, R. (1963), Elastic properties of reinforced solids: some theoretical principles, *Journal of the Mechanics and Physics of Solids*, 11, 357-372.
- Kanit, T., Forest, S., Galliet, I., Mounoury, V., and Jeulin, D. (2003), Determination of the size of the representative volume element for random composites: statistical and numerical approach, *International Journal of Solids and Structures*, 40, 3647-3679.
- Milani, M., Rubino, J.G., Müller, T. M., Quintal, B., and Holliger, K. (2014), Velocity and attenuation characteristics of P-waves in periodically fractured media as inferred from numerical creep and relaxation tests, *Exp. Abst. 84th Meet. Soc. Expl. Geophys.*, pp. 2882-2887.
- Quintal, B., Steeb, H., Frehner, M., and Schmalholz, S. (2011), Quasi-static finite element modeling of seismic attenuation and dispersion due to wave-induced fluid flow in poroelastic media, *Journal of Geophysical Research*, 116, B01, 201.
- Rubino, J., Ravazzoli, C., and Santos, J. (2009), Equivalent viscoelastic solids for heterogeneous fluid-saturated porous rocks, *Geophysics*, 74, N1-N13.

P 7.26**Seismic energy dissipation due to wave-induced fluid flow in fractured network: comparison of laboratory data from creep tests with numerical simulations**Céline Mallet¹, Béatriz Quintal¹, Eva Caspari¹ & Klaus Holliger¹¹ *Institute of Earth Sciences, University of Lausanne, CH-1015 Lausanne (celine.mallet@unil.ch)*

The geophysical and hydraulic characterization of fractured rocks is widely regarded as something like an ultimate objective. Yet it has a lot of applications, such as, the sustainable use of groundwater, the production of hydrocarbons and geothermal energy, the storage of nuclear waste... Recent evidences indicate that the attenuation of seismic waves, in such environments, is not only sensitive to the presence of fractures per se, but also to the parameters defining the corresponding fracture networks, (like the fracture interconnectivity). This in turn may offer the perspective of linking seismic observations to the hydraulic properties of fractured rocks. To further explore this and to test and complement the few existing numerical studies, we confront them to laboratory data from creep tests performed on thermally cracked water-saturated glass samples. We consider glass because this material can provide an useful reference when compared to more complex material such as rocks. Especially, studies on cracked glass samples play a key role in understanding the fundamentals of fracture effects.

The 2D geometry of the crack network is digitized based on corresponding SEM pictures from vertical cuts through the cylindrical samples. Together with the well-known physical properties of the non-fractured glass matrix, this forms the basis for our corresponding numerical simulations. The comparison of the observed and simulated seismic attenuation indicates that our 2D model is able to represent the basic characteristics of the laboratory observations, notably, the overall shape and frequency dependence of the attenuation curves. However, the predicted attenuation amplitudes are, overall, ~75% higher than the observed ones. Some of this discrepancy might be attributed to poorly constrained rock physical properties, such as the compressibility of the cracks. Moreover, the comparison of the attenuation behavior of a simpler 3D model to that of a corresponding 2D model indicates that this difference might be also due to the 2D simplification of the real 3D structure.

REFERENCES

- Rubino, G., Ravazzoli, C., & Santos, J. 2009: Equivalent viscoelastic solids for heterogeneous fluid-saturated porous rocks, *Geophysics*, 74, N1-N13.
- Quintal, B., Steeb, H., Frehner, M. & Schmalholz, S. 2011: Quasi-static finite element modeling of seismic attenuation and dispersion due to wave induced fluid flow in poroelastic media, *Jr of Geophysical Research*, 116, B01201.
- Mallet, C., Fortin, J., Gueguen, Y. & Bouyer, F. 2015: Brittle creep and subcritical crack propagation in glass submitted to triaxial conditions, *Jr of Geophysical Research*, 10.1002/2014JB011231.

P 7.27**Laboratory evidence for Krauklis wave resonance in fractures**Pei-Ju Rita Shih¹ and Marcel Frehner¹¹ *Geological Institute, ETH Zurich, Sonneggstrasse 5, CH-8092 Zurich
(pei-ju.shih@erdw.ethz.ch, marcel.frehner@erdw.ethz.ch)*

Krauklis waves are of major interest since they can lead to resonance effects in fluid-filled fractured rocks. This resonant behavior should lead to strong frequency dependence for seismic body waves, enabling the identification of Krauklis wave-related signals in the coda of recorded seismograms (Korneev, 2008). Aki et al. (1977) and Chouet (1996) used this resonance effect to show the potential of volcanic eruption forecasting by recording long-period volcanic tremor signals, which provide information of the state of fluid in the subsurface. Tary et al. (2014) identified and interpreted the observed resonances during hydraulic fracturing activities. The frequency content of the recorded seismic signals contains useful information for understanding the reservoir formation. The characteristics of Krauklis waves might be one of the keys to reveal properties of fluid-bearing fractured rocks.

Frehner (2014) demonstrates that body waves are capable of initiating Krauklis waves and that the initiation strongly depends on the incident wave mode (P- or S-wave) and fracture orientation. This study also shows that incident S-waves may carry more information about fractures. Here we combine numerical modeling results with laboratory experiments to study and visualize fracture-related effects on seismic wave propagation. We present a laboratory study that mimics similar conditions as in the numerical experiments (Frehner, 2014) of a homogenous medium containing a single well-defined fracture. We record the signals obtained from propagating ultrasonic waves along a sample without a fracture and samples with a fracture with different inclination angles of 30°, 45°, and 60°.

Figure 1 presents the spectrograms of the receiver data. The presence of the fracture induces elevated amplitudes at low frequencies in the coda after the first arrival (150 μ s onwards, Figure 1b, c, and d). The spectrogram for the case of 45° fracture inclination exhibits relatively larger amplitude around 0.1 MHz (200 μ s, Figure 1c) as compared to the cases of 30° and 60°. This fracture-related effect is very narrow-banded exhibiting a signature frequency around 0.1 MHz and decays relatively slowly over time. The observed signature frequency is independent of the fracture orientation and lower than the used source frequency (i.e., 1 MHz). We interpret this effect as a resonance in the fracture. The resonance frequency is an intrinsic property of the fracture size and elastic properties. In addition, we plan to employ an analytical solution (Lipovsky and Dunham, 2015) to verify our laboratory results by investigating the relationship between the fracture width, fracture length, resonance frequency, and quality factor. The ultimate goal is to identify relationships between the recorded seismic signal and the fracture properties (e.g., geometry and orientation).

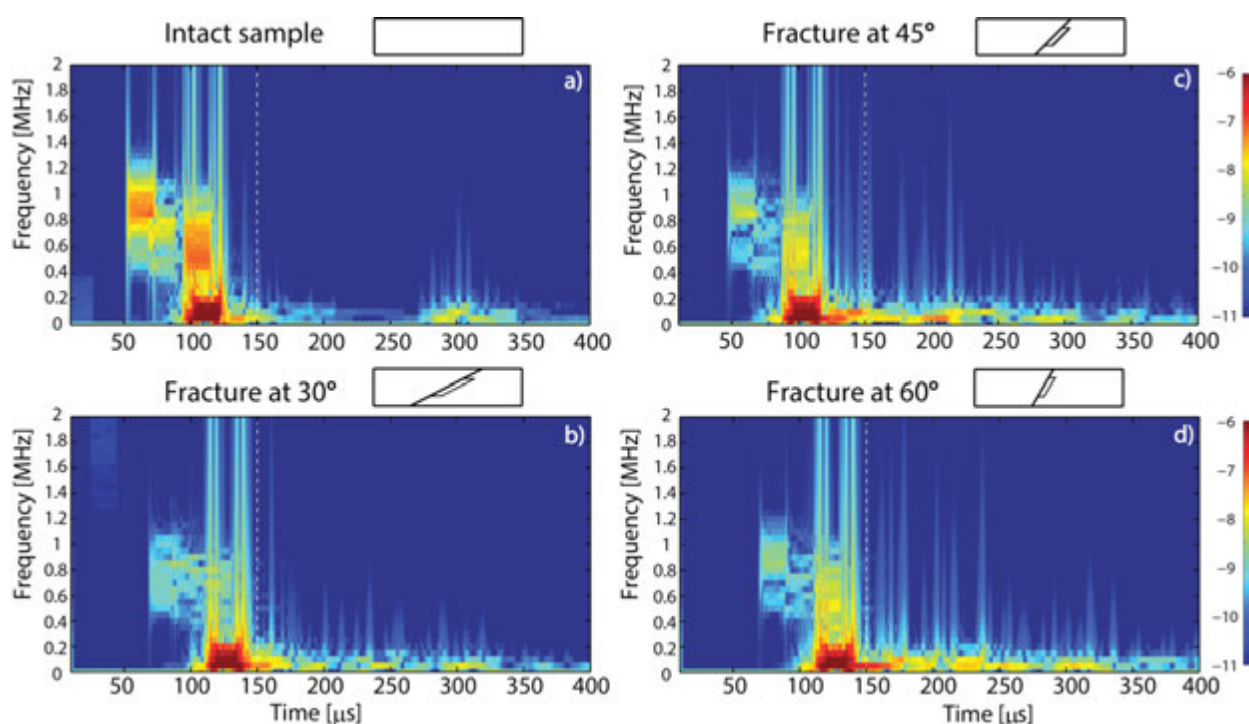


Figure 1. Spectrograms of receiver time signals generated by an S-wave with a dominant source frequency of 1 MHz propagating through the intact sample (a) ,and through fractured samples with a fracture inclination angle of 30° (b), 45° (c), and 60° (d), respectively.

REFERENCES

- Aki, K., Fehler, M. & Das, S. 1977: Source mechanism of volcanic tremor: Fluid-driven crack models and their application to the 1963 Kilauea eruption, *Journal of Volcanology and Geothermal Research*, 2, 259–287.
- Chouet, B.A. 1996: Long-period volcano seismicity: Its source and use in eruption forecasting, *Nature*, 380, 309–316.
- Frehner, M. 2014: Krauklis wave initiation in fluid-filled fractures by seismic body waves, *Geophysics*, 79, T27–T35.
- Lipovsky, B.P. & Dunham, E.M. 2015: Vibrational modes of hydraulic fractures: Inference of fracture geometry from resonant frequencies and attenuation, *Journal of Geophysical Research*, 120, 1080–1107.
- Korneev, V. 2008: Slow waves in fractures filled with viscous fluid, *Geophysics*, 73, N1–N7.
- Tary, J.B., Van der Baan, M. & Eaton, D.W. 2014: Interpretation of resonance frequencies recorded during hydraulic fracturing treatments, *Journal of Geophysical Research*, 119, 1295–1315.

P 7.28

Laboratory measurements of seismic attenuation of partially saturated Berea sandstone for a range of confining pressures

Samuel Chapman¹, Nicola Tisato², Beatriz Quintal¹ and Klaus Holliger¹

¹ University of Lausanne, Institute of Earth Sciences, Lausanne, Switzerland (samuel.chapman@unil.ch)

² University of Toronto, Civil Engineering Department, Toronto, Canada; previously at ETH Zurich, Department of Earth Sciences, Zurich, Switzerland

A number of physical mechanisms, commonly in the form of pressure diffusion related to wave-induced fluid flow or WIFF, can cause attenuation of seismic waves in fluid-saturated rocks (Mavko et al., 2009). The magnitude and frequency dependence of these forms of seismic attenuation strongly depend on the physical properties of the pore fluid, such as the viscosity, and the degree of saturation. The corresponding details tend to differ drastically from one mechanism to another. While most of these attenuation mechanisms have been analytically or numerically explored for idealized scenarios (e.g., Müller et al., 2010), there is a general lack of low-frequency experimental studies. Experiments at seismic frequencies (less than 100 Hz) are essential to help us verify these models and to assess their pertinence in real rocks.

We measure the extensional-mode attenuation and Young's modulus of a Berea sandstone sample at seismic frequencies (0.5-50 Hz) for a range of water saturation levels (~0-99%) and confining pressures (2-25 MPa). For dry conditions and water saturation levels of about 50%, attenuation is negligible and frequency independent, while it is frequency dependent for saturation levels above 80%, peaking between 1 and 20 Hz (Figure 1). Increasing the confining pressure on the sample from 2 to 25 MPa causes a reduction of the overall attenuation, reduces its frequency dependence, and shifts the attenuation peak to higher frequencies. The observed frequency-dependent attenuation is characteristic of attenuation caused by mesoscopic wave-induced fluid flow (WIFF) in response to a heterogeneous, patchy-type, water distribution in the porespace.

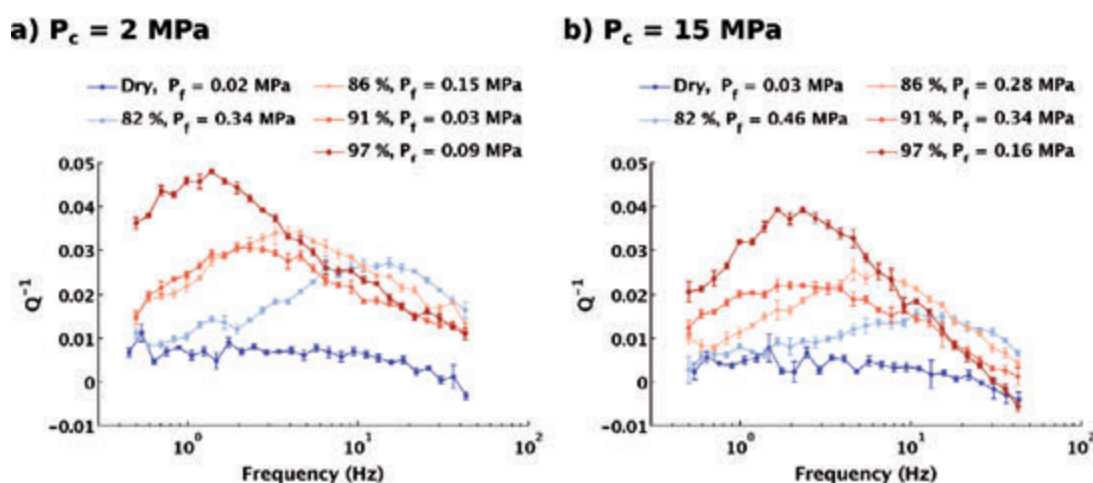


Figure 1. Extensional-mode attenuation Q^{-1} for: confining pressures 2 MPa (a) and 15 MPa (b). The legends provides the water saturation, from dry conditions to 97%, and the corresponding fluid pressures P_f .

REFERENCES

- Müller, T. M., B. Gurevich, and M. Lebedev 2010: Seismic wave attenuation and dispersion resulting from wave-induced flow in porous rocks – A review: Geophysics, 75, A147-A164.
- Mavko, G., T. Mukerji, and J. Dvorkin 2009: The rock physics handbook: Cambridge University Press.

8. Modeling in Geomorphology

C. Graf, I. Gärtner-Roer, N. Kuhn, R. Delaloye, M. Keiler, C. Scapozza, J. Müller, C. Levy, F. Herman, S. Castelltort, B. Staub

Swiss Geomorphological Society (SGS)

TALKS:

- 8.1 Costa A., Molnar P., Schlunegger F., Stutenbecker L., Lane S.N., Bakker M.: The relation between suspended sediment loads and climate in a regulated Alpine catchment.
- 8.2 Lambert R., King G.E., Herman F., Valla P.G.: Investigating K-feldspar luminescence thermochronometry for application in the Mont Blanc massif
- 8.3 Lehmann B., Valla P.G., King G. & Herman F.: OSL-surface exposure dating as a tool to constrain post-LGM glacier fluctuations in the Western Alps
- 8.4 Scapozza C., Castelletti C., Arrigo S., Ambrosi C.: The future from the past: numerical modeling of potential landslides triggering based on their historical evolution on the upper Cassarate catchment
- 8.5 Valla P.G., Herman F., Simon-Labric T., Braun J., Shuster D.L., Reiners P.W., Fellin M.G., Champagnac J.-D. & Baumgartner L.P.: Time-transgressive latitudinal impact of glaciations on mountain erosion since the Late Miocene
- 8.6 Vouillamoz N., Ottowitz D., Santoyo J.C., Joswig M., Mosar J.: Nanoseismic monitoring of landslides induced seismic events (slidequakes): New case study at the Pechgraben landslide – Upper Austria

POSTERS:

- P 8.1 Ambrosi C., Scapozza C., Lifa I., Heimgartner M., Spataro A., Cannata M.: Sustainable erosion control using Wood Wool
- P 8.2 Darvishi khatooni, J.: Distribution of lead in Khuzestan plain sediments, Iran
- P 8.3 Dufresne A., Prager C., Bösmeier A.S.: Morphology and emplacement processes of a large carbonate rockslide – rock avalanche (Tschirgant, Austria)
- P 8.4 Jalilian T., Darvishi khatooni J.: Karst Process in Bistoon of Kermanshah Province
- P 8.5 Krenz J., Greenwood P., Kuhn B., Heckrath G., Foster I., Boardman J., Meadows M., Kuhn N.: Modelling Carbon erosion in the Great Karoo Region, South Africa
- P 8.6 Micheletti N., Lane S.N., Lambiel C.: Coupling aerial imagery, hydropower intakes data and climatic indicators to investigate the changing climate effects on geomorphic dynamics of high mountain environments
- P 8.7 Prudat B., Bloemertz L., Kuhn N.J.: Ehenge: marginalized soil with high water use efficiency
- P 8.8 Silva T.A., Girardclos S., Loizeau J.L.: How much sediment is stored in the Rhone delta, canyon and fan system (Lake Geneva, Switzerland/France) since 1889?
- P 8.9 Valla P.G., Lajeunesse E., Delunel R., Gayer E., Allemand P., Delacourt C.: Orographic precipitations and landscape evolution in Basse Terre Island, Guadeloupe archipelago (Lesser Antilles Arc)
- P 8.10 Winterberg S., Willett S.: Dynamic reorganisation of Alpine river catchments analysed with χ -mapping

8.1

The relation between suspended sediment loads and climate in a regulated Alpine catchment.

Anna Costa¹, Peter Molnar¹, Fritz Schlunegger², Laura Stutenbecker², Stuart N. Lane³, Maarten Bakker³

¹ *Institute of Environmental Engineering, ETH Zürich, Stefano-Franscini-Platz 3, CH-8093 Zürich (costa@ifu.baug.ethz.ch)*

² *Institute of Geological Sciences, University of Bern, CH-3012 Bern*

³ *Institute of Earth Surface Dynamics, University of Lausanne, CH-1015 Lausanne*

The amount of sediment reaching the outlet of a catchment is function of the spatial and temporal distribution of sediment supply and transport capacity. In an Alpine environment many factors determine the rates of sediment production, transfer and deposition. While at long time scales geological forcing plays a crucial role in shaping the landscape, at shorter time scales, rainfall and runoff influence erosion and sediment transport. The amount of precipitation contributes to discharge and affects sediment transport capacity. The spatial and temporal distribution of rainfall impacts soil moisture and, as a consequence, on runoff and potential transport. Hillslope erosion is influenced by high intensity rainfall. Temperature is also a key variable, especially in mountainous environments: glacier and snow melting play a crucial role in fine sediment production and in the transport capacity of the fluvial system.

In this context, we analyse the correlation between suspended sediment loads at the outlet of the Upper Rhône basin and spatially distributed climatic data such as precipitation and temperature. The aim is to get a better understanding of basin-scale sediment-related processes, which is at the basis of the modelling framework that will be developed to investigate the decrease of sediment supply into Lake Geneva, after widespread dam construction (Loizeau et al., 2000). Turbidity data measured continuously at Port du Scex, a hydrometric station located on the Rhône River just upstream of Lake Geneva, are considered as a proxy for suspended sediment concentration. Gridded datasets are used to compute total daily precipitation and mean daily air temperature over the entire basin and over about 40 tributary catchments. The relation between fine sediment loads and climatic conditions is analysed by estimating the Spearman's rank correlation coefficient between turbidity, precipitation and temperature time series, assuming different time lags. The analysis is applied at the monthly scale. In order to identify a possible hierarchy of factors driving fine sediment production and transport processes, different geomorphological parameters are considered such as: mean elevation, area, glacier covered fraction, mean slope, curvature, main aspect, mean hillslope length, and topographic index, as explanatory variables.

Results show that there is a stronger correlation between turbidity and temperature than precipitation. This is likely related to the fact that temperature-driven processes such as snow and glacier melting are similarly distributed at basin scale, while the signal of more localized precipitation events might be dampened before reaching the catchment outlet. Highest correlations are found at the similar time lags for each sub-catchments (Figure 1), providing information of the concentration time of the basin, which is between 2 and 4 days on the average. The relation between temperature and fine sediment loads, as well as the time lag of maximum correlation, depend on the month, indicating that different processes drive sediment supply and transfer throughout the year. Although the strength of correlation between turbidity and temperature varies between the different tributary catchments, it is possible to identify a spatial pattern driven by geomorphological characteristics such as slope and elevation for some months (Figure 2).

The present work is part of the research project SEDFATE funded by the SNF Sinergia Programme, which aims at quantifying the human impacts on the observed reduction of suspended sediment inflows to Lake Geneva.

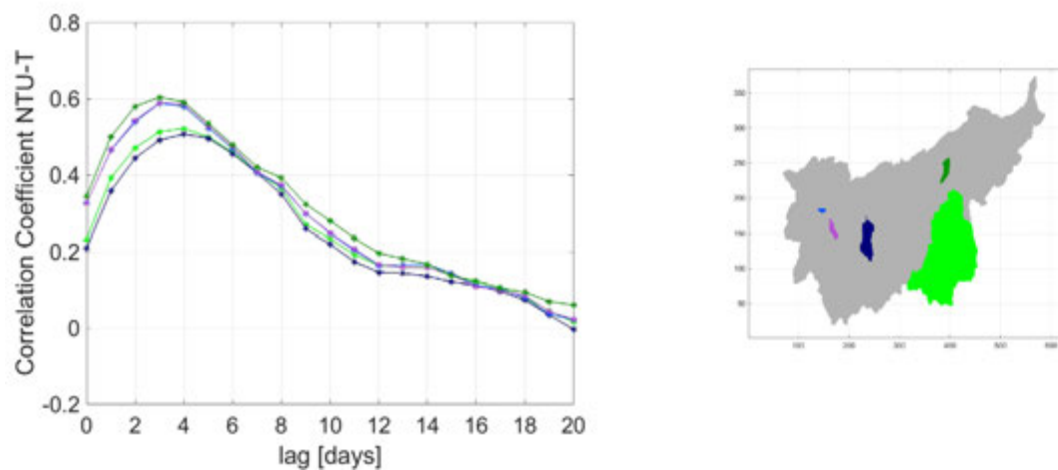


Figure 1. Example of correlation coefficients between turbidity and sub-catchment mean daily temperature for September. Each sub-catchment is a different line in the correlogram.

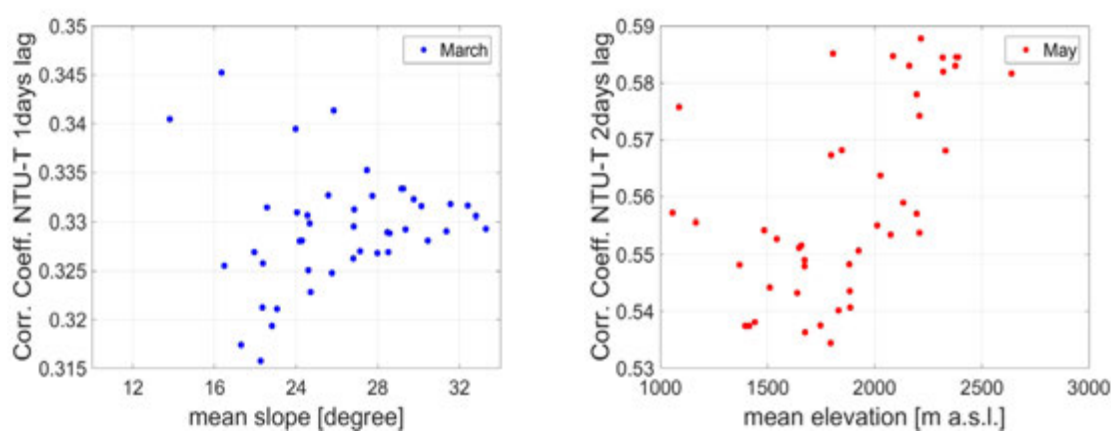


Figure 2. Correlation coefficients between turbidity and sub-catchments mean daily temperature as a function of mean slope (left) and mean elevation (right).

REFERENCES

Loizeau, J.-L. & Dominik, J. 2000: Evolution of the Upper Rhone River discharge and suspended sediment load during the last 80 years and some implications for Lake Geneva, *Aquatic Sciences*, 62, 54-67.

8.2

Investigating K-feldspar luminescence thermochronometry for application in the Mont Blanc massif

Renske Lambert¹, Georgina King^{1,2}, Frédéric Herman¹ & Pierre Valla¹

¹ *Institute of Earth Surface Dynamics, University of Lausanne, Batiment Géopolis, Quartier Mouline, CH-1015 Lausanne (renske.lambert@unil.ch)*

² *Institute of Geography, University of Cologne, Albertus-Magnus-Platz, 50923 Köln*

Luminescence dating has the potential to quantify the recent exhumation history of mountain ranges as a low-temperature thermochronometer. During rock exhumation, electrons get trapped through exposure to ionizing radiation whilst elevated temperatures cause thermally stimulated detrapping. The resulting luminescence signals measured in the laboratory can be used to constrain rock thermal histories through modelling of the kinetic parameters of electron trapping and detrapping. Here, we investigate and model laboratory kinetic processes of the luminescence of K-feldspar and assess their extrapolation over geological timescales.

Samples were taken from the actively eroding Mont Blanc massif in the European Alps, along a 12 km long tunnel with ambient temperatures of 10-35 °C. In this setting rapid exhumation rates have been found during the last 2 million years (up to ~2 km/Myr), however, we intend to increase the temporal resolution to sub-Quaternary timescales using luminescence thermochronometry. Infra-red stimulated luminescence signals at 50 °C (IR50) and at 225 °C (post-IR IRSL225) of K-feldspar extracted from Mont Blanc tunnel samples were measured and our first results reveal a thermal signature from which rock cooling rates can be derived. Isothermal decay experiments show non-exponential decay, but interestingly, experiments with a range of regenerative doses reveal first-order kinetics. The observed thermal decay pattern is well-described by a model based on a physically plausible distribution of the density of states.

Ultimately, we intend to use the IR50 and post-IR IRSL225 signals of K-feldspar as dual thermochronometers to determine the late-Quaternary cooling history of the Mont Blanc massif. Moreover, the luminescence signals may give insights into local thermal field evolution, before the influence of postglacial hydrothermal flow.

8.3

OSL-surface exposure dating as a tool to constrain post-LGM glacier fluctuations in the Western Alps

Benjamin Lehmann¹, Pierre G. Valla¹, Georgina King² & Frederic Herman¹

¹ *Institute of Earth Surface Dynamics, Faculty of Geosciences and Environment, University of Lausanne, CH-1012 Lausanne (benjamin.lehmann@unil.ch)*

² *Institute of Geography, University of Cologne, D-50923 Cologne, Germany*

Providing tight spatial/temporal constraints on late-Pleistocene glacier fluctuations remains an important challenge for understanding glacier response to climate change. In most mountainous settings, paleo-glacier reconstructions are limited because they lack precise temporal constraint, which would enable their use as a paleoclimate proxy. OSL-surface exposure dating has been recently proposed [Sohbati et al., 2011] and offers the potential to improve paleo-glacier reconstruction. Because the OSL signal is sensitive to light, OSL-signal bleaching within a rock sample depends on its exposure time and environmental conditions, and can therefore be used to date the exposure time of glacially-polished bedrock or erratic boulders. However, successful application of this technique first requires calibration and validation.

Here, we focus on the Mer de Glace glacier (Mont Blanc massif, France) where the post-LGM glacier dynamics remain poorly constrained with numerous short glacier re-advances occurring during the mid-Pleistocene and Holocene [LeRoy et al., 2015]. First, we calibrated the different parameters involved in OSL surface exposure dating. We have sampled a vertical transect of polished bedrock surfaces with known exposure ages (from 10 to 165 years) from the Montenvers train station (1913 m a.s.l.) to the present-day position of the Mer de Glace (1600 m a.s.l.). OSL data from rock slices show increasing exposure age with elevation which is consistent with glacier thinning since the Little Ice Age. Moreover, our results show the importance of the bedrock lithology and exposure conditions in controlling the different model parameters. Secondly, we sampled the Trelaporte transect where exposed bedrock surfaces are of uniform lithology. Here, we will apply similar approach on a much longer timescale, from the Last Glacial Maximum (LGM, ~24 ka, Coutterand et al., 2006) to the present day. In summary, OSL-surface exposure dating applied to periglacial environments appears to be a promising method for studying past glacier fluctuations and surface weathering rates, and can be used as paleoclimate proxy in mountainous environments.

REFERENCES

- Sohbati, R., Murray A., Jain M., Buylaert J.-P., and Thomsen K. (2011), Investigating the resetting of OSL signals in rock surfaces, *Geochronometria*, 38 (3), 249_258, doi:10.2478/s13386-011-0029-2.
- Le Roy, M., Nicolussi, K., Deline, P., Astrade, L., Edouard, J.-L., Miramont, C., Arnaud, F. (2015), Calendar dated glacier variations in the western European Alps during the Neoglacial: the Mer de Glace record, Mont Blanc massif, *Quaternary Science Review* 108 (2015) 1-22, doi:10.1016
- Coutterand S., Buoncristiani J.-F. (2006), Paléogeographie du dernier maximum glaciaire du Pléistocène récent de la région du Massif du Mont Blanc, France, *Quaternaire*, 17, (1), 2006, p. 35-43

8.4

The future from the past: numerical modeling of potential landslides triggering based on their historical evolution on the upper Cassarate catchment

Cristian Scapozza¹, Claudio Castelletti¹, Samuel Arrigo¹ & Christian Ambrosi¹

¹ *Istituto scienze della Terra (IST), Scuola Universitaria Professionale della Svizzera Italiana (SUPSI), Campus Trevano, CH-6952 Canobbio*

In mountain environments subject to intensive pastoralism since the second half of 20th century, modifications in land use derived from the abandon of alpine pastures and natural reforestation may have had a significant effect on the number and surface of shallow landslides. Four study sites in the upper Cassarate catchment (Southern Swiss Alps) were analysed for quantify their evolution in the last century. The aim of this study is then to produce numerical scenarios of evolution of shallow landslides based on historical data for an assessment of the present situation and an evaluation of their future evolution.

The diachronical mapping based on historical analysis allowed the evolution of the number and surface of shallow landslides to be quantified (Figure 1). For two sites (Alpe Rompiago and Alpe Pietrarossa), surface variations shows a slight increase in the area of shallow landslides in the decades before 1950. For the second half of 20th century, data shows a slow and gradual decrease in surface area, which in 2012 is less than a half compared to 1950. In the two other study sites (Alpe Cottino and Cima di Foiorina), the increase in shallow landslides surface since 1923 is significant.

Evolution of shallow landslides was compared with a database of 55 mass movements occurred in the catchment between 1900 and 2014. Thanks to the quantification of an antecedent standardized precipitation index (IPAS), allowing the characterization of the state of moisture/drought of the near surface, it was also possible to calculate triggering thresholds of observed shallow landslides based on the state of ground moisture at the beginning of the rainfall event. Thresholds based on an exponential relationship between the sum of precipitation and the IPAS minimal value provides the highest correlation coefficients. The correspondence rate with the shallow landslides historical dataset is higher than 90%. Positive predictive values of the triggering thresholds are lower than 5%, probably due to the very limited number of days with landslides (55) with respect to the total number of days analysed (42'003 = 115 years). Despite this point, negative predictive values are higher than 99.96%, indicating that it is very unlikely to have a landslide if it was not predicted.

Four scenarios of shallow landslide triggering were finally implemented thanks to numerical modeling of potential instability zones was performed thanks to the TRIGRS program (Transient Rainfall Infiltration and Grid-Based Regional Slope-Stability). This model is able to evaluate the effect of rainfall events on the temporal evolution of the slope stability considering local geotechnical characteristics and infiltration processes. Validation of the model was performed thanks to scenarios related with potential conditions of instability under different rainfall durations and intensities and ground moisture conditions. A final calibration of this model based on the adjustment of cohesion and angle of internal friction parameters, allowed maps of zones of potential aggravation of observed shallow landslides, and zones of potential triggering of new instabilities, to be produced.

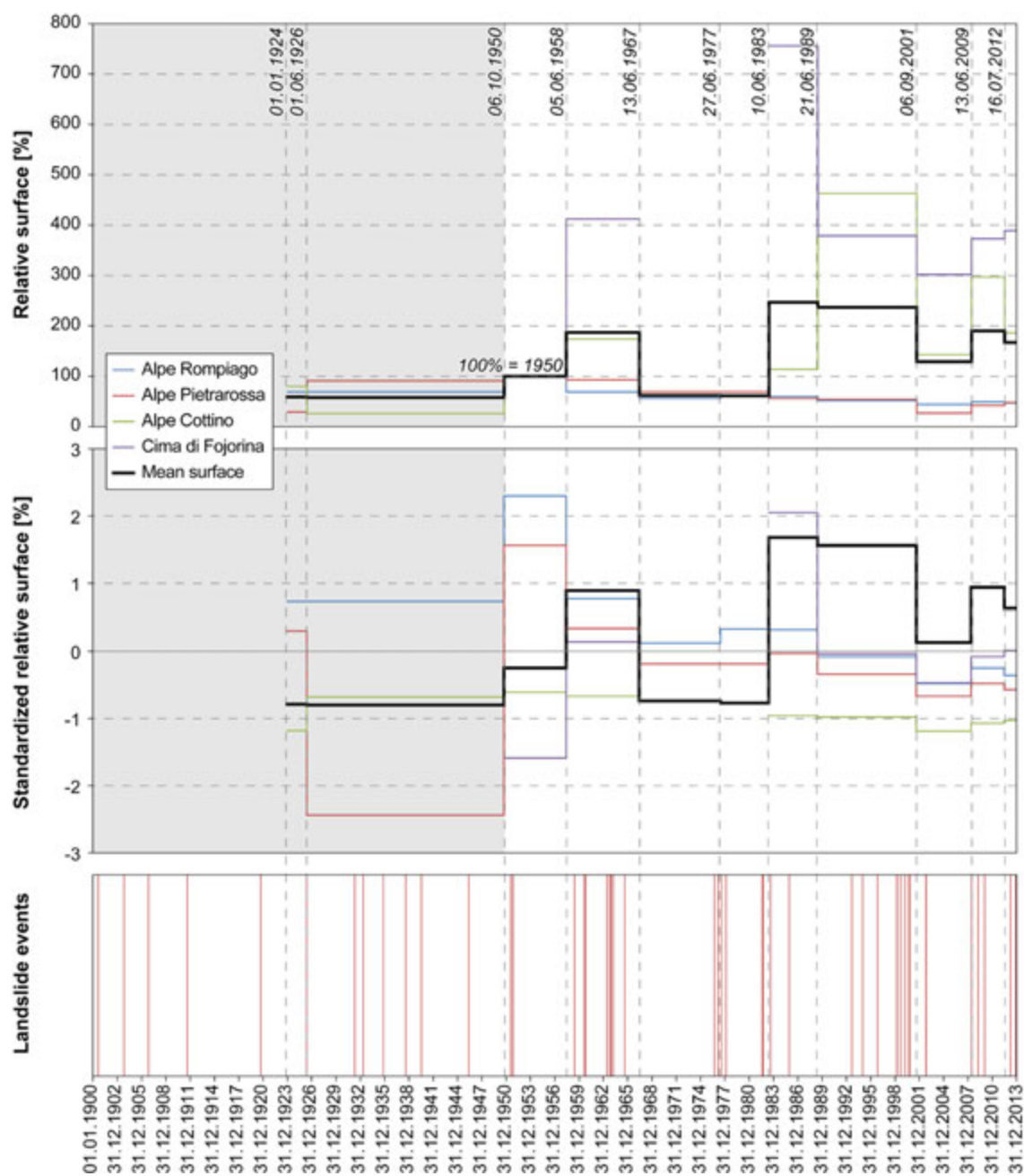


Figure 1. Evolution of absolute and standardized landslide surface and frequency diagram of the historical landslide events recorded in the upper Cassarate catchment. In grey, data calculated on terrestrial oblique photographs.

8.5

Time-transgressive latitudinal impact of glaciations on mountain erosion since the Late Miocene

Pierre G. Valla^{1,2}, Frédéric Herman¹, Thibaud Simon-Labric^{1,3}, Jean Braun³, David L. Shuster^{4,5}, Peter W. Reiners⁶, Maria G. Fellin⁷, Jean-Daniel Champagnac² and Lukas P. Baumgartner⁸

¹ *Institute of Earth Surface Dynamics, University of Lausanne, CH-1015 Lausanne (pierre.valla@unil.ch)*

² *Geological Institute, ETH Zürich, CH-8092 Zürich*

³ *Institute of Earth Sciences, University of Grenoble, F-38400 Grenoble*

⁴ *Department of Earth & Planetary Science, University of California, USA-94720 Berkeley*

⁵ *Berkeley Geochronology Center, USA-94707 Berkeley*

⁶ *Department of Geosciences, University of Arizona, USA-85721 Tucson*

⁷ *Institute for Geochemistry and Petrology, ETH Zürich, CH-8092 Zürich*

⁸ *Institute of Earth Sciences, University of Lausanne, CH-1015 Lausanne*

Whether Late Cenozoic climate cooling and onset of glaciations has had a global impact on mountain erosion is one of the most fundamental questions in Earth Sciences (Molnar and England, 1990; Zhang et al., 2001; Willenbring and von Blanckenburg, 2010). Recent evidence points towards a global and synchronous increase in mountain erosion and global sedimentation rates at 4-2 Ma (Zhang et al., 2001; Herman et al., 2013). However, paleoclimate and sediment records (e.g. Zachos et al., 2001) suggest a progressive migration of glaciations from high- to mid-latitudes since the Oligocene period, with intensification from the Late Miocene toward present. Such a global and synchronous increase in erosion rates appears thus contradictory to the progressive climate cooling and an observed equatorward migration of glaciations during the Late Cenozoic.

Here we use low-temperature thermochronometry (apatite (U-Th-Sm)/He and ⁴He/³He dating) and numerical modeling to constrain Late Cenozoic erosion histories in southern Patagonian Andes (Torres del Paine) and southern Alaska (Granite Range, Chugach-St. Elias Range). These high-latitude settings have been tectonically-quiescent since at least the Late Miocene, and are in turn suitable environments to quantitatively assess any climate forcing on mountain erosion. Our results reveal that erosion rates significantly increased at ~8-6 Ma, in line with reported onset of glaciations at these sites. More importantly, this marked increase also appears to be synchronous in both the southern and northern hemispheres. Finally, our findings demonstrate a latitudinal migration of increased mountain erosion during the Late Cenozoic, implying that progressive climate cooling exerted a primary control on mountain erosional processes and sediment production.

REFERENCES

- Herman, F. et al. 2013: Worldwide acceleration of mountain erosion under a cooling climate. *Nature*, 504, 423-426.
- Molnar, P. & England, P. 1990: Late Cenozoic uplift of mountain ranges and global climate change: chicken or egg? *Nature*, 346, 29-34.
- Willenbring, J.K. & von Blanckenburg, F. 2010: Long-term stability of global erosion rates and weathering during late-Cenozoic cooling. *Nature*, 465, 211-214.
- Zachos, J., Pagani, M., Sloan, L., Thomas, E. & Billups, K. 2001: Trends, rhythms, and aberrations in global climate 65 Ma to present. *Science*, 292, 686-693.
- Zhang, P., Molnar, P. & Downs, W.R. 2001: Increased sedimentation rates and grain sizes 2-4 Myr ago due to the influence of climate change on erosion rates. *Nature*, 410, 891-897.

8.6

Nanoseismic monitoring of landslides induced seismic events (slidequakes): New case study at the Pechgraben landslide - Upper Austria

Naomi Vouillamoz¹, David Ottowitz² (& group), Juan Carlos Santoyo¹, Manfred Joswig¹, Jon Mosar³

¹ Institut für Geophysik, Universität Stuttgart, Azenbergstr. 16, DE-70174 Stuttgart
(naomi.vouillamoz@geophys.uni-stuttgart.de)

² Geologische Bundesanstalt, Fachabteilung Geophysik, Neulinggasse 38, A-1030 Vienna
The landslide working group of the Geological Survey of Austria refers to Birgit Jochum, Stefan Pfeiler & Robert Supper

³ Sciences de la Terre, Département de Géosciences, Université de Fribourg, Ch. Du Musée 6, CH-1700 Fribourg

Key dynamics influencing unstable slope mass movements can be investigated with the most precise timing by seismic monitoring, which brings a unique insight into the mechanisms driving the slope movement. Recently, a newly developed method named nanoseismic monitoring (Joswig, 2008) enabled the observation of various landslide induced seismic events at creeping softrock slope instabilities (e.g. Walter et al., 2013; Tonnellier et al., 2013). Nanoseismic monitoring combines several seismological approaches that extend the capabilities of seismic analysis (event detection, evaluation and location) down to the background noise threshold.

This project aims at investigating brittle deformation source processes associated to landslide creep by using nanoseismic monitoring. In this perspective, the Pechgraben landslide in upper Austria has been selected to carry out a first (feasibility) measurement campaign of about two weeks in October 2015. The Pechgraben landslide is a historical slope instability that has been reactivated after heavy rainfalls in summer 2013 on a 7ha surface. Following its reactivation, the landslide has been routinely operated through multi-disciplinary monitoring methods including UAV, GPS, cameras, fractures measurements, geoelectrics, soil humidity, soil temperature, precipitation monitoring, inclinometers and piezometers, as part of the TEMPEL/LAMOND landslide network of the FP7 project SafeLand (see Supper et al., 2014).

By applying nanoseismic monitoring on a such extensively investigated and documented creeping softrock landslide, our objective is to (i) characterize the spatiotemporal occurrence of brittle deformation within the landslide body (ii) investigate how the brittle deformation relates to slope dynamics and water-dependent material properties and (iii) interpret the driving source processes.

REFERENCES

- Joswig, M. 2008. Nanoseismic monitoring fills the gap between microseismic networks and passive seismic. special topic, Leveraging Technology, first break 26, 117–124.
- Supper, R., Ottowitz, D., Jochum, B., Kim, J.-H., Römer, A., Baron, I., Pfeiler, S., Lovisolo, M., Gruber, S., & Vecchiotti, F. 2014: Geoelectrical monitoring: an innovative method to supplement landslide surveillance and early warning. Near Surface Geophysics 12, pp. 133-150. DOI: 10.3997/1873-0604.2013060.
- Tonnellier, A., Helmstetter, A., Malet, J.-P., Schmittbuhl, J., Corsini, A. & Joswig, M. 2013. Seismic monitoring of soft-rock landslides: the Super-Sauze and Valoria case studies. Geophysical Journal International 193 (3), pp. 1515–1536. DOI: 10.1093/gji/ggt039.
- Walter, M., Gombert, J., Schulz, W., Bodin, P., Joswig, M. (2013). Slidequake Generation versus Viscous Creep at Softrock-landslides: Synopsis of Three Different Scenarios at Slumgullion Landslide, Heumoes Slope, and Super-Sauze Mudslide. Journal of Environmental & Engineering Geophysics 18 (4), pp. 269–280. DOI: 10.2113/JEEG18.4.269.

P 8.1

Sustainable erosion control usin Wood Wool

Christian Ambrosi¹, Cristian Scapozza¹, Imad Lifa², Michel Heimgartner², Alessio Spataro¹ & Massimiliano Cannata¹

¹ *Istituto scienze della Terra (IST), Scuola Universitaria Professionale della Svizzera Italiana (SUPSI), Campus Trevano, CH-6952 Canobbio ([name.surname]@supsi.ch)*

² *Institut für Bauen im alpinen Raum (IBAR), Hochschule für Technik und Wirtschaft Chur (HTW), Pulvermühlestrasse 80, CH-7000 Chur (Imad.Lifa@htwchur.ch)*

Several shallow landslides occurred in the Southern Swiss Alps in November 2014. Shallow landslides were triggered by heavy rainfalls on steep slopes in loose sediments. Most of these phenomena lead to a change in the slope stability causing a series of instabilities such as surface erosion. In particular, steep slopes hardly find a natural equilibrium state moving toward a situation of progressive degradation of surface stability.

Vegetation is one of the main systems for natural protection against erosion by stabilizing the slopes and adjusting their water content. Once the roots of plant and grass are grown up, the soil erosion will be stopped.

This process can be supported by the use of the Wood Wool for the production of erosion control mats. Protection against erosion by Wood Wool is a method known and widely used in the United States. At the opposite, in Switzerland the Wood Wool has been replaced in the last decades either by synthetic materials or by imported natural fibers as coconut and jute. The use of wood has the advantage of (i) re-employ a natural material already present in the area, (ii) to be 100% biodegradable and (iii) to support local economies in mountains regions.

Focus of this applied research, funded by the Swiss Commission for Technology and Innovation (KTI/CTI), is to evaluate the conditions to re-introduce the Wood Wool as a slope stability controller. Four different kind of Wood Wool are tested in the framework of this project. We specified the material characteristics that best fit to different geotechnical characteristics of the areas such as: Wood Wool type (different percentage of diverse wood as pine, beech, fir or ash), supporting material (polypropylene or jute) and the choice of the type of local plants for sowing on the Wood Wool mats. These properties were quantitatively evaluated by the use of a Riegl VZ-400 Terrestrial Laser Scanner (TSL), able to quantify the development of the vegetative state on different types of Wood Wool and to quantify also modification of the ground surface for evaluating erosion control.



Figure 1. Installation of the Wood Wool mats on a test site in Gramiröi (Val Leventina, Canton Ticino).

P 8.2

Distribution of lead in Khuzestan plain sediments, Iran

Javad darvishi khatooni¹

¹ Geological survey of Iran (Javaddarvishi2007@yahoo.com)

Iran is located in the west of Asia, and in the arid and semi-arid belts (Hojati et al. 2011). The annual rainfall ranges from 224 to 275 mm, and the central Iran has remarkable dust emission sources, which are one of the most prominent dust sources in the dust belt. The southern parts of Khuzestan province, especially the low elevations and coastal areas, experience tropical weather. The annual mean of maximum temperature in the warm period is about 50 °C (in July) and the minimum winter temperature is 9 °C (in February).

In this research 71 surface sediment samples were taken for sedimentology and sedimentary geochemistry investigation. These samples were analysed in the geological survey of Iran laboratory. Sieve analyses, laser analyses, calcimetry, mineralogy (XRD), morphoscopy, morphometry and chemical analyses (ICP & AAS) have been done. The Results show that silt and clay size sediments are dominated that have suitable potential to wide distance and long time transportation. Sediments type in Khozestan plain is Slightly gravelly sandy mud, Slightly gravelly mud, Gravelly muddy sand, Slightly gravelly sand, Sandy mud (Darvishi khatooni, 2014). The origin of some anomalies lead, Can be of some chemicals and non- chemical in war or industrial waste in the area (alcohol and oil and petroleum contamination) or agricultural pesticides (sugar cane companies, etc.).

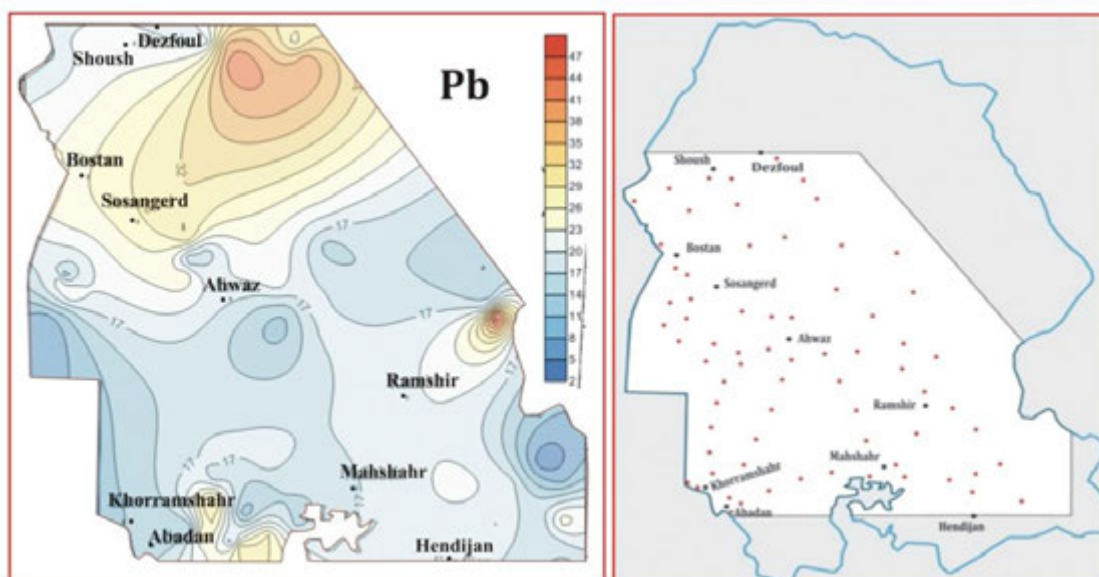


Figure 1. Distribution of lead in Khuzestan plain sediments

REFERENCES

- Darvishi khatooni, J. 2014: Study wind sediments Khuzestan province. Geological survey of Iran. Internal report.
 Hojati S, Khademi H, Faz Cano A, Landi A (2011) Characteristics of dust deposited along a transect between central Iran and the Zagros Mountains. Catena J 88:27–36.

P 8.3

Morphology and emplacement processes of a large carbonate rockslide – rock avalanche (Tschirgant, Austria)

Anja Dufresne¹, Christoph Prager² & Annette S. Bösmeier³

¹ *Geologie, University of Freiburg, Albertstr. 23b, D-79104 Freiburg (anja.dufresne@geologie.uni-freiburg.de)*

² *alpS GmbH, Grabenweg 68, A-6020 Innsbruck*

³ *Geographie, University of Freiburg, Werthmannstr. 4, D-79098 Freiburg*

Catastrophic rockslope failure from the southeast side of the Tschirgant ridge (Tyrol, Austria) 3-3.3 ka ago (Ostermann and Prager, 2014) resulted in a deposit 200-250 Mm³ in volume spread over an area of at least 9.8 km² (Patzelt, 2012). Two different emplacement modes of rock sliding and spreading can still be identified morphologically in the deposit. Longitudinal ridge axes on the central rockslide deposit point straight back to the source scarp, thus these sliding blocks travelled along the main rockslope failure direction without being affected by runout path topography. The orientations of longitudinal ridges of the rock avalanche part, on the other hand, evidence motion change to radial spreading. These ridges are present exclusively in competent lime- and dolostones (Wetterstein Fm), whereas weaker siliciclastic-carbonate beds (Raibl Group) cannot form high ridges. Yet, offset clayshale marker beds document lobe formation also in Raibl deposits. Extensive field mapping shows that the source stratigraphy was preserved in that the initial sub-vertical configuration of lithological units in the Tschirgant mountain ridge was translated into a radial, sub-horizontal geometry of broken, highly fragmented, spread, and sheared granular mass during rock avalanche deposition. These morphological signatures plus sedimentological characteristics provide valuable insights into the emplacement dynamics of large rockslides and rock avalanches.

REFERENCES

- Ostermann, M. & Prager, C. 2014: Major Holocene rock slope failures in the Upper Inn- and Ötz valley region (Tyrol, Austria). In: From the Foreland to the Central Alps, Kerschner, H., Krainer, K. & Spötl, C. (eds), DEUQUA Excursions, 116-126.
- Patzelt, G. 2012. The rock avalanches of Tschirgant and Haiming (Upper Inn Valley, Tyrol, Austria), comment on the map supply. *Jahrbuch der Geologischen Bundesanstalt* 152(1-4), 13-24.

P 8.4

Karst Process in Bistoon of Kermanshah Province

Tahere Jalilian¹, Javad Darvishi khatooni²

¹ Department of Geomorphology, University of shahid Beheshti(tg_7434@yahoo.com)

² Geological survey of Iran

In mountainous massif of Parav - Bistoun, Various forms of the karst landscapes such as karrens, uvalas, dolines, caves and soon have emerged due to specific lithology and tectonic. The Depressions are interesting because of great influence of fractures on them and their dimensions. Thus, in this study, morphotectonic consideration of depressions an important part of karstic studies has been marked.

The area has various depressions with different dimentions. The biggest depression has depth of 115 m and diameter of 180 m. It shows azimuth angle of 30 degrees. Other karstic forms of area are caves, which recognized as the deepest cave in the whole Middle East and have depth and length of about 751 and 1361m, respectively(Jafarbeyglou etal, 2011). Prav-Bisetoon massif composed of limestone and is located in over thrusted Zagros (high-broken), west of Iran at Kermanshah province. The main form is Karsts in sinkholes which the formation and development is affected by thrust, Faults and fractures in this region. The land form provides appropriate conditions for feeding and development of ground water resources and has influenced region hydrogeology. Topographic maps, Digital elevation model, ETM+ and LISS (III) images and field work were used. The sinkholes were identified accordingon field observations, algorithm of topographic maps, Radar images, thermal Indicatorsand reflection images. Sensitivity analyses of sinkholes have done based on field work, Standardization of variables, Preparation itstable locations Matching and statistical methods. The Results were shown, 183 sinkholes and their Regression models of Sensitivity to collapse. An assessment method was done on location analysis of sinkholes due to lineaments, faults, rivers channel and statistical tests(FIG 1).

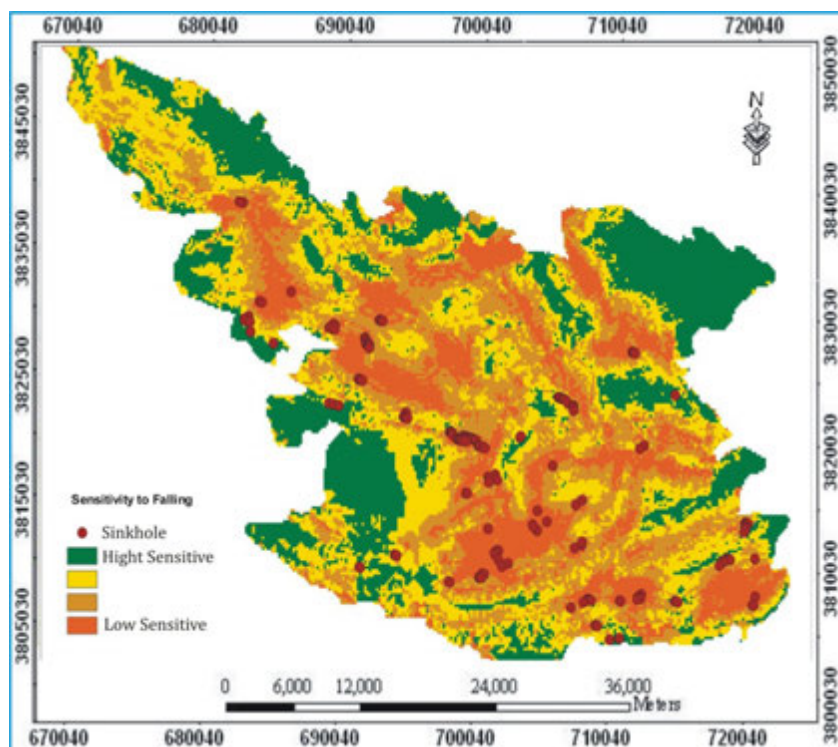


Figure 1. Sensitivity to Falling in Prav-Bisetoon

REFERENCES

- Ford D. and Williams P. 2007: Karst Hydrogeology and Geomorphology, John Wiley & Sons Ltd1-562.
 Jafarbeyglou m. Moghimi E. Safari F. 2011: Evaluating morphotectonic karst sinks in Parav - Bistoun mass using DEM, Geography and Environmental lanning Journal 22th. Year, vol. 44, No.4, Winter 2012.

P 8.5

Modelling Carbon Erosion in the Great Karoo Region, South Africa

Juliane Krenz¹, Philip Greenwood¹, Brigitte Kuhn¹, Goswin Heckrath², Ian Foster³, John Boardman⁴, Mike Meadows⁵, Nikolaus Kuhn¹

¹ *Department of Environmental Sciences, Physiogeographie and Environmental Change, University of Basel, Klingelbergstrasse 27, 4056 Basel, Switzerland (juliane.krenz@unibas.ch)*

² *Department of Agroecology, Aarhus University, Blichers Allé 20, Postboks 50, 8830 Tjele, Denmark*

³ *School of Science and Technology, University of Northampton, Newton Building, NN2 6JD Northampton, United Kingdom*

⁴ *Environmental Change Institute, Oxford University Centre for the Environment, South Parks Road, OX1 3QY Oxford, United Kingdom*

⁵ *Department of Environmental and Geographical Sciences, University of Cape Town, Private Bag X3, Rondebosch 7701, South Africa*

Work undertaken in the seasonally arid upland areas of the Great Karoo region of South Africa has established a link between land degradation and overgrazing that began in the second half of the 18th century when European farmers first settled the area. Ongoing land use change and shifting rainfall patterns resulted in the development of badlands on foot slopes of upland areas and gully systems in valley bottoms. As a consequence of agricultural intensification and overgrazing accompanied by a higher water demand many small reservoirs were constructed, most of which are now filled with sediment. The deposited material serves as an environmental archive to analyse land use changes during the last 100 years, with a special focus on erosion and deposition of soil-associated carbon (C). It is assumed that erosion causes an initial flush of carbon rich soil which was subsequently stored and buried off-site, but the net-effect of erosive processes on carbon dioxide emissions is still unknown. In this project preliminary results, from an investigation to determine whether land degradation in the Karoo has resulted in a shift from a net sink of C to a net source of C, are presented. Firstly, surface cover was mapped via drone imagery and ground-truthing to assess the extent of erosion. Drone imagery serves to create a high-resolution elevation model as a base for detailed erosion modelling using spatially distributed deposition and erosion models (WaTEM and/or RUSLE Modul IDRISI Selva) in later stages. Secondly, sediment deposits from silted-up reservoirs were analysed for varying physicochemical parameters to analyse and reconstruct erosion and deposition. Total Carbon (TC) content was recorded and the sharp decrease in TC content with decreasing depth suggests that land degradation during and after post-European settlement probably led to accelerated erosion of the relatively fertile surface soils, and this presumably resulted in the rapid in-filling of reservoirs with carbon-rich surface material.

P 8.6

Coupling aerial imagery, hydropower intakes data and climatic indicators to investigate the changing climate effects on geomorphic dynamics of high mountain environments

Natan Micheletti¹, Stuart N. Lane¹ & Christophe Lambiel¹

¹ *Institute of Earth Surface Dynamics, University of Lausanne, Geopolis UNIL Mouline, CH-1015 Lausanne (natan.micheletti@unil.ch)*

With the general consensus that has been reached about the inevitability of current climate warming, increased attention is now being given to the consequences of such change. Alpine landscapes are likely to be particularly sensitive to climate change, because of: (1) the vulnerability of permafrost and glacial and nival processes to changes in atmospheric temperature and precipitation; (2) their heritage in terms of large amounts of potentially mobile sediment; and (3) the steep slopes that may sustain sediment mobilization. To observe the impact of climate change upon high mountain areas, two unique datasets available from the 1960s to present were derived for a number of adjacent basins in the south-western Swiss Alps: (1) archival aerial images processed to generate high precision digital elevation models (DEMs) and corrected ortho-photograph, and so identify significant changes in elevation and surface displacement velocities at the decadal scale; and (2) long term records of sediment export based upon the flushing of sediment from hydropower intakes. These findings were interpreted in a climatic context by extrapolation or modelling using data from meteorological stations near the region of interest and in a geomorphic context using a geomorphological map. The results show distinct geomorphic responses to cold and warm period and to changes in rates of precipitation and snow cover and favour the hypothesis that some elements of the landscape are sensitive to climate change. Further, whilst changes in atmospheric temperature remain a key controlling factor upon glacial and periglacial dynamics, precipitation and snow cover prove critical in controlling rock glacier behaviour and can induce acceleration of surface displacements even under cold atmospheric conditions. Nevertheless, coupling these findings with hydropower intakes data unveils strong evidence of transport capacity limitation in these systems, which translates in impeded propagation of the climate change signal throughout the landscape. Effectively, the level of geomorphic activity within basins is orders of magnitude higher than the volume of sediment exported from the basins. Hence, despite climatically-driven enhanced sediment production within these basins, signs of sensitivity to climate change generally remain predominantly confined because of the impeded contribution of sensitive elements to the drainage system.

P 8.7

Ehenge: marginalized soil with high water use efficiency

Brice Prudat¹, Lena Bloemertz¹ and Nikolaus J. Kuhn¹

¹ *Physical Geography and Environmental Change, University of Basel, Klingelbergstrasse 27, CH-4056 Basel (brice.prudat@unibas.ch)*

Farmers of North-Central Namibia classify local soils mainly based on hydraulic characteristics and production potential. In that context, Ehenge is a common soil type. These (eutric protoargic) Arenosols are nutrient-poor with loose sand layers (Ap, B, E) overlying thin duripans (Bt, Bg) that lie at several decimetres of depth. Despite their low nutrient content, the ehenge soils are usually used for cereal production because they sustain the growth of crops for longer dry periods than some more nutrient-rich soils. This characteristic is attributed to the combination of the sand texture and the duripan, generating rapid infiltration, but protection from evaporation and drainage from the root zone of the pearl millet. Our objective is to calibrate a model to calculate plant water availability in this soil over the growing season in order to evaluate the impact of climate change on agricultural potential of these soils. From March to June 2014, we recorded soil water content data every minute at different depth (5, 25, 45 and 55 cm) and rainfall amount.

The new model will help to anticipate and alleviate the effect of climate change on agricultural potential of these soils. The presence of duripan is commonly considered to be a limiting factor for agricultural development but our results on the hydrology of the ehenge demonstrate that this soil has a large potential especially if rainfall get more irregularly distributed in coming years.

P 8.8

How much sediment is stored in the Rhone delta, canyon and fan system (Lake Geneva, Switzerland/France) since 1889?

Tiago Adrião Silva^{1,3}, Stéphanie Girardclos^{2,3} & Jean-Luc Loizeau^{1,3}

¹ *Institute F.-A. Forel, University of Geneva (Tiago.Adriao@unige.ch);*

² *Section of Earth and Environmental Sciences, Faculty of Sciences, University of Geneva;*

³ *Institute for Environmental Sciences, University of Geneva.*

The Rhone River sublacustrine delta was first described in 1892 (Forel 1892) through the analysis of bathymetric data collected by Swiss and French engineers in 1886/89. In 2013/14, a multibeam campaign was carried out and for the first time since 1889 a new high resolution image of the whole lake bed was produced. Comparison between these datasets allows a qualitative and quantitative assessment of the changes in Lake Geneva bottom morphology in the last 128 years.

To assess the distribution of sedimentation/erosion rates in the lake a comparative study was carried out in a GIS environment between the historical bathymetry and the recent multibeam bathymetric data. A map with the distribution of sediment thickness deposited/eroded in the last 128 years resulted from this comparison and showed a maximum deposition of +52m in the proximal delta and a maximum erosion of -27m in the active sublacustrine canyon bed. A more detailed study was undertaken in a selected area in the eastern part of the lake and sediment thickness was recalculated to sedimentation rates. The map confirms the presence of three high sedimentation rate zones that had already been hypothesized by previous authors (Giovannoli 1990; Loizeau 1991) and adds further data to their morphology and exact sedimentation pattern.

In proximity to the Rhone River mouth a high sedimentation zone 1800m wide and 3400m long is observed and interpreted as resulting from interflows and overflows from the Rhone discharge into the lake; a second zone occupies two 200m wide areas around the levees on each side of the main canyon for approximately 5km. These zones are interpreted as overspill deposits that occur during large underflows and turbiditic currents flowing through the canyon; a third fan-shaped distal zone occurs at the end of the main canyon, at depths >290m. This fan-shaped zone has an area of 11km² and seems to result from sediment transported by underflows coming from the Rhone River that bypass the proximal areas of the lake through the main sublacustrine canyon. In our study area these three zones of high sedimentation rates comprise 23% of the surface and account for 60% of the total sediment accumulated there in the last 128 years.

Overall, our results show that during the last century 3.9*10⁸ tons of sediment have been deposited in the studied area, corresponding to an average input of 3.1*10⁶ tons per year. This results seems to be in fair agreement with data from previous studies on the sediment supply from the Rhone River, which is the main sediment source of the lake and specifically of our study area (Loizeau and Dominik, 2000).

Further work will focus on the correlation of 25 sediment cores collected in 2014/15 in order to build a detailed chronological framework for the past ca. 100 years necessary to reconstruct and characterize in detail the sediment fluxes coming from the Rhone River catchment upstream Lake Geneva. This research project is developed under the scope of the Sedfate project (SNF nr. 147689) which aims at the quantification of the impact of anthropogenic activities in the last ca. 100 years on the erosion and sediment transfer in the Rhone River catchment down to Lake Geneva.

REFERENCES

- Forel, F.-A., 1892. *Le Léman* (Tome 1). Ed. Rouge, Lausanne (Switzerland).
- Giovannoli, F., 1990. Horizontal transport and sedimentation by interflows and turbidity currents in Lake Geneva, in: Tilzer, M.M., Serruya, C. (Eds.), *Large lakes: ecological structure and function*. Springer-Verlag, Berlin, pp. 175-195.
- Loizeau, J.-L., 1991. *La sédimentation récente dans le delta du Rhône, Léman: processus et évolution*, unpublished PhD thesis. Institut Forel, Faculté des Sciences. Université de Genève, Genève, p. 209.
- Loizeau, J.-L., Dominik, J., 2000. Evolution of the Upper Rhone River discharge and suspended sediment load during the last 80 years and some implications for Lake Geneva. *Aquatic Sciences*, 62, 54-67.

P 8.9**Orographic precipitations and landscape evolution in Basse Terre Island, Guadeloupe archipelago (Lesser Antilles Arc)**

Pierre G. Valla¹, Eric Lajeunesse², Romain Delunel³, Eric Gayer², Pascal Allemand⁴ & Christophe Delacourt⁵

¹ *Institute of Earth Surface Dynamics, University of Lausanne, CH-1015 Lausanne (pierre.valla@unil.ch)*

² *Institut de Physique du Globe, Université Sorbonne Paris Cité, F-75005 Paris*

³ *Institute of Geological Sciences, University of Bern, CH-3012 Bern*

⁴ *Laboratoire de Géologie de Lyon Terre-Planète-Environnement, Université de Lyon, F-69100*

⁵ *Institut Universitaire Européen de la Mer, Université de Bretagne Occidentale, F-29280 Plouzané*

Understanding the respective role of endogenic and exogenic processes in the Earth's Surface evolution remains a scientific challenge. This is in part due to the intrinsic differences in spatial and temporal scales at which they operate. Tropical volcanic islands offer interesting natural environments to investigate such interactions. They are small-scale settings compared to larger-scale mountain belts, with relative spatially uniform basaltic/andesitic lithologies. They are also affected by a well-defined climatic forcing with stable tropical humid climate. Finally, detailed information on the volcanic activity exists, with precise and independent knowledge of both the timing and spatial extent of eruptive events (i.e. dating of lava flow and topographic reconstruction of the initial volcanic edifice).

Here, we study the Basse Terre Island (Guadeloupe archipelago, Lesser Antilles Arc). It is composed of four successive andesitic edifices (Samper et al., 2007) that reveal the progressive southward migration of the volcanic activity from ~3 Ma until present-day. This unique setting offers a tight temporal framework for the quantification of erosional processes and landscape evolution after cessation of the volcanism. Tropical humid climate is characterized by eastern trade-winds and strong orographic precipitations (Gaillardet et al., 2011) and storm events (Allemand et al., 2014). We present morphometric analysis conducted on high-resolution DEMs (25- and 5-m scale) that we combine with reconstruction of the volcanic activity from the literature (e.g. Samper et al., 2007) and modern precipitation data (source MeteoFrance). Our preliminary results show that topographic relief decreases with edifice age (erosional destruction) but more importantly that the precipitation patterns closely follow the island topography. This spatial correlation illustrates the co-evolution of island topography and orographic effect. Detailed analysis of the drainage network and river profiles will exemplify how erosional processes closely interact in the long-term island evolution.

REFERENCES

- Allemand, P., Delacourt, C., Lajeunesse, E., Devauchelle, O., & Beauducel, F. 2014: Erosive effects of the storm Helena (1963) on Basse Terre island (Guadeloupe - Lesser Antilles Arc). *Geomorphology*, 206, 79-86.
- Gaillardet, J., Rad, S., Louvat, P., Rivé, K., Gorge, C., Allègre, C.J., & Lajeunesse, E. 2011: Orography-driven chemical denudation in the Lesser Antilles: evidence for a new feedback mechanism stabilizing atmospheric CO₂. *American Journal of Science*, 311, 851-894.
- Samper, A., Quidelleur, X., Lahitte, P., and Mollex, D. 2007: Timing of effusive volcanism and collapse events within an oceanic arc island: Basse-Terre, Guadeloupe archipelago (Lesser Antilles Arc). *Earth and Planetary Science Letters*, 258, 175-191.

P 8.10

Dynamic reorganisation of Alpine river catchments analysed with χ -mapping

Sascha Winterberg¹, Sean D. Willett²

¹ *Geologisch Institut, Departement Erdwissenschaften, ETH Zürich, Sonneggstrasse 5, CH-8092 Zürich (sascha.winterberg@erdw.ethz.ch)*

² *Geologisch Institut, Departement Erdwissenschaften, ETH Zürich, Sonneggstrasse 5, CH-8092 Zürich*

The drainage network in the Alps is an inherited network from the combined forces of erosion and alpine tectonics that created differential uplift. River courses are therefore subject of ongoing evolution. This causes significant changes in erosion and deposition patterns that induce a feedback on the geodynamics itself. Migration of the drainage divide and capture of other river catchments leads to a positive feedback and forms dominating river systems.

We analysed the topography of the Alps using the high resolution SRTM 1 arc second data. A steady state river channel proxy was used to calculate at each point on the river network an equilibrium elevation (Willett et al., 2014). The according χ -value integrates drainage area below each point to a common baselevel (Perron and Royden, 2013). Comparing χ -values reveals the current state of the reorganisation of the river network.

Our calculation revealed that most of the observed drainage reorganisations are currently going on in the Danube catchment. It loses catchment area against the Rhine in the west and Adda/Adige in the south. Rivers draining to the tectonic external side to the north or northwest respectively loose catchment to rivers draining to the southern tectonic internal side. The western Alps that show a recent rapid uplift from thermochronometric ages (Fox et al., 2015) show only minor river course reorganisation.

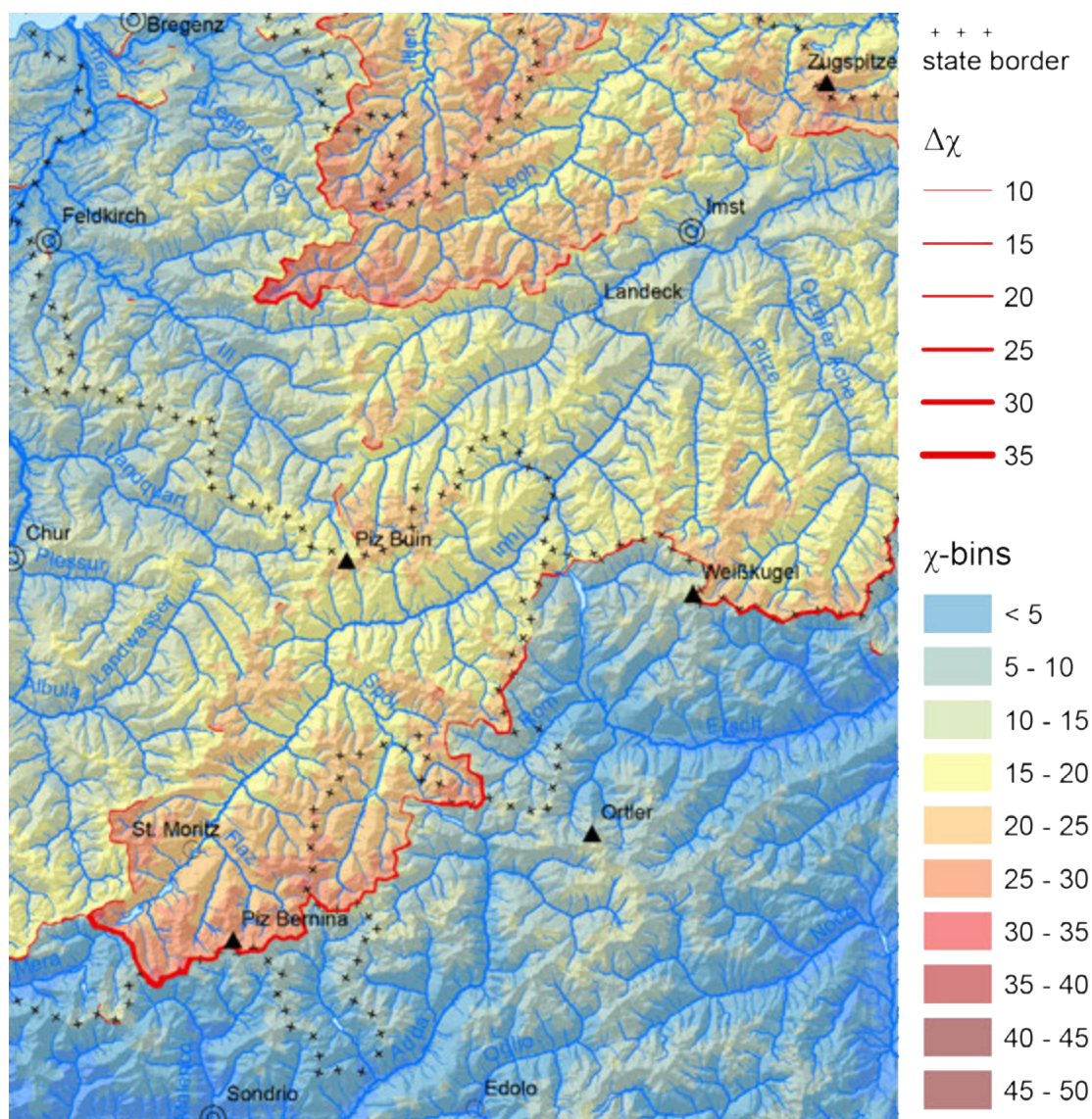


Figure 1. Extract of the Arlberg Engadine region from the Alpine χ -map 1:1'000'000. Baselevel for the calculation is 250 m a.s.l. and the data source is the SRTM 1" from USGS. Threshold area for rivers is 1 km². To better visualize the χ -values the catchments are coloured respective to χ of the respective river.

The unsteady drainage divides of the upper Engadine and the Lechtal is marked by the high $\Delta\chi$.

REFERENCES

- Fox, M., Herman, F., Kissling, E., and Willett, S. D., 2015, Rapid exhumation in the Western Alps driven by slab detachment and glacial erosion: *Geology*, p. G36411. 36411.
- Perron, J. T., and Royden, L., 2013, An integral approach to bedrock river profile analysis: *Earth Surface Processes and Landforms*, v. 38, no. 6, p. 570-576.
- Willett, S. D., McCoy, S. W., Perron, J. T., Goren, L., and Chen, C.-Y., 2014, Dynamic reorganization of river basins: *Science*, v. 343, no. 6175, p. 1248765.

9. Quaternary environments: landscapes, climate, ecosystems, human activity during the past 2.6 million years

Philippe Rentzel, Christine Pümpin

Swiss Society for Quaternary Research (CH-QUAT)

TALKS:

- 9.1 Brönnimann D., Rentzel P., Sedlmeier J., Wick L., Marti R.: Late Glacial and early Holocene soil formation and morphogenetic processes in Dittingen – Schachletetal (canton Basle-Land, Switzerland)
- 9.2 Diaz N., Dietrich F., King G., Valla P., Sebag D., Herman F., Verrecchia E.P.: Reconstructing 20 ka of history using multi-dating on pedogenic carbonate nodules
- 9.3 Grischott R., Kober F., Hippe K., Lupker M., Ivy-Ochs S., Hajdas I., Christl M.: Climate control on alpine denudation in the Holocene – Clues from two converse datasets of paleo-CWDR
- 9.4 Kuhlemann, J., Ivy-Ochs, S., Anselmetti, F., Glotzbach, C., Rahn, M.: Tracing a glacial 2.5 Ma profile from Corsica
- 9.5 Litty C., Schlunegger F.: Controls on pebbles size and shape in streams of the Swiss Alps
- 9.6 Rodrigues L., Lombardo U., Veit H.: Linking soil properties and pre-Columbian agricultural strategies in the Bolivian Lowlands
- 9.7 Steiner B., Ismail-Meyer K., Heitz-Weniger A., Gross E., Akeret Ö., Antolin F., Schären G., Jacomet S., Rentzel P.: Transdisciplinary study of waterlogged archaeological deposits: the example of the lakeshore settlement of Zug-Riedmatt (Switzerland)
- 9.8 Thew N., Furrer H.: A new deposit dating from the Eemian Interglacial at Niederweningen (Zürich) and the associated mollusc faunas
- 9.9 Vattioni S., Hajdas I., Strasser M., Grischott R., Sormaz T.: Lake level reconstruction of Lake Sils, Engadine valley
- 9.10 Vogel H., Russell J.M., Bijaksana S., Crowe S., Fowle D., Haffner D., King J., Marwoto R., Melles M., von Rintelen T., Stevenson J., Watkinson I. & the TDP science team: The Lake Towuti Drilling Project: A new, ~1 million year record of Quaternary climate and ecosystem dynamics from the Indo-Pacific
- 9.11 Wirsig C., Ivy-Ochs S., Reitner J., Christl M., Vockenhuber C., Bichler M., Reindl M.: Quantifying subglacial erosion rates at Goldbergkees, Hohe Tauern (Austria) with cosmogenic ^{10}Be and ^{36}Cl
- 9.12 Wuscher P., Koehler H., Moine O., Bachellerie F., Basoge F., Griselin S., Schneider N., Boës E., Diemer S., Sévêque N.: Palaeolithic in the plaine of Alsace and in the Vosgian foreland: state of art, taphonomy and landscape-use archaeology
- 9.13 Ziehmer M.M., Nicolussi K., Schlüchter C., Leuenberger M.: Novel Insights from Multi-Millennial Tree Ring Isotope Records of the Early and Mid-Holocene

POSTERS:

- P 9.1 Kalbe, J., Pümpin, C., Jagher, R.: Nadaouiye Aïn Askar – Mid-Pleistocene Palaeocology in a Spring fed Wetland of El Kowm Oasis in the Central Syrian Desert.
- P 9.2 Wegmüller F., Koehler H., Pümpin C., Wuscher P., Sévêque N.: New results of excavations at the Middle Palaeolithic site of Mutzig-Rain (Alsace, France)
- P 9.3 Antolín F., Balbo A., Colonese A., Huchet J.-B., López O., Jacomet S., Manganelli G., Palomo A., Piqué R., Terradas X., Zanchetta G.: An interdisciplinary approach to site formation processes through profile sampling at the Neolithic lakeshore settlement of La Draga (Banyoles, Spain)
- P 9.4 Claude A., Akçar N., Ivy-Ochs S., Schlunegger F., Kubik P.W., Christl M., Vockenhuber C., Rahn M., Dehnert A., Schlüchter C.: Long-term bedrock incision rates in the northern Swiss Alpine Foreland inferred from reconstructed Deckenschotter chronologies
- P 9.5 Reber R., Schlunegger F.: Confluence area of the Aare and the Valais Paleoglaciers Lobes
- P 9.6 Märki L., Cogez A., Herman F.: Glacial erosion and dust transport to the Southern Ocean : coupling between erosion on climate
- P 9.7 Hippe K., Fontana A., Hajdas I., Ivy-Ochs, I.: Reconstructing Alpine glacier activity during 50-20 ka BP by high-resolution radiocarbon dating of the Cormor alluvial megafan (Tagliamento glacier, NE Italy)
- P 9.8 Luetscher M., Ivy-Ochs S., Hof M.: Reconstructing the last deglaciation at Sieben Hengste, Switzerland
- P 9.9 Boxleitner M., Maisch M., Walthard P., Ivy Ochs S., Brandova D., Egli M.: Lateglacial and Holocene glacier development and landscape evolution in Meiental, Uri (CH)
- P 9.10 Wüthrich L., Hepp J., Schäfer I.K., Lutz S., Sirocko F., Zech M., Zech R.: A Late Glacial / Early Holocene climate reconstruction using stable isotopes in biomarkers from the Gemündener Maar, Germany
- P 9.11 Ivy-Ochs S., Martin S., Campedel P., Viganò A., Alberti S., Rigo M., Vockenhuber C.: Age and geomorphology of the Marocche (Trentino, Italy)
- P 9.12 Kronig O., Ivy Ochs S., Hajdas I., Christl M., Schlüchter C.: Late Holocene evolution of the Triftjégletscher constrained with ¹⁰Be exposure and radiocarbon dating
- P 9.13 Aksay S., Ivy-Ochs S., Hippe K., Grämiger L., Vockenhuber C.: The geomorphological evolution of a landscape in a tectonically active region: The Sennwald Landslide
- P 9.14 Mozafari Amiri N., Sümer Ö., Tikhomirov D., Özkaymak Ç., Uzel B., Ivy-Ochs S., Vockenhuber Ch., Sözbilir H., Akçar N.: Holocene destructive seismic periods in Western Anatolia: pace tracking beyond historical data
- P 9.15 Strupler M., Anselmetti F.S., Hilbe M., Fleischmann T., Kopf A.J., Strasser M.: Geotechnical properties of submerged slopes in Lake Zurich and the influence of their spatial variability on slope stability
- P 9.16 Darvishi khatooni J.: Reconstruction of sedimentary environments, climate and water level change of Urmia lake in the Holocene
- P 9.17 Haghipour N., Eglinton T., McIntyre C., Hunziker D., Darvishi Khatooni J., Mohammadi A.: Paleo-climate and paleo-environment reconstruction based on a high-resolution, multi-proxy record from Lake Urmia (NW Iran)
- P 9.18 Hunziker D., Vasconcelos C.: Paleohydrology, paleoenvironment and biomineralization in Lagoa Pitanguinha, Rio de Janeiro, Brazil
- P 9.19 Haas M., Zech R., Szidat S., Salazar G., Bliedtner M.: Radiocarbon dating of leaf waxes in the Kurtak loess paleosol sequence, Central Siberia
- P 9.20 Schäfer I.K., Schweri L.I., Tananaev N., Zech R.: Leaf wax patterns and compound specific isotope analyses in a permafrost section near Igarka, Northern Siberia
- P 9.21 Ismaylova L.: Scientific-Methodological Approaches Of Revelation Of Landscape-Recreation Potential Of Mountain Geosystems (On example of Southern slopes of the Greater Caucasus)

9.1

Late Glacial and early Holocene soil formation and morphogenetic processes in Dittingen – Schachletetal (canton Basle-Land, Switzerland)

David Brönnimann¹, Philippe Rentzel¹, Jürg Sedlmeier², Lucia Wick¹, Reto Marti²

¹ *Integrative Prehistory and Archaeological Science IPAS, University of Basel, Spalenring 14, 4055 Basel, Switzerland*

² *Kantonsarchäologie Baselland, Amtshausgasse 7, 4410 Liestal, Switzerland*

In 1996, well preserved deer bones, antler and some bones of black grouse were found in a filled karst crack (Rentzel et al. 1999). Those animal remains were discovered in the course of an expansion of a limestone quarry in the Jura Mountains near Dittingen (canton Basle-Land, Northwest Switzerland). The site is situated in a gully of a dry valley beneath a loess covered high plain. In the framework of an archaeological excavation, the karst crack filling and overlying sediments (hill-washed loess, soils and colluviums) were documented. Samples for granulometry, chemical analysis, micromorphology and palynology were analysed in order to reconstruct morphogenetic and soil formation processes. The animal remains deriving from the karstic fissure were radiocarbon dated to the early Bølling Interstadial (14'800 to 14'200 cal. BP). In addition the palynological study shows that the overlying gully sediments were deposited between the Younger Dryas and the Middle Ages.

The interdisciplinary investigation of the sediments revealed new insights into early soil formation processes and morphogenetic events in periglacial environments (Brönnimann et al. 2015). The new results clearly show that soil formation started immediately after the permafrost melted in the early Late Glacial. Decalcification and clay illuviation quickly developed in the course of intense vertical water flow through the sediment due to meltwater. As shown in other studies (Guélat 2000) luvisol development took place during the Lateglacial Interstadial (Bølling-Allerød-Interstadial). This means that a rethinking of the widespread idea of extraordinary fertile soils (black earth, Chernozem) at the Neolithic in Northwestern Switzerland (appearance of the first farmers) is needed. New research shows that instead of fertile Chernozem in Early Holocene, deeply decalcified, acid soils are observed, which had to be intensely prepared for agriculture (Brönnimann & Rentzel in prep.).

REFERENCES

- Brönnimann, D. & Rentzel, P. (in prep.): Die Bodenbeschaffenheit zur Zeit des Frühneolithikums. In: Der jungsteinzeitliche Siedlungsplatz Gächlingen-Goldacker. (Altorfer, K., Hartmann, C., Haydon, E.). Beiträge zur Schaffhauser Archäologie.
- Brönnimann, D., Rentzel, P., Sedlmeier, J., Wick, L., 2015: Karstspalte Schachlete: Ein Archiv der spätglazialen und holozänen Landschafts- und Klimageschichte. In: Die letzten Wildbeuter der Eiszeit. Neue Forschungen zum Spätpaläolithikum im Kanton Basel-Landschaft (Sedlmeier, J.). Schriften der Archäologie Baselland 51 (Basel) 210–241.
- Guélat, M., 2000: Approche Micromorphologique. In: Dernier cycle glaciaire et occupations paléolithiques à Alle, Noir Bois (Jura, Suisse) (Aubry, D., Guélat, M., Detrey, J.). Cahier d'archéologie jurassienne 10 (Porrentruy) 61–80.
- Rentzel, P., Sedlmeier, J., Steppan, K., Wick, L., 1999: Die spätglaziale Karstspaltenfüllung im Schachletetal bei Dittingen BL. Archäologie Schweiz 22 (1), 8–12.

9.2

Reconstructing 20 ka of history using multi-dating on pedogenic carbonate nodules

Nathalie Diaz¹, Fabienne Dietrich¹, Georgina King^{1, 2}, Pierre Valla¹, David Sebag³, Frédéric Herman¹
& Eric P. Verrecchia¹

¹ *Institute of Earth Surface Dynamics, University of Lausanne, Switzerland (corresponding author nathalie.diaz@unil.ch)*

² *Institute of Geography, University of Cologne, Germany*

³ *Department of Geosciences and Environment, University of Rouen, France & IRD, Hydrosociences Montpellier, University of Ngaoundéré, Cameroon*

Carbonate nodules associated with clay-rich soils were recently found near Maroua (northern Cameroon). They are located along the granitic watershed of the Mayo Tsanaga (Fig. 1). Clay-rich soils can occur as mima-like mounds or buried sediments. The presence of carbonate accumulation in such geological settings is unexpected and may act as a sink in the continental carbon (C) budget. The mechanism leading to their formation is thus a crucial point of investigation.

We propose that the nodules have a pedogenic origin and are related to vertisolisation processes, possibly inherited from the African Humid Period (AHP). Their present-day geomorphological settings demonstrate their relic-nature, which might result from this paleo-pedogenesis combined with later erosion (Diaz et al., *in review*). However, these assumptions are based on field and microscale observations but lack age constraints. Here we use optically stimulated luminescence dating (OSL) and radiocarbon dating to constrain the proposed environmental evolution chronology of the nodules.

Carbonate nodules are composed of 57±8% of calcite (CaCO₃) and 43±8% of other minerals, mainly quartz, feldspars, phyllosilicates and oxides, resulting in a residual soil fraction. OSL is used to date the trapped K-feldspars to constrain the deposition of the soil parent material, while radiocarbon dating (¹⁴C) of carbon from calcite is used to date carbonate nodule formation.

We show that the soil parent material was deposited between 18 ka and 12 ka BP, during the Bossoumian dry period (20–15 ka BP; Hervieu, 1969) and the earlier and drier stage of the AHP (c.14.8 ka – 11.5 ka BP; e.g. Armitage et al., 2015). The nodules precipitated at the end of the AHP between 7 ka and 5 ka BP. The initiation of vertisolisation was probably effective from 11.5 ka to 5.5 ka BP (the main humid period; e.g. Armitage et al., 2015), because this process requires wet climatic conditions (Diaz et al., *in review*). A gap in OSL ages at the mound surface may be an indication of detrital erosion after the carbonate formation, thus leading to the present-day mima-like mound landscape.

These results provide further support to the proposed scenario for the formation of pedogenic carbonate nodules and landscape evolution. They are the result of complex sedimentary processes related to Late Pleistocene and Holocene climatic changes. This knowledge is essential for our understanding of mechanisms leading to carbonate precipitation in such unfavourable geological settings and to assess their implication in the continental C cycle.

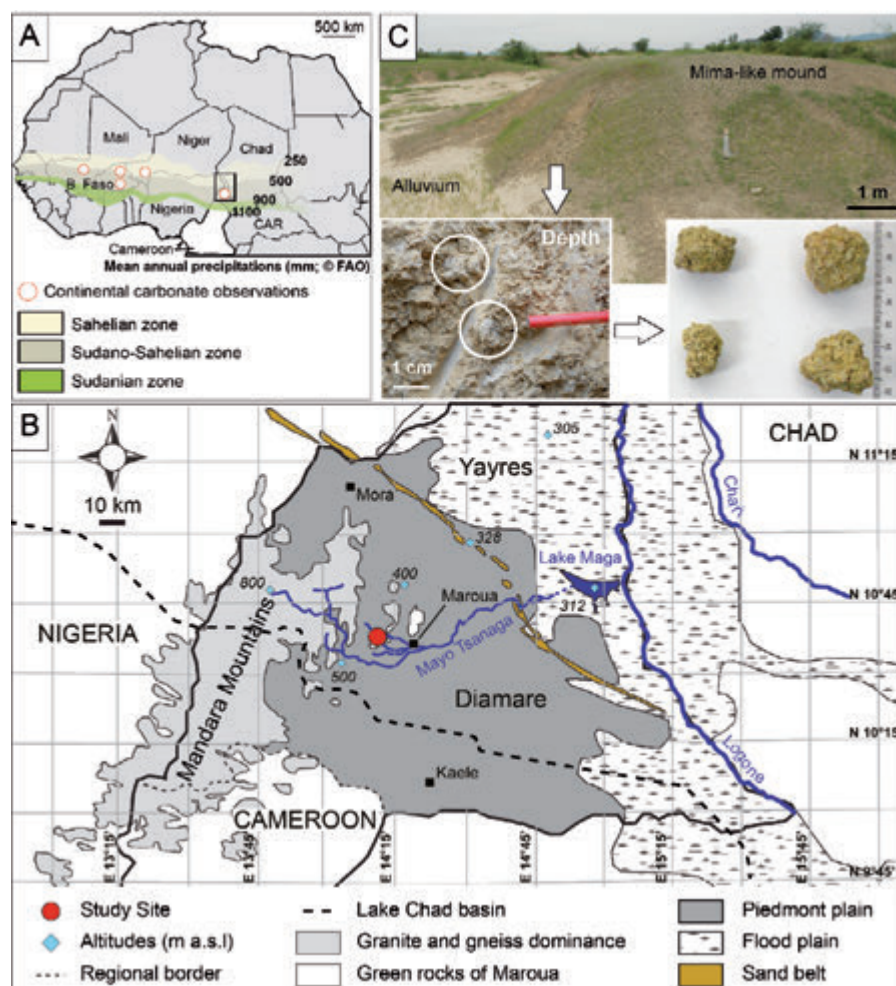


Figure 1. Study site location and illustration. A) Location of continental carbonate observation sites in Africa. B) Settings of the study site located in the Diamare piedmont along the Mayo Tsanaga watershed mainly granitic and gneissic. C) Example of a metric mima-like mound and centimetric carbonate nodules associated.

REFERENCES

- Armitage, S. J., Bristow, C. S., Drake, N. A. 2015: West African monsoon dynamics inferred from abrupt fluctuations of Lake Mega-Chad, PNAS, vol. 112 no. 28, 8543-8548
- DeMenocal, P.B., Ortiz, J., Guilderson, T., Adkins, J., Sarnthein, M., Baker, L., Yarusinsky, M. 2000: Abrupt Onset and Termination of the African Humid Period: Rapid Climate Responses to Gradual Insolation Forcing. *Quaternary Science Reviews* 19, 347-361.
- Diaz, N., Dietrich, F., Cailleau, C., Sebag, D., Ngounou Ngatcha, B. & Verrecchia E. P. 2015: Can Mima-like Mounds be Palaeo-Vertisols (Chad Basin, Far North Region of Cameroon)?, *Geomorphology*, in review.
- Hervieu, J. 1969: Le Quaternaire du Nord-Cameroun Schéma d'Evolution Géomorphologique et Relations avec la Pédogenèse. ORSTOM, Paris, France, 38 pp.

9.3

Climate control on alpine denudation in the Holocene – Clues from two converse datasets of paleo-CWDR

Reto Grischott¹, F. Kober², K. Hippe³, M. Lupker¹, S. Ivy-Ochs³, I. Hajdas³, M. Christl³

¹ *Geologisches Institut, ETH Zurich, Sonneggstrasse 5, CH-8092 Zürich (reto.grischott@erdw.ethz.ch)*

² *NAGRA, Hardstrasse 73, 5430 Wettingen*

³ *Labor für Ionenstrahlphysik, ETH Zürich, Otto-Stern-Weg 5, CH-8093 Zürich*

Beryllium-10 (¹⁰Be) concentrations in active stream sediments have provided useful synoptic views of catchment-wide denudation rates (CWDR). Commonly, inferred denudation rates were assumed to be constant over the characteristic time period e.g. a few thousand years over which they integrate. However, little is known about the variability of denudation and their driving forces on the 10³ to 10⁴ yr timescale caused by climatic variability in alpine catchments. Further, potential bias by glacial sediments on the riverborne nuclide inventory has been argued but not quantified on the Holocene timescale. Here we present a 6 kyr long record of ¹⁰Be paleo-CWDR retrieved from sediment cores and a three year timeseries from the active stream in the Fedoz Valley (Eastern Switzerland). We find a decreasing trend of paleo-CWDR from 0.9 mm/yr at 6 kyr BP to 0.5 mm/yr at present day which correlates with decreasing summer temperatures but not with extreme precipitation records and glacier fluctuations. Frost cracking is proposed to be the dominant geomorphic process driving denudation. Intense frost cracking is occurring in a narrow altitude band below the altitude of the 0°C mean annual air temperature (MAAT, (Hales and Roering, 2007)). The position of this altitude indicates on the hypsometric curve how much of the catchment area is affected by intense frost cracking and thus is responsible for a high sediment production. This mechanism might explain why a higher denudation rate in the Middle Holocene seems to be reasonable because the 0°C-MAAT was significantly higher. Our data are compared with another alpine paleo-CWDR dataset from a lower altitude range in the Austrian Alps which show a lower denudation rate in the Middle Holocene than in the Late Holocene, as has been commonly proposed by soil studies (Giguët-Covex et al., 2011). The apparently contrasting datasets in terms of trends in paleo-CWDR confirm previous findings of a strong dependency of occurrence and intensity of geomorphic processes on the altitude range. Fluctuations of climatic proxies like temperature and precipitation might provoke converse denudational responses in different altitude ranges. Therefore, a detailed assessment of catchment processes and their driving forces is needed to compare different catchments with each other. The results of our study indicate that global predictions of denudation due to climate change might be complex.

REFERENCES

- Giguët-Covex, C., Arnaud, F., Poulenard, J., Disnar, J. R., Delhon, C., Francus, P., David, F., Enters, D., Rey, P. J., and Delannoy, J. J., 2011, Changes in erosion patterns during the Holocene in a currently treeless subalpine catchment inferred from lake sediment geochemistry (Lake Anterne, 2063 m a.s.l., NW French Alps): The role of climate and human activities: *Holocene*, v. 21, no. 4, p. 651-665.
- Hales, T. C., and Roering, J. J., 2007, Climatic controls on frost cracking and implications for the evolution of bedrock landscapes: *Journal of Geophysical Research-Earth Surface*, v. 112, no. F2.

9.4

Tracing a glacial 2.5 Ma profile from Corsica

Joachim Kuhlemann¹, Susan Ivy-Ochs², Flavio Anselmetti³, Christoph Glotzbach⁴ & Meinert Rahn¹

¹ Swiss Federal Nuclear Safety Inspectorate (ENSI), Industriestrasse 19, CH-5600 Brugg (joachim.kuhlemann@ensi.ch)

² Ion Beam Physics, ETH Zürich, Otto-Stern-Weg 5, CH-8093 Zürich

³ Institute of Geol. Sciences, University of Bern, Baltzerstrasse 1+3, CH-3012 Bern

⁴ Institute of Geology, Leibniz Universität, Callinstrasse 30, DE-30167 Hannover

The Mediterranean island of Corsica has undergone multiple phases of glaciation (Kuhlemann et al. in prep.), and these periods of glacial erosion had a distinct influence on the island's morphology, not only in the mountainous central part (Kuhlemann et al. 2008), but also down to its coastline. We here report on preliminary work on what we believe to be one of the rare relics exposing a profile from MIS 100 to MIS 6, which would cover a morphological memory of 2.5 Ma years. The features of this locality are described and compared to many other localities of similar features on Corsica.

Several steep valleys on Corsica show the existence of distinct plateaus in the slope of the valley, formed mainly by granitic rocks. The observed plateaus show characteristic vertical distances which increase with distance from the coast. In the Golo valley (south of Monte Cinto, the tallest mountain on Corsica), staircases along the valley slope were attributed to MIS zones that are thought to cause glacial events on Corsica (Fig. 1). Even though speculative in one locality, these staircases can be observed at several other places (Porto, Rau de Lonca, Vivario-Tattone, Tavaroz-Rizzanese, Rau de Misognu, Niolu), even close to the coastline. They are accompanied by kolk caves, roches moutonnées, potential traces of former glacial striae, eskers (near Calvi-Calenzana), carvets of glacial scours and traces of ice inlets along the coast line (e.g. at the mouths of the Travu, Porto and the Fango rivers).

One old terrace (suggested to be MIS 82) was dated using cosmogenic nuclides, including a minor amount of post-glacial erosion (in the range of few cm). Results will be discussed in the light of a long-term morphological evolution of Corsica.

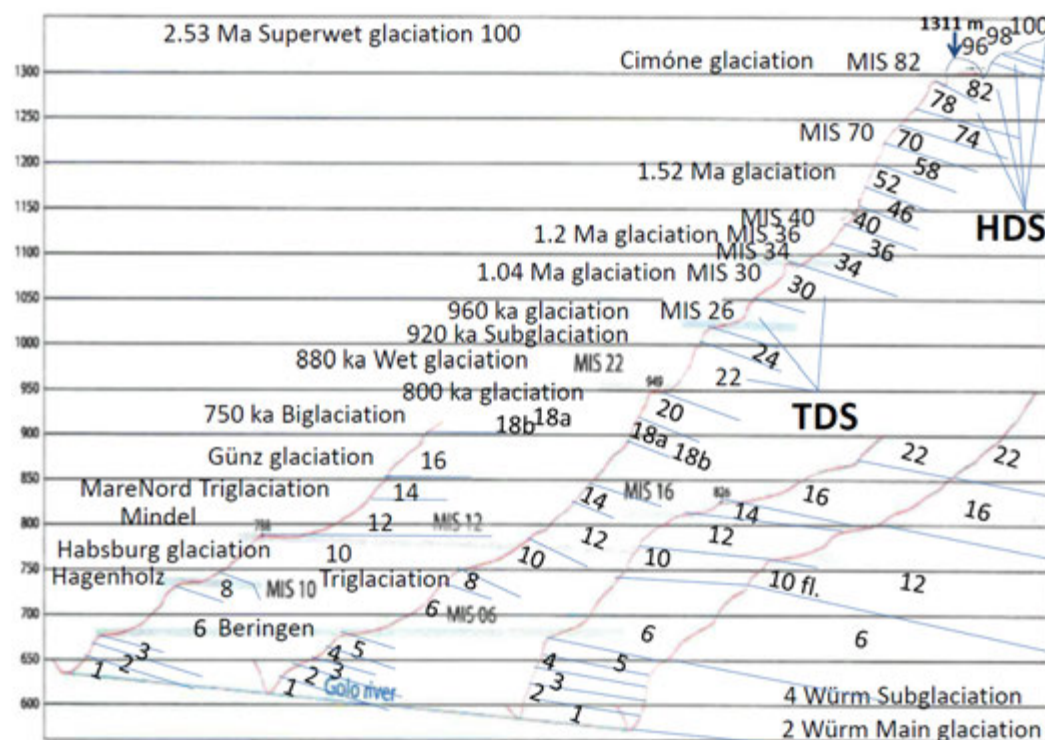


Figure 1. Glacial terraces along valley slopes of the Golo river, with attributed MIS events (including Alpine and proposed names for glacial periods). HDS and TDS mark the assumed period of Höhere and Tiefere Deckenschotter glaciation in the Northern Alps (Kuhlemann & Rahn 2013). The arrow near top right marks the locality of the dated sample.

REFERENCES

- Kuhlemann, J., Rohling, E., Krumrei, I., Ivy-Ochs, S. & Kucera, M. 2008: Regional Synthesis of Mediterranean Atmospheric Circulation During the Last Glacial Maximum. *Science* 321, 1338–1340.
- Kuhlemann, J. & Rahn, M. 2013: Plio-Pleistocene landscape evolution in Northern Switzerland. *Swiss Journal of Geosciences* 106, 451–467.

9.5

Controls on pebbles size and shape in streams of the Swiss Alps

Camille Litty, Fritz Schlunegger

*Institute of Geological Sciences, University of Bern, Baltzerstrasse 1+3, 3012 Bern
(camille.litty@geo.unibe.ch)*

Rivers in the Swiss Alps have been analyzed to determine the relationships between fluvial processes and grain size and shape to emphasize the factors controlling the grain characteristics. 18 bars of gravel-bed rivers have been sampled. At each site the long axis and the intermediate axis of about 500 pebbles have been measured. In addition the morphometric properties of each river basin have been studied. Looking for correlation between grain size and shape and other fluvial properties the study shows that grain size and shape are mainly controlled by the lithology on which the rivers are mainly flowing but not controlled by erosion rate, hydrology or basins metric properties. Deposits of rivers flowing on sedimentary lithology are better sorted and the pebbles are more rounds and have smoother surface than the deposits of rivers flowing on metamorphic lithology. This lack of correlation between grain size and shape and the other studied factors are mainly explained by the fact that the rivers are supply limited. Remarkably for all these different pebbles size and river/basin properties, the ratio of the intermediate axis and the long axis only ranges between 0.63 and 0.72 without any relationships with the lithology. This ratio named the elongation E is not impacted by any of the analyzed river processes in the studied rivers.

9.6

Linking soil properties and pre-Columbian agricultural strategies in the Bolivian Lowlands

Leonor Rodrigues¹, Umberto Lombardo² & Heinz Veit¹

¹ *Institute of Geography, University of Berne, Hallerstrasse 12, CH-3012 Bern (leonor.rodrigues@giub.unibe.ch)*

² *University of Pompeu Fabra, Ramon Trias Fargas 25-27, Mercè Rodoreda ES-08005 Barcelona.*

Our study aims to further our understanding of pre-Columbian agricultural systems in the Llanos de Moxos, Bolivia. The Llanos de Moxos, a seasonally inundated savannah located in the southernmost part of the Amazon basin, is an important area for the study of pre-Columbian human-environment interactions in the region. Increasing research shows that several cultures settled in the LM at different times, building a variety of earthworks (Denevan, 2001; Erickson, 2008; Lombardo et al., 2011; Prümers and Jaimes Betancourt, 2014). One of the most striking examples are the thousands of hectares of pre-Columbian raised fields found in the LM. Raised fields are elevated agricultural earth platforms. Why they were built and how they were managed in the past are a matter of debate. Some authors suggest that raised fields were a form of highly productive agriculture able to sustain large populations (Walker, 2004; Erickson, 2008; Whitney et al., 2014), others believe that fields were built as a mitigation strategy against severe floods during periods of frequent extreme events (Lombardo et al., 2011b; Rodrigues et al., 2014). Different types of raised fields have been studied and excavated at four different places in the Llanos de Moxos in the Bolivian Amazon; the morphology, texture and geochemistry of the soils of these fields and the surrounding area were analysed. Differences in field design have often been associated with cultural and technological diversity. Our results suggest that differences in field shape, height and layout are primarily the result of an adaptation to the local edaphology. By using the technology of raised fields, pre-Columbian people were able to drain and cultivate soils with very different characteristics, making the land suitable for agriculture and possibly different crops. This study also shows that some fields in the Llanos de Moxos were built to prolong the presence of water, allowing an additional cultivation period in the dry season and/or in times of drought.

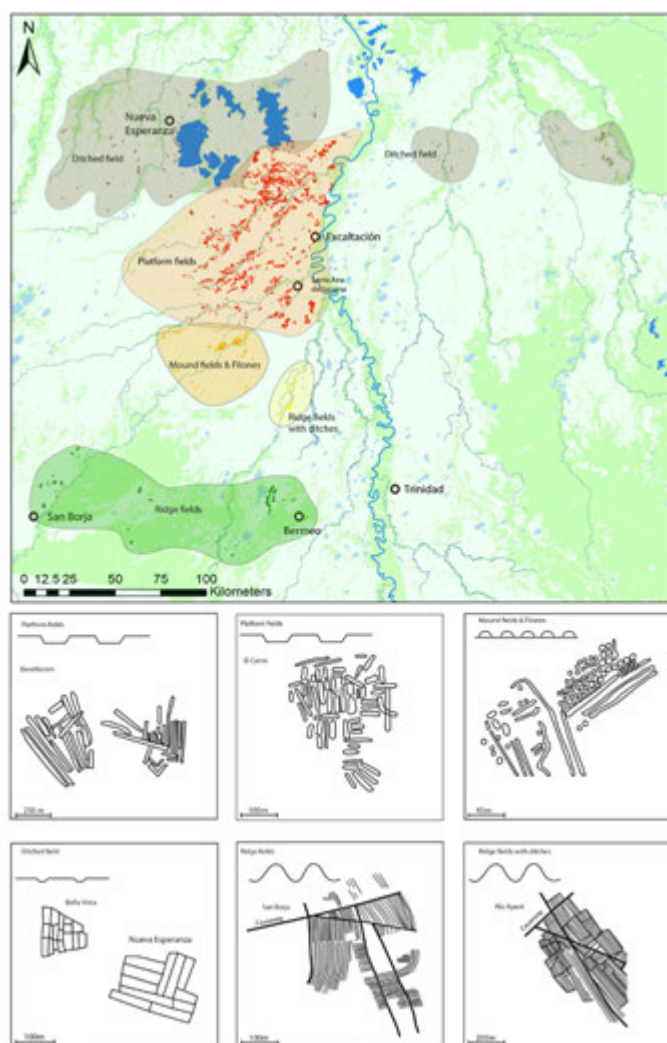


Figure 1. Different types of raised fields in the study area Llanos de Moxos, Bolivia.

REFERENCES

- Denevan, W.M., 2001. Cultivated landscapes of native Amazonia and the Andes. Oxford University Press.
- Erickson, C.L., 2008. Amazonia: the historical ecology of a domesticated landscape. In: , The handbook of South American archaeology. Springer, pp. 157–181.
- Pamir, J., Balen, D. & Herak M. 2002: Origin and geodynamic evolution
- Lombardo, U., Canal-Beeby, E., Veit, H., 2011b. Eco-archaeological regions in the Bolivian Amazon. *Geographica Helvetica* 66 (3), 173–182.
- Lombardo, U., Canal-Beeby, E., Fehr, S., Veit, H., 2011a. Raised fields in the Bolivian Amazonia: a prehistoric green revolution or a flood risk mitigation strategy? *Journal of Archaeological Science* 38 (3), 502–512.
- Prümers, H., Jaimes Betancourt, C., 2014. 100 años de investigación arqueológica en los Llanos de Mojos. *Arqueoantropológicas* (4), 11–53.
- Walker, J.H., 2004. Agricultural Change in the Bolivian Amazon 13. Center for Comparative Arch.
- Whitney, B.S., Dickau, R., Mayle, F.E., Walker, J.H., Soto, J.D., Iriarte, J., 2014. Pre-Columbian raised-field agriculture and land use in the Bolivian Amazon. *Holocene* 24 (2), 231–241.

9.7

Transdisciplinary study of waterlogged archaeological deposits: the example of the lakeshore settlement of Zug-Riedmatt (Switzerland)

Bigna Steiner¹, Kristin Ismail-Meyer¹, Annekathi Heitz-Weniger¹, Eda Gross², Örne Akeret¹, Ferran Antolin¹, Gishan Schären², Stefanie Jacomet¹, Philippe Rentzel¹

¹ *Integrative Prähistorische und Naturwissenschaftliche Archäologie, University of Basel, Spalenring 145, CH-4055 Basel (bigna.steiner@unibas.ch)*

² *Amt für Denkmalpflege und Archäologie, Kanton Zug, Hofstrasse 15, CH-6300 Zug*

At Zug-Riedmatt, excellently preserved waterlogged organic layers were conserved in a depth of 6m, below the deltaic deposits of the river Lorze into lake Zug. The layers have been accumulated during Neolithic settlement activities between 3200 and 3100 cal BC. Even though only a small part of the site was excavated, an exceedingly dense recovery technique was used, ensuring that profile columns could be investigated in detail in the laboratory. Using a microarchaeological methodological approach, 78 profile columns were documented and subsampled following the defined layers in an intensive cooperation between archaeobotany, palynology, micromorphology, archaeozoology, geochemistry and archaeology. All disciplines involved simultaneously analyse the same samples and actively exchange their results, experiences and ideas. The aim is to understand layer formation and degradation processes from different perspectives with a focus on taphonomy. Our talk provides an insight into the transdisciplinary discussion of a selected profile column 96 regarding archaeobotany, palynology and micromorphology. Do we jointly observe events like flooding or desiccation and can we make a statement about the seasonality in the different layers? The microarchaeological approach shows that complex, hard to solve questions emerge, which have to be discussed in detail between the involved disciplines.

9.8

A new deposit dating from the Eemian Interglacial at Niederweningen (Zürich) and the associated mollusc faunas

Nigel Thew¹ & Heinz Furrer²

¹ *Section d'archéologie et paléontologie, Office de la Culture, République et Canton du Jura, Hôtel des Halles – CP 64, CH-2900 Porrentruy 2 (nigel.thew@jura.ch)*

² *c/o Mammutmuseum Niederweningen (heinz.furrer-paleo@bluewin.ch)*

During the inspection of new trenches being dug for house construction at the western end of the village of Niederweningen, (Zürich), HF documented and sampled four peat beds in April-May 2015. The site is situated about 350 m NW of the famous localities near Niederweningen railway station, where many bones from Late Pleistocene mammals, including mammoths, have been discovered since the 19th century. Two major peat units have been documented within the Wehntal valley where the village is situated. Both are associated with mammal bones and the base of the lower peat also contains numerous pieces of wood. The mammoth remains from the upper peat have been radiocarbon dated to ~45 k BP and ~39 k BP (Furrer et al. 2007, Hajdas et al. 2009). The lower peat, which has only been detected in boreholes, was correlated with the Eemian Interglacial by Welten (1988) and in a study of borehole NW07 by Anselmetti et al. (2010). In a more recent study of borehole NW09, however, it was concluded that this peat could equally well be associated with the second of the Early Würm interstadials (Dehnert et al. 2012).

In the short-lived exposures of spring 2015, HF recognized several lens-like deposits of grey tufaceous silt that lay unconformably beneath the lowest of the four peats beds. These silts were seen to contain crystalline and limestone pebbles, redeposited fragments of travertine, mollusc shells and organic material. They seem to have been deposited within a series of shallow, linear depressions eroded into underlying blue-grey laminated lacustrine silts. Three samples were taken in two columns (A: 2 samples, and B: 1 sample) 65 m apart. These were subsequently wet sieved to allow a

provisional analysis. Tufaceous sediments such as these have never previously been documented in the Niederweningen area, and both the size and frequency of the tufaceous concretions, as well as the richness of the molluscan remains is remarkable. In addition to the mollusc shells, the silts were found to contain numerous small wood fragments, some uncarbonised seeds, rare fish bones and a moderate frequency of worm granules. Some of the travertine fragments bear the impressions of leaves from trees and other plant material. The uncarbonised seeds recovered from sample NW15/3 (Column B) include a hazel (*Corylus*) nut and seeds from both elder (*Sambucus* sp.) and blackberry or raspberry (*Rubus* sp.). Analysis of the plant macroremains, pollen and wood fragments is ongoing.

When NT inspected the mollusc shells, it was immediately apparent that this material represents an important new record for Switzerland. The molluscs are both abundant and well-preserved, despite considerable fragmentation. The rich assemblage of 52 terrestrial species and 16 aquatic taxa is typical for central European interglacial sites. The presence of the marker species *Aegopis vorticillus*, *Discus perspectivus* and *Pagodulina pagodula* shows that the tufaceous silts correspond to a previous interglacial, while their position within the dated sequence at Niederweningen means that they must correspond to the Eemian. Of further note is the virtual absence of pioneer species such as *Discus ruderratus*, as seen in a sequence of Eemian deposits analysed from a site at Yverdon-Les Tuileries (Thew unpublished), and a lack of any of the taxa that appear during the final part of the Eemian at sites studied in eastern France and southern Germany. This means that these faunas probably belong within the optimum phase of the Eemian, between around 125 and 120 k BP, when largely deciduous forests attained their maximum development. Sample NW15/3 of Column B has a noticeably more diverse terrestrial fauna than the two samples from Column A, including the presence of the three key interglacial marker species, which may suggest that the fauna from this sample is somewhat younger.

The terrestrial species suggest that the local environment consisted of mature, essentially deciduous, rather damp woodland with an understory of tall herbs. The rather abundant aquatic fauna, together with the fragments of travertine, indicates that the silts accumulated near to ground-water springs that fed small, slow-flowing streams and shallow marshy pools with abundant water plants. The streams and pools seem to have been flanked by damp marshy ground largely overshadowed by trees that tolerate wet conditions, such as alder. The forest was somewhat denser near Column B, possibly because the area around Column A was significantly wetter (the samples from Col A have a much more abundant aquatic fauna), or due to the fauna from Column B representing a somewhat younger, more advanced stage of forest development. The three interglacial marker species can all be found living to the east of Switzerland, in Austria, the Czech Republic, Slovakia and Hungary, so it is possible that the climate during the last interglacial was more continental than that of today.

REFERENCES

- Anselmetti, F.S., Drescher-Schneider, R., Furrer, H., Graf, H.R., Lowick, S.E., Preusser, F., and Riedi, M.A. 2010: A ~180'000 years sedimentation history of a perialpine overdeepened glacial trough (Wehntal, N-Switzerland). *Swiss Journal of Geosciences*, 103, 345–361.
- Dehnert, A., Lowick, S.L., Preusser, F., Anselmetti, F.A., Drescher-Schneider, R., Graf, H.R., Heller, F., Horstmeyer, H., Kemna, H.A., Nowaczyk, N.R., Züger, A., and Furrer, H. 2012: Evolution of an overdeepened trough in the northern Alpine Foreland at Niederweningen, Switzerland. *Quaternary Science Reviews*, 34, 127–145.
- Furrer, H., Graf, H.R., and Mäder, A. 2007: The mammoth site of Niederweningen, Switzerland. *Quaternary International*, 164/165, 85–97.
- Hajdas, I., Michczyński, A., Bonani, G., Wacker, L., and Furrer, H. 2009: Dating bones near the limit of the Radiocarbon dating method: Study case mammoth from Niederweningen, ZH Switzerland. *Radiocarbon*, 51, 675–680.
- Welten, M. 1988: Neue pollenanalytische Ergebnisse über das Jüngere Quartär des nördlichen Alpenvorlandes der Schweiz (Mittel- und Jungpleistozän). *Beiträge zur Geologischen Karte der Schweiz*, 162, 1–40.

9.9

Lake level reconstruction of Lake Sils, Engadine valley

Sandro Vattioni¹, Irka Hajdas², Michael Strasser^{1,3}, Reto Grischott¹, Trivun Sormaz⁴

¹ *Geologisches Institut, ETH Zürich, Sonneggstrasse 5, CH-8092 Zürich, (sandrov@student.ethz.ch)*

² *Laboratory of Ion Beam Physics, ETH Zürich, Otto-Stern-Weg 5, CH-8093 Zurich*

³ *Institut für Geologie, Universität Innsbruck, Innrain 52, A-6020 Innsbruck*

⁴ *Laboratory of Dendrochronology, Archaeological Service of Canton Grison, Loestrasse 26, CH-7000 Chur*

Lake level changes influence lacustrine and fluvial sedimentation processes and therefore also the appearance of landscape. In summer 2011, the Archaeological Service of Canton Grisons found several tree trunks in about 2.5 meters depth close to the eastern shoreline of Lake Sils. Some of these tree trunks were in a standing position and some of them were just lying on the bottom of the lake. It can be assumed that some of these tree trunks grew there when the lake level was lower than today.

Previous studies have proposed that the lake level was significantly lower in the Middle Holocene and continuously rose between 3000 and 2000 years BP (Grischott et al., in prep.) and other studies reported a tsunami, which occurred 700 AD (Blass et al., 2005). Both scenarios were plausible since they could have led to the death of the trees. Therefore, in this study we dated these tree trunks using radiocarbon dating and dendrochronology to test these possible scenarios.

The results reveal four different groups of ages of the trees. The first group of trees, which dates to the 8th century BC and the second one, which dates to Roman times indicate two lake level minima of about 3 meters below the present lake level. This lake level correlates with climate data like glacier fluctuations (Holzhauser et al., 2005), which indicate glacier advances at these times. These advancing glaciers could have brought more bed load to the fan delta of Sils, which is damming Lake Sils. Therefore, the lake level was subsequently higher dammed during this time and the trees drowned.

The two younger groups of trees with Medieval ages and the one with an early 20th century ages, can be related to human activities. The trees from Medieval period were identified as piles of fish traps (German: "Reusen"), which can be related to the local fishing history.

None of the tree trunks can be related to the tsunami of 700 years AD and neither do the results support the hypothesis of a constant lake level rise between 2000 and 3000 years BP. More likely, the lake level was about 3 meters lower than today until about 200 AD, followed by a lake level rise to about today's level, which was reached at about 300 AD (Wohlwend, 2010).

This study, which combines dendrochronology with radiocarbon dating, shows high potential for the reconstruction of the Quaternary landscape history in the Alpine regions.

REFERENCES:

- Blass A., Anselmetti F. S., Grosjean M. and Sturm M., 2005, The last 1300 years of environmental history recorded in the sediments of Lake Sils (Engadine, Switzerland): *Eclogae Geologicae Helvetiae*, v. 98, no. 3, p. 319-332.
- Grischott R., Kober F., Lupker M., Hippe K., Ivy-Ochs S., Hajdas I., Salcher B., Christl M., in preparation, Limited variability in erosion and sediment transport for the last 6 ky in an alpine glaciated catchment, Geological Institute, ETH Zürich.
- Holzhauser, H., Magny, M., and Zumbühl, H.J., 2005, Glacier and lake-level variations in west-central Europe over the last 3500 years. *The Holocene* 15, 789-801.
- Wohlwend, S., Anselmetti, F. and Gilli, A., 2010, Shoreline deposits around Lej da Segl (Upper Engadine, Switzerland), Traces of a Prehistoric Tsunami?, master thesis, D-Erdw, ETH Zürich.

9.10

The Lake Towuti Drilling Project: A new, ~1 million year record of Quaternary climate and ecosystem dynamics from the Indo-Pacific

Hendrik Vogel¹, James M. Russell², Satria Bijaksana³, Sean Crowe⁴, David Fowle⁵, Douglas Haffner⁶, John King⁷, Ristiyanti Marwoto⁸, Martin Melles⁹, Thomas von Rintelen¹⁰, Janelle Stevenson¹¹, Ian Watkinson¹² & the TDP science team

¹ *Institute of Geological Sciences and Oeschger Centre for Climate Change Research, University of Bern, 3012 Bern, Switzerland (hendrik.vogel@geo.unibe.ch)*

² *Brown University, Providence, USA*

³ *Institut Teknologi Bandung, Bandung, Indonesia*

⁴ *University of British Columbia, Vancouver, Canada*

⁵ *University of Kansas, Lawrence, USA*

⁶ *University of Windsor, Windsor, Canada*

⁷ *University of Rhode Island, Kingston, USA*

⁸ *LIPI Biology, Bogor, Indonesia*

⁹ *University of Cologne, Köln, Germany*

¹⁰ *Museum f. Naturkunde Berlin, Germany*

¹¹ *Australian National University, Canberra, Australia*

¹² *Royal Holloway, London, UK*

Lake Towuti (2.5°S, 121°E) is a, 560 km², 200-m deep tectonic lake at the downstream end of the Malili lake system, a set of five, ancient (1-2 MYr) tectonic lakes in central Sulawesi, Indonesia. Lake Towuti's location in central Indonesia provides a unique opportunity to reconstruct long-term paleoclimate change in a crucially important yet understudied region- the Indo-Pacific warm pool (IPWP), heart of the El Niño-Southern Oscillation. The Malili Lakes have extraordinarily high rates of floral and faunal endemism, and the lakes are surrounded by one of the most diverse tropical forests on Earth. The ultramafic (ophiolitic) rocks and lateritic soils surrounding Lake Towuti provide metal substrates that feed a diverse, exotic microbial community, analogous to the microbial ecosystems that operated in the Archean Oceans.

In May-July 2015 we recovered a total of ~1200 m of sediment drill core from 3 different sites in the Lake Towuti basin in the framework of the ICDP Towuti Drilling Project. Our deepest hole bottomed out at ~170 meters below lake floor in coarse fluvial gravel. Seismic data along with borehole geophysical data, initial lithological and petrophysical data collected in the field and available data from our 2010 piston cores imply that the lake existed continuously for the last ~600 kyr and discontinuously for up to 1 Myr. These assumptions are so far of course only based on a very rough age-depth calculation. Due to the fact that we found numerous up to several 10s of centimeter thick tephra layers we hope that we can refine our chronology using absolute radiometric techniques. Core processing and sub-sampling for various different analyses to be conducted by >40 TDP science team members is still in progress and will ultimately help to achieve the primary goals of our initiative:

- (1) Document the timing, frequency, and amplitude of orbital- to millennial-scale changes in (hydro-)climate in the Indo-Pacific Warm Pool across multiple glacial-interglacial cycles;
- (2) Understand how variations in terrestrial hydrology and temperature in central Indonesia respond to changes in the mean state of the ENSO system, the monsoons, high-latitude forcing, and insolation;
- (3) Analyze the long-term stability and resilience of rainforest vegetation to changes in climate, greenhouse gases, and fire frequency;
- (4) Study the extent, biogeography, and metabolism of microbial life in the sediments of a non-sulfidic, ferruginous basin, and their relationships to carbon cycling, redox metal deposition, and the concentration of metal ore minerals;
- (5) Study the effects of climate-driven changes in the aquatic environment on both lacustrine microbial populations, and the geobiosphere within the lake's sediment;
- (6) Determine the age of Lake Towuti, and the ensuing rates of speciation of Towuti's endemic fauna and flora;
- (7) Identify the timing of past lake level fluctuations in Towuti, changes in hydrological connections among the Malili Lakes, and how these influenced biological colonization events, habitat stability, and modes of speciation (sympatric, allopatric).

9.11

Quantifying subglacial erosion rates at Goldbergkees, Hohe Tauern (Austria) with cosmogenic ^{10}Be and ^{36}Cl

Christian Wirsig¹, Susan Ivy-Ochs¹, Jürgen Reitner², Marcus Christl¹, Christof Vockenhuber¹, Mathias Bichler², Martin Reindl

¹ Ion Beam Physics, ETH, 8093 Zurich (wirsig@phys.ethz.ch)

² Sedimentology, Geological Survey of Austria, 1030 Wien

Cirques and troughs are ubiquitous landforms of glacial erosion in glaciated mountain ranges like the Alps. Yet, the processes of erosion on the cirque or valley floor that are responsible for their formation are poorly quantified. In this study we use concentrations of cosmogenic ^{10}Be and ^{36}Cl to determine in-situ subglacial erosion depths in the recently deglaciated bedrock at Goldbergkees in the Eastern Alps (Austria). We sampled inside of the footprint of the Goldbergkees; an area that has been ice free since the glacier melted back at the end of the Little Ice Age (LIA) about 150-100 years ago. Our sampling strategy was aimed at studying glacial abrasion rates therefore we avoided plucked surfaces. The youngest exposure ages match the known exposure time after the LIA (< 150 years). Yet many of the analyzed bedrock surfaces have apparent exposure ages that are thousands of years older than the known exposure time after the end of the LIA. This shows that inherited cosmogenic nuclides that accumulated during ice-free periods between the end of the Lateglacial and the beginning of late Holocene advances (ca. 4 ka) are present. In that light the measured nuclide concentrations can be better understood as representing subglacial erosion depths, rather than exposure times. Based on the cosmogenic nuclide concentrations we were able to quantify the thicknesses of bedrock that were removed by subglacial erosion at each sampling spot during the late Holocene. The bedrock of the 'youngest' surfaces was deeply eroded by the Goldbergkees down to >300 cm during the late Holocene. In contrast, bedrock at the margin of the LIA ice extent was eroded <35 cm. These values convert to subglacial erosion rates on the order of 0.1 mm/yr to 5 mm/yr. Erosion depths along transverse and longitudinal profiles show a patchy pattern, likely strongly influenced by local controls exerted by small-scale bed topography and bedrock erodibility. Interestingly, erosion rates are fastest at the turn from cirque floor to sidewall, just as predicted by glacial erosion models (Harbor, 1992). The depth of bedrock erosion is directly reflected in relative differences in nuclide concentration between ^{10}Be and ^{36}Cl due to the different shapes of their production rate depth profiles. Even though apparent ^{36}Cl ages tend to be older than ^{10}Be ages, calculated erosion rates are identical. This reinforces our interpretation that the dominant influence on measured nuclide concentrations is erosion, not exposure time.

REFERENCES

Harbor, J.M. 1992: Numerical modeling of the development of U-shaped valleys by glacial erosion, Geological Society of America Bulletin, 104, 1364-1375.

9.12

Palaeolithic in the plaine of Alsace and in the Vosgian foreland: state of art, taphonomy and landscape-use archaeology

Patrice Wuscher¹, H  lo  se Koehler², Olivier Moine³, Fran  ois Bachellerie⁴, Florian Basoge⁵, , Sylvain Griselin⁶, Nathalie Schneider⁷, Eric Bo  s⁸, Simon Diemer⁹ and No  mie S  v  que¹⁰

¹ *P  le d'Arch  ologie Interd  partemental Rh  nan et UMR7362/Laboratoire Image, Ville, Environnement - LIVE, 2 all  e Thomas Edison - ZA Sud - CIRSUD, 67600 S  lestat, France (patrice.wuscher@pair-archeologie.fr)*

² *P  le d'Arch  ologie Interd  partemental Rh  nan et UMR7041/ArScan, 2 all  e Thomas Edison - ZA Sud - CIRSUD, 67600 S  lestat, France*

³ *Centre National de la Recherche Scientifique, UMR8591/Laboratoire de G  ographie Physique de Meudon, Batiment Y, 1 place Aristide Briand, 92195 Meudon, France*

⁴ *Antea Arch  ologie et UMR5199/PACEA, 11 rue de Zurich, 68440 Habsheim*

⁵ *P  le d'Arch  ologie Interd  partemental Rh  nan, 2 all  e Thomas Edison - ZA Sud - CIRSUD, 67600 S  lestat, France*

⁶ *Institut National de Recherches Arch  ologiques Pr  ventives, UMR7041/ArScan, 10 rue d'Altkirch, 67000 Strasbourg, France*

⁷ *Institut National de Recherches Arch  ologiques Pr  ventive, UMR7362/Laboratoire Image, Ville, Environnement - LIVE, 10 rue d'Altkirch, 67000 Strasbourg, France*

⁸ *Institut National de Recherches Arch  ologiques Pr  ventives, UMR7044/Archim  de, 10 rue d'Altkirch, 67000 Strasbourg, France*

⁹ *PhD student, University of Strasbourg, France*

¹⁰ *PhD student, University of Lille, France*

Human strategies and population movements facing climatic and/or landscape (resources and constraints) changes during the Pleistocene are crucial questions in archaeology. However, despite the significant progresses in the reconstruction of both climatic and environmental changes on the European continent realised these last decades, the chronological mapping of Human occupations remains a difficult work even at the regional scale due to taphonomy and to the presence or not of archaeologists involved in the Palaeolithic periods. Then, for some regions the quality of Palaeolithic sites maps remains highly questionable.

In Alsace, the isolated character of the few Pleistocene sites prevents any regional overview of the history of Palaeolithic occupations. Recent excavations (Mutzig, Morschwiller...) raised up this question. We propose therefore to compile and criticize the available data about the stratigraphic successions and archaeological sites in order to elaborate regional models of conservation and location of archaeological sites. These models will be enhanced and tested during the preventive archaeological surveys. Finally, we will try to approach the history of human territorial strategies during the Pleistocene and to compare the regional trends with the nearby regions.

The preliminary results of the project allows to discuss the nature and the age of the geomorphological units in the French part of the Rhine graben and to examine the distribution of archaeological sites. This distribution is linked to the history of the research but also to geology, geomorphology and geography.

9.13

Novel Insights from Multi-Millennial Tree Ring Isotope Records of the Early and Mid-Holocene

Malin Michelle Ziehmer¹, Kurt Nicolussi², Christian Schlüchter³, Markus Leuenberger¹

¹ *Climate and Environmental Physics, Physics Institute & Oeschger Center for Climate Change Research, University of Bern, Sidlerstr. 5, CH-3012 Bern (ziehmer@climate.unibe.ch)*

² *Alpine Tree-Ring Group, Institute of Geography, University of Innsbruck, Innrain 52, A-6020 Innsbruck*

³ *Institute of Geological Sciences & Oeschger Center for Climate Change Research, University of Bern, Baltzerstrasse 1+3, CH-3012 Bern*

The reconstruction of Holocene climate, its evolution and variability in the Alps is mainly based on low frequency archives such as glacier and tree line fluctuations. Investigated low-frequency records expose an evolution of Holocene climate from a generally warm Early and Mid to a relatively cool Late Holocene. High resolution records are rare and often do not indicate a general long-term trend; causes and mechanism behind this disagreement are not fully understood yet.

However; recent finds of wood remains of long-lived trees in Alpine glacier forefields changed the concept of Holocene glacier variability as well as the present understanding of Holocene climate dynamics. They prove that glaciers in the Alps were relatively small and short in their extension during the Early and Mid-Holocene (Joerin et al., 2008; Nicolussi and Schlüchter, 2012). Therefore, these wood remains prove that the natural variability of postglacial climate is still not sufficiently known. However; such knowledge is essential for climate model input and the ability to disentangle natural from anthropogenic influences on the Earth's climate.

Therefore, the study aims at establishing highly resolved isotope records from the mentioned, calendar-dated wood remains covering the past 9000 years. Samples are collected in glacier forefields in the Alps covering a broad SW- NE transect. Wood samples are separated into 5-year tree ring blocks from which cellulose is extracted and crushed by ultrasonic homogenization (Boettger et al., 2007; Laumer et al., 2009). Stable isotopes of carbon, oxygen and hydrogen are simultaneously measured using a recently developed method by Loader et al. (2015). Stable isotope records, containing of a sample replication of four samples per 5-year tree ring block, allow to establish stable isotope chronologies over the entire Holocene.

During the Early and Mid-Holocene, the investigated multi-millennial tree ring isotope records (9000 to 6000 yr b2k) display novel insights into the high frequency archive of tree rings from glacial wood remains. Further, the carbon, oxygen and hydrogen records reveal interesting low frequency variability as well expected offsets between the measurements of individual trees which are also investigated separately by sampling site, tree species as well as age structure and growth trend. The measured Deuterium records reveal a species- specific isotope signature for the investigated species *Larix decidua* and *Pinus cembra*, which is not resembled in the carbon and oxygen records. Further, first comparisons with reconstructions of solar and orbital parameters show a correlation between the long-term variability displayed by the carbon isotope records and the reconstructed solar irradiance during the Early and Mid-Holocene (Steinhilber et al., 2009). This is – though to a lesser degree – resembled by the species-dependent hydrogen isotope variations.

REFERENCES

- Boettger, T., et al. 2007: Wood cellulose preparation methods and mass spectrometric analyses of delta C-13, delta O-18, and nonexchangeable delta H-2 values in cellulose, sugar, and starch: An interlaboratory comparison, *Analytical Chemistry*, 79, 4603-4612.
- Joerin, U.E. et al. 2008: Holocene optimum events inferred from subglacial sediments at Tschierwa Glacier, Eastern Swiss Alps, *Quaternary Science Reviews*, 27, 337-350.
- Laumer, W., et al. 2009: A novel approach for the homogenization of cellulose to use micro-amounts for stable isotope analyses, *Rapid Communications in Mass Spectrometry*, 23, 1934–1940.
- Loader, N.J., et al. 2015: Simultaneous Determination of Stable Carbon, Oxygen, and Hydrogen Isotopes in Cellulose, *Analytical Chemistry*, 87, 376-380.
- Nicolussi K., & C. Schlüchter 2012: The 8.2 ka event - Calendar-dated glacier response in the Alps, *Geology*, 40, 819-822.
- Steinhilber, F., Beer, J. & C. Fröhlich 2009: Total solar irradiance during the Holocene, *Geophysical Research Letters*, 36, L19704.

P 9.1

Nadaouiye Aïn Askar – Mid-Pleistocene Palaeocology in a Spring fed Wetland of El Kowm Oasis in the Central Syrian Desert.

Johannes Kalbe¹, Christine Pümpin², Reto Jagher²

¹ *Institute of Earth- and Environmental Science, Karl-Liebknecht-Straße 24-25, 14476 Potsdam-Golm, Germany*

² *University of Basel, Integrative prähistorische und naturwissenschaftliche Archäologie (IPNA), Spalenring 145, CH-4055 Basel*

The site of Nadaouiye Aïn Askar is an ancient artesian spring in the oasis of El Kowm, Central Syria. The oasis, consists of several dozens of local wetlands that were active at least since the lower Pleistocene. The area has steadily been frequented by humans for at least 1.8 million years. The Nadaouiye Aïn Askar site covers environmental human history from about 550 ka to 150 ka in a continental setting. Excavations exposed a deep stratigraphy with a succession of sedimentary units with a strong limnic component, containing a unique succession of artefact assemblages assigned to the Acheulean techno-complex. Unit VI, attributed to Marine Isotope Stage 13, is rich in ostracod valves and was chosen for a preliminary environmental study. From these sediments *Heterocypris salina*, *H. incongruens*, *Ilyocypris bradyi*, *I. inermis*, *I. gibba*, *Darwinula stevensoni*, *Plesiocypridopsis cf. newtoni*, *Fabaeformiscandona cf. rawsoni*, *Candonopsis cf. kingsleyi*, *Pseudocandona sp.*, *Trajanocypris sp.*, *Physocypris sp.* and *Mixtacandona sp.* could be documented the first time for Middle Pleistocene wetlands of the arid environment of Northern Arabia. Data from these microfossils and geochemical proxies indicate three cycles, changing the wetland from paludine conditions into a pond fed by an effluent with increasing salinity in the course of sedimentation. The high mineralisation of the spring waters permits the discussion about early human adaptability to brackish waters for drinking water, which are common features within the steppe and desert environments along the “out-of-Africa”-corridor through the Arabian Peninsula and into the eastern Mediterranean.

P 9.2

New results of excavations at the Middle Palaeolithic site of Mutzig-Rain (Alsace, France)

Fabio Wegmüller¹, Héloïse Koehler², Christine Pümpin¹, Patrice Wuscher² & Noémie Sévêque³

¹ *Institut für Prehistorie und Archäologische Science (IPAS) University of Basel Switzerland, (fabio.wegmueller@unibas.ch, christine.puempin@unibas.ch)*

² *Pôle d'Archéologie Interdépartemental Rhénan (PAIR) Sélestat (F) (heloise.koehler@pair-archeologie.fr, patrice.wuscher@pair-archeologie.fr)*

³ *Laboratoire Préhistoire et Quaternaire, Université de Lille (noemie.seveque@etu.univ-lille3.fr)*

The site of Mutzig “Rain” was discovered by chance in 1992 during construction works. Subsequently several test trenches were made in the surrounding area between 1992 and 1996. This test trenches brought to light a large Middle Paleolithic site. Since 2009, systematic excavations have been carried out by the Pôle d'Archéologie Interdépartemental Rhénan (PAIR), the Universities of Strasbourg, Basel, Cologne and Lille. During this excavation different layers with a rich archaeological and paleontological record were discovered documented. The abundant lithic and faunal assemblages are well preserved and date back to the Mousterian period ca. 90,000 years ago. This poster aims to present the newest results from the ongoing excavation in Mutzig and to discuss the chronological position of the site, the site formation processes and the interpretations of the archaeological finds.

P 9.3

An interdisciplinary approach to site formation processes through profile sampling at the Neolithic lakeshore settlement of La Draga (Banyoles, Spain)

Ferran Antolín¹, Andrea Balbo², André Colonese³, Jean-Bernard Huchet⁴, Oriol López⁵, Stefanie Jacomet¹, Giuseppe Manganelli⁶, Antoni Palomo⁵, Raquel Piqué⁵, Xavier Terradas², Giovanni Zanchetta⁷

¹ *Integrative prähistorische und naturwissenschaftliche Archäologie (IPNA), University of Basel, Spalenring 145, CH-4055 Basel (ferran.antolin@unibas.ch)*

² *Spanish National Research Council, CSIC-IMF, Egipcíques 15, 08001 Barcelona.*

³ *Dept. of Archaeology, University of York, B/S Block, Wentworth Way, YO10 5DD York*

⁴ *Muséum national d'Histoire naturelle, UMR 7209 du CNRS, Archéozoologie, Archéobotanique: sociétés, pratiques et environnements, case postale 56, 55 rue Buffon, 75005 Paris*

⁵ *Dept. of Prehistory, Universitat Autònoma de Barcelona, Campus de Bellaterra, 08193 Bellaterra*

⁶ *Sezione di Scienze Ambientali, University of Sienna, Via P.A. Mattioli 4 - 53100 Siena*

⁷ *Dipartimento di Scienze della Terra, University of Pisa, via S. Maria 53, 56126 Pisa*

To date, La Draga is the only lake-dwelling site that is known in the Iberian Peninsula. It is dated to the last third of the VIth millennium cal BC and at least two settlement phases were distinguished within this period (Palomo et al 2014): the first phase would correspond to a real pile-dwelling settlement; the second would probably be on wet land, but not on water. Farming was well established in the settlement and a rich assemblage of archaeobiological data has been investigated (Antolín et al. 2014).

Excavations at La Draga began in 1990 but a new project started in 2010. A specific sampling strategy was applied to target new research questions (Antolín et al. 2013), combining surface bulk samples with profile samples. Plant macros (preserved both charred and uncharred), soil micromorphological analyses, malacological (including isotopic analyses) and insect remains were investigated from three profile columns.

The integration of all this data allows a combined approach to site formation processes never performed before for an Early Neolithic lake settlement. Our results are preliminary due to the low surface of the settlement represented in our profile columns but they mean a step forward for scientific archaeological investigations in the region and the comprehension of the site formation processes at the site.

REFERENCES

- Antolín, F., Blanco, À., Buxó, R., Caruso, L., Jacomet, S., López, O., Marlasca, R., Palomo, A., Piqué, R., Saña, M., & Terradas, X., 2013: The application of systematic sampling strategies for bioarchaeological studies in the Early Neolithic lakeshore site of La Draga (Banyoles, Spain), *Journal of Wetland archaeology* 13, 29-49.
- Antolín, F., Buxó, R., Jacomet, S., Navarrete, V., & Saña, M., 2014: An integrated perspective on farming in the early Neolithic lakeshore site of La Draga (Banyoles, Spain), *Environmental Archaeology* 19, 241-255.
- Palomo, A., Piqué, R., Terradas, X., Bosch, A., Buxó, R., Chinchilla, J., Saña, M., & Tarrús, J., 2014: Prehistoric occupation of Banyoles lakeshore: results of recent excavations at La Draga site, Girona, Spain, *Journal of Wetland Archaeology* 14, 58-73.

P 9.4

Long-term bedrock incision rates in the northern Swiss Alpine Foreland inferred from reconstructed Deckenschotter chronologies

Anne Claude¹, Naki Akçar¹, Susan Ivy-Ochs², Fritz Schlunegger¹, Peter W. Kubik², Marcus Christl², Christof Vockenhuber², Meinert Rahn³, Andreas Dehnert³ & Christian Schlüchter¹

¹ *Institute of Geological Sciences, University of Bern, Baltzerstrasse 1-3, CH-3012 Bern, (anne.claude@geo.unibe.ch)*

² *Laboratory of Ion Beam Physics (LIP), ETH Zurich, Otto-Stern-Weg 5, CH-8093 Zurich*

³ *Swiss Federal Nuclear Safety Inspectorate ENSI, Industriestrasse 19, CH-5200 Brugg*

At the beginning of the Quaternary the Swiss Alpine Foreland was assumed to be made up of a low relief landscape with advancing piedmont glaciers. The broad valleys were later filled with proximal braided river sediments, i.e. the Deckenschotter. They cover Tertiary Molasse or Mesozoic bedrock with an erosional unconformity and are referred as the Höhere (Higher; HDS) and Tiefere Deckenschotter (Lower; TDS) based on their distinct topographical positions. The difference in elevation suggests that the two Deckenschotter units are separated from each other by a period of significant incision. In the period between HDS and TDS deposition, an incision of approximately 80-100 m into formerly deposited gravels and 30-110 m into bedrock are observed. Even deeper incision into the bedrock was observed after TDS deposition with values between 140 and 260 m.

The evolution of landscape change during the Quaternary merits special importance in modelling the long-term safety of the deep geological repositories for nuclear waste disposal in the northern Alpine Foreland. To shed light on this evolution, timing of the Swiss Deckenschotter needs to be unravelled. In this study, we reconstructed the chronology of HDS at four locations: Mandach (AG), Siglistorf (AG), Stadlerberg (ZH) and Irchel (ZH) with cosmogenic depth-profile and isochron-burial dating techniques. Our results showed that proximal braided rivers started to deposit gravels prior to 2 Ma while incising the Molasse bedrock with long-term incision rates up to 0.2 mm/a. This regime continued until around 1 Ma, when incision rates accelerated up to 0.3-0.5 mm/a. This increase in bedrock incision rates can be correlated to the Mid-Pleistocene Revolution, which marks the transition from 41 ka to 100 ka glacial/interglacial cycles. During the Mid-Pleistocene Revolution, a reorganization of the drainage network occurred in the northern Alpine Foreland with a significant lowering of the base level of stream channels, which is also recorded by the increase in incision rates in our data.

REFERENCES

- Graf, H.R. (1993). Die Deckenschotter der zentralen Nordschweiz. Dissertation, ETH Zürich, 187 pp.
- Kuhlemann, J. & Rahn, M. (2013). Plio-Pleistocene landscape evolution in Northern Switzerland. *Swiss Journal of Geosciences*, 106, 451-467.
- Häuselmann, P., Granger, D.E., Jeannin, P.-Y., Lauritzen, S.-E. (2007). Abrupt valley incision at 0.8 Ma dated from cave deposits in Switzerland. *Geology*, 35, 143-146.
- Heuberger, S. & Naef, H. (2014). NAB 12-35: Regionale GIS-Kompilation und -Analyse der Deckenschotter-Vorkommen im nördlichen Alpenvorland. Nagra Arbeitsbericht.
- Maslin, M.A. & Ridgwell, A.J. 2005: Mid-Pleistocene revolution and the 'eccentric myth'. *Geological Society, London, Special Publications* 247, 19-34.

P 9.5

Confluence area of the Aare and the Valais Paleoglacier Lobes

Regina Reber¹, Fritz Schlunegger¹

¹ *Institut für Geologie, Universität Bern, Baltzerstrasse 1+3, CH-3012 Bern (rreber@geo.unibe.ch)*

We will present a high-resolution reconstruction of the erosional features in the Molasse bedrock beneath the Bern area. This area has been covered by large Alpine glaciers during the Last Glacial Maximum and previous Pleistocene glaciations. This area has also been explored by thousands of drillings for geothermal and geotechnical explorations. Our reconstruction will be based on the results of previous studies (Dürst Stucki et al., 2010; 2013). With our enhanced resolution in our study area we will be able to use cross-cutting relationships between the tunnel valley system beneath Bern and orientations and extents of paleo-glaciers in the region in an effort to infer differences in prevailing moisture sources mainly between LGM times and earlier glaciations of unknown age.

REFERENCES

- Stucki, M. D., Reber, R., & Schlunegger, F. 2010. Subglacial tunnel valleys in the Alpine foreland: an example from Bern, Switzerland. *Swiss Journal of Geosciences*, 103(3), 363-374.
- Stucki, M. D., & Schlunegger, F. 2013. Identification of erosional mechanisms during past glaciations based on a bedrock surface model of the central European Alps. *Earth and Planetary Science Letters*, 384, 57-70.

P 9.6

Glacial erosion and dust transport to the Southern Ocean : coupling between erosion on climate

Lena Märki¹, Antoine Coge¹, Frédéric Herman¹

¹ *Institut des Dynamiques de la Surface Terrestre, Université de Lausanne, Bâtiment Geopolis, Quartier Unil-Mouline, CH-1015 Lausanne*

Glacial and interglacial fluctuations of the last 700 kyrs have been accompanied by changes in climatic parameters, continental erosion and biogeochemical cycles. The relations and respective influences between them are still debated since there are no unique causal relationships. In particular it remains an open question whether chemical weathering varied during the last glacial-interglacial cycles and had or not an influence on the climate by consuming atmospheric CO₂. In this paper we examine a mechanism in which increased glacial erosion over Patagonian Andes during glacial periods enhanced the dust transport to the Southern Ocean, where iron fertilization enhanced biologic productivity, CO₂ consumption and further cooling. If the causal relationships between CO₂ variations, biologic productivity in the Southern Ocean, and nutrients supply by dusts have been already well studied, it remains unclear which role is played by glacial erosion over Patagonia. We studied the precise provenance of the sediments by measuring a precise North-South profile of Nd isotopes in the sediments delivered from the Patagonian Andes. We correlate the location of the erosion hotspot of the last glacial-interglacial cycle with the composition of the glacial dusts exported to Antarctica. Moreover we show, using mineralogy data in a core of the Southern Atlantic Ocean, that the material delivered to the Southern Ocean is fresher and has a higher potential for nutrients (especially Fe) delivery during glacial times, consistently with a glacial provenance. Altogether these observations, and others reported from the literature, suggest an indirect control of climatic fluctuations by glacial erosion over the last glacial-interglacial cycles.

P 9.7

Reconstructing Alpine glacier activity during 50-20 ka BP by high-resolution radiocarbon dating of the Cormor alluvial megafan (Tagliamento glacier, NE Italy)

Kristina Hippe¹, Alessandro Fontana², Irka Hajdas¹ & Susan Ivy-Ochs¹

¹ *Laboratory of Ion Beam Physics, ETH Zürich, Otto-Stern-Weg 5, CH-8093 Zürich, (hippe@phys.ethz.ch)*

² *Department of Geoscience, University of Padua, Via Gradenigo 6, I-35131 Padova*

We present more than 130 radiocarbon ages from a series of about 55 peat and macrofossil samples taken from a drilling core (PNC1, 65 m) at the site of Piancada on the eastern Venetian-Friulian Plain, SE Alpine foreland. The drilling site is located in the distal part of the Cormor alluvial megafan, one of the main outwashes of the southern Alpine Tagliamento glacier onto the foreland basin during the Last Glacial Maximum (LGM; Fontana et al. 2014). Due to the immediate connection between outwash fan and glacier, the fan sedimentary sequence provides an exceptional record of changes in rate and character of sedimentation caused by fluctuating glacier activity and, thus, by variations in climate.

The stratigraphic sequence of the core shows an alternation of silt and clay deposits with intercalated peaty and humic horizons. These organic layers of 5-40 cm thickness represent phases of enhanced accumulation of plant remains because of locally inactive fluvioglacial sedimentation and the formation of a fen environment. For radiocarbon dating, samples were taken every few centimetres to decimetres between 4 to 33 m depth. Obtained ¹⁴C ages range from ~50-20 cal ka BP, providing a detailed chronology of LGM and pre-LGM fluvioglacial sediment deposition in the Cormor alluvial megafan. These data allow to directly identify periods of glacier advance and withdrawal with a unique chronological precision.

To assess the effect of sample preparation on the resulting radiocarbon ages, 30 samples were separated into various fractions and treated with different pre-treatment laboratory protocols. The classical ABA (acid-base-acid) protocol and two different ABOX treatments (using K₂Cr₂O₇ or H₂SO₄ for the final acid step) were applied on bulk peat samples of varying organic particle size as well as on separated macrofossils. With regard to the size and/or type of the organic particle, no systematic age differences were observed. However, some samples indicate a shift towards younger ages after ABOX treatment. Few samples also suggest the incorporation of particles containing old carbon (too old ages). These results emphasize the necessity of a careful material selection and treatment for accurate, high-resolution radiocarbon chronologies.

REFERENCES

Fontana, A., Monegato, G., Zavagno, E., Devoto, S., Burla, I. & Cucchi F. 2014: Evolution of an Alpine fluvioglacial system at the LGM decay: The Cormor megafan (NE Italy), *Geomorphology*, 204, 136-153.

P 9.8

Reconstructing the last deglaciation at Sieben Hengste, Switzerland

Marc Luetscher^{1,2}, Susan Ivy-Ochs³ & Maric Hof⁴

¹ *Austrian Academy of Sciences, Inst. for Interdisciplinary Mountain Research, ICT, Technikerstr. 21a, A-6020 Innsbruck (marc.luetscher@uibk.ac.at)*

² *University of Innsbruck, Inst. of Geology, Innrain 52, A-6020 Innsbruck*

³ *ETH-Zurich, Labor f. Ionenstrahlphysik (LIP), Otto-Stern-Weg 5 8093 Zuerich*

⁴ *ch. du Lazé, 1806 St-Légier*

The Sieben Hengste karst extends between 1700 and 2000 m a.s.l. in Central Switzerland and hosts one of the most extensive speleological network of Western Europe (Häuselmann and Jeannin, 2004). The karst aquifer encompasses the 200 m-thick Schrattenkalk Formation (Barremian to Aptian; Urgonian facies), a Cretaceous platform limestone formed in the Helvetic realm. The geological structure follows a monoclinial slope dipping to the southeast at about 15-30° and is delineated to the east by a large normal fault whose throw reaches up to 1000 m.

Several lines of evidence, including alignments of erratic boulders and glacial striations, point to an ice-covered hydrological catchment during the Last Glacial Maximum (LGM), with an Equilibrium Line Altitude estimated at ca. 1250 m a.s.l. Despite the elevated altitude, continuous speleothem growth between 30 and 14.7 ka suggests that part of the system must have acted as a talik during the LGM (Luetscher et al., 2015). To better understand the thermal response of such a system, we attempt a reconstruction of the local glacier dynamics during the LGM. Here, we report preliminary surface exposure ages (³⁶Cl) obtained on two erratic boulders deposited at the margin of the carbonate outcrop.

REFERENCES

- Häuselmann, P., & Jeannin, P.-Y., 2004. Sieben Hengste, Switzerland. In Gunn (ed.), *Encyclopedia of Caves and Karst Science*, Fitzroy Dearborn, 647-649.
- Luetscher M., Boch R., Sodemann H., Spötl C., Cheng H., Edwards R.L., Frisia S., Hof F., Müller W., 2015. North Atlantic storm track changes during the Last Glacial Maximum recorded by Alpine speleothems. *Nature Communications*, 6:6344.

P 9.9

Lateglacial and Holocene glacier development and landscape evolution in Meiental, Uri (CH)

Max Boxleitner¹, Max Maisch¹, Peter Walthard¹, Susan Ivy Ochs², Dagmar Brandova¹, Markus Egli¹

¹ *Geographisches Institut, Universität Zürich, Winterthurerstrasse 190, CH-8050 Zürich (max.boxleitner@geo.uzh.ch)*

² *Labor für Ionenstrahlphysik, ETH Zürich, Otto-Stern-Weg 5, CH-8093 Zürich*

The aim of our study in Central Switzerland, based on a multimethodical approach, is to develop a refined relative morphostratigraphy and absolute chronology of the local glacial development and the landscape history of the Meiental after the LGM. By identifying the glacial remnants we based our study on the preliminary work by Renner (1982) and Spillmann et al. (2011).

Against the backdrop of the general interregional synchronicity of climatic events our findings will contribute to the understanding of the climate history in Switzerland and the Alps during the Lateglacial and the Holocene and its regional anomalies.

The highly unstable climatic period of the alpine Lateglacial is characterized by a general vanishing of the ice masses after the LGM and numerous glacier re-advances during repeated cold phases (stadials). Among other glacial and periglacial landforms (i.e. rock glaciers) especially moraines can be found as witnesses of these processes in the Meiental. As terrestrial archives they contain direct or indirect information about the glacier extent and other relevant parameters such as the paleo-ELA at a certain time in the past. ¹⁰Be dating of boulders allows us to attribute the moraines to a distinct time period.

Based on Digital Elevation Models and geomorphological mapping we have collected more than 20 samples from moraines of comparable and/or different ages in the Meiental for ¹⁰Be analysis. These samples were processed in the laboratory and first results nicely confirm and support the supposed attribution to the regional equivalents of the Egesen (YD), Daun and Clavadel-stadials (pre Bölling).

REFERENCES

- Renner, F.B. 1982: *Beiträge zur Gletschergeschichte des Gotthardgebietes und dendroklimatologische Analysen an fossilen Hölzern*. Vol. 8. Universität Zürich.
- Spillmann, P., Labhart, T., Brücker, W., Renner, F., Gisler, C. & Zraggen A. 2011: Geologie des Kantons Uri. Naturforschende Gesellschaft Uri – Bericht Nr. 24, 224 S.

P 9.10

A Late Glacial / Early Holocene climate reconstruction using stable isotopes in biomarkers from the Gemündener Maar, Germany

Lorenz Wüthrich^{1,2}, Johannes Hepp³, Imke Kathrin Schäfer^{1,2}, Selina Lutz¹, Frank Sirocko⁴, Michael Zech³, Roland Zech^{1,2}

¹ *Institute of Geography, University of Bern, CH-Bern*

² *Oeschger Center for Climate Change Research, University of Bern, CH-Bern*

³ *Institute of Agronomy and Nutritional Sciences, Martin Luther University Halle- Wittenberg, D-Halle*

⁴ *Institute for Geosciences, Johannes Gutenberg-University, D-Mainz*

Lake sediments are valuable archives for the reconstruction of past changes in climate and vegetation. In the present study, we analyse samples from the Gemündener Maar, a lake situated in the western Eifel, Germany, for their isotopic composition of n-alkanes (²H) and sugars (¹⁸O). Both isotopes can be used to reconstruct the isotopic composition of precipitation. But this approach is hampered by evaporative enrichment of leaf water. The solution for this problem might be the combination of both isotopes, which allows calculating not only the isotopic composition of paleo-precipitation but also relative humidity (rh) based on reconstructed d-excess of leaf water. Preliminary results suggest that the rh was lower during the Younger Dryas compared to the very humid Allerød. The onset of the Holocene was even drier than the Younger Dryas, except for one very humid spell. Only with the transition Preboreal/Boreal, rh increased again. Apart from the analysis of isotopic composition, different chain lengths of n-alkanes are used to reconstruct paleovegetation.

P 9.11

Age and geomorphology of the Marocche (Trentino, Italy)

Susan Ivy-Ochs¹, Silvana Martin², Paolo Campedel³, Alfio Viganò³, Silvio Alberti², Manuel Rigo², and Christof Vockenhuber¹

¹ *Ion Beam Physics, ETH, 8093 Zurich (ivy@phys.ethz.ch)*

² *Geosciences Department, University of Padua, 35133 Padua*

³ *Geological Survey of the Province of Trento, 38121 Trento*

As a consequence of the steep high valley walls and the presence in part of structurally compromised rock, numerous rock avalanche deposits are found in the Adige and Sarca River valleys (northern Italy). With a view to understanding predisposition and triggering factors of massive rock avalanches in this seismically active region, we are studying the geomorphology and timing of several rock avalanches in the River Sarca-Lake Garda area (Marocche, Monte Spinale, Lago di Tovel, Lago di Molveno, San Giovanni and Torbole). Amongst the most extensive of these deposits, with an area of 13 km² and a volume of about 10⁹ m³, are the Marocche. Marocche deposits cover the lower Sarca valley north of Lake Garda for a length of more than 8 km with a deposit thickness of about 200 m. Both collapse and bedding parallel sliding are a consequence of dip slopes and the extreme relief on the right side of the valley of nearly 2000 m from the bedrock below the valley floor to the peaks combined with the zones of structural weakness. The rock avalanches developed within carbonate rocks of Mesozoic age, mainly limestones of the Jurassic Calcarei Grigi Group. The main scarps are located on the western side of the lower Sarca Valley, along the steep faces of Mt. Brento and Mt. Casale. The presence of these scarps is strictly related to the Southern Giudicarie and the Ballino fault systems. The former is here constituted by regular NNE-directed ESE-vergent thrust faults. The latter has been reactivated as normal faults. These complicated structural relationships favored complex failure mechanisms, including rock slide and massive collapse. At the Marocche itself, based on field relationships and analysis of lidar imagery, we differentiate two large rock avalanches: the Marocca di Kas in the south, which overlies and in part buries the Marocche (s.s.) in the northern sector. Previous mapping had suggested up to five rock avalanches in the Marocche area where we differentiate two. In spite of hypotheses suggesting failure of the rock avalanches onto stagnating late Pleistocene glaciers, preliminary ³⁶Cl exposure dating results for numerous boulders of the two deposits suggests middle and late Holocene ages. The latter are well comparable with post-Roman ages proposed by Trener in 1924 based on the presence of artifacts found at the base of the younger Marocche deposits during construction of hydroelectric tunnels early in the last century.

P 9.12

Late Holocene evolution of the Triftjegletscher constrained with ^{10}Be exposure and radiocarbon dating

Olivia Kronig¹, Susan Ivy Ochs¹, Irka Hajdas¹, Markus Christl¹, Christian Schlüchter²

¹ Laboratory of Ion Beam Physics (LIP), ETH Zurich, Otto-Stern-Weg 5, 8093 Zurich, Switzerland

² Institute of Geological Sciences, University of Bern, Baltzerstrasse 1+3, 3012 Bern, Switzerland

Glacial landforms record the history of past glacial fluctuations. A detailed documentation of those landforms allows for a reconstruction of the climatic change forming them. Although there is a lot recent research on Holocene glacier reconstruction in the Alps, a consistent statement about glacier fluctuation in the Alps is difficult to find. This is because Alpine glaciers reacted in different time scales to the climatic changes (response time) due to local climatic conditions, size of the glaciers and topography. Therefore, it is important to investigate more glacier forefields to improve the overall knowledge about the history of glacier fluctuations in the Alps. The aim of this work was to acquire an overview of different evolutionary stages during the Holocene of the the Triftjegletscher and the Oberseegletscher east of Zermatt (VS) in the Valais Alps, Switzerland (Fig. 1).

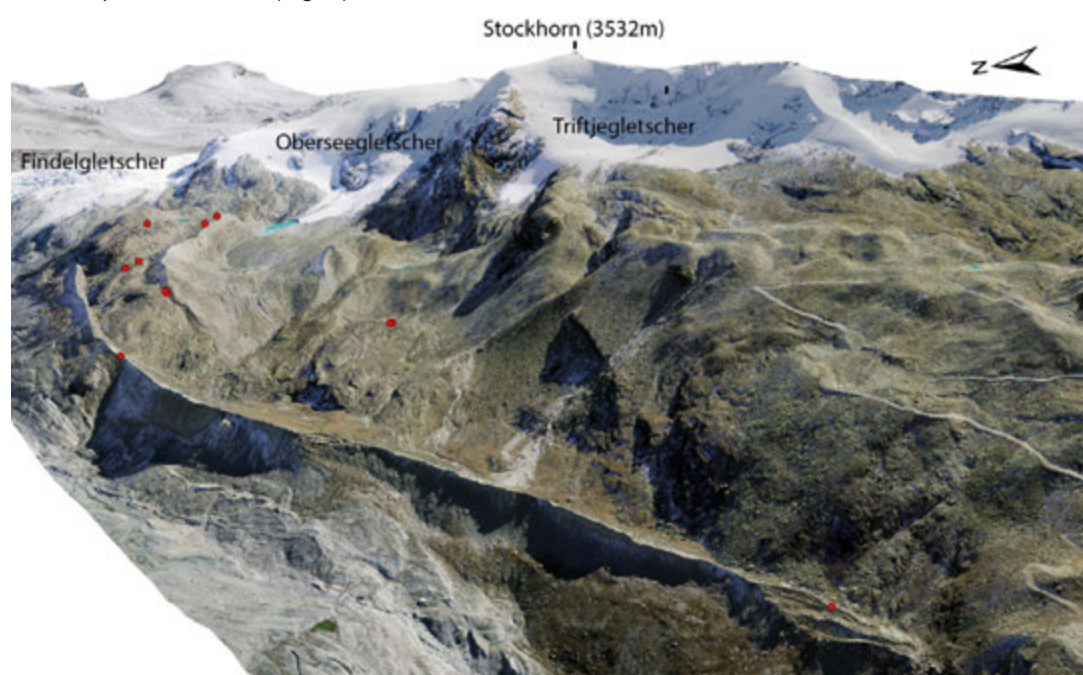


Figure 1. View to the south-east of the study area. Besides the remnants of the Oberseegletscher and the Triftjegletscher the most prominent landforms are visible; the big left lateral moraine of the Findelgletscher in the low left part and the two lateral moraines of the ancient Oberseegletscher. As a scale, the length of the visible Findelgletscher moraine is approximately 2.6 km. The red dots show the sample locations. The image was created based on the Swissimage 25 and the swissALTI3D, reproduced by permission of swisstopo (JA100120).

Although this location offers a range of glacial landforms of various glacial periods, this area has not been a part of any study thus far. A combined approach of precise geological and geomorphological observations, consisting of a detailed mapping of the study area, ^{10}Be exposure and radiocarbon dating were applied to obtain a better understanding of the local glacial history. Where field research and cross-cutting relations between glacial landforms give a relative history of the study area, exposure dating completes these observations by adding absolute ages to the glacial landforms.

Outside of the Little Ice Age (LIA) extents, documented by the Dufour map published in 1863, a total of twelve samples of boulders on moraines and bedrock were taken. Based on the gained results, four tentative important steps of the Holocene evolution until the LIA could be distinguished. An early Holocene stage, which documents the decay of the Egesen glaciers where the first parts of the study area became ice free. This was followed by a phase with no recordings and two glacier advancing periods in the late Holocene. A first advance around a thousand years ago, confirmed by several moraine ages and a bigger more extensive readvance during the LIA based on one ^{10}Be exposure and the radiocarbon age, and as shown on the historical maps. This later advance destroyed or overprinted the earlier landforms in most parts of the area, but still are visible in one place as overrun moraines. The youngest history of the study area since the LIA can nicely be observed in the field as approximately 1 m high moraine ridges, which can be assigned to the 1920s and 1980s advances with the help of maps, aerial photos and glacier monitoring done by the Versuchsanstalt für Wasserbau (VAW).

The interaction of fieldwork with ^{10}Be exposure and radiocarbon dating resulted in a nearly complete retrospection of the glacier fluctuation of the Triftjegletscher and the Oberseegletscher and helps to enhance the knowledge about the Alpine glacier history.

P 9.13

The geomorphological evolution of a landscape in a tectonically active region: the Sennwald landslide

Selçuk Aksay¹, Susan Ivy-Ochs², Kristina Hippe², Lorenz Grämiger¹ & Christof Vockenhuber²

¹ *Geological Institute, ETH Zurich, Sonneggstrasse 5, CH-8092, Zurich (selcukaksay@gmail.com)*

² *Labor für Ionenstrahlphysik (LIP), HPK, ETH Zurich, Otto-Stern-Weg 5, 8093 Zurich*

In this study, we investigate a pre-historical landslide in the Rhine valley in Sennwald, St. Gallen (Switzerland). Our study comprises detailed mapping of landform features, thin section analysis of landslide boulder lithologies, landslide volume estimation, numerical DAN-3D run-out modelling, surface exposure dating using the cosmogenic nuclide ³⁶Cl, and the spatial and temporal relationship of the event. Driving factors of the Sennwald landslide are also displayed with the recognition of geological and tectonic setting, earthquake frequency analysis and the slope deformation phenomena. In the Sennwald landslide, 92 million m³ of Lower Cretaceous limestones detached from the south-eastern wall of the Säntis Nappe and slid with a maximum travel distance of ~4'500 m and a "fahrboeschung" angle of 15° along the SE-dipping sliding plane almost parallel to the orientation of the bedding plane. Numerical run-out modelling results match the extent and the thickness of landslide deposits as observed in the field. Besides, velocities of maximum 90 m/s were obtained from the numerical run-out modelling. The exposure ages, the distribution of limestone boulders in the accumulation area, and the numerical run-out modelling support the hypothesis that the landslide was a single catastrophic event. The bedrock stratigraphy was preserved as geologically the top layer in the bedrock package travelled the farthest and the bottom layer the nearest during the landslide. The exposure ages imply that the rock failure occurred during the middle Holocene, a period of increased neotectonic activity in Eastern Alps (Prager et al., 2007). This time period also coincides with notably wet climate, which has been suggested as an important trigger for landslides around this age across the Alps (Zerathe et al., 2014).

REFERENCES

- Prager, C., Zangerl, C., Brandner, R., Patzelt, G., 2007. Increased rockslide activity in the Middle Holocene? New evidences from the Tyrolean Alps (Austria). *Landslides and climate change, challenges and solutions*. Taylor and Francis, London: 25-34.
- Zerathe, S., Lebourg, T., Braucher, R., & Bourlès, D. (2014). Mid-Holocene cluster of large-scale landslides revealed in the Southwestern Alps by ³⁶Cl dating. Insight on an Alpine-scale landslide activity. *Quaternary Science Reviews*, 90, 106-127.

P 9.14

Holocene destructive seismic periods in Western Anatolia: pace tracking beyond historical data

Nasim Mozafari Amiri¹, Ökmen Sümer², Dmitry Tikhomirov¹, Çağlar Özkaymak³, Bora Uzel², Susan Ivy-Ochs⁴, Christof Vockenhuber⁴, Hasan Sözbilir² & Naki Akçar¹

¹ *Institute of Geological Sciences, University of Bern, Baltzerstrasse 3, 3012 Bern, Switzerland
(nasim.mozafari@geo.unibe.ch)*

² *Department of Geological Engineering, Dokuz Eylül University, 35160 İzmir, Turkey*

³ *Department of Geological Engineering, Afyon Kocatepe University, Ahmet Necdet Sezer Kampusü, 03200 Afyonkarahisar, Turkey*

⁴ *Swiss Federal Institute of Technology, Institute for Particle Physics, Otto-Stern-Weg 5, 8093 Zürich, Switzerland*

The Western Anatolian Extensional Province is one of the most seismically active regions in the world with several major horst-graben systems which are formed as a result of approximately N-S extensional regime since the Early Miocene. The Büyük Menderes graben is one of these main tectonic structures, where the 37 km long NE-SW trending normal Priene-Sazlı fault is the main fault segment in its westernmost part built in carbonates.

In order to evaluate the destructive ruptures of the major faults and forecast the probable future earthquakes, a complete seismic data over a large time scale is required. However, the oldest historical earthquake in the Eastern Mediterranean and Middle East dates back to 464 B.C. and the instrumental earthquake data are only available for the last century. We used fault scarp dating with cosmogenic ³⁶Cl concentration to reconstruct the timing of paleoearthquakes and enlarge the existing seismic data records. 117 samples were collected on the Priene-Sazlı fault surface. The fault surface, colluvium and the top surface dip were measured 52, 20 and 31 degrees, respectively. The scarp rock and colluvium density were also evaluated 2.4 and 1.5 g/cm³, in turn. A new Matlab® code was used to reconstruct timing of the past ruptures and their related vertical displacements.

Our result shows the occurrence of five periods of high seismic activity in the Priene-Sazlı fault around 2, 3, 7, 8 and 11 kyr ago since the Late Pleistocene which are compatible with the existing seismic data. The ruptures remarks slip rate of approximately 1 mm/yr through the entire activity period of the fault. Priene-Sazlı fault is considered as a seismogenic fault which is capable of generating earthquake with magnitude of maximum 6.9.

P 9.15

Geotechnical properties of submerged slopes in Lake Zurich and the influence of their spatial variability on slope stability

Michael Strupler¹, Flavio S. Anselmetti², Michael Hilbe², Timo Fleischmann³, Achim J. Kopf³ & Michael Strasser^{1,4}

¹ *Geologisches Institut, ETH Zürich, Sonneggstrasse 5, CH-8092 Zürich (michael.strupler@erdw.ethz.ch)*

² *Institut für Geologie und Oeschger Centre for Climate Change Research, Universität Bern, Baltzerstrasse 1+3, CH-3012 Bern*

³ *MARUM - Center for Marine Environmental Sciences, D- 28195 Bremen*

⁴ *Institut für Geologie, Universität Innsbruck, Innrain 52, A-6020 Innsbruck*

Numerous subaquatic slope failures have occurred in the perialpine lakes of Switzerland since the deglaciation after the Last Glacial Maximum, and some of these have caused devastating tsunamis (e.g. Schnellmann et al., 2002; Kremer et al., 2012). A key part of hazard assessments, which will help to reduce potential future damage on infrastructure and communities induced by these processes, are subaquatic slope-stability analyses. As those require knowledge of several geotechnical and morphological properties, they are often subject to large uncertainty. Slope-stability models are usually based on data from only few sampling locations, which are assumed to represent characteristics of the entire slope. Hence, the spatial variability of the geotechnical parameters within a slope and the resulting uncertainty of the models often remains poorly constrained.

We present a high-resolution geotechnical dataset taken on a submerged slope in the up to 136 m deep main basin of Lake Zurich. The 'Oberrieden' study area (~2 km²) shows three distinct subaquatic landslides with well-defined head-scars, translation areas and mass-transport deposits with known ages. The failures have been assigned to different trigger mechanisms ranging from human-induced shore loading to earthquake shaking (Nipkow, 1927; Strasser, 2008).

Landslide features were detected on a 3.5 kHz pinger seismic reflection dataset and a 1 m DTM from 300 kHz multibeam bathymetry. Both datasets were used as basis for targeted coring and *in situ* geotechnical testing. A total of 8 Kullenberg-system piston cores (4 cores /km²) and 22 (11 cores /km²) short gravity cores were taken, and 39 Cone Penetration Tests (CPT) (~20 CPT samples /km²) were performed in the study area. The high density of sediment cores and CPT sites in a well-known area and the subsequent high-resolution measurements of the most important geotechnical parameters allow us to identify their distribution patterns and spatial variability within different sedimentological units.

A preliminary slope-stability analysis is presented, based on the acquired input data. Results show the importance of including spatial variability when modelling slope stabilities. The findings of this study can be extended in a further step to a basin-wide extent and transferred to other perialpine lakes in order to produce a subaquatic hazard map.

REFERENCES

- Kremer, K., Simpson, G. & Girardclos, S. 2012: Giant Lake Geneva tsunami in ad 563. *Nature Geoscience* 5. 756–757.
- Nipkow, H.F. 1927: Über das Verhalten der Skelette planktischer Kieselalgen im geschichteten Tiefenschlamm des Zürich- und Baldeggersees. *Neue Beiträge zur Biologie der Planktondiatomeen und zur biomorphose der subalpinen Seen*. Diss. Naturwiss. ETH Zürich, Nr. 455.
- Schnellmann, M., Anselmetti, F.S., Giardini, D., McKenzie, J.A., and Ward, S.N. 2002. Prehistoric earthquake history revealed by lacustrine slump deposits. *Geology* 30, 1131–1134.
- Strasser, M. 2008. Quantifying Late Quaternary Natural Hazards in Swiss Lakes: Subaquatic Landslides, Slope Stability Assessments, Paleoseismic Reconstructions and Lake Outbursts. *Beiträge zur Geologie der Schweiz, Geotechnische Serie*, 95, (published by Schweizerischen Geotechnischen Kommission SGK - ISBN 978-3-907997-30-7).

P 9.16**Reconstruction of sedimentary environments, climate and water level change of Urmia lake in the Holocene**

Javad darvishi khatooni¹

¹ *Geological survey of Iran (Javaddarvishi2007@yahoo.com)*

Urmia Lake is one of the biggest and salt over-saturated Lakes in the world. It is located at the northwestern part of Iran. This environmental hazard is one of the most significant geological problems of Iran. In this research, 28 sedimentary undisturbed cores having a maximum depth of 9 meters, and totally more than 200m were prepared by Auger coring method. Sedimentary facies were separated by color, grain size, sedimentary fabrics and evaporative minerals (Darvishi khatooni and Mohammadi, 2011). With regard to vertical sedimentary facies (from surface to sub-surface areas) changes, geography, climatic conditions and lake water level fluctuation were re-constructed. Facies are from Lake, Lagoon and Mud plain environments. Coring and verification of lake sub environment sedimentary facies indicate that sequential drying up tracks are visible in the coastal areas of Urmia lake. However, the main part of the lake had watery environment (6.5m of the lake floor sediments) for 13000 years (Darvishi khatooni et al, 2011). According to the dating by isotope carbon-14 method deposition rate is between 0.7 to 0.8 mm per year, but this rate is varies in different parts of the lake (1.0 to 1 mm per year). Wet years or droughts has direct effect on the various elements in the sediment. According to the proportions of these elements can identified the period of wet years or droughts, according to sedimentary geochemistry. Generally, the many facies and environmen changes at the Urmia lake, is under the influence of climatic, environmental and structural conditions.

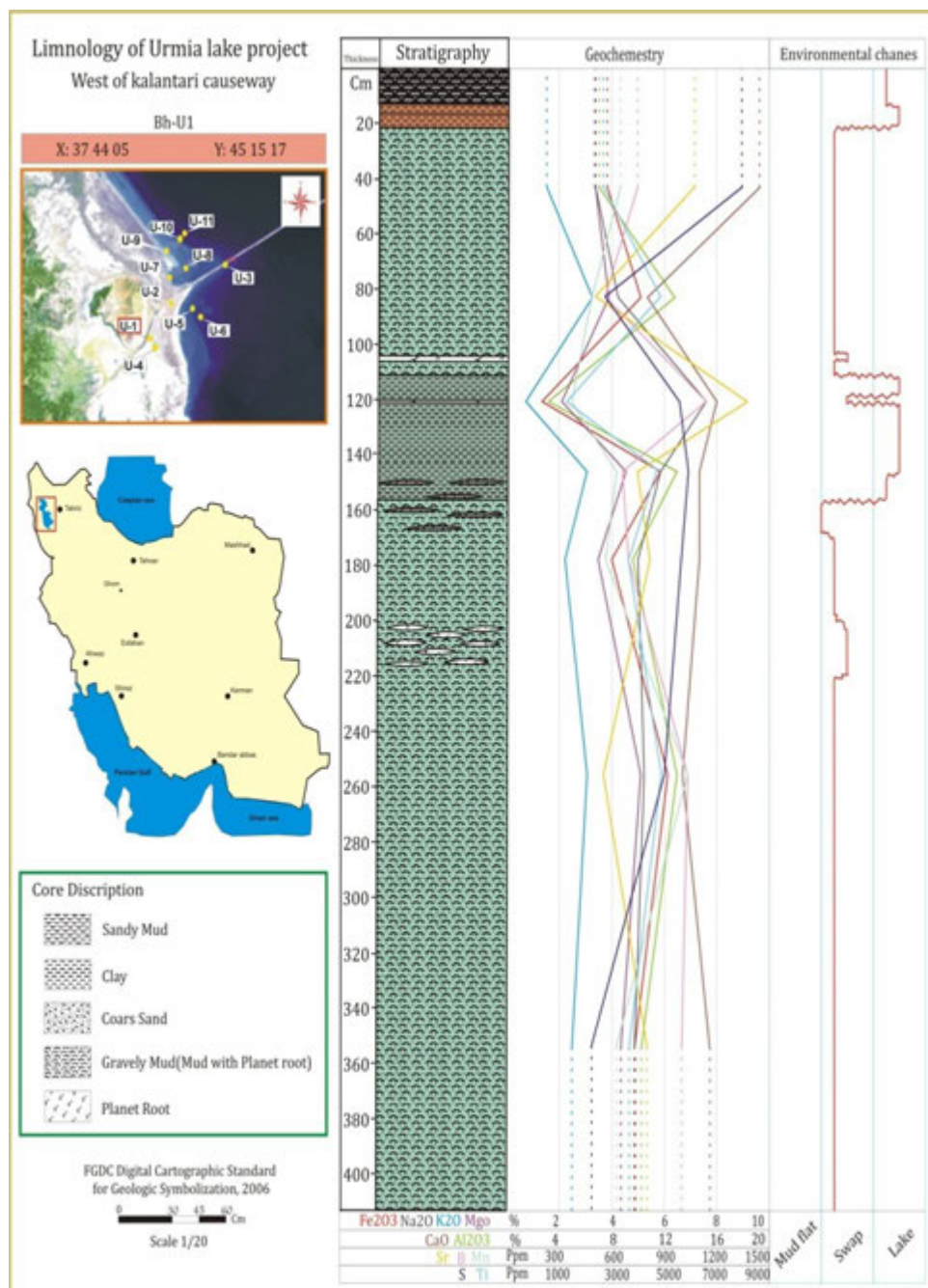


Figure 1. An example of one of the cores taken from the west of the Urmia lake, stratigraphic column, the relative change in the water level, sedimentary environment and sediment geochemistry.

REFERENCES

- Darvishi khtooni, J., Mohammadi, A., 2011. Report of limnology and paleolimnology of Urmia lake, phase III: paleoclimatology, paleoecology and paleogeography, geological survey of Iran. With out report number, 120 p(in persian).
- Darvishi khatouni, J., Mohammadi, A., Salehipure Milani, A., 2011. Effects of development projects on the level of Lake. 1th Urmia lake Environment Student Congress. Zanjan. Iran(in persian).

P 9.17

Paleo-climate and paleo-environment reconstruction based on a high-resolution, multi-proxy record from Lake Urmia (NW Iran)

Negar Haghipour¹, Timothy Ian Eglinton¹, Cameron McIntyre^{1, 2}, Daniela Hunziker³, Javad Darvishi Khatooni⁴ & Ali Mohammadi³

¹ *Geological Institute, Biogeosciences, ETH (negar.haghipour@erdw.ethz.ch)*

² *Laboratory of Ion Beam Physics, ETH Zurich*

³ *Geological Institute, ETH Zurich*

⁴ *Geological Survey of Iran, Marine Geology department*

Lake Urmia, in northwest Iran, is the largest saline lake in the Middle East with a surface area of ~ 5000 km². Historical documents mention its existence since at least 2000 years BC, and palynological investigation of a 100 m-long core suggested that the lake contains a sedimentary record spanning the last 200 ka. Despite this potential as an archive of paleo-climate and paleo-environmental information, there has been no molecular organic geochemical investigation or precise dating of these sediments. As part of an exploratory study, we have analyzed material from 3 recently collected, 8 m-long cores from the eastern, western and middle parts of the lake, with the aim of gaining insight into past depositional and environmental conditions from biomarker signatures preserved in Lake Urmia sediments.

The main objectives were to 1) constrain major source(s) of organic matter and gain insights into carbon cycle and depositional processes from bulk isotopic ($\delta^{13}\text{C}_{\text{org}}$, $\Delta^{14}\text{C}_{\text{org}}$) and molecular information, 2) determine the applicability of molecular proxies derived from glyceroldialkylglycerol tetraethers, GDGTs for paleo-temperature reconstruction and 3) reconstruct the paleo-vegetation and hydrology from compound-specific stable isotopes ($\delta^{13}\text{C}$ and δD of n-alkanes and fatty acids).

The age model based on 30 calibrated radiocarbon dates shows variation of sedimentation rates between early Holocene (~0.2 mm/a) and middle Holocene (~1.6 mm/a). The TOC and $\delta^{13}\text{C}_{\text{org}}$ also show a remarkable shift between early and middle Holocene.

The hydrocarbon fractions are dominated by long-chain n-alkanes, with n-C₂₉ and C₃₁ as the dominant homologues in most of the analysed samples from the three cores. Based on the n-alkane distribution, we distinguish two main types; Type 1 mainly includes samples deeper than ca 4 m (CPI= 10.2, ACL= 30); it is characterized by a terrestrial higher plant source; Type 2 comprises mainly shallower samples (CPI=1.5, ACL = 27.3) which may suggest an increased contribution of aquatic plants. Preliminary GDGT analyses indicate low BIT values, which suggest little input of soil-derived branched-GDGTs. The fact that Urmia Lake is large and little affected by in situ production of iso-GDGTs from methanogenic Euryarchaeota makes the measured TEX₈₆ proxy reliable. From 9-11 ka samples show low organic productivity probably due to cold and arid climate. Before 3 ka, slight increase in organic productivity indicates warmer/wetter conditions.

P 9.18**Paleohydrology, paleoenvironment and biomineralization in Lagoa Pitanguinha, Rio de Janeiro, Brazil**

Daniela Hunziker¹, Crisogono Vasconcelos¹

¹ *Climate Geology, Geological Institute, ETH Zürich, Sonneggstrasse 5, CH-8092 Zürich, (daniela.hunziker@erdw.ethz.ch)*

Microbialites are biogenic sedimentary bodies that form mainly by the activity of cyanobacteria since the Arcean until the present. Thrombolites form associated with microbial mats in Lagoa Pitanguinha, a hypersaline coastal lagoon about 100km to the east of Rio de Janeiro (Brazil). This lagoonal system developed as a result of climate related sea level fluctuations in the quaternary. Lagoa Pitanguinha resulted from the last episode of regression in Holocene initiated around 7000 years ago. Since then, the changes of hydrology and microbial activity in this environment is preserved in the sediment record. Modern microbial mats and thrombolites produce different carbonates as a result microbial activity and environmental conditions. The goal of this study is to elaborate the evolution history of Lagoa Pitanguinha with respect to climate changes and local hydrology. Then we want to correlate the changes in sedimentology with phases of increased microbial carbonate precipitation to elucidate the most relevant factors. A sediment core shows the dominance of microbial mats in the uppermost 10 cm and lower levels with several sparsely distributed thinly laminated carbonate layers. A combination of different approaches using XRF elemental analysis, X-ray diffraction, stable isotope analysis on carbon and carbonates will be conducted to investigate environmental changes. Petrography, electron microscopy and stable isotope analysis on microbialites will shed light on the processes involved in their formation. Combining both concepts indicates how and to what extent environmental and climatic changes influence microbial activity and related carbonate precipitation.

P 9.19

Radiocarbon dating of leaf waxes in the Kurtak loess-paleosol sequence, Central Siberia

Mischa Haas¹, Roland Zech², Sönke Szidat³, Gary Salazar³, Marcel Bliedtner²

¹ Department of Earth Sciences, ETH Zürich, Sonneggstrasse 5, CH-8092 Zürich (mihaas@student.ethz.ch)

² Geographical Institute and Oeschger Centre for Climate Change Research, University of Bern, Hallerstrasse 12, CH-3012 Bern

³ Department of Chemistry & Biochemistry and Oeschger Centre for Climate Change Research, University of Bern, Freiestrasse 3, CH-3012 Bern

Loess-paleosol sequences (LPS) are valuable, more or less continuous archives for Quaternary climate and environmental changes. However, precise and reliable chronologies are key to every paleo-reconstruction. So far, LPS are generally dated using luminescence analyses with ~10% uncertainties or radiocarbon analyses e.g. on charcoal, macrofossils of terrestrial plants, total organic carbon (TOC) or chemical fractions. Over the last few years, new proxies were introduced in LPS research, so called leaf wax lipid biomarkers which are persistent and hardly decomposable molecular components produced by higher terrestrial plants. Leaf waxes like *n*-alkanes are accumulated syndepositionally on the topsoil after litter fall and preserved over long periods of time. Häggi et al. (2014) recently corroborated the stratigraphic integrity and the great potential of leaf wax biomarkers for dating LPS.

We tested a newly developed prep-GC (Brechtbühler AG, Prep9000) to collect specific *n*-alkane homologues and to establish a compound-specific radiocarbon age chronology for the key LPS Kurtak, Central Siberia. Recoveries were generally very low (33% ± 13%, *n*=30), so we had to mainly date zeolite-cleaned total *n*-alkane fractions. Two compound-specific and thirteen *n*-alkane fractions from selected samples were measured on a MICADAS (Mini Carbon Dating System) accelerated mass spectrometry (AMS) system with an online-coupled Elemental Analyzer (EA). The results were corrected for both a constant contamination of 0.91 µg C (Fm 0.72) and a memory effect of 0.2%. Nevertheless, ages for the MIS 2 loess range from 16.3 to 22.8 ky, and ages for the MIS 3 paleosol range from 27.3 to 48.6 ky, respectively. This is in good agreement with independent age control based on luminescence and radiocarbon dating, corroborating the stratigraphic integrity of leaf waxes and the great potential to use compound-specific ¹⁴C analysis for establishing late Quaternary chronologies in LPS back to 30 – 40 ky.

REFERENCES

Häggi, C., Zech, R., McIntyre, C., Zech, M., and Eglinton, T., 2014, On the stratigraphic integrity of leaf-wax biomarkers in loess paleosols: Biogeosciences, v. 11, no. 9, p. 2455-2463.

P 9.20**Leaf wax patterns and compound specific isotope analyses in a permafrost section near Igarka, Northern Siberia**

Imke Kathrin Schäfer¹, Lea Illona Schweri¹, Nikita Tananaev² & Roland Zech¹

¹ *Institute of Geography and Oeschger Centre for Climate Change Research, University of Bern, Hallerstrasse 12, CH-3012 Bern (imke.schaefer@giub.unibe.ch)*

² *Igarka Geocryology Laboratory, Melnikov Permafrost Institute, Merzlotnaya St., 36, RU-677010 Yakutsk*

Long chain *n*-alkanes and *n*-alcanoic acids are essential constituents of leaf waxes in higher plants. They are preserved in soils and sediments and can be used as biomarkers for paleovegetation and paleoclimate reconstruction. Here we present the results of leaf wax analyses from a permafrost outcrop at the left banks of the Yenisei River near the city of Igarka, Northern Russia. Fluvio-glacial sediments are exposed in the lower part of the outcrop and probably date back to ~60 ka. The upper part consist of aeolian sediments deposited since, overprinted by various pedogenetic processes. First results indicate a continuous contribution of deciduous trees to the vegetation during the last glacial. Compound specific deuterium and radiocarbon analyses are in progress in order to investigate changes in paleoclimate and to establish a robust chronology.

P 9.21

Scientific-Methodological Approaches Of Revelation Of Landscape-Recreation Potential Of Mountain Geosystems (On example of Southern slopes of the Greater Caucasus)

L.A. Ismaylova

Azerbaijan National Academy of Sciences, Institute of Geography named after acad. H.Aliyev, H.Javid str. 31, Baku, AZ1143, Azerbaijan

The rapid development in terms of recreation of mountainous in recent years areas increased interest in the study of mountains that characterized by high dynamism and sensitivity to anthropogenic factors.

The complexity of geological structure, sharp change of the relief, horizontal and vertical differentiation of the slope incline, exposition, absolute altitude and periodic change of mezo-micro climate conditions within mountainous areas has formed geosystems with complex structure - functional characteristics. Wrong anthropogenesis interference influences to this type of mountain structures causes sharp ecological disbalance within landscapes that results in rapid activation hazardous natural processes such as floods, landslides, collapse, erosion etc.

The study in GIS environment of the modern landscapes of the area between Filfilichay-Girdimanchay area of high flood hazardous Demiraparanchay's basin will make more efficient use of the areas that are rich in recreational potential and will allow develop tourism complexes on the basis of the landscape planning.

Research area. Demiraparanchay basin was chosen as an example area for research purposes. Floody Demiraparanchay basins' area is 596 km², length 69 km and starts from the 3850 m height on the southern slope of the Greater Caucasus range. The water flow rate of the river 40-60% supported by ground waters. Annual average water debit is 3-10 m³/sec. Flow of the river comes 26% in spring, 23% in autumn, 35% in summer and 16% in winter.

The data that have been registered as elements of tourism-recreation potential were analyzed in Geographic information system and evaluated by five point scale system. Here, 1st point scale was accepted as very favorable, 2nd as favorable, 3rd as middle favorable, 4th as less favorable, 5th as very small favorable. During evaluation of recreational potential of landscapes, the special attention has been given to development opportunities of tourism potential in this area.

For example, 1st point scale zone of foothills and low mountains with forest and scrub forest, meadow and forest landscape is very profitable for different types of tourism and recreation opportunities.

Demiraparanchay river is the most dangerous flood risk river in the Southern slope of the Greater Caucasus after Shinchay and Kischay rivers. The intensity of exo-dynamic processes within rivers' basin, regular floods and landslides here has strongly influenced formation of the surrounding areas and landscapes, strongly affected landscape inner differentiation and increased landscape-ecological tension here.

Geological structure, lithology composition of the rocks strongly affected formation of modern landscapes of the Demiraparanchay basin. The prevalence of gravitational – tectonic ruptures in this area has intensively influenced formation of landslides, sets of valley-ravines and rock falls in this area. During estimation of recreation potential of the areas, the following criteria goes into consideration: relief of the area (relative height, incline, degree of decomposition of the area, watershed and river profile and so on), area's climate indicators, richness and species of vegetation, water resources, natural landscape diversity, anthropogenic changes within the area and possibilities of creation of transport infrastructures for the area.

For the purpose of reduction of mountainous geosystems' degradation level, along with mitigation of the negative influences coming from anthropogenic activity and to prevent overweight of the landscapes we analyzed the sustainability of the landscapes from anthropogenic changes, and for the area that are subject for the recreation development we have plotted 1:100 000 scale maps of landscapes and recreation potential along with map of soils use on the basis of field works data and using GIS based pictures from several satellites (Landsat 7 ETM+, SPOT 1-4, OrbView-3 and others). In conclusion, it is outlined to compile a landscape planning program where the complex measures for this area will be highlighted (Figure 1).

REFERENCES

- ANTIPOV, A.N., SEMENOV, YU., M. Russian School of Landscape Planning // *Annals of Agrarian Science*. – 2005. – Vol. 3, № 2
- GOLDBERG, M., AI VO M., KARAM, G. Theanalysis of Landsat imagery using an expert system: forestry applications// *Proc. Auto Carto 6*. -1984.- p.493-503

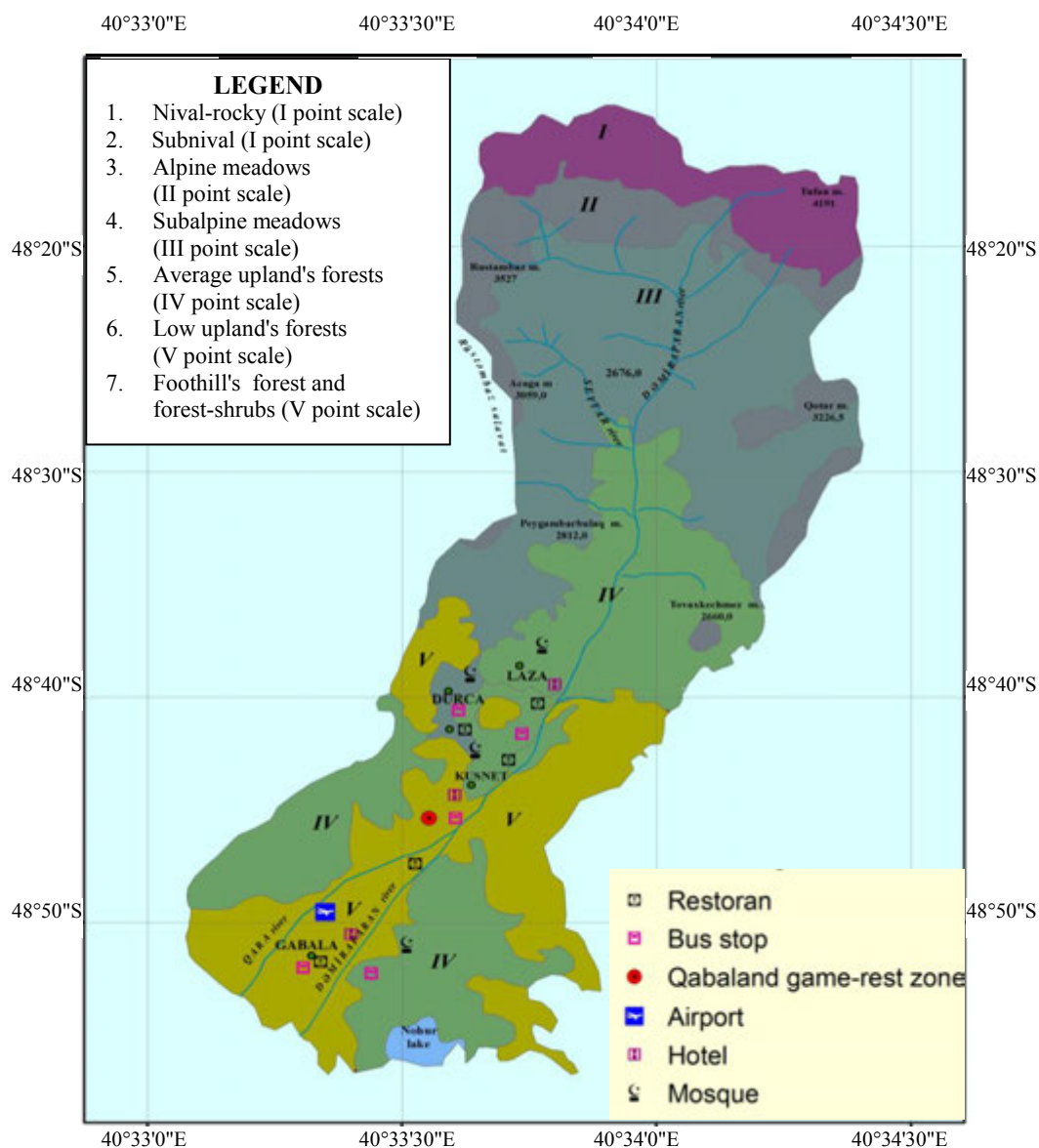


Figure 1 Map of of estimation of recreation potential and torism opportunities of the Demiraparanchay river basin landscapes according to landscape zones (M 1: 100 000)

I - very favorable, II - as favorable, III - as middle favorable, IV - as less favorable,

V - as very small favorable

10. Palaeontology

M. Schwikowski, A. Bauder, M.Lüthi, J. Alean, Martin Heggli, Jeannette Nötzli

Swiss Snow, Ice and Permafrost Society

TALKS:

- 10.1 Becker P., Jouvet G., Seguinot J., Funk M.: Glacier extent and climate conditions in the Alps at the Last Glacial Maximum: A glaciological modelling approach
- 10.2 Bohleber P. (solicited): Long-term atmospheric temperature and mineral dust variability recorded in the Colle Gnifetti multi core array
- 10.3 Dal Farra A., Schwikowski M.: Effect of particulate matter on the albedo of alpine glaciers
- 10.4 Gäggeler H.W. (solicited): Historic Reminiscences that led to the Colle Gnifetti ice core program and accompanying atmospheric studies
- 10.5 H. Machguth, H.H. Thomsen, A. Weidick, J. Abermann, A.P. Ahlstrøm, M.L. Andersen, S.B. Andersen, D. van As, R.J. Braithwaite, A.A. Bjørk, J. Box, C.E. Bøggild, M. Citterio, P. Clement, W. Colgan, R.S. Fausto, K. Gleie, B. Hasholt, B. Hynek, N.T. Knudsen, S.H. Larsen, S.H. Mernild, H. Oerter, O.B. Olesen, K. Steffen, M. Stober, S. Sugiyama, R.S. van de Wal: Old data in help of modern science; restoring Greenland's melt history
- 10.6 Haeberli W. (solicited): A temperate-cold debate and the initiation of ice core drilling/glaciology research on Colle Gnifetti
- 10.7 Hoelzle M. (solicited): Three decades of englacial temperature measurements on Colle Gnifetti, Monte Rosa
- 10.8 Licul A., Herman F., Podladchikov Y., Räss L., Omlin S.: Full Stokes glacier modeling on graphic cards
- 10.9 Lüthi M.P. (solicited): Colle Gnifetti: challenges of modeling the ice flow
- 10.1 Mazzotti G., Moeser D., Jonas T.: Modelling snow cover below coniferous canopies: The effect of snow interception
- 10.11 Preiswerk L.E., Anandakrishnan S., Beutel J., Burkett P.G., Dalban Canassy P., Funk M., Limpach P., Marchetti E., Meier L., Neyer F., Walter F.: Monitoring unstable parts in the ice covered Weissmies northwest face
- 10.12 Rastner P., Mölg N., Bolch T., Pau F.: A new glacier inventory for the Pamir-Karakoram region
- 10.13 Schwikowski M. (solicited): European pollution history recorded in Colle Gnifetti ice cores
- 10.14 Simioni S., Sidler R., Dual J., Schweizer J.: Measuring and modeling wave propagation and weak layer failure due to explosive loading in snow

POSTERS:

- P 10.1 Bosson J.-B., Capt M., Fischer M., Micheletti N., Lane S., Lambiel C.: Internal structure, dynamics and genesis of a small heavily debris-covered glacier system (Tsarmin Glacier; Arolla, Vs)
- P 10.2 Delaney I., Weidmann Y., Huss M.: Erosion Rates and Processes in a Glacier's Forefield Over a 28 Year Period
- P 10.3 Dizerens C., Hüsler F., Wunderle S.: Webcam imagery rectification and snow classification – potential for complementing satellite-derived snow maps over Switzerland
- P 10.4 Gaume J., van Herwijnen A., Chambon G., Schweizer J.: Dynamic crack propagation in weak snowpack layers: from field experiments to discrete element modeling
- P 10.5 Gindraux S., Farinotti D., Fischer M., Bösch R.: Accuracy assessment of UAV photogrammetry on Alpine glaciers
- P 10.6 Kronenberg M., Barandun M., Hoelzle M., Huss M., Farinotti D., Azisov E., Usabaliev R., Gafurov A., Petrakov D., Käab A.: Mass balance reconstruction for Glacier No. 354, Tien Shan, from 2003 to 2014
- P 10.7 Licciulli C., Bohleber P., Wagenbach D., Eisen O., Gagliardini O., Hoelzle M.: Supplementing ice core time series at Colle Gnifetti with a 3D full Stokes ice flow model using Elmer/Ice
- P 10.8 Lucas C., Hajnsek I., Bühler Y., Marino A.: Observation of snow properties and avalanches with new polarimetric and interferometric ground radar
- P 10.9 H. Machguth, M. MacFerrin, D. van As, J. E. Box, C. Charalampidis, W. Colgan, R. S. Fausto, H.A.J. Meijer, E. Mosley-Thompson, R.S.W. van de Wal: Successive and intense melt rapidly decreases Greenland meltwater retention in firn
- P 10.10 Nötzli J., Delaloye R., Phillips M. & the PERMOS Scientific Committee: First results from PERMOS after the hot summer 2015
- P 10.11 Paul F.: Fifty years of glacier surges in the central Karakoram
- P 10.12 Proksch M., Löwe H., Schneebeli M.: A local calibration approach to derive snow structural parameters from SnowMicroPen measurements.
- P 10.13 Ragettli S., Bolch T., Immerzeel W., Pellicciotti F.: Glacier changes in a Nepalese catchment and hydrological impacts
- P 10.14 Seguinot J., Bauder A., Funk M., Jouvett G., Limpach P., Neyer F., Ryser C., Sugiyama S. and Weidmann Y.: Measurements of ice dynamical properties of Bowdoin Glacier, Northwest Greenland
- P 10.15 Tilg A.-M., Marty C., Klein G.: An automatic algorithm for validating snow depth measurements of IMIS stations
- P 10.16 Tognini P., Inglese M., Ferrario A., Ubaldi M., Testa P.: Role of glacial caves in the evolution of glaciers: examples on the Forni Glacier (I), Morteratsch and Aletsch Glacier (CH)
- P 10.17 Vieli A., Lüthi M., Moreau L., Joughin I., Reisser M., Mercenier R., Rohner C.: Long-term dynamics and forcing of a tidewater outlet glacier in West Greenland

- P 10.18 Werder M., Huss M.: Towards the volumes of all the glaciers in the world 2.0
- P 10.19 Azisov E., Kronenberg M., Barandun M., Hoelzle M., Usabaliev R.: Glacier Monitoring on Golubin Glacier since 2011
- P 10.20 Avak S.E., Birrer M., Wälle M., Bartels-Rausch T., Schwikowski M., Eichler A.: Development of a Cryocell for High-Resolution Trace Element Analysis of Ice Cores Using LA-ICP-MS
- P 10.21 Bartels-Rausch T., Orlando F., Huthwelker T., Waldner A., Ammann M.: The nature of frozen salt solutions: A new in-situ XPS approach
- P 10.22 Edebeli J., Ammann M., Eichler A., Schneebeli M., Bartels-Rausch T.: Temperature dependence of ozone loss by reaction with NaBr-films in coated-wall flow-tubes
- P 10.23 Hoffmann H., Greulich S., Schock M., Stricker P., May B. Bohleber P., Wagenbach D.: Organic carbon investigations at ice cores from Colle Gnifetti – lessons learned and future challenges
- P 10.24 Stopelli E., Conen F., Zimmermann L., Morris C.E., Alewell C.: Ice nuclei and the landscape-precipitation feedbacks: an example from the Arctic environment
- P 10.25 Uglietti C., Zapf A., Jenk T., Szidat S., Salazar G., Hardy D.R., Schwikowski M.: The debate on the basal age of Kilimanjaro's plateau glaciers
- P 10.26 Waldner A., Orlando F., Birrer M., Ammann M., Huthwelker T., Bartels-Rausch T.: Acidic trace gas adsorption on ice: XPS analysis with the new NAPP experimetal cell at SLS
- P 10.27 Osmont D., Sigl M., Schmidely L., Wendl I., Isaksson E., Schwikowski M.: A 250-year black carbon record from the Lomonosovfonna ice core, Svalbard

10.1

Glacier extent and climate conditions in the Alps at the Last Glacial Maximum: A glaciological modelling approach

Patrick Becker¹, Guillaume Jouvét¹, Julien Seguinot¹, Martin Funk¹

¹ *Versuchsanstalt für Wasserbau, Hydrologie und Glaziologie (VAW), ETH Zürich, Hönggerberggring 26, CH-8093 Zürich (becker@vaw.baug.ethz.ch)*

About 20,000 years before present at the end of the Würm glaciation, glaciers in the Alps have reached their maximum extent and wide parts of the forelands were covered by ice. The climate conditions during the Last Glacial Maximum (LGM) are not fully understood. We reconstruct the Alpine ice cap at the LGM using numerical simulations of the ice flow. For this purpose we use the Parallel Ice Sheet Model (PISM) to simulate the glacier flow. PISM is a hybrid model superposing a Shallow Ice Approximation and a Shallow Shelf Approximation at the base as a pseudo sliding-law. For this reason, PISM is capable to simulate the time evolution of a large scale ice sheet for millennia by accounting for the dynamics of ice, englacial temperature, bedrock temperature, lithosphere deformation and surface mass balance. The latter is computed using a positive degree day model that is forced by climate data.

For reconstruction of the alpine ice cap we apply temperature cooling and precipitation reduction to present-day climate data. Our obtained glacier extent reconstructions will be constrained to geomorphological reconstructions of the glacier extent to study the prevailing climate conditions at the LGM. Further, we discuss our results with respect to non-glaciological studies.

10.2

Long-term atmospheric temperature and mineral dust variability recorded in the Colle Gnifetti multi core array

Pascal Bohleber^{1,2}

¹ *Climate Change Institute, University of Maine, Orono, ME 04469 USA (pascal.bohleber@maine.edu)*

² *Institut für Umweltphysik, Heidelberg University, Im Neuenheimer Feld 229, D-69120 Heidelberg*

Based on the first reconnaissance and ice coring activities at Colle Gnifetti (4450 m asl, Monte Rosa summit) the exceptional potential of this small firn saddle was already recognized as being the only drilling site in the European Alps that may offer ice core records over the last millennium and beyond. Due to an ice thickness of not much exceeding 100 m, the archiving of long-term records at Colle Gnifetti (CG) only becomes possible due to its exceptionally low net accumulation rates. The latter are a result of substantial snow loss driven by wind erosion, causing snow deposition to be characterized by a strong seasonal bias and pronounced spatio-temporal variability. Consequently, a robust interpretation of such long-term records is strongly challenged by depositional noise associated with a highly irregular annual layer stratigraphy.

Over the course of 40 years, an unique ice core array, including several drillings to bedrock, has been established and still continues to expand at CG. This multi-core array plays a key role for the reliable identification of atmospheric signals, following the reasoning that, opposed to local depositional noise, atmospheric signals have to have a common imprint on the variability of all cores.

To assist the time series comparison of multiple ice cores, ground-penetrating radar (GPR) has been deployed for extensive mapping of internal isochrone reflections between the CG drilling sites. However, observable internal GPR reflections are found restricted roughly to the firn zone (< 30 m) thus limiting the GPR assisted time series comparison to roughly the last 100 years or so.

Focusing on the instrumental time period first, it has been demonstrated how the depositional noise caveat is most evident in case of the relatively weak stable water isotope trends, in particular regarding their climatic significance in terms of the underlying temperature changes. The search for a common signal among the isotope time series of different CG cores has revealed a shared, temperature-related variability dominating in their supra-decadal signal components.

At present, two main challenges still lie ahead to fully exploit Colle Gnifetti's unique potential for long-term temperature reconstruction: (1) A quantitative interpretation of the shared isotope variability in the CG ice cores calls for an improved understanding of a peculiar high sensitivity value found when attempting to calibrate the isotope signal against instrumental temperature. (2) In combination with a relatively large vertical strain rate and rapid layer thinning, annual layer counting gets increasingly ambiguous as of approximately 100 years. As a consequence, the common signal investigation becomes flawed by substantial, yet hard to quantify uncertainty in the core's age-depth scales.

Regarding (2), remedy may come from novel sub-mm impurity analyses deployed for improved annual layer identification in combination with absolute age information provided by micro-radiocarbon analyses. By this means, shared variability in water isotopes and mineral dust was recently identified, for the first time, over the last millennium among two CG ice cores. As to ultimately contribute to other long-term proxy reconstructions for the Alpine realm, however, the high isotope sensitivity, the decisive role of upstream effects and a near-bedrock isotope anomaly still need to be specifically addressed.

This contribution is devoted to Dietmar Wagenbach (Institute of Environmental Physics, Heidelberg University), who unexpectedly passed away in December 2014. Dietmar's ingenious and passionate commitment to Colle Gnifetti's many intricate challenges has inspired generations of students and co-workers in Heidelberg and elsewhere.

10.3

Effect of Particulate Matter on the Albedo of Alpine Glaciers

Anna Dal Farra^{1,2,3}, Margit Schwikowski^{1,2,3}

¹ *Laboratory of Radiochemistry and Environmental Chemistry, Paul Scherrer Institut, CH-5232 Villigen PSI
(anna.dal-farra@psi.ch)*

² *Department of Chemistry and Biochemistry, University of Bern, Freiestrasse 3, CH-3012 Bern*

³ *Oeschger Centre for Climate Change Research, University of Bern, Falkenplatz 16, CH-3012 Bern*

It is known that glaciers worldwide are melting and that the reduction of their surface albedo is a major contributing factor. Snow albedo can be reduced by the presence of particles, which can accelerate melting by absorbing the sunlight and converting it into heat [Warren et al., 1985; Jacobson, 2004]; it has been shown that the same process is true for the albedo of bare ice [Qu et al, 2014].

To study this phenomenon we focused on Plaine Morte glacier (a wide and flat glacier located between the cantons of Valais and Bern) already subject of many studies [Huss et al, 2013] where we collected fourteen samples and took reflectance spectra with Fieldspec4 ASD. We selected this glacier because it presents a strong negative mass balance and has been snow free during the summer for the past ten years. The exposed bare ice results in the lowering of glacier albedo, partly because ice has a lower albedo than snow but principally because the snow free surface reveals an accumulation of a dark and well distributed particulate matter which is primarily composed of:

- Mineral dust (from local or distant sources)
- Soot, (deposited by wet or dry deposition)
- Organic matter (algae, bacteria and decomposition products)

These are the key players in the albedo lowering phenomenon and their contribution depends on the quantity in which they are present on the glacier and on their light absorbing properties.

To quantify the presence of these three components on the glacier's surface a thermal optical method was employed. This method quantifies the fraction of organic carbon (OC) and of elemental carbon (soot). The sample is combusted according to a specific protocol (Swiss_4S) [Zhang, 2012] and the CO₂ emitted at the different temperatures is detected. The measurements show that for the analyzed samples the soot and the organic matter range respectively around 1% and 3.5% revealing the preponderance, in the glacier particulate matter, of mineral dust (Fig. 1.b)

To determine the relative albedo lowering property of each component a hyperspectral imaging spectrometer was employed. This instrument allows the collection of images in which for every pixel a reflectance spectrum is captured. At 100 X magnification a pixel is about 130 nm and the spectra collected are of wavelengths 400 to 1000 nm. Numerous reflectance spectra were collected for particles of organic material, soot and several different minerals. An average spectrum was defined for the three components and their integral was calculated (Fig. 1.a). The ratio between the three averages suggests that soot and organic matter reflected the least while minerals the most. Considering the link between absorption and reflection (1):

$$(1 = \alpha + \rho + \tau) \quad (1)$$

We can assume that their ratio will be valid for each component's albedo lowering property (Fig. 1.c). This way we obtained both the average quantity of each component on the glacier and their relative albedo lowering property.

Combining the two results we obtain a measure of which component contributes more to the lowering of surface albedo in the case of Plaine Morte glacier (Fig.1.d).

The results suggest that the primary cause of albedo reduction in Plaine Morte is the large presence of mineral dust; the organic matter and the soot are both indeed higher absorbents but are present on the glacier in lower quantities.

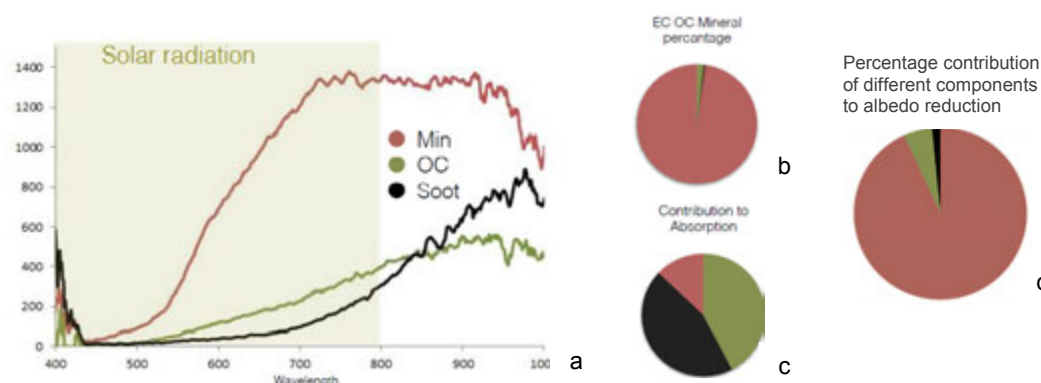


Figure 1. a) Average reflectance spectra for the three components. b) Composition of particulate matter. c) Albedo lowering properties. d) Percentage contribution of the different components to albedo reduction.

REFERENCES

- Warren S.G., Wiscombe W.J. 1985: A model for the spectral albedo of snow. II: snow containing atmospheric aerosols, *Journal of the Atmospheric Sciences* 37, 2712-2733
- Jacobson M.Z., 2004: Climate response of fossil fuel and biofuel soot, accounting for soot's feedback to snow and sea ice albedo and emissivity, *Journal of Geophysical Research: Atmospheres* 109, 21201 1-15
- Qu, B., Ming, J., Kang, S.-C., Zhang, G.-S., Li, Y.-W., Li, C.-D., Zhao, S.-Y., Ji, Z.-M., and Cao, J.-J. 2014: The decreasing albedo of the Zhadang glacier on western Nyainqentanglha and the role of light-absorbing impurities, *Atmos. Chem. Phys.*, 14, 11117-11128
- Huss, M., Voinesco, A., Hoesle, M. 2013: Implication of climate change on glacier de la Plaine Morte, Switzerland, *Geographica Helvetica* 68, 227-237
- Y. L. Zhang, N. Perron, V. G. Ciobanu, P. Zotter, M. C. Minguillón, L. Wacker, A. S. H. Prévôt, U. Baltensperger, and S. Szidat. 2012: On the isolation of OC and EC and the optimal strategy of radiocarbon-based source apportionment of carbonaceous aerosols, *Atmospheric Chemistry and Physics*, 12, 10841–10856

10.4

Historic Reminiscences that led to the Colle Gnifetti ice core program and accompanying atmospheric studies

Heinz W. Gaeggeler

¹ Labor für Radio- und Umweltchemie, Paul Scherrer Institut, CH-5232 Villigen (heinz.gaeggeler@psi.ch)

In the early 1970th Hans Oeschger and his group from Bern University started an extensive glaciological activity aiming at exploring the suitability of glacier ice from the Swiss Alps as archive of environmental information. Early field studies were performed at the Unteraargletscher, the Ewigschneefeld, the Jungfrauoch, the Plaine Morte and, finally, the Colle Gnifetti. The outcome of these studies were published in several progress reports and publications (e.g. refs [1-4]).

As final conclusion of these early activities it was realized that temperate glaciers are not suited for preservation of environmental species contained in ice while cold glaciers such as e.g. the Grenzgletscher on Colle Gnifetti are. Therefore, later ice core drill campaigns concentrated on Colle Gnifetti (4450 m asl). Some exceptions are studies performed at Fiescherhorn as well as at Col du Dome. The latter two places, however, did not enable investigations back in time over several millennia.

To complement paleoatmospheric studies at Colle Gnifetti two groups performed *in-situ* and continuous measurements at this high altitude site. The group from Heidelberg University (D. Wagenbach et al.) conducted continuous glacier surface measurements and determined the atmospheric composition (e.g. [5]) while a group from Paul Scherrer Institut (H.W.G. et al.) measured the total amount of aerosol particles in air with a time resolution of 30 min (e.g. [6]). Both projects yielded important information in order to interpret ice core data.

REFERENCES

- [1] U. Schotterer, R. Finkel, H. Oeschger, U. Siegenthaler, M. Wahlen, G. Bart, H. Gäggeler, H.R. von Gunten, Isotope measurements on firn and ice cores from alpine glaciers, Proc. Grenoble Symp. on Isotopes and Impurities in Snow and Ice, Aug./Sept. 1975: Actes du Colloque de Grenoble, IAHS Publ. No 118 (1977) 232-236
- [2] H. Oeschger, U. Schotterer, B. Stauffer, W. Haeberli, H. Röthlisberger, First results from alpine core drilling projects, Z. Gletscherkunde und Glazialgeol. Bd. 13, H.1/2 (1977) 193-208
- [3] H. Gäggeler, ²¹⁰Po(²¹⁰Pb) dating on the Colle Gnifetti Core of 1976 (appendix to ref. [2])
- [4] H. Oeschger, U. Schotterer, Die im Eis gespeicherte Information über die Geschichte von Naturvorgängen, Jahrbuch der Schweiz. Naturforschenden Gesellschaft, wiss. Teil (1978) 30- 46
- [5] S. Preunkert, D. Wagenbach, An automated recorder for air/firn transfer studies of chemical aerosol species at remote glacier sites, Atmos. Env., **32**, No 23 (1998) 4021 – 4030
- [6] H.W. Gäggeler, U. Baltensperger, D.T. Jost, M. Emmenegger, M. Schwikowski, Continuous background aerosol monitoring at high-alpine sites, Proc. EUROTRAC Symp. 1990, P. Borrell (Ed), SPB Academic Publishing, The Hague, The Netherlands (1991) 55-56

10.5

Old data in help of modern science; restoring Greenland's melt history

Horst Machguth^{1,2}, Henrik H. Thomsen¹, Anker Weidick¹, Jakob Abermann³, Andreas P. Ahlstrøm¹, Morten L. Andersen¹, Signe B. Andersen¹, Dirk van As¹, Roger J. Braithwaite⁴, Anders A. Bjørk⁵, Jason Box¹, Carl E. Bøggild⁶, Michele Citterio¹, Poul Clement¹, William Colgan⁷, Robert S. Fausto¹, Karin Gleie¹, Bent Hasholt⁸, Bernhard Hynek⁹, Niels T. Knudsen¹⁰, Signe H. Larsen¹, Sebastian H. Mernild¹¹, Hans Oerter¹², Ole B. Olesen¹, Konrad Steffen¹³, Manfred Stober¹⁴, Shin Sugiyama¹⁵ and Roderik S. van de Wal¹⁶

¹ Geological Survey of Denmark and Greenland GEUS, København, Denmark (horst.machguth@geo.uzh.ch)

² World Glacier Monitoring Service (WGMS), Department of Geography, University of Zurich, Zurich, Switzerland

³ Asiaq Greenland Survey, Nuuk, Greenland

⁴ The University of Manchester, Manchester, United Kingdom

⁵ Centre for GeoGenetics, Natural History Museum of Denmark, University of Copenhagen, Copenhagen, Denmark

⁶ Centre for Arctic Technology, Danish Technical University, Kgs. Lyngby

⁷ Department of Earth and Space Science and Engineering, York University, Toronto, Ontario, Canada

⁸ Department of Geosciences and Natural Resource Management, University of Copenhagen, Copenhagen, Denmark

⁹ Zentralanstalt für Meteorologie und Geodynamik (ZAMG), Vienna, Austria

¹⁰ Institute for Geoscience, Aarhus University, Aarhus, Denmark

¹¹ Glaciology and Climate Change Laboratory, Centro de Estudios Científicos (CECs), Valdivia, Chile

¹² Alfred Wegener Institute (AWI), Bremerhaven, Germany

¹³ Swiss Federal Institute for Forest, Snow and Landscape Research (WSL), Birmensdorf, Switzerland

¹⁴ Stuttgart University of Applied Sciences, Stuttgart, Germany

¹⁵ Institute of Low Temperature Science, Hokkaido University, Sapporo, Japan

¹⁶ Institute for Marine and Atmospheric Research Utrecht (IMAU), Utrecht, The Netherlands

Glacier surface mass balance measurements on Greenland started more than a century ago. While accumulation measurements have been compiled in a number of studies, no comprehensive overview of the data from the ablation zone of the ice sheet and from the local glaciers exists. These data are missing in the evaluation of modelled glacier mass balance, but also bare the potential of specifying changes in glacier melt independently from modelled data.

Here we present a comprehensive database of glacier surface mass balance observations from the ablation zone of the Greenland ice sheet and the local glaciers. The database covers a time span of 123 years and contains a total of ~3000 mass balance observations from 46 sites (Fig. 1). For each individual observation X, Y and Z coordinates, starting and ending dates and quality flags are provided. Sources are given for all entries and metadata.

Data were mostly collected from grey literature and unpublished archive documents. The majority of the data have not been published before and were thus inaccessible to the scientific community.

The data in the publicly available database are useful to improve our understanding of the melt on the ice sheet; but they also tell a compelling story of the history of Greenland research, of political and economic interests, Cold War legacy, and of creativity and endurance to overcome natural and technical limitations while measuring in the field.

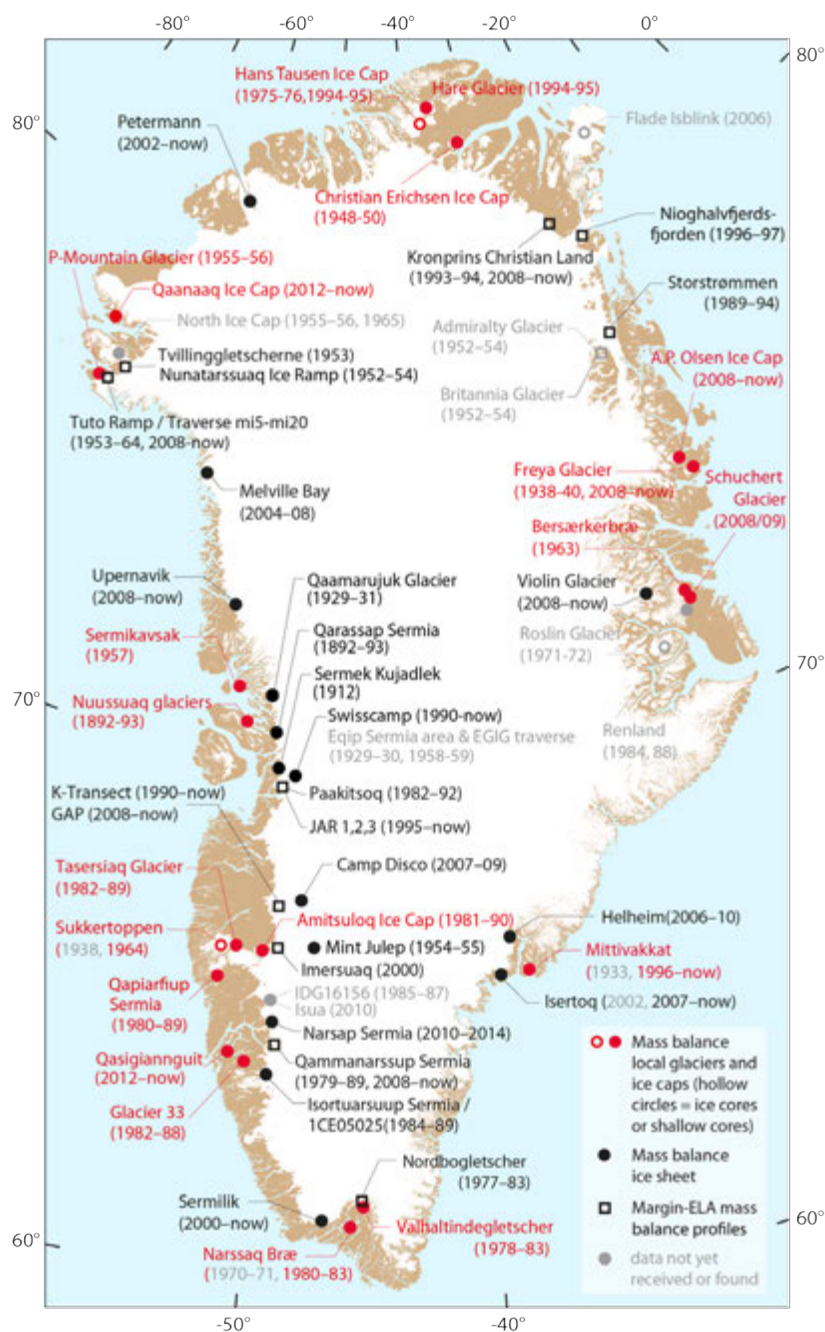


Figure 1. Map of the Greenland glacier surface mass balance observations contained in the database.

10.6

A temperate-cold debate and the initiation of ice core drilling/glaciology research on Colle Gnifetti

Wilfried Haeberli¹

¹ Department of Geography, University of Zurich, Winterthurerstrasse 190, CH-8057 Zurich, Switzerland
(wilfried.haeberli@geo.uzh.ch)

The initiation of core drilling and accompanying glaciological research on the cold firn/ice saddle of Colle Gnifetti, Monte Rosa, 4450 m a.s.l. (Figure 1), followed a debate and new insights in the mid 1970s concerning thermal conditions of Alpine glaciers. The existence of cold firn and ice on the highest Alpine summits had indeed been known for a long time already from observations in firn/ice tunnels: Vallot reported a mean temperature of -16.7°C for the summit ice cap of Mont Blanc in 1893 and Fisher temperatures down to -13.3°C near the ice-bedrock interface at Silbersattel, Monte Rosa, in 1952. Based on borehole temperature measurements in the tongue of Hintereisferner by Hess around 1900 and in the Jungfraufirn by Perutz in the late 1940s, however, the opinion nevertheless prevailed that the glaciers of the Alps are generally temperate, i.e. at phase-equilibrium or melting temperature.

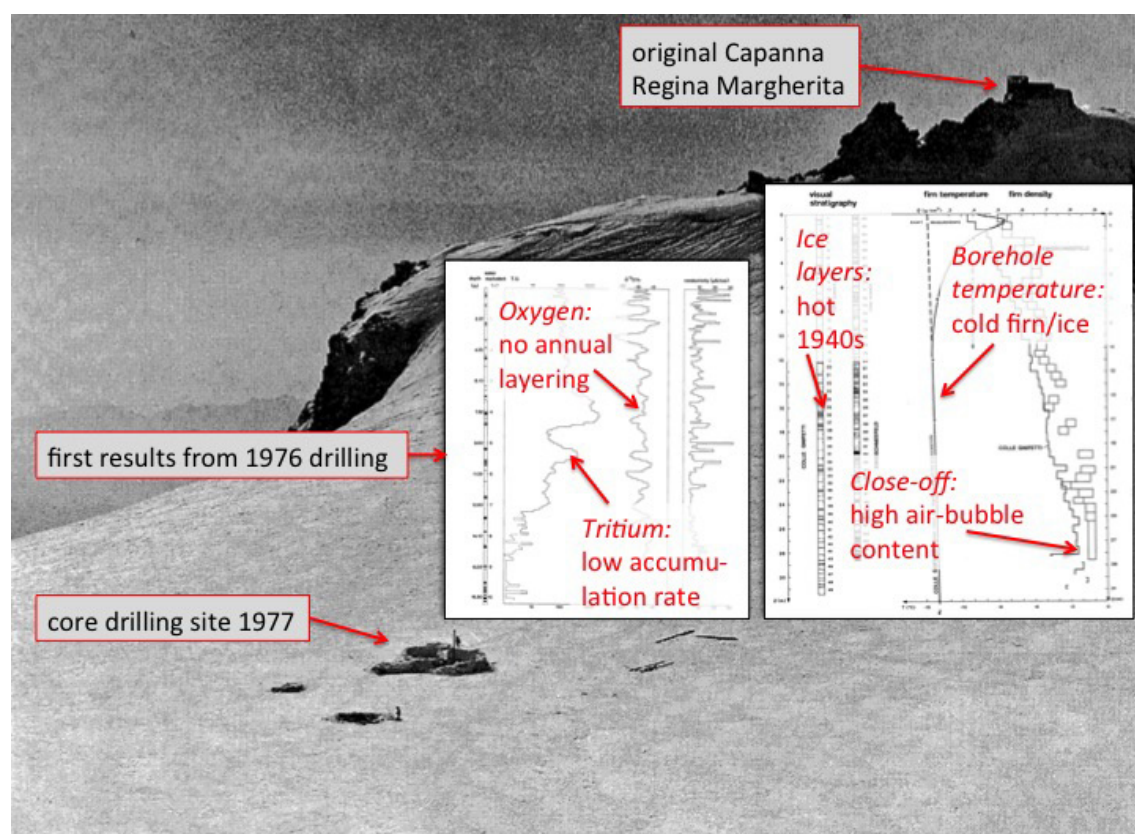


Figure 1: Colle Gnifetti, 4450 m a.s.l., on Monte Rosa in 1977 with the drill site 1977 and first principal insights from the 1976 core drilling (after Oeschger et al. 1978).

Shallow core drillings and borehole temperature measurements at various altitudes of Mont Blanc in 1973 together with temperature measurements in a deep borehole drilled 1974 into the polythermal tongue of Grenz glacier in the Swiss Alps documented the occurrence of cold and polythermal ice not only at highest altitudes but also in glacier ablation areas (Haeberli 1976, Lliboutry et al. 1976). The cold part of the Grenz glacier tongue was recognized to be “white” ice with a high air bubble content advected from the cold high-altitude accumulation area around Colle Gnifetti (cf. the numerical modelling by Blatter and Haeberli 1984) with a “recrystallization-infiltration” firn facies (melting-refreezing limited to the uppermost annual snow layer). With this it had become clear that good conditions existed at Colle Gnifetti for ice core drilling and corresponding environmental reconstructions.

The first firn/ice cores from Colle Gnifetti were recovered in 1976 and 1977 (Oeschger et al. 1978). Together with borehole temperature measurements and in-situ density determination of the cores, the first analyses confirmed that (1) the mean firn/ice temperature was close to -14°C and, hence, indeed far below melting temperature, (2) close-off (firn-ice transition) at a density of about 0.85 g/cm^3 was at greater depth than in temperate firn and indicated about 10% air content in the ice, (3) ice layer formation from melting/refreezing was limited to near-surface snow excluding perturbations by deeply percolating melt water, (4) a low accumulation rate of about 0.35 m water equivalent per year was determined from tritium, Sahara dust, ice layer concentration in the hot 1940s and $^{210}\text{Po}/^{210}\text{Pb}$, opening the possibility for the existence of relatively old ice (centuries to millennia) at greater depth, but (5) annual layering was not to be expected (^{18}O). These first experiences and insights encouraged further ice core drilling/analyses and glaciological research (accumulation patterns under the effect of strong wind erosion, borehole temperature monitoring, high-resolution radio-echo sounding, numerical model calculation of glacier flow and age, etc.) on cold high-Alpine firn and ice for many years to come (cf., for instance, Wagenbach et al. 2012).

Dietmar Wagenbach (Institute of Environmental Physics at the University of Heidelberg), who unexpectedly died in 2014, had joined the 1977 core drilling and later became one of the main drivers and scientific leaders of long-term work on Colle Gnifetti. The present contribution is devoted to his memory.

REFERENCES

- Blatter, H. and Haeberli, W. 1984. Modelling temperature distribution in Alpine glaciers. *Annals of Glaciology* 5, 18-22.
- Haeberli, W. 1976. Eistemperaturen in den Alpen. *Zeitschrift für Gletscherkunde und Glazialgeologie* XI (2), 201-220.
- Oeschger, H., Schotterer, U., Stauffer, B., Haeberli, W. and Röthlisberger, H. 1978. First results from Alpine core drilling projects. Appendix 1: $^{210}\text{Po}/^{210}\text{Pb}$ dating on the Colle Gnifetti core 1976 (H. Gäggeler). Appendix 2: Sahara dust in the Alps – a short review (W. Haeberli). *Zeitschrift für Gletscherkunde und Glazialgeologie* XIII (1-2), 193-208.
- Wagenbach, D., Bohleber, P. and Preunkert, S. 2012. Cold Alpine ice bodies revisited: What may we learn from their impurity and isotope content? *Geografiska Annaler: Series A, Physical Geography* 94, 245-263. doi:10.1111/j.1468-0459.2012.00461

10.7

Firn and ice temperatures at Colle Gnifetti, Monte Rosa, Switzerland/Italy

M. Hoelzle¹

¹ Department of Geosciences, University of Fribourg, CH-1700 Fribourg

A range of firn and ice temperature measurements was acquired in the Monte Rosa in the past three decades. These temperature measurements revealed no evidence of warming at the firn saddle of Colle Gnifetti at 4452 m a.s.l. between 1982 and 1991. From 1991 to present an increase of the englacial temperatures is observed, may indicating that the amount of infiltrating and refreezing meltwater at Colle Gnifetti has probably increased in the more recent past. This is confirmed by six existing boreholes with measured temperature down to bedrock, which were drilled in 1982, 1995, 2003 and 2005 and 2013. All the observed temperature profiles show a slight bending to warmer temperatures in their uppermost part indicating a warming of the firn, which can be related to the observed atmospheric warming in the 20th century. However, most drill sites on Colle Gnifetti are still located in the recrystallisation-infiltration zone, especially on the northern slope.

A stronger warming than on Colle Gnifetti was found at locations beneath on Grenzgletscher from 1991 to 2008. This warming is one order of magnitude greater than the atmospheric warming and can be explained only by a strong increase in the latent heat input by infiltrating and refreezing meltwater. The observations indicate that since 1991, an important firn area beneath Colle Gnifetti has already undergone a firn facies change from the recrystallisation-infiltration to the cold infiltration zone due to an increasing supply of surface melt energy.

10.8

Full Stokes glacier modeling on graphic cards

Aleksandar Licul¹, Frédéric Herman¹, Yuri Podladchikov², Ludovic Räss² and Samuel Omlin²

¹ *Institute of Earth Surface Dynamics, University of Lausanne, CH-1015 Lausanne, Switzerland (aleksandar.licul@unil.ch)*

² *Institute of Earth Sciences, University of Lausanne, CH-1015 Lausanne, Switzerland*

In the last decade, there has been a rapid development of ice flow models following the publication of the fourth IPCC report (Solomon et al., 2007) and an increased access to high performance computing facilities. The IPCC report revealed that ice sheet flow models did not provide an accurate description of polar ice sheet discharge (Gagliardini et al., 2013 and Pattyn et al., 2008). This was mostly because ice flow models were based on asymptotic approximations of the Stokes equations. In particular, Pattyn et al. (2008) showed through an inter-comparison exercise (so-called ISMIP-HOM inter-comparison) that one of the most important prerequisites for an ice flow model is to include an accurate description of the complex state of stress in the ice. Therefore, solving Stokes equations, or at least a higher-order asymptotic formulation, is essential, especially in areas where the basal topography and slipperiness vary greatly. Despite providing a more accurate description of ice flow, the application of these models is still limited by computation time. Applications are therefore limited to short timescales and relatively low resolution. To overcome this constrain, we investigate the potential of GPU acceleration in glacier modeling.

The goal of this research is to develop a three-dimensional Stokes solver and apply it to glacier flow. We numerically solve the Stokes momentum balance equations together with the incompressibility equation. We also take into account strong nonlinearities for ice rheology.

We have developed a fully three-dimensional numerical MATLAB application based on an iterative finite difference scheme with preconditioning of residuals. Differential equations are discretized on a regular staggered grid. We have ported it to C-CUDA to run it on GPU's in parallel, using MPI.

We demonstrate the accuracy and efficiency of our developed model by manufactured analytical solution test for three-dimensional Stokes ice sheet models (Leng et al., 2013) and by comparison with other well-established ice sheet models on diagnostic ISMIP-HOM benchmark experiments (Pattyn et al., 2008).

In future work we will apply our solver to real world applications and we will implement the free surface evolution capabilities.

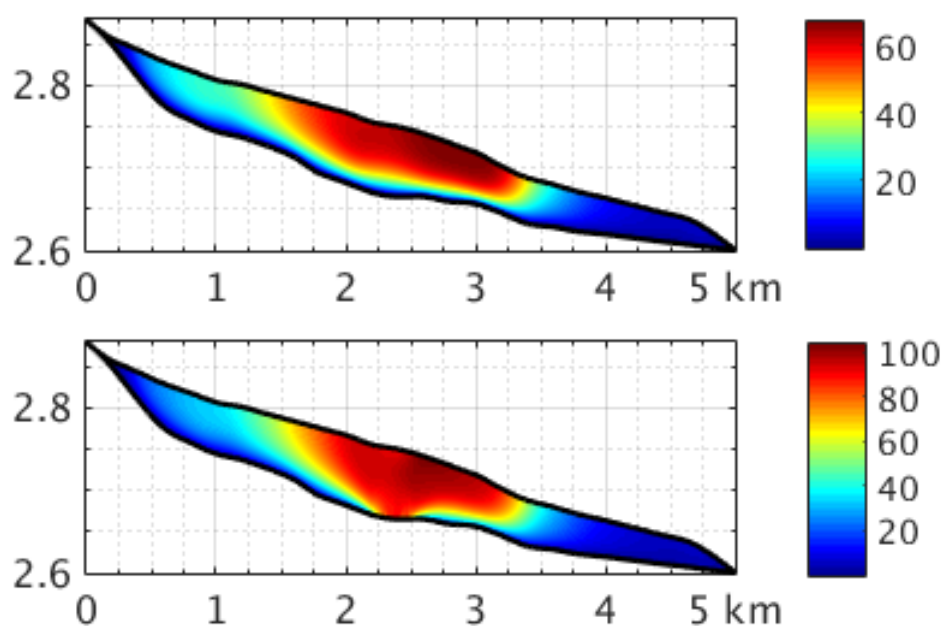


Figure 1. Simulation results for ISMIP-HOM Experiment E (Haut Glacier d'Arolla): L2-norm of the velocity (ma^{-1}) (top) Case I without sliding zone (bottom) Case II with sliding zone

REFERENCES

- Gagliardini, O., Zwinger, T., Gillet-Chaulet, F., Durand, G., Favier, L., de Fleurian, B., Greve, R., Malinen, M., Martín, C., Råback, P., Ruokolainen, J., Sacchetti, M., Schäfer, M., Seddik, H., and Thies, J.: Capabilities and performance of Elmer/Ice, a new-generation ice sheet model, *Geosci. Model Dev.*, 6, 1299–1318, doi:10.5194/gmd-6-1299-2013, 2013, 1125
- Leng, W., Ju, L., Gunzburger, M. & Price, S., 2013. Manufactured solutions and the verification of three-dimensional Stokes ice-sheet models. *Cryosphere* 7, 19–29.
- Pattyn, F., Perichon, L., Aschwanden, A., Breuer, B., de Smedt, B., Gagliardini, O., Gudmundsson, G.H., Hindmarsh, R.C.A., Hubbard, A., Johnson, J.V., Kleiner, T., Kononov, Y., Martin, C., Payne, A.J., Pollard, D., Price, S., Rckamp, M., Saito, F., Souk, O., Sugiyama, S. & Zwinger, T., 2008. Benchmark experiments for higher-order and full-Stokes ice sheet models (ISMIPh). *The Cryosphere* 2, 95–108.
- Solomon, S., Qin, D., Manning, M., Chen, Z., Marquis, M., Averyt, K., Tignor, M., and Miller, H.: *The physical science basis*, New York and Cambridge: Cambridge University Press, 235–337, 2007.

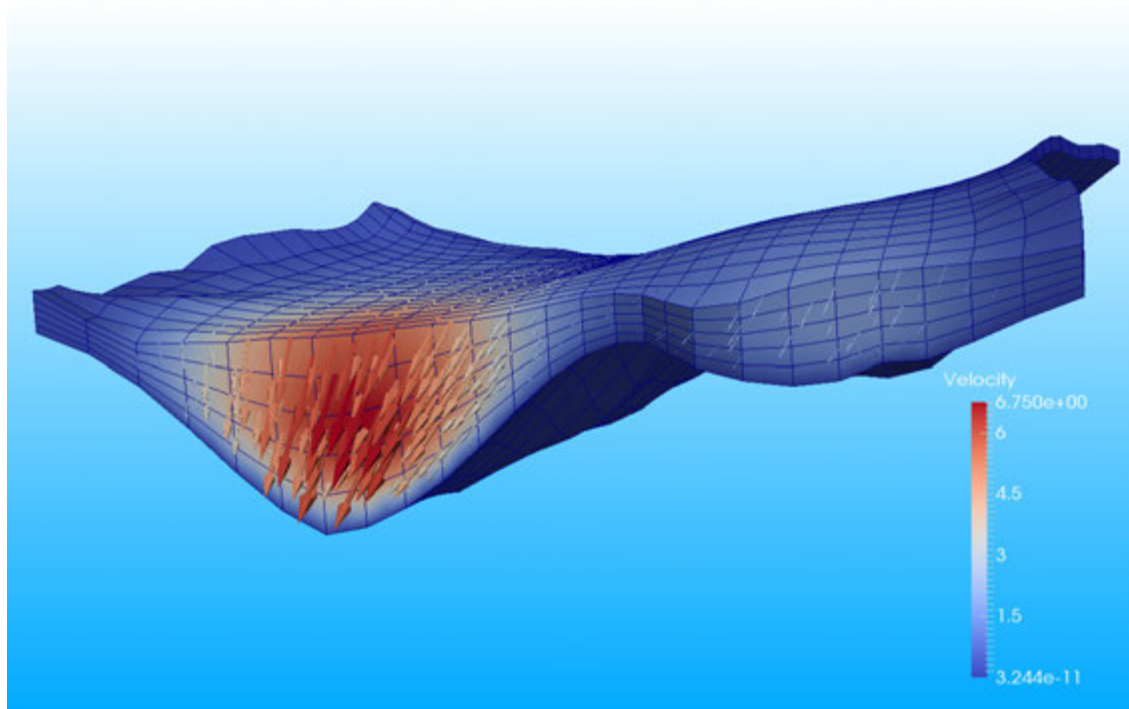
10.9

Colle Gnifetti: challenges of modeling the ice flow

Martin P. Lüthi

Department of Geography, 3G, University of Zurich, 8057 Zurich, Switzerland

Colle Gnifetti in the Monte Rosa massif of the Alps is a very high, saddle-shaped glacier where several ice cores have been drilled for climatological investigations. Dating these ice cores is notoriously difficult due to missing annual layers. Therefore, age-dating approaches based on ice flow models are necessary. I will discuss the challenges of ice flow modeling of this small glacier. The main difficulties include the rheology of compressible firn, the advection-diffusion of heat, the glacier geometry, the thermal boundary conditions, and the stress boundary conditions on the sides of the domain. The saddle-shaped geometry poses additional problems since the position of the saddle point might move due to external forcing or internal instabilities. Finally, ice flow modeling and age-dating approaches of different complexity are reviewed and compared.



Results from a 3D Finite Element ice flow model of Colle Gnifetti.

10.10

Modelling snow cover below coniferous canopies: The effect of snow interceptionGiulia Mazzotti^{1,2} David Moeser¹, Tobias Jonas¹¹ *Snow Hydrology Research Group, WSL Institute for Snow and Avalanche Research SLF, Flüelastrasse 11, CH-7260 Davos Dorf (giulia.mazzotti@slf.ch)*² *Laboratory of Hydraulics, Hydrology and Glaciology, Swiss Federal Institute of Technology Zurich ETHZ, Hönggerbergstr. 26, CH-8093 Zürich*

Understanding forest snow processes that affect the water balance of forested basins is of high importance in hydrological applications. The presence of the forest alters snow accumulation and ablation processes, thus giving rise to a high spatial heterogeneity of the below-canopy snow cover. The process of snow interception by the canopy has been found to be one of the main drivers of this variability.

The amount of intercepted snow in the canopy has traditionally been expressed as function of solid precipitation and generalized canopy characteristics. Most snow cover models integrate an interception model by Hedstrom and Pomeroy (Hedstrom & Pomeroy, 1998). However, a new model for snow interception has recently been developed by Moeser et al. based on interception measurements from single storm events (Moeser et al, 2015). By including more diversified canopy parameters in its parametrization, the model aims at an improved prediction of the process and its variability in space.

In this study both interception models were intercompared at several forested sites with varying canopy characteristics. To allow a straight comparison, both interception models were integrated with the Factorial Snow Model (FSM), a multi-model framework for energy balance-type snow cover modelling. Driving meteorological data was assembled and extrapolated to the modelled sites. Snow measurements for validation were collected during field campaigns. The model could be applied to 3 open sites and 1237 forest points at which the canopy characteristics were derived from LiDAR data.

The new Moeser model was found to produce results that vary substantially between points, while only little variability resulted for the Hedstrom and Pomeroy model. The spatial heterogeneity observed for the Moeser model corresponds well to the pattern of canopy structure and reflects the measured variability of the below-canopy snow cover.

REFERENCES

- Hedstrom, N.R., & Pomeroy, J. 1998: Measurements and Modeling of Snow Interception in the Boreal Forest. *Hydrologic Processes*, 12, 1611-1625.
- Moeser, D., et al. 2015: Improved Snow Interception Modeling Using Canopy Parameters Derived from Airborne LIDAR Data. *Water Resources Research* 2015 (accepted).

10.11

Monitoring unstable parts in the ice covered Weissmies northwest face

Lukas E. Preiswerk^{1,2}, Sridhar Anandakrishnan³, Jan Beutel⁴, Peter G. Burkett³, Pierre Dalban Canassy^{1,5}, Martin Funk¹, Philippe Limpach⁶, Emanuele Marchetti⁷, Lorenz Meier⁸, Fabian Neyer⁸ & Fabian Walter¹

¹ *Laboratory of Hydraulics, Hydrology and Glaciology, ETH Zürich, Switzerland, preiswerk@vaw.baug.ethz.ch*

² *Institute of Geophysics, ETH Zürich, Switzerland*

³ *Department of Geosciences and Earth and Environmental Systems Institute, Pennsylvania State University, USA*

⁴ *Computer Engineering and Networks Laboratory, ETH Zürich, Switzerland*

⁵ *now at GEOTEST AG, Zollikofen, Switzerland*

⁶ *Institute of Geodesy and Photogrammetry, ETH Zürich, Switzerland*

⁷ *Department of Earth Sciences, University of Firenze, Italy*

⁸ *GEOPRAEVENT AG, Zürich, Switzerland*

The glacierized northwest face of Weissmies gives rise to Triftgletscher in the Saas valley (Switzerland). Recently, climate-induced glacier thinning has weakened the buttressing effect of the steep ice masses on this glaciated face, creating new glacier instabilities (Fig. 1). In addition, high melt rates may have warmed the previously cold subglacial environment by releasing latent heat due to refreezing of meltwater. This process reduces the basal friction between ice and bedrock and further promotes instability. The situation is critical, because a ski resort, mountaineers climbing on the normal route to the popular Weissmies peak, and – in the case of a large event – human infrastructure in the Saas valley are exposed to the danger of a glacier break-off.

In 2014, a monitoring campaign was initiated. The ultimate goal is the detection of break-off precursors, such as exponentially increasing surface velocities (Failletaz et al., 2015). Since October 2014, an interferometric radar provides real-time measurements of surface displacements in line-of-sight. At the same time, photogrammetric processing of images from an automatic camera yields velocities in the plane normal to line-of-sight. L1-GPS sensor systems with wireless data transmission, installed directly on the unstable glacier part, serve as high-precision ground truth measurements of surface displacements. Finally, infrasound and seismometer arrays monitor acoustic and seismic emissions of even small-scale ice avalanches and englacial fracture development.

Here we discuss the results obtained so far. Despite an initial spring acceleration, the unstable glacier mass did not undergo a large-scale break-off event, in fact it decelerated during the unusually warm summer months. This is particularly surprising as surface velocities of other parts of the glacier steadily increased. An explanation remains elusive but likely involves subglacial processes and bedrock topography. Nevertheless, our results allow us to draw important conclusions regarding the suitability of different approaches to monitoring unstable glaciers.

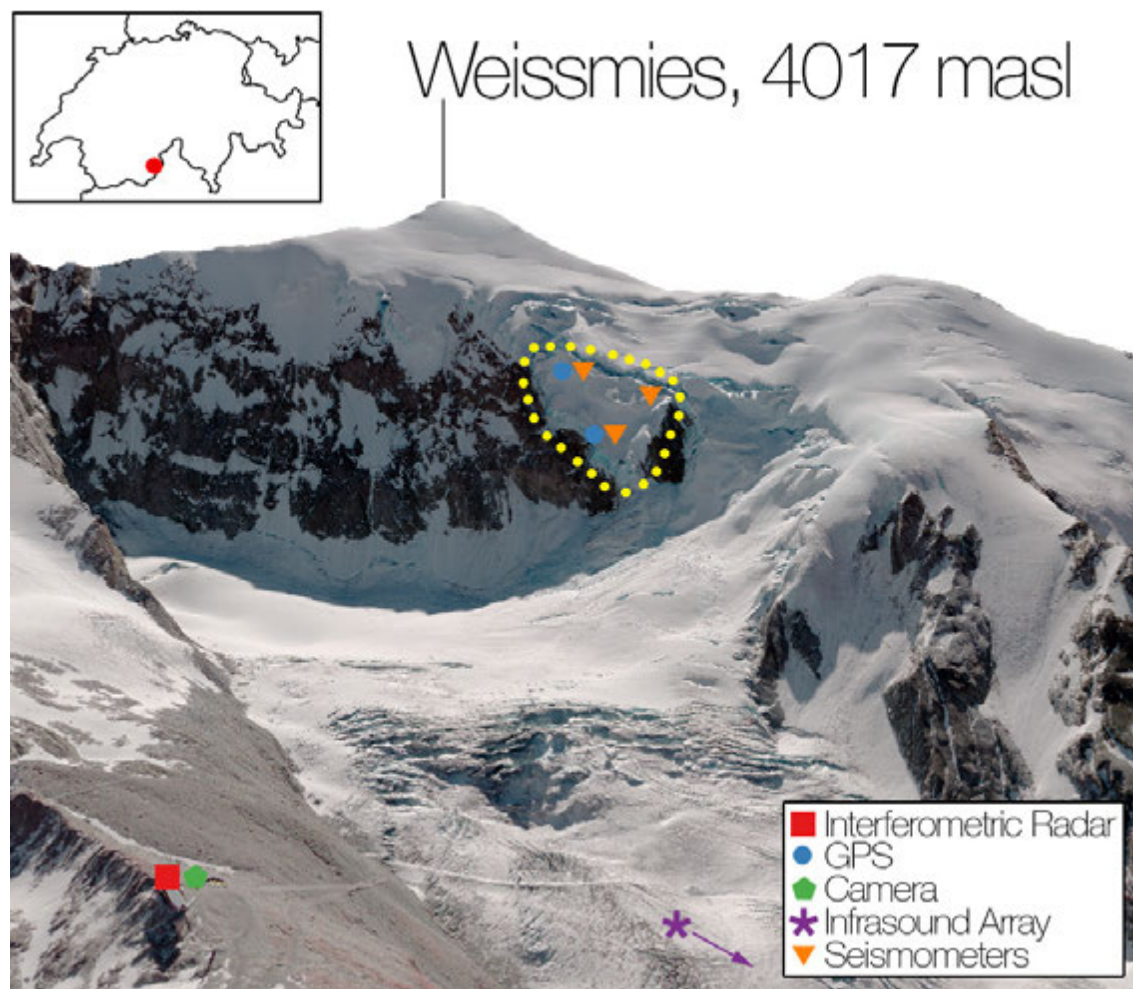


Figure 1. Trift glacier at Weissmies with an overview of the measurement methods. The unstable part of the glacier is circled in yellow dots.

REFERENCES

Faillettaz, J., Funk, M. & Vincent, C. 2015: Avalanching glacier instabilities: Review on processes and early warning perspectives. *Reviews of Geophysics*, doi:10.1002/2014RG000466

10.12

A new glacier inventory for the Pamir-Karakoram region

Philipp Rastner¹, Nico Mölg¹, Tobias Bolch^{1, 2} and Frank Paul¹

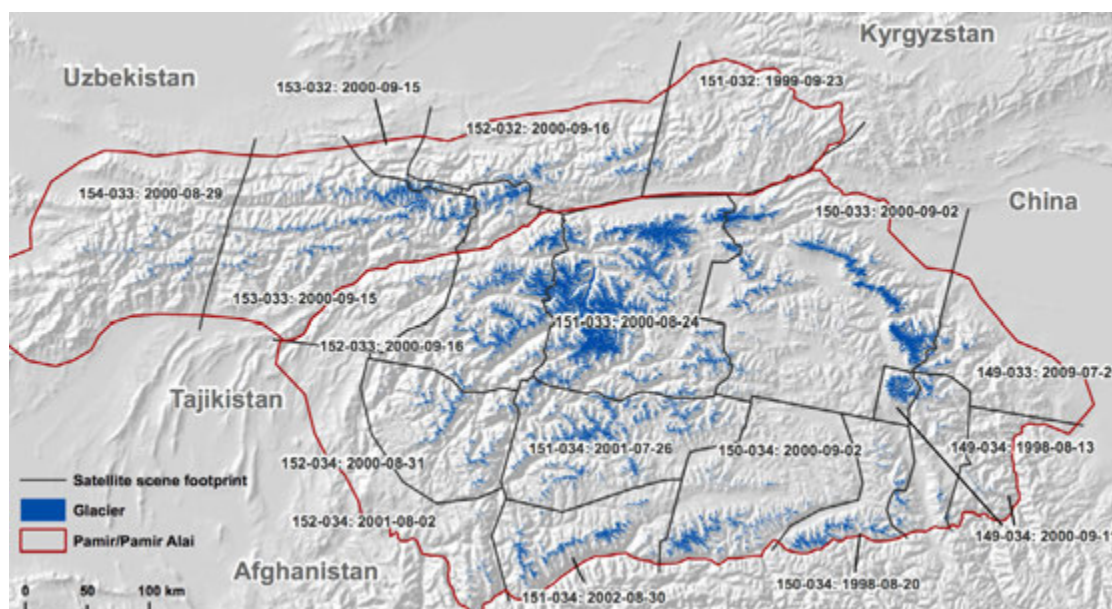
¹ Department of Geography, University of Zurich, Winterthurerstr. 190, CH-80567 Zurich (philipp.rastner@geo.uzh.ch)

² Institute for Cartography, Technical University Dresden, 01062 Dresden, Germany

High-quality glacier inventories are required as a reference dataset to determine glacier changes and model their reaction to climate change, among others. In particular in High Mountain Asia such an inventory was missing for several heavily glacierized regions with reportedly strongly changing glaciers. As a contribution to GLIMS and the Randolph Glacier Inventory (RGI) we have mapped all glaciers in the Karakoram and Pamir region within the framework of ESAs Glaciers_cci project (Paul et al. 2015). Glacier mapping was performed using the band ratio method (TM3/TM5) and manual editing of Landsat TM/ETM+ imagery acquired around the year 2000 (e.g. Rastner et al. 2012). Drainage divides were derived from the ASTER GDEM II and manually corrected to calculate topographic parameters.

Creating a glacier inventory in this region has several challenges, among others: (a) frequent seasonal snow at high elevations, (b) debris-covered glacier tongues, and (c) surging glaciers that are sometimes connected to much larger glaciers. We addressed (a) by utilizing multi-temporal imagery (not everywhere successful) and (b) by using coherence images derived from the ALOS PALSAR microwave sensor (Frey et al. 2012). In total, more than 30 Landsat scenes were processed for both regions (Figure 1). For issue (c) we decided to manually disconnect surge-type glaciers in case they are connected at the date of image acquisition. For these glaciers parameters such as area, length, minimum and mean elevation or mean slope can strongly vary between their minimum and maximum extent in a surge cycle.

All glaciers larger 0.02 km² cover an area of about 21,700 km² in the Karakoram and about 11,800 km² in the Pamir region (Fig. 1). Most glaciers are in the 0.1-0.5 km² size class for Pamir, whereas for the Karakoram they are in the class <0.1 km². Glaciers between 1 and 5 km² contribute more than 30% to the total area in Pamir, whereas for the Karakoram region it is only 17%. The mean glacier elevation in the Karakoram (Pamir) region is 5426 (4874) m. A comparison with other recently published inventories reveals differences in the interpretation of glacier extents (mainly in the accumulation region) that would lead to large area changes if unconsidered for change assessment across different inventories.



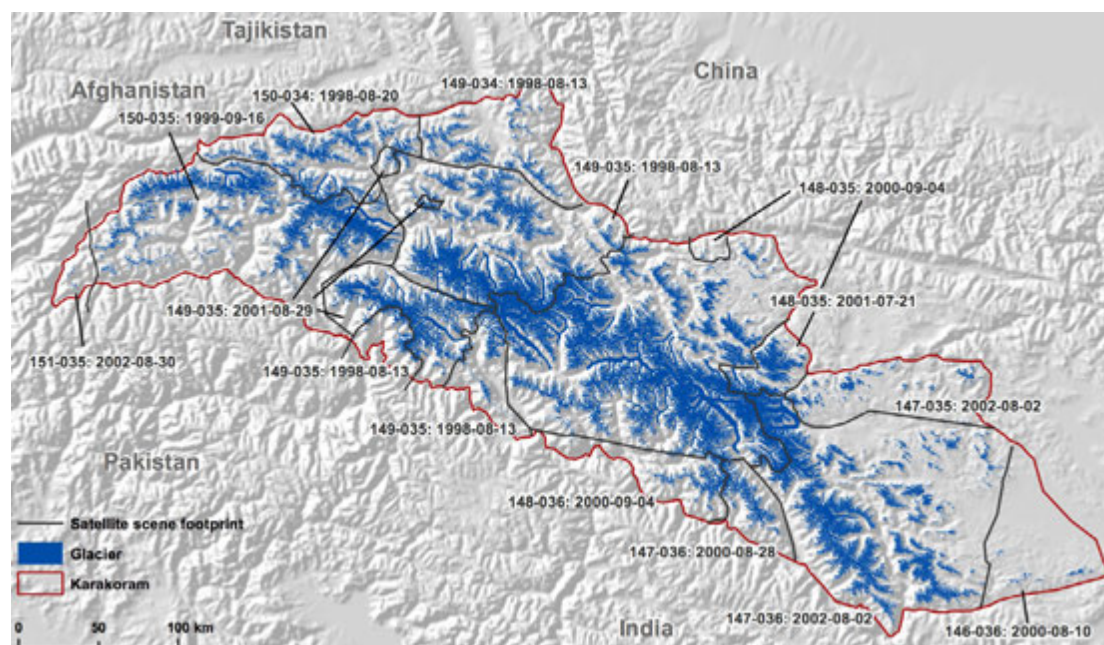


Figure 1. The new glacier inventories for the Pamir (top) and Karakoram (bottom) mountain ranges with footprints of the satellite scenes used to map the glaciers. The numbers give path-row and date (yyyy-mm-dd) of each scene.

REFERENCES

- Paul, F. & 24 others 2015: The Glaciers Climate Change Initiative: Algorithms for creating glacier area, elevation change and velocity products. *Remote Sensing of Environment*, 162, 408-426.
- Rastner, P., Bolch, T., Mölg, N., Machguth, H., Le Bris, R. & Paul, F. 2012: The first complete inventory of the local glaciers and ice caps on Greenland. *The Cryosphere*, 6, 1483-1495.
- Frey, H., Paul, F. & Strozzi, T. 2012: Compilation of a glacier inventory for the western Himalayas from satellite data: Methods, challenges and results. *Remote Sensing of Environment*, 124, 832-843.

10.13

European pollution history recorded in Colle Gnifetti ice cores

Margit Schwikowski^{1,2}

¹ *Paul Scherrer Institut, CH-5232 Villigen (margit.schwikowski@psi.ch)*

² *Department of Chemistry and Biochemistry and Oeschger Centre for Climate Change Research, University of Bern, CH-3012 Bern*

With the first ice cores collected on Colle Gnifetti, Monte Rosa in 1976 the potential of this glacier to contain a record of environmental and climatic information was already recognised. After 40 years of research there is overwhelming evidence that the Colle Gnifetti glacier is unique in the Alps as natural archive of past atmospheric composition. This is due to the fact that Colle Gnifetti is the highest glacier saddle in the Alps and has very cold firn and ice temperatures between -9°C and -14°C, implying absence of melt water percolation. The glacier is frozen to the bedrock and has low annual net snow accumulation rates because of preferential wind erosion of dry winter snow. That combination suggested that long time scales are accessible.

Meanwhile this assumption was confirmed by applying a new radiocarbon-based dating technique, revealing a core collected on Colle Gnifetti in 2003 to cover most of the Holocene with indication for late Pleistocene ice present at the very bottom. The last 2000 years correspond to 76 m of the 82 m long core, whereas the older part is strongly compressed.

The array of ice cores from Colle Gnifetti allowed the reconstruction of air pollution levels in Europe, which show a dramatic increase of anthropogenic emissions starting with the onset of industrialization in the middle of the 19th century and the reduction in emissions of certain pollutants since regulatory measures were put into effect in the 1970ies. This strong impact due to human activities is visible in the concentrations of primary pollutants (e.g. heavy metals copper, lead, zinc, plutonium, and carbonaceous particles as well as organic substances) and of secondary pollutants formed in the atmosphere after emission of precursor gases (e.g. sulfate, nitrate, ammonium).

10.14

Measuring and modeling wave propagation and weak layer failure due to explosive loading in snow

Stephan Simioni¹, Rolf Sidler², Jürg Dual³ and Jürg Schweizer¹

¹ *WSL Institute for Snow and Avalanche Research SLF, Davos, Switzerland (simioni@slf.ch)*

² *Simon Fraser University, Burnaby, Canada*

³ *Institute of Mechanical Systems, ETH Zürich, Switzerland*

Avalanche control by explosives is a key temporary preventive measure. While explosive avalanche control is widely used, little is known about the mechanism involved in releasing avalanches in such a way.

We therefore performed experiments with explosive charges over a snowpack. We installed microphones above the snowpack to measure near-surface air pressure and accelerometers within three snow pits to measure snowpack acceleration. We also recorded displacement of the snow cover in each pit with high speed cameras to detect weak layer failure. If weak layer failure occurred, we also assessed if it was caused by crack propagation through the snowpack or by the direct impact of the air pressure wave above the snowpack. We compared these results to air pressure and snowpack acceleration data to estimate magnitudes required to cause weak layer failure in a given snowpack. In addition, we used a model to perform two-dimensional numerical simulations of wave propagation in a Biot-type porous material. The accelerations measured in the snowpack best correlated with the modeled acceleration of the air relative to the ice frame. Locations of snow failure were identified in the simulation by comparing the axial and deviatoric stress field of the simulation to the corresponding snow strength. The identified snow failure locations corresponded well with the observed failure locations in the experiment.

The results of this comparison are an important step towards quantifying the effectiveness of avalanche control by explosives.

P 10.1

Internal structure, dynamics and genesis of a small heavily debris-covered glacier system (Tsarmine Glacier; Arolla, VS)

Jean-Baptiste Bosson¹, Maxime Capt¹, Mauro Fischer², Natan Micheletti¹, Stuart Lane¹ & Christophe Lambiel¹

¹ *Institut des dynamiques de la surface terrestre (IDYST), Université de Lausanne, Bâtiment Géopolis UNIL Mouline, CH-1015 Lausanne (jeanbaptiste.bosson@gmail.com)*

² *Département des Geosciences, Université de Fribourg, Chemin du Musée 4, CH-1700 Fribourg*

Glaciers are considered among the best climate indicators. However, the response of individual glaciers to similar changes in the regional climate forcing varies significantly, pointing to the importance of the geometrical setting of the glacier and local topoclimatic factors. If the importance of the latter becomes predominant, more complex processes, feedbacks and nonlinearities influence the response to climate variations. Empirical results are required to understand these local controls and to better integrate them in large-scale modelling. This contribution explores the effects of the glacier size, topography, permafrost conditions, debris-cover, distal sediment accumulations and lake development on the decadal to seasonal behaviour of the small, heavily debris-covered, Tsarmine glacier (46°03'N, 7°31'E; 0.49 km²; 2600-3070 m a.s.l.; Arolla Valley, Valais). Internal structure, dynamics and genesis of the glacier were investigated with Electrical Resistivity Tomography, Ground Penetrating Radar, Digital Photogrammetry and differential GPS between 2011 and 2015.

Tsarmine glacier corresponds to avalanche cones and a heavily debris-covered tongue. Mean ice thickness is 15 m and ice volume, a third of which was lost between 1967 and 2012, is 4×10^6 m³. The debris-cover reverses the ablation gradient and Tsarmine is becoming a flatter and stagnant downwasting glacier. In comparison with larger local glaciers, Tsarmine has a specific decadal behaviour in time (divergence of mass balance since the 2000s) and space (inverted ablation pattern). Between 1999 and 2012, average geodetic mass balance stabilized around -0.3 m w.e.yr⁻¹ and Tsarmine did not experience the acceleration of ice loss generally observed on nearby glaciers. Noticeable seasonal variations of ice motion and surface lowering showed the strong control of air temperature and water circulation on this probably largely temperate glacier. The Holocene fluctuations of this glacier have been progressively restricted by the distal sediment accumulation. Nowadays, dead ice, ice-free debris and a lake are present downslope the glacier tongue. In the northwestern margin, where the ice flow is slower and the debris input was the highest during the Holocene, a rock glacier has developed. Deformed by LIA advance, this ice-cored and ice-cemented body is decoupling from the upslope vanishing glacier. Creep accelerated in the last decades, probably in relation with the air temperature increase. However, this zone is weakly coupled with seasonal climate variations and mean surface lowering was close to zero between 2011 and 2014.

P 10.2

Erosion Rates and Processes in a Glacier's Forefield Over a 28 Year Period

Ian A. Delaney¹, Yvo Weidmann¹ & Matthias Huss¹

¹ *Laboratory of Hydraulics, Hydrology and Glaciology (VAW), ETH-Zürich, Hönggerberggring 26, CH 8090 Zürich*

Glacially fed hydropower reservoirs in the Swiss Alps have experienced substantial increases in sedimentation recently. This sedimentation causes reduced reservoir capacity, turbine abrasion and increased need for sediment flushing, all of which reduce the efficiency and economic viability of hydropower in the region. Although the issue is largely attributed to regional glacier retreat, there is a need for greater understanding of the specific processes that contribute to the increased sedimentation. To evaluate these processes we examine the Griesgletscher catchment, which lies in the central Swiss Alps and its runoff feeds a hydropower reservoir.

The recent exposure of the glacier's fore-field (roughly 1986) due to the glacier's retreat beyond the reservoir's margin, along with its simple catchment area make it an ideal location to examine pro-glacial erosion. Here we present an annual time-series from 1986-2014 of digital elevation model (DEM) created from aerial photographs of the Griesgletscher's forefield. Comparison of DEMs from subsequent years yields erosion volumes and sediment balance over the 28-year period for the pro-glacial area. Bathymetry of the pro-glacial reservoir for select years allows us to speculate if the erosion of the recently exposed glacier forefield is the sole source of sediment to the reservoir, or if alternative processes such as increased glacial erosion or mobilization of sub-glacial sediments could contribute. We correlate erosion amounts with runoff volumes from the Griesgletscher and changes in the glacier's morphology and coverage. Additionally, implementation of the Glacier Evolution Runoff Model allows us to examine the variability in the glacier's runoff on the hourly to daily scale. By examining these relationships, we constrain the processes contributing to the erosion of the Griesgletscher's pro-glacial area.

P 10.3

Webcam imagery rectification and snow classification – potential for complementing satellite-derived snow maps over Switzerland

Céline Dizerens¹, Fabia Hüsler^{1,2} & Stefan Wunderle¹

¹ *Institute of Geography and Oeschger Centre for Climate Change Research, University of Bern, Hallerstrasse 12, CH-3012 Bern (celine.dizerens@giub.unibe.ch)*

² *Department of Geography, University of Zurich, Winterthurerstr. 190, CH-8057 Zurich*

The spatial and temporal variability of snow cover has a significant impact on climate and environment and is of great socio-economic importance for the European Alps. Satellite remote sensing data are widely used to study snow cover variability and can provide spatially comprehensive information on snow cover extent. However, cloud cover strongly impedes the surface view and hence limits the number of useful snow observations. Outdoor webcam images offer a unique potential for complementing satellite-derived snow retrieval under cloudy conditions and provide a high temporal and spatial resolution to obtain small-scale snow information.

The overall aim of this work is to develop a robust procedure to generate a snow cover extent data set based on webcam images. We use daily and freely available webcam imagery of Swiss landscapes and apply and improve existing approaches dealing with the positioning of photographs within a terrain model, the appropriate rectification and the automatic snow classification of such photographs. Since no information about the different webcam sensors and its lenses are available, the key issue is to automatically derive extrinsic and intrinsic webcam parameters such as the principal point or focal length of the webcam image. The rectification procedure then requires a mapping relating two-dimensional pixels in the webcam images to three-dimensional points in a high-resolution digital elevation model. The automatic classification of snow finally uses threshold values as well as a statistical analysis of the image. The resulting snow cover maps have the same resolution as the available elevation model and indicate for every grid cell whether the cell is snow-covered, snow-free or not visible from the webcams' positions.

P 10.4

Dynamic crack propagation in weak snowpack layers: from field experiments to discrete element modeling

J. Gaume¹, A. van Herwijnen¹, G. Chambon² J. Schweizer¹.

¹ WSL Institute for Snow and Avalanche Research SLF Davos, Switzerland

² IRSTEA, Grenoble, France

Email : johan.gaume@slf.ch

Dry-snow slab avalanches are generally caused by a sequence of fracture processes including (1) failure initiation in a weak snow layer underlying a cohesive slab, (2) crack propagation within the weak layer and (3) tensile fracture through the slab which leads to its detachment.

During the past decades, theoretical and experimental work has gradually led to a better understanding of the fracture process in snow involving the collapse of the structure in the weak layer during fracture. This now allows us to better model failure initiation and the onset of crack propagation, i.e. to estimate the critical length required for crack propagation. On the other hand, our understanding of dynamic crack propagation and fracture arrest propensity is still very limited. For instance, it is not uncommon to perform field measurements with widespread crack propagation on one day, while a few days later, with very little changes to the snowpack, crack propagation does not occur anymore. Thus far, there is no clear theoretical framework to interpret such observations, and it is not clear how and which snowpack properties affect dynamic crack propagation.

To shed more light on this issue, we performed numerical propagation saw test experiments applying the discrete element (DE) method and compared the numerical results with field measurements based on particle tracking. The goal is to investigate the influence of weak layer failure and the mechanical properties of the slab on crack propagation and fracture arrest propensity. Crack propagation speeds and distances before fracture arrest were derived from the displacement field for different snowpack configurations and mechanical properties. Then, the relation between mechanical parameters of the snowpack was taken into account so as to compare numerical and experimental results, which were in good agreement, suggesting that the simulations can reproduce crack propagation in PSTs. Finally, an in-depth analysis of the mechanical processes at play was carried out which led to suggestions for minimum column length in field PSTs.

P 10.5

Accuracy assessment of UAV photogrammetry on Alpine glaciers

Saskia Gindraux¹, Daniel Farinotti¹, Mauro Fischer², Ruedi Bösch¹

¹ *Swiss Federal Institute for Forest, Snow and Landscape Research WSL, Zürcherstrasse 111, 8903 Birmensdorf (saskia.gindraux@wsl.ch)*

² *Department of Geosciences, University of Fribourg, Ch. du Musée 4, 1700 Fribourg*

In recent years, Unmanned Aerial Vehicle (UAV) based surveys have become very popular due to the fast evolution of automated close-range photogrammetry techniques and the emergence of consumer-friendly, ready-to-use UAV platforms. Such platforms, together with Structure-from-Motion (SfM) techniques, allow obtaining high-resolution datasets such as orthophotos and Digital Elevation Models (DEMs). This offers a new range of application possibilities in many different research areas including forestry, agriculture, archeology, biology and hydrology. In the glaciological context, UAV photogrammetry is promising not only because of its low cost, but also due to its portability and facility of use in the field. Compared to in-situ measurements, UAV surveys are time-saving and also cover potentially dangerous areas (e.g. Ryan et al., 2015).

Several studies report extraordinary resolution and accuracy of their UAV-based SfM applications. For example, horizontal and vertical accuracies in the order of 9-30 cm and 2 to 80 cm respectively, are claimed in the studies by d'Oleire Oltmanns et al. (2012) and De Michele et al. (2015). Ground sampling distances in the order of 2-8 cm are reported in different works (e.g. Fonstad et al., 2013). These accuracies and resolutions, however, are often assessed only roughly through the comparison of sparse ground control points (e.g. Whitehead et al., 2013). A rigorous accuracy assessment on snow and glacier surfaces, e.g. based on the comparison with a benchmark technique such as Light Detection And Ranging (LiDAR), is missing to date.

Here we present the first results of a study, which aims to perform a thorough accuracy assessment of the SfM method over snow and ice. We flew our UAV on three different glaciers in the Swiss Alps (Findelenglacier, Griesglacier and St-Annafrim). Fixed targets, as well as continuous transects have been measured with a differential GPS, allowing the comparison of the SfM derived DEM with thousands of ground-truth points. Moreover, during the St. Annafrim flights, high-resolution terrestrial LiDAR scans were acquired with the new ultra-long range Riegl VZ-6000 device, allowing to assess the quality of high-resolution DEMs from different sources.

REFERENCES

- De Michele, C., Avanzi, F., Passoni, D., Barzaghi, R., Pinto, L., Dosso, P., Ghezzi, A., Gianatti, R., and Della Vedova, G. (2015). Microscale variability of snow depth using U.A.S. technology. *The Cryosphere Discussions*, 9(1):1047-1075.
- d'Oleire Oltmanns, S., Marzol, I., Peter, K., and Ries, J. (2012). Unmanned Aerial Vehicle (UAV) for Monitoring Soil Erosion in Morocco. *Remote Sensing*, 4(12):3390-3416.
- Fonstad, M. A., Dietrich, J. T., Courville, B. C., Jensen, J. L., and Carbonneau, P. E. (2013). Topographic structure from motion: a new development in photogrammetric measurement. *Earth Surface Processes and Landforms*, 38(4):421-430.
- Ryan, J. C., Hubbard, A. L., Box, J. E., Todd, J., Christo_ersen, P., Carr, J. R., Holt, T. O., and Snooke, N. (2015). UAV photogrammetry and structure from motion to assess calving dynamics at Store Glacier, a large outlet draining the Greenland ice sheet. *The Cryosphere*, 9(1):1-11.
- Whitehead, K., Moorman, B. J., and Hugenholtz, C. H. (2013). Brief Communication: Low-cost, on-demand aerial photogrammetry for glaciological measurement. *The Cryosphere*, 7(6):1879-1884.

P 10.6

Mass balance reconstruction for Glacier No. 354, Tien Shan, from 2003 to 2014

Marlene Kronenberg¹, Martina Barandun¹, Martin Hoelzle¹, Matthias Huss^{1,2}, Daniel Farinotti^{3,4}, Erlan Azisov⁶, Ryskul Usabaliev⁵, Abror Gafurov⁴, Dmitry Petrakov⁶ & Andreas Käb⁶

¹ Department of Geosciences, University of Fribourg, Chemin de Musée 4, CH-1700 Fribourg (marlene.kronenberg@unifr.ch)

² Laboratory of Hydraulics, Hydrology and Glaciology (VAW), ETH Zurich, Zurich, Switzerland

³ Swiss Federal Institute for Forest, Snow and Landscape Research (WSL), Birmensdorf, Switzerland

⁴ German Research Center for Geoscience (GFZ), Potsdam, German

⁵ Central Asian Institute of Applied Geosciences (CAIAG), Bishkek, Kyrgyzstan

⁶ Faculty of Geography, Lomonosov Moscow State University, Moscow, Russia

⁷ Department of Geosciences, University of Oslo, Oslo, Norway

Long-term mass balance observations on glaciers in data sparse regions are crucial to understand consequences of climate change. Furthermore, melt-water from glaciers is an important contributor to the water cycle and is essential for the dry lowlands of Central Asia.

Glaciers located in the Akshiirak Range, Inner Tien Shan, Kyrgyzstan have suffered from important area and mass losses since the onset of comprehensive investigations in the 1940s. Past scientific activities in this area focussed mainly on glacier area and volume changes detected with the help of airborne photographs and satellite imagery. From 1985 to 1989, in the framework of the Soviet Glacier monitoring strategy, mass balance measurements were carried out on Sary-Tor glacier located in the Akshiirak Range. However, today Sary-Tor glacier is situated within the area of gold mining activities and access is restricted. Therefore, in the context of a general (re-)establishing of long-term mass balance observations in Central Asia, a new glacier monitoring network was set up on Glacier No. 354, Akshiirak Range within the projects Capacity Building and Twinning for Climate Observing System (CATCOS) and Central Asian Water (CAWa) in 2010.

This study presents an analysis of measured mass balance for the period 2011-2014 and a reconstruction of seasonal mass balance from 2003 to 2010 for Glacier No. 354 using a distributed accumulation and temperature-index melt model driven by daily air temperature and precipitation data from a nearby meteorological station. The model is calibrated with in-situ measurements of annual mass balance collected from 2011 to 2014 and with complementary winter accumulation measurements performed in May 2014.

From 2003 to 2014, a cumulative mass loss of -4.78 ± 0.98 m w.e. was found. For the period 2003-2012, the cumulative mass balance of -3.59 ± 0.89 m w.e. could be validated with an independent geodetic mass loss of -4.34 ± 0.67 m w.e. The subseasonal model performance was evaluated with observations of the snow-cover depletion pattern observed on satellite images. For Glacier No. 354 a mass balance series at high temporal resolution could be produced for a decade for which only little is known about glacier mass changes in the Akshiirak range.

P 10.7

Supplementing ice core time series at Colle Gnifetti with a 3D full Stokes ice flow model using Elmer/Ice

Carlo Licciulli¹, Pascal Bohleber^{1,2} Dietmar Wagenbach^{1,†} Olaf Eisen^{3,1} Olivier Gagliardini^{4,5} Martin Hoelzle⁶

¹ *Institute of Environmental Physics, University of Heidelberg, Heidelberg, Germany, (carlo.licciulli@iup.uni-heidelberg.de)*

² *Climate Change Institute, University of Maine, USA*

³ *Alfred Wegener Institute Helmholtz Centre for Polar and Marine Research, Bremerhaven, Germany*

⁴ *CNRS, LGGE (UMR5183), Grenoble, France*

⁵ *Univ. Grenoble Alpes, LGGE (UMR5183), Grenoble, France*

⁶ *Department of Geosciences, University of Fribourg, Fribourg, Switzerland*

[†] *deceased*

The cold glacier saddle Colle Gnifetti (CG) is the unique drilling site in the European Alps offering ice core records substantially exceeding the instrumental period. However, the full exploitation of the unique potential of this site is hampered by depositional noise and, combined with a complex flow regime, upstream-effects. Here we present results from an ongoing new sophisticated flow modeling attempt, i.e. 3D full Stokes with consideration of firn rheology, fully thermo-mechanically coupled, utilizing the finite element software Elmer/Ice. In view of our latest ice core drilled to bedrock in 2013, a major objective is to map source trajectories of existing ice core sites in order to evaluate potential upstream effects. An additional focus is to assist in finding a reliable age scale, especially targeting depths where annual layers can no more be counted. This includes the calculation of isochronous surfaces for intercomparison of different drilling sites within the CG multi core array.

Previous numerical ice flow models of CG have been developed by W. Haeberli, S. Wagner, M. Lüthi (Lüthi & Funk 2000, 2001) and H. Konrad (Konrad et al. 2013). The level of accuracy of these previous works was mainly limited by the not well known bedrock topography and englacial temperatures. However, since the work of M. Lüthi several new temperature profiles are available (Hoelzle et al. 2011) and additional GPR measurements have been performed extensively (Bohleber 2011). Ongoing measurements will provide more precise information about the surface flow velocity, surface topography and their stationarity. In addition, two new ice cores have been drilled on CG, in 2005 and 2013. The 2013 drilling project employs a unique approach of combining multiple state-of-the-art methods in ice core analysis, for example new ultra-high resolution impurity analysis for detecting highly thinned annual layers as well as analysis of ice microstructure. All these new data sets together with the nowadays higher available computing power motivated a new model attempt at CG, the only way to evaluate potential upstream effects.

Model input quantities comprise density profiles measured at the ice core sites, surface topography and GPR based bedrock topography. The model accuracy is limited especially by the latter, due to an uncertainty of typically 15%. Additional limitations arise from other model parameters, that are not directly constrained by measurement, for example the mechanical stress on the glacier boundaries. To achieve better constraints, the model input quantities are iteratively adjusted to provide the best fit between model derived and directly measured quantities.

Here we present first results regarding the model validation based on comparison with empirical data, using for this purpose the measured surface velocities and borehole temperatures.

Finally we discuss the next steps in building our model approach, which include comparing model results with ice core derived depth-dependent information like e.g. the observed layer thinning or the measured vertical age distribution as well as to use a flow law taking into account ice anisotropy, as observational evidence suggests.

REFERENCES

- Bohleber, P. 2011: Ground-penetrating radar assisted ice core research: The challenge of Alpine glaciers and dielectric ice properties. Dissertation, Universität Heidelberg.
- Hoelzle, M., Darms, G., Lüthi, M. & Suter, S. 2011. Evidence of accelerated englacial warming in the Monte Rosa area, Switzerland/Italy. *Cryosphere*, 5(1), 231–243 (doi: 10.5194/tc-5-231-2011).
- Konrad, H., Bohleber, P., Wagenbach, D., Vincent, C. & Eisen, O. 2013: Determining the age distribution of Colle Gnifetti, Monte Rosa, Swiss Alps, by combining ice cores, ground-penetrating radar and a simple flow model. *Journal of Glaciology*, 59(213).
- Lüthi, M., & Funk, M. 2000: Dating of ice cores from a high Alpine glacier with a flow model for cold firn. *Ann. Glaciol.*, 31:69–79.
- Lüthi, M., & Funk, M. 2001: Modelling heat flow in a cold, high altitude glacier: interpretation of measurements from Colle Gnifetti, Swiss Alps. *J. Glaciol.*, 47:314–324.

P 10.8

Observation of snow properties and avalanches with new polarimetric and interferometric ground radar

Célia Lucas¹, Irena Hajnsek², Yves Bühler³, Armando Marino⁴

¹ *Institute of Environmental Engineering (IfU), ETH Zürich, 8093 Zürich, Switzerland*

² *Microwaves and Radar Institute, German Aerospace Center (DLR), Germany*

³ *Institute for Snow and Avalanche Research (SLF), Flüelastrasse 11, CH-7260 Davos Dorf, Switzerland*

⁴ *Department of Engineering and Innovation, Open University*

The investigation of snow properties with field measurements is often complicated by the topography and inaccessibility of mountainous regions. The use of radar remote sensing techniques for cryospheric research is promising as it reduces the necessity of direct field measurements. It also allows large scale instead of localized, point-like measurements. In this context, the research efforts have primarily focused on space-borne data. This allows for broad coverage, but has the drawbacks of often large revisit times to a scene and coarse resolutions, which cannot satisfyingly reflect the complicated and often very small scale variable snow properties.

A novel ground-based radar system gives us new perspectives in the field of snow research by solving several of the satellite remote sensing drawbacks. KAPRI, our **Ku-band Advanced Polarimetric Radar Interferometer**, has been used in the winter season 2014/2015 to monitor the slope of Dorfberg, close to Davos Dorf, on several test days. After investigation of the first dataset, there will be a fixed installation at the same test site for the winter season 2015/2016 which will give us a continuous dataset over the the daily and the seasonal cycles in alpine snow.

With a resolution of 0.75 m in azimuth direction and 6.9 m in range direction at a 1 km distance, an analysis of the small scale heterogeneities in the snow, due to factors like sun and shade, local slope steepness, local snow depth and grain size are possible.

Avalanche monitoring with the means of remote sensing has been explored by several authors [eg. Caduff et al., 2015, Eckerstorfer et al., 2014] but still offers a large range of potential improvements. By exploiting the high temporal and spatial resolution as well as the full polarimetric nature of KAPRI, new methodologies for automatic avalanche detection and warning can be developed, making use of interferometric coherence on one hand and polarimetric change detectors [Marino et al., 2013] on the other hand.

With this poster, we want to display first promising results of our campaign to the cryosphere community and discuss further possible applications of this novel tool.

REFERENCES

- Marino, A., Cloude, S. & Lopez-Sanchez, J.M. 2013: A new polarimetric change detector in radar imagery, IEEE Transactions on geoscience and remote sensing, vol. 51, no.5, pp. 2986-3000
- Eckerstorfer, M., Malnes, E., Domaas, U. & Brattlien, K. 2014: Avalanche Debris Detection Using Satellite-Borne Radar and Optical Remote Sensing, International Snow Science Workshop 2014 Proceedings, Banff, Canada
- Caduff, R., Wiesmann, A., Bühler, Y. & Pielmeier, C. 2015: Continuous monitoring of snowpack displacement at high spatial and temporal resolution with terrestrial radar interferometry, AGU Geophysical Research Letters, vol. 42, pp. 813-820

P 10.9

Successive and intense melt rapidly decreases Greenland meltwater retention in firn

Horst Machguth^{1,2}, Mike MacFerrin³, Dirk van As², Jason E. Box², Charalampos Charalampidis², William Colgan⁴, Robert S. Fausto², Harro A.J. Meijer⁵, Ellen Mosley-Thompson⁶ and Roderik S.W. van de Wal⁷

¹ World Glacier Monitoring Service, Department of Geography, University of Zurich, Zurich, Switzerland (horst.machguth@geo.uzh.ch)

² Geological Survey of Denmark and Greenland GEUS, København, Denmark

³ Cooperative Institute for Research in Environmental Sciences (CIRES), University of Colorado at Boulder, Boulder, USA

⁴ Department of Earth and Space Science and Engineering, York University, Toronto, Ontario, Canada

⁵ Centre for Isotope Research (CIO), Energy and Sustainability Research Institute Groningen (ESRIG), University of Groningen, Groningen, the Netherlands

⁶ Department of Geography, Ohio State University, Columbus OH, USA

⁷ Institute for Marine and Atmospheric Research Utrecht (IMAU), University of Utrecht, Utrecht, the Netherlands

About half of the current mass loss of the Greenland ice sheet is attributed to runoff from surface melt. At higher elevations, however, melt does not automatically equal runoff, because meltwater refreezes in the porous near-surface snow and firn. Recent studies suggest that all or most firn pore space is available for meltwater storage, which would make the firn an important buffer against Greenland's surface melt contribution to sea level rise.

Here, we challenge the notion that all firn pore space is available for meltwater retention based on field observations (Fig. 1), analysed in the context of historical legacy data. Our observations frame the recent exceptional melt summers of the years 2010 and 2012 and reveal a distinctive pathway of firn changes induced by successive and intensive melt. At the lower end of the pathway, where melt is most abundant, porous firn loses its capability to retain meltwater.

At 67°N, in the lower percolation zone of the western flank of the ice sheet, the formation of thick near-surface ice layers ("regime (3)" in Fig. 1) renders 32±10% of firn pore space inaccessible and forces meltwater to enter the surface discharge system rather than percolating and being retained in the underlying firn. As a direct consequence, ice sheet mass loss is intensified; in summer 2012 11±4% of total runoff originated in the zone of thick near-surface ice layers (~1680 to 1870 m a.s.l.).

Strong evidence suggests that the above described processes take place over extended areas of the lower Greenland percolation zone.

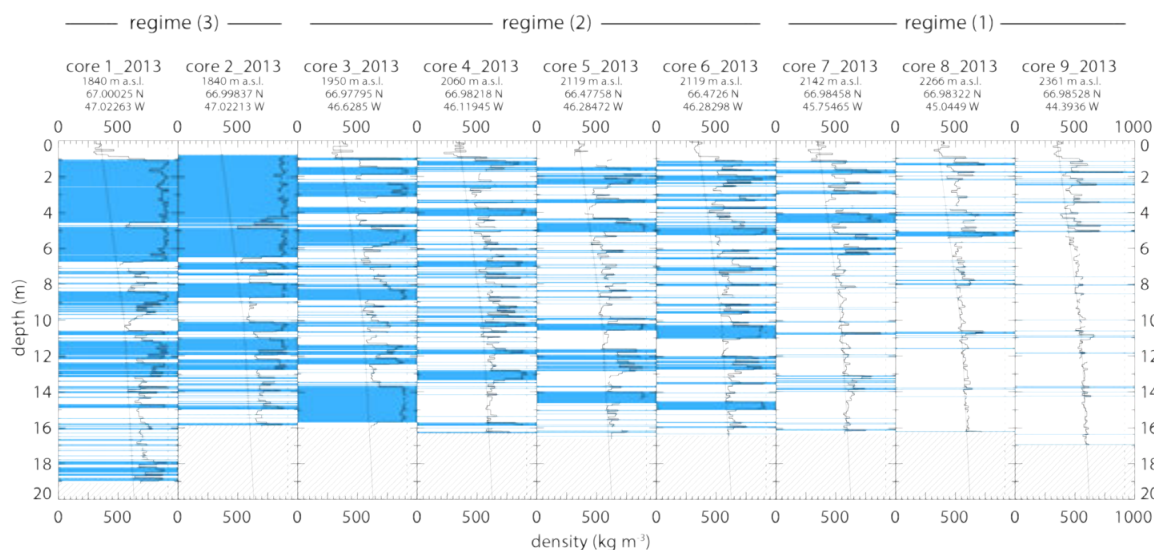


Figure 1. Stratigraphy of the nine major firn cores drilled in late April to mid May 2013. Ice lenses are in blue and given at 1 cm vertical resolution. Density at 10 cm resolution is in black. The dotted vertical line indicates the density of pure ice (917 kg m⁻³); the thin inclined line denotes dry firn density. Dashed areas mark the end of the cores. The association of each core with three hypothesized firn regimes is indicated at the top.

P 10.10

First results from PERMOS after the hot summer 2015

Jeannette Nötzli¹, Reynald Delaloye², Marcia Phillips¹ & the PERMOS Scientific Committee

¹ WSL Institute for Snow and Avalanche Research SLF, Flüelastrasse 11, CH-7260 Davos Dorf (jeannette.noetzli@slf.ch)

² Department of Geosciences, University of Fribourg, Chemin du Musée 4, CH-1700 Fribourg

Air temperatures in summer 2015 were about 2.5 °C higher than the mean 1981–2010 and 1°C higher than during previous record summers, except for the extreme summer 2003 (MeteoSwiss 2015). In and/or following the year 2003 record values were reported for nearly all observation elements and sites in the permafrost monitoring network PERMOS: surface and subsurface temperatures, active layer thickness, creep velocities and electrical resistivities (PERMOS 2007). In addition, a large number of rock falls was reported from high elevation areas that were possibly related to enlarged active layer thicknesses in bedrock permafrost.

We will present first results from the permafrost measurements from summer 2015 and compare it to the data from the year 2003. Such summer heat waves lead to an increase of the mean annual ground surface temperature (MAGST) of ca. 0.5–1 °C. For the ground thermal regime in snow covered areas, however, also winter conditions are important. Winter 2002/2003 was one of the two warmest at the ground surface since the beginning of systematic measurements in the late 1990s. In winter 2014/2015 conditions were colder because of a later and longer lasting snow cover. MAGST values in 2015 hence seem to not exceed those from 2003. During the previous six years however continuously warm to very warm permafrost conditions were recorded compared to the 10–15 years of measurement and a resulting cumulative effect has already been observed in the underground. Permafrost temperatures at 10–20 m depth were significantly higher before the 2015 heat wave than before the one in 2003. Due to the inertia of heat diffusion, the response of permafrost underground below the uppermost meters will mainly be observed in 2016. The winter 2015/2016, in particular the timing of the first thicker snow cover, will be of importance as it can balance or enhance the effects of summer 2015.

REFERENCES

- MeteoSwiss 2015: Zweitwärmster Sommer seit Messbeginn. <http://www.meteoschweiz.admin.ch/home/aktuell/meteoschweiz-blog.subpage.html/de/data/blogs/2015/8/zweitwaermster-sommer-seit-messbeginn.html> (accessed on 26. August 2015).
- PERMOS 2007: Permafrost in Switzerland 2002/2003 and 2003/2004. Vonder Muehll, D., Noetzli, J., Roer, I., Makowski, K. and Delaloye, R. (Eds). Glaciological Report (Permafrost) No. 4/5 of the Cryospheric Commission of the Swiss Academy of Sciences and Department of Geography, University of Zurich, 106 pp.

P 10.11

Fifty years of glacier surges in the central Karakoram

Frank Paul¹

¹ Department of Geography, University of Zurich, Winterthurerstr. 190, CH-80567 Zurich (frank.paul@geo.uzh.ch)

The Pamir and Karakoram mountain ranges are one of the places on Earth with a high abundance of surge-type glaciers (Sevestre & Benn 2015; Copland et al. 2011; Kotlyakov et al. 2008). Thereby, analysis of multi-temporal satellite images and local field evidence revealed that a large number of glaciers in the central Karakoram are currently (last 15 years) surging (Rankl et al. 2014; Hewitt 2007) or have done so in the past and now surge again (Copland et al. 2011). It was speculated that the recent high surge activity in this region is also an expression of climatic changes (e.g. increased winter precipitation), which was named the 'Karakoram Anomaly'. However, only some of the more recent surges have been analysed and described in detail (e.g. Hewitt 2007) and an overall and/or detailed analysis of individual surges going back to the 1960s is missing despite available satellite images.

For this study a large number of declassified satellite images from the Corona (1961, 1965, 1969, 1971) and Hexagon (1973, 1980) missions were analysed in combination with a more or less complete (near-annual) time series of Landsat images (1989 to 2015) to reveal the timing of individual surges and identify previous surges for 25 glaciers. The resulting fifty-year time-series revealed that most of the currently surging glaciers have also surged in the 1950s and 1960s and that the previous and current appearance of surges is in most cases very similar. The analysis also showed a large variety in the timing of the surges (from very fast and short-lived to very slow and long-lasting) with a partly complex interaction between surging tributaries and blocked main glaciers. Also the repeat cycles vary greatly, from one glacier that is surging every 20 to 25 years (Figure 1) to another one (just 8 km away on the opposite side of the valley) that is advancing since 50 years. In contrast to most other regions in the world, many of the surging glaciers in this specific region are comparably small, steep and debris free.

The large variety of glacier surges and surge-type glaciers that was found in this small region confirms initial observations forwarded in a previous study by Meier and Post (1969). It also stresses the principle difficulties in clearly discriminating surge-type glaciers from others.

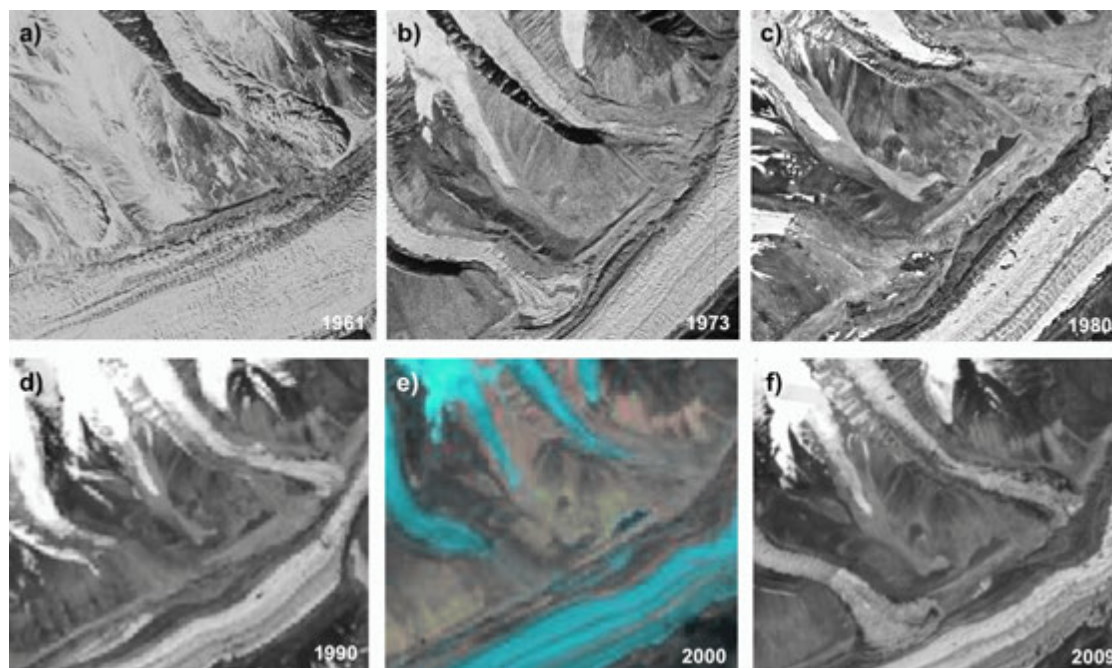


Figure 1. Repeat surges of two small glaciers in the Sarpo Lago basin as revealed by time-series of satellite images. While the glacier to the lower left surged two times over the period 1961–2009, its similar-sized northern neighbour (to the upper right in each image) surged three times. Images are from a) Corona, b) and c) Hexagon, d) Landsat TM, e) Landsat ETM+ (with glaciers in light blue) and f) the panchromatic band from ETM+. The region covers about 4 km by 3 km.

REFERENCES

- Copland, L., Sylvestre T., Bishop M.P., Shroder, J.F., Seong Y.B., Owen L.A., Bush A., & Kamp, U. 2011: Expanded and recently increased glacier surging in the Karakoram, *Arct. Antarct. Alp. Res.*, 43, 503–516.
- Hewitt, K. 2007: Tributary glacier surges: an exceptional concentration at Panmah Glacier, Karakoram Himalaya, *J. Glaciol.*, 53, 18–188.
- Meier, M.F. & Post, A. 1969: What are glacier surges?, *Can. J. Earth Sci.*, 6, 807–817.
- Rankl, M., Kienholz C. & Braun M. 2014: Glacier changes in the Karakoram region mapped by multimission satellite imagery, *Cryosphere*, 8, 977–989.
- Sevestre, H. & Benn D.I. 2015: Climatic and geometric controls on the global distribution of surge-type glaciers: implications for a unifying model of surging. *J. Glaciol.*, 61 (228), 646–662.
- Kotlyakov, V.M., Osipova G.B. & Tsvetkov D.G. 2008: Monitoring surging glaciers of the Pamirs, central Asia, from space, *Ann. Glaciol.*, 48, 125–134.

P 10.12

A local calibration approach to derive snow structural parameters from SnowMicroPen measurements

Martin Proksch¹, Henning Löwe¹, Martin Schneebeli¹

¹ WSL Institute for Snow and Avalanche research SLF, Flüelastrasse 11, CH-7260 Davos Dorf (proksch@slf.ch)

Snow permanently influences many facets of science and society as it is immutably bound to climatology, hydrology, natural hazards, numeric weather prediction or public transport. It becomes apparent from this, that a precise measurement of snow physical parameters is of major importance. However, snow measurements are typically limited by one of the following issues, i.e. coarse resolution, extensive measurement times or subjectivity of the observer. Here we present a measurement method based on a local calibration for the SnowMicroPen (SMP). The SMP is a high resolution penetrometer, which allows full meter profiles to be measured in less than one minute in an observer independent way, and as such a promising tool for snow measurements. Due to its short measurement times, the instrument is in addition suited to measure the spatial variability of the snowpack. We present an approach to calibrate the instrument in order to derive three of the main snow structural parameters, density, correlation length and the specific surface area (SSA) from SMP measurements. The calibration is based on the assimilation of measurements from other instruments, such as density cutters or micro-computed tomography (μ CT). We show that after applying the local calibration, the SMP derived parameters are in good agreement with the target variables derived from the other instruments. A specific advantage of the local calibration approach is its flexibility to account for local conditions of a specific snow environment, even though practical limitations arise for rapidly changing snow conditions or different target instruments for calibration.

P 10.13

Glacier changes in a Nepalese catchment and hydrological impacts

Silvan Ragettli¹, Tobias Bolch^{2,3}, Walter Immerzeel⁴, Francesca Pellicciotti^{1,5}

¹ *Institute of Environmental Engineering, ETH Zürich, Stefano-Franscini-Platz 5, 8093 Zürich (ragettli@ifu.baug.ethz.ch)*

² *University of Zurich, Department of Geography, Zurich, Switzerland*

³ *Institute for Cartography, Technische Universität Dresden, Dresden, Germany*

⁴ *Utrecht University, Department of Physical Geography, Utrecht, The Netherlands*

⁵ *Northumbria University, Department of Geography, Newcastle upon Tyne, UK*

Himalayan Glaciers are showing a heterogeneous response to climate change. Most of them are losing mass at rates similar to glaciers elsewhere, but satellite remote sensing studies show that heavily debris-covered glaciers with stagnant low-gradient termini typically have stable fronts. It is known that debris thickness above a critical value of few cm reduces ablation. However, several remote sensing studies have shown that many Himalayan debris-covered glaciers do not thin at lower rates than clean ones, also when in the same elevation range. Strong surface lowering of debris-covered glaciers has been explained by high air temperatures and enhanced melting on exposed ice cliffs and beneath supraglacial lakes and reduced ice flux. Anomalous glacier changes in some parts of the Himalaya on the other hand may be attributed to topography and climate: the debris-covered tongues are often avalanche-fed and therefore respond more quickly to increased precipitation.

In this study we use a unique set of high resolution digital elevation models (DEMs) obtained from satellite (e.g. Spot 6) and UAV imagery for the Upper Langtang catchment in Nepal. The catchment has an area of 350 km², with a total glacier portion of ~34%, of which 27% is debris covered. DEMs are available from the years 2006, 2009, 2010, 2013, 2014 and 2015 which allows studying glacier evolution over several years. The high resolution of the DEMs also allows making detailed estimates about the role of avalanches or supraglacial cliffs for glacier mass balance. The geodetic mass balances in combination with simulations by a glacio-hydrological model show that mass balances of debris-covered and debris-free glaciers in the valley are both negative and are similar. However, we show that mass loss is significantly reduced by thick debris cover, even if cliffs indeed contribute to a significant percentage of the total thinning over the tongues.

The glacio-hydrological model simulations allow assessing the role played by glaciers for runoff. To inform our choice of model parameters we make use of a unique set of ground data combined with high resolution satellite observations. The systematic integration of detailed information on physical processes enhances the capacity of the model to unravel the full water balance of the study catchment. The multi-variable model validation against catchment runoff, remotely sensed snow cover and geodetic glacier mass balances further increases confidence in the model. We show that at present about 26% of annual catchment runoff originate from ice melt. Snowmelt is the most important component representing 40% of all sources, followed by rainfall (34%). 9% of total water inputs originate from sub-debris ice melt, and 5% originate from melted avalanched snow. We then use the model to make projections of twenty-first century runoff and glacier changes considering the newest climate change scenarios. We show that global warming leads to an increase in future icemelt and a peak in glacier runoff by mid-century. The increase in total icemelt is due to higher ablation rates due to higher air temperatures and large areas currently located above the equilibrium-line altitude that will contribute to melt. Debris-covered glacier area will disappear at a slower pace than non-debris covered area. Still, due to the relative climate insensitivity of melt rates below thick debris, the contribution of sub-debris icemelt to runoff will not exceed 10% at all times.

P 10.14**Measurements of ice dynamical properties of Bowdoin Glacier, Northwest Greenland**

Julien Seguinot¹, Andreas Bauder¹, Martin Funk¹, Guillaume Jouvét¹, Philippe Limpach², Fabian Neyer², Claudia Ryser¹, Shin Sugiyama³ and Yvo Weidmann¹

¹ *Laboratory of Hydraulics, Hydrology and Glaciology, ETH Zürich, CH-8093 Zürich (seguinot@vaw.baug.ethz.ch)*

² *Geodesy and Geodynamics Lab, ETH Zürich, CH-8093 Zürich*

³ *Institute of Low Temperature Science, Hokkaido University, JP-060-0819 Sapporo*

The observed rapid retreat of ocean-terminating glaciers in southern Greenland may propagate to the north in the near future. Hence, tidewater glaciers in this area, some of which have remain stable for decades, are expected to start retreating rapidly through iceberg calving in the coming years, thus allowing a monitoring and investigation of ice dynamical changes starting from the early stages of retreat.

Here, we present measurements of ice dynamical properties from Bowdoin Glacier (77° 42' N; 68° 35' W), a tidewater outlet glacier located at the northwestern margin of the Greenland Ice Sheet. The glacier surface experiences lowering at a rate of 1.5 m/a since 2007. A rapid calving front retreat of 260 m/a was also observed since 2008, while no significant changes occurred during the previous 20 years. From July 2014 to July 2015, we monitored subglacial water pressure changes in boreholes, internal ice deformation through tilt sensors at different depths, englacial ice temperature profiles from the glacier bed to the surface, and high resolution surface motion from GPS records. These observations will be used to validate a numerical ice flow model for tidewater glaciers, aiming for a better understanding of iceberg calving processes in relation to changes in internal ice dynamics.

P 10.15

An automatic algorithm for validating snow depth measurements of IMIS stations

Anna-Maria Tilg¹, Christoph Marty¹, Geoffrey Klein^{2,3}

¹ WSL Institute for Snow and Avalanche Research SLF, Flüelastrasse 7, CH - 7260 Davos Dorf (anna-maria.tilg@slf.ch)

² Institut de Géographie, Université de Neuchâtel, Espace Louis Agassiz 1, CH - 2000 Neuchâtel

³ Swiss Federal Institute for Forest, Snow and Landscape Research WSL

The stations of the IMIS network (Interkantonaless Mess- und Informationssystem) deliver halfhourly meteo- and snowdata. These stations are located in remote areas in the Swiss Alps between 1500 and 3000 m asl. and were originally set up for the avalanche warning service. Since the 1990s more than 110 stations have been installed. In the meantime the data is also useful for ecosystem modeling, climatic or hydrological applications. All these disciplines are interested in accurate snow depth data.

Unfortunately, automatic snow depth measurements might be affected for instance by malfunctioning due to blowing snow events or instrument anomalies. In addition, the ultrasonic snow depth sensor cannot differ between snow and vegetation on the ground. Therefore, an automatic algorithm has been developed to detect and remove outliers in the snow data and to distinguish between snow covered and snow free ground.

Outliers and other obvious sensor problems such as a unique snow depth value over a week, are tried to detect with filters of MeteoIO (Bavay & Egger, 2010). These filters among others allow to check if the snow depth data are between specific thresholds, or if the change rate between two halfhourly values is unusually high.

A distinction between snow covered and snow free ground with the help of the snow surface temperature (SST) seems to be promising. SST is used because more IMIS stations have SST than ground surface temperature (GST) and SST has less suspect data than GST. Using thresholds for minimum, maximum and mean SST lead to a realistic evolution of snow depth during a hydrological year.

REFERENCES

Bavay, M., & Egger T. 2012: MeteoIO – A Meteorological Data Pre-Processing Library for Numerical Models, Geophysical Research Abstracts Vol. 1, EGU2012-11477.

P 10.16

Role of glacial caves in the evolution of glaciers: examples on the Forni Glacier (I), Morteratsch and Aletsch Glacier (CH)

Paola Tognini¹, Mauro Inglese¹, Andrea Ferrario², Margherita Ubaldi², Paolo Testa³

¹ Gruppo Grotte Milano CAI-SEM, via A. Volta 22, 20122 Milano, Italy; Progetto Speleologia Glaciale (paolatognini@iol.it)

² Gruppo Grotte Saronno CAI-SSI, via G. Parini, 54, 21047 Saronno (VA), Italy; Progetto Speleologia Glaciale

³ Gruppo Speleologico CAI Varallo, via Durio, 14, 13019 Varallo (VC), Italy; Progetto Speleologia Glaciale

All the Alpine glaciers are presently affected by huge ice mass losses, with great reduction in volume and retreating of the glacier snouts. Ice mass reduction goes together with changing in morphology, stress distribution and subsequent jointing. Constant monitoring and observations through time of glacial caves point out as recent glacier changing is affecting also on the evolution of en-glacial caves systems and on the formation of contact caves.

It is in fact well demonstrated that glacial caves strictly depend on the distribution of stress through the ice mass and on air and water flow entering the caves: every change in one of these factors causes a change in the morphology of caves. On the other hand, the existence of glacial caves has a control on the evolution of the glaciers themselves, by breakdown and collapse of caves causing sometimes huge losses of ice mass, and by a more criptic process of “erosion” under ice by sublimation and melting processes inside caves. The evolution of glacial caves can also control some peculiar features on the glaciers surface, such as sinkholes and collapse dolines, unroofed canyons, englacial deposits causing the formation of glaciers cones, etc...

Some examples of Forni and Morteratsch Glaciers show the important role glacial caves may have in the evolution of a glacier, mainly in the snout zone. On these two big glaciers it has been observed the way the evolution of very large contact caves is leading to the collapse of large areas at the snout during the last few years: thanks to the breakdown of large glacial galleries, at the snout huge ice masses are suddenly lost, together with a considerable reduction in length. The collapse of large sub-glacial caves thus dramatically and suddenly changes glacier morphology at the snout. Examples on Morteratsch, Aletsch and Forni Glaciers also show the important, though still poorly investigated, role sub- and en-glacial sublimation and melting processes play in glacier ice mass loss.

Glacial caves therefore play a significant role in the evolution of alpine temperate glaciers, being responsible for rapid and spectacular retreats and for considerable ice loss: information given by the study of en- and sub-glacial caves may thus help in forecasting glacier evolution in the very next future.



The collapse of a huge subglacial contact cave in 2010 caused a dramatic change and the loss of a huge ice mass at the snout of Morteratsch Glacier (Photo By Mauro Inglese)

REFERENCES

Eraso A. 1992: Internal glacier melting and naled ice ice generated by air circulation. Proposal of an enthalpy-entropy diagram for quantitative calculations, Proceedings of 2th Int. Symposium Glacier Caves and Glacial Karst in High Mountains and Polar Regions, UIS, 10-16 Feb. Midzygorze, Silesian University Sosnowies, 29-42

- Eraso A., Dominguez M.C. 2007: Subpolar glacier network as natural sensors of global warming evolution, Proceedings of 8th Int. Symposium Glacier Caves and Glacial Karst in High Mountains and Polar Regions, UIS, Sosnowies, 29-47
- Ferrario A., Inglese M., Testa P., Tognini P. 2012: Progetto Speleologia Glaciale: ricerche per conoscere, esplorare e documentare le cavità glaciali dell'arco alpino, *Speleologia*, 67, Società Italiana di Speleologia, 26-34
- Mavlyudov B. R. 1991: The influence of air flows on glacier caves forming, Proceedings of 1st Int. Symposium Glacier Caves and Glacial Karst in High Mountains and Polar Regions, UIS, 1-5 October, 1990, Madrid, 199-206
- Mavlyudov B. R. 1992: Ice evaporation in the glacier caves (Kagware Glacier, South Tibet), Proceedings of 2nd Int. Symposium Glacier Caves and Glacial Karst in High Mountains and Polar Regions, UIS, 10-16 February, Midzygorze, Silesian University Sosnowies, 81-91
- Tognini P. 2009: L'evoluzione delle grotte glaciali del Ghiacciaio dei Forni, *Il Grottesco* n. 55, Bollettino del Gruppo Grotte Milano CAI-SEM, 89-95
- Tognini P., 201: Role of subglacial caves in the evolution of glacier in the snout area. Two examples on the Forni Glacier (Valtellina, I) and Morteratsch Glacier (CH). Proceeding of the 5th Int. Workshop on Ice Caves IWIC-V, 16-23 September, 2012, Barzio, 23
- Tognini P., Ferrario A., Inglese M., Mangiagalli C. 2012: Criocarsismo e speleologia glaciale. In: Bonardi L., Rovelli E., Scotti R., Toffaletti A., Urso M., Villa F. 2012: I ghiacciai della Lombardia: evoluzione e attualità. Servizio Glaciologico Lombardo, Hoepli, 51-58

P 10.17**Long-term dynamics and forcing of a tidewater outlet glacier in West Greenland**

Andreas Vieli¹, Martin Lüthi¹, Luc Moreau², Ian Joughin^{3,1}, Moritz Reisser¹, Röemy Mercenier¹, Christoph Rohner¹

¹ *Department of Geography, University of Zurich, Winterthurerstrasse 190, CH-5057 Zurich (andreas.vieli@geo.uzh.ch)*

² *Chamonix, France*

³ *Polar Science Center, University of Washington, USA*

Dynamic changes of ocean-terminating outlet glaciers such as terminus retreat and flow acceleration are responsible for about half of the current mass loss of the Greenland ice sheet. Although these changes seem related to the general warming in recent decades, the detailed link between external forcing from the atmosphere and/or ocean and glacier response is not well understood. Further, existing observations of tidewater outlet glacier change also show strong temporal fluctuations and are mostly limited to the last two decades of satellite observations.

Here we present and analyze a detailed long-term record of flow and geometry evolution of Egi Sermia, an ocean terminating outlet glacier in West Greenland. This historic record starts in 1912 and has, due to its proximity to the main access route for early expeditions to the ice sheet, a decadal or higher resolution. Observations from satellites and ground based radar interferometry further complement this data set on front positions and flow velocities for the two recent decades.

The front and flow speed of Egi Sermia was more or less stable between 1912 with a slow retreat phase between 1920 to the 1960, followed by a slight readvance in the 1980s. In 2007 the terminus started to retreat rapidly and in a step wise fashion by more than 3km to present and almost quadrupled its flow speed at the terminus. A comparison with surface mass balance and atmospheric temperature records suggests a close relation of the long-term evolution of Egi Sermia to atmospheric forcing, perhaps reflecting the relatively shallow fjord depths. However, due to the close relation between the atmospheric and oceanic time-series, the influence of oceanic forcing cannot be excluded. In contrast, the recent rapid retreat phase and acceleration seems to be linked to a changing regime in the calving process and geometric effects.

P 10.18**Towards the volumes of all the glaciers in the world 2.0**

Mauro Werder, Matthias Huss

Versuchsanstalt für Wasserbau, Hydrologie und Glaziologie (VAW), ETH Zürich, 8093 Zürich (werder@vaw.baug.ethz.ch)

Knowledge about ice thickness and volume is indispensable for studying ice dynamics, future sea-level rise due to glacier melt or their contribution to regional hydrology. Accurate measurements of glacier thickness require on-site work, usually employing radar techniques. However, these field measurements are time consuming, expensive and sometimes downright impossible.

The model of Farinotti et al. (2009) calculates ice thicknesses by using a mass conservation approach fed by estimates of the surface mass balance. The presented model extends this by also incorporating assimilation of surface flow speed measurements, which are becoming available world-wide through remote sensing. This extension has the potential to improve the accuracy of the ice thickness predictions for all the glaciers world-wide. We present the new assimilation strategy and assess the model performance using glaciers of the Antarctic Peninsula with well known bed topography. The final goal of the project is to provide new thickness and volume estimates for all of the glaciers in the world.

REFERENCES

Farinotti, D., Huss, M., Bauder, A., Funk, M., and Truffer, M. (2009). A method to estimate the ice volume and ice-thickness distribution of alpine glaciers. *Journal of Glaciology*, 55(191):422-430.

P 10.19

Glacier Monitoring on Golubin Glacier since 2011

Erlan Azisov¹, Marlene Kronenberg², Martina Barandun², Martin Hoelzle² & Ryskul Usabaliev¹

¹ *Central Asian Institute of Applied Geosciences (CAIAG), Bishkek, Kyrgyzstan*

² *Department of Geosciences, University of Fribourg, Fribourg, Switzerland*

During the Soviet Union many glaciers in Central Asia were monitored continuously until the mid-90s (Unger-Shayesteh and others, 2013). With the collapse of the USSR the scientific programs stopped abruptly on all glaciers located in Kyrgyzstan. Within the projects CATCOS and CAWa the WGMS, the GFZ Potsdam, the University of Fribourg and the Central Asian Institute for Applied Geosciences joined their efforts to re-establish the glacier monitoring on four selected Kyrgyz Glaciers (Golubin, Suyok Zapadnyi, Abramov Glacier and Glacier No. 354) in 2010 respectively 2011 (WGMS, 2013). Since then, the measurements are annually carried out under joined efforts of an international team of scientists. The collected glaciological data is submitted regularly to the WGMS and meteorological data from newly installed automatic weather stations in close vicinities to the monitored glaciers are openly accessible on the CAWa homepage (Schoene and others, 2013).

Golubin Glacier is a well accessible Tien Shan glacier in the Ala Archa basin in Kyrgyzstan (5.5 km²) (Fig. 1). Records of length changes reach back to 1861, and continuous glaciological, hydrological and atmospheric studies were performed between 1958 and the late 1990's. Mass balance measurements and length change observations have been re-established in 2010. The ablation stake network includes 15 stakes and each year between 2 to 5 snow-pits are dug to measure density and snow depth in the accumulation area (fig. 2). Snow depth probings are additionally carried out to improve the spatial coverage of measurements in the accumulation zone. Field surveys are usually conducted once a year, preferably at the end of summer. However, due to logistic reasons this was not always possible and some surveys were carried out in late July or early August. Mass balance is thus measured in the floating date system. We analysed the glaciological data with the simple profile and contour-line methods. Results of both methods are compared for the period from 2011 to 2015.

We could identify that the changing measurement period affects the result strongly and suggest correcting the mass balance data to match the hydrological year. We plan to apply a calibrated mass balance model after Huss and others (2009) to do a homogenization of the new data since 2010 and a re-analysis of the existing mass balance data back to the 1960s.



Figure 1. Location of Golubin Glaciers is indicated in Red

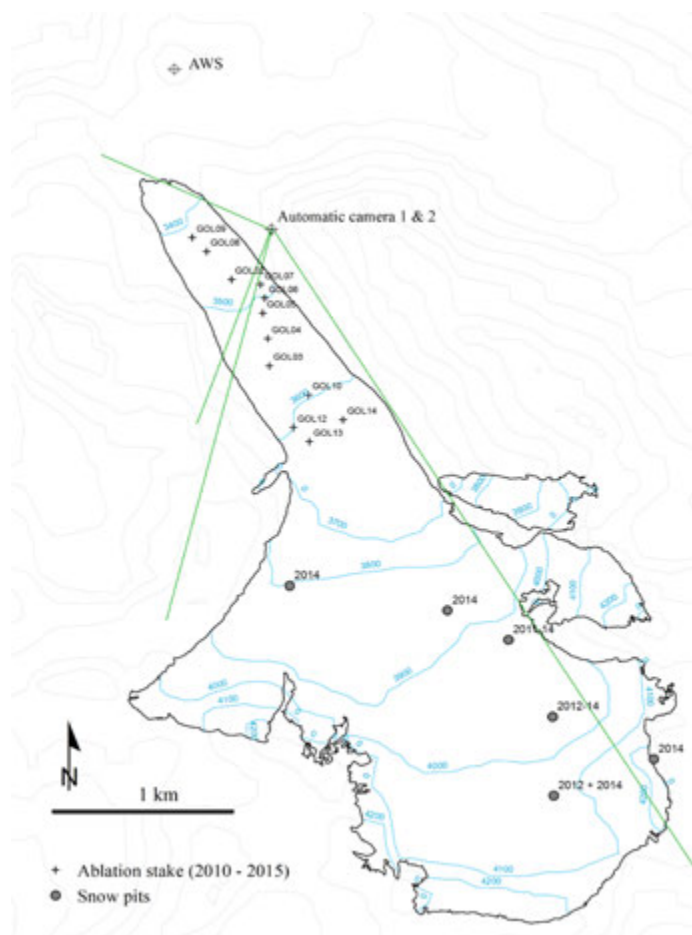


Figure 2. Stake network and snow-pit location at Golubin Glacier.

REFERENCES

- Huss, M., Bauder, A., & Funk, M. (2009). Homogenization of long-term mass-balance time series. *Annals of Glaciology*, 50(50), 198-206.
- Schöne, T., Zech, C., Unger-Shayesteh, K., Rudenko, V., Thoss, H., Wetzel, H. U., ... & Zubovich, A. (2013). A new permanent multi-parameter monitoring network in Central Asian high mountains—from measurements to data bases. *Geoscientific Instrumentation, Methods and Data Systems*, 2(1), 97-111.
- Unger-Shayesteh, K., Vorogushyn, S., Farinotti, D., Gafurov, A., Duethmann, D., Mandych, A., & Merz, B. (2013). What do we know about past changes in the water cycle of Central Asian headwaters? A review. *Global and Planetary Change*, 110, 4-25.
- WGMS, (2013). *Glacier Mass Balance Bulletin No. 12 (2010-2011)*. Ed. Zemp, M., Nussbaumer, S. U., Naegeli, K., Gärtner-Roer, I., Paul, F., Hoelzle, M., & Haeberli, W., ICSU (WDS)/IUGG (IACS)/UNEP/UNESCO/WMO, World Glacier Monitoring Service, Zurich, Switzerland, 106 pp.

P 10.20

Development of a Cryocell for High-Resolution Trace Element Analysis of Ice Cores Using LA-ICP-MS

Sven Erik Avak,^{1,2,3} Mario Birrer,¹ Markus Wälle,⁴ Thorsten Bartels-Rausch,¹ Margit Schwikowski,^{1,2,3} and Anja Eichler^{1,2}

¹ Laboratory of Radiochemistry and Environmental Chemistry, Paul Scherrer Institute, CH-5232 Villigen PSI (sven.avak@psi.ch)

² Oeschger Centre for Climate Change Research, University of Bern, CH-3012 Bern

³ Department of Chemistry and Biochemistry, University of Bern, CH-3012 Bern

⁴ Institute of Geochemistry and Petrology, ETH Zurich, CH-8092 Zurich

Past changes of atmospheric pollution can be reconstructed from ice core trace element records of cold mountain glaciers. Due to the current global temperature increase glaciers at low and mid altitudes are in danger to turn into polythermal ones, where postdepositional processes like percolation of melt water alter the information originally stored in those environmental archives. The preservation of impurities with respect to melt water depends on whether they are located at grain boundaries or embedded into the matrix. Laser ablation inductively coupled plasma mass spectrometry (LA-ICP-MS) is the method of choice for the direct *in situ* chemical analysis of trace elements at high spatial resolution in ice (Sneed *et al.*, 2015). However, applications with glacial ice samples show that some obstacles still remain. The quantification of signals and the internal standardization are not yet matured (Reinhardt *et al.*, 2001, Della Lunga *et al.*, 2014). Here, we present the setup of a newly designed cryocell compatible to a commercially available laser ablation system. This cryocell is able to simultaneously hold ice samples and frozen standard solutions for quantifying concentration differences between grain boundaries and ice grain interiors. Furthermore the development and optimization of frozen standards for calibration will be discussed. Once this analytical technic is established, this will smooth the way to investigate the potential of ice cores from polythermal glaciers as archives of past atmospheric pollution.

REFERENCES

- Sneed, S. B., Mayewski, P. A., Sayre, W. G., Handley, M. J., Kurbatov, A. V., Taylor, K. C., Bohleber, P., Wagenbach, D., Erhardt, T. & Spaulding, N. E. 2015: New LA-ICP-MS cryocell and calibration technique for sub-millimeter analysis of ice cores, *Journal of Glaciology*, 61, 233-242.
- Della Lunga, D., Müller, W., Rasmussen, S. O. & Svensson, A. 2014: Location of cation impurities in NGRIP deep ice revealed by cryo-cell UV-laser-ablation ICPMS, *Journal of Glaciology*, 60, 970-988.
- Reinhardt, H., Kriews, M., Miller, H., Schrems, O., Lüdke, C., Hoffmann, E. & Skole, J. 2001: Laser ablation inductively coupled plasma mass spectrometry: a new tool for trace element analysis in ice cores, *Fresenius' Journal of Analytical Chemistry*, 370, 629-636.

P 10.21

The nature of frozen salt solutions: A new in-situ XPS approach

Thorsten Bartels-Rausch, Fabrizio Orlando, Thomas Huthwelker, Astrid Waldner, Markus Ammann

Paul Scherrer Institute, Switzerland

Sea salt, and in particular its major halide, chloride, is an important reactant in the atmosphere. Chloride in air-borne sea salt aerosol is – once chemically converted to a molecular halogen (Cl_2 , BrCl) and released to the atmosphere – well known as important atmospheric reactant, driving large-scale changes to the atmospheric composition and in particular to ozone levels in remote areas, but also in coastal mega cities [1,2]. Similar chemistry has been proposed for sea salt deposits in polar snow covers [3]. A crucial factor determining the overall reactivity is the local physical environment of the chloride ion. For example, the reactivity of liquid aerosols decreases significantly upon crystallization [1,4,5]. Surprisingly, the phases of NaCl-containing systems are still under debate [4], partially due to the limited availability of in situ measurements directly probing the local environment at the surface of frozen NaCl-water binary systems.

Using core electron spectroscopy of the oxygen atoms in water, we previously showed that these systems follow the phase rules at the air-ice interface [5]. This finding contrasts some earlier observations, where the presence of liquid-like Cl below the eutectic point of bulk solutions [6] was postulated (see Ref. [4] and references therein). In the present study, we present new electron yield near-edge X-ray absorption fine structure spectroscopy (NEXAFS) data obtained at near-ambient pressures up to 20 mbar of NaCl and NaBr frozen solutions. The method is sensitive to small changes in the local environment of the chlorine and the bromine atom. The measurements reported in this section were performed at the PHOENIX beamline at SLS. The study indicates frapant differences in the phases of NaCl- or NaBr-water mixtures at temperatures blow the freezing point for the surface of the ice vs. the bulk. This has signifiant impact on modeling chemical reactions in snow or ice and it's environmental consequences.

REFERENCES

- [1] J.P.D. Abbatt, J.L. Thomas, K. Abrahamsson, C. Boxe, A. Granfors, A.E. Jones, M.D. King, A. Saiz-Lopez, P.B. Shepson, J. Sodeau, D.W. Toohey, C. Toubin, R. von Glasow, S.N. Wren, X. Yang, Halogen activation via interactions with environmental ice and snow in the polar lower troposphere and other regions, *Atmospheric Chemistry and Physics*, 12 (2012) 6237-6271.
- [2] H.D. Osthoff, J.M. Roberts, A.R. Ravishankara, E.J. Williams, B.M. Lerner, R. Sommariva, T.S. Bates, D. Coffman, P.K. Quinn, J.E. Dibb, H. Stark, J.B. Burkholder, R.K. Talukdar, J. Meagher, F.C. Fehsenfeld, S.S. Brown, High levels of nitrly chloride in the polluted subtropical marine boundary layer, *Nature Geoscience*, 1 (2008) 324-328.
- [3] T. Koop, A. Kapilashrami, L.T. Molina, M.J. Molina, Phase transitions of sea-salt/water mixtures at low temperatures: Implications for ozone chemistry in the polar marine boundary layer, *Journal of Geophysical Research: Atmospheres*, 105 (2000) 26393-26402.
- [4] T. Bartels-Rausch, H.W. Jacobi, T.F. Kahan, J.L. Thomas, E.S. Thomson, J.P.D. Abbatt, M. Ammann, J.R. Blackford, H. Bluhm, C. Boxe, F. Domine, M.M. Frey, I. Gladich, M.I. Guzmán, D. Heger, T. Huthwelker, P. Klán, W.F. Kuhs, M.H. Kuo, S. Maus, S.G. Moussa, V.F. McNeill, J.T. Newberg, J.B.C. Pettersson, M. Roeselová, J.R. Sodeau, A review of air-ice chemical and physical interactions (AICI): Liquids, quasi-liquids, and solids in snow, *Atmospheric Chemistry and Physics*, 14 (2014) 1587-1633.
- [5] C.E. Kolb, R.A. Cox, J.P.D. Abbatt, M. Ammann, E.J. Davis, D.J. Donaldson, B.C. Garrett, C. George, P.T. Griffiths, D.R. Hanson, M. Kulmala, G. McFiggans, U. Pöschl, I. Riipinen, M.J. Rossi, Y. Rudich, P.E. Wagner, P.M. Winkler, D.R. Worsnop, C.D. O'Dowd, An overview of current issues in the uptake of atmospheric trace gases by aerosols and clouds, *Atmospheric Chemistry and Physics*, 10 (2010) 10561-10605.
- [6] A. Křepelová, T. Huthwelker, H. Bluhm, M. Ammann, Surface Chemical Properties of Eutectic and Frozen NaCl Solutions Probed by XPS and NEXAFS, *ChemPhysChem*, 11 (2010) 3859-3866.
- [7] Y. Cheng, H. Su, T. Koop, E. Mikhailov, U. Pöschl, Size dependence of phase transitions in aerosol nanoparticles, *Nat Commun*, 6 (2015).

P 10.22

Temperature dependence of ozone loss by reaction with NaBr-films in coated-wall flow-tubes

Jacinta Edebeli¹, Markus Ammann, Anja Eichler¹, Martin Schneebeli² & Thorsten Bartels-Rausch¹

¹ *Laboratory of Radio and Environmental Chemistry, Paul Scherrer Institute, 5232 Villigen, Switzerland*

² *Institute for Snow and Avalanche Research SLF, Flüestrasse 11, CH-7260 Davos Dorf Switzerland*

The application of coated wall flow tube (CWFT) to heterogeneous interactions is a well-established experimental method [1]. This method has been applied to observing the kinetics and uptake of compounds from the gas phase over frozen [2,3], and dry surfaces [3] as well as for photolysis studies in doped ice [4]. In this work, we apply CWFT in observing the dependence of ozone loss on temperature over NaBr-citric acid mixture. Citric acid was used as a viscous matrix to facilitate coating of flow tube and to dilute the NaBr. The loss of ozone attributed to the production of reactive bromine species from salt solutions has been explained by heterogeneous reactions (both light dependent and light independent). One of such set of reactions, which we studied, is presented below:



The temperature dependence of ozone depletion studies in brominated systems remains an unanswered research question in this topic of study [6]. The goal of this study was to attempt answering this question using a simple but established experimental setup.

REFERENCES

1. Bartels-Rausch, T., Huthwelker, T., Gäggeler, H.W., Ammann, M. 2005: Atmospheric pressure coated-wall flow-tube study of acetone adsorption on ice. *J. Phys. Chem. A*, 109, 4531-4539.
2. Bartels-Rausch, T., Brigante, M., Elshorbany, Y.F., Ammann, M., D'Anna, B., George, C., Stemmler, K., Ndour, M., Kleffmann, J. 2010: Humic acid in ice: Photo-enhanced conversion of nitrogen dioxide into nitrous acid. *Atmospheric Environment* 44, 5443-5450.
3. Holmes, N.S., Adams, J. W., Crowley, J.N. 2001: Uptake and reaction of HOI and IONO₂ on frozen and dry NaCl/NaBr surfaces and H₂SO₄. *Phys. Chem. Chem. Phys.* 3, 1679 – 1687.
4. Haag, W.R. and Hoigné, J. 1983: Ozonation of bromide-containing waters: Kinetics of formation of hypobromous acid and bromate. *Environ. Sci. Technol.* 17, 261-267 In Oum, K.W., Lakin M. J., Finlayson-Pitts, B.J. 1998: Bromine activation in the troposphere by the dark reaction of O₃ with seawater ice. *Geophys Res. Lett* 25, 3923-3926.
5. Abbatt, J. 1994: Heterogeneous reaction of HOBr with HBr and HCl on ice surfaces at 228 K. *Geophys Res. Lett* 21 665-668 In Oum, K.W., Lakin M. J., Finlayson-Pitts, B.J. 1998: Bromine activation in the troposphere by the dark reaction of O₃ with seawater ice. *Geophys Res. Lett* 25, 3923-3926.
6. Abbatt J., Thomas, J.L., Abrahamsson, K.A., Boxe, C., Granfors, A., Jones, A.E., King, M.D., Saiz-Lopez, A., Shepson, P.B., Sodeau, J., Toohey, D. W., Toubin, C., von Glasow, R., Wren, S.N., Yang, X. 2012. Halogen activation via interactions with environmental ice and snow in the polar lower troposphere and other regions. *Atmos. Chem. Phys.* 12, 6237-6271.

P 10.23

Organic carbon investigations at ice cores from Colle Gnifetti – lessons learned and future challenges

Helene Hoffmann¹, Steffen Greilich³, Martin Schock³, Phil Stricker³, Barbara May³, Pascal Bohleber^{1,2} & Dietmar Wagenbach[†]

¹ *Institut für Umweltphysik, Universität Heidelberg, Im Neuenheimer Feld 229, 69120 Heidelberg (helene.hoffmann@iup.uni-heidelberg.de)*

² *Climate Change Institute, University of Maine, Orono, ME 04469, USA*

³ *formerly at: Institut für Umweltphysik, Universität Heidelberg, Im Neuenheimer Feld 229, 69120 Heidelberg*

[†] *deceased 2014*

Organic carbonaceous aerosols contribute an important fraction to the global atmospheric aerosol budget. However, especially source attributions are still not very well understood. Due to its low net accumulation rate, the cold high Alpine glacier saddle of Colle Gnifetti, offers unique long-term ice core records, that can be used to investigate those organic species potentially over the last millenium and beyond.

At the Institute of Environmental Physics in Heidelberg, measurements of organic carbon in ice samples have been carried out for more than fifteen years. The original emphasis was on analysis of the dissolved organic carbon fraction (DOC), revealing a significant rise in concentration during the 20th century likely caused by increased anthropogenic fossil fuel burning. Of special interest is also an increase in DOC concentrations near bedrock, which remains poorly understood so far.

Recent studies explored the opportunity of dating ice cores via micro-radiocarbon analysis of the dissolved and the particulate organic carbon fraction (POC). This is especially relevant for ice cores from Colle Gnifetti, where conventional stratigraphic are very limited. A major challenge in dating via ¹⁴C is the small concentration of organic carbon in these ice samples, ranging from 10-50µg carbon per kg ice in the POC and 50-100µg carbon per kg ice in the DOC fraction, which makes sample preparation cumbersome and susceptible to contamination.

Here we present the latest developments in DOC and POC micro radiocarbon dating performed on CG ice cores drilled in 2005 and 2013. We focus on a rigorous analysis of potential age biasing effects, comprising in situ production in the DOC fraction and reservoir effects like the input of old Saharan dust in the POC fraction.

P 10.24

Ice nuclei and the landscape-precipitation feedbacks: an example from the Arctic environment

Emiliano Stopelli¹, Franz Conen¹, Lukas Zimmermann¹, Cindy E. Morris², Christine Alewell¹

¹ *Environmental Geosciences, University of Basel, Bernoullistrasse 30, CH-4056 Basel (emiliano.stopelli@unibas.ch)*

² *INRA, UR0407 Pathologie Végétale, F-84143 Montfavet Cedex, France*

The Arctic is considered with growing concern as one of the areas on Earth most sensitive to climate change. One of the greatest uncertainties in climate modelling involves the behavior of clouds, with direct implications for the determination of their radiative budget and the distribution of precipitation. Clouds in the Arctic region are generally characterised by low droplet concentrations, mirroring low abundance of cloud condensation nuclei (CCN) and leading to low-intensity precipitation events. Particles acting as ice nucleators (IN) catalyse the aggregation of water molecules into ice, increasing the chance for precipitation. Therefore, a change in IN numbers and composition may have strong impacts on climate in the Arctic.

To understand how many IN are present in the Arctic atmosphere and to identify possible sources of such particles, in July 2015 we collected samples at the Haldde Observatory, Norway (69°55'45" N, 22°48'30" E, 905 m a.s.l.). A portable PM₁₀ sampler was used to collect particles from the atmosphere and the abundance of IN active at moderate supercooling temperatures (≥ -15 °C) which deposited on the filters was determined. We also collected samples of material with high potential for becoming airborne and for acting as IN, such as soil from a highland subject to melting-thawing cycles and some leaf litter from a surface progressively uncovered from snow melting. Results indicate that, based on the temperature of activity of the particles, it is mainly litter which can potentially account for the IN we observed on PM₁₀ filters at Haldde.

These preliminary results indicate that simple methodology based on PM₁₀ filters has a high potential for broad application, specifically in studying how precipitation patterns are impacted by IN and which are the potential local and faraway sources of such particles. This is of fundamental relevance in glaciological and hydrological studies, since it allows the determination of how IN contribute to the renewal of snowpacks and water reservoirs. Secondly, this example suggests feedbacks linking landscapes and atmosphere in the frame of climate change in the Arctic. Snowmelt in the Arctic region can increase the extent of areas of litters that are exposed to wind and grazing and reduce the snow coverage. This can potentially change the origin of ice particles in the atmosphere, for instance from ice crystals from snowpacks blown by wind to airborne IN from leaf litter. Such IN may then promote a different freezing of clouds, changing their lifetime, radiative properties, and ultimately the occurrence of precipitation in the Arctic region.

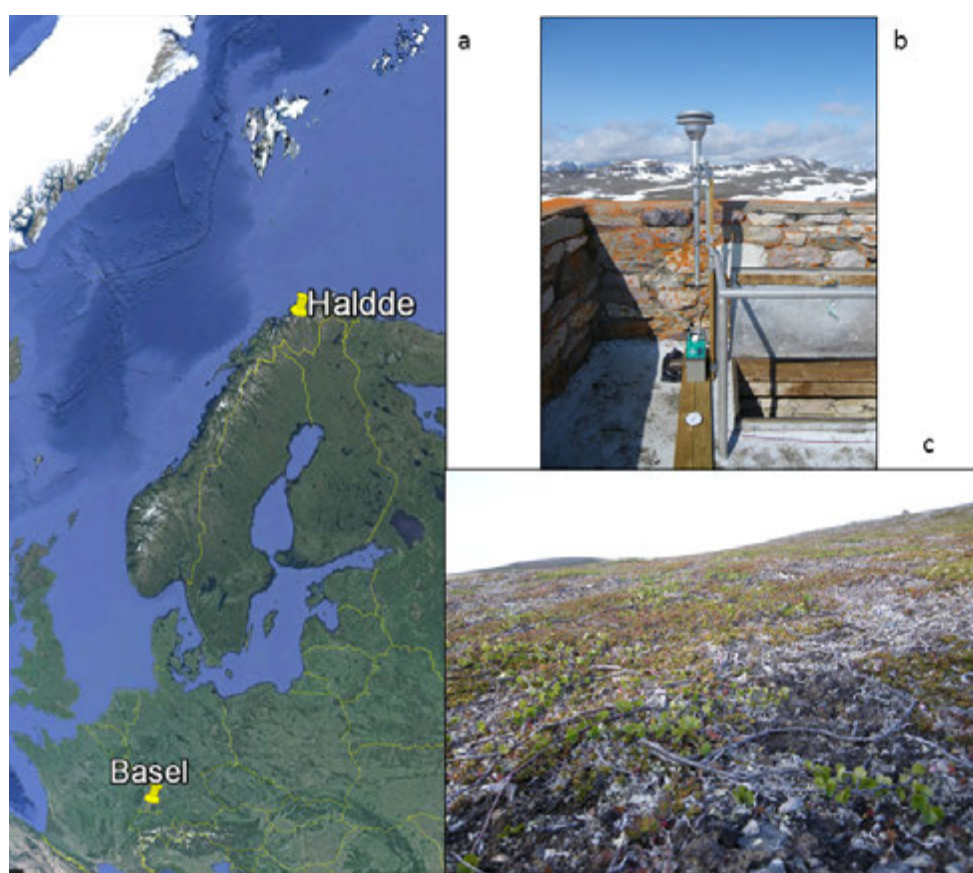


Figure 1. a) Location of the Haldde sampling site; b) Portable PM₁₀ sampler; c) Highland subject to freeze-thawing cycles where soil samples were collected.

REFERENCES

- Bigg, E. K., 1996. Ice forming nuclei in the high Arctic. *Tellus B*, 48, 223-233.
- Conen, F. *et al.*, 2012. Atmospheric ice nucleators active ≥ -12 °C can be quantified on PM₁₀ filters. *Atmospheric Measurement Techniques* 5, 321-327.
- Creamean, J.M. *et al.*, 2015. Impact of interannual variations in sources of insoluble aerosol species on orographic precipitation over California's central Sierra Nevada. *Atmospheric Chemistry and Physics*, 15, 6535-6548.
- Gayet, J.-F., *et al.*, 2009. On the onset of the ice phase in boundary layer arctic clouds. *Journal of Geophysical Research*, 114, 1-15.
- Prenni A. J., *et al.*, 2007. Can ice-nucleating aerosols affect arctic seasonal climate? *Bulletin of the American Meteorological Society*, 88, 541-550.

P 10.25

The debate on the basal age of Kilimanjaro's plateau glaciers

C. Uglietti^{1,2,3}, A. Zapf^{1,2,3†}, T. Jenk^{1,2,3}, S. Szidat^{1,2,3}, G. Salazar², D.R. Hardy⁴, M. Schwikowski^{1,2,3}

¹ *Laboratory of Radiochemistry and Environmental Chemistry, Paul Scherrer Institute, Villigen, 5232, Switzerland*

² *Department of Chemistry and Biochemistry, University of Bern, Switzerland*

³ *Oeschger Center for Climate Research, University of Bern, Switzerland*

⁴ *Department of Geosciences, University of Massachusetts, Amherst, MA 01003, USA*

[†] *Deceased*

Radiocarbon dating is a powerful tool when the annual layers counting in the lowermost segments of high altitude ice cores is constrained by ice flow-induced thinning limits, but the organic material amount in the ice can be a limiting factor. We present a radiocarbon dating approach using carbonaceous aerosols enclosed in the ice to help resolve the controversy about the age of the Kilimanjaro's plateau glaciers. Paleoclimate reconstructions based on six ice cores drilled in 2000 assigned a basal age of 11'700 years. A recent study claims recurring cycles of waxing and waning controlled primarily by atmospheric moisture and an absence of the ice bodies was suggested for 1200 AD. Solving the dispute of the interval for the extinction of the Kilimanjaro ice might have implications for the understanding of the climate variability in the tropics.

A stratigraphic sequence of 45 horizontal short cores was collected in 2011 from the exposed vertical ice cliffs at the margins of the Northern Ice Field (NIF). The insoluble carbonaceous particles were filtrated and combusted by means of a thermo-optical OC/EC analyser and ¹⁴C was analysed using the compact radiocarbon AMS system 'MICADAS'.

The results of ¹⁴C calibrated ages span between modern ages at the surface to 1200 AD at the bottom, thus supporting the hypothesis that the ice on Kilimanjaro's plateau has come and gone recurrently throughout the Holocene. It is possible that the cores collected further from the margin of the NIF contained older, relict ice, implying hiatuses, and a non-continuous record.

P 10.26

Acidic trace gas adsorption on ice: XPS analysis with the new NAPP experimetal cell at SLS

Astrid Waldner^{1,2} Fabrizio Orlando¹, Mario Birrer¹, Markus Ammann¹, Thomas Huthwelker¹ & Thorsten Bartels-Rausch¹

¹ *Paul Scherrer Institut, 5232 Villigen PSI, Switzerland (astrid.waldner@psi.ch)*

² *Institute of Atmospheric and Climate Science, ETH Zurich, 8092 Zurich, Switzerland*

Acidic trace gases, such as HCl, HNO₃ and formic acid, play an important role in stratospheric and tropospheric chemistry. The presence of ice in form of cirrus clouds or snow disturbs this chemistry. The molecular processes of the interaction of acidic trace gases with ice are still a matter of debate. It has been proposed that the disordered interface at the ice surface, the premelting region, influences the underlying processes (Dash 2006). However neither a quantification of the uptake is possible nor a molecular picture of the uptake is available (Bartels-Rausch 2014, Huthwelker 2006). Among others this severe lack of knowledge hinders the development of global models that would allow predicting changes to the large-scale effects in the near future.

The understanding of how dopants can modify the structure of the ice's water molecules network is herein of fundamental importance. Former laboratory based studies indicate that the surface of ice can become increasingly disordered upon adsorption of acids at temperatures of less than 243 K. It was further shown that the uptake of acidic gases significantly increased in presence of this disordered surface layer, also called quasi-liquid layer. But so far, direct experimental observations under environmentally relevant conditions of the ice surface and of the adsorption of trace gases to it are very limited. In this study, we take advantage of the high surface and analytical sensitivity as well as the chemical selectivity of photoemission and absorption spectroscopy performed at near ambient pressure conditions to overcome this limitation in environmental science. The usage of the surface sensitive spectroscopic methods X-ray Photoelectron Spectroscopy (XPS) allows us to analyse the acidic trace gas adsorption on ice on a molecular level. The depth concentration profile and dissociation degree of the dopant can be directly probed. Due to the aim to perform measurements close to atmospheric conditions the Near-Ambient-Pressure-Photospectroscopy endstation (NAPP) solid chamber was optimized.

Here we present first analysis of the uptake of formic acid on ice as show in figure 1. Acidic trace gases, such as formic acid, are some of the most abundant oxygenated volatile organic compounds in the atmosphere and major contributors to free acidity in precipitation (Chebbi 1996). Depth profiles based on C 1s and O 1s XPS of ice in presence of formic acid indicate that the dosed acid stays at the ice surface. The obtained results are compared to former analysis of the uptake of further trace gases.

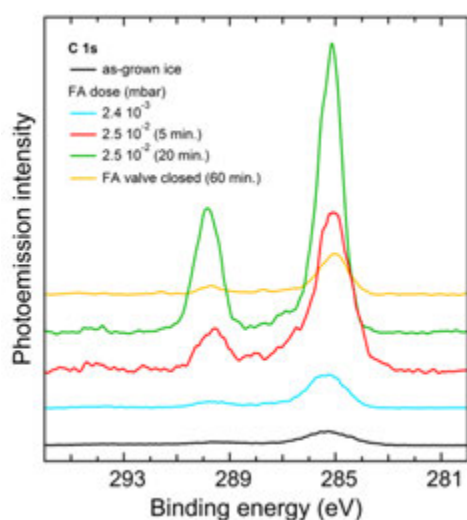


Figure 1. C 1s XPS spectra measured during formic acid uptake on the ice surface at 223 K and 0.042 mbar partial water vapor pressure in the analysis cell. The measurements were performed at the PHOENIX beamline of PSI/SLS with a photon energy of 2200 eV. The C 1s spectra indicate nicely the uptake and release of the formic acid on the ice. (Orlando 2015)

REFERENCES

- Dash, J. G., Rempel, A. W., Wettlaufer, J. S 2006: The physics of premelted ice and its geological consequences. *Rev. Mod. Phys.* 78, 695.
- Bartels-Rausch, T., H.-W. Jacobi, T. F. Kahan, J. L. Thomas, E. S. Thomson, J. P. D. Abbatt, M. Ammann, J. R. Blackford, H. Bluhm, C. Boxe, F. Domine, M. M. Frey, I. Gladich, M. I. Guzmán, D. Heger, Th. Huthwelker, P. Klán, W. F. Kuhs, M. H. Kuo, S. Maus, S. G. Moussa, V. F. McNeill, J. T. Newberg, J. B. C. Pettersson, M. Roeselová, and J. R. 2014: A review of air-ice chemical and physical interactions (AICI): liquids, quasi-liquids, and solids in snow. *Atmos. Chem. Phys.* 14, 1587-1633.
- Huthwelker, T., Ammann, M., Peter, T. 2006: The uptake of acidic trace gases. *Chem. Rev.* 106, 1375-1444.
- Chebbi, A., Carlier, P. 1996: Carboxylic acids in the troposphere occurrence, sources and sinks: A review. *Atmos. Env.* 30, 24.
- Orlando, F., Waldner, A., Bartels-Rausch, T., Birrer, M., Lee, M., Proff, C., Huthwelker, T., Kleibert, A., Bokhoven, J., Ammann, M. 2015: Environmental photochemistry of oxide surfaces and the nature of frozen salt solutions: A new in situ XPS approach. Submitted to: *Topics in Catalysis*

P 10.27

A 250-year black carbon record from the Lomonosovfonna ice core, Svalbard

Dimitri Osmont^{1,2,3}, Michael Sigl^{1,2,3}, Loïc Schmidely³, Isabel Wendl^{1,2,3}, Elisabeth Isaksson⁴, Margit Schwikowski^{1,2,3}

¹ *Laboratory of Radiochemistry and Environmental Chemistry, Paul Scherrer Institut, CH-5232 Villigen PSI
(dimitri.osmont@psi.ch)*

² *Department of Chemistry and Biochemistry, University of Bern, Freiestrasse 3, CH-3012 Bern*

³ *Oeschger Centre for Climate Change Research, University of Bern, Falkenplatz 16, CH-3012 Bern*

⁴ *Norwegian Polar Institute, Framsenteret, 9296 Tromsø, Norway*

Ice cores retrieved from polar and high-mountain glaciers are a very powerful tool to reconstruct paleoclimates due to the fact that glaciers behave as climate archives by trapping chemical information from the atmosphere. Among the studied compounds, Black Carbon (BC), as other atmospheric aerosol constituents, has been of growing interest for the last years because of its potential impact on global warming and human health.

BC consists of aggregates of small carbon spherules produced by the incomplete combustion of fossil fuels and biofuels (including wildfires) from both anthropogenic and natural origin (Bond et al., 2013). BC strongly absorbs visible light and therefore contributes directly to the warming of the atmosphere, and indirectly via the reduction of the snow albedo.

Our work is part of an inter-disciplinary project (SNF Sinergia "Paleo fires") aiming at reconstructing regional paleofire histories for the last 2000 years in order to understand the complex relationship between climate, fires and humans, by measuring BC and other fire tracers in ice cores from mountain glaciers. BC was analysed with a Single Particle Soot Photometer (SP2) according to the protocol given by Wendl et al. (2014). Here we present a 250-year BC record from the Lomonosovfonna ice core, drilled in Svalbard in 2009.

The BC record clearly shows an anthropogenic influence since the beginning of the industrial revolution. BC concentrations were slowly rising from a natural background after 1800 and increased sharply after 1870. Peak values were observed around 1880 and 1900 probably due to coal emissions in Western Europe and Northern America, in agreement with the findings of McConnell et al. (2007) in an ice core from Greenland. After a decline between the two World Wars owing to the economic crisis, BC emissions dramatically increased after the Second World War because of the economic growth and the extensive use of coal and oil. The highest values were found between the 1950s and the 1980s, followed by a clear decline due to the implementation of cleaner technologies and stricter environmental policies. Some sharp peaks with sub-annual resolution can be attributed to strong forest fires occurring in the Northern Hemisphere, such as the 1994 biomass burning event, also detected by Dibb et al. (1996) in Greenland.

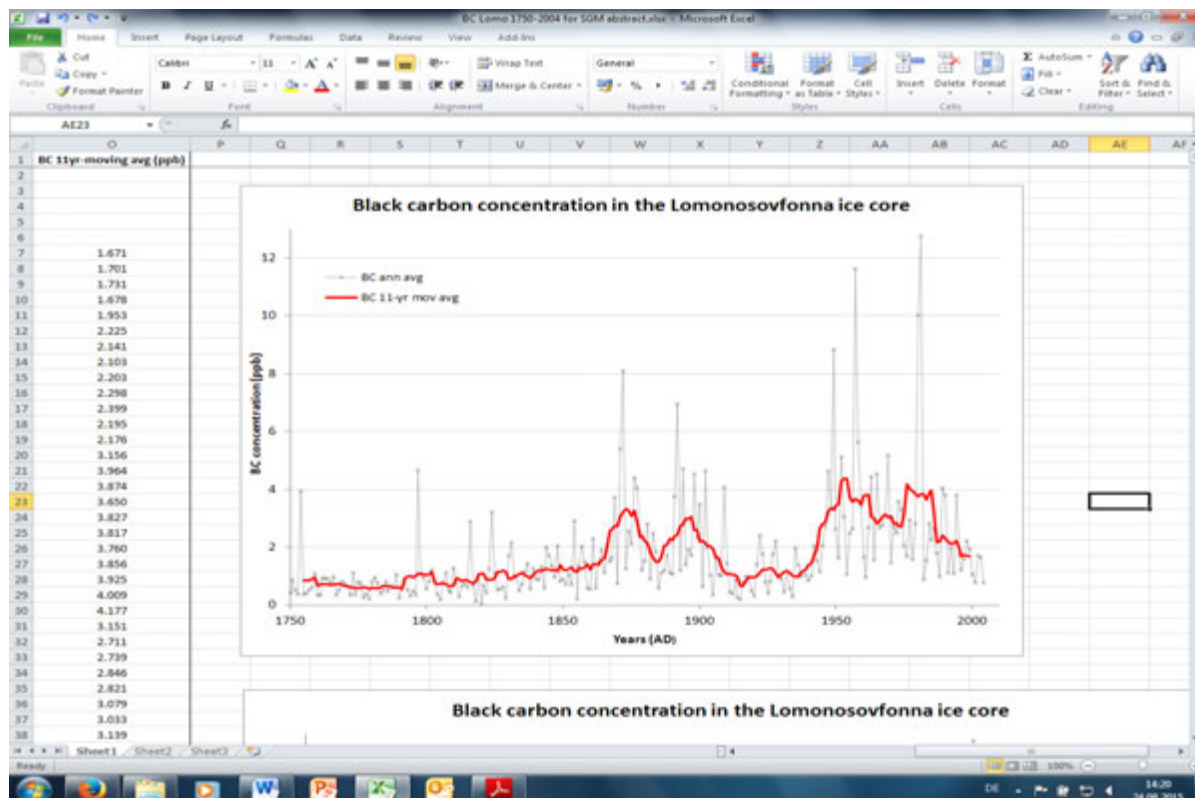


Figure 1. Black carbon (BC) record from the Lomonosovfonna ice core spanning 1750-2004 AD. Dashed black line represents the annual averages, bold red line the 11-year moving averages.

REFERENCES

- Bond, T. C., Doherty, S. J., Fahey, D. W., Forster, P. M., Berntsen, T., DeAngelo, B. J., Flanner, M. G., Ghan, S., Kärcher, B., Koch, D., Kinne, S., Kondo, Y., Quinn, P. K., Sarofim, M. C., Schultz, M. G., Schulz, M., Venkataraman, C., Zhang, H., Zhang, S., Bellouin, N., Guttikunda, S. K., Hopke, P. K., Jacobson, M. Z., Kaiser, J. W., Klimont, Z., Lohmann, U., Schwarz, J. P., Shindell, D., Storelvmo, T., Warren, S. G. & Zender, C. S. 2013: Bounding the role of black carbon in the climate system: A scientific assessment. *Journal of Geophysical Research: Atmospheres*, 118, 5380-5552.
- Dibb, J. E., Talbot, R. W., Whitlow, S. I., Shipham, M. C., Winterle, J., McConnell, J. & Bales R. 1996: Biomass burning signatures in the atmosphere and snow at Summit, Greenland: an event on 5 August 1994. *Atmospheric Environment*, 30, 4, 553-561.
- McConnell, J. R., Edwards, R., Kok, G. L., Flanner, M. G., Zender, C. S., Saltzman, E. S., Banta, J. R., Pasteris, D. R., Carter, M. M. & Kahl, J. D. W. 2007: 20th-century industrial black carbon emissions altered Arctic climate forcing. *Science*, 317, 1381-1384.
- Wendl, I. A., Menking, J. A., Färber, R., Gysel, M., Kaspari, S. D., Laborde, M. J. G. & Schwikowski, M. 2014: Optimized method for black carbon analysis in ice and snow using the Single Particle Soot Photometer. *Atmospheric Measurement Techniques*, 7, 2667-2681.

11. Hydrology, Limnology and Hydrogeology

Bruno Schädler, Tobias Jonas, Ole Rössler, Michael Sinreich, Massimiliano Zappa

*Schweizerische Gesellschaft für Hydrologie und Limnologie,
Schweizerische Gesellschaft für Hydrogeologie
Schweizerische Hydrologische Kommission*

TALKS:

- 11.1 Brunner P.: Keynote: Bridging the conceptual gaps between hydrology and hydrogeology
- 11.2 Griessinger N., Jonas T., Seibert J.: The value of snow data assimilation for hydrological modelling in alpine catchments
- 11.3 Khayrat K., Jenny P.: A Multi-Scale Pore Network Model for Two-Phase Flow In Porous Media
- 11.4 Molnar P., Dzubakova K., Pfäffli M., Pellicano R., Fatichi S., Burlando P.: Monitoring riparian vegetation water stress in the Maggia River, Switzerland
- 11.5 Niayifar A., Perona P.: Efficient ecologic and economic operational rules for dammed systems by means of nondominated sorting genetic algorithm II
- 11.6 Rickenmann D.: Keynote: Possible impact of climate change on brown trout (*Salmo trutta fario*) recruitment
- 11.7 Schilling O.S., Brunner P., Hunkeler D., Gerber C., Purtschert R., Kipfer R.: Using multiple isotopic tracers to measure the influence of groundwater abstraction on groundwater-surface water interactions in the Emmental
- 11.8 Speich M., Scherstjanoi M., Zappa M., Lischke H.: FORHYCS – A distributed ecohydrological model for assessing global change impact on forests and water resources
- 11.9 Traber D., Gmünder C.: Hydrodynamic model of deep flow systems in Northern Switzerland
- 11.10 Tron S., Perona P., Gorla L., Schwarz M., Laio F., Ridolfi L.: Analytical model to predict the root profile in fluvial ecosystems: experimental validation and GUI
- 11.11 Vennemann T.W., Spangenberg J.E., Sprecher L., Khanh Ngo T.M.: The carbon cycle of Lake Geneva during late-summer stratification
- 11.12 Wanner P., Hunkeler D., Parker B., Chapman S., Aravena R.: Applying Compound-Specific Isotope Analysis (CSIA) to identify biodegradation of chlorinated hydrocarbons in low permeability sediments
- 11.13 Wüest A. : Keynote: Potentials and limits of three dimensional modelling in lakes

POSTERS:

- P 11.1 Diem S., Masset O., Poppei J.: Using natural tracers for transport model calibration
- P 11.2 Gianni G., Richon J., Vogel A., Perrochet P., Brunner P.: Identification of Transience in Streambed Hydraulic Conductivity
- P 11.3 Käser D.H., Hunkeler D.: Rethinking the role of alluvial groundwater in sustaining mountain baseflow: a mesoscale study based on continuous measurements of fluxes and storage
- P 11.4 Schneeberger R., Waber H.N., Mäder U.K., Kober F., Herwegh M.: Hydrogeology at Grimsel Test Site: hydrochemistry and flow paths
- P 11.5 Benoit L., Mariethoz G.: High resolution rain gauges for fine scale temporal rain intensity monitoring
- P 11.6 Carlier C., Cochand F., Wirth S., Staudinger M., Seibert J., Stölzle M., Stahl K., Weiler M., Hunkeler D., Brunner P.: Hydrogeological and topographic controls on watershed vulnerability to droughts
- P 11.7 de Palézieux L., Löw S., Zwahlen P.: Mountain slope hydrogeology in deep-seated gravitational slope deformations near Poschiavo, CH
- P 11.8 Dib I., Chettah W., Dib H., Hamed Y.: Risque de contamination des eaux souterraines par les nutriments et qualité hydrochimique : cas de la plaine GADDAINE-AIN YAGHOUT (Nord-Est de BATNA), ALGERIE
- P 11.9 Kerrou J., Negro F.: The influence of faults on groundwater flow and mass transport dynamics in the area of Neuchâtel
- P 11.10 Pera S., Tognini P., Inglese M., Ferrario A., Testa P.: Dye tracing test at Morteratsch Glacier (CH) to investigate englacial drainage flowpaths and to evaluate possible G.L.O.F. risk
- P 11.11 Pera S., Bronzini S., Molignani P.: Assessing surface water contribution to groundwater recharge: An example from Traversagna Valley, Ticino.
- P 11.12 Santos A.C., Schaeffli B., Portela M.M., Manso P., Schleiss A., Rinaldo A.: Characterization of flow duration curves in Switzerland
- P 11.13 Weber, S., Wanner, C., Wersin, P.: Temporal and spatial analysis of the redox plume in the groundwater at Aarberg, Switzerland
- P 11.14 Zermatten M.-A., Bruner P., Renard P.: The influence of aquifer heterogeneity on drawdown and transmissivity estimation
- P 11.15 Werthmüller S., Surbeck H., Ryser R.: Airborne exploration of anomalous high uranium contents in water and soil in the region of the "Lyssbach" – Canton of Bern
- P 11.16 Kaveh Firouz A., Burg J.-P.: Geomorphological analysis of the drainage system along the North Tabriz Fault

11.1

Bridging the conceptual gaps between hydrology and hydrogeology

Philip Brunner¹

¹ Centre d'hydrogéologie et de géothermie (CHYN), University of Neuchâtel, Emile-Argand 1, CH-2000 Neuchâtel
(philip.brunner@unine.ch)

Hydrology and hydrogeology have to a certain extent developed as independent scientific disciplines. This separate development is reflected in the conceptual models of the two communities: Hydrological models typically simulate surface processes in a detailed way, but simplify groundwater flow processes. Hydrogeologists, on the other hand, often reduce the complexity and dynamics of the surface to a simple boundary condition. As surface water and groundwater form a natural continuum, this separation has been an impediment for a holistic understanding of the water cycle. However, recent developments in fully-coupled, physically based models allow for a better integration of the two domains. In this presentation two examples to illustrate this point are shown. In the first example a model simulating surface water-groundwater interactions as well as the feedback mechanisms with riparian vegetation is presented. The model was calibrated using tree ring data. In the second example a new approach for the full spatial and temporal deconvolution of a hydrograph is presented. Both examples illustrate the importance to integrate surface and subsurface flow processes in a holistic way.

11.2

The value of snow data assimilation for hydrological modelling in alpine catchments

Nena Griessinger^{1, 2}, Tobias Jonas¹, Jan Seibert²

¹ WSL Institute for Snow and Avalanche Research SLF, Flüelastrasse 11, CH-7260 Davos Dorf, (nena.griessinger@slf.ch)

² Department of Geography, University of Zurich, Winterthurerstrasse 190, CH-8057 Zurich

Snow models have been developed with a wide range of complexity depending on the purpose of application. For avalanche research or snow studies on a small scale, simulating processes within the snowpack are of great interest and importance. Since snowmelt often is a major contribution to runoff, modelling snow processes is also important for flood or drought forecasting, reservoir operation and inland waterway management, as well as ecological concerns such as river and lake protection.

For computational reasons and due to limited data availability, many hydrological models use the temperature-index (TI) method which only requires precipitation and temperature data as input. This method may fail to accurately describe the accumulation and melt of seasonal snow. In particular, predicted melt-out dates can be biased due to cumulative modelling errors over the entire winter season. In this study we address the question, whether the performance of hydrological models based on the TI method vary by integrating data from external dedicated snow model variations.

We used the hydrological model HBV in the version HBVlight as framework for our tests. While HBV usually uses the TI approach, we in this study replace this by different snow model approaches. To analyze the impact of integrating an external snow model, four variations were applied. a) Using full capabilities of the external snowmelt model including the assimilation of observational snow data, b) using the snowmelt model with data assimilation switched off, c) using a downgraded version of the snowmelt model with constant day degree factor, d) using no snowmelt model and force all precipitation to be rain. Model runs were conducted for 20 catchments at different elevation levels within Switzerland for the hydrological years 1999 – 2013 using a 1km model grid resolution.

Our results show that at low elevations the hydrological model performance, specifically the Nash-Sutcliffe model efficiency coefficient during the melt-out season and the efficiency for peak flows within the melt-out season, did not differ depending on the snow model version chosen. Regarding higher elevation levels, model performance decreased when applying the least complex snow model version. Here, the differences between the three other versions were small. At the highest elevation level, best model performance was obtained by using the snowmelt data calculated with snow data assimilation. This findings show that with increasing elevation of catchments the value of assimilating observational snow data grows.

11.3

A Multi-Scale Pore Network Model for Two-Phase Flow In Porous Media

Karim Khayrat¹, Patrick Jenny¹

¹ *Institute of Fluid Dynamics, Department of Mechanical and Process Engineering, ETH Zurich, Sonneggstrasse 3, CH-8092 Zurich (khayratk@ifd.mavt.ethz.ch)*

Pore network models are important tools in studying the effects of pore-scale phenomena on two-phase flow through porous media. However, these simulators have a time complexity of order N^2 for N pore bodies, which limits their usage to small domains. Quasi-static pore network simulators, which assume capillary dominated flow, are more efficient with a time complexity of order $N \log N$, but are unable to capture phenomena caused by viscous effects such as viscous fingering and stable displacement.

For numerous common flow scenarios, capillary forces are dominant at the pore scale and viscous forces at larger scales. In order to take advantage of this behaviour, we propose a multi-scale pore-network method for two phase flow. In our solution algorithm, the pore network is divided into several smaller subnetworks. The algorithm to advance the fluid interfaces within each subnetwork consists of three steps: 1) A meso-scale mass balance equation for the subnetworks is first solved. In this step, both the viscous and capillary forces are taken into account. 2) The fluid-fluid interfaces within each subnetwork is advanced either by a dynamic network model or a quasi-static network model, depending on the local capillary number. 3) The transmissibilities for the meso-scale equation are updated based on the updated fluid configurations in each subnetwork. For this purpose the methodology of the existing multi-scale finite volume (MSFV) method is employed.

An important feature of the multi-scale pore-network method is that it is straightforward to parallelize the solution algorithm. Validation studies are presented and compared to results obtained with an existing dynamic pore network model.

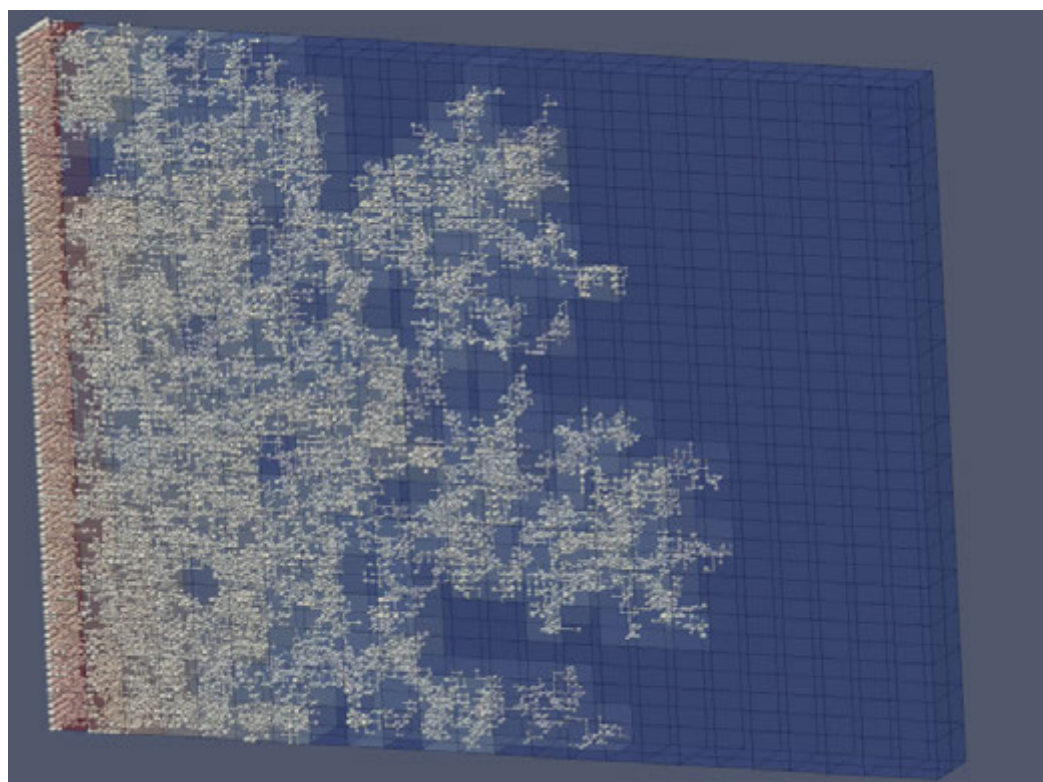


Figure 1. Simulation of viscous fingering for viscosity ratio 10 using the multiscale pore network model. Grid cells encapsulate different coupled subnetworks. Shown in white are subnetworks tubes that are filled with invading non-wetting fluid. The meso-scale saturation of non-wetting fluid is shown in color (red 0.74, blue 0).

REFERENCES

- Løvoll, G., et al. "Influence of viscous fingering on dynamic saturation–pressure curves in porous media 86.1 (2011): 305-324.
- P Jenny, SH Lee, HA Tchepi. "Adaptive fully implicit multi-scale finite-volume method for multi-phase flow and transport in heterogeneous porous media." *Journal of Computational Physics* 217.2 (2006): 627-641.

11.4

Monitoring riparian vegetation water stress in the Maggia River, Switzerland

Peter Molnar¹, Katarina Dzubakova², Matthias Pfäffli¹, Riccardo Pellicano¹, Simone Fatichi¹ & Paolo Burlando¹

¹ *Institute of Environmental Engineering, ETH Zurich, CH-8093 Zurich (molnar@ifu.baug.ethz.ch)*

² *Stream Biofilm and Ecosystem Research Lab, EPF Lausanne, CH-1015 Lausanne*

Riparian vegetation on gravel bars and banks in braided Alpine rivers plays an important ecological role in riverine habitat creation. Riparian vegetation patches vary along rivers according to channel morphology, sediment supply, and hydrological dynamics. Furthermore, vegetation plays an active role in shaping channels by protecting banks, generating deposition areas, and influencing surface-groundwater exchanges (e.g. Gurnell et al., 2012). Water stress and flood disturbance are the major hydrological factors impacting riparian vegetation distribution. Low groundwater levels and soil moisture, as well as frequent and erosive flooding, are potentially detrimental to riparian vegetation establishment and growth. In this study, we investigate the feedback between hydrology and vegetation erosion/growth in the Maggia River in Switzerland on the basis of a new terrestrial camera monitoring system with near-infrared sensitivity, 2d hydrodynamic river/aquifer modelling, and plant scale measurement of growth rates by dendrometers and tree ring dating.

At the reach scale we demonstrate the sensitivity of a customer-grade digital camera system to objectively separate different surfaces (gravel, water, vegetation) and to quantify vegetation activity by means of the normalized difference vegetation index (NDVI). We monitor the progression of vegetation activity estimated by NDVI through four years, water stress is evident in periods with low precipitation and streamflow, e.g. spring and early summer in 2011 (Figure 1). We also quantify the immediate response of riparian vegetation to the five largest floods in our monitoring period on three distinct floodplain units. We find both a negative (damage) and positive (enhancement) response of vegetation within 1 week following the floods, with a selective impact determined by pre-flood vegetation vigour, geomorphological setting, and intensity of the flood forcing (Dzubakova et al., 2014). Most affected are saplings and young plants within the inundation zone with high flow velocity.

At the plant scale we observe the effects of water stress using dendrometers installed on four *Populus nigra* and *Salix eleagnos* species on a gravel bar in spring 2015. First data are indicating that growth rates are reacting rapidly to climatic conditions given by solar radiation, precipitation, air temperature and vapour pressure deficit. A longer-term perspective on water stress is provided by tree ring growth increments which were sampled on several trees in the study area in 2014 and which indicate a weak correlation between tree ring increments and early season precipitation.

We conclude that vegetation response to flood disturbance may be effectively monitored by terrestrial photography with near-infrared sensitivity and by plant scale growth measurement. This type of monitoring can be useful for calibrating-validating stochastic riparian zone disturbance models (e.g., Perona et al., 2009) as well as for long-term assessments in river management and restoration projects in Alpine rivers affected by hydropower regulation (e.g. Molnar et al., 2008).

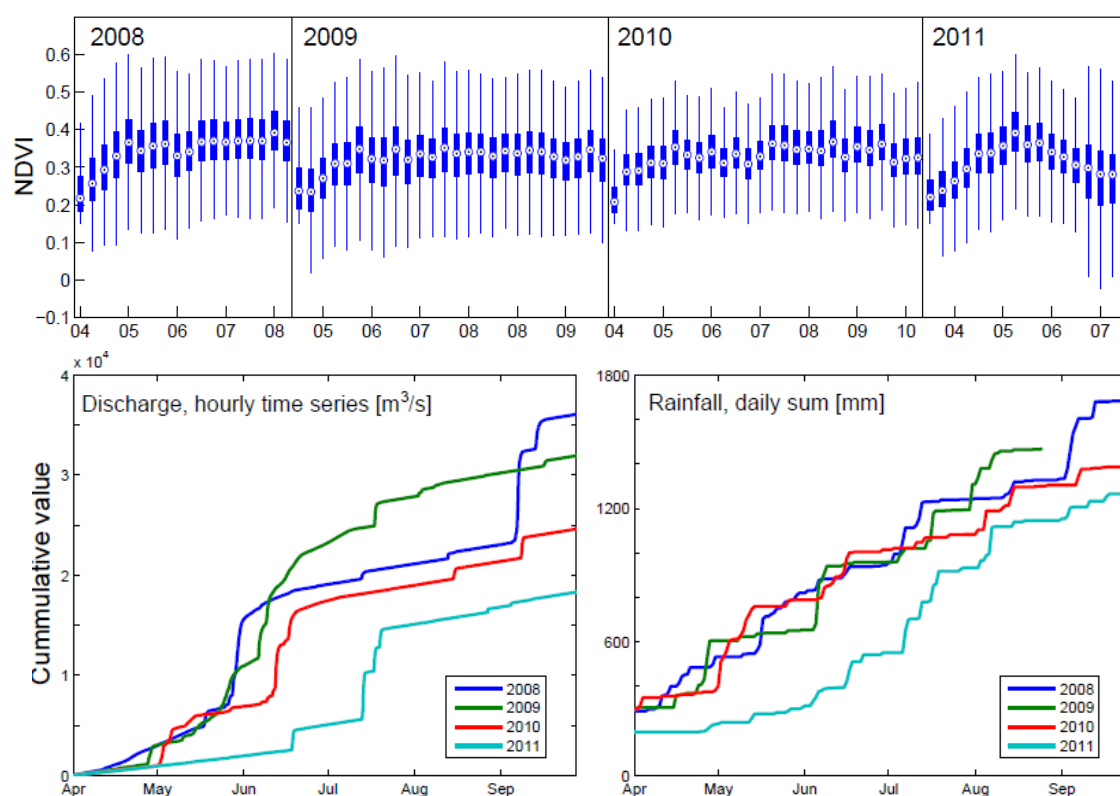


Figure 1. Boxplots of NDVI estimated over a gravel bar in the Maggia river for the period 2008-2011 (top). Cumulative discharge and rainfall in the studied years starting from 1 April in the growing season (bottom).

REFERENCES

- Dzubakova, K., Molnar, P., Schindler, K., & Trizna, M. 2015: Monitoring of riparian vegetation response to flood disturbances using terrestrial photography, *Hydrol. Earth Systems Sci.*, 19, 195-208.
- Gurnell, A.M., Bertoldi, W. & Corenblit, D. 2012: Changing river channels: The roles of hydrological processes, plants and pioneer fluvial landforms in humid temperate, mixed load, gravel bed rivers, *Earth Science Reviews*, 111, 129-141.
- Molnar, P., Favre, V., Perona, P., Burlando, P., Randin, C., & Ruf, W. 2008: Floodplain forest dynamics in a hydrologically altered mountain river, *Peckiana*, 5, 17-24.
- Perona, P., Molnar, P., Savina, M., & Burlando, P. 2009: An observation-based stochastic model for sediment and vegetation dynamics in the floodplain of an Alpine braided river, *Water Resour. Res.*, 45.

11.5

Efficient ecologic and economic operational rules for dammed systems by means of nondominated sorting genetic algorithm II

Amin Niayifar¹ and Paolo Perona¹

¹ Institute of Environmental Engineering, EPFL-ENAC, Lausanne, Switzerland (amin.niayifar@epfl.ch)

The natural flow regime and in turn the riparian ecosystems with its biodiversity can be severely affected by water impoundment by dams. Ensuring future ecosustainable exploitation of the water resource from mountain streams requires innovative operational strategies. As an alternative to classic minimal flow releases, we seek for flow release rules which generate dynamic environmental flows while maintaining an economically efficient energy production.

For dammed systems, we build the ecological and economical efficiency plot for non-proportional flow release rules and compare them to others, including traditional one based on one or more constant thresholds for minimal flow. As for the case of small hydropower plants (Razurel et al. 2015), a family of nonlinear functions is used to realize non-proportional redistribution flow releases. These rules allocate a fraction of water to the riverine environment depending on current reservoir inflows and storage. Differently from small hydropower, this fraction is then modified by introducing a correction factor that reflects the current volume of stored water in the reservoir.

In order to compute the riverine ecological benefits associated to the resulting dynamic environmental flows, we integrate the Weighted Usable Area (WUA) for fishes together with Richter's hydrological indicators. Then, nondominated sorting genetic algorithm II (NSGA-II) are applied to an ensemble of non-proportional and minimal flow redistribution rules in order to generate the Pareto frontier showing the system performances in the ecologic and economic efficiency space.

This fast and elitist multiobjective optimization method is eventually applied to a case study. It is found that for certain hydropower systems a consistent improvement of the global efficiency is possible. In particular, we find solutions where non-proportional dynamic flow releases ensure maximal power production on the one hand, while conciliating ecological sustainability on the other hand. This amelioration in the environmental indicator is found to be mainly due to a better use of the reservoir storage dynamics, which enables to capture and laminate flood events while recovering part of them for energy production. Furthermore, by comparing the constant minimum flow releases with non-proportional ones in terms of Richter's hydrological indicators, it is found that non-proportional flow redistribution rules determine a reduced impact on the natural flow regime. In conclusion, adopting such new operational policies would unravel a spectrum of globally-efficient performances of the dammed system when compared with those resulting from policies based on constant minimum flow releases.

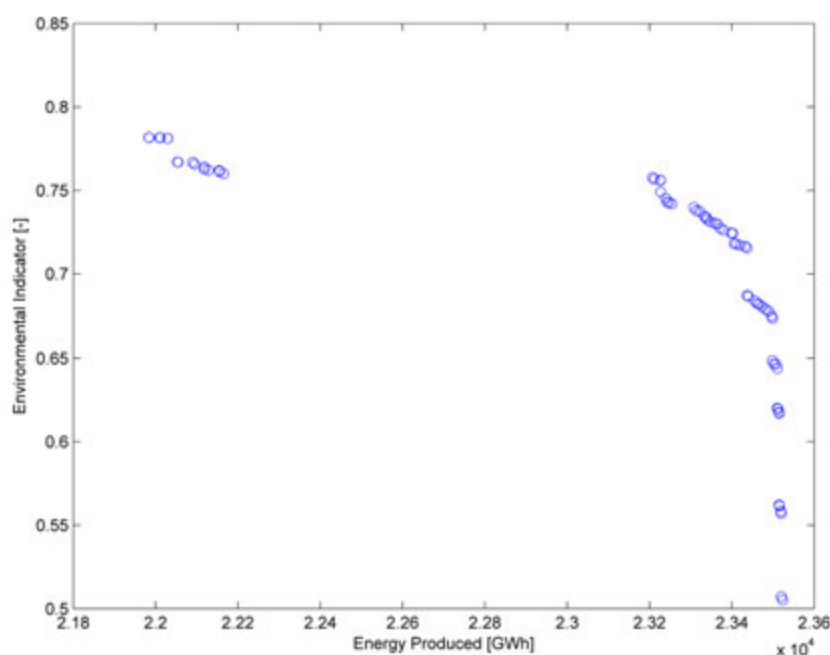


Figure 1. Economy and ecology efficiency Pareto's frontier using NSGA-II

REFERENCES

- [1] Razurel, P., Gorla, L., Crouzy, B., Perona, P. (2015). Non-Proportional water repartition rules for flow diversions, Journal of water resource management (Accepted in revision)

11.6

Possible impact of climate change on brown trout (*Salmo trutta fario*) recruitment

Dieter Rickenmann¹, Armin Peter², Julian Junker², Florian U. M. Heimann¹, Christoph Hauer³, Jens M. Turowski¹, Massimiliano Zappa¹, Alexandre Badoux¹

¹ WSL Swiss Federal Institute for Forest, Snow and Landscape Research, Zürcherstrasse 111, 8903 Birmensdorf, Switzerland (dieter.rickenmann@wsl.ch)

² EAWAG Swiss Federal Institute of Aquatic Science and Technology, Seestrasse 79, 6047 Kastanienbaum, Switzerland

³ University of Natural Resources and Life Sciences, Muthgasse 107, 1190 Vienna, Austria

The annual discharge pattern in rivers is expected to change as a result of climate warming. This has an impact on bedload transport and consequently on aquatic life, because coarse sediments in streams provide important habitat for many species including brown trout (*Salmo trutta fario*). We used a multiple model approach to assess for the Kleine Emme catchment in Switzerland how predicted discharge changes affect bedload transport and the vulnerable early life stages of brown trout who spawn in the top gravel layer of the river bed. Future discharge scenarios predict an increased frequency of flood occurrence in winter and long-lasting low-flow periods in summer. As a result, bed erosion will become more frequent during winter, leading to less stable spawning grounds and deeper scouring. On the other hand, during summer an improvement in habitat diversity can be expected, which is advantageous for the young-of-the-year fish.

REFERENCES

- Junker, J., Heimann, F.U.M., Hauer, C., Turowski, J.M., Rickenmann, D., Zappa, M., & Peter, A. 2015. Assessing the impact of climate change on brown trout (*Salmo trutta fario*) recruitment, *Hydrobiologia*, 751, 1–21.
- Badoux, A., Peter, A., Rickenmann, D., Junker, J., Heimann, F., Zappa, M., & Turowski, J.M. 2014. Geschiebetransport und Forellenhabitate in Gebirgsflüssen der Schweiz: mögliche Auswirkungen der Klimaänderung, *Wasser, Energie, Luft*, 106(3), 200–209.

11.7

Using multiple isotopic tracers to measure the influence of groundwater abstraction on groundwater-surface water interactions in the Emmental

Oliver S. Schilling¹, Philip Brunner¹, Daniel Hunkeler¹, Christoph Gerber², Roland Purtschert² & Rolf Kipfer³

¹ *Centre d'hydrogéologie et de géothermie (CHYN), Université de Neuchâtel (UniNE), Rue Emile-Argand 11, CH-2000 Neuchâtel (oliver.schilling@unine.ch)*

² *Climate and Environmental Physics, University of Bern (UniBE), Sidlerstrasse 5, CH-3012 Bern*

³ *Water Resources and Drinking Water, EAWAG, Überlandstrasse 133, CH-8600 Dübendorf*

Around 45% of drinking water for the Swiss capital Bern and its surroundings is extracted groundwater of the alluvial aquifer in the immediate vicinity of the highly dynamic, pre-alpine Emme River. The Emme is the main source of recharge to this alluvial aquifer. The high transience of the Emme, coupled with frequent extreme events, particularly droughts, requires a solid understanding of the local surface water-groundwater (SW-GW) interactions. In a collaborative effort between UniNE, UniBE, EAWAG, and the water works of the Canton of Bern (WVRB), groundwater abstraction was reduced during one week to the smallest technically possible rate (approx. 200 l/s) after a long period of high groundwater abstraction (approx. 350 l/s). This controlled transient forcing of the river-aquifer system provided an ideal framework to study SW-GW interactions, and to compare a wide range of methods and approaches to monitor and quantify the exchanges between the river and the aquifer. Besides standard chemical and physical measurements (e.g. of pressure, temperature, electrical conductivity, ions, pH and stable H₂O isotopes), a number of innovative approaches were employed during the experiment: Distributed Temperature Sensing (DTS) on the riverbed to detect locations of GW exfiltration, a combination of widely used unstable isotopic tracers (²²²Rn ($T_{1/2}$ =3.8d), ³H/³He ($T_{1/2}$ =12.4y) and a never before employed natural tracer for SW-GW interactions (³⁷Ar ($T_{1/2}$ =35d)). Moreover, stream water gauging to measure exfiltration using a fluorescent tracer, freeze-core-sampling of the riverbed, as well as geophysical measurements on the geological structure of the streambed were employed. The applied methods, with a focus on the unstable isotopic tracers, are presented. In particular, we show how ³⁷Ar can provide an ideal complement to the standard unstable isotopic tracers in order to ensure measuring of the right temporal and spatial scale.

11.8

FORHYCS – A distributed ecohydrological model for assessing global change impact on forests and water resources

Matthias Speich^{1,2}, Marc Scherstjanoi¹, Massimiliano Zappa¹, Heike Lischke¹

¹ *Swiss Federal Institute for Forest, Snow and Landscape Research WSL, Zuercherstrasse 111, CH-8903 Birmensdorf (matthias.speich@wsl.ch)*

² *Department of Environmental Systems Science, ETH Zurich, ETH Zentrum, CH-8092 Zurich*

Important effects of a changing climate are expected on the forests and water resources of Switzerland in the present century. Previous modeling studies predict a change in both seasonal and inter-annual hydrological conditions for most catchments. In particular, an increase in the frequency of summer droughts is expected. Observed effects of increasing drought stress on forests include biomass reduction as a result of extreme dry spells and a change in local species composition due to an alteration of the long-term drought conditions. Furthermore, modeling studies suggest range shifts and local disappearance of tree species as a result of warming and increased drought. To date, hydrological climate impact modeling studies for the whole of Switzerland treat vegetation dynamics in a simplified manner, using prescribed and time-invariant parameter values for key vegetation variables such as leaf area, which greatly influence hydrological processes. We introduce a coupled ecohydrological model simulating both hydrological processes and vegetation dynamics, with an explicit formulation of the couplings between the two.

The newly developed model consists of a coupling between a rainfall-runoff model (PREVAH; see e.g. Schattan et al. 2011) and a forest-landscape model (TreeMig; Lischke et al. 2006), both of which have previously been applied for climate impact studies in Switzerland. Both models are spatially distributed and operate on a regular grid, with a cell size currently set at 200 m. The hydrological model calculates the water balance of each cell at a sub-daily temporal resolution, while the forest-landscape model simulates tree species distribution and vegetation dynamics with an annual time step. Among the bioclimatic drivers of the forest model is a yearly drought stress index, which influences tree growth and mortality. This index is obtained from the ratio of actual to potential evapotranspiration as simulated by the hydrological model. In its original version, TreeMig uses a drought stress index based on an empirical, temperature-based evapotranspiration applied at a monthly time step. It is expected that the higher temporal resolution and a more robust method for estimating evapotranspiration (Penman-Monteith) in the coupled model lead to more reliable values for drought stress. The water and energy budget of each cell is greatly influenced by vegetation properties. The most important vegetation descriptors in PREVAH are leaf area index (LAI) and fractional vegetation cover. In the coupled model, these are derived from the number and height distribution of trees, using allometric relationships with species-specific parameters. In stand-alone PREVAH, those two variables are prescribed for each land cover class and varied monthly. In this case as well, it is expected that the more process-based formulation and increased temporal resolution leads to a better model performance.

In this presentation, we outline the coupling concept of the new model. Special attention is given to theoretical considerations on an ecologically sensible definition of drought stress and potential evapotranspiration. Furthermore, we present the results of an application of the new model to the Navisence catchment (Valais). Due to a steep altitudinal gradient and complex topography, this catchment is characterized by a high spatial heterogeneity of hydro-climatic conditions and is thus well suited to examine and illustrate the behavior of the new model under different conditions. We compare the simulation results of the coupled model with those of the stand-alone versions of PREVAH and TreeMig to assess the effect of transient vegetation simulations and of the improved drought stress index calculation. We present both the spatially distributed results (tree species distribution, biomass, evapotranspiration, soil moisture) and the simulated discharge.

In a further step, the model presented here shall be used for a Switzerland-wide ensemble study with different climate and land use change scenarios to assess global change impact on forests and water resources in the near (2021-2050) and distant future (2070-2099).

REFERENCES

- Lischke, H., Zimmermann, N.E., Bolliger, J., Rickebusch, S., & Löffler, T.J. 2006: TreeMig: A forest-landscape model for simulating spatio-temporal patterns from stand to landscape scale. *Ecol. Model.* 199, 409–420.
- Schattan, P., Zappa, M., Lischke, H., Bernhard, L., Thürig, E., & Dieckkrüger, B. 2013: An approach for transient consideration of forest change in hydrological impact studies. In: *Climate and Land Surface Changes in Hydrology*, Proceedings of H01, IAHS-IAPSO-IASPEI Assembly, Gothenburg, Sweden, July 2013 (IAHS Publ. 359), 311-319.

11.9

Hydrodynamic model of deep flow systems in Northern Switzerland

Daniel Traber¹, Christian Gmünder²

¹ *Nagra, Hardstrasse 73, CH-5430 Wettingen (daniel.traber@nagra.ch)*

² *Simultec AG, Hardturmstrasse 261, CH-8005 Zürich (cg@simultec.ch)*

In Northern Switzerland, thermal springs indicate the existence of deep reaching groundwater flow systems, as for example the Baden springs. In the last years, the deep aquifers were of increasing interest for the sequestration of CO₂ or for geothermal energy production. The presented model was elaborated in the framework of the Swiss Sectoral Plan to establish deep geological repositories for radioactive waste (Gmünder et al. 2014).

A 3D geological model based on seismic profiles, borehole data and isopach maps is a basis of the work. The model extends from the Bodensee area in the East to the area of Olten in the West. In the North, it includes the outcrops of the Muschelkalk in the Wutach area. The southern margin is striking parallel to the Alpine deformation front and was chosen based on preliminary 2D models. This geometry was implemented in the numerical code FEFLOW in order to perform stationary hydrodynamic modelling. The model includes 15 hydrogeological layers of regional importance from Mittlerer Muschelkalk up to the Quaternary. The regional fault structures are represented by 20 discrete faults. They are implemented as 3 parallel rows of elements; this allows to test different scenarios of their hydraulic properties. In order to minimize the number of elements, the faults were distorted into the vertical maintaining the outcrop positions and the elevations of hydrogeologic units.

Once the geometry of the hydrogeological 3D model had been implemented, it was a versatile tool to model the flow systems and to test scenarios. Hydraulic conductivities have been assigned to the hydrogeological units based on measured values taking into account the tectonic regime, major facies changes and depth. The inspection of the available data showed that the Muschelkalk aquifer (middle triassic carbonates) is typically characterized by elevated conductivities down to c. 400 m below sea level (c. 800 m below ground). In contrast, the zone of elevated conductivities of the Malm aquifer appears to be restricted to a comparably shallow zone (c. 200 m below ground). The potential hydraulic impact of the regional fault zones was studied in scenarios: C1 considers the displacement at the faults only. Additional scenarios simulate sealing respectively transmissive faults.

In C1, the general flow direction in Malm and Muschelkalk aquifer is from the southern margin and from the elevated outcrops in Folded and Tabular Jura towards the large river valleys where the units crop out typically below Quaternary gravel aquifers (Figs. 1 & 2). For the Malm aquifer, the particle tracking highlights the exchange with the Molasse: In the south western model area recharge occurs from the Molasse, in the north east, Malm groundwater exfiltrates via Molasse into Untersee. In the case of the Muschelkalk aquifer south of the Jura Main Thrust, the model shows converging flow lines towards the outcrops in the Aare-, Reuss- and Limmat-valley. This explains at least partly the occurrence of thermal springs in this area.

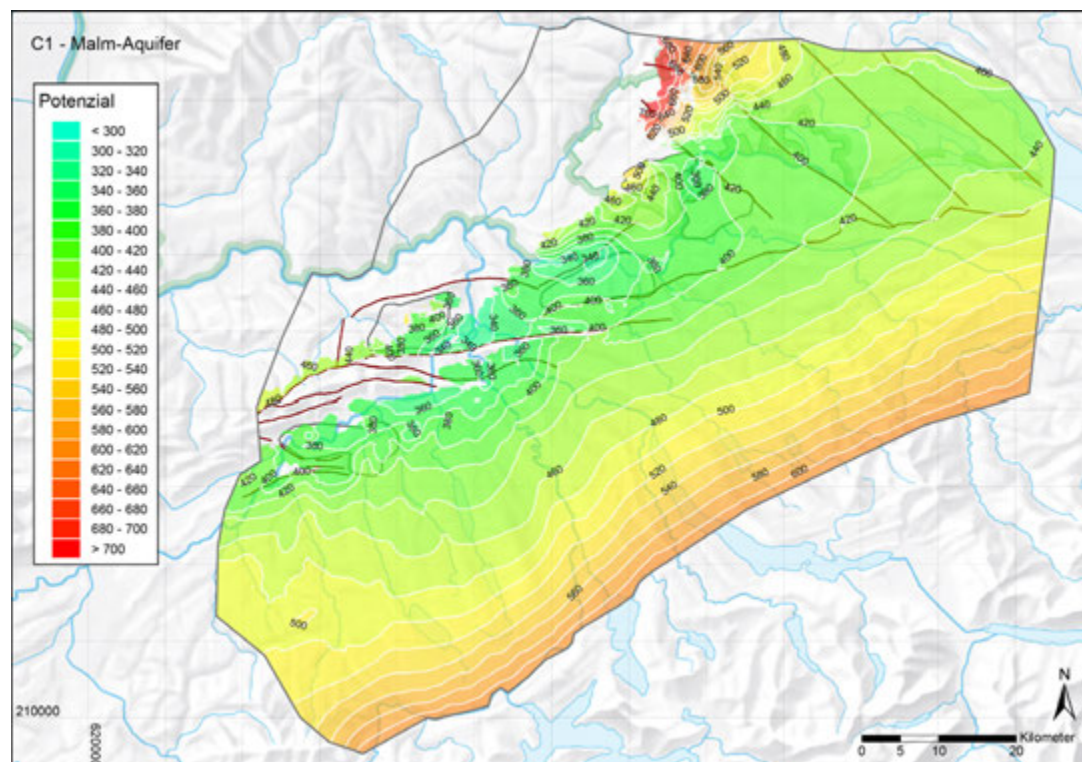


Figure 1. Simulated hydraulic heads in the Malm aquifer. Modelling case C1 (see text).

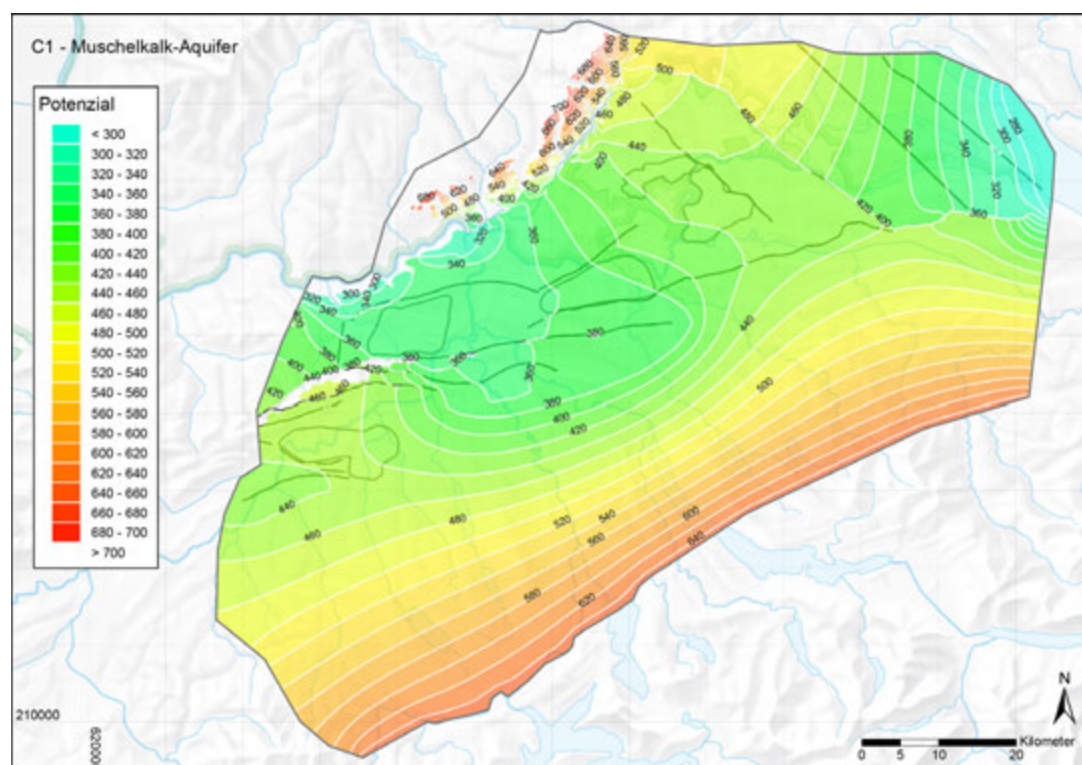


Figure 2. Simulated hydraulic heads in the Muschelkalk aquifer. Modelling case C1 (see text).

REFERENCES

Gmünder, C. Malaguerra, F., Nusch, S., & Traber, D. 2014: Regional Hydrogeological Model of Northern Switzerland. Nagra Working Report NAB 13-23. Nagra, Wetztingen, Switzerland (available via www.nagra.ch).

11.10

Analytical model to predict the root profile in fluvial ecosystems: experimental validation and GUI

Tron S.¹, Perona P.¹, Gorla L.¹, Schwarz M.², Laio F.³, and Ridolfi L.³

¹ *Institute of Environmental Engineering, EPFL-ENAC, Lausanne, Switzerland*
(stefania.tron@epfl.ch)

² *Bern University of Applied Science, HAFL, Zollikofen, Switzerland*

³ *Department of Environment, Land and Infrastructure Engineering, Politecnico di Torino, Turin, Italy*

In riparian environments plant root systems are recognized to play a crucial role in several processes. For example, through mineral absorption, they contribute to enhance the water quality of the river by reducing the concentration of nitrogen, phosphorus, and in some cases also of heavy metals. From a mechanical perspective, roots increase the soil cohesion contributing to riverbank stability thus influencing the morphologic evolution of the river belt. Moreover, plant roots contribute to preserve the belowground biodiversity and the whole riparian ecosystem functioning. These processes explain the importance of knowing and predicting how roots are distributed within the soil. Generally, many factors may concur to shape the root system structure: soil temperature, water and nutrient availability, soil compaction, etc. However, in the riparian zone, where the availability of nutrients is not a limiting factor, the main drivers for the root development are likely aerotropism and hydrotropism. The availability of water and oxygen in this zone are mainly determined by the random fluctuations of the river level.

In this work, we show some recent results obtained by Tron et al (2015). A collection of root measurements from field and outdoor controlled experiments is used to demonstrate that the vertical root density distribution of riparian plants can be described by a simple analytical expression (Tron et al., 2014). This function links the stochastic fluctuations of the water table to the related dynamics of root growth and decay. As shown in Figure 1, the model is able to predict very well the measured vertical density distribution of root profiles by using physically based parameters describing soil, water table, and plant properties at the measurement site. These promising results prove that the root architecture of riparian plants mirrors the availability of water and oxygen in the soil as driven by random fluctuation of the river stages.

The model predicts the root adaptability to different hydrological and pedological scenarios and has, thus, several potential applications. Among them it can be used to assess the impact of climate change projections of river stage variability on the riparian vegetation, as well as the impact of river regulation, e.g. due to the impoundment of the basin headwaters. As well, the model can be applied to predict roots development in cuttings that are used for bank stability reinforcement in bioengineering restoration projects.

In order to promote the use of the model to a larger professional and scientific audience we present a Graphical User Interface that we recently developed. This tool allows for the estimation of the vertical density distribution of roots by just entering a simple description of site hydrology, soil surface elevation, vegetation type, and soil granulometry.

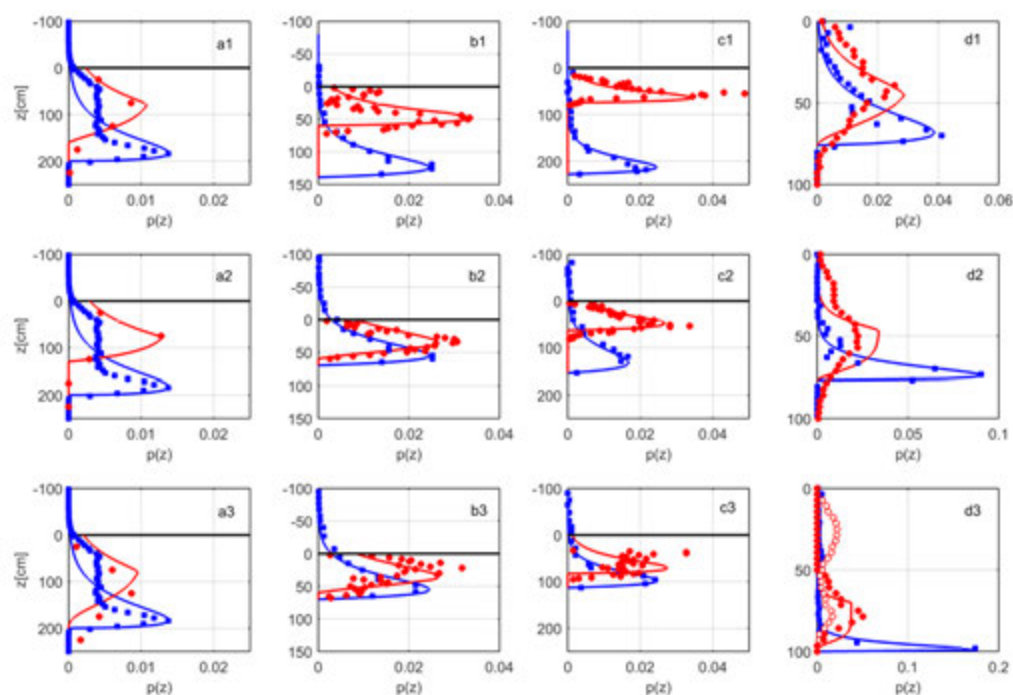


Figure 1. Normalized measured and modeled root profiles (red circles and lines) and corresponding water table distributions (blue squares and lines). Three representative examples are shown for each root dataset. Sets of measured root systems and soil level (black line): riverbank of the Rhone river (a1,a2,a3), island of the Thur river in 2009 (b1,b2,b3) and 2010 (c1,c2,c3), and outdoor experiment in Lausanne (d1,d2,d3). The original root profile in panel (d3) is shown with red empty circles, while the full circles show the root profile without root growth at the surface.

REFERENCES

- Tron, S., Perona, P., Gorla, L., Schwarz, M., Laio, F., & Ridolfi, L. (in Press) The signature of randomness in riparian plant root distributions. *Geophys. Res. Lett.*
- Tron, S., Laio, F., & Ridolfi, L. 2014: Effect of water table fluctuations on phreatophytic root distribution, *J. Theor. Biol.*, 360, 102-108.

11.11

The carbon cycle of Lake Geneva during late-summer stratification

Torsten W. Vennemann¹, Jorge E. Spangenberg¹, Lucie Sprecher¹ & Thi Mai Khanh Ngo¹

¹ *Institute of Earth Surface Dynamics, University of Lausanne, Geopolis, CH-1015 Dorigny (Torsten.Vennemann@unil.ch)*

Three depth profiles from the middle of Lake Geneva towards the Bay of Vidy were sampled in the middle of September 2014 and the samples were analyzed for their chemical and isotopic composition, including the stable carbon isotope composition of dissolved inorganic carbon (DIC) and that of particulate organic carbon (POC), as well as for their total chlorophyll content. The aim was to characterize the carbon cycling within this Alpine lake during a period of lake stratification. The three profiles share the same overall features with a well-mixed, warm, relatively low conductivity and rain water influenced epilimnion (top 5 m), followed by a well-developed thermo- and chemocline (7 to about 30 m) or metalimnion, and a cold, higher conductivity hypolimnion (Figure 1). While most pronounced in the profile along the central axis of the deep lake, the metalimnion in all three profiles also shows a clear interflow layer at between 12 to 23 m depth that is interpreted to represent a high proportion of Rhone river water, clearly recognized by the changes in the H- and O-isotope composition of water (e.g. Halder et al., 2013). In September 2014 though, this can also be recognized by changes in temperature, conductivity, pH, as well as $\delta^{13}\text{C}$ values of DIC for the deep lake profile as well as the intermediate depth profile, but only in the H- and O-isotope composition in the Bay of Vidy.

In all three profiles, the temperature, pH, carbonate content as well as the $\delta^{13}\text{C}$ values of DIC change perfectly in concert with depth; the latter changing from about -3.2‰ (VPDB) in the epilimnion, down to -7.6‰ in the hypolimnion (Fig. 2). In contrast, POC concentrations and the $\delta^{13}\text{C}$ values thereof do not change in concert with any of the above-mentioned parameters, even though the POC concentrations are always highest at the surface and decrease with depth. $\delta^{13}\text{C}$ values of POC average -24‰ in the epilimnion, decreasing to -30‰ in the metalimnion just to increase again to an average of -26‰ in the hypolimnion (Fig. 2). A brief excursion towards values of about -27‰ can be recognized in the interflow layer of the metalimnion. The difference in C-isotope composition between the DIC and POC, $\Delta(\text{DIC-POC})$, changes from about 20 in the surface waters to about 25 in the metalimnion and returns to about 19 in the epilimnion. Collectively, these changes in the inorganic and particulate organic carbon concentrations and their isotopic compositions can be interpreted to indicate that the DIC in the deep lake is largely externally derived from the drainage basin while its change in concentration and isotopic composition in the surface layers is directly related to the solubility of CO_2 as a function of temperature (and pH), but less so by the biochemical parameters and direct photosynthetic uptake of carbon in this low-productivity lake. Lake Geneva is undersaturated with respect to atmospheric partial pressures of CO_2 from spring to late fall and it is suggested that diffusive atmospheric CO_2 invasion, dissolution and mixing processes in the epi- and metalimnion control $\delta^{13}\text{C}$ values of DIC. The POC is interpreted to be dominated by terrestrial organic matter largely derived from the riverine inputs but some contributions of autochthonous POC are important in the lower epilimnion and upper metalimnion as indicated by the low $\delta^{13}\text{C}$ values in layers with or just below those with the highest measured chlorophyll contents.

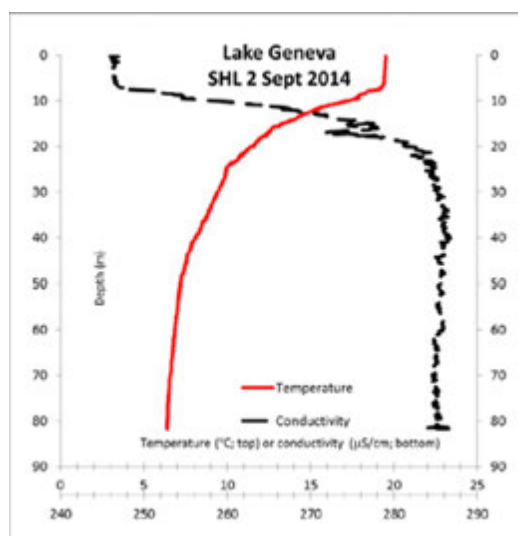


Figure 1. Variation in temperature and conductivity as a function of depth for a profile in the center of Lake Geneva.

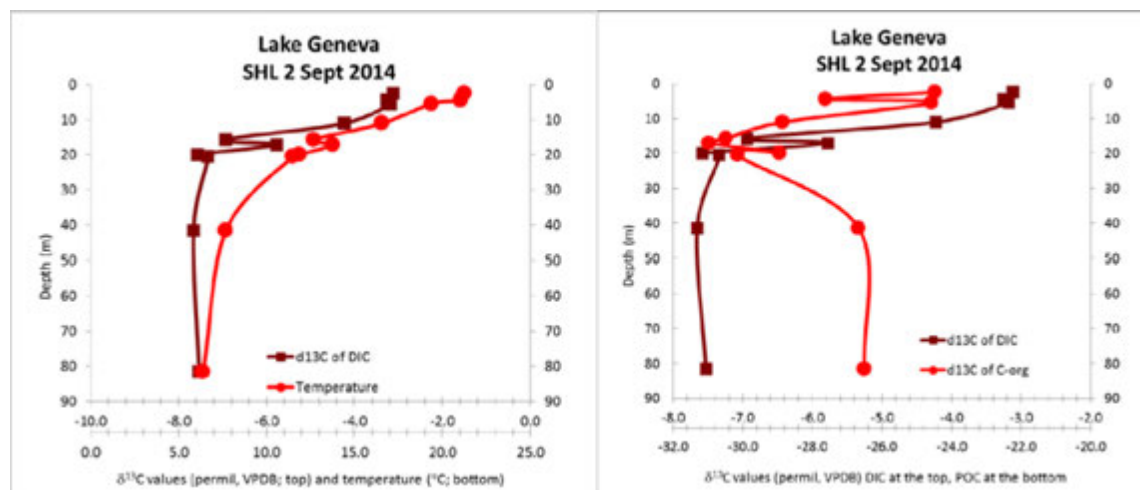


Figure 2. Variation in C-isotope composition of the DIC and temperature as a function of depth (left) and C-isotope composition of DIC and POC as a function of depth (right) for a profile in the center of Lake Geneva.

REFERENCES

Halder, J., Decrouy, L. & Vennemann, T.W. 2013: Mixing of Rhône River water in Lake Geneva (Switzerland–France) inferred from stable hydrogen and oxygen isotope profiles. *Journal of Hydrology*, 477, 152-164.

11.12

Applying Compound-Specific Isotope Analysis (CSIA) to identify biodegradation of chlorinated hydrocarbons in low permeability sediments

Philipp Wanner¹, Daniel Hunkeler¹, Beth Parker², Steven Chapman², Ramon Aravena³

¹ Centre for Hydrogeology & Geothermics (CHYN), University of Neuchâtel, Rue Emil Argand 11, CH-2000 Neuchâtel, Switzerland (philipp.wanner@unine.ch)

² School of Engineering, University of Guelph 50, Stone Road East, Guelph, Ontario, Canada N1G 2W1

³ Department of Earth Sciences, University of Waterloo, 200 University Avenue West, Waterloo, Ontario, Canada N2L 3G1

As a result of improper use and disposal, chlorinated solvents are major subsurface contaminants. Due to the high density and low viscosity, chlorinated solvents migrate through the unsaturated zone into aquifer systems and often accumulate on top of low permeability sediments. With time chlorinated solvents diffuse into these low permeable units, which then potentially serve as a long-term contaminant source to the adjacent aquifer. However, due to the presence of more reducing conditions in these units, (bio)degradation might occur, which reduces the risk of long-term groundwater contamination. Compound-specific stable isotope analysis (CSIA) is increasingly used to quantify (bio)degradation processes in aquifer systems affecting organic contaminants. This method makes use of isotope effects associated with (bio)degradation. In contrast to aquifers, it is not yet clear to what extent CSIA can also be used for tracking (bio)degradation in saturated low permeability sediments, where transport is likely diffusion dominated.

To address this gap of knowledge, several detailed C and Cl isotope ratio profiles of chlorinated solvents were determined for a contaminated clayey aquitard underlying a sandy aquifer. The contaminant source originated from a controlled-solvent release on top of the aquitard 14.5 years ago. Large shifts towards lighter isotope signature (e.g. 23‰ for C isotopes in TCE) of compound-specific isotope ratios were observed in the isotope ratio profiles, suggesting that (bio)degradation of chlorinated solvents is also occurring in saturated low permeability sediments. Furthermore, the results of numerical modeling gained more insight into the governing processes and allowed us to determine (bio)degradation rates affecting chlorinated solvents in the clayey aquitard.

Our findings demonstrate that CSIA is also applicable in saturated low permeability sediments for the identification of reactive processes. Moreover, our results revealed that (bio)degradation is potentially superimposed on diffusion and thus, it is difficult to identify based on concentration profiles only. Therefore, isotope information is an important complement additionally to concentration data to identify (bio)degradation in low permeability sediments.

11.13

Potential and limits of three-dimensional modelling in lakes

Alfred Wüest^{1,3}, George S. Constantinescu^{2,3} & Damien Bouffard³

¹ Eawag, Aquatic physics, Seestrasse 79, 6047 Kastanienbaum (alfred.wueest@eawag.ch)

² IIHR—Hydroscience & Engineering, University of Iowa, 100 C. Maxwell Stanley Hydraulics Laboratory, Iowa City, Iowa 52242-1585

³ Laboratoire de physique des systèmes aquatiques, EPFL ENAC IIE APHYS, GR A0 402 (Bâtiment GR), Station 2, 1015 Lausanne

Often the spatial resolution of models are much more detailed than of the measured data, but still not fine enough for adequately describing ecologically relevant processes. Especially, three-dimensional lake models are usually “over- and underqualified” for most problems. With the continuously increasing computing power, we can handle now fascinating applications, which allow describing and analysing interesting limnological processes with high resolution. In this talk three such examples with completely different length scales will be presented and the relevance for the lake ecology is shown.

P 11.1

Using natural tracers for transport model calibration

Samuel Diem¹, Olivier Masset¹ & Joachim Poppei¹

¹ *AF-Consult Switzerland Ltd, Groundwater Protection and Waste Disposal, Täferstrasse 26, CH-5405 Baden
(samuel.diem@afconsult.com)*

Riverbank filtration provides an important drinking water resource in several European countries. Within this context, groundwater flow and transport modeling is a valuable tool for the risk assessment of existing and planned drinking water wells close to rivers, as it quantitatively links flow paths, travel times and the fraction of infiltrated river water. However, the calibration of flow and transport models requires both head and concentration observations in order to reduce the predictive uncertainty of transport simulations.

The conventional approach to obtain concentration observations for river – groundwater systems is to inject a pulse of artificial tracer into the river and observe its breakthrough at selected observation wells after infiltration and transport through groundwater. These breakthrough curves contain information on the travel times and the fraction of freshly infiltrated river water. As an efficient and cost-effective alternative, one may take advantage of existing natural tracers in the river, such as fluctuations of electrical conductivity (EC): Analyzing measured EC time series in the river and in observation wells by deconvolution allows the reconstruction of breakthrough curves from a tracer test without the need of injecting any artificial tracer mass into the river.

In our presentation, we introduce the deconvolution method and demonstrate its application to measured EC time series in a river – groundwater system in the Aare Valley between the cities of Olten and Aarau in northern Switzerland. Furthermore, we compare the resulting travel time distributions (breakthrough curves) with those obtained in a former conventional tracer test. Finally, we show how we use the results from both the tracer test and the EC time series analysis to calibrate a 3D groundwater flow and transport model.

P 11.2

Identification of Transience in Streambed Hydraulic Conductivity

G. Gianni¹, J. Richon², A. Vogel³, P. Perrochet¹, P. Brunner¹

¹ *Centre d'hydrogéologie et de géothermie (CHYN), Université de Neuchâtel (UniNE), Rue Emile-Argand 11, CH2000 Neuchâtel*

² *Bureau d'études Géologiques SA, Rue de la Printse 4, CH-1994 Aproz*

³ *Service des routes, transports et cours d'eau, Section Protection contre les Crues du Rhône, Rue des Creusets 5, CH1950 Sion*

Streambed hydraulic conductivity controls the interactions between surface and groundwater. Streambed properties are often subjected to transience due to deposition and erosion processes. However, monitoring this transience using current field methods remains challenging. Here we present a straightforward method to detect transience in streambed hydraulic conductivity. Input data are time series of stream stage and near stream groundwater head. The method is based on the inversion of a floodwave response. This method is applied on dataset from the Rhône River and its alluvial aquifer (Valais, Switzerland). The results show causality between climatic events driven fluvial dynamics, such as flood (100-year flood event of October 2000) or heatwave (2003), and variations in the streambed hydrogeological properties.

P 11.3

Rethinking the role of alluvial groundwater in sustaining mountain baseflow: a mesoscale study based on continuous measurements of fluxes and storage

Daniel H. Käser, Daniel Hunkeler¹

¹ Centre d'Hydrogéologie et de Géothermie de Neuchâtel, Rue Emile-Argand 11, CH-2000 Neuchâtel (daniel.kaeser@unine.ch)

In mountainous regions, alluvial aquifers cover a minor fraction of the landscape. Unlike headwater riparian zones, they are rarely associated with the extensive network of first order streams. As a result, such aquifers are not thought to contribute significantly to seasonal water storage, but are considered rather as a transmission zone between the catchment and the channel network.

The present research challenges this conception and investigates whether alluvial aquifers may provide sufficient storage to sustain extended baseflow. This study focuses on a 6 km² alluvial plain located in the peri-alpine region of Emmental (Switzerland). The plain covers only 3% of catchment area. However, the underlying material is highly permeable and exhibits relatively high storativity values.

The methodological setup relies on surface and subsurface water-level measurements conducted during one year. Twenty-six observation wells were equipped with pressure loggers and three coupled gauging stations were installed to monitor simultaneously river and alluvial groundwater discharge at key locations. This approach provided continuous estimations of both total catchment outflow and groundwater storage variations for the main catchment (196 km²) and for a sub-catchment (52 km²). The key results pertain to the study's driest month and may be summarized as follow:

- At the end of the dry spell, alluvial groundwater storage sustained a considerable fraction of catchment outflow. Depletion, which occurred mostly in the highest part of the aquifer, supported:
 - 35% of the total catchment outflow
 - 75% of the sub-catchment outflow
- During this same period, the river gauging stations missed a substantial part of outflow (the subsurface component). This represented :
 - 15% of the total catchment outflow
 - 85% of the sub-catchment outflow
- During this same period, the discharge ratio 'groundwater:river' varied spatially along the valley: the aquifer conveyed 15% of total outflow at the outlet (196 km²) and 100% (0.45 m³/s) only 4 km upstream (186 km²)

The role of mountainous alluvial aquifers in seasonal water storage appears indeed to be overlooked. Characterization of the aquifer-catchment linkage may be challenging. Yet, as this study shows, continuous monitoring solutions in appropriate locations might help constrain flux estimations and provide significant insight into the system's functioning. In particular, coupled river/groundwater gauging stations could prove useful for monitoring total catchment outflow and thus improve the reliability of rainfall-runoff models, especially for drought predictions.

P 11.4

Hydrogeology at Grimsel Test Site: hydrochemistry and flow paths

Raphael Schneeberger¹, H. Niklaus Waber¹, Urs K. Mäder¹, Florian Kober², Marco Herwegh¹

¹ *Institute of Geological Sciences, University of Bern, Baltzerstrasse 1, 3012 Bern, Switzerland*
(raphael.schneeberger@geo.unibe.ch)

² *Nagra, Hardstrasse 73, 5430 Wettingen*

Knowledge about fluid percolation through crystalline rocks is of importance within the framework of radioactive waste disposal, geothermal energy and groundwater supply projects. The underground laboratory at the Grimsel Test Site (GTS, www.grimsel.com), operated by Nagra, offers a unique possibility to investigate fluid flow in crystalline rocks based on structural data combined with long-term hydrochemical and hydrological monitoring.

The area is composed of the Central Aar Granite (CAGr) and the Grimsel Granodiorite (GRGr), which are both cut by meta-basic dykes. During the Alpine orogeny these rocks underwent greenschist metamorphic and tectonic overprint (Steck, 1968). This resulted in the formation of two steeply dipping shear zone networks, one dipping towards SE and the other towards SSW (Wehrens, 2015). The last, cataclastic stage of the Alpine deformation produced discrete zones of increased permeability and thus led to a channelling of the fluid flow through the crystalline rocks.

The present study focuses on a systematic hydrochemical monitoring of the groundwater collected from packed-off borehole sections in order to relate hydrochemical differences to the different structural features in the CAGr and GRGr. Over a one year period of sampling no statistically relevant seasonal trends were observed in the chemical and isotopic composition of the various groundwaters. This suggests homogenisation and attenuation of such variable infiltration signals along flow paths (up to 520 m rock overburden). Such homogenisation is in agreement with low tritium activities (0.6–4.8 TU) obtained earlier for few localities, which indicate average subsurface residence times in the order a few decades (Keppler, 1996).

Groundwater at all localities at the GTS is alkaline, of a similar $\text{Na-Ca-CO}_3\text{-F-(SO}_4\text{)}$ chemical type, has low total mineralisation ($\text{TDS} = 57 \pm 7 \text{ mg/L}$), partial pressures of CO_2 below that of the atmosphere and is of meteoric origin. Over the entire monitoring period, groundwater collected in the southern, GRGr-dominated part has higher pH-values and higher concentrations in Na, K, Li, and Cl, but lower concentrations in Ca, SO_4 and NO_3 compared to groundwater collected in the northern, CAGr-dominated part of the GTS. Similarly, the ratios of Na/Cl , Na/K , Li/Cl , $\text{SO}_4\text{/Cl}$, Sr/Ca , and Ca/Mg differ markedly between the two hydrogeological systems. In contrast, concentrations of Al, Si and F are remarkably similar between the two groups suggesting a similar solubility control in both systems. In combination with the lower $\delta^{18}\text{O}$ and $\delta^2\text{H}$ values of the southern, GRGr-dominated groundwater, which indicate a higher infiltration area, differences in the chemical composition can be related to longer flow paths and residence time and consequently intensified water-rock interaction.

The results indicate that despite small differences in groundwater composition, the systematic long-term hydrochemical survey in combination with structural data allows deciphering different hydrogeological systems in crystalline rock environments.

REFERENCES

- Keppler, A. (1996). *Hydrogeologische, hydrochemische und isotopenhydrologische Untersuchungen an den Oberflächen- und Kluftwässern im Grimselgebiet, Schweiz (unpublished PhD thesis)*. Ludwig-Maximilian-Universität, München, Germany.
- Steck, A. (1968). Die alpidischen Strukturen in den Zentralen Aaregraniten des westlichen Aarmassivs. *Eclogae Geol. Helv.*, 61(1), 19–48.
- Wehrens, P. (2015). *Structural evolution in the Aar Massif (Haslital transect): Implications for mid-crustal deformation (unpublished PhD thesis)*. University of Bern, Bern, Switzerland.

P 11.5

High resolution rain gauges for fine scale temporal rain intensity monitoring

Lionel Benoit¹ & Grégoire Mariéthoz¹

¹ *Institut des Dynamiques de la Surface Terrestre (IDYST), University of Lausanne, Quartier Mouline, Batiment Geopolis, CH-1015 Lausanne (lionel.benoit@unil.ch)*

Nowadays, most in-situ measurements of rainfall are derived from tipping bucket rain gauges. Their operating principle, based on the tilt of a bucket once it is filled, results in discrete measurements of the integrated cumulative rain. In most operating tipping bucket networks, the bucket volume is equivalent to 0.1 to 0.254mm rainfall, which leads to relatively coarse cumulative rain measurements. Deriving rainfall rates with such data presents several drawbacks:

- The temporal resolution is limited by the time needed to fill the bucket.
- The precision is limited by the discrete volume of the bucket.
- The onset and the end of the rain event cannot be precisely timed.

These coarse measurements can in turn induce inaccuracy in rain rate maps generated from rain gauge data and then propagate throughout the whole hydrological analysis. Tips interpolation algorithms have been developed to partially mitigate these drawbacks, but rain gauges complementary to tipping buckets and based on different operating principles are requested to monitor rain rates at fine temporal scale.

Here we propose to investigate the use of drop counting rain gauges for rain rates measurements with a high temporal resolution. To this end, drip-loggers from driptych (www.driptych.com) are used. They allow recording each drop of water exceeding a given energy threshold as an event, and to count the number of events during a given integration time, usually from 10 sec to 1 min. On one hand, drip-loggers are used equipped with a funnel (127mm in diameter) that generates calibrated drops, each one corresponding to 0.01mm of rain. This leads to rain gauges called pluviates, with a resolution one order of magnitude higher than that of tipping buckets. On an other hand, drips-loggers are used alone to record the number of 'big drops' falling during the rain, but the threshold of 'big drops' definition as well as the actual size of the drops generating events remains unknown. This leads to a relative rain intensity sensor, which needs a calibration using a co-located rain gauge to derive the actual rain intensity.

A tipping bucket, a pluviometer and a relative rain intensity sensor were set up on the roof of the University of Lausanne during the summer of 2015. A procedure for rain intensity sensor calibration was developed. Collected data are used to evaluate the capabilities of each sensor for rain intensity measurement with a high temporal resolution, defined here as 1 min or smaller time integration period. The benefits and drawbacks of each method are evaluated in the light of several criteria: 1) accuracy of rain rate and total amount measurement, 2) temporal resolution, 3) duration of the smallest detectable event and 4) timing of rainfall event onset/end.

Finally, the design of a mobile rain intensity measurement system is proposed, taking into account the capability of the rain measurement evaluated in this study. The setting is based on a relative rain intensity sensor set up on a drone flying between points equipped with pluviometers. The ground-based rain gauges are then used for the calibration of the data acquired by the flying sensor.

P 11.6**Hydrogeological and topographic controls on watershed vulnerability to droughts**

Claire Carlier¹, Fabien Cochand¹, Maria Staudinger², Jan Seibert², Michael Stölzle³, Kerstin Stahl³, Markus Weiler³, Stefanie Wirth¹, Daniel Hunkeler¹, Philip Brunner¹

¹ Centre for Hydrogeology and Geothermics, University of Neuchâtel, Rue Emile-Argand 11, CH-2000 Neuchâtel (claire.carlier@unine.ch)

² Hydrology and Climate Unit, University of Zurich, Winterthurerstrasse 190, CH-8057 Zürich

³ Chair of Hydrology, University of Freiburg, Fahnbergplatz, D-79098 Freiburg

The frequency and intensity of periods with scarce water availability are likely to increase under changing climatic conditions. Even temperate and relatively humid regions like Switzerland are subject to seasonal and regional effects of such low-flow events. In order to manage water supply in the future, regions vulnerable to droughts therefore need to be identified.

Groundwater, as one of the main fresh water reservoirs, greatly impacts hydrological catchment dynamics, especially during droughts. Numerous studies have analysed watershed processes, however, they have mainly concentrated on surface flows and streamflow statistics. In fact, classical hydrological models oversimplify groundwater flow processes, leading to poor reproduction of low flows.

Our approach is thus to improve the understanding of low-flow watershed dynamics by considering all relevant physical processes: surface runoff, saturated and unsaturated subsurface flow, the interaction between surface water and groundwater, snowmelt and evapotranspiration. With the physically based numerical model HydroGeoSphere, synthetic models are developed to quantify how basin properties control low-flow dynamics independently from each other and from meteorological conditions. Geological, hydrogeological, topographic and geomorphological characteristics as well as soil properties are tested. 59 Swiss gauged watersheds are then used in order to validate the identified interdependency between basin features and low-flow dynamics. Once the control of watershed characteristics on low flow generating mechanisms is identified, drought sensitivity indicators can be developed, an essential tool for water resources management of ungauged basins under dry conditions.

P 11.7**Mountain slope hydrogeology in deep-seated gravitational slope deformations near Poschiavo, CH**

Larissa de Palézieux¹, Simon Löw¹, Peter Zwahlen²

¹ Geological Institute, ETH Zurich, Sonneggstrasse 5, CH-8092 Zurich (dlarissa@student.ethz.ch)

² Büro für Technische Geologie, Grossfeldstrasse 74, CH-7320 Sargans

A large number of mountain slopes in the Swiss Alps exhibit deep-seated gravitational slope deformations (DSGSD). In DSGSDs, rock mass bodies with sizes at the scale of the mountain flank are slowly displaced over several hundreds of meters without failing catastrophically (Crosta et al., 2013). The size and type of movement leads to characteristic phenomenological features (Figure 1).

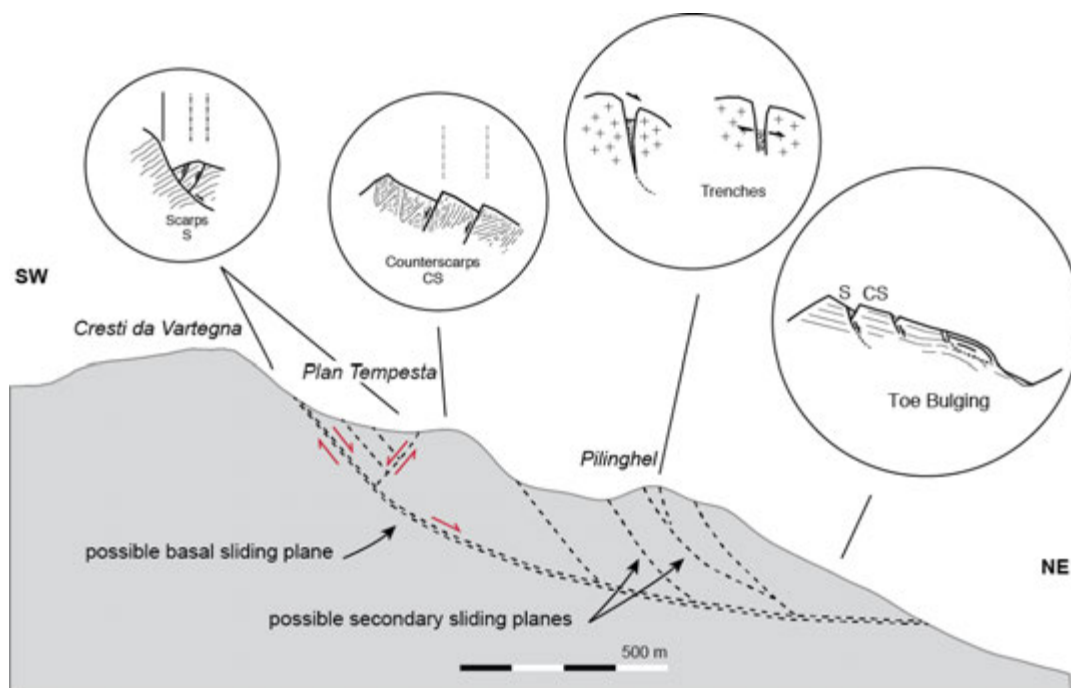


Figure 1. Topographic cross-section through the investigated DSGSD near Poschiavo, Switzerland (location on figure 2). Feature sketches (after Agliardi et al., 2001) are linked to example locations of their occurrence: the main scarp (Cresti da Vartegna), counterscarps towards the front edge of the DSGSD head (Plan Tempesta), trenches, ridges, and troughs spaced at a 2–5 m in the second main body (Pilinghel), and slight bulging at the DSGSD foot. The basal rupture plane is interpreted to be a discontinuous combination of sliding planes, rather than a single, well-defined sliding plane.

The hydrogeology of mountain slopes in alpine regions is generally not very well understood and even less so in DSGSDs. The rock mass in such slope deformations is disturbed and disintegrated, which strongly increases hydraulic permeability and thus alters the local hydrogeologic conditions. In the studied mountain slopes southwest of Poschiavo, surface run-offs are scarce and even completely missing between two torrents at the altitude of the DSGSDs (Figure 2). Below DSGSDs, surface water appears from springs only at lower altitudes (below ca. 1700 m a.s.l.).

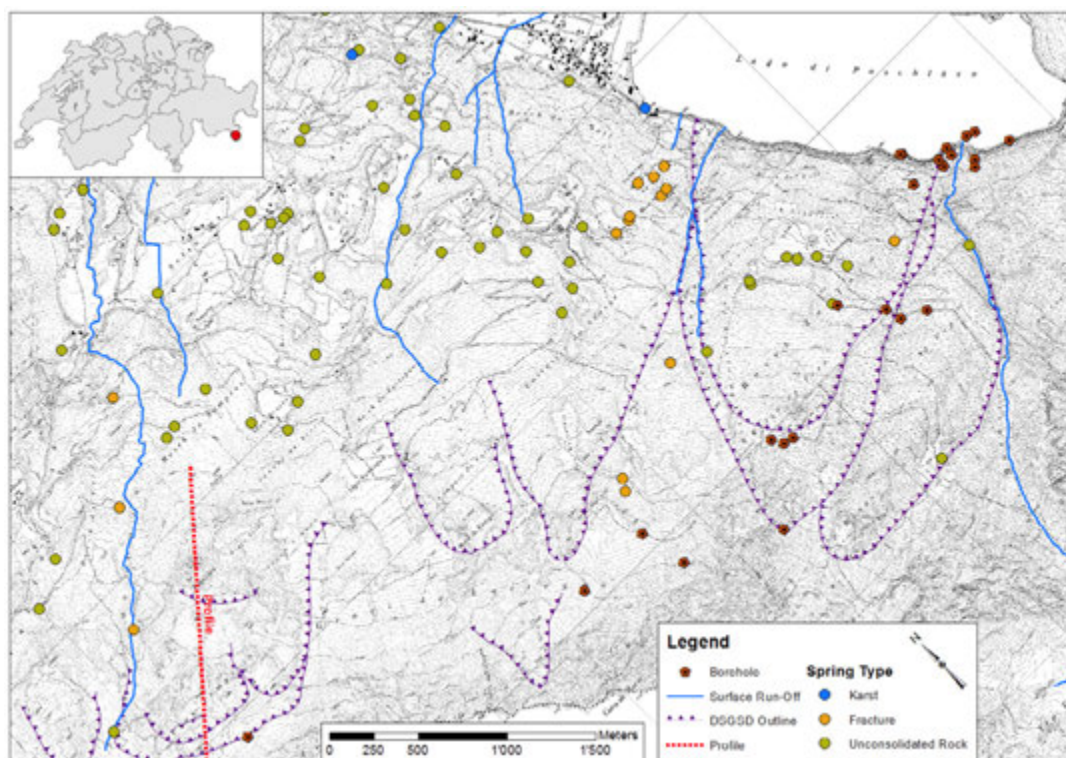


Figure 2. Topographic map of the study area showing the two torrents, the springs classified by type and the outlines of the DSGSDs (after Figi, 2014).

Within the scope of planning a hydropower pump storage plant in the Poschiavo valley by Lagobianco SA (Repower AG), numerous boreholes with depths of 50 to 300 m were drilled in the years 2010/2012. In several boreholes Lugeon and packer tests were executed at various depths and/or pore water pressure sensors installed, which have been recording regularly ever since. Most of the boreholes intersect DSGSDs. The retrieved drill cores contain the whole range from fractured but 'in-situ' rock mass over highly fragmented rock mass residues to kakirite zones of several tens of meters thickness. In some boreholes, the rock mass is disintegrated to a degree where the permeability is too high for any water to remain in the borehole, thus making drilling difficult and hydraulic testing impossible (Figli, 2014).

The study links the hydrogeological data to the phenomenological observations in terms of spatial distribution of the DSGSDs, rock mass permeability, and surface run-off and gives a first understanding of the hydrogeologic conditions in alpine regions containing DSGSDs.

REFERENCES

- Agliardi, F., Crosta, G. & Zanchi, A. 2001: Structural constraints on deep-seated slope deformation kinematics. *Engineering Geology* 59, 83–102.
- Crosta, G. B., Frattini, P. & Agliardi, F. 2013: Deep seated gravitational slope deformations in the European Alps. *Tectonophysics* 605, 13–33.
- Figli, D., Brunold, F. & Zwahlen, P. 2014: Felskennwerte - Kennwertebericht, Projekt Lagobianco. Büro für Technische Geologie AG, Sargans.

P 11.8

Risque de contamination des eaux souterraines par les nutriments et qualité hydrochimique : cas de la plaine GADDAINE-AIN YAGHOUT (Nord-Est de BATNA), ALGERIE

Imane Dib¹, Wahid Chettah¹, Henia Dib¹ & Younes Hamed²

¹ *Département des Sciences Géologiques, Université des Frères Mentouri de Constantine, route de Ain El Bey 25000, Constantine, Algérie (dib.imen@yahoo.fr)*

² *Laboratoire Eau Energie et Environnement (L3E), Institut National des ingénieurs de Sfax (ENIS).*

Dans la plupart des régions arides et semi-arides dans le monde, la disponibilité de suffisamment d'eau douce est devenue un facteur limitant de développement. Dans les régions d'Afrique du Nord, où la rareté de l'eau a toujours été un problème dominant, l'interférence du cycle de l'eau naturelle en raison de la surexploitation de ressources en eau souterraine pour satisfaire les besoins de l'agriculture et des activités domestiques ainsi que des changements de l'utilisation de la terre ont provoqué la réduction de l'eau disponible. Quant à notre région d'étude (plaine de Gadaïne - Ain Yaghout), l'utilisation intensive des pesticides, des engrais chimiques et des rejets d'eaux usées dans les fosses septiques ne sont que quelques exemples d'activités anthropiques qui mènent à la contamination des eaux souterraines. En plus, le facteur interaction eau-roche et la durée de cette interaction ont abouti à la détérioration des ressources en eau dans cette région.

Les objectifs de notre étude étaient d'évaluer les caractéristiques et la distribution spatio-temporelle des deux indicateurs de pollution (concentration des éléments nutritifs et la salinité) et leurs origines (naturelle ou anthropique) ainsi que déterminer les principaux facteurs de migration de l'azote à travers le sol vers les eaux souterraines de la zone d'étude.

Pour atteindre ces objectifs, cinquante échantillons d'eau souterraine de l'aquifère Mio-plio-quaternaire ont été prélevés en Mai 2009 (période des hautes eaux) et en Septembre 2009 (période des basses eaux). La mesure in situ de la conductivité électrique donne des valeurs variant entre 1941 et 7260 $\mu\text{S}/\text{cm}$ et qui restent supérieures aux limites des normes de potabilité fixées par l'OMS ($\sigma < 1500 \mu\text{S}/\text{cm}$). L'analyse chimique des éléments suivants : Na^+ , K^+ , Mg^{2+} , Ca^{2+} , Cl^- , HCO_3^- et SO_4^{2-} et le report de ces résultats sur le diagramme de Piper montre que 60 % des points d'eau ayant un faciès « Chloruré sodique et potassique ou sulfaté sodique » et 40 % des points ont un faciès « Chloruré et sulfaté calcique et magnésien ». La dominance des chlorures et des sulfates est confirmée par des graphes traduisant la relation « $r \text{HCO}_3^- / r (\text{SO}_4^{2-} + \text{Cl}^-)$ - conductivité électrique » et la relation « $r \text{Cl}^- / r \text{SO}_4^{2-}$ - conductivité électrique ».

Les principales sources de chlorure dans les eaux souterraines sont les minéraux liés à des dépôts évaporitiques existants dans les chotts salés et les formations triasiques (comme le gypse ($\text{CaSO}_4 \cdot 2\text{H}_2\text{O}$) présentes dans la plaine. Les concentrations du chlorure dans la zone d'étude varient entre 226 et 1913 mg / l, ces valeurs font l'anion principal dans l'eau étudiée. L'existence de sulfate dans l'eau souterraine provient de la décomposition des matières organiques dans le sol. La valeur du SO_4^{2-} dans la zone d'étude varie entre 93 et 591 mg / l. Près de 96% des échantillons dépassent la limite souhaitable de Cl^- (250 mg / l), et 84% d'eux dépassent la norme de SO_4^{2-} (250 mg / l), (selon l'OMS, 2008).

Pour les cartes représentant la distribution spatio-temporelle des nitrates, la méthode d'interpolation par Krigeage a été utilisée. Les concentrations maximales des NO_3^- en Mai et Septembre sont 112,92 mg / l et 133,09 mg / l respectivement, cependant, elles sont plus élevées que leurs normes respectives de l'OMS (50 mg/l). Pour les valeurs de nitrites sont supérieures aux normes (0.1mg/l) dans les puits situés au Nord et à l'Est de la zone d'étude. En mai, la concentration d'ammonium maximale est de 0,96 mg / l. Cette concentration augmente en Septembre pour atteindre environ 1,03 mg / l (>0,5 mg / l) dans les puits situés dans le nord et le centre de la zone d'étude.

En Septembre, la majorité des échantillons ont des concentrations plus élevée que ceux du mois de mai ce qui augmente le risque de contamination des eaux souterraines par les nutriments. Dans la zone d'étude, ces échantillons ont été principalement prises à proximité des zones urbaines et agricoles où les rejets des eaux usées domestiques, la décharge des effluents d'élevage et l'application des engrais ont le potentiel de polluer non seulement le sol, mais aussi les eaux souterraines par la perte des nitrates et leurs migration vers ces eaux. Cette migration est influencée principalement par les caractéristiques du sol, la nature et la quantité des engrais appliquée ainsi les techniques d'irrigation utilisées.

REFERENCES

- Rouabhia, A., Baali, F., Fehdi, CH., Kherici, N. & Djabri, L. 2008: Hydrochemical and isotopic investigation of a sandstone aquifer groundwater in a semi-arid region, El Ma El Abiod, Algeria. *Journal of Environmental Geology* (Springer) Environ Geol. N°: 254. doi 10.1007/s00254-008-1451-5.
- Hamed, Y. 2009: Caractérisation hydrogéologique, hydrochimique et isotopique du système aquifère de Moularés-Tamerza. Thèse de doctorat, Université de Sfax, (280p).
- Hamed, Y., Awad, S. & Ben Sâad, A. 2013: Nitrate contamination in groundwater in the Sidi Aïch-Gafsa Oasis region, Southern Tunisia, *Environ Earth Sci.* doi 10.1007/s12665-013-2445-5.
- Hamed, Y., Dhahri, F. 2013: Hydro-geochemical and isotopic composition of groundwater and meteoric water, with emphasis on sources of salinity, in the aquifer system in Northwestern Tunisia, *Journal of African Earth Sciences*. <http://dx.doi.org/10.1016/j.jafrearsci.2013.02.004>.
- Vila, J.M. 1977: Notices explicatives des cartes géologiques 1/50 000 d'Ain Yaghout et d'El Madher," Ministère de l'énergie, Algérie.
- World Health Organization (WHO), "Guidelines for Drinking Water Quality," third ed. Vol 1, Recommendations, Geneva, 2008, (515 p).
- Gundogdu, K.S., Guney, I. 2007 : Spatial analyses of groundwater levels using universal kriging," *J. Earth Syst. Sci.* 116 (1), 49-55

P 11.9

The influence of faults on groundwater flow and mass transport dynamics in the area of Neuchâtel

Jaouher Kerrou¹ & François Negro¹

¹ The Centre for Hydrogeology and Geothermics (CHYN), University of Neuchâtel, Rue Emile-Argand 11, CH-2000 Neuchâtel – Suisse (jaouher.kerrou@unine.ch)

The knowledge of the role of faults on a regional scale on groundwater flow and mass transport dynamics is very important to better evaluate the groundwater resources and their vulnerability; and also to evaluate the role of such structures on regional geothermal potential. The main objectives of this study are (i) to evaluate the ability of an equivalent porous media model to simulate regional groundwater flow in highly karstified and faulted aquifer system; and (ii) to point out the effects of major faults (e.g. St-Blaise, la Ferrière and Yverdon faults) on the groundwater flow in the multi-layered aquifer of the central Jura in the area of Neuchâtel.

In this study, a 3D hydrogeological numerical model was used (Kerrou and Negro, 2014). It was elaborated based on a large number of studies have been conducted on the geology and the groundwater resources in the region of Neuchâtel (e.g. Kiraly, 1973; Pasquier et al., 1999, 2006; Negro and Kerrou 2014). The model of 2200 Km² area extends from the Pontarlier fault to the city of Biel and from the Doubs river to the Lake of Neuchâtel. It represents a multi-layered system of 10 hydrogeological units from Trias to Tertiary age including the two main regional aquifers, namely the upper Malm and the Dogger. Only major faults relevant for groundwater flow have been included. The 3D Finite element steady state flow model was calibrated by adjusting the inflow fluxes and the hydraulic conductivities of the outcropping formations against hundreds of hydraulic heads and springs flow rates measurements. The depth-dependent hydraulic parameters of the main aquifers were calibrated by inverse modelling using PEST algorithm. Once the model was calibrated without active faults, it was used to evaluate the effects of faults on groundwater flow dynamics.

From a conceptual point of view, the role of the faults on groundwater flow, i.e. transmissive or barrier was defined based on their orientation relative to principal stress. The NW directed thrusts were considered to be impervious, whereas the NNE-SSW strike slip faults were considered to be transmissive. Afterward, the estimation of the hydraulic conductivity of transmissive faults was realised by sensitivity analysis using a combination of trial and error and automated inverse methods. Vertically, the hydraulic parameters of the faults depend on the affected lithology. For different distributed faults parameters the reproduced potentiometric surface by the model was compared to measured hydraulic heads. The comparison was also evaluated in term of groundwater fluxes in some springs. The impact of permeable faults on the interaction between multi-layered aquifers with different water qualities was evaluated.

The results showed that the numerical model reproduced well the main flow directions (Fig. 1) and that the equivalent medium approach can be used to simulate groundwater flow at the scale of Neuchâtel Canton. With regards to faults, first results showed that these tectonic structures have a local effect on hydraulic head distributions, however, they represent a preferential flow path for mass transport.

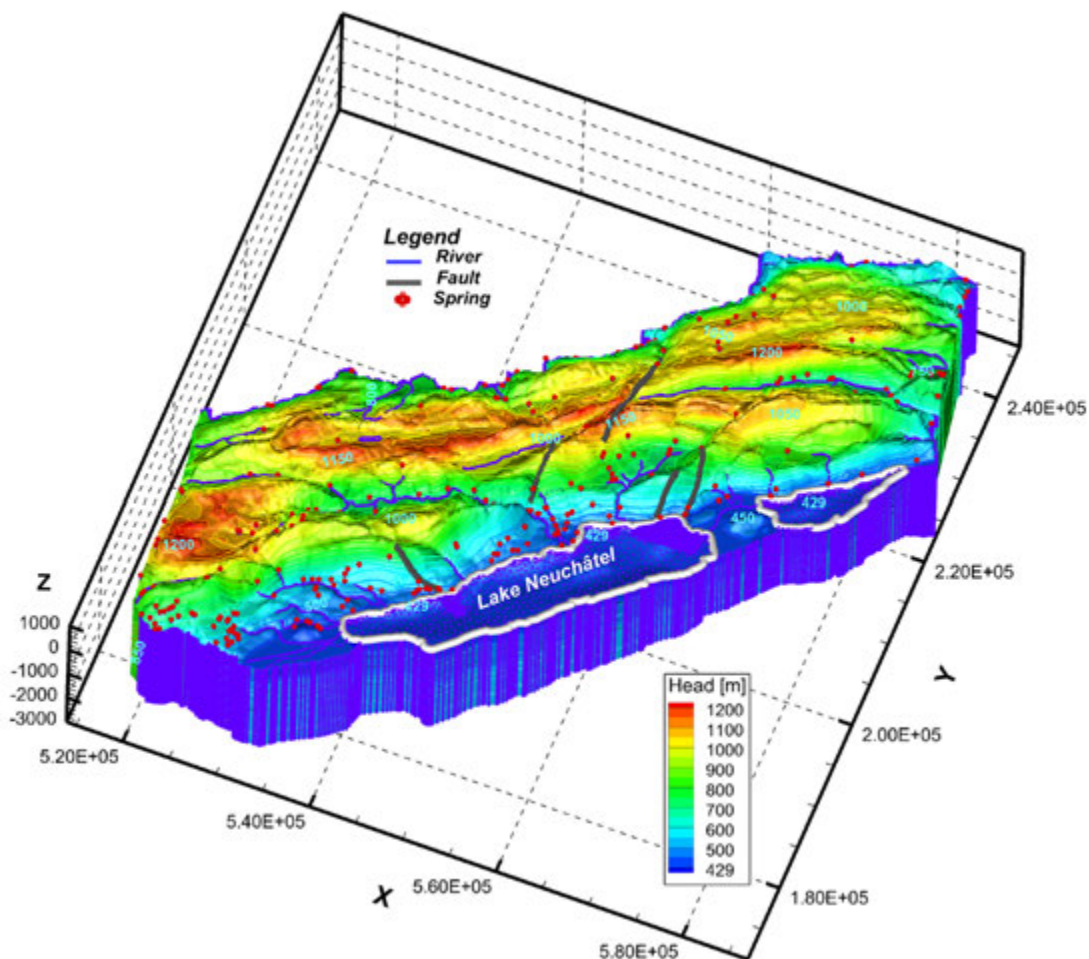


Figure 1. Simulated hydraulic heads (iso-contours).

REFERENCES

- Kerrou J., Negro F. (2014) Regional hydrogeological modelling of the central Jura in the area of Neuchâtel. Part 2 : 3D groundwater flow and mass transport modelling. Swiss Geoscience Meeting 2014, Nov. 2014 Fribourg, Suisse.
- Kiraly, L., 1973 : Notice et carte hydrogéologique du canton de Neuchâtel. Bulletin de la Société Neuchateloise de Sciences Naturelles, 96.
- Negro F., Kerrou J. (2014) Regional hydrogeological modelling of the central Jura in the area of Neuchâtel. Part 1 : 3D geological modelling. Swiss Geoscience Meeting 2014, Nov. 2014 Fribourg, Suisse.
- Pasquier, F., Bouzelboudjen, M. & Zwahlen, F., 1999 : Carte Hydrogéologique de la Suisse, Sarine, feuille n° 6. Commission Géotechnique Suisse et Service Hydrologique et Géologique National.
- Pasquier, F., Zwahlen, F. & Bichet, V., 2006 : Carte hydrogéologique de la Suisse, Vallorbe-Léman nord, feuille n° 8. Commission géotechnique suisse.

P 11.10

Dye tracing test at Morteratsch Glacier (CH) to investigate englacial drainage flowpaths and to evaluate possible G.L.O.F. risk

Sebastian Pera¹, Paola Tognini², Mauro Inglese², Andrea Ferrario³, Paolo Testa⁴

¹ *Earth Sciences Institute, University of Applied Sciences and Arts of Southern Switzerland, Via Trevano, CH-6952 Canobbio (sebastian.pera@supsi.ch)*

² *Gruppo Grotte Milano CAI-SEM, via A. Volta 22, 20122 Milano, Italy; Progetto Speleologia Glaciale*

³ *Gruppo Grotte Saronno CAI-SSI, via G. Parini, 54, 21047 Saronno (VA), Italy; Progetto Speleologia Glaciale*

⁴ *Gruppo Speleologico CAI Varallo, via Durio, 14, 13019 Varallo (VC), Italy; Progetto Speleologia Glaciale*

With an area of about 16 km² and a length of 7 km, the Morteratsch Glacier (Graubünden, CH) is the largest glacier in the Central Alps and the longest in the Bernina Massif. It is a typical valley glacier, built up by the confluence of Vadret da Morteratsch and Vadret da Pers. Both tongues contain well developed en-glacial caves systems and big sub-glacial caves exist (or have been existing till 2010) at the snout.

The glacier morphology let us infer the possibility that “steps” in the bedrock could be responsible for the formation of en- or sub-glacial lakes, which could create a high GLOF (Glacial Lake Outburst Flow) risk.

In the upper ice fragile horizon (150-200 m deep), water moves through en-glacial conduits, so that hydrodynamic inside a temperate glacier is similar to karst water circulation: it can thus be investigated with hydrogeological methods normally used in karst systems.

In September 2012 a dye tracing test was organized, with the aim to evaluate GLOF risk for the Morteratsch Glacier. Two different dyes (Uranine and Aminorhodamine G) have been injected simultaneously into two different sinkholes, in the Vadret da Morteratsch and in the Vadret da Pers. The use of a fluorometer with data logger in the outlet at the snout allowed a detailed and continuous restitution graph to be obtained, which allowed to estimate both the development and efficiency of the en-glacial karst drainage system and the possibility of en- and sub-glacial lakes or storage basins to exist inside or below the glacier.

The restitution graphs are significantly different in the two cases:

- the Vadret da Morteratsch en-glacial flow path exhibits a first arrival of the dye through a well developed caves system, and two minor later peaks probably due to less efficient secondary caves flow paths;
- the Vadret da Pers en-glacial flow path exhibits a similar first arrival peak through a quite well developed caves system, but most dye arrives later, as pointed out by a second wide peak, which indicates a high dye retention, together with dilution and homogenization processes which are well compatible with the existence of an en- or sub-glacial basin or lake, where the dye is temporarily stopped and dispersed. This result is compatible with other Authors' investigations (Frey et alii., 2010; Cook & Swift, 2012), who infer the probability of bedrock overdeepening and related sub-glacial basins to exist in Morteratsch Glacier.

A dye tracing test alone cannot distinguish between en- or sub-glacial basins (GLOF risk being much higher in the former case): it can only show if en- or sub-glacial lakes are related to the active water circulation of the injected cave system, but this method surely enables to highlight a potentially risky situation. In the studied case of the Morteratsch Glacier, a GLOF risk is therefore quite low, or null, in the Vadret da Morteratsch tongue, but rather higher in the Vadret da Pers tongue. Dye tracing tests could therefore be an efficient, quick and easy method to evaluate possible GLOF risk, especially in the present retreat phase.

ACKNOWLEDGEMENTS

A special thank to whom who helped on the field and during data interpretation: Bulat Mavlyudov, Marco Menichetti, Eleonora Beccaluva, Davide Corengia, Silvano Franchi, Valeria Nava, Ursula Taranto, Margherita Ubaldi

REFERENCES

- Cook S.J., Swift D.A. 2012: Subglacial basins: their origin and importance in glacial systems and landscapes, *Earth Science Reviews*. 115, 332-372
- Ferrario A., Inglese M., Testa P., Tognini P. 2012: Progetto Speleologia Glaciale: ricerche per conoscere, esplorare e documentare le cavità glaciali dell'arco alpino, *Speleologia*, 67, Società Italiana di Speleologia, 26-34
- Frey H., Haeberli W., Linsbauer C., Huggel C., Paul F. 2010: A multi-level strategy for anticipating future glacier lake

- formation and associated hazard potentials, *Natural Hazards and earth System Sciences*, 10, 339-352
- Tognini P. 2012: Evidence of a subglacial lake in a contact cave on the Forni Glacier (Italy), *Proceeding of the 5th International Workshop on Ice Caves IWIC-V*, 16-23 September, 2012, Barzio, 26
- Tognini P., Ferrario A., Inglese M., Mangiagalli C. 2012: Criocarsismo e speleologia glaciale. In: Bonardi L., Rovelli E., Scotti R., Toffaletti A., Urso M., Villa F. 2012: I ghiacciai della Lombardia: evoluzione e attualità. Servizio Glaciologico Lombardo, Hoepli, 51-58
- Tognini P. 2002: Considerazioni teoriche sulla struttura e sul funzionamento degli acquiferi endo-e sottoglaciali: il contributo della speleologia glaciale, *Terra Glacialis* n. 5, 33-64

P 11.11

Assessing surface water contribution to groundwater recharge: An example from Traversagna Valley, Ticino.

Sebastian Pera¹, Simona Bronzini¹, Paolo Molignani²

¹ *Earth Sciences Institute, University of Applied Sciences and Arts of Southern Switzerland, Via Trevano, CH-6952 Canobbio (sebastian.pera@supsi.ch)*

² *Geoturrita SAGL, Via C. Molo 9, CH-6900 Bellinzona*

Tracer tests are widely used to evaluate a variety of hydrogeological issues. By using them it is possible to know groundwater flow velocity, study transport of dissolved solids, evaluate porosity of aquifers, etc. while discharge measurements allow tracer recovery calculations and are also routinely used to study hydrology of watersheds.

Arbedo Castione water distribution system relies entirely on groundwater from a small aquifer located in the Traversagna Valley, before its confluence with the Ticino River. The aquifer was formed after the sediments carried by the Traversagna river (mostly gravel, sand and blocks) arriving to a screen dam, completely filled it. 5 drains were therefore drilled within the aquifer starting from the screen dam to exploit it. Those drains used for drinking water provide a continuous discharge of roughly 0.03 m³/s (Pedrozzi, 1990). Given the small surface/volume of the aquifer of about 0.012 Km² / 3*10⁵ m³, and considering the fact that it is limited by gneiss which could be considered as impervious, the Traversagna River should play a role in recharge of the aquifer besides meteoric events, to maintain piezometric levels and therefore the observed discharge from drains.

In order to study the contribution of the Traversagna River to recharge, discharge measurements by using an electronic gauge were performed in date 5.3.2015, in 3 points see figure 1: Upstream (Q1) where the river leaves the gneiss and start to flow through the alluvial sediments, at the spillway (Q2) of the screen dam and downstream after the drains (Q3). A tracer test was also performed in April 2015 with continuous injection of a solution containing 200 g/l of Uranine in the river at point U1. River discharge was measured and tracer injection rate was determined in order to reach a constant concentration in the river of 500 ppb. That concentration was maintained for approximately 30 min. 3 fluorimeters Ggun from Neuchâtel University for continuous tracer monitoring were placed. One in top of the screen dam at the spillway (F1) to analyse the tracer leaving the area through the Traversagna river, the second (F2) in the basin collecting water from the drains, and the third (F3) between the overflow pipe of the drains and the screen dam to get the tracer leaving the aquifer through holes in the dam placed at lower level respect to the spillway. Water conductivity and pH were also measured in the river and in the drains.

According with the results, water conductivity in the river and from the drains present almost no difference with 266 µS/cm and 245 µS/cm respectively, pH values are also similar with 8.28 and 8.20 units indicating that is almost the same water. The contribution of river to recharge is confirmed by discharge measurements. In Q1 discharge was 0.255 m³/s in Q2 180 m³/s and in Q3 0.270 m³/s. Indicating that the river contributed with 0.075 m³/s to the recharge at the time of the measure. Concerning the tracer test, river discharge at the moment of injection was in Q1 of 0.45 m³/s, a concentration of 450 ppb was reached and maintained approximately constant during 25 minutes. Uranine started to arrive to the drains 3.5 hours after tracer injection, reaching a peak of 3.3 ppb 48 hours after injection with a tail reaching values of 0.12 ppb 10 days after injection.

The study shows that the Traversagna river plays a decisive role in recharging the aquifer, with both significant volumes and quick links with the drains providing drinking water to Arbedo - Castione. In terms of management and protection special attention should be paid to the Traversagna River since it is the main source of recharge and any pollution will quickly reach the drains.

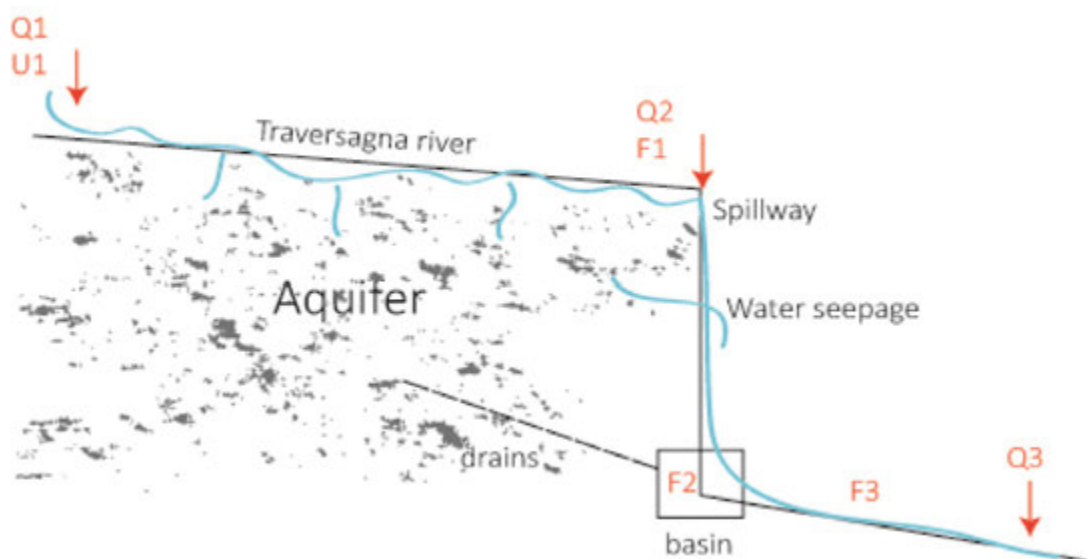


Figure 1. Cross section showing the aquifer, the position discharge measurements (Q), tracer injection point (U1) and fluorimeters position (F)

REFERENCES

Pedrozzi, P. 1992: Relazione geologica protezione captazioni comunali d'acqua potabile del Comune di Arbedo Castione. Studio di geologia Geol. P. Pedrozzi.

P 11.12

Characterization of flow duration curves in Switzerland

Ana Clara Santos ^{1,2,3}, Bettina Schaepli ^{1,2}, Maria Manuela Portela ³, Pedro Manso ², Anton Schleiss ², Andrea Rinaldo ^{1,4}

¹ *Ecole Polytechnique Fédérale de Lausanne (EPFL), School of Architecture, Civil and Environmental Engineering (ENAC), Laboratory of Ecohydrology (ECHO) CH-1015 Lausanne (anaclara.santos@epfl.ch),*

² *EPFL - ENAC, Hydraulic Constructions Laboratory (LCH),*

³ *Instituto Superior Tecnico (IST), Centre for Hydrosystems Research (CEHIDRO), Lisbon, Portugal,*

⁴ *Dipartimento di Ingegneria Civile, Edile ed Ambientale, Università di Padova, Italy;*

A flow duration curve (FDC) represents the percentage of time, a discharge in a stream section is equalled or exceeded. It is a very useful tool in engineering and between its uses there are the studies for hydropower production. This project is part of the Swiss Competence Center on Supply of Electricity (SCCER-SoE), and the focus of the study is on the application of FDCs for hydropower production. In this field, FDCs can be used to determine the volume of water available for electricity production and to select design discharges. Usually, they are estimated based on sufficiently long observed discharges time series, but many catchments are ungauged and we have to look for alternative solutions.

To be able to establish FDCs for ungauged sites, the first step is to understand the available information about gauged catchments, their hydrological regimes and what leads to those regimes. In Switzerland, we can distinguish sixteen discharge regimes (Weingartner and Aschwanden, 1992), defined based on the patterns of the distribution of the discharge over the year and the drivers of those patterns. Those same characteristics and drivers influence the FDCs. Accordingly, we started the characterization of FDCs in Switzerland with catchments that represent the natural regimes in the country and that can be considered natural, meaning that they have not experienced much engineering (notably, catchments without dams and lakes that can regulate the discharge or with significant water withdrawals), and that have available data for a representative period.

For those chosen catchments, we selected homogeneous discharge time series data as stated in Hänggi and Weingartner (2012) to study the form of the curves and to classify them according to this form. We also studied the mechanisms of discharge production to be able to construct models for the ungauged sites in the future.

The characterization included the construction of nonparametric complete FDCs, annual and seasonal FDCs. The curves were also standardised to allow their comparison and their uncertainties have been estimated.

REFERENCES

- Weingartner, R., Aschwanden, H., 1992. Discharge regime – the basis for the estimation of average flows. In: *Hydrological Atlas of Switzerland*, Plate 5.2. Swiss Federal Office for the Environment, Bern, CH.
- Hänggi, P., Weingartner, R., 2012. Variations in discharge volumes for hydropower generation in Switzerland, *Water Resources Management*, 26, pp. 1231–1252

P 11.13

Temporal and spatial analysis of the redox plume in the groundwater at Aarberg, Switzerland

Samuel Weber¹, Christoph Wanner¹, Paul Wersin¹

¹ *Institute of Geological Sciences, University of Bern, Baltzerstrasse 1+3, CH-3012 Bern (saemiweber@students.unibe.ch)*

The Seeland aquifer is a very important source of water for drinking as well as for industrial and agricultural purposes. It mainly consists of gravels and sands with only small amounts of fine-grained material. This study concentrates on the eastern central part of the aquifer between Aarberg and Lyss. The hydrology in this area is strongly influenced by bank filtration that occurs in the Hagneck-Kanal to the southwest and the Alte Aare River, which runs through the study area.

The sugar factory at Aarberg has been producing sugar for more than 100 years. Open ponds along the Alte Aare River were used to dispose wastewater and sludge from the sugar beet processing until the 1980ies. These wastes released large amounts of organic carbon, which was oxidized in the subsurface by different microbially-mediated redox processes. The main electron acceptors are dissolved oxygen, nitrate, iron and manganese. Due to leaking ponds a substantial part of the aquifer is characterized by manganese and iron reducing conditions as well as by elevated ammonium concentrations and increased alkalinity. All these processes deteriorate the water quality in the aquifer.

The aim of this study is to unravel the temporal evolution of the redox-plume in the study area. To do so, water analyses from a long-term monitoring of up to 60 years were analyzed in detail. Time series from different observation boreholes all show maximum concentration of reduced species in the 1950ies and 1960ies, with a later trend towards more oxidizing conditions. In addition to the analyses of historical data, we also performed two sampling campaigns to assess the current state of the redox plume in detail. Results from both campaigns show areas with different attenuation progress of the redox plume. Areas close to the deposits have generally higher concentrations of reducing species. However, the local concentrations are strongly variable. For instance, the area to the west of the Alte Aare generally features low concentrations of reduced species, while the area to the east of the Alte Aare (i.e., north-west of Lyss) shows higher iron, manganese and ammonium concentrations. We suspect that this variability is caused by heterogeneous river infiltration along the Alte Aare River. Accordingly, the influx of oxygen-rich river water is likely higher in the western area, which results in an increased attenuation of the reducing conditions when compared to the area east of the Alte Aare.

Whether the wastes of the sugar factory are responsible for the large-scale reducing conditions north of Lyss is not completely resolved. Forests and swampy areas along the Alte Aare River as well as organic rich sediments could be another source of organic matter.

P 11.14

The influence of aquifer heterogeneity on drawdown and transmissivity estimation

Marc-Antoine Zermatten¹, Philip Bruner¹ & Philippe Renard¹

¹ *Faculté d'hydrogéologie et de géothermie (CHYN), Université de Neuchâtel, Rue Emile-Argand 11, CH-2000 Neuchâtel*

Aquifer tests such as the method of Jacob assume homogeneous subsurface properties. However, aquifers rarely are homogeneous, and therefore the estimation of parameters such as transmissivity could be biased. A range of studies have analysed the influence of heterogeneity on drawdown. To the best of our knowledge, all of these approaches were based on simple, multi-Gaussian realisations of aquifer heterogeneity that do not consider the connectivity of facies. In this study, we analyse the effect of heterogeneity on the aquifer drawdown using a highly realistic geological model that correctly represent facies connectivity. This geological model was developed by *Lopez et al. [2008]* and is based on the reproduction of deposition and erosion processes of a fluvial environment.

We use this geological model to simulate drawdown near a pump. The drawdown data obtained provide the basis for a comparison with the Jacob method to estimate aquifer transmissivity. We conclude that, in an anisotropic environment, the transmissivity estimated using Jacob's method is equal to the effective transmissivity for flow parallel to the geological structures. This indicates that the Jacob method is a good way to approximate transmissivity in heterogeneous environments. However, our results also indicate the importance of using multiple boreholes for such an analysis. Also, to obtain stable results using the Jacob method, the aquifer tests have to be carried out over relatively long time period.

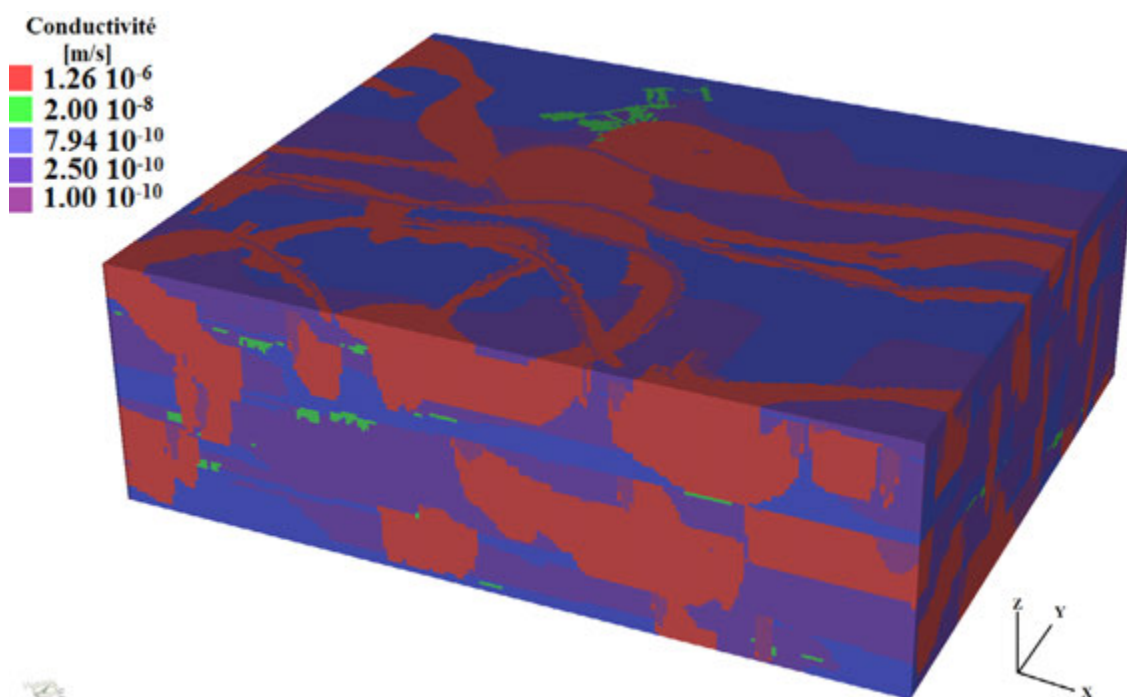


Figure 1. 3D hydrogeological model based on highly realistic heterogeneity distribution.

REFERENCE

Lopez S., Cojan I., Rivoirard J., Galli A., 2008, Process-based stochastic modelling: meandering channelized reservoirs, Spec. Publ. Int. Assoc. Sedimentol., 40, 139-144

P 11.15

Airborne exploration of anomalous high uranium contents in water and soil in the region of the “Lyssbach” – Canton of Bern

Simon Werthmüller¹, Heinz Surbeck² & Rico Ryser³

¹ *Geologische Beratungen SCHENKER KORNER RICHTER AG, Büttenehalde 42, 6006 Luzern
(simon.werthmueller@fsgeolog.ch)*

² *Nucfilm GmbH, Fineta, 1792 Cordast*

³ *Amt für Wasser und Abfall des Kantons Bern (AWA), Gewässer- und Bodenschutzlabor (GBL), Reiterstrasse 11, 3011 Bern*

The water and soil protection laboratory of the Canton of Bern detected anomalous high uranium concentrations in the creek “Lyssbach” at the locality of Lätti between between Lyss and Schönbühl (canton of Bern) as part of the standard water monitoring program. Values up to 45 µg/l of dissolved uranium in creekwater and at up to 400 µg/l in groundwater samples have been measured. The average concentration of dissolved uranium in Swiss creeks is in the range of a few µg/l (Baertschi & Keil 1992).

Water samples were collected from the “Lyssbach” and from groundwater inflows in the creek to explore the possible uranium source. Two suspicious contaminated sites were evaluated using a radiation detector as a payload of a octocopter (Figure 1). Airborne radiation mapping turned out to be a very effective and low budget instrument to detect anomalous radiation areas within short time.

It was possible to scan several 100'000 m² within a day with a resolution of approximately 10 m² and a detection limit of the flying Na(Ti) detector ~ 50 cps. In order to increase the resolution to 2 m² within the resulting anomalous radiation, the area was measured with the same detector by foot. Soil samples, taken from core drillings, were analysed by gamma spectrometry and X-ray fluorescence spectroscopy, watersamples by alphaspectrometry. In addition, piezometer measurements were made. The resulting radiation map is shown in Figure 2. The obtained uranium concentrations of the soil samples showed a max. value of 220 ppm U at a depth from 0.60 m. The uranium content of the watersample from the piezometer (420 µg U/l) showed the same value as earlier (Schmidt 2013) measurements from the drainagewater.

Several possible uranium sources could be evaluated, based on a historical investigation: disposal sites, fertilisers / waste of fertiliser production or geogene origin. The deposition age of the solid uranium compounds in the soil could be estimated to 10'000 years b.p., based on the ratio of Ra-226 and Th-234. Therefore any present-day anthropogenic origin of the uranium compounds can be excluded. However, during in the past 150 years the redox conditions may have changed by draining the swampy fields to gain agricultural land. This could have caused the input of oxygen into the soil to remobilize the uranium.



Figure 1: Octocopter with a radiation detector as payload.

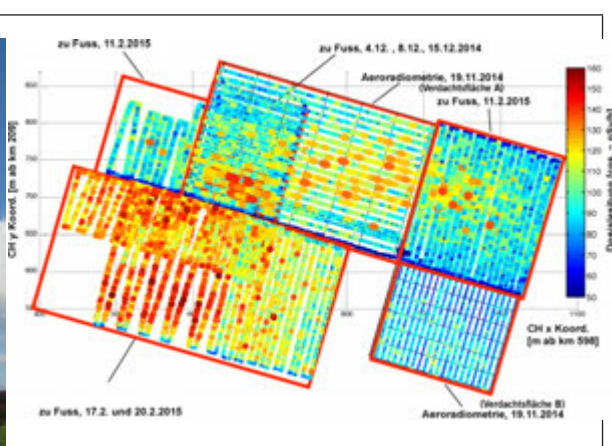


Figure 2: Radiationmap

REFERENCES

- Baertschi, P. & Keil, R. (1992). Urangelhalte von Oberflächen-, Quell- und Grundwässern der Schweiz Beiträge zur Geologie der Schweiz. Kleinere Mitteilungen; Nr. 94
- Franziska Schmidt (2013): Schwermetalle im Lyssbach – Herkunft und Bedeutung, BSc thesis, Dept. Earth Sciences, ETH-Zurich, 2013

P 11.16**Geomorphological analysis of the drainage system along the North Tabriz Fault**

Amaneh Kaveh Firouz¹, Jean-Pierre Burg¹

¹ *Geological Institute, ETH Zurich, Sonneggstrasse 5, CH-8092 Zurich, Switzerland (amaneh.kaveh@erdw.ethz.ch)*

The Urmia Basin in NW Iran is part of the active tectonic zone between the colliding Arabian and Eurasian plates. During the last glacial-interglacial cycles the base level has been documented to fluctuate between 10 to 30 meter (Stevens and Djamali, 2012). Moreover, one of the most active strike-slip faults, the Tabriz Fault, occurs to the north of the lake. Therefore, the Urmia Lake area provides a promising example to understand the response of lake level changes to tectonics in the surrounding landscape.

We carried out the morphometric analysis of river profiles using the 90 m Digital Elevation Model. Results show that the stream crossing the Tabriz Fault is characterized by a knickpoint channel steepness between 26.1 and 34.5 on both sides of the knickpoints whereas the concavity index varies between 0.72 and 13 upstream and downstream of the knickpoint, respectively. We interpret the knickpoint as a response to recurrent movement along the Tabriz Fault as documented in historical record.

REFERENCES

Stevens, Lora R., and Djamali M. 2012: Hydroclimatic variations over the last two glacial/interglacial cycles at Lake Urmia, Iran. *J Paleolimnol*, 47, 645-660.

13. The International Year of Soils: open session on soil security

Nikolaus J. Kuhn, Stéphane Burgos, Emmanuel Frossard, Frank Hagedorn, Elena Havlicek, Jens Leifeld, Pascal Walther, Andreas Papritz, Urs Steiger

*National Research Programme «Sustainable Use of Soil as a Resource» (NRP 68)
Swiss Soil Science Society*

TALKS:

- 13.1 Arata L., Meusburger K., Alewell C.: Soil erosion assessment in Swiss mountainous areas using Fallout Radionuclides (^{137}Cs , $^{239+240}\text{Pu}$)
- 13.2 Bader C., Leifeld J., Müller M., Schulin R.: Assessing the carbon sequestration potential of Miscanthus cropping on managed organic soils
- 13.3 Gosheva S., Müller M., Walther L., Zimmermann S., Niklaus P., Beatriz R., Domínguez G., Abiven S., Hagedorn F.: SOM storage and pool distribution along climatic and altitudinal gradients in Swiss forest soils
- 13.4 Menichetti L., Leifeld J., Kätterer T.: Exploring mean residence time and distribution of SOC pools in a long term experiment in Switzerland through explicit radiocarbon model structures
- 13.5 Solly E.F., Brunner I., Herzog C., Schöning I., Schrumpf M., Fritz H.S., Susan E.T., Hagedorn F.: Unravelling the “real age” of tree fine roots
- 13.6 Studer M.S., Gonzalez Dominguez B.R., Niklaus P. A., Abiven S.: Effect of climate change on plant-soil-atmosphere carbon cycling: plant vs. soil organic matter derived CO_2 effluxes
- 13.7 van der Voort T.S., Zell C., McIntyre C., Hagedorn F., Fisher L., Eglinton T.: Insights into soil organic matter stability using temporal, fraction- and compound-specific radiocarbon analysis

POSTERS:

- P 13.1 Kuhn N.J., Hu Y., Bloemertz L., Xiao L., He J., Li H., Greenwood P.: Conservation tillage and sustainable intensification of agriculture: regional vs. global benefits analysis
- P 13.2 González Domínguez B.R., Studer M.S., Niklaus P.A., Abiven S.: Losses of organic carbon from Swiss forest soils in relation to climate, soil properties and landscape characteristics
- P 13.3 Tresch S.: Soil quality indicators of urban gardens in Zurich

13.1

Soil erosion assessment in Swiss mountainous areas using Fallout Radionuclides (^{137}Cs , $^{239+240}\text{Pu}$)

Laura Arata¹, Katrin Meusburger¹ & Christine Alewell¹

¹ *Environmental Geosciences, University of Basel, Bernoullistrasse 32, CH-4056 Basel (laura.arata@unibas.ch)*

The combined pressure of land use and climate change has resulted in accelerated soil erosion rates in Alpine grasslands. To efficiently mitigate and control soil losses by erosion and reduce their environmental impacts in Alpine grasslands, reliable and validated methods for comprehensive data generation on the magnitude and spatial extent of soil erosion are needed. Sheet erosion, which is one of the main forms of erosion affecting Swiss Alpine grasslands, is particularly difficult to quantify.

Among other methods to estimate the role of sheet erosion in the degradation processes of Alpine soils, the application of the Fallout Radionuclides (FRN) as soil tracers showed very promising results (e.g. Konz et al. 2012). So far, applications of FRNs in the Alps as soil erosion tracers include ^{137}Cs (half-life: 30.2 years) (Konz et al., 2012), ^{239}Pu (^{239}Pu [half-life = 24110 years] and ^{240}Pu [half-life = 6561 years]) (Alewell et al., 2014).

The classical approach of the FRN method is based on a qualitative comparison: the inventory (total radionuclide activity per unit area) at a given sampling site is compared to that of an undisturbed reference site, where no soil redistribution processes have occurred since the main deposition of the selected FRN. To derive quantitative estimates of soil erosion and deposition rates from FRN measurements specific conversion models are needed.

This traditional reference-site approach encounters a number of limitations in the Alps, especially related to the selection of suitable reference sites and to the use of ^{137}Cs , the most widely used FRN for soil erosion studies. First, finding undisturbed slopes with no erosional activity during the last 30 years (time since ^{137}Cs fallout) is challenging. Second, the application of ^{137}Cs in alpine grasslands is compromised by the high heterogeneity of the fallout at the reference sites, which is most likely due to its origin from the Chernobyl accident.

To overcome the above described limitations, our research focuses on three main aims:

1. To replace the classical ^{137}Cs approach, where an undisturbed reference site is compared to erosional sites, with a repeated sampling approach (Porto et al., 2014), where we re-sample sites which have already been measured for ^{137}Cs inventories in the past. In this way the spatial reference is replaced by a temporal.
2. To apply airborne gamma measurements to map ^{137}Cs distribution over selected alpine study areas. Having an overview of the ^{137}Cs concentration in the study areas allows to identify suitable reference sites. Moreover, to upscale the application of ^{137}Cs as soil tracer for soil erosion assessment would help to validate results of soil erosion risk models.
3. To investigate the application of Pu isotopes in alpine grasslands, and to design a valid conversion model to estimate soil redistribution rates from Pu inventories. In the alpine valleys the origin of Plutonium fallout is mainly linked to the nuclear bomb tests, which took place from 1954 to the mid-1960s, and therefore $^{239+240}\text{Pu}$ deposition is not connected to few specific rain events, which results in a more homogeneous distribution of $^{239+240}\text{Pu}$ in the alpine soils (Alewell et al., 2014).

The quantification of Alpine soil erosion rates will be crucial in the near future for alpine grassland management, as it might increase management efficiency towards a more sustainable land use.

REFERENCES

- Alewell, C., Meusburger, K., Juretzko, G., Mabit, L., Ketterer, M. E., 2014. Suitability of $^{239+240}\text{Pu}$ and ^{137}Cs as tracers for soil erosion assessment in mountain grasslands. *Chemosphere*, 103, 274-280.
- Konz, N., Prasuhn, V., & Alewell, C., 2012. On the measurement of alpine soil erosion. *Catena*, 91, 63-71
- Porto, P., Walling, D. E., Alewell, C., Callegari, G., Mabit, L., Mallimo, N., ... & Zehringer, M. (2014). Use of a ^{137}Cs re-sampling technique to investigate temporal changes in soil erosion and sediment mobilisation for a small forested catchment in southern Italy. *Journal of environmental radioactivity*, 138, 137-148.

13.2

Assessing the carbon sequestration potential of *Miscanthus* cropping on managed organic soils

Cedric Bader^{1/3}, Jens Leifeld¹, Moritz Müller² Rainer Schulin³

¹ Agroscope INH, Reckenholzstrasse 191, CH-8046 Zürich, (cedric.bader@agroscope.admin.ch)

² HAFL, Berner Fachhochschule, Länggasse 85, CH-3052 Zollikofen

³ D-USYS, ETH Zürich, Universitätstrasse 16, CH 8092 Zürich

The organic soils of peatlands represent a major terrestrial carbon sink. Agricultural use of organic soils requires drainage and thus changes conditions in these soils from anoxic to oxic. As a consequence, organic carbon that had been accumulated over millennia is rapidly mineralized, so that these soils are converted from a CO₂ sink to a source. The peat mineralisation rate depends mainly on drainage depth and on cultivation type. Several studies stated that *Miscanthus*, a C4 bioenergy plant, shows potential for carbon-sequestration in mineral soils because of its root system, absence of tillage and preharvest litterfall (Dondini et al (2009), Zimmermann et al (2011), Poeplau & Don (2014)). The major aim of our study was to determine the amount of C4-derived carbon in a managed organic soil and thus to quantify whether also organic soils with *Miscanthus* sequester new carbon. Additionally, we analysed the isotopic composition of respired CO₂ emitted from incubated organic soil samples cultivated with *Miscanthus*. We examined soil samples from different soil depths down to 1 m of two adjacent fields cultivated either with *Miscanthus* (since 20 years) or perennial grass. Both sites are located in the Bernese Lakeland. The $\delta^{13}\text{C}$ values of the soil imply, that the highest share of *Miscanthus* derived carbon lies around 17.8 % and is situated in a depth of 10-20 cm. To assess the influence of *Miscanthus* on respired CO₂, we incubated soil samples at 20°C and 10°C for 9 months. During the first month, soil respiration rates were slightly smaller for the samples from the *Miscanthus* field, but became similar to the soil from perennial grass over longer incubation periods. To analyse the isotopic CO₂ composition, we trapped CO₂ of the soil samples from a depth of 0-30 cm during the first 600 hours of incubation at 20°C. We precipitated it as BaCO₃ and measured its $\delta^{13}\text{C}$ value. CO₂ of the soil samples mainly originated from *Miscanthus* (17-98 %). Hence, C4-derived carbon is more actively mineralized than peat-derived carbon. However, the share of *Miscanthus* derived CO₂ shows no correlation with the amount of C4-derived soil carbon. After 20 years of *Miscanthus* cropping on an organic soil we found a substantial contribution of C4-derived soil carbon. Nevertheless the sequestration rate is 1.3-2 times smaller than on mineral soils used for studies by Dondini et al (2009) and Zimmermann et al. (2011).

REFERENCES

- Dondini, Marta, Kees-Jan Van Groenigen, Ilaria Del Galdo, und Michael B. Jones. 2009: Carbon Sequestration under *Miscanthus*: A Study of ^{13}C Distribution in Soil Aggregates, *GCB Bioenergy* 1, 321-330.
- Poeplau, Christopher, und Axel Don. „Soil Carbon Changes under *Miscanthus* Driven by C4 Accumulation and C3 Decomposition – toward a Default Sequestration Function.“ *GCB Bioenergy* 6): 327–38.
- Zimmermann, Jesko, Jens Dauber, und Michael B. Jones. „Soil Carbon Sequestration during the Establishment Phase of *Miscanthus* × *Giganteus*: A Regional-Scale Study on Commercial Farms Using ^{13}C Natural Abundance.“ *GCB Bioenergy* 4, : 453–61.

13.3

SOM storage and pool distribution along climatic and altitudinal gradients in Swiss forest soils

Sia Gosheva^{1, 2}, Mirjam Müller^{1, 3}, Lorenz Walthert¹, Stephan Zimmermann¹, Pascal Niklaus², Beatriz R. González Domínguez³, Samuel Abiven³, Frank Hagedorn¹

¹ Forest Soils and Biogeochemistry, Swiss Federal Institute of Forest, Snow and Landscape Research (WSL), Zürcherstrasse 111, CH-8903 Birmensdorf (sia.gosheva@wsl.ch)

² Institute of Evolutional Biology and Environmental Studies, University of Zurich, Winterthurerstrasse 190, CH-8057 Zurich

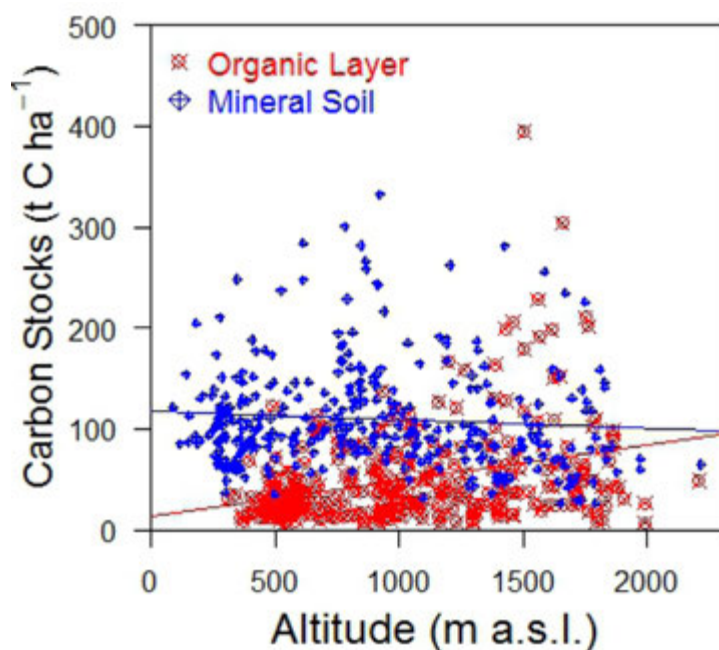
³ Soil Science and Biogeochemistry Unit, Department of Geography, University of Zurich, Winterthurerstrasse 190, CH-8057 Zurich

Soil organic matter (SOM) plays a key role for a number of soil and ecosystem functions, but our quantitative understanding of the driving factors is still uncertain. SOM consists of a continuum of compounds ranging from slightly altered plant residues, the so-called particulate OM (POM), to mineral-associated OM. POM is the most rapidly cycling and hence labile fraction in SOM. Therefore, it might respond particularly sensitive to climate change. For Swiss grasslands, Leifeld et al. 2009 observed higher SOM contents and an increasing contribution of POM with increasing elevation suggesting that climate exerts a major control on SOM stability and storage. Little is known, however, for forest soils where a substantial fraction of POM is stored in the organic layer.

In our study, we explore the controlling factors of SOM stocks and the distribution of POM in the organic layer as well as within mineral soils of Swiss forests. We hypothesize that SOM storage increases with increasing elevation. Furthermore, we expect elevational changes to be larger for SOM properties (contribution of POM, SOM depth distribution, and C/N ratio) than for SOM stocks.

We examined the SOM stocks in the organic layer and the mineral soil of 1000 soil profiles. Mineral soils (0-20cm) from a subset of 54 sites were separated into free light fraction (fLF), occluded light fraction (oLF), fine heavy fraction (fHF), and coarse heavy fraction (cHF). The sites, all located in Swiss forests, were distributed along a great altitudinal gradient ranging between 277 and 2207 m a.s.l., mean annual temperatures (MAT) ranging between 0.6 and 11.9 °C, and mean annual precipitation (MAP) between 704 and 2340 mm.

In the organic layer C-stocks increased with an increase in elevation (Figure 1) and with a decrease in MAT. MAP had no impact on the organic layer; however, in the mineral soil, C-stocks increased with an increasing MAP, but they were not influenced by neither altitude nor MAT. These elevational changes occurred on both calcareous and acidic bedrock.



Similarly to the organic layer, we found an increase in all SOM-fractions except in cHF with an increasing elevation and MAP. MAT showed a smaller impact as compared to MAP and altitude. Our results indicate that climatic conditions exert a significant control on SOM stocks and quality. In particular MAT is important for the organic layer and MAP for the POM in the mineral soil. Consequently, a warmer and drier climate could lead to a deterioration of SOM, especially at high elevations. This could possibly cause a redistribution of carbon pools and C losses from forest soils.

Figure 1. Relationship C-stocks vs. altitude

REFERENCES

Leifeld J., Zimmermann M., Fuhrer J., & Conen J. 2009: Storage and turnover of carbon in grassland soils along an elevation gradient in the Swiss Alps, *Global Change Biology*, 15(3), 668-679.

13.4

Exploring mean residence time and distribution of SOC pools in a long term experiment in Switzerland through explicit radiocarbon model structures

Lorenzo Menichetti¹, Jens Leifeld¹, Thomas Kätterer²

¹ Agroscope, Climate / Air Pollution Group, Reckenholzstrasse 191, CH 8046 Zürich (Switzerland).

Lorenzo.Menichetti@agroscope.admin.ch

² Sveriges Lantbruksuniversitet, Inst för Ekologi, Box 7044, 75007 Uppsala (Sweden). Thomas.Katterer@slu.se

Modelling soil organic carbon (SOC) dynamics is of paramount importance to face several of the challenges of the present century, linked with the need to reduce atmospheric greenhouse gases, to maintain or enhance soil fertility, and to mitigate the impact of climate change on other ecosystem services.

SOC dynamics are the result of different, partially unknown, interacting processes and controls at the pedon and ecosystem scale. This complexity translates in SOC models as high number of degrees of freedom and high number of latent variables to be inferred. In consequence, SOC model parameters interact strongly, generating an equifinality problem. In order to minimize equifinality and to better deal with the lack of data to constrain parameters, one of the good practices in SOC modelling is to prioritize model simplicity. This criterion in itself is rather simple, but difficult to implement. It defines an elusive optimum point over the bias/variance trade off, balancing the adherence of the model to reality (model complexity) with its predictive power and potential to generalize (model simplicity).

The time scale of SOC turnover is mostly in the range of years to centuries, hence direct turnover measurements are difficult or impossible to design. Thus, robust proxy variables are needed to improve the precision of estimating latent variables. In this respect, carbon radioisotope measurements can serve as a proxy for SOC ages both at annual to decadal (bomb peak based) and centennial to millennial time scales (radio decay based).

Since the first attempts to utilize radiocarbon measurements in SOC models, at the end of the last century, there seems to be a discrepancy between what is indicated by isotope data and by SOC kinetic models. This suggests that contemporary SOC models are missing key processes, and indicates structural uncertainties of SOC models. These uncertainties need to be considered, but are difficult to quantify.

To tackle these problems, we studied SOC dynamics and kinetics in the ZOFÉ experiment, a >60-years old controlled cropland experiment situated in Zürich (Oberholzer et al., 2014) by utilizing SO^{14}C measurements in the framework of different SOC model structures. The different model structures, built starting from a “mother” structure (the two-pool model ICBM, Andren & Kätterer, 1997), present small variations in order to represent different processes. We first added an inert pool (structure 2) to the basic ICBM structure (structure 1), in order to represent slower SOC. We then considered this third pool as decaying with similar kinetics as the others (structure 3). We then added a term representing interactions between SOC and the microbial C pool both to the basic ICBM structure (structure 4) and to the inert pool structure (structure 5).

The use of different model structures allows us also to explore model structural uncertainty and to compare different estimates of SOC initial distributions and kinetics in the experiment. This multiple structure approach can improve greatly the robustness of the estimates. Together with structural uncertainty, we took care of parameter uncertainty and equifinality by implementing each calibration in a formal Bayesian framework.

All model structures have been then extended to explicitly represent a total C pool and a ^{14}C pool in order to combine the information coming from the measured total SOC and SO^{14}C data streams to constrain more accurately the models. In order to investigate the effect of the information from the two data streams on the parameter calibration over the different structures, all the models are calibrated over a gradient of weights assigned to the two data streams. This way we assessed the sensitivity of different SOC kinetics hypotheses to the SO^{14}C data stream.

Results define a clear picture for the ZOFÉ experiment. All model structures indicated a dramatic change following an initial land use change, followed then by a smaller but constant C loss in the three treatments considered in our study. The mean residence times of the C pools defined in our models was robust for the younger SOC (varying between 0.9 and 1.1 years), but highly sensitive to model structure for the older SOC (varying between 20 and 70 years).

Those two model structures that include a microbial control parameter, influenced by substrate availability (structure 4 and 5) performed the best. This suggests an interaction between substrate input rate and SOC turnover that should be considered in SOC models.

Our results indicate that explicit SO^{14}C modeling has the potential to identify key controls of SOC turnover in agricultural soils.

REFERENCES

- Andren, O., & Katterer, T. (1997). ICBM : The Introductory Carbon Balance Model for Exploration of Soil Carbon Balances. *Ecological Applications*, 7(4), 1226–1236.
- Oberholzer, H. R., Leifeld, J., & Mayer, J. (2014). Changes in soil carbon and crop yield over 60 years in the Zurich Organic Fertilization Experiment , following land-use change from grassland to cropland. *Journal of Plant Nutrition and Soil Science*, 493, 696–704.

13.5

Unravelling the “real age” of tree fine roots

Emily F. Solly¹, Ivano Brunner¹, Claude Herzog¹, Ingo Schöning², Marion Schrumpf², Fritz H. Schweigruber¹, Susan E. Trumbore², Frank Hagedorn¹

¹ Swiss Federal Research Institute WSL, Zürcherstrasse 111, CH-8903 Birmensdorf (emily.solly@wsl.ch)

² Max Planck Institute for Biogeochemistry, Hans-Knoell-Str. 10, DE-07745 Jena

Estimating the turnover time of tree fine roots is crucial for modelling soil organic matter dynamics, but it is one of the biggest challenges in soil ecology and one of the least understood aspects of the belowground carbon cycle. The methods used - ranging from radiocarbon to ingrowth cores and root cameras (minirhizotrons) - yield very diverse pictures of fine root dynamics with turnover rates reaching from less than one year to decades. These have huge implications on estimates of carbon allocation to root growth and maintenance and on the persistence of root carbon in soils before it is decomposed or leached. We will present a new approach, involving dendrochronological techniques, which unravels the “real age” of fine roots and reconciles the debate on root turnover in recent years.

For a range of forests with diverse water and nutrient limitations we find that the annual growth rings in the secondary xylem of thin transversal sections have a mean root “ring age” of 1.5 - 2 years (Figure 1). However, radiocarbon estimates of mean “carbon ages”, which define the time elapsed since structural carbon was fixed from the atmosphere, average around a decade. We relate this dramatic difference not to methodological bias, but rather to a time lag between C assimilation and production of fine root tissues due to the storage of older carbon components in trees. We further observed that the root ring age increases with root diameter although it does not appear to be related to the branching order. Our findings indicate that both the physiological and radiocarbon ages must be modelled jointly in forest ecosystems, if we want to correctly account for the inputs of root litter into the soil organic matter pool and quantify the carbon persistence times in soils.

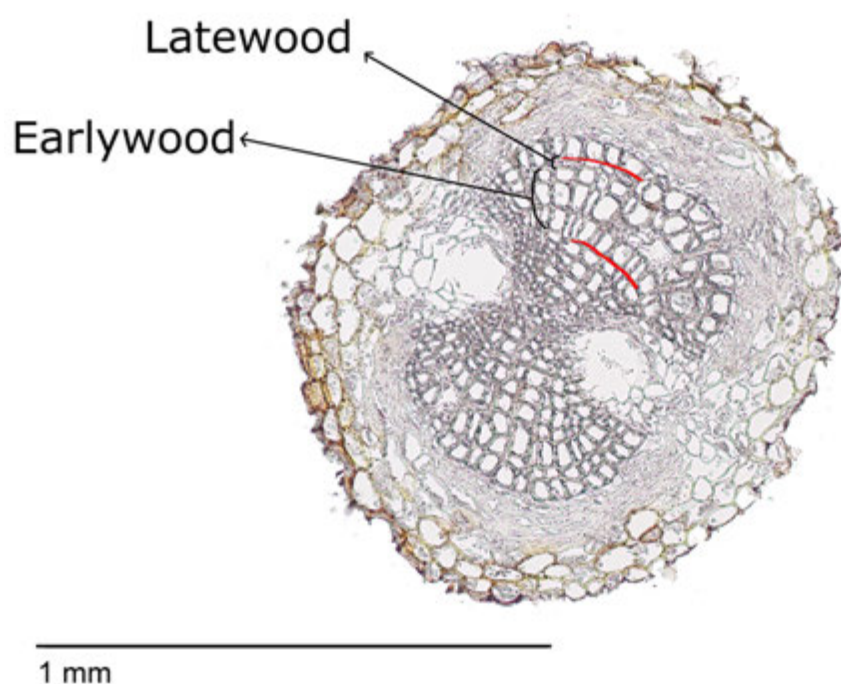


Figure 1. Example of fine root microscopic section of a pine (*Pinus sylvestris* L.) fine root. The earlywood and latewood cells in a yearly growth ring are highlighted.

13.6

Effect of climate change on plant-soil-atmosphere carbon cycling: plant vs. soil organic matter derived CO₂ effluxes

Mirjam S. Studer¹, Beatriz R. Gonzalez Dominguez^{1,2}, Pascal A. Niklaus², Samuel Abiven¹

¹ Department of Geography, Soil Science and Biogeochemistry, University of Zurich, Winterthurerstr. 190, CH-8057 Zurich (mirjam.studer@geo.uzh.ch)

² Institute of Evolutionary Biology and Environmental Studies, University of Zurich, Winterthurerstr. 190, CH-8057 Zurich

The effect of future multifactorial climate change on plant-soil C fluxes and thus on the current carbon (C) stocks is still largely unknown (Kreyling and Beier, 2013). The overall goal of this project, which is part of the Swiss National Research Program 68, is to estimate the drivers of the vulnerability of Swiss soil organic carbon (SOC) stocks to climate change. The vulnerability is defined as the likelihood of a soil to lose its organic carbon due to the influence of external factors. The objective of the experiment presented here was to study the effect of plants on the soil CO₂ efflux under current and future climate in order to identify potential feedback mechanism between climate and the plant-soil C cycle.

The vulnerability of soil organic matter was quantified as the ratio between the soil respiration rate and its C content, whereby a high ratio indicates a high potential vulnerability. We grew poplar plants in two soils with similar SOC content, but different CO₂ efflux rates for five weeks in two climate chambers (described in Studer et al., 2014). We used stable isotope techniques to distinguish the plant-derived from the SOC-derived CO₂ efflux. The plant shoots, which were hermetically sealed from the roots and the soil, were continuously labelled with 10.6 at.% ¹³C-CO₂. The plant soil system were acclimatised at current conditions (22 °C air and soil temperature, 400 ppm CO₂, 34 mm week⁻¹ precipitation, 60 % relative air humidity) for 11 days before we started to simulate in one of the chambers the climate predicted for Switzerland for the period 2070-2100 (+4 °C temperature, +550 ppm CO₂ concentration, -18 % precipitation and -9 % relative air humidity).

The initial results indicate that the total soil CO₂ efflux rate was increased under future climate conditions by 62 and 43 % (+1.1 and +1.4 μmol CO₂ m⁻² s⁻¹), while the plant-derived CO₂ efflux was increased by 95 and 76 % (+0.4 μmol CO₂ m⁻² s⁻¹ in both soils) in the soils with low and high potential vulnerability, respectively. Thus 37 and 29 % of the change in total soil CO₂ efflux was due to a change in plant-C mineralization. This indicates that the plant-soil C fluxes in the soil classified as less vulnerable (low CO₂ efflux/C content ratio) were affected more strongly by climate change, but that the overall quantitative change in the SOM mineralization was still larger in the more vulnerable soil (1.0 vs. 0.7 μmol CO₂ m⁻² s⁻¹) that is characterized by a high mineralization rate compared to the C content under the current climate conditions.

The preliminary conclusions of this experiment are that future climate will have a massive effect on the plant-soil C fluxes and thus endanger the current Swiss SOC stocks. Upcoming sample and data analysis will focus on the question if the plant is a major driver of the soil organic matter vulnerability due to rhizosphere priming effect.

REFERENCES

- Kreyling, J. and Beier, C. 2013: Complexity in Climate Change Manipulation Experiments, *Bioscience*, 63, 763–767.
 Studer, M. S., Siegwolf, R. T. W. and Abiven, S. 2014: Carbon transfer, partitioning and residence time in the plant-soil system: a comparison of two ¹³CO₂ labelling techniques, *Biogeosciences*, 11, 1637–1648.

13.7

Insights into soil organic matter stability using temporal, fraction- and compound-specific radiocarbon analysis

Tessa S. van der Voort¹, Claudia Zell¹, Cameron McIntyre^{1,2}, Frank Hagedorn³, Lorena Fisher¹, Timothy Eglinton¹

¹ *Institute of Geology, ETH Zürich, Sonneggstrasse 5, 8092 Zürich, Switzerland*

² *Department of Physics, Laboratory of Ion Beam Physics, ETH Zurich, Schaffmatstrasse 20, 9083 Zurich*

³ *Forest soils and Biogeochemistry, Swiss Federal Research Institute WSL, Zürcherstrasse 111, 8903 Birmensdorf, Switzerland*

Understanding controls on the stability of soil organic matter (SOM) has garnered attention in recent years in the context of its vulnerability to, and role in climate change, as well as its importance in soil function. Radiocarbon has proven to be a powerful tool for assessing SOM dynamics and is increasingly used in studies of carbon turnover. However, soil heterogeneity and complex underlying processes render it challenging to determine dynamics of different carbon pools from single time-point bulk radiocarbon signals alone. This project aims to improve the understanding of processes that influence SOM stability and vulnerability over time on a bulk level as well as on a carbon-pool specific level. This is done by investigating the change in bulk radiocarbon signature in soils over time as well as measuring the abundance and radiocarbon signatures of density fractions (free light fraction, occluded light fraction, heavy fraction) and molecular markers of vascular plant and microbial organic matter (lignin, plant waxes, glycerol dialkyl glycerol tetraethers). Our goal is to examine the turnover and fate of these specific biologically-derived components and to evaluate their utility as tracers of carbon flow and turnover within soils. We focus on soil profiles from specific well-studied sites that form part of the Long-Term Forest Ecosystem Research (LWF) program of the Swiss Federal Institute for Forest, Snow and Landscape research (WSL).

Preliminary results reveal marked soil-dependant changes in radiocarbon signature over time as well as strong variations in the abundance and radiocarbon age of different molecular markers as a function of both soil type and depth. Radiocarbon age relationships between specific markers and density fractions imply both distinct and evolving modes of association within the soil matrix. Ultimately, data emanating from this combined compound- and fraction-specific approach may serve to improve carbon turnover models by constraining the size and age of different SOM pools, enhancing our ability to assess SOM stability and to predict vulnerability to change.

P 13.1

Conversation tillage and sustainable intensification of agriculture: regional vs. global benefits analysis

Nikolaus J. Kuhn¹, Yaxian Hu¹, Lena Bloemertz¹, Liangang Xiao¹, Jin He², Hongwen Li² & Philip Greenwood¹

¹ *Physical Geography and Environmental Change Research Group, University of Basel, Klingelbergstrasse 27, CH-4056 Basel (nikolaus.kuhn@unibas.ch)*

² *Conservation Tillage Research Center, China Agricultural University, Qinghua East Road 17, Beijing 100083, China*

Climate change is expected to affect both the amount of global crop production, and annual variability in food supply. Agriculture is a major source of greenhouse gas emissions, but also considered to mitigate climate change. Conservation tillage, as a climate-smart agricultural practice, is repeatedly reported to mitigate net greenhouse gas emissions by increasing soil organic carbon (SOC). However, with reduced tillage, less litter is moved from the surface deeper into the soil profile, so SOC increase is very likely constrained to topsoil layers. Further adaptation benefits, such as increasing crop yield and resilience to famine, have recently been questioned after averaging yields from field studies. However, such global averaging masks the geographic extent individual studies apply to. This paper attempts a holistic regional analysis on the benefits of conservation tillage, in particular its fundamental principle no-tillage (NT), on the Chinese Loess Plateau. Based on a review of almost 20 years of conservation tillage plot experiments, the potential of NT to increase SOC stock and to adapt to lower but more variable rainfall in the future has been assessed. The results show that the difference of total SOC stocks between NT and CT decreased with soil depth, confirming that the SOC benefits of NT are concentrated to the immediate topsoil still subject to direct seeding. The topsoil achieved maximum SOC stocks after about 10 years of NT. Crop yields, on the other hand, increased by up to 20% for years with average and below average precipitation. In addition, the misrepresentation of study locations in previous report suggests that as a result of global averaging, the negative results of NT in SOC stock increase from the under-represented humid regions outweighed the positive effects from the over-represented drylands. Therefore, given the size of the Loess Plateau and its relevance for food security in China, our analysis illustrates the need to assess the benefits of a tillage pattern for each combination of eco-region and farming system, weighed by their area and the affected population, rather than just using a global average for policy development on sustainable productivity.

P 13.2

Losses of organic carbon from Swiss forest soils in relation to climate, soil properties and landscape characteristics

Beatriz R. González Domínguez^{1, 2}, Studer Mirjam S.¹, Pascal A. Niklaus² & Samuel Abiven¹

¹ *Department of Geography, University of Zurich, CH-8057 Zurich, Switzerland.*

² *Institute of Evolutionary Biology and Environmental Studies, University of Zurich, CH-8057 Zurich, Switzerland.*

In a changing climate, the mineralization of previously stabilized organic carbon can become one of the largest feedbacks from terrestrial ecosystems to the atmosphere (Lal, 2004). For this reason, it is of interest to understand the vulnerability of this carbon in relation to drivers. In this study, soil organic matter (SOM) vulnerability is defined as the likelihood of a soil to lose its organic carbon due to the influence of external factors. In this study, SOM vulnerability is quantified as the ratio between the respiration and the organic carbon content of the soil.

The objective of this study is twofold: firstly, to develop a robust statistical approach to allow the investigation of SOM vulnerability at large scales and, secondly, to determine whether climate, soil properties and/or terrain characteristics are driving the vulnerability of organic matter of Swiss forest soils.

The hypothesis of this research is that the main variables driving SOM vulnerability are climate (i.e. temperature and soil moisture proxy), soil (i.e. pH and % clay) and terrain (i.e. slope and aspect). Based on this hypothesis, 54 study sites, all part of the Swiss Federal Institute for Forest, Snow and Landscape Research (WSL) network, were selected to introduce a balanced combination of the variables and to enable a powerful hypothesis testing. To accomplish this, first we spread all sites from the WSL database according to their climatic data during the period 1981-2010. Then, we spread these sites spatially by incorporating the productive regions of Switzerland (Schwaab et al., 2015). Finally, we carried out a principal coordinates analysis with soil and terrain data before selecting the sites that were going to be part of the study.

Three non-overlapping topsoil (i.e. 20 cm) composites were collected within 40 x 40 m² plots at the 54 sites selected. Soils were sieved at 2 mm and incubated in the lab for 6 months under aerobic and controlled conditions of moisture and temperature (25 °C). Carbon vulnerability was investigated by quantifying heterotrophic respiration and soil water extractable organic carbon.

The first results from the regression analysis show a systematic influence of the drivers investigated on SOM vulnerability. Unexpectedly, soil properties play a more significant role than terrain characteristics and even climate.

A systematic influence of drivers on SOM vulnerability leaves a door open to produce predictive tools/models for regional scales. These tools could assist in the assessment of the risk of soils becoming increasing net sources of CO₂ into the atmosphere.

REFERENCES

- Lal R. 2004. Soil carbon sequestration impacts on global climate change and food security. *Science* (New York, N.Y.) 304: 1623–1627.
- Schwaab J, Bavay M, Davin E, Hagedorn F, Hüsler F, Lehning M, Schneebeli M, Thürig E, Bebi P. 2015. Carbon storage versus albedo change: Radiative Forcing of forest expansion in temperate mountainous regions of Switzerland. *Biogeosciences* 12: 467–487.

P 13.3

Soil quality indicators of urban gardens in Zurich

Simon Tresch^{1, 3}, Andreas Fliessbach¹, Marco Moretti² & Claire Le Bayon³

¹ *Department of Soil Sciences, Research Institute of Organic Agriculture (FiBL (simon.tresch@fibl.org))*

² *Biodiversity and Conservation Biology, Swiss Federal Research Institute WSL)*

³ *Functional Ecology Laboratory, Institute of Biology, University of Neuchâtel*

For the first time in human history the majority of people lives in urban areas. It is vital to understand urban ecology because urban ecosystems provide important ecosystem services like (i) supporting services (e.g. nutrient cycling, decomposition of organic matter, water cycling), (ii) regulating services (air quality, climate regulation, natural hazard regulation) & (iii) provisioning service (e.g. food, fibre, pollination, fresh water, fertile soils). Urban gardens provide a great part of the green space in urban areas in many countries and are therefore essential for their functioning. However, soil quality in an urban context is poorly investigated.

This study is part of an interdisciplinary project called “Strategies for Better Gardens: Integrated Analysis of Soil Quality, Biodiversity and Social Value of Urban Gardens” (www.bettergardens.ch). Four research groups, two from the Swiss Federal Research Institute WSL and two from the Research Institute of Organic Agriculture (FiBL) are collaborating closely to analyse the economy, sociology, above ground biodiversity and soil quality in urban gardens. New strategies to preserve urban green spaces and to safeguard the soils underneath have to include ecosystem services and respect soil functions (such as filter, absorption, decomposition) that help to build and conserve above and below ground life in the cities.

As a first step, soil quality indicators of 80 private and allotment gardens in the city of Zurich will be analysed in situ and under controlled conditions. In situ measures comprise penetration resistance and decomposition of plant material in litterbags and a standardised tea bag approach. Important soil biological indicators like microbial biomass (Cmic, Nmic) and a multi-substrate respiration method (MicroResp), for developing a community level physiological profile of soil microorganisms, will be established. Together with relevant chemical and physical soil properties soil quality can be compared. Statistical correlation of the measured soil quality indicators, vegetation and soil fauna parameters will build the basement for further functional decomposition experiments on a selected sub-group of gardens. Established ecosystem services like nutrient cycling and comminution of organic material and their link to the multiple ecological and social functions of urban gardens will be taken into consideration to provide a comprehensive synthesis showing the interdisciplinary research in the multi-stakeholder environment of the cities.

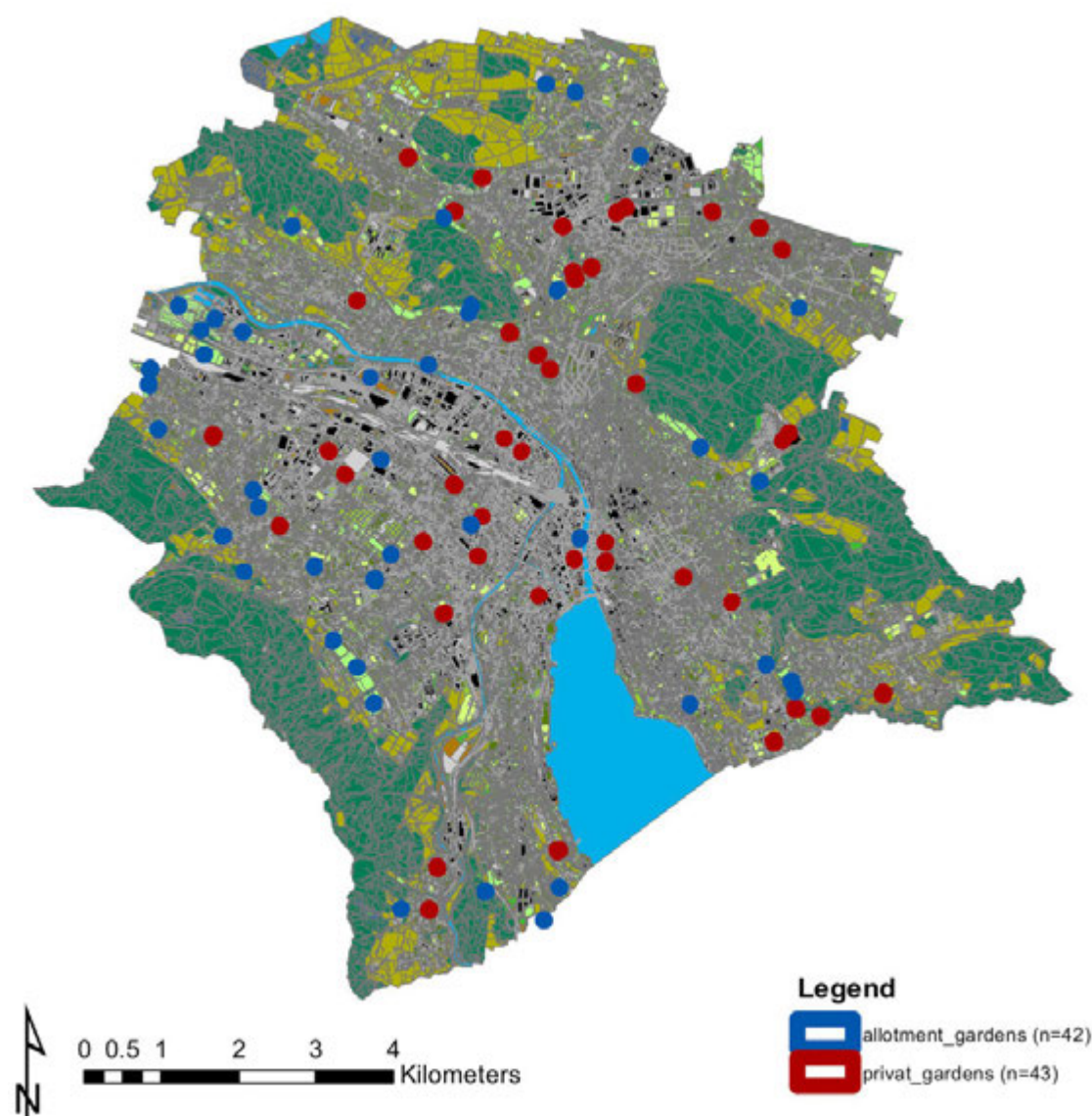


Figure 1. Research plots located in the urban area of Zurich (n=85).

REFERENCES

- Millennium Ecosystem Assessment. 2005: Ecosystems and Human Well-being: Biodiversity Synthesis. World Resources Institute, Washington, DC.
- Lin B.B., Philpott S.M. & Jha S. 2015: The future of urban agriculture and biodiversity-ecosystem services: Challenges and next steps. *Basic and applied ecology*, 16, 189-201.
- Keuskamp J. A., Bas J J Dingemans, Lehtinen T., Sarneel J. M. & Hefting M.M. 2013: Tea Bag Index: A Novel Approach to Collect Uniform Decomposition Data across Ecosystems. *Methods in Ecology and Evolution*, 4, 1070–75.
- Campbell C. D., Chapman S. J., Cameron C. M., Davidson M. S. & Potts J.M. 2003: A Rapid Microtiter Plate Method To Measure Carbon Dioxide Evolved from Carbon Substrate Amendments so as To Determine the Physiological Profiles of Soil Microbial Communities by Using Whole Soil. *Applied and Environmental Microbiology*, 69, 3593–99.

14. Biogeochemistry of aquatic and terrestrial realms

Helge Niemann, Jakob Zopfi, Moritz Lehmann, Franz Conen,
Katrin Meusburger, Christine Alewell

TALKS:

- 14.1 Auderset A., Martinez-Garcia A., Haug G., Eglinton T., Tiedemann R.: Early Pliocene Sea Surface Temperature Reconstruction in the North Atlantic
- 14.2 Bigalke M., Kusonwiriawong C., Abgottspon F., Wilcke W.: Fate of Cu in flooded soils: a stable isotope approach
- 14.3 Birkholz A., Meusburger K., Schindler Wildhaber Y., Mabit L., Alewell C.: Apportionment of sediment sources in a small river of the Swiss plateau using CSIA of plant wax lipids
- 14.4 Huang J.-H., Jia B., Tang Y., Tian L., Franz L., Alewell C.: Impact of Fish Farming on Phosphorus in Reservoir Sediments
- 14.5 Le Faucheur S., Freiburghaus A., Dranguet P., Slaveykova V.I.: Mercury impacts towards periphyton
- 14.6 Lehmann M.F., Simona M., Wyss S., Blees J., Frame C.H., Niemann H., Veronesi M., Zopfi, J.: Powering up the "bio-geochemical engine": The impact of exceptional mixing events on fixed-nitrogen and methane turnover in a deep meromictic lake
- 14.7 Morlock, M., Vogel, H., Nigg, V., Russell, J.M., Bijaksana, S. & the TDP science team: Erosion intensity and element cycling under changing hydroclimatic conditions during the past ~60 kyr BP in the catchment of tropical Lake Towuti, Indonesia
- 14.8 Müller B.: Interaction between the Bacterium *Pseudomonas fluorescens* strain CHA0, its genetic derivatives and vermiculite: Effects on chemical, mineralogical and mechanical properties of vermiculite
- 14.9 Nelson D.B., Kahmen A.: Exploring the links between plant waters and leaf wax isotopes from a European sample network
- 14.10 Spangenberg J.E., Schweizer M., Zufferey V.: Molecular and isotopic changes in leaf lipids of plants living under abiotic stress conditions – implications for organic geochemical proxies
- 14.11 Steinle L., Maltby J., Engbersen N., Zopfi J., Bange H., Kock A., Lehmann M., Treude T., Niemann H.: Environmental controls on aerobic methane oxidation in coastal waters (SW-Baltic Sea)
- 14.12 Weber Y., Sinninghe Damsté J.S., Schubert C.J., Gilli A., Lehmann M.F., Niemann H.: Potential and constraints of lipid-based paleo-thermometry in lake sediments: New insights on the sources of branched GDGTs
- 14.13 Wigganhauser M., Wilcke W., Bigalke M., Imseng M., Müller M., Rehkämper M., Murphy K., Kreissig K., Frossard E.: Isotopic fractionation of Cd in agricultural soil-plant systems

POSTERS:

- P 14.1 Schomburg A., Guenat C., Brunner P., Verrecchia E. P., Le Bayon R.-C.: Applicability of Rock-Eval pyrolysis to quantify ecosystem engineers' impact on soil structure formation in a carbonate-rich pre-alpine floodplain
- P 14.2 Stern B., Giglio E., Vogel H., Anselmetti F., Lovas R., Niemann H., Lehmann M. F.: Eutrophication and re-oligotrophication of Lake Sempach over the last 150 years: Assessing the impact on calcium carbonate nucleation and redox-sensitive metals in the sediments
- P 14.3 Naeher S., Huguet A., Roose-Amsaleg C.L., Laverman A.M., Fosse C., Lehmann M.F., Derenne S., Zopfi J.: Geochemical constraints on anaerobic ammonium oxidation (anammox) in a riparian zone of the Seine Estuary
- P 14.4 Su G., Niemann H., Zopfi J., Lehmann M.F.: Potential role of nitrate, iron and manganese reduction during anaerobic methane oxidation in lacustrine sediments
- P 14.5 Moinecourt C., Dranguet P., Zonta R., Slaveykova V.I., Le Faucheur S.: Response of periphyton communities to metals, including Hg, in the lagoon of Venice.
- P 14.6 Richner D., Niemann H., Steinle L., von Deimling J.S., Urban P., Hoffmann J., Schmidt M., Treude T., Lehmann M.F.: Short-term variations of methane and methanotrophic activity in a coastal inlet (Eckernförde Bay, Germany)
- P 14.7 Blattmann T., Wen K., Li J., Zhao Y., Zhang Y., Wacker L., Michael Plötze., Liu Z., Eglinton T.: Tracing Pathways of Organic Matter Transport in the Modern South China Sea
- P 14.8 Nigg V., Vogel H., Morlock M., Anselmetti F., Russell J.M., Bijaksana, S.: Understanding grain-size effects on element geochemistry and mineralogy in sedimentary records from Lake Towuti, Sulawesi, Indonesia
- P 14.9 Ladd S.N., Dubois N., Schubert C.: Sedimentary abundance and isotopic composition of algal lipid biomarkers in lakes of variable Phosphorous concentration in central Switzerland
- P 14.10 Freymond C.V., Kündig N., Peterse F., Buggle B., Giosan L., Filip F., Eglinton T.I.: From source to sink – biomarker transport along the Danube River
- P 14.11 Tischer J., Zopfi J., Frame C.H., Lehmann M.F.: Nitrogen cycling and N₂O production in the water column of the ferruginous meromictic Lake La Cruz (Spain)
- P 14.12 Ley M., Lehmann M., Niklaus P., Frey B., Kuhn Th., Luster J.: Microhabitat effects on N₂O emissions from floodplain soils under controlled conditions
- P 14.13 Kalvelage T., Normandeau C., Li W., Wallace D.W.R.: A time series of nitrogen speciation and nitrogen isotope fractionation during nitrification in a eutrophic coastal embayment
- P 14.14 Frame C., Lau E., Nolan J., Goepfert T., Lehmann M.F.: Acidification enhances N₂O production by aquatic ammonia oxidizing microorganisms
- P 14.15 Cojean A., Zopfi J., Robertson E., Thamdrup B., Lehmann M.F.: Estimation of O₂ influence on benthic nitrogen cycling in the south basin of Lake Lugano, Switzerland

14.1

Early Pliocene Sea Surface Temperature Reconstruction in the North Atlantic

Alexandra Auderset¹, Alfredo Martinez-Garcia¹, Gerald Haug¹, Timothy Eglinton¹ & Ralf Tiedemann²

¹ *Geological Institute, ETH Zürich, Sonneggstrasse 5, CH-8092 Zürich (audersea@student.ethz.ch)*

² *Marine Geology and Paleontology, Alfred Wegener Institute, Am Alten Hafen 26, D-27568 Bremerhaven*

Several recent studies examine in the final closure of the Central American Gateway (CAG), approximately 4.6 Ma ago, and discuss the resulting change in ocean circulation and its influence on global climate. Paleooceanographic models suggest this event strengthened northward heat and salt transport via the Gulf Stream, which is considered one of the prerequisites for ice sheet growth in the Northern Hemisphere. Corresponding intensification of the Atlantic Meridional Overturning Circulation (AMOC) has been confirmed based on deep sea (benthic) records (Haug and Tiedemann, 1998), however reconstructions of changes in sea surface temperature (SST) remain equivocal.

Here we present new records of SST change in the early Pliocene (5.3 - 3.9 Ma) in the North Atlantic using $U_{37}^{K'}$ ratio of C_{37} alkenones synthesized by unicellular algae (Haptophyta) and TEX_{86} based on C_{86} glycerol dialkyl glycerol tetraethers (GDGTs) derived from planktonic archaea.

Measurements indicate that the timing of the closure of the CAG coincides with an increase in SST as recorded in GDGTs signatures (Figure 1), and that this warming of the North Atlantic is accompanied by an increase in salinity that is reflected in reconstructed $\delta^{18}O$ values for seawater. Attendant changes in continental vegetation type in North America, linked to an increase in moisture transport, is also inferred from a decrease in average chain length of terrestrial plant wax-derived *n*-alkanes.

SST changes recorded by $U_{37}^{K'}$ values reflect the progressive intensification of the Northern Hemisphere glaciation during the Early Pliocene, and also imply significant influence of seasonality on this proxy signal. We infer that alkenone production of coccolithophores (and hence corresponding SST values imparted to the sedimentary record), is the highest during late spring when the cold, low-salinity Labrador Current strengthens, and extends to core location DSDP 609 in the North Atlantic, resulting in markedly contrasting proxy signals relative to TEX_{86} .

Overall, this study provides improved insights into the timing and impact of the closure of the CAG on ocean circulation and climate in the Northern Hemisphere. Additionally, it highlights the contrasting signals recorded by two TEX_{86} and $U_{37}^{K'}$ SST proxies, underlining the importance of careful and informed interpretation of these and other signals embedded in sedimentary records.

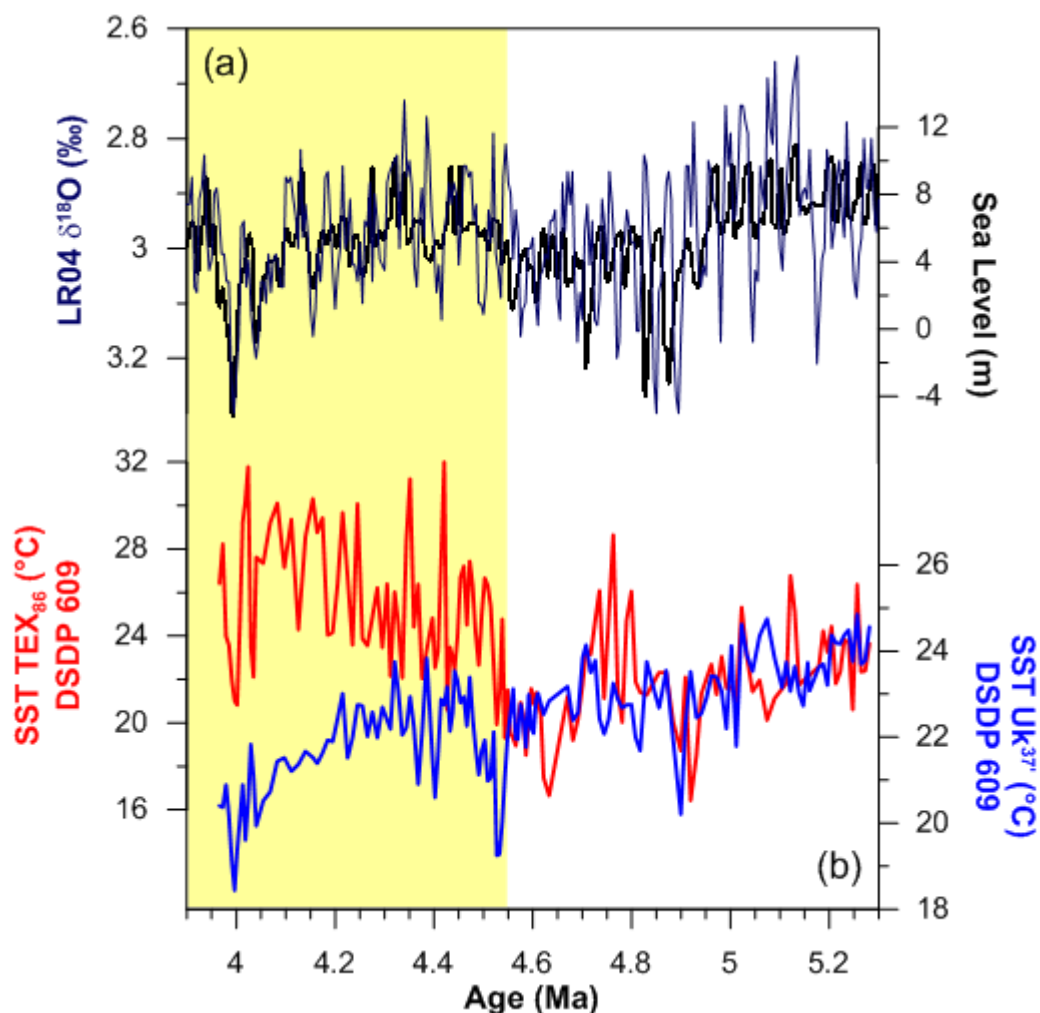


Figure 1. (a) Early Pliocene changes in $\delta^{18}\text{O}$ after Lisiecki and Raymo, 2005 (dark blue line) and relative sea level changes after Rohling et al., 2014 (black line) (b) Sea surface temperatures using TEX₈₆ (red line) and U_{37'}^K (blue line) from Site DSDP 609.

REFERENCES

- Haug, G. H. and Tiedemann, R. (1998). Effect of the formation of the isthmus of panama on atlantic ocean thermohaline circulation. *Nature*, 393(6686):673–676
- Lisiecki, L. E. and Raymo, M. E. (2005). A pliocene-pleistocene stack of 57 globally distributed benthic $\delta^{18}\text{O}$ records. *Paleoceanography*, 20(1).
- Rohling, E. J., et al. „Sea-level and deep-sea-temperature variability over the past 5.3 million years.“ *Nature* 508.7497 (2014): 477-482.

14.2

Fate of Cu in flooded soils: a stable isotope approach

Moritz Bigalke¹, Charirat Kusonwiriawong¹, Florian Abgottspon¹, Wolfgang Wilcke²

¹ *Institute of Geography, University of Bern, Hallerstrasse 12, CH-3012 Bern, (moritz.bigalke@giub.unibe.ch)*

² *Institute of Geography and Geoecology, Karlsruhe Institute of Technology (KIT), Reinhard-Baumeister-Platz 1, D-76131 Karlsruhe.*

Cu is an essential micronutrient for plants, animals and humans but can also be a pollutant if it occurs in high concentrations. Speciation and mobility of Cu in soils is strongly influenced by the redox conditions in soils because Cu can assume redox states between 0 and +2 in soil. If soils get water saturated e.g., by flooding, oxygen supply is inhibited and redox potential decreases, which causes an initial release of Cu (Weber et al., 2009).

We conducted microcosm experiments to study the response of Cu in a calcareous floodplain soil to flooding. We sampled soil water at different times after flooding and separated the colloidal (0.02-10 μm) and dissolved (<0.02 μm) fraction. Redox potential (Eh), pH, concentrations of H_2S , organic and inorganic C, major ions, and metals as well as $\delta^{65}\text{Cu}$ values were determined in the two solution fractions. Furthermore, we determined Cu partitioning in soil with a five-step sequential extraction procedure (F1: NH_4NO_3 -extractable, F2: NaOAc-extractable, F3: NH_4Ox -extractable, F4: hot $\text{H}_2\text{O}_2/\text{NH}_4\text{OAc}$ -extractable, and F5: residual fraction) and also determined Cu concentrations and $\delta^{65}\text{Cu}$ values in each of the five fractions. Cu concentrations in soil solutions showed a peak in metal concentrations 2-6 days after flooding. The Cu release was strongly dominated by the colloidal fraction (>80%; 0.02-10 μm). After 6 days, however, Cu concentrations in solution started to decrease until the end of the experiment on Day 40. The $\delta^{65}\text{Cu}$ values of total Cu in solution first decreased and then increased back to the initial value suggesting equilibration with Cu pools from solid soil after initial release. The fractionation between dissolved and colloidal Cu ($\Delta^{65}\text{Cu}_{\text{dissolved-colloidal}}$) ranged from $-0.26 \pm 0.13\text{‰}$ to $1.57 \pm 0.04\text{‰}$ indicating reduction of colloidal Cu. The temporal course of $\Delta^{65}\text{Cu}_{\text{dissolved-colloidal}}$ indicated that colloidal Cu^{2+} was initially reduced to Cu^+ and Cu^0 and finally immobilized as Cu^+ , probably in the form of Cu_xS .

The partitioning of Cu in the solid soil changed strongly in response to flooding. The Cu concentrations in F1-F3 decreased while they increased in F4-F5. Overall, 73% of the total Cu was redistributed among the five studied fractions. Before flooding, $\delta^{65}\text{Cu}$ values in F1-F4 followed the estimated bonding strengths of Cu in the respective fractions, indicating equilibrium distribution of Cu at the beginning of the experiment (under oxic conditions). The total variation in $\delta^{65}\text{Cu}$ values among F1-F5 changed strongly from $0.83 \pm 0.18\text{‰}$ on Day 0 to a maximum of $2.18 \pm 0.17\text{‰}$ on Day 7. This change indicated the reduction of Cu^{2+} . The strongest variations in $\delta^{65}\text{Cu}$ values occurred in F3 ($0.09 \pm 0.07\text{‰}$ to $1.43 \pm 0.13\text{‰}$) and F4 ($-0.24 \pm 0.07\text{‰}$ to $0.55 \pm 0.07\text{‰}$), while flooding had no or small effects on the $\delta^{65}\text{Cu}$ values of F1, F2 and F5. Our results suggest a direct transfer of Cu from F3 to F4 because both, the Cu concentration changes and changes in $\delta^{65}\text{Cu}$ values were balanced between the two fractions. The responses of Cu partitioning and $\delta^{65}\text{Cu}$ values to flooding are in line with the formation of Cu_xS or other reduced Cu species and reduction of Cu associated to Fe (oxyhydr)oxides and organic matter. Our results fit findings from hydromorphic soils (Bigalke et al., 2010, 2011, 2013) and wetlands (Babcsanyi et al., 2014), where significant shifts towards heavier $\delta^{65}\text{Cu}$ have been reported compared to oxic weathered soils. This shift can be explained by the release and leaching of reduced Cu colloids with light $\delta^{65}\text{Cu}$ values.

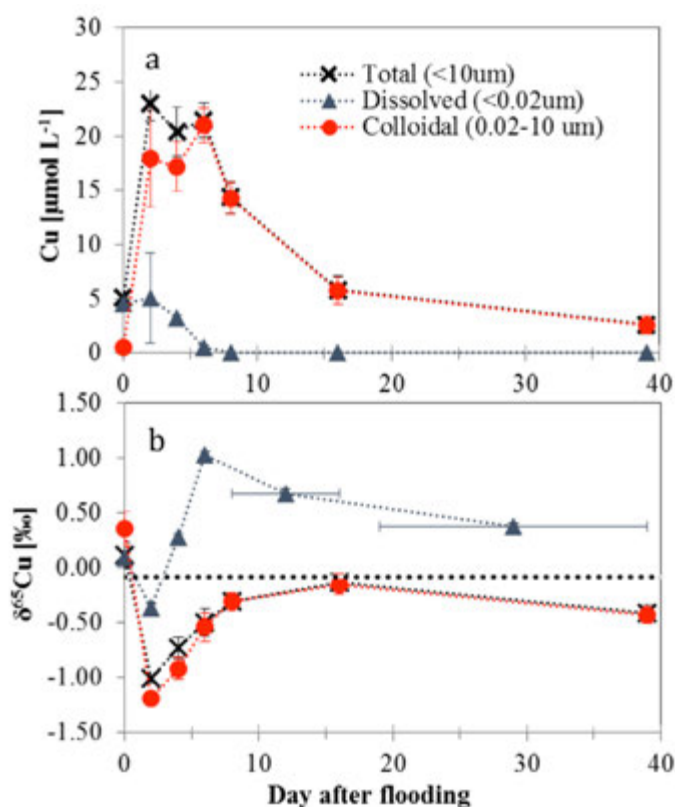


Figure 1: Total, colloidal and dissolved a) Cu concentrations and b) $\delta^{65}\text{Cu}$ values in the soil solution.

REFERENCES

- Babcsanyi, I., Imfeld, G., Granet, M., Chabaux, F. 2014. Copper Stable Isotopes To Trace Copper Behavior in Wetland Systems. *Environmental Science & Technology* 48, 5520-5529.
- Bigalke, M., Kersten, M., Weyer, S., Wilcke, W. 2013. Isotopes trace biogeochemistry and sources of Cu and Zn in an intertidal soil. *Soil Sci. Soc. Am. J.* doi:10.2136/sssaj2012.0225.
- Bigalke, M., Weyer, S., Wilcke, W. 2010. Stable Copper Isotopes: A Novel Tool to Trace Copper Behavior in Hydromorphic Soils. *Soil Sci. Soc. Am. J.* 74, 60-73.
- Bigalke, M., Weyer, S., Wilcke, W. 2011. Stable Cu isotope fractionation in soils during oxic weathering and podzolization. *Geochim. Cosmochim. Acta* 75, 3119-3134.
- Weber, F.A., Voegelin, A., Kaegi, R., Kretzschmar, R. 2009. Contaminant mobilization by metallic copper and metal sulphide colloids in flooded soil. *Nat Geosci* 2, 267-271.

14.3

Apportionment of sediment sources in a small river of the Swiss plateau using CSIA of plant wax lipids

Axel Birkholz¹, Katrin Meusburger¹, Yael Schindler Wildhaber², Lionel Mabit³, Christine Alewell¹

¹ Environmental Geosciences, Department Environmental Sciences, University of Basel, Bernoullistrasse 30, CH-4056 Basel (axel.birkholz@unibas.ch)

² Water Quality Section, Federal Office for the Environment FOEN, CH-3063 Ittigen

³ Soil and Water Management and Crop Nutrition Laboratory, FAO/IAEA Agriculture & Biotechnology Laboratories, A-2444 Seibersdorf

The prediction and/or modeling of sediment pathways to freshwater ecosystems is becoming increasingly important for catchment managers, as sediments remain one of the major ecological threats to aquatic biota and hydrosystem sustainability.

The authors have tested a sediment source apportionment approach in a Swiss river using compound specific stable isotope analysis (CSIA). The river Enziwigger is located on the Swiss plateau near Lucerne. $\delta^{13}\text{C}$ signatures of plant waxes – in this study long-chain fatty acids (FA) – of possible sediment sources (i.e. arable land, pasture and forest) were analyzed and compared to the $\delta^{13}\text{C}$ signatures of river suspended sediments (base flow, storm flow) at three different river sampling spots. Using a mixing calculation based on n tracers to differ $n+1$ sources, sediment source contributions have been differentiated. In case a unique analytical solution was not possible, the mixing model software IsoSource was applied. FA concentration was used to calculate the proportional contributions of the different source areas to the sediment yield. This is the first existing investigation of sediment source apportionment using CSIA based only on the difference between C3 vegetation cover.

As an outlook, the authors would like to present as well the concept of a planned study at the hypertrophic Swiss lake Baldeggersee. Diffuse pollution from agricultural practices and livestock breeding is the main origin of this hypertrophic status. The catchment setup will be used as an application-oriented example to further explore the potential of using compound specific stable isotope (CSSI) technique as catchment management tool.

14.4

Impact of Fish Farming on Phosphorus in Reservoir Sediments

Jen-How Huang¹, Binyang Jia², Ya Tang³, Liyan Tian¹, Leander Franz⁴, and Christine Alewell¹

¹ *Department of Environmental Sciences, University of Basel, Bernoullistrasse 30, CH-4056 Basel, Switzerland (jen-how.huang@unibas.ch)*

² *Chengdu Academy of Environmental Sciences, Chengdu 610072, People's Republic China.*

³ *College of Architecture and Environment, Sichuan University, Chengdu 610065, People's Republic China.*

⁴ *Mineralogy and Petrography, University of Basel, CH-4056 Basel, Switzerland*

Global aquaculture production has grown at an average rate of 8.8% annually since 1980 and is expected to further increase in the future (FAO 2012). Fish farming in cages is considered to be an intensive or semi-intensive farming technique. The production process releases a large amount of residual food and excreta into the water. The majority of these by-products would become part of the sediments, ultimately leading to long-term accumulation. Fish farming increases not only phosphorus sedimentation but also changes phosphorus speciation e.g., accumulation of Ca-bound phosphorus (Ishii et al. 2008; Uede 2007) and biological activities in sediments e.g., an increment of alkaline phosphatase activity in lake sediments (Zhou et al. 2001). Still, the current understanding about the influence of fish farming in cages on phosphorus mobility and speciation in the sediments is very limited.

Fish farming has seriously influenced the aquatic environment in Sancha reservoir in SW China since 1985 and has been strongly restricted since 2005. Thus, phosphorus speciation using sequential extraction in a sediment core dated between 1945 and 2010 at cm-resolution and in surface sediments from Sancha reservoir may allow us track how fish farming impacts phosphorus dynamics in lake sediments. Additionally, the mineral composition of sediments, fish feed and water-purification reagents, the most important additives of fish farming, were analysed using laser particle analyzer, XRD, FT-IR and Raman spectroscopy. Batch experiments were performed to quantify phosphate adsorption behaviour to sediments at different depths, fish feed and water-purification reagents and the release kinetics of P from fish feed.

Fish farming shifts the major binding forms of phosphorus in sediments from organic to residual phosphorus, which mostly originated from fish feed. Sorption to metal oxides and association with organic matters are important mechanisms for phosphorus immobilisation with low fish farming activities, whereas calcium-bound phosphorus had an essential contribution to sediment phosphorus increases under intensive fish farming. Notwithstanding the shifting, the aforementioned phosphorus fractions are usually inert in the lake environment, therefore changing phosphorus mobility little. The use of fish feed and water-purification reagents, the most important additives for fish farming, introduce not only phosphorus but also large amounts of sand-sized minerals such as quartz into the lake, to which phosphorus weakly sorbs. The sand-sized minerals as additional sorbents increase the pool of easily mobilisable phosphorus in sediments, which will slow down the recovery of reservoir water due to its rapid re-mobilisation.

REFERENCES

- FAO. 2012: The state of world fisheries and aquaculture. In F. a. A. D. Food and Agriculture Organisation of the United Nations (Ed.), (pp. 209). Rome.
- Ishii, Y., Komatsu, N., Harigae, S., Yabe, T., Watanabe, K., Negishi, M., & Iwasaki, J. 2008: Characteristics of fractional phosphorus distribution in sediment of fish farming area at Lake Kasumigaura, Japan. *Nippon Suisan Gakkaishi*, 74, 607-614.
- Uede, T. 2007: Chemical characteristics and forms of phosphorus compounds in sediment of fish farming areas. *Nippon Suisan Gakkaishi*, 73, 62-68.
- Zhou, Y., Li, J., Fu, Y., & Zhang, M. 2001: Kinetics of alkaline phosphatase in lake sediment associated with cage culture of *Oreochromis niloticus*. *Aquaculture*, 203, 23-32.

14.5

Mercury impacts towards periphyton

S  verine Le Faucheur¹, Aline Freiburghaus¹, Perrine Dranguet¹ & Vera I. Slaveykova¹

¹ *University of Geneva, Institute F.-A. Forel, Uni Carl Vogt, 66 Boulevard Carl-Vogt, CH-1211 Gen  ve 4
(severine.lefaucheur@unige.ch)*

Periphyton are communities of microorganisms, which colonize hard substrata (rock, plant, sediment etc.) in natural waters. They are known to be involved in the biogeochemical cycle of major elements (C, N, P) and trace metals including mercury (Hg). Indeed Hg can experiment several transformations following its accumulation by periphyton such as methylation and reduction of its inorganic form (Hg^{II}) or demethylation of its methylated species (CH₃Hg). All these processes are known to be mostly biologically mediated, suggesting that periphyton composition will be an important driver of Hg transformations. One of the various parameters that would influence periphyton composition is the concentration of Hg itself in their ambient water. The present study thus aimed to assess the impact of Hg towards periphyton composition in relation to their Hg accumulation and their sensitivity to Hg.

To that end, periphyton were colonized in four flow-through microcosms containing Geneva Lake water spiked with 20 pM, 200 pM and 2 nM Hg^{II}. One control microcosm was not contaminated with Hg. After 7 weeks of colonization, periphyton composition was assessed using chlorophyll a content, ash free dry mass (AFDM), microscopic observation with DAPI staining to distinguish between abiotic and biotic fractions as well as with pyrosequencing. Total and non-extractable Hg (i.e. after a cysteine washing step) contents were both analyzed in periphyton. A second set of experiment was additionally performed with the cultivated periphyton, which were further exposed to 2 nM Hg^{II} for 24 h and examined for damage on their membrane permeability using propidium iodide (PI) and cellular oxidative stress using CellRox® green.

Chlorophyll a content decreased from 4.7 ± 0.1 mg/g dw in periphyton grown in control microcosm to 2.9 ± 0.1 mg/g dw in those grown in 2 nM Hg^{II}. In contrast the percentage of AFDM remained similar amongst the treatments (~ 60%), except for the two-fold decrease at 20 pM Hg^{II}. Microscopic analysis evidenced an increase of the biotic fraction upon Hg exposure, whereas a shift in the microbial communities was further revealed with taxonomic analysis, from an algal dominated community (87%) in control periphyton to a bacterial dominated community (69%) in those cultivated into 2 nM Hg^{II}. Total accumulated Hg concentrations increased with increasing Hg concentration in culture media, from 0.33 ± 0.01 nmol/g dw in control periphyton to 18 ± 0.6 nmol/g dw in periphyton grown in 2 nM Hg^{II}. Moreover a large proportion (> 60%) of that accumulated Hg was non-extractable. Finally membrane permeability was observed to be less impacted in periphyton cultivated in Hg compare to those from the control microcosm whereas oxidative stress was found to be the highest in pre-exposed biofilms.

The present study demonstrates the strong influence of Hg on periphyton communities, even at environmentally relevant concentrations, which could further modify its biotransformation in aquatic systems.

14.6

Powering up the “biogeochemical engine”: The impact of exceptional mixing events on fixed-nitrogen and methane turnover in a deep meromictic lake

Lehmann M.F., Simona M., Wyss S., Blee J., Frame C.H., Niemann H., Veronesi M., Zopfi, J.

The Lake Lugano North Basin has been meromictic for several decades, with anoxic waters below 100m depth. Two consecutive cold and windy winters in 2005 and 2006 induced exceptional deep mixing, leading to a transient oxygenation of the whole water column. With the ventilation of deep waters and the oxidation of large quantities of reduced solutes, the lake's total redox-balance turned positive, and the overall hypolimnetic oxygen demand of the lake strongly decreased. The fixed nitrogen (N) inventory was reduced by ~30% (~1000 t). The water-column turnover induced the nitrification of the previously NO_3^- -free deep hypolimnion by oxidation of large amounts of legacy NH_4^+ and by mixing with NO_3^- -rich subsurface water masses. Sediments with a strong denitrifying potential, but NO_3^- -starved for decades, were brought in contact with NO_3^- -replete waters, invigorating benthic denitrification and rapid fixed N loss from the lake in spite of the overall more oxygenated conditions. Similarly, a large microbial aerobic CH_4 oxidation (MOx) potential in the hypolimnion was capitalized upon ventilation of the deep basin. Almost all CH_4 , which had been built up over more than 40 years (~2800 t), was removed from the water column within 30 days. However, boosted MOx could only partly explain the disappearance of the CH_4 . The dominant fraction (75%) of the CH_4 evaded to the atmosphere, through storage flux upon exposure of anoxic CH_4 -rich water to the atmosphere.

14.7

Erosion intensity and element cycling under changing hydroclimatic conditions during the past ~60 kyr BP in the catchment of tropical Lake Towuti, Indonesia

Marina Morlock¹, Hendrik Vogel¹, Valentin Nigg¹, James M. Russell², Satria Bijaksana³ & the TDP science team

¹ *Institute of Geological Sciences and Oeschger Centre for Climate Change Research, University of Bern, 3012 Bern, Switzerland (marina.morlock@geo.unibe.ch)*

² *Department of Geological Sciences, Brown University, Providence, RI 02912*

³ *Faculty of Mining and Petroleum Engineering, Institut Teknologi Bandung, Bandung 40132, Indonesia*

The tropics are a zone of intense chemical weathering, and lateritic weathering horizons can be up to several 10s and even 100s of metres thick. When only considering non-anthropogenic aspects, weathering and erosion rates in the lower latitudes are mainly driven by hydrological factors such as the seasonality and intensity of precipitation, but are also influenced by other factors such as vegetation cover. While there is an extensive body of research on contemporary processes controlling weathering and erosion in the tropics, very little is known about the influence of climatic changes on these processes on glacial-interglacial time-scales. It is expected that varying hydroclimatic conditions lead to changes in the weathering and erosion rates and greatly influence terrestrial element cycling. The direction of change and more quantitative estimates of the rates of changes are, however, widely unknown.

Lake Towuti (560 km² surface area; 203 m max. water depth) is part of the Malili Lake System, a chain of five tectonic lakes in Sulawesi, Indonesia. Embedded in the ultramafic East Sulawesi Ophiolite, the lake is highly ferruginous but poor in sulphur. The lake is among the least productive tropical lakes on Earth (ultraoligotrophic). This provides the floor for exceptional yet interesting biogeochemical cycles and a unique lake fauna. More than 60% of fish and snail species are endemic to the lake. In May-July 2015, sediment drill cores of the entire lacustrine sediment infill have been recovered from Lake Towuti in the course of the ICDP Towuti Drilling Project. Initial lithological data and chronological estimates along with reflection seismic datasets imply uninterrupted lacustrine sedimentation in the past 600,000 years. These new sedimentary records provide the unique opportunity to study changes in element cycling and weathering intensity under changing climatic conditions in a confined tropical catchment over several glacial-interglacial cycles.

Up until to date we examined the geochemical and clay-mineralogical variations in the modern Lake Towuti system as well as in two short sediment piston cores recovered in 2010, which date back 30,000 and 60,000 years, respectively. In order to perform a source-to-sink analysis, we collected catchment-characteristic bedrock samples with profiles of their overlying laterites and 85 samples of surface sediments evenly spread across the lake. We calculated the Chemical Index of Alteration (CIA) as a measure of the degree of chemical weathering. The index is based on the relative accumulation of the less mobile Al_2O_3 relative to more easily soluble Na_2O , K_2O , and $\text{CaO}_{\text{silicate}}$ in a weathered substrate, e.g. bedrock, soil or sediment (Nesbitt & Young 1982).

Preliminary results show that weathering intensity increases from bedrock (mean CIA 6.9 ± 4.0 , least weathered) across river bedload of the 15 inlets (mean CIA 66.9 ± 22.4) to the sediments in the deepest basin of the lake (mean CIA 85.2 ± 2.6 , most weathered). In the past 60,000 years, CIA values are highest between 35,000 and 15,000 yrs BP. Illite was the most abundant clay mineral in marine isotope stage 3 (MIS 3), followed by kaolinite in MIS 2 and smectite in the Holocene (Figure 1). When comparing these datasets to our vegetation ($\delta^{13}\text{C}$ of terrestrial leaf waxes) and runoff (Ti concentrations) proxy time-series (Russell et al. 2014) for the same period we find that more intensely weathered material reached the lake during glacial periods of MIS 2 and 4, which are climatically characterized by reduced runoff and vegetation cover. In contrast, less weathered material reached the lake during phases with increased runoff and a dense, closed canopy rainforest vegetation. This points towards a more surficial erosion primarily delivering weathered substrates during dry glacial phases and deeper erosion and mobilization of less weathered substrates during wet interglacial phases. These findings imply that erosion and element cycling are mainly driven by changes in precipitation amount and terrestrial runoff in Towuti's catchment.

Additional, on-going geochemical and clay-mineralogical analysis on samples collected from weathering/laterite profiles will help to better quantify the depth of incision and to draw conclusions about the weathering intensity under different hydroclimatic conditions in the past ~600,000 years.

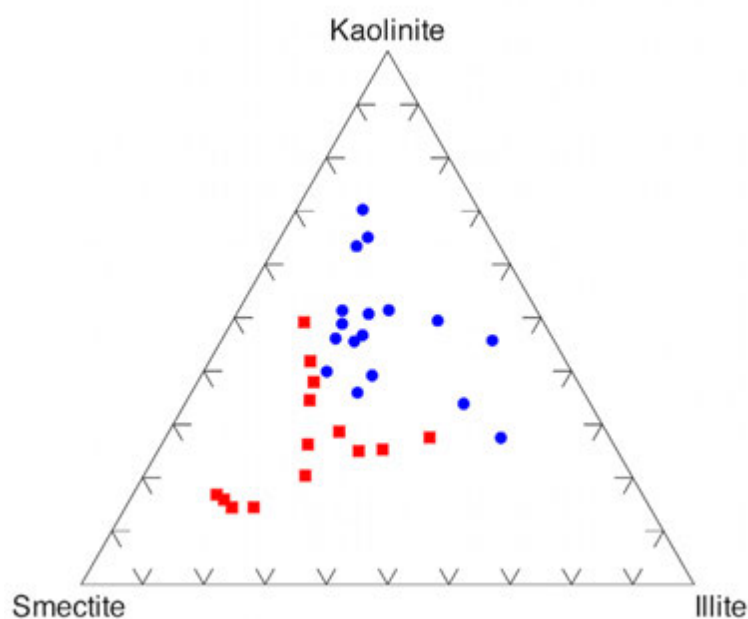


Figure 1. Clay mineral distribution in the two sediment cores for the past 30,000 years. Blue circles indicate samples from the last glacial (15,000-30,000 yrs BP) while red squares indicate samples younger than 15,000 years BP.

REFERENCES

- Nesbitt, H.W. & Young, G.M. 1982: Early Proterozoic climates and plate motions inferred from major element chemistry of laterites, *Nature*, 299, 715-717.
- Russell, J.M., Vogel, H., Konecky, B.L., Bijaksana, S., Huang, Y., Melles, M., Wattrus, N., Costa, K. & King, J.W. 2014: Glacial forcing of central Indonesian hydroclimate since 60,000 y BP, *PNAS*, 111, 5100-5105.

14.8

Interaction between the Bacterium *Pseudomonas fluorescens* strain CHA0, its genetic derivatives and vermiculite: Effects on chemical, mineralogical and mechanical properties of vermiculite

Barbara Müller

Universität Basel, 4056 Basel

email: bar.mueller@unibas.ch

Using bacteria of the strain *Pseudomonas fluorescens* wild type CHA0 and its genetic derivative strains CHA77, CHA89, CHA400, CHA631 and CHA661 (which differ in one gene only) the changes in chemical, mineralogical and rheological properties of the clay mineral vermiculite affected by microbial activity were studied in order to test whether the individually different production of metabolites by the genetically engineered strains may alter the clay mineral vermiculite in distinct ways. With the novel strategy of working with living wild type bacteria, their genetic derivatives and clay, the following properties of the mineral altered by the various strains of *Pseudomonas fluorescens* were determined: grain size, X-Ray diffraction pattern, intercrystalline swelling with glycerol, layer charge, CEC, BET surface and uptake of trace elements. Laser ablation inductively coupled plasma mass spectrometry (LA-ICP-MS) was used to determine the changes in major, minor and trace elements of the clay vermiculite affected by microbial activity. Among all analyzed trace elements, Fe, Mn and Cu are the most interesting. Fe and Mn are taken up from the clay mineral by all bacterial strains whereas Cu is only removed from vermiculite by strains CHA0, CHA77, CHA400 and CHA661. The latter mentioned strains all produce the antibiotics 2,4-diacetylphloroglucinol and monoacetylphloroglucinol which can complex Cu efficiently. Therefore the alteration of only one gene of the bacteria is causing significant effects on the clay mineral.

14.9

Exploring the links between plant waters and leaf wax isotopes from a European sample network

Daniel B. Nelson¹ & Ansgar Kahmen¹

¹ *Department of Environmental Sciences - Botany, University of Basel, Schönbeinstrasse 6, CH-4056 Basel
(daniel.nelson@unibas.ch)*

Applications of sedimentary plant wax $^2\text{H}/^1\text{H}$ values as a climate proxy is predicated on an empirical relationship with mean annual precipitation isotope values. Efforts towards mechanistic understanding of the processes by which plants take up water and modify its $^2\text{H}/^1\text{H}$ composition before preserving the signal in the leaf cuticle have indicated varying levels of importance for the effects of leaf water enrichment through transpiration, the timing of leaf wax synthesis, and the influence of species/phenotype/plant functional type. In many cases the magnitude of these effects has been demonstrated to be much larger than potential changes in the precipitation isotope signal targeted for reconstruction. These observations cast doubts on the fidelity of the climate signal preserved in sedimentary leaf wax $^2\text{H}/^1\text{H}$ values, yet, despite these concerns, seemingly viable climate records that corroborate results from independent proxies have been produced from these data.

We address the disconnect between individual plant and ecosystem-integrated sedimentary $^2\text{H}/^1\text{H}$ values through a two-season-long sampling campaign (2014 and 2015) encompassing more than 20 sites over the European continent. We measured precipitation, soil, xylem, and leaf water isotope values at each site at approximately 5-week intervals over each growing season, and used these data along with meteorological data from co-located eddy covariance flux towers to calculate continuous leaf water isotope values using a mechanistic leaf water model. By assessing the source water pools in detail, we investigate the role for modification of this signal up to the point directly preceding biosynthesis at a spatial scale that is relevant for gridded climate data sets. We also measured leaf, end of season leaf litter, and A-horizon soil leaf wax $^2\text{H}/^1\text{H}$ values in each season to assess the individual, season integrated, and long term integrated hydrogen isotope signal at each site.

Our results confirm clear differences in the importance of leaf water enrichment for monocots and dicots. For trees we find that the highest correlation coefficient between summer xylem water monthly mean precipitation isotope climatology occurs in December. From these observations, and the measured leaf wax $^2\text{H}/^1\text{H}$ ratios at each site we calculate continental scale predictions for plant water and plant wax $^2\text{H}/^1\text{H}$ values that can be visualized in maps of the spatial isotope distributions as isoscapes. At this scale, coherent signals emerge that help to link the water isotope signal in plants with the ecosystem-integrated signal in sediments.

14.10

Molecular and isotopic changes in leaf lipids of plants living under abiotic stress conditions – implications for organic geochemical proxies

Jorge E. Spangenberg¹, Marc Schweizer¹ & Vivian Zufferey²

¹ *Institute of Earth Surface Dynamics IDYST, University of Lausanne, Géopolis, CH-1015 Lausanne
(jorge.spangenberg@unil.ch)*

² *Agroscope, Institute of plant production sciences IPV, Pully, CH-1009 Pully*

The understanding of the molecular (e.g. distribution of *n*-alkanoic and *n*-alkanes) and isotopic ($\delta^{13}\text{C}$ and $\delta^2\text{H}$ values) response of leaf lipids to environmental stresses is of prime relevance for the correct interpretation of organic geochemical paleo-proxies based on terrestrial plant biomarkers.

In the today's rapidly changing environment plants are exposed to various abiotic stresses including drought, high or low temperatures, freezing, strong winds, high salinity, nutrient imbalance, radiation damage, oxidative stress, oxygen deficiency, high soil CO_2 concentrations (acidification), and metal toxicity. As plants cannot escape from the surrounding conditions, they must adapt to them by a series of physiological/molecular responses. Variations in the chemistry,

mobilization and deposition of extracellular lipids (epicuticular waxes) seem to module the response of plants to stress, particularly to drought (Cameron et al., 2006). The epicuticular waxes consist predominantly of homologous series of long-chain *n*-alkanes, *n*-alkan-1-ols, *n*-alkanoic acids, esters, aldehydes, secondary alkanols, ketones, and cyclic compounds. Among these plant biomarkers, *n*-alkanes, *n*-alkan-1-ols and *n*-alkanoic acids distribution and their isotopic composition ($\delta^{13}\text{C}$ and $\delta^2\text{H}$ values) are the most utilized to trace vascular-plant derived biomass in modern and fossil soils, sediments and sedimentary rocks.

In this work, we investigate the changes in the major chemistry of epicuticular waxes from leaves during development of a single plant species exposed to drought controlled by monitoring the soil water status and leaving all the other key environmental variables (such as soil type, temperature, CO_2 concentration, light, radiation, canopy management) constant. Several irrigation treatments have been conducted in Leytron (Agroscope-IPV experimental station) since 2004 on an homogeneous plantation of field-grown grapevine (*Vitis vinifera* L.): cultivars of white grape Chasselas and red grape Pinot noir. Three soil water status conditions were set as follows: drip irrigation (9 L/m²/week), no irrigation and no irrigation with waterproof non-reflecting plastic cover on soil in order to eliminate the infiltration of water from precipitation events during summer (maximizes plant evapotranspiration). The local natural soil was the only source of nutrients for the plants. Estimates of the plant water stress were obtained from different field and laboratory measurements (e.g., shoot growth rate, relative water content, leaf-stem water potential, stomatal and hydraulic conductance, leaf-canopy temperature, xylem sapflow, and $\delta^{13}\text{C}$ values of the berry sugar). The sugar $\delta^{13}\text{C}$ values in must at harvest of Chasselas varied from -27.6 to -22.5‰ during ten growing seasons (2003 to 2012) with different water conditions. These results motivated a study on possible similar response of the epicuticular waxes.

During the 2014 growing season leaves of Chasselas and Pinot Noir were collected (in triplicate) monthly during the growing season (plant/leaf development stages between June and September) in different successive zones (heights, different age) in the shoot (basal, median and apical) and three water-stress conditions. Only leaves showing no signs of damage, apparent alteration or surface debris were suitable for the analysis of epicuticular wax lipids. The sample set includes a total of 60 leaves for each plant variety (Chasselas, Pinot Noir). One leaf was used for stable C and N isotope analysis of the whole leaf tissue, a second leaf for surface epicuticular lipid analysis and the third was saved for future studies. The $\delta^{13}\text{C}$ values of the whole leaf powders for Chasselas varied from -29.0 to -25.6‰ ($-27.4 \pm 0.9\text{‰}$, $n = 24$) and for Pinot Noir from -28.5 to -25.3‰ ($-27.0 \pm 0.8\text{‰}$, $n = 24$); the $\delta^{15}\text{N}$ values for Chasselas varied from 0.5 to 4.0‰ ($1.8 \pm 0.9\text{‰}$, $n = 24$) and for Pinot Noir from -0.2 to 3.6‰ ($1.7 \pm 1.1\text{‰}$, $n = 24$). Analysis of specific regions from the same leaf show that $\delta^{13}\text{C}$ and $\delta^{15}\text{N}$ values vary by up to 1.4‰ and 1‰ respectively within a single leaf. The leaf surface lipid extractions were performed by briefly dipping the (washed and dried) whole leaf in solvents of decreasing polarity (MeOH and CH_2Cl_2 mixtures). The acid and neutral lipids were separated by alkaly hydrolysis and LC for determination of the distribution of alkanolic acids and neutral lipids by GC-MS, GC-FID and compound specific $^{13}\text{C}/^{12}\text{C}$ analysis of the individual *n*-alkanoic acids and *n*-alkanes by GC-C-IRMS. The epicuticular lipids of leaves ($n=21$ Chasselas, $n=21$ Pinot Noir) were extracted and their lipid fractions analyzed by GC-MS and GC-FID. Clear differences are observed in the distribution of lipids for both varieties. Saturated *n*-alkanoic acids occur in the C_{14} - C_{30} range with even/odd C number predominance and maxima at C_{24} (Chasselas) or C_{16} (Pinot Noir). The *n*-alkanes typically occur in the C_{21} - C_{31} range with characteristic odd/even C number predominance and maxima at C_{25} (Chasselas) or C_{27} (Pinot Noir). Differences in the relative abundances of polyunsaturated C_{18} acids (18:3, 18:2), saturated acids (16:0 and 18:0), PUFA/SA ratio, and $\text{C}_{31}/\text{C}_{27}$ *n*-alkane ratio vary clearly with plant variety (cultivar) and leaf age. The degree of C_{18} acid unsaturation decreased and the $\delta^{13}\text{C}$ values of the individual *n*-alkanoic acids increased in both plant varieties during water stress.

The variable bulk $\delta^{13}\text{C}$ and $\delta^{15}\text{N}$ values within the leaves and between the varieties of a single plant species, as well as the distribution, concentration and $\delta^{13}\text{C}$ values of lipids are not necessarily correlated with the soil water content and temperature. This clearly indicate that the use of bulk organo-isotopic composition and terrestrial plant biomarkers from soil/sedimentary rocks in paleoecological, paleoceanographic, paleolimnologic, and paleoclimatic studies may be problematic/debatable.

REFERENCE

Cameron, K.D., Teece, M.A., Smart, L.B., 2006. Increases accumulation of cuticular wax and expression of lipid transfer protein in response to periodic drying events in leaves of tree tobacco. *Plant Physiology* 140, 176-183.

14.11

Environmental controls on aerobic methane oxidation in coastal waters (SW-Baltic Sea)

Lea Steinle^{1,2}, Johanna Maltby², Nadine Engbersen¹, Jakob Zopfi¹, Hermann Bange², Annette Kock², Moritz Lehmann¹, Tina Treude³, Helge Niemann¹

¹ *Aquatic and Stable Isotope Biogeochemistry, Department of Environmental Sciences, University of Basel, Bernoullistrasse 30, CH-4056 Basel (lea.steinle@unibas.ch)*

² *Helmholtz Centre for Ocean Research, GEOMAR, Wischhofstr. 1-3, D-24148 Kiel*

³ *University of California Los Angeles, Dept. of Earth, Planetary, and Space Sciences & Atmospheric and Ocean Sciences, 595 Charles Young Drive East, CA 90095, Los Angeles*

Coastal waters contribute more than 75 % to the global oceanic methane emissions. An important process that modulates the liberation of methane to the atmosphere is the aerobic oxidation of methane (MOx), mediated by methane oxidising bacteria (MOB) in the water column. Coastal oceans are highly dynamic systems with strong fluctuations, for example, in temperature, salinity, and oxygen concentrations, all of which are potential key environmental factors controlling MOx. To further our knowledge on the regulation of MOx by environmental variables, we conducted a two-year time-series study with measurements of methane concentrations, MOx rates, the composition of the MOB community, and physicochemical parameters of the water column at the Boknis Eck Station, located in a coastal inlet of the SW-Baltic Sea (BE, 54°31.823 N, 10°02.764 E, 28 m water depth). In addition, we investigated the influence of temperature and oxygen on MOx in controlled laboratory incubation experiments. At BE, seasonal stratification and organic matter degradation causes hypoxia (March-Sept) or even anoxia (Aug/Sept) in bottom waters. Methane is produced year-round in the sediments, leading to accumulation of large amounts of methane in bottom waters, and supersaturation with respect to the atmospheric equilibrium even in surface waters (Bange et al., 2010). Rapid changes in water mass properties are common, and mostly due to episodic storm-induced inflow of saline North Sea.

We found that factors impacting the extent of MOx and/or the composition of the MOB community are a) perturbations of the water column caused by storm events, currents or seasonal mixing, b) temperature and c) oxygen concentration. a) Perturbations of the water column after storm events led to a decrease in MOx, probably caused by replacement of stagnant waters at BE with a high standing stock of MOB by newly inflowed N-Sea waters with a lower abundance of MOB. Community fingerprinting (DGGE) confirmed that the regular MOB community in BE waters changed dramatically after storm events. b) An increase in temperature generally led to higher MOx rates, attesting to a mesophilic community. However, laboratory incubations indicated the presence of psychrophilic MOB-community after a strong storm event. c) In spite of ubiquitously high methane concentrations (> 20 nM) throughout the water column, MOB communities were most active in bottom waters (1-5 nM/day), where usually also the lowest oxygen concentrations are found (sometimes <1 µM). Laboratory experiments with methane-rich (~ 100 µM) water from BE and variable oxygen concentrations (0.2 - 220 µM) confirmed maximum MOx rates at sub-micromolar O₂ concentrations. Additionally, the metabolic fate of methane-carbon at low (<0.5 µM) and high (~200 µM) O₂ concentrations was investigated in incubations with ¹⁴C-labelled methane. In the high-O₂ experiments, the percentage of methane-carbon incorporation into biomass was significantly higher than in low-O₂ experiments, suggesting a differential partitioning of catabolic versus anabolic processes as a function of O₂.

REFERENCES

Bange, H.W., Bergmann, K., Hansen, H. P., Kock, A., Koppe, R., Malien, F., Ostrau, C. 2010: Dissolved methane during hypoxic events at the Boknis Eck Time Series Station (Eckernförde Bay, SW Baltic Sea). *Biogeosciences* 7: 1279-1284.

14.12

Potential and constraints of lipid-based paleo-thermometry in lake sediments: New insights on the sources of branched GDGTs

Yuki Weber¹, Jaap S. Sinninghe Damsté^{2,3}, Carsten J. Schubert⁴, Adrian Gilli⁵, Moritz F. Lehmann¹, Helge Niemann¹

¹ Dept. of Environmental Sciences, University of Basel, Bernoullistrasse 30, 4056 Basel, Switzerland

² Department of Marine Organic Biogeochemistry, Royal Netherlands Institute for Sea Research (Royal NIOZ), P.O. Box 59, 1790 AB Den Burg, Texel, The Netherlands

³ Utrecht University, Department of Geosciences, The Netherlands

⁴ Eawag, Swiss Federal Institute of Aquatic Science and Technology, Department of Surface Waters - Research and Management, Seestrasse 79, 6047 Kastanienbaum, Switzerland

⁵ Geological Institute, ETH Zurich, Sonneggstrasse 5, 8092 Zurich, Switzerland

Branched glycerol dialkyl glycerol tetraethers (brGDGTs) comprise a series of 16 different bacterial membrane lipids that are ubiquitous in soils and peat, as well as in sediments and suspended particulate matter (SPM) of lakes. The relative distribution of brGDGTs in soils changes systematically with ambient temperature and pH, making them promising proxy indicators for paleoclimatic reconstructions. It was assumed initially that in lacustrine deposits, brGDGTs mainly originate from allochthonous soil organic matter, thus reflecting the integrated mean annual air temperature (MAAT) within the watershed. Most recent research, however, strongly suggests that the brGDGTs used for paleo-thermometry can also be produced in situ within lakes, leading to offsets in reconstructed MAAT of >10°C.

Thus, the brGDGTs present in lacustrine sedimentary archives can originate from two distinct sources, both of which display inconsistent MAAT-brGDGT relationships, hampering the use of brGDGTs for quantitative paleotemperature reconstructions. Furthermore, the identity, ecological niche and carbon substrate of the aquatic source organisms are unknown, which additionally complicates the interpretation of brGDGT-based proxy signals in lacustrine environments.

By applying an improved HPLC-MS method, our recent analyses of sediments from a small, eutrophic alpine lake (Lake Hinterburg, Switzerland) revealed the presence of a novel, brGDGT molecule (Weber et al. 2015). This novel compound could not be detected in soils of the catchment and was characterised by a strongly ¹³C-depleted carbon isotope composition of about -47 ‰. Similarly, all other major brGDGTs in the sediment showed low $\delta^{13}\text{C}$ values of about -43 ‰, strongly contrasting the C-isotopic composition of brGDGTs of catchment soils (-27 ‰).

These findings raise two fundamental questions: (1) Are lake-derived brGDGTs generally more depleted in ¹³C with respect to their allochthonous counterparts? And (2) Does the $\delta^{13}\text{C}$ of sedimentary brGDGTs serve as a reliable indicator for lacustrine in situ production of brGDGTs?

To further explore the distribution and stable C isotope composition of brGDGTs in freshwater lakes, we analysed SPM in a vertical profile from meromictic northern basin of Lake Lugano (Switzerland). The novel brGDGT (firstly identified in Lake Hinterburg) contributed up to 20% to the total brGDGT pool below the oxic/anoxic interface, but was completely absent in the oxic part of the water column (Fig. 1 A).

Moreover, the relative abundances of the two main brGDGT subgroups (i.e., 5-methyl- and 6-methyl brGDGT isomers) showed opposite patterns below and above the redoxcline. These stark compositional changes were accompanied by a negative shift in the brGDGT's $\delta^{13}\text{C}$ from -34 ‰ in the mixolimnion to -41 ‰ in the anoxic monimolimnion, suggesting that two distinct brGDGT-producing bacterial communities with differing redox requirements and possibly different C sources co-exist within the water column of Lake Lugano.

In order to study the impact of aquatic brGDGT production on sedimentary proxy records, we investigated the composition and ¹³C content of brGDGTs in surface sediments of 33 lakes from the Swiss alpine region. In ~60 % of the studied sediment samples, the $\delta^{13}\text{C}$ of the extracted brGDGTs ranged between -34 ‰ and -45 ‰, indicating a predominantly aquatic origin (Fig. 1 B). However, in one third of the lake sediments, $\delta^{13}\text{C}$ > -30 ‰ suggest a substantial contribution of brGDGTs from an allochthonous soil source.

Our data demonstrate the great potential of compound-specific C isotope analysis to constrain the origin of brGDGTs in lake sediments, possibly allowing the identification of freshwater environments that are particularly suited for brGDGT-based paleoenvironmental reconstructions.

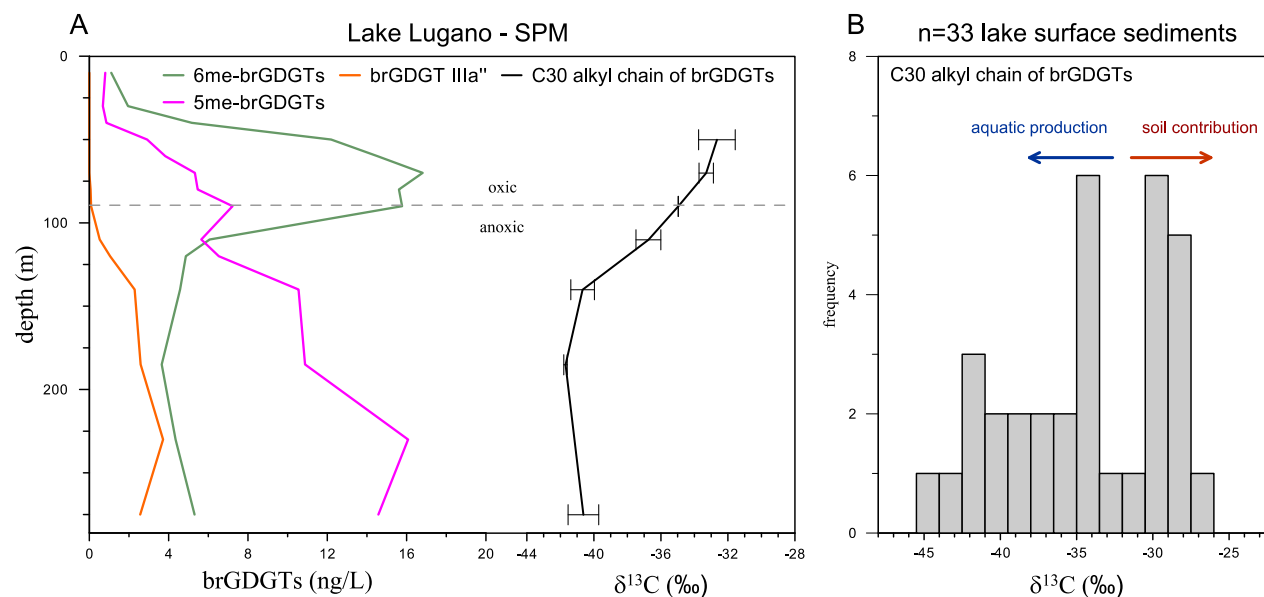


Figure 1. (A) Water column concentrations of the two main brGDGT subgroups (green and pink) and the novel brGDGT (orange), as well as the average C isotope composition of brGDGTs ($\delta^{13}\text{C}$), determined by the analysis of their C30 alkyl chains in suspended particles (SPM) from the water column of Lake Lugano. (B) Histogram of the $\delta^{13}\text{C}$ of brGDGTs in surface sediments of 33 lakes from the Alpine Region.

REFERENCES

- Weber Y., De Jonge C., Rijpstra W. I. C., Hopmans E. C., Stadnitskaia A., Schubert C. J., Lehmann M. F., Sinninghe Damsté J. S. and Niemann H. 2015: Identification and carbon isotope composition of a novel branched GDGT isomer in lake sediments: Evidence for lacustrine branched GDGT production. *Geochim. Cosmochim. Acta*, 154, 118-129.

14.13

Isotopic fractionation of Cd in agricultural soil-plant systems

Matthias Wigganhauser¹, Wolfgang Wilcke², Moritz Bigalke³, Martin Imseng³, Michael Müller⁴, Mark Rehkämper⁵, Katy Murphy⁵, Katharina Kreissig⁵, Emmanuel Frossard¹

¹ Institute of Agricultural Sciences, ETH Zurich, Eschikon 33, CH-8315 Lindau, Switzerland
(matthias.wigganhauser@usys.ethz.ch)

² Institute of Geography and Geoecology, Karlsruhe Institute of Technology (KIT), P.O. Box 6980, D-76049 Karlsruhe

³ Geographic Institute, University of Bern, Hallerstrasse 12, CH-3012 Bern

⁴ Swiss Soil Monitoring Network (NABO), Agroscope, Reckenholzstrasse 191, CH-8046 Zürich

⁵ Department of Earth Science & Engineering, Imperial College, UK-London SW7 2AZ

Cadmium (Cd) is a hazardous trace element for humans. Since Cd has a long biological half life time, a small but continuous intake of Cd can lead to accumulation in human bodies, causing reduced kidney function or weakening of bones. In agriculture, Cd cycling is of particular interest as comparatively high amounts of Cd have been introduced to agro-ecosystems especially via phosphate fertilizers which can lead to increased Cd concentrations in agricultural soils. Although no essential use of Cd for plants is known, plants take up small amounts of Cd which can then enter the food chain. The underlying processes behind the transport of Cd from the soil into edible plant parts are not yet fully understood.

Stable metal isotopes ratios provide a novel tool to study plant uptake and transfer mechanisms in soil-plant systems. Several studies have established preliminary conceptual models of stable isotope fractionation in soil-plant systems of metals such as Ca, Fe, Cu and Zn. For Cd, processes such as evaporation, sorption, precipitation and biological uptake show isotopic fractionation. However, the fractionation of Cd isotopes in soil-plant systems has not been investigated and may potentially provide useful information about plant uptake and transfer processes of this non-essential element.

We grew wheat (*Triticum aestivum* L., cv. "Fiorina") under controlled conditions in a growth chamber on three soils which differed in pH, organic matter and clay content. All soils were sampled from the Swiss soil monitoring network (NABO) and represent non contaminated agricultural soils. The wheat was supplied with sufficient water and nutrients. We sampled bulk soil, rhizosphere soil, roots, shoots and grains after the plants reached full maturity. In addition, plant available Cd was extracted from the bulk soils using $\text{Ca}(\text{NO}_3)_2$. Prior to measurements of Cd isotopic composition by MC-ICP-MS, the digested samples were purified using anion exchange and extraction chromatography. A double spike was used to correct for instrumental mass bias.

Cadmium isotopes were significantly fractionated between bulk soil and the plant-available Cd pool in which Cd was enriched in heavy isotopes compared to the bulk soil Cd ($\delta^{114/110}\text{Cd}_{\text{NIST3108}}$ in bulk soil -0.06‰ to 0.09‰, plant available pool = 0.1‰ to 0.5‰). In the wheat, shoots (0.09‰ to 0.45 ‰) were enriched in heavy isotopes compared to the roots (-0.14‰ to 0.13‰) and grains (0.59‰ to 0.8‰) were further enriched in heavy isotopes compared to the shoots. These results show that Cd isotopes are significantly fractionated on their way from the solid soil to the wheat grains.

At the conference, the results will be discussed (i) comparing isotopic fractionation of Cd in soil-wheat systems with terrestrial Cd isotopic fractionation (e.g. rocks, sediments, seawater), (ii) comparing isotopic fractionation in soil-plant systems with that of chemically similar elements such as Zn and Ca, and (iii) presenting a preliminary conceptual model describing Cd isotopic fractionation in soil-wheat systems.

P 14.1

Applicability of Rock-Eval pyrolysis to quantify ecosystem engineers' impact on soil structure formation in a carbonate-rich pre-alpine floodplain

Andreas Schomburg¹, Claire Guenat², Philip Brunner³, Eric P. Verrecchia⁴ & Renée-Claire Le Bayon¹

¹ *Institut de biologie, Laboratoire d'écologie fonctionnelle, University of Neuchâtel, Rue Emile-Argand 11, CH-2000 Neuchâtel (andreas.schomburg@unine.ch)*

² *Laboratoire des systèmes écologiques (ECOS-WSL), École Polytechnique Fédérale de Lausanne (EPFL), CH-1015 Lausanne*

³ *Centre d'hydrogéologie et d'hydrothermie (CHYN), University of Neuchâtel, Rue Emile-Argand 11, CH-2000 Neuchâtel*

⁴ *Institut des dynamiques de la surface terrestre, University of Lausanne, Géopolis, CH-1015 Lausanne*

Natural and restored pre-alpine floodplains are highly dynamic ecosystems that host an elevated biodiversity and provide a wide range of ecosystem services. Frequent flood events perturb the ecosystem balance, leading to a restructuration of the ecosystem community and reset the pedogenesis processes. A certain degree of soil stability is required to attenuate unconsolidated sediment erosion processes and therefore to maintain the ecosystem balance. Plants and earthworms as ecosystem engineers are able to improve the soil structure stability by creating water stable macro-aggregates that stabilise the alluvial sediments. The engineering effect of plants and earthworms may vary in different floodplain habitats depending on the distance to the river, the flood frequency, the soil development state and the physico-chemical properties of the soil. However, the hydrological and pedological controls on these dynamics remain poorly understood. In this regard, a reliable method is required to quantify the relative importance of biological agents for improving the soil stability. The interactions between plants and earthworms in soil and the soil aggregation mechanisms were frequently investigated in microcosms under controlled conditions. Spectroscopical methods such as near infrared spectroscopy (NIRS) were applied as indicators to identify signatures of biogenic structures produced by ecosystem engineers during the aggregate formation.

Spectroscopical applications are, however, inappropriate in the presence of low amounts of organic matter and high total carbonate contents. In this study, we test the applicability of the Rock-Eval pyrolysis method to distinguish soil aggregates according to their origin from plants or earthworms. Sixty subsurface soil aggregate samples were taken in 3 different floodplain habitats (Pioneer Vegetation, Willow bush and Alluvial forest) including 5 replicates. Soil physico-chemical properties will be determined to generate a structure of different variables describing the preconditions for the soil aggregate formation. The dependency of soil aggregation on abiotic environmental components will be reflected using PCA analysis. The results might give an approach to improve floodplain management strategies with regard to the increasing number of recent floodplain restoration projects in Switzerland and worldwide. The link between the recovery of the river species diversity and the flood protection function of the floodplain ecosystem may thus be established.

Keywords: Rock-Eval pyrolysis, ecosystem engineers, soil aggregation, natural and restored floodplains

REFERENCES

- Acreman, M. C.; Riddington, R.; Booker, D. J. (2003): Hydrological impacts of floodplain restoration: a case study of the River Cherwell, UK. *Hydrology and Earth System Sciences* 7: 75-85.
- Bottinelli, N.; Capowiez, Y.; Hallaire, V.; Ranger, J.; Jouquet, P. (2013): Inability of Near Infrared Reflectance Spectroscopy (NIRS) to identify belowground earthworm casts in no-tillage soil. *Applied Soil Ecology* 70: 57-61.
- Fournier, B.; Samaritani, E.; Shrestha, E.; Mitchell, E. A. D.; Le Bayon, R.-C. (2012): Community ecology of earthworm in a restored floodplain and potential as bioindicators of river restoration. *Applied Soil Ecology* 59: 87-95.
- Saenger, A.; Cécillon, L.; Sebağ, D.; Brun, J.-J. (2013): Soil organic carbon quantity, Chemistry and thermal stability in a mountainous landscape: A Rock-Eval pyrolysis survey. *Organic Geochemistry* 54: 101-114.

P 14.2

Eutrophication and re-oligotrophication of Lake Sempach over the last 150 years: Assessing the impact on calcium carbonate nucleation and redox-sensitive metals in the sediments

Benjamin Stern¹, Elena Giglio¹, Hendrik Vogel², Flavio Anselmetti², Robert Lovas³, Helge Niemann¹, Moritz F. Lehmann¹

¹ *Aquatic and Stable Isotope Biogeochemistry, University of Basel, Bernoullistrasse 30, CH-4056 Basel (benjamin.stern@stud.unibas.ch)*

² *Institute of Geological Sciences & Oeschger Centre for Climate Change Research, University of Bern, Baltzerstrasse 1+3, CH-3012 Bern*

³ *Kanton Luzern, Umwelt und Energie (uwe), Oberflächengewässer, Libellenrain 15, CH-6002 Luzern*

Eutrophication of freshwater environments due to nutrient loading can have detrimental ecological effects, such as excessive algal growth, water-column hypoxia or anoxia, biodiversity loss, as well as large-scale fish kills and/or reproduction failure. While nutrient and oxygen levels in modern lakes are often monitored, knowledge on the trophic and oxygenation state of lakes beyond historic times relies on proxy indicators preserving chemical/physical water-column characteristics of the past. For example, direct links have been invoked between phosphate levels and the size of authigenic CaCO_3 particles (through the inhibiting effect of PO_4^{3-} as surface inhibitors during nucleation). Analogously, bottom water oxygenation seems to directly affect the concentration of redox-sensitive metals (e.g. V, Mo) in lake sediments. The applicability of either sediment proxy to sedimentary archives for paleoenvironmental reconstruction, however, requires solid ground-truthing in modern environments. In this regard, long-term hydro- and biogeochemical data sets from ongoing monitoring programs are extremely valuable for the calibration of these paleolimnological proxies and for testing their sensitivity towards environmental change.

Here, we investigate past oxygenation and phosphate levels in Lake Sempach, Switzerland. Similar to many other Swiss lakes, Lake Sempach turned eutrophic and subsequently hypoxic/anoxic in the deep hypolimnion in the mid-20th century, as a result of elevated sewage and/or agricultural fertilizer loading. The strong reduction in nutrient loading since the 1980ies led to a re-oligotrophication of Lake Sempach and in 1984, an aeration-system was installed in order to re-oxygenate the bottom water. The well-documented (monitoring since the 1950s) trophic and redox history of Lake Sempach makes this system consequently an ideal study site for testing sedimentary proxy indicators for past phosphate and oxygen levels. From the center of the lake, we retrieved a 90 cm long sediment core. A sediment age model was developed using radiometric dating methods (Cs-137 and Pb-210) and by counting sediment varves, demonstrating that our core provides an undisturbed sediment record from 1690 to 2015. We investigated the down-core grain-size distribution of calcium carbonate nucleoids at a resolution of 1 centimeter (corresponding to ~5 years). We also measured redox sensitive trace metals (V, Mo,) using an ITRAX X-Ray Fluorescence (XRF)-Scanner at a resolution of 200 μm , (corresponding to ~0.1 years). We observed a clear positive relationship between the size of CaCO_3 particles and phosphate concentrations. Moreover, the concentrations of V and Mo were doubled with the start of anoxia and euxinic sediment conditions (1936 – 1985) and decreased again once the aeration in 1984 started. Hence our results demonstrate the good responsiveness of the investigated proxy parameters to recent environmental changes in Lake Sempach both during the eutrophication and re-oligotrophication periods, and thus underline their potential for reconstructing the eutrophication history of lake environments in the past.

P 14.3

Geochemical constraints on anaerobic ammonium oxidation (anammox) in a riparian zone of the Seine Estuary

Sebastian Naeher², Arnaud Huguet², Céline L. Roose-Amsaleg², Annet M. Laverman², Céline Fosse³, Moritz F. Lehmann¹, Sylvie Derenne² & Jakob Zopfi¹

¹ *Aquatic and Stable Isotope Biogeochemistry, Department of Environmental Sciences, University of Basel, Bernoullistrasse 30, CH-4056 Basel (jakob.zopfi@unibas.ch)*

² *METYS, Sorbonne Universités, UPMC, 4 Place Jussieu, 75252 Paris 05, France*

³ *Chimie ParisTech, 11 rue Pierre et Marie Curie, 75231 Paris 05, France*

Anammox, the microbial anaerobic oxidation of ammonium to molecular nitrogen with nitrite as oxidant is the second biogeochemical process after denitrification that closes the global nitrogen cycle. While the importance of anammox is well recognized for marine environments, e.g. coastal upwelling areas, its role in the terrestrial N-cycle is not well constrained to date.

We studied the abundance, community structure, and activity of anammox bacteria in intertidal sediments and irregularly flooded soils of a riparian zone in the Seine Estuary, France (Naeher et al., 2015). The combination of i) molecular biological analyses of anammox bacterial 16S rRNA and hydrazine oxidoreductase (*hzo*) genes, ii) quantification of specific ladderane lipids and, iii) ¹⁵N-isotope label incubation experiments revealed that anammox bacteria were ubiquitous in the studied ecosystem. Their diversity was low and the anammox community was dominated by *Candidatus* 'Brocadia'. The abundance of anammox bacteria, as assessed by copy numbers of anammox bacterial 16S rRNA genes, was generally lower in the more oxygenated soils than in the intertidal sediments.

The C₂₀-ladderane fatty acid with five cyclobutane moieties was found in sediments and soils, while others were only detected in the wetland sediments. This is the first detection of ladderanes in soils without prior enrichment. The differential ladderane distribution is due to intra-genus differences rather than abiotic factors (e.g. temperature).

A low but consistent contribution of anammox to the total N₂ production (< 8%) highlights its dependence on nitrite supply from denitrification. As a consequence, the dependence of denitrification on the quality and stoichiometry of organic matter seems to be passed on to the anammox bacterial community.

Our study suggests that anammox in riparian zones barely contributes to mitigating N eutrophication in riverine systems, leaving denitrification as the most important N-eliminating process in these environments.

REFERENCE

Naeher S., Huguet A., Roose-Amsaleg C. L., Laverman A. M., Lehmann M. F., Derenne S. & Zopfi J. 2015: Molecular and geochemical constraints on anaerobic ammonium oxidation (anammox) in a riparian zone of the Seine Estuary (France). *Biogeochemistry*. 123, 237–250.

P 14.4

Potential role of nitrate, iron and manganese reduction during anaerobic methane oxidation in lacustrine sediments

Guangyi Su¹, Helge Niemann¹, Jakob Zopfi¹ & Moritz F. Lehmann¹

¹ *Department of Environmental Sciences, University of Basel, Bernoullistrasse 30, CH-4056 Basel (guangyi.su@unibas.ch)*

Freshwater habitats such as lakes are important sources of methane (CH₄), a potent greenhouse gas to the atmosphere. Traditionally, sulfate reduction coupled to anaerobic oxidation of methane (AOM) has been considered as the dominant methane consuming process in anoxic marine environments. Sulfate concentrations are typically low in lakes and recent investigations have revealed that AOM may also be coupled to alternative electron acceptors like nitrate/nitrite (Raghoebarsing et al. 2006) or iron and manganese oxides (Beal et al. 2009), but knowledge about the significance of these processes in natural environments is still limited.

We initiated a project to study AOM coupled to alternative electron acceptors in two eutrophic Swiss lakes with contrasting sediment biogeochemistry: Lake Sempach and Lake Lugano. Geochemical profiles in Lake Sempach show high concentrations of CH₄, as well as of dissolved ferrous iron and manganese. Methane oxidation rates measurement using ¹⁴CH₄ radiotracer incubations revealed CH₄ turnover in the zone where concentration profiles indicate iron/manganese reduction, thus providing putative evidence for iron/manganese-driven AOM. Moreover, comparison of winter and summer methane oxidation profiles indicate strong seasonal variation of AOM activity. In Lake Lugano, porewaters at both Figino and Melide sites show much higher concentrations of methane and dissolved iron/manganese than in Lake Sempach. As in Lake Sempach, higher AOM rates occurred where relatively lower concentrations of dissolved iron/manganese were observed, while in Lake Lugano different Fe and Mn conditions between Figino (higher Fe²⁺) site and Melide site (higher Mn²⁺) did not induce significantly distinct AOM rates.

To further understand the role of various potential electron acceptors for AOM in lakes, laboratory incubation experiments were conducted with sediment slurries from Lake Sempach, which were amended with ¹⁴C-labeled methane and differential amounts of amorphous manganese and iron oxides, nitrate and sulfate. Assessing the magnitude of methane oxidation as a function of electron acceptor types and concentrations will provide further insights into the potential and relative importance for AOM and the associated electron acceptors in lacustrine environments.

REFERENCES

- Raghoebarsing A. A., et al. 2006. A microbial consortium couples anaerobic methane oxidation to denitrification. *Nature* 440:918–921.
- Beal, E. J., et al. 2009. Manganese- and iron-dependent marine methane oxidation. *Science* 325:184–187.

P 14.5

Response of periphyton communities to metals, including Hg, in the lagoon of Venice.

Carmen Moinecourt¹, Perrine Dranguet¹, Roberto Zonta², Vera I. Slaveykova¹, Séverine Le Faucheur¹.

¹ University of Geneva, Institute F.A. Forel, Uni Carl Vogt, 66 Boulevard Carl-Vogt, CH-1211 Genève 4, Switzerland

² ISMAR Istituto di Scienze Marine / Arsenale - Tesa 104, Castello 2737/F, 30122 Venezia, Italy

Periphyton is a biological layer of microorganisms, which colonize various substrata in natural water (rivers, lakes, sea). It is mainly composed of microalgae, bacteria and fungi embedded in a polysaccharide matrix (Donlan, 2002). Biofilms are good bioindicators due to their position at the base of the food chain, short live cycle and fast answer to environmental changes (Gold and al., 2002). Moreover they can give a good representation of the bioaccumulation path of toxicants by their positions at the interface between the water and the sediments (Serra and al., 2009).

The lagoon of Venice is subject for many years to anthropogenic pollution coming from the industrial site of porto Marghera (refinery, metallurgy), and the city of Venice (transportation, wastewater) (Zonta and al., 2007). The aim of our study was to evaluate the bioavailability of metals (Cu, Zn, Pb, As, Co, Ni, Cr), including Hg, present in the lagoon, using marine biofilms and to assess which parameters drive metal accumulation in periphyton.

To that end, colonisation boxes containing 150 microscope slides were immersed in water at 1.50 m depth at six different sampling sites representing a gradient of pollution, i.e. a low-impacted site (Santa Maria del Mare), two highly-impacted industrial (Porto Marghera) and urban sites (channel of Venice city) and two less affected sites situated in the area of glass production (Murano Island) and of marine currents influenced by the city (San Clemente Island). Samples of water were taken at each site to measure metals, Hg and methylmercury (MeHg) concentrations in water and suspended matters. Specific metal and Hg DGTs were fixed 7 days at the same place and depth than the colonization set-ups to quantify labile metals and Hg concentrations at each site. The colonized slides were collected after 40 days of immersion and analysed for their concentrations in total and intracellular metals, Hg and MeHg as well as their chlorophyll a content and ash-free dry mass (AFDM). Periphyton composition was further analysed by epifluorescent microscopy with DAPI staining to quantify the biotic fraction.

Periphyton collected at the low impacted sites (St Maria del Mare) contained more algae (0.75 ± 0.09 g chl a/g dw) than those collected in the channel of Venice city (0.02 ± 0.01 g chl a/g dw). The inorganic fraction was very high in periphyton from the most polluted sites such as Murano (81 ± 2 %) and the industrial zone (75 ± 3 %). Total accumulated Hg measured in periphyton suggested that one of the main source of Hg for the Lagoon was coming from the city with the highest quantities of Hg found in the channel (2.6 ± 0.2 ppm), Murano (1.4 ± 0.4 ppm) and San Clemente (1.05 ± 0.16 ppm), the two last sites being influenced by the marine currents from the city. For comparison, the lowest impacted site contained 0.7 ± 0.3 ppm Hg. Obtained results will allow us to evaluate metals and Hg bioavailability for primary producers in the lagoon of Venice.

REFERENCES

- Donlan, R. M. 2002: Biofilms: Microbial Life on Surfaces. *Emerging Infectious Diseases* 8, 881–890.
- Gold, C., Feurtet-Mazel, A., Coste, M. & Boudou, A. 2002 : Field transfer of periphytic diatom communities to assess short-term structural effects of metals (Cd, Zn) in rivers. *Water Research* 36, 3654–3664.
- Serra, A., Corcoll, N. & Guasch, H. 2009 : Copper accumulation and toxicity in fluvial periphyton: The influence of exposure history. *Chemosphere* 74, 633–641.
- Zonta, R. and al. 2007: Sediment chemical contamination of a shallow water area close to the industrial zone of Porto Marghera (Venice Lagoon, Italy). *Marine Pollution Bulletin* 55, 529–542.

P 14.6**Short-term variations of methane and methanotrophic activity in a coastal inlet (Eckernförde Bay, Germany)**

Dominik Richner¹, Helge Niemann¹, Lea Steinle^{1/2}, Jens Schneider von Deimling², Peter Urban², Jasper Hoffmann², Mark Schmidt², Tina Treude^{2/3}, and Moritz F. Lehmann¹

¹ *University of Basel, Dept. of Environmental Sciences, Stable Isotope Geochemistry and Aquatic Biogeochemistry Group, Basel, Switzerland (d.richner@stud.unibas.ch)*

² *GEOMAR Helmholtz Centre for Ocean Research Kiel, Department of Marine Biogeochemistry, Düsternbrooker Weg 20, 24105 Kiel, Germany*

³ *University of California, Los Angeles, Department of Earth, Planetary and Space Sciences & Department of Atmospheric and Ocean Sciences, Math Sciences Building 7127, Los Angeles, CA 90095-1565, USA*

Large quantities of methane are produced in anoxic sediments of continental margins and may be liberated to the overlying water column and, potentially, to the atmosphere where it contributes to global warming. However, microbially mediated methane oxidation in sediments and the water column mitigates the contribution of marine environments to the atmospheric methane budget. In anoxic sediments, specialised archaea can oxidise methane with sulphate (anaerobic oxidation of methane; AOM). In addition, aerobic bacteria at the sediment surface and the water column have the potential to consume methane (aerobic oxidation of methane; MOx) that has bypassed the anaerobic benthic microbial filter. However methane cycling in (aerobic) marine waters is not well constrained. Particularly little is known with respect to the key physical, chemical and biological factors that modulate the spatiotemporal variability of MOx activity. Here we show rate measurement data from Eckernförde Bay (E-Bay), a coastal inlet with seasonal hypoxic/anoxic bottom water (SW Baltic Sea, Germany). In autumn 2014, we observed strong fluctuations in the methane cycle dynamics at time scales of hours to days: Anoxic bottom waters in a trough in the northern part of the bay contained extremely high methane concentrations of up to 800 nM, which sharply declined at the midwater redox interface (though methane remained supersaturated with respect to the atmospheric equilibrium throughout the water column at all times). The methane decrease at the redox interface was related to highly active MOx communities, consuming methane under microoxic conditions at rates of up to 40 nM/d. About 12 hours later, methane concentrations and the extend of bottom water anoxia were markedly reduced. MOx rates were also reduced in the northern but strongly elevated in the southern part of the bay. A few days later, bottom water anoxia, high methane loading and MOx activity was partially re-established. The observed spatiotemporal dynamics could be related to storm-associated water-column mixing and rapid re-stratification, as well as current-induced translocation of methanotrophic communities.

P 14.7**Tracing Pathways of Organic Matter Transport in the Modern South China Sea**

Thomas Blattmann¹, Ke Wen², Jianru Li², Yulong Zhao², Yanwei Zhang², Lukas Wacker³, Michael Plötze⁴, Zhifei Liu² & Timothy Eglinton¹

¹ *Institute of Geology, ETH Zurich, Sonneggstrasse 5, CH-8092 Zurich (thomas.blattmann@erdw.ethz.ch)*

² *State Key Laboratory of Marine Geology, Tongji University, Siping Road 1239, CN-200092 Shanghai*

³ *Ion Beam Physics, ETH Zurich, Otto-Stern-Weg 5, CH-8093 Zurich*

⁴ *Institute for Geotechnical Engineering, ETH Zurich, Stefano-Franscini-Platz 3, CH-8093 Zurich*

The South China Sea, one of the largest marginal seas bordering the Pacific, exhibits marked, large-scale spatial gradients in clay mineralogy as a consequence of diverse sources of terrigenous material emanating from Taiwan, the Chinese mainland, and the Philippines. Strong contrasts in smectite, kaolinite, chlorite, and illite assemblages, enables phyllosilicate composition to serve as an excellent provenance indicator (Liu et al., 2010). Stable carbon and radiocarbon isotopic compositions can be used to constrain different sources of organic matter (e.g., marine phytoplankton, soils, and eroding rocks). Given that organic matter exhibits a strong affinity for phyllosilicates, with sorption to mineral surfaces and other interactions influencing organic matter transport and stability (Keil & Mayer, 2014), we hypothesize that coupled investigations of organic matter and clay mineral composition will yield key insights into factors controlling source and fate of organic matter in the modern ocean.

Here, we present preliminary results from an investigation of stable carbon and radiocarbon isotopic compositions of bulk organic matter intercepted by time-series sediment traps deployed at two locations in the South China Sea, and evaluate these measurements in the context of hydrographic, sedimentological and clay mineralogical information. In particular, carbon isotopic fingerprints are used to provide initial insights into source-to-sink transport processes and organic matter cycling in the South China Sea.

REFERENCES

- Keil, R. & Mayer, L. 2014: Mineral Matrices and Organic Matter, in Turekian, H. ed., *Treatise on Geochemistry* (Second Edition): Oxford, Elsevier, 337-359.
- Liu, Z., Li, X., Colin, C. & Ge, H. 2010: A high-resolution clay mineralogical record in the northern South China Sea since the Last Glacial Maximum, and its time series provenance analysis, *Chinese Science Bulletin*, 55, 4058-4068.

P 14.8

Understanding grain-size effects on element geochemistry and mineralogy in sedimentary records from Lake Towuti, Sulawesi, Indonesia

Valentin Nigg¹, Hendrik Vogel¹, Marina Morlock¹, Flavio Anselmetti¹, James M Russell², Satria Bijaksana³

¹ *Institute of Geological Sciences and Oeschger Centre for Climate Change Research, University of Bern, 3012 Bern, Switzerland (valentin.nigg@students.unibe.ch; hendrik.vogel@geo.unibe.ch)*

² *Department of Geological Sciences, Brown University, Providence, RI 02912*

³ *Faculty of Mining and Petroleum Engineering, Institut Teknologi Bandung, Bandung 40132, Indonesia*

Measurements of grain-size variability in sedimentary records are commonly used to better understand transport processes and energies during the time of deposition. The impact of grain-size variability and changing depositional modes on elemental and mineralogical proxies used to reconstruct climatic and environmental change over time is, however, commonly neglected. We examined the influence of grain-size variability on element geochemistry and mineralogy in sedimentary records from Lake Towuti in order to groundtruth previously suggested proxies for changes in the region's hydroclimate and erosion.

Lake Towuti (2.5°S, 121°E) is a 560 km²-large and 200-m deep lake at the downstream end of the Malili lake system, a set of five ancient (1-2 Ma) tectonic lakes located in central Sulawesi, Indonesia. Its location provides an important opportunity to reconstruct long-term hydroclimatic change in equatorial Indonesia in the center of the Indo-Pacific warm pool. The lake's catchment is in many ways unique because it predominantly consists of ultramafic rocks of the East Sulawesi Ophiolite. The bedrock is intensely weathered to several 10s of metres thick, highly evolved lateritic soils. Substrates and solutes released from these catchment rocks and soil profiles are deposited or through pass Lake Towuti, with the style and type of erosion and weathering exerting strong control on the sediment composition in the lake.

Sediment piston cores recovered from Lake Towuti in 2010 and reaching back to ~60 kyr BP document the value of the climatic signal preserved in Towuti's sediments through pronounced changes in sedimentary geochemistry and mineralogy (Russell et al. 2014, Costa et al. 2015, Tamuntuan et al. 2015). Russell et al. (2014) applied titanium (Ti) as elemental tracer for terrestrial runoff and the carbon isotopic composition of terrestrial plant leaf waxes ($\delta^{13}\text{C}_{\text{wax}}$) as indicator for moisture-balance-driven changes in vegetation surrounding Lake Towuti. The coherent signal produced by these datasets implies that the region experienced significant changes in moisture availability, with interstadial/interglacial periods of marine isotope stage 3 (MIS 3) and the Holocene being characterized by wetter and stadial/glacial periods of MIS 4 and 2 being characterized by substantially drier conditions (Russell et al. 2014).

We performed grain-size, geochemical and mineralogical analyses on sediment samples at a 2000 yr spacing and on grain-size separates from the 2010 piston cores to study the effects of grain-size variability on element and mineral concentrations in Lake Towuti across the documented changes in the region's hydroclimate. We find two distinct grain-size distribution end-members. One is defined by a unimodal grain-size distribution, with a grain-size maximum in the 5-30 μm range, and connected to wet climate conditions of MIS 3 and the Holocene. The other grain-size distribution shows a bimodal pattern, with two grain-size maxima in the 5-30 and 50-150 μm range, and coincident with drier climates of MIS 2 at Lake Towuti. We interpret these changes in grain-size distribution as being primarily a result of lake-level forced changes in shore-line proximity of our coring sites and delta progradation of the major rivers feeding the lake. Hence, we assume lower lake-levels during the MIS 2 dry phase compared to wetter phases of MIS 3 and the Holocene. Data evaluation and interpretation is still ongoing but one important finding of our analyses with respect to grain-size effects on element geochemistry in Lake Towuti is that Ti concentration are seemingly not affected by grain-size variability. This is an important finding because Ti is one of the most important proxy indicators for hydroclimatic changes in sedimentary records from Lake Towuti and ~1200 m of sediment drill cores, possibly reaching back 1 million years in time, have been recovered in course of the ICDP Towuti Drilling Project in May-July 2015. Further evaluation and refinement of our datasets will help to groundtruth and establish additional proxies not only for the region's hydroclimate but also for erosion of catchment soils and element cycling.

REFERENCES

- Costa, K.M., Russell, J.M., Vogel, H., Bijaksana, S. 2015: Hydrological connectivity and mixing of Lake Towuti, Indonesia in response to paleoclimatic changes over the last 60,000 years. *Paleogeography, Paleoclimatology, Palaeoecology*, 417, 467-475.
- Russell, J., Vogel, H., Konecky, B.L., Bijaksana, S., Huang, Y., Melles, M., Wattrus, N., Costa, K. & King, J.W. 2014: Glacial forcing of central Indonesian hydroclimate since 60,000 y B.P. *PNAS* vol. 111 no. 14, 5100-5105.
- Tamuntuan, G., Bijaksana, S., King, J., Russell, J., Fauzi, U., Maryunani, K., Afa, N. & Safiuddin, L.O. 2015: Variation of magnetic properties in sediments from Lake Towuti, Indonesia, and its paleoclimatic significance. *Paleogeography, Paleoclimatology, Palaeoecology*, 420, 163-177.

P 14.9

Sedimentary abundance and isotopic composition of algal lipid biomarkers in lakes of variable Phosphorous concentration in central Switzerland

S. Nemiah Ladd¹, Nathalie Dubois² & Carsten Schubert¹

¹ Surface Waters Research and Management – Biogeochemistry group, Eawag, Seestrasse 79, CH-6047 Kastanienbaum (nemiah.ladd@eawag.ch)

² Surface Waters Research and Management – Sedimentology group, Eawag, Überlandstrasse 133, CH-8600 Dübendorf

During much of the 20th century, lakes in the Swiss central plateau experienced increasing anthropogenic phosphorous loading due to residential and agricultural pollution. The resulting eutrophication created hypoxic and anoxic events, harmful algal blooms, and fish kills, reducing the economic and aesthetic value of the lakes. Concerted remediation efforts by the Swiss government have significantly reduced phosphorous concentrations in most lakes and reversed previous eutrophication. However, in many sites phosphorous concentrations remain elevated above their preindustrial levels. High quality monitoring of lake nutrient levels since the 1950s, along with several lakes of wide-ranging phosphorous concentrations in close proximity, make central Switzerland an ideal location for studying the ways in which nutrient loading affects the organic composition of lacustrine sediments. Results of such studies can be used to develop proxies of eutrophication in sites where historical data is sparser, and to reconstruct historical phosphorous concentrations in Swiss lakes from the time before record keeping began.

We analyzed the distributions of algal lipid biomarkers from surface sediment and sediment traps collected in the spring of 2015 from ten lakes with variable phosphorous concentrations in central Switzerland. Sedimentary lipid distributions from these lakes confirm that biomarkers associated with algal and cyanobacterial sources are more abundant in the sediment of lakes with greater phosphorous loading. The dry sedimentary concentration of biomarkers such as brassicasterol (primarily diatom source) and diplopterol (cyanobacteria source), as well as the less source specific short-chain *n*-alkanols, linearly increase from 0.4 – 1.2 µg/g as total phosphorous in the upper water column increases by 1 µg/L over a range of 7 – 50 µg/L. Additionally, the abundance of cholestanol to cholesterol increases linearly as phosphorous concentrations increase, indicating greater rates of anaerobic respiration in the sediments of more eutrophic lakes.

We also present preliminary hydrogen isotope data from these biomarkers. Hydrogen isotopes of algal lipids primarily reflect the source water in which the algae grew, and this relationship has been developed as a paleohydrologic proxy. However, laboratory cultures of marine algae demonstrate that they discriminate more against ²H under nutrient replete conditions. We present the first field assessment of how nutrient availability influences ²H fractionation in freshwater algae, and demonstrate how such measurements can be used to infer past information about anthropogenic nutrient loading.

P 14.10**From source to sink – biomarker transport along the Danube River**

Chantal V. Freymond¹, Nicole Kündig¹, Francien Peterse², Björn Buggle¹, Liviu Giosan³, Florin Filip⁴ & Timothy I. Eglinton¹

¹ *Geological Institute, ETH Zürich, Sonneggstrasse 5, CH-8092 Zürich
(Chantal.Freymond@erdw.ethz.ch, Timothy.Eglinton@erdw.ethz.ch)*

² *Geochemistry, Utrecht University, Netherlands*

³ *Geology & Geophysics, Woods Hole Oceanographic Inst., MA, USA*

⁴ *Department of Geography, University of Bucharest, Bucharest, Romania*

Organic carbon (OC) discharged by rivers and buried in continental margin sediments represents an important carbon sink and a valuable record of information on past environmental variations on the continents. In this context, it is crucial to understand the sources of carbon in river basins and the factors that influence biomarker signals during transport from the continental source to the oceans. In this study, we adopt a source-to-sink approach where concentration and compositional variations in plant wax fatty acids and branched glycerol dialkyl glycerol tetraethers (brGDGTs) in fine-grained (<63 µm) river sediment deposits from the Danube River are investigated. We sampled along the Inn River, the largest tributary to the Danube in the upper basin, doubling the discharge of the Danube at the confluence, and further the Danube River to the delta at its terminus. In combination with compound-specific stable carbon and hydrogen isotope measurements and ultimately biomolecular ¹⁴C dating of the plant wax fatty acids, we seek to establish geochemical “fingerprints” of the largest tributaries and follow the evolution of these signatures through the river basin, from headwater tributaries to the ocean. Spatial trends in biomarker concentrations along the river are set in context with mineralogical characteristics of the fluvial sediments and assessed through normalization to mineral-specific surface area. Surface area-normalized total organic carbon, plant wax and brGDGT concentrations are initially low in the upper Inn River, increasing from the headwaters down to the Danube. After the confluence, the Danube shows a clear trend to decreasing values (ng compound m⁻²) from the upper to the lower catchment, raising the question of initial loading and further gradual unloading of the available mineral surface area and underlining the importance of organo-mineral interactions within the transport of organic carbon along a river transect. The distributions of brGDGTs, a group of soil bacterial membrane lipids that has been shown to record local environmental parameters, reflect the trend of increasing air temperature from the upper to the lower reaches of the Danube. This trend suggests an increasing contribution of soil organic carbon from tributaries joining the lower Danube basin to the OC that is finally delivered to the delta.

P 14.11

Nitrogen cycling and N₂O production in the water column of the ferruginous meromictic Lake La Cruz (Spain)

Jana Tischer¹, Jakob Zopfi¹, Caitlin H. Frame¹, Moritz F. Lehmann¹

¹ *Aquatic and Stable Isotope Biogeochemistry, Department of Environmental Sciences, University of Basel, Bernoullistrasse 30, CH-4056 Basel (jana.tischer@unibas.ch)*

Ferruginous meromictic lakes are rare systems, with only a handful of known representatives worldwide. They are considered potential modern analogues for an ancient Archean ferruginous Ocean, and may therefore represent valuable model ecosystems to study biogeochemical processes during early Earth history, in particular, the interaction between the iron (Fe) and other element cycles such as the nitrogen (N) cycle. Meromictic lakes are known for their complex N cycling within redox transition zones with aerobic (nitrification) and anaerobic (organotrophic or chemolithotrophic denitrification, anammox) N transformation processes occurring in close vicinity. Nitrous oxide (N₂O), for example, can be produced as intermediate or byproduct by some of these processes, but can also be produced by abiotic reactions, e.g. by ferrous Fe reducing nitrite. Stable N isotope ratios can be used as tracers for the production, consumption and transport of N₂O, as well as the possible dissolved inorganic N substrates involved.

In context of its exceptional water chemistry, we studied the N cycling in the meromictic, ferruginous Lake La Cruz in the Central Iberian Ranges in Spain, combining i) general water chemical and detailed N species characteristics ii) N₂O and NO₃⁻ isotope measurements and iii) ¹⁵N-isotope label incubation experiments, which were performed to identify and quantify N₂ and N₂O production pathways in the lake water column, respectively.

First results show maximum N₂O concentrations (16 nmol/L) at the oxic-anoxic interface and complete consumption within the anoxic water column. The N₂O peak corresponds to the depth of decreasing nitrate concentrations towards the chemocline, suggesting incomplete denitrification as main N₂O producing pathway, but based on the bulk dual N-versus-O isotope signature, other production mechanisms cannot be excluded at this point. The N₂O in the anoxic zone was enriched in the heavy isotopes ($\delta^{15}\text{N-N}_2\text{O} = 11.0\text{‰}$, $\delta^{18}\text{O-N}_2\text{O} = 49.0\text{‰}$) with respect to the shallow-water N₂O, indicating isotope fractionation during denitrification. We will also analyze the intramolecular ¹⁵N distributions (site preferences) of N₂O for better constraining the source of N₂O, testing specifically for possible abiotic production through the reaction of nitrification intermediates and ferrous and/or ferric Fe. Planned ¹⁵N incubation experiments will additionally provide information about the existence and activity of denitrifying and anammox bacteria, and possible dependencies on reduced Fe in the lake water column.

REFERENCES

- Frame, C.H., Deal, E., Nevison, C.D., Casciotti, K.L. 2014: N₂O production in the eastern South Atlantic: Analysis of N₂O stable isotopic and concentration data, *Global Biogeochemical Cycles*, 28, 1262-1278.
- Walter, X. A., Picazo-Mozo, A., Miracle, M.R., Vicente, E., Camacho, A., Aragno, M. & Zopfi, J. 2014: Phototrophic Fe(II)-oxidation in the chemocline of a ferruginous meromictic lake, *Frontiers in Microbiology*, 5, 1-9.

P 14.12

Microhabitat effects on N₂O emissions from floodplain soils under controlled conditions

Martin Ley^{1, 3}, Moritz Lehmann¹, Pascal Niklaus², Beat Frey³, Thomas Kuhn¹ and Jörg Luster³

¹ *Department of Environmental Sciences, University of Basel, Bernoullistrasse 30, CH-4056 Basel
(martin.ley@unibas.ch)*

² *Institute of Evolutionary Biology and Environmental Studies, University of Zürich, Winterthurerstrasse 190, CH-8057 Zurich
(pascal.niklaus@ieu.uzh.ch)*

³ *Forest Soils and Biogeochemistry, Swiss Federal Institute for Forest, Snow and Landscape Research WSL,
Zürcherstrasse 111, CH-8903 Birmensdorf (martin.ley@wsl.ch)*

Semi-terrestrial soils such as floodplain soils are considered to be potential hotspots of nitrous oxide (N₂O) emissions. The quantitative assessment of N₂O release from these hotspots under field conditions, and of the microbial pathways that underlie net N₂O production (ammonium oxidation, nitrifier-denitrification, and denitrification) is challenging because of their high spatial and temporal variability. The production and consumption of N₂O appears to be linked to the presence or absence of micro-niches, providing specific conditions that may be favorable to either of the relevant microbial pathways. Flood events have been shown to trigger moments of enhanced N₂O emission through a close coupling of niches with high and low oxygen availabilities. Such microhabitat effects might be related to soil aggregate formation, root soil interactions and the degradation of organic matter accumulations. In order to assess how these factors can modulate N₂O production and consumption under simulated flooding/drying conditions, we have set up a mesocosm experiment with N-rich floodplain soils comprising different combinations of soil aggregate size classes and inert matrix material. These model soils were either planted with willow (*Salix viminalis* L.), mixed with leaf litter or left untreated. At several time points throughout simulated flood events, we measured the net N₂O efflux rate. In addition, soil water content, redox potential as well as C and N substrate availability were monitored. In order to gain insight into the sources of, and biogeochemical controls on N₂O production, we will measure the bulk isotopic signature of the produced N₂O as well as its intramolecular Nitrogen-15 site preference. In combination with the analysis of the microbial DNA by qPCR, we will investigate the treatment effects on the microbial communities. Those findings will be linked to the isotopic signatures of the emitted N₂O. Therefore our study helps to increase our limited understanding of how microhabitats affect the occurrence of high N₂O emissions from floodplain soils.

P 14.13**A time series of nitrogen speciation and nitrogen isotope fractionation during nitrification in a eutrophic coastal embayment**

Tim Kalvelage¹, Claire Normandeau², William Li³ & Douglas R.W. Wallace²

¹ *Institute of Biogeochemistry and Pollutant Dynamics, Aquatic Chemistry Group, ETH Zurich, Universitätsstrasse 16, CH-8092 Zurich (tim.kalvelage@usys.ethz.ch)*

² *Department of Oceanography, CERC.OCEAN Group, Dalhousie University, 1355 Oxford Street, Halifax B3H 4R2, Canada*

³ *Bedford Institute of Oceanography, Fisheries and Oceans Canada, 1 Challenger Drive, Dartmouth B2Y 4A2, Canada*

In aquatic environments, processes and conditions affecting distribution and isotopic compositions of nitrogen (N) compounds are complex and highly variable in both space and time. Verification studies that can be used to test understanding of mechanisms through comparison of both N species concentrations and N isotopic signals with microbial N sources and sinks are rare. A particularly effective approach is to exploit naturally occurring “experiments”, in which temporally changing physical and hydrochemical conditions drive changes in N cycling that can be followed through observation of temporal changes in N concentrations and isotopic ratios. Here, we present an annual cycle of both physical and biogeochemical parameters obtained in the frame of the Bedford Basin Time Series, a coastal monitoring program in the Northwestern Atlantic near Halifax, Canada.

During spring and early summer, high export production and remineralization of phytoplankton-derived organic matter resulted in increasing levels of particulate N and accumulation of ammonium (NH_4^+) in the basin bottom waters (60m). Elevated bottom water nitrate (NO_3^-) concentrations as well as an increase in $\delta^{15}\text{N-NH}_4^+$ and a corresponding decrease in $\delta^{15}\text{N-NO}_3^-$ clearly indicated active NH_4^+ and nitrite (NO_2^-) oxidation. In mid-summer, inflow of more saline Scotian Shelf water into the basin was observed and nitrifying activity markedly increased, likely driven by an increase in temperature and/or bottom water oxygen concentrations. Decreasing surface productivity in autumn was followed by a decline in subsurface NH_4^+ concentrations and a complete oxidation of the NH_4^+ pool to NO_3^- . The N isotopic compositions of NH_4^+ , NO_2^- , and NO_3^- followed a Rayleigh-type fractionation, with a fractionation factor for NH_4^+ oxidation of ~15 ‰.

P 14.14

Acidification enhances N₂O production by aquatic ammonia oxidizing microorganisms

Caitlin Frame¹, Evan Lau², Joe Nolan², Tyler Goepfert³ & Moritz Lehmann¹

¹ *Departement Umweltwissenschaften, University of Basel, Bernoullistrasse 30, 4056 Basel, Switzerland*
(caitlin.frame@unibas.ch)

² *Department of Natural Sciences and Mathematics, West Liberty University, 208 University Drive, West Liberty, WV 26074, USA*

³ *Helmholtz Center for Ocean Research, GEOMAR, Wischhofstrasse 1-3, 24148 Kiel, Germany*

Human activity has accelerated emission of the powerful greenhouse gas nitrous oxide (N₂O). Ammonia oxidizing microorganisms are an important source of N₂O in aquatic environments, but the impact that acidification has on their rate and mechanism of N₂O production is not well understood. The south basin of Lake Lugano (Switzerland) is a eutrophic system whose ammonia oxidizer community is dominated by the bacterial genus *Nitrosospira* in the shallow hypolimnion. Incubations of water drawn from 17m with either 1 micromolar ¹⁵NH₄⁺ or 1 micromolar ¹⁵NO₂⁻ were used to measure the rate and mechanism of N₂O production under four sets of O₂ concentrations and pH values: 1) 290 micromolar O₂, pH 7.54, 2) 70 micromolar O₂, pH 7.54, 3) 290 micromolar O₂, pH 7.20, and 4) 70 micromolar O₂, pH 7.20.

Measured ammonia oxidation rates were similar among all of the incubation conditions, ranging from 0.48 +/- 0.02 to 0.54 +/- 0.02 micromolar/day. By contrast, the rate of N₂O production was substantially higher at pH 7.20 than it was at pH 7.54. The rate of N incorporation from added ¹⁵NH₄⁺ into N₂O was higher than the rate of N incorporation from added ¹⁵NO₂⁻ in all experiments. At 290 micromolar O₂, reduction of the pH from 7.54 to 7.20 increased the rate at which NH₄⁺-derived N was incorporated into N₂O from 0.013 +/- 0.009 nM/day to 0.042 +/- 0.009 nM/day. In incubations where the O₂ was reduced to 70 micromolar, the rate of NH₄⁺-derived N incorporation increased from 0.031 +/- 0.009 nM/day at pH 7.54 to 0.059 +/- 0.01 nM/day at pH 7.20.

The increase in N₂O production with reduced pH was partially due to an increased incorporation of N from added NO₂⁻. At pH 7.20 and 290 micromolar O₂, the N incorporation from added NO₂⁻ was 0.007 +/- 0.005 nM/day and at 70 micromolar O₂, it was 0.009 +/- 0.004 nM/day. At pH 7.54, N incorporation from added NO₂⁻ was not significantly different from zero at either O₂ concentration. The production of m/z 45N₂O (¹⁵N¹⁴N¹⁶O or ¹⁴N¹⁵N¹⁶O) and not m/z 46N₂O (¹⁵N¹⁵N¹⁶O) during ¹⁵NO₂⁻ incubations is consistent with a 'hybrid' N₂O formation mechanism whereby NO₂⁻ or one of its derivatives is reduced by an intermediate of ammonia oxidation such as NH₂OH to N₂O. It is not consistent with N₂O formation by nitrifier denitrification (i.e. reduction of 2NO₂⁻ to N₂O).

Both 46N₂O and 45N₂O were produced during the ¹⁵NH₄⁺ experiments. Although this makes it clear that much of the N incorporated into N₂O was derived from NH₃ oxidized during these experiments, the ¹⁵N distribution of the N₂O could be explained by either hybrid N₂O formation by reaction of NH₂OH and (mainly) intracellular NO₂⁻ or by autooxidation of 2NH₂OH. We favor the first explanation, since the abiotic reaction of NH₂OH with NO₂⁻ accelerates as the pH drops toward the pKa of HNO₂ (2.8), whereas autooxidation of NH₂OH tends to accelerate as pH increases. Furthermore, previous studies have observed that enzyme extracts of ammonia oxidizing bacteria that convert NH₂OH and NO₂⁻ to N₂O have a pH optimum of 5.75 (Hooper, 1968).

REFERENCES

Hooper A. 1968: A nitrite-reducing enzyme from *Nitrosomonas europaea*, *Biochimica et Biophysica Acta*, 162, 49-65.

P 14.15**Estimation of O₂ influence on benthic nitrogen cycling in the south basin of Lake Lugano, Switzerland**

Adeline Cojean¹, Jakob Zopfi¹, Elizabeth Robertson², Bo Thamdrup², Moritz F. Lehmann¹,

¹ *Department of Aquatic and Stable Isotope Biogeochemistry, University of Basel, Bernoullistrasse 32, CH-4056 Basel (adeline.cojean@unibas.ch)*

² *Nordic Centre for Earth Evolution, Institute of Biology, University of Southern Denmark DK-5230 Odense M, Denmark*

Nitrogen (N) is an essential element for all living organisms, and high N loading in lakes can lead to eutrophication and excessive algal growth, leading to water column suboxia or anoxia. The microbially mediated removal of fixed N can help to mitigate N loading in lakes. Sediments represent a particularly important sink for reactive N via N₂ production either by denitrification or anammox. The dissimilatory reduction of nitrate to ammonium (DNRA) has been shown to be an important process in some environments. The relative partitioning between DNRA and N loss through denitrification or anammox is an important factor in the N budget of aquatic systems. In contrast to denitrification, DNRA returns reduced N to the system in a bioavailable form favored by primary producers. While coastal sediments have been well studied, a complete understanding of N transformation and elimination processes in lacustrine benthic systems is still lacking. Since all nitrate reduction (organotrophic and chemolithotrophic) and anammox is thought to be inhibited by oxygen, redox conditions are likely a significant controlling factor. Exact O₂ inhibition thresholds, however, are uncertain, and probably different for the respective N transformation pathways. Moreover, recent work has shown that denitrification (and DNRA) can be coupled to the oxidation of reduced iron species, but the quantitative importance of this process in freshwater environments is uncertain. The south basin of Lake Lugano is an ideal area to study benthic redox reactions because of its recent eutrophication during the second part of the last century, leading to seasonally anoxic conditions in the deep hypolimnion. The goal of this study was to determine N turnover rates under variable microaerobic oxygen concentrations in the muddy sediments of two sites in the south basin, Figino (iron-rich) and Melide (iron-poor), and to investigate the potential role of Fe in nitrate reduction. Conducting laboratory slurry experiments with ¹⁵N additions (¹⁵NO₃, ¹⁵NH₄), we determined the production of ¹⁵N-N₂ via denitrification and/or anammox as well as DNRA rates under controlled oxygen conditions (e.g., 0, 1, 2, 3, 4 and 0, 4, 8 μM of O₂ for Figino and Melide, respectively). At both sites anammox was measured only under anoxic conditions, yet rates were insignificant compared with those of denitrification. Partial inhibition of denitrification and DNRA by microaerobic levels of O₂ was also observed, yet with an apparently greater O₂ tolerance by DNRA bacteria. Overall higher ¹⁵N-N₂ production rates in Figino sediments, with higher Fe²⁺ concentrations, than in Melide hint at a coupling of denitrification and Fe²⁺ reduction. Ongoing slurry incubation work with Fe²⁺ amendments will help to assess the potential contribution of Fe²⁺-dependent denitrification to total nitrate reduction and fixed N loss in the Lake Lugano sediments.

15. Atmospheric Processes and Interactions with the Biosphere

Christof Ammann, Stefan Brönnimann, Lutz Merbold, Peter Waldner

*ACP – Commission on Atmospheric Chemistry and Physics,
ProClim – Forum for Climate and Global Change,
IGBP- Swiss Committee*

TALKS:

- 15.1 Aebi Ch., Gröbner J., Kämpfer N., Vuilleumier L.: Cloud radiative effect depending on cloud type and cloud fraction at three sites in Switzerland
- 15.2 Davin E., Maisonnave E., Seneviratne S.: Evaluation of a Regional Climate Model with improved land surface processes representation
- 15.3 Eugster M.: Global Precipitation Measurement (GPM): An example of how NASA brings current research into classrooms
- 15.4 Felber R., Neftel A., Ammann C.: The importance of organic carbon fluxes for the determination of a pasture carbon budget
- 15.5 Hörtnagl L., Bahn M., Buchmann N., Dias-Pinez E., Eugster W., Kiese R., Klumpp K., Ladreiter-Knauss T., Wohlfahrt G., Zeeman M., Merbold L.: Management influence on GHG fluxes over Central European grasslands
- 15.6 Juszak I., Iturrate-Garcia M., Schaepman-Strub G.: Influence of Arctic tundra vegetation on radiation and soil fluxes
- 15.7 Klein G., Vitasse Y., Filippa G., Marty C., Rixen C., Rebetez M.: Spatiotemporal patterns of snowmelt dates in the Swiss Alps shown by a new data processing method
- 15.8 Merbold L., Decock C., Hoertnagl L., Fuchs K., Eugster W.: No memory effects of restoration on N₂O exchange above an intensively managed grassland in Switzerland
- 15.9 Mystakidis S., Davin L.E., Gruber N. & Seneviratne I.S.: Hydrological and biogeochemical constraints on carbon cycle projections
- 15.10 Oney B., Gruber N., Henne S., Leuenberger M., Emmenegger L., Brunner D.: Determining the regional biospheric signal in CO₂ measurements using CO as a quantitative tracer for anthropogenic CO₂
- 15.11 Osterwalder S., Sommar J., Riedi J., Huang J.-H., Åkerblom, S., Nilsson M.B., Bishop K., Alewell C.: Elemental mercury evasion from contaminated and background soils in Switzerland and Sweden
- 15.12 Pfister C.: 500 years of weather data for surfing
- 15.13 Reimann S., Vollmer M.K., Schoenenberger F., Henne S., Brunner D. & Emmenegger L.: New halogenated greenhouse gases in the atmosphere: from anesthetics to mobile air conditioning
- 15.14 Zink K., Berchet A., Brunner D., Emmenegger L.: Simulating air pollution on the city scale
- 15.15 Zscheischler J., Blanken P., Bohrer G., Clark K., Desai A., Fatichi S., Hollinger D., Keenan T., Novick K.A., Wolf S., Seneviratne S.I.: Short-term weather variability is an important control of interannual variability in carbon and water fluxes in temperate forests

POSTERS:

- P 15.1 Buri A., Cianfrani C., Pradervand J-N., Guisan A.: Predicting plant distribution in an heterogeneous Alpine landscape: does soil matter?
- P 15.2 Ghiggi G., Mariethoz G., Berne A.: A Multiple Point Statistics Approach to Combine Weather Radar and Rain-Gauge Data
- P 15.3 Paul S., Ammann C., Alewell C., Leifeld J.: CO₂ and CH₄ exchange of a degrading fen, Seeland, Switzerland

15.1

Cloud radiative effect depending on cloud type and cloud fraction at three sites in Switzerland

Christine Aebi^{1,2}, Julian Gröbner¹, Niklaus Kämpfer², Laurent Vuilleumier³

¹ *Physikalisch-Meteorologisches Observatorium Davos, World Radiation Center, Dorfstrasse 33, CH-7260 Davos Dorf (christine.aebi@pmodwrc.ch)*

² *Oeschger Center for Climate Change Research and Institute of Applied Physics, University of Bern, Sidlerstrasse 5, CH-3012 Bern*

³ *Federal Office of Meteorology and Climatology MeteoSwiss, Chemin de l'Aérologie, CH-1530 Payerne*

Radiative transfer of energy in the atmosphere and the influence of clouds on the radiation budget remain the greatest sources of uncertainty in the simulation of climate change. Small changes in cloudiness and radiation can have large impacts on Earth's climate. Depending on the wavelength range, the effect of clouds on the radiation budget can have an opposing sign and may result in either a cooling or a warming of the atmosphere. For assessing this cloud effect and the corresponding changes, frequent and more precise radiation and cloud observations are necessary.

The role of clouds on the surface radiation budget is studied in order to quantify the longwave, shortwave and the total cloud radiative effect (CRE) depending on the atmospheric composition (e.g. temperature and integrated water vapour), the fractional cloud cover and the cloud type. The study is performed for three different sites in Switzerland at three different altitude levels: Payerne (490 m asl), Davos (1'560 m asl) and Jungfraujoch (3'580 m asl).

On the basis of data of visible all-sky camera systems at the three aforementioned stations in Switzerland, up to six different cloud types are distinguished (Cirrus-Cirrostratus, Cirrocumulus-Alto cumulus, Stratus-Altostratus, Cumulus, Stratocumulus and Cumulonimbus-Nimbostratus). These cloud types are classified with a modified algorithm of Heinle et al. (2010). This cloud type classifying algorithm is based on a set of statistical features describing the colour (spectral features) and the texture of an image (textural features) (Wacker et al., 2015). The calculation of the fractional cloud cover is based on spectral information of the all-sky camera data. The radiation data are taken from measurements with pyranometers and pyrgeometers at the different stations.

First we calculate the longwave and shortwave CRE for cases where only one cloud type is present. This calculation is performed for the two stations Jungfraujoch and Payerne and the six different cloud types separately. On the basis of case studies we get a better understanding about the influencing factors on the CRE. In a second step we expand the study in order to calculate a climatology over a whole year of the longwave and shortwave CRE and its sensitivity to integrated water vapour, cloud cover and cloud type for the three above-mentioned stations in Switzerland. For the calculation of the shortwave and longwave CRE the corresponding cloud-free reference models developed at PMOD/WRC are used (Wacker et al., 2013). As the study is restricted to daytime data so far (due to cameras measuring in the visible), we are developing an all-sky thermal infrared cloud cam (IRCCAM), which enables nighttime measurements and analyses as well.

REFERENCES

- Heinle, A., Macke A. & Srivastav A. 2010: Automatic cloud classification of whole sky images, *Atmospheric Measurement Techniques*.
- Wacker, S., Gröbner J. & Vuilleumier L. 2013: A method to calculate cloud-free long-wave irradiance at the surface based on radiative transfer modeling and temperature lapse rate estimates, *Theoretical and Applied Climatology*.
- Wacker, S., Gröbner J., Zysset C., Diener L., Tzoumanikis P., Kazantzidis A., Vuilleumier L., Stöckli R., Nyeki S. & Kämpfer N. 2015: Cloud observations in Switzerland using hemispherical sky cameras, *Journal of Geophysical Research*.

15.2

Evaluation of a Regional Climate Model with improved land surface processes representation

Edouard Davin¹, Eric Maisonnave² & Sonia Seneviratne¹

¹ *Institute for Atmospheric and Climate Science, ETH Zurich, CH-8092 Zurich (edouard.davin@env.ethz.ch)*

² *CERFACS, 31100 Toulouse, France*

The representation of land surface processes and fluxes in climate models critically affects the simulation of near-surface climate over land. Here we present an evaluation of a Regional Climate Model (COSMO-CLM) augmented by a state-of-the-art Land Surface Model (CLM4.0). Given the relatively simple land surface module included in the original COSMO-CLM, this coupling with CLM4.0 aims at improving the representation of land surface processes in the model system.

We performed historical simulations over Europe with this newly developed coupled system following the EURO-CORDEX intercomparison protocol. We then evaluate simulations performed with our coupled system, the standard COSMO-CLM and other EURO-CORDEX RCMs against various observational datasets of temperature, precipitation and surface fluxes. Overall, the results indicate that the coupled system outperforms both the standard COSMO-CLM and the other EURO-CORDEX models in simulating sensible, latent and radiative fluxes as well as 2-meter temperature across different seasons and regions. The performance improvement is particularly strong for turbulent fluxes and for daily maximum temperatures and more modest for daily minimum temperature, indicating that land surface processes affect daytime more than nighttime temperatures. The coupled system also alleviates a long-standing issue of overestimation of interannual summer temperature variability present in all EURO-CORDEX models. For precipitation, the coupling does not result in any clear improvement, suggesting that land processes are more critical for the simulation of surface temperature than for precipitation. Finally, we show that several factors contribute to the performance improvements achieved with the coupled system. In particular the representation of ground heat flux plays an important role, an aspect that has received so far only very little attention from the climate and land modelling community.

15.3

Global Precipitation Measurement (GPM): An example of how NASA brings current research into classrooms

Markus Eugster

Sekundarschule, Schoentalstrasse 2, 9244 Niederuzwil (markus.eugster@schule-uzwil.ch)

In a nutshell

With monthly webinars NASA succeeded in inspiring teachers and students of the current GPM mission, in explaining complex technology and fundamental processes in the Earth's systems to the public and probably in influencing some students in their choice of field of study.

The GPM mission

The GPM = Global Precipitation Measurement mission is a joint venture of NASA and JAXA (Japan Aerospace Exploration Agency) and is a constellation of ten satellites that collaborate to get a worldwide precipitation picture every three hours. The GPM core observatory carries a microwave imager (GMI) and a dual-frequency precipitation radar (PR) and orbits our planet at 407km every 93min. Unlike its predecessor, TRMM, it covers a wider area up to the polar circles and can even detect snowfall.

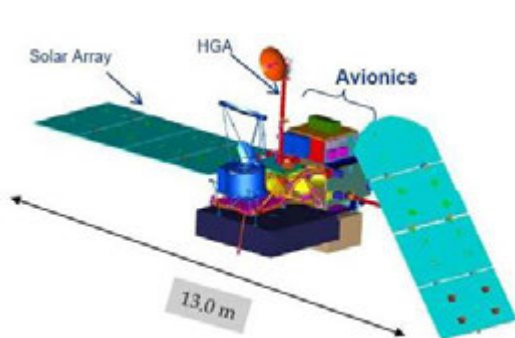


Figure 1: The GPM core observatory

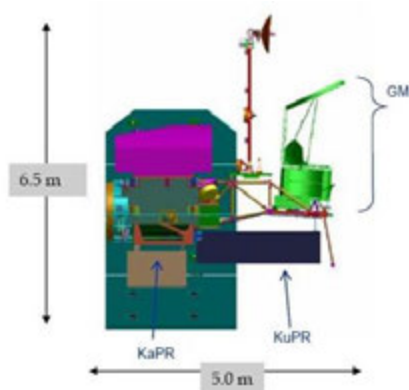


Figure 2: The satellite's instruments

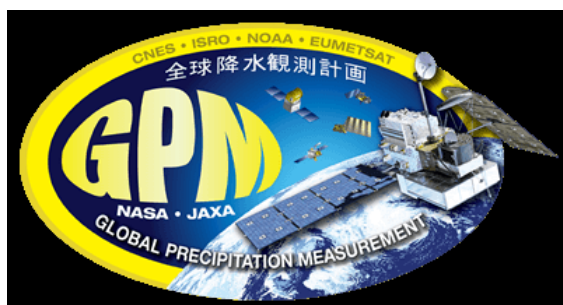


Figure 3: The GPM logo

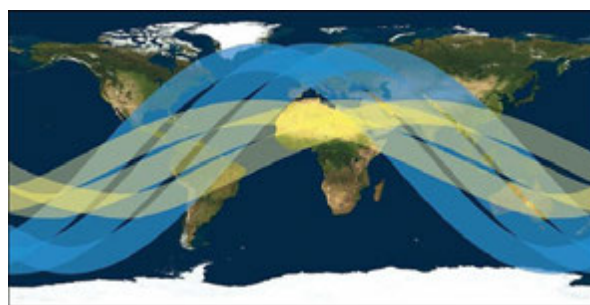


Figure 4: yellow: TRMM; blue: GPM

NASA's educational program

NASA employs a handful of specialists who develop educational material such as videos, lesson plans, student capture sheets, presentations, teachers' guides, etc. NASA collaborates with the GLOBE program (Global Learning and Observations to Benefit the Environment): a GLOBE precipitation measurement campaign served as ground validation.

Concept of the GPM master teacher program

After the application the participants were chosen in a test webinar with all the candidates. About 20 candidates formed the GPM master teacher cohort. We met in monthly webinars. Each time there was a presentation of an involved scientist with an opportunity to ask questions and two or three short presentations of the participants. After a pre-assessment we used some of the NASA materials (texts, pictures, activities, experiments, videos, IQuests) in our lessons and checked the success with post-assessments. We proposed improvements and developed additional material, gave feedback in surveys and kept an online journal about all our GPM related activities.

Side effects

We could make contact to NASA scientists, collaborate with other master teachers, learn more about GPM mission applications and gain insight into other NASA fields of research.

References

About GPM: <http://pmm.nasa.gov/GPM>

Educational resources: <http://pmm.nasa.gov/education/>

Connection to GLOBE: <http://www.globe.gov/web/gpm/>

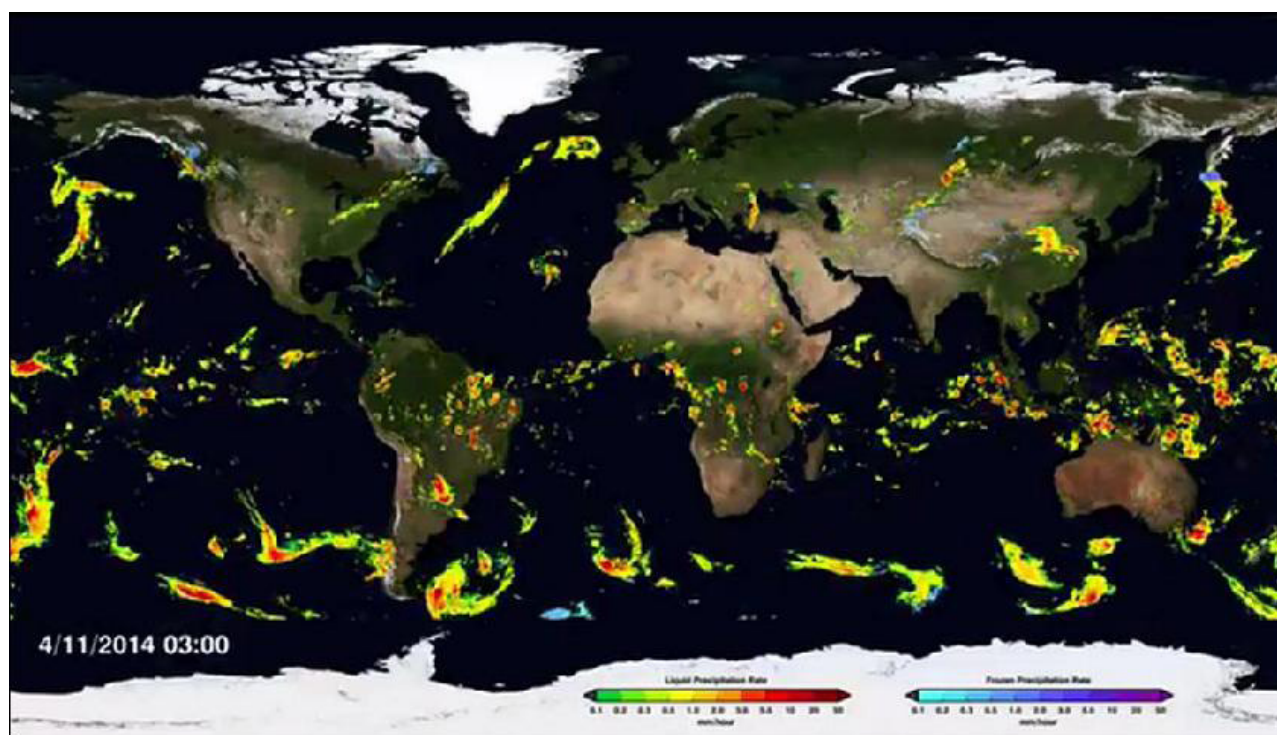


Figure 5: Still taken in the first GPM animation of worldwide precipitation

Source Fig. 1 – 5: NASA / GPM

15.4

The importance of organic carbon fluxes for the determination of a pasture carbon budget

Raphael Felber¹, Albrecht Neftel¹ & Christof Ammann¹

¹ Agroscope Research Station, Climate and Air Pollution Group, Reckenholzstrasse 191, CH-8046 Zürich
(raphael.felber@agroscope.admin.ch)

Grasslands act as sinks and sources for greenhouse gases (GHG) and are, in conjunction with livestock production systems, responsible for a large share of agricultural GHG emissions. Soil carbon (C) sequestration is considered as a potential important mechanism to mitigate GHG emissions of the agricultural sector (Soussana et al, 2010). For shorter time periods the carbon sequestration can be determined by the net ecosystem carbon budget (NECB) approach, which describes the change of soil C as the sum of all relevant import and export C fluxes. These fluxes include the CO_2 exchange (net ecosystem exchange NEE), the CH_4 exchange as well as carbon exported and imported into the system in slurry and products (e.g., export of grass or export as milk).

In our study we evaluated and compared two approaches (Fig. 1) to calculate the NECB for a grazed pasture in Switzerland. Approach (a) includes the cows in the system boundaries, whereas the system boundaries of approach (b) comprises the soil only; the cows remove C while grazing and return C by the excreta. NEE and the CH_4 loss from cows and soil was measured using the eddy covariance method. In few existing studies two procedures have been suggested to determine the annual NEE of grazed pasture: (a) treating the cow respiration as part of total ecosystem respiration (Soussana et al., 2007) and gap fill the entire flux dataset including cow contributions; and (b) discarding all cases with cows in the footprint (Skinner, 2008) and gap filling the remaining dataset. These two approaches correspond to the NEEs of the two investigated system boundaries. For a reliable allocation of the fluxes for the two systems, cows were equipped with GPS devices. The detailed position information together with a footprint analysis allowed on one hand a reliable distinction between fluxes with and without cow contributions and on the other hand the determination of cow emissions during grazing (Felber et al, 2015). Organic C fluxes were directly measured or determined from the cow C budget.

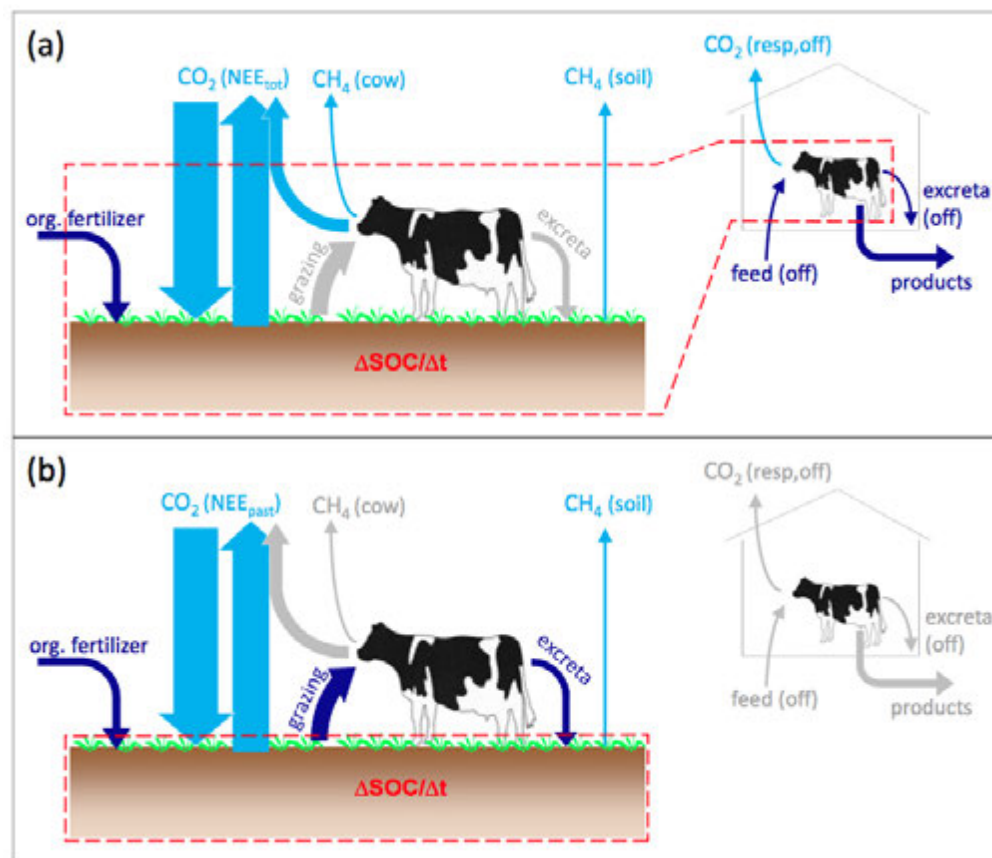


Figure 1. Illustrations of the two approaches to determine soil carbon change of a pasture system using different system boundaries (dashed red lines) and the relevant carbon fluxes (coloured arrows).

Both approaches yielded very similar results indicating a near-neutral C budget, but with considerable uncertainties. The NECB uncertainty was mainly associated to the uncertainty of the NEE determination. Additionally the detailed analysis of the organic carbon fluxes revealed their importance in both approaches. These C fluxes showed considerably lower uncertainties compared to the NEE uncertainty.

REFERENCES

- Felber, R., Munger, A., Neftel, A. & Ammann, C. 2015: Eddy covariance methane flux measurements over a grazed pasture: effect of cows as moving point sources, *Biogeosciences*, 12, 3925-3940.
- Skinner, R.H. 2008: High biomass removal limits carbon sequestration potential of mature temperate pastures, *Journal of Environment Quality*, 37, 1319-1326.
- Soussana, J.F., Allard, V., Pilegaard, K., Ambus, P., Amman, C., Campbell, C., Ceschia, E., Clifton-Brown, J., Czobel, S., Domingues, R., Flechard, C., Fuhrer, J., Hensen, A., Horvath, L., Jones, M., Kasper, G., Martin, C., Nagy, Z., Neftel, A., Raschi, A., Baronti, S., Rees, R.M., Skiba, U., Stefani, P., Manca, G., Sutton, M., Tuba, Z. & Valentini, R. 2007: Full accounting of the greenhouse gas (CO₂, N₂O, CH₄) budget of nine European grassland sites, *Agriculture, Ecosystems & Environment*, 121, 121-134.
- Soussana, J.F., Tallec, T. & Blanfort, V. 2010: Mitigating the greenhouse gas balance of ruminant production systems through carbon sequestration in grasslands, *Animal*, 4, 334-350.

15.5

Management influence on GHG fluxes over Central European grasslands

Lukas Hornagl¹, Michael Bahn², Nina Buchmann¹, Eugenio Dias-Pinez³, Werner Eugster¹, Ralf Kiese³, Katja Klumpp⁴, Thomas Ladreiter-Knauss², Georg Wohlfahrt², Matthias Zeeman³ and Lutz Merbold¹

¹ *ETH Zurich, Institute of Agricultural Sciences, Zurich, Switzerland (lukas.hoertnagl@usys.ethz.ch)*

² *University of Innsbruck, Institute of Ecology, Innsbruck, Austria*

³ *Karlsruhe Institute of Technology (KIT), Institute of Meteorology and Climate Research, Karlsruhe, Germany*

⁴ *INRA, Grassland Ecosystem Research, Clermont-Ferrand, France*

Agricultural management practices and land use change at grassland sites can have a strong impact on annual carbon dioxide (CO₂), methane (CH₄) and nitrous oxide (N₂O) budgets. At the same time emissions of CH₄ and N₂O can contribute to an increase of the global warming potential (GWP) of an ecosystem by offsetting concurrent CO₂ uptake in terms of CO₂-equivalents. It is therefore necessary to quantify long-term fluxes of all three compounds in order to reliably assess the climatic impact of management activities and the effectiveness of greenhouse gas (GHG) mitigation strategies.

In this presentation we give an overview of the GHG exchange of eleven managed Central European grassland sites along an elevation and land use intensity gradient. Fluxes of the three major GHGs CO₂, CH₄ and N₂O were calculated using the eddy covariance or chamber technique. The investigated grasslands were different with regard to the amount of fertilizer input, frequency of cuts and grazing duration and intensity.

In this presentation we focus on time periods when measurements of all three compounds were available and investigate common features among observed CH₄ and N₂O exchange patterns at the different grassland sites. We analyze these observations in relation to management activities and concurrently measured biotic / abiotic parameters. For field sites where long-term measurements are available we evaluate the impact of CH₄ and N₂O fluxes on the annual GWP.

15.6

Influence of Arctic tundra vegetation on radiation and soil fluxes

Inge Juszak¹, Maitane Iturrate-Garcia¹ & Gabriela Schaepman-Strub¹

¹ *Institute of Evolutionary Biology and Environmental Studies, University of Zurich, Winterthurerstrasse 190, CH-8057 Zurich (inge.juszak@ieu.uzh.ch)*

Vegetation changes such as shrub encroachment have been observed in the Arctic tundra and further changes are predicted due to climate change (Myers-Smith et al. 2015). These changes feed back to climate through altering the surface energy balance. Shrubs can reduce the albedo and thus enhance air and soil temperature warming at the larger scales (Lawrence & Swenson 2011). On the other hand, shrubs may cool the permafrost soil locally through shading (Blok et al. 2010). We asked in how far the shortwave radiation budget of two widespread tundra vegetation types explained soil heat fluxes and active layer thickness.

We measured time series of soil heat flux and temperature as well as radiation fluxes above and below two vegetation types, dwarf shrubs (*Betula nana*) and sedges (*Eriophorum angustifolium*) at the Kytalyk field site, North-East Siberia (70.8°N, 147.5°E). Additionally, we measured reflected and below canopy transmitted photosynthetically active radiation, active layer thickness, vegetation height and leaf area index at eight plots per vegetation type. We found a lower growing season albedo of dwarf shrubs (0.15) as compared to sedges (0.17). However, sedges shaded the soil more efficiently than dwarf shrubs, the average growing season transmittance was 0.28 and 0.36 for sedges and shrubs, respectively. We measured deeper active layers and higher soil heat fluxes below sedges as compared to dwarf shrubs.

Our data suggests that neither the above canopy radiative balance nor soil shading explains the reduced soil heat flux and active layer thickness below dwarf shrubs as compared to sedges. However, we found differences between shrub and sedge soil properties, such as thermal conductivity and soil albedo, which may partly explain the observed differences between soil heat fluxes.

REFERENCES

- Blok, D., Heijmans, M. M. P. D., Schaepman-Strub, G., Kononov, A. V., Maximov, T. C. & Berendse, F. 2010: Shrub expansion may reduce summer permafrost thaw in Siberian tundra, *Global Change Biology*, 16, 1296-1305
- Lawrence, D. M. & Swenson, S. C. 2011: Permafrost response to increasing Arctic shrub abundance depends on the relative influence of shrubs on local soil cooling versus large-scale climate warming, *Environmental Research Letters*, 6, 045504
- Myers-Smith, I. H., Elmendorf, S. C., Beck, P. S. A., Wilmking, M., et al. 2015: Climate sensitivity of shrub growth across the tundra biome, *Nature Climate Change*, 5, 887-891

15.7

Spatiotemporal patterns of snowmelt dates in the Swiss Alps shown by a new data processing method

Geoffrey Klein^{1,2}, Yann Vitasse^{1,2,3}, Gianluca Filippa⁴, Christoph Marty³ & Christian Rixen³, Martine Rebetez^{1,2}

¹ *University of Neuchâtel, Institute of Geography, Neuchâtel, Switzerland*

² *WSL Swiss Federal Institute for Forest, Snow and Landscape Research, Neuchâtel, Switzerland*

³ *WSL Institute for Snow and Avalanche Research SLF, Group Mountain Ecosystems, Davos, Switzerland*

⁴ *ARPA Valle d'Aosta, Saint-Christophe(AO), Italy*

In alpine terrains, climate change is expected to cause major modifications on the environment, in particular through changes in the snow conditions. The effects of the temperature increase on the snowpack and snowmelt timing are critical for alpine ecosystems (Wheeler et al. 2014), as well as for winter tourism (Rixen et al. 2011) or hydrological regimes (Confortola et al. 2013). Despite the expected relevance of the snowmelt time in spring, snowmelt patterns are still largely missing in scientific literature, due to lack of in-situ measurements at high elevation.

Here, we analyzed snow height and temperature data from 123 automatic meteorological stations located in remote areas from 1600 to 3000 m asl in the Swiss Alps over the period 1993-2014. We developed an algorithm based on manual data processing to accurately determine the snowmelt date. We then described the spatial and temporal patterns of the snowmelt date over the study period and in connection with some longer series originating from traditional manual observations since the 1950's.

The algorithm procedure for the analysis of the automatic series consisted in first removing outliers from snow depth, ground surface and snow surface temperature, and then filling short data gaps based on the temperature measured before and after the missing data.

Finally, the annual spring snowmelt date was set for each station, as the first full snow-free day of the spring/summer period (Jonas et al. 2008).

This method gave robust snowmelt dates with only a few outliers that were discarded.

The method developed here provides accurate snowmelt dates that could be further investigated particularly in connection with alpine plant growth and phenology.

REFERENCES

- Confortola, G., Soncini, A., & Bocchiola, D. 2013: Climate change will affect hydrological regimes in the Alps, *Journal of Alpine Research* 101-3.
- Jonas, T., Rixen, C., Sturm, M. & Stoeckli, V. 2008: How alpine plant growth is linked to snow cover and climate variability, *Journal of Geophysical Research-Biogeosciences*, 113(G3).
- Rixen, C., Teich, M., Lardelli, C., Gallati, D., Pohl, M., Putz, M. & Bebi, P. 2011: Winter Tourism and Climate Change in the Alps: An Assessment of Resource Consumption, Snow Reliability, and Future Snowmaking Potential, *Mountain Research and Development*, 31(3), 229-236.
- Wheeler, J.A., Hoch, G., Cortés, A.J., Sedlacek, J., Wipf, S. & Rixen, C. 2014: Increased spring freezing vulnerability for alpine shrubs under early snowmelt, *Oecologia*, 1-11.

15.8

No memory effects of restoration on N₂O exchange above an intensively managed grassland in Switzerland

Lutz Merbold¹, Charlotte DeCock¹, Lukas Hörtnagl¹, Kathrin Fuchs¹, Werner Eugster¹

¹ *Department of Environmental Systems Science, Institute of Agricultural Sciences, ETH Zurich, Switzerland*
(lutz.merbold@usys.ethz.ch)

Here we present three consecutive years of eddy covariance flux measurements of N₂O, CH₄ and CO₂ carried out in intensively managed grassland in Switzerland (Chamau, CHA). Our measurements of greenhouse gas (GHG) concentrations were based on a recently developed continuous-wave quantum cascade laser spectrometer to measure the concentrations of N₂O and CH₄ and an open-path infrared gas analyzer to measure the concentrations of CO₂ and H₂O. We investigated the magnitude of these trace gas emissions during a year of major disturbance (grassland restoration - including ploughing, harrowing, sowing as well as fertilization with inorganic and organic fertilizers in 2012) and the two following years representing business as usual (up to 6 harvests events per year which are followed by organic fertilizer application, 2013 and 2014).

We observed large peaks of N₂O (up to 50 nmol m⁻² s⁻¹ compared to < 5 nmol m⁻² s⁻¹ as the background flux) in 2012 (Merbold et al. 2014) during thawing of the soils after the long winter period and after re-sowing as well as inorganic fertilizer application at the beginning of the summer season. N₂O emissions following harvest and organic fertilizer application at the end of 2012 and in 2013 as well as 2014 ranged between 2 and 7 nmol m⁻² s⁻¹ and background fluxes were no larger than 1 nmol m⁻² s⁻¹.

Fluxes of N₂O were primarily controlled by soil water content and temperature, while management activities lead commonly to larger variation of N₂O fluxes during several days after the management event when compared to the background flux measured during periods without management. Annual flux budgets were dominated by CO₂ emissions and N₂O emissions contributed largely to the annual budget in 2012 but to a much lesser extend in the post-disturbance years (2013/2014). CH₄ flux contribution to the annual budget was negligible.

We conclude that grassland restoration results in large N₂O emissions, while not leading to larger N₂O emissions in subsequent years. Still, such specific time periods of enhanced N₂O emissions need to be considered in decadal greenhouse gas budget estimates due to the fact that a single year can offset previous carbon and nitrogen sinks. We further highlight the potential of recently developed quantum cascade laser spectrometers that are coupled to an eddy covariance system as a powerful tool to determine N₂O flux variation and changes in magnitudes at an unprecedented precision. Only if these systems are deployed for sufficient time periods (several years) researchers are enabled to identify periods of large N₂O emissions at ecosystem scale, which may not be captured with conventional chamber approaches.

15.9

Hydrological and biogeochemical constraints on carbon cycle projections

Stefanos Mystakidis ^{1,3} Edouard L. Davin ¹, Nicolas Gruber ^{2,3} & Sonia I. Seneviratne ^{1,3}

¹ *Institute for Atmospheric and Climate Science, ETH Zurich, Universitätsstrasse 16, CH-8092 Zurich (stefanos.mystakidis@env.ethz.ch)*

² *Environmental Physics, Institute of Biogeochemistry and Pollutant Dynamics, ETH Zurich, Universitätsstrasse 16, CH-8092 Zurich*

³ *Center for Climate Systems Modeling, ETH Zurich, Universitätsstrasse 16, CH-8092 Zurich*

The terrestrial biosphere is currently acting as a sink for about a quarter of the total anthropogenic CO₂ emissions. However, the future fate of this sink in the coming decades is very uncertain, as current Earth System Models (ESMs) simulate diverging responses of the terrestrial carbon cycle to upcoming climate change. Here, we use observation-based constraints of water and carbon fluxes to reduce uncertainties in the projected terrestrial carbon cycle response derived from simulations of ESMs conducted as part of the 5th phase of the Coupled Model Intercomparison Project (CMIP5). We find in the ESMs a clear linear relationship between present-day Evapotranspiration (ET) and Gross Primary Productivity (GPP), as well as between these present-day fluxes and projected changes in GPP, thus providing an emergent constraint on projected GPP. Constraining the ESMs based on their ability to simulate present-day ET and GPP leads to a substantial decrease of the projected GPP and to a 50% reduction of the associated model spread in GPP by the end of the century. Given the strong correlation between projected changes in GPP and in NBP in the ESMs, applying the constraints on Net Biome Productivity (NBP) reduces the model spread in the projected land sink by more than 30% by 2100. Moreover, the projected decline in the land sink is at least doubled in the constrained ensembles and the probability that the terrestrial biosphere is turned into a net carbon source by the end of the century is strongly increased. This indicates that the decline in the future land carbon uptake might be stronger than previously thought, which would have important implications for the rate of increase of the atmospheric CO₂ concentration and for future climate change. Emergent constraints on global carbon cycle feedbacks will also be discussed.

15.10

Determining the regional biospheric signal in CO₂ measurements using CO as a quantitative tracer for anthropogenic CO₂

Brian Oney^{1,2}, Nicolas Gruber^{2,3}, Stephan Henne¹, Markus Leuenberger⁴, Lukas Emmenegger^{1,2} & Dominik Brunner^{1,2}

¹ Empa, Lab. for Air Pollution/Environmental Technology, Überlandstr. 129, CH-8053 Dübendorf

² ETH Zurich, Center for Climate Systems Modeling, Universitätsstr. 16, CH-8092 Zurich

³ ETH Zurich, Inst. of Biogeochemistry und Pollutant Dynamics, Universitätsstr. 16, CH-8092 Zurich

⁴ Univ. of Bern, Physics Inst., Climate and Environmental Division,
and Oeschger Centre for Climate Change Research, Sidlerstrasse 5, CH-3012 Bern

When inversely modeling the biospheric CO₂ flux using CO₂ concentration measurements on a regional scale, the anthropogenic (CO_{2,A}) and background (CO_{2,BG}) components need to be estimated and subtracted from the measured CO₂ to derive the residual biospheric signal (CO_{2,B}). The estimation of CO_{2,A} and CO_{2,BG} often entails employing an anthropogenic emission inventory and an atmospheric transport model, both of which are plagued by random and systematic uncertainties. Here, we present a method to circumvent these issues using collocated measurements of carbon monoxide (CO) as a quantitative tracer of CO_{2,A} and estimating the CO₂ background concentrations from measurements. To this end, background CO₂ and CO signals are derived from measurements at the remote, high altitude site Jungfraujoch (3580 m asl), and CO measurements from the target site (at low altitude) above this CO background are converted into CO_{2,A} using a site-specific CO:CO₂ ratio derived from observed wintertime CO and CO₂. To demonstrate this method's plausibility, we apply it to two CarboCount-CH measurement sites in the Swiss Plateau, and compare with CO₂ concentrations directly simulated with the Lagrangian transport model FLEXPART-COSMO for reference. Evaluating wintertime timeseries shows that the measurement-based CO₂ concentration estimates perform much better than modeled estimates (e.g. R: 0.48 to 0.95; Figure 1). During summertime, the residual measurement-based CO_{2,B} shares many similarities with the residual model-based CO_{2,B} and the values directly simulated with the Vegetation Photosynthesis and Respiration Model (VPRM) as the biospheric flux inventory in the FLEXPART-COSMO simulation (Figure 2). However, the residual measurement-based CO_{2,B} indicates a weaker uptake of CO₂ over the Swiss Plateau than predicted when using the model-based method, and much weaker than directly modeled by FLEXPART-COSMO with VPRM. In conclusion, given the wintertime evaluation, the proposed method improves the ability to estimate biogenic CO₂ signals, which has implications for the magnitude of the Swiss biospheric CO₂ flux.

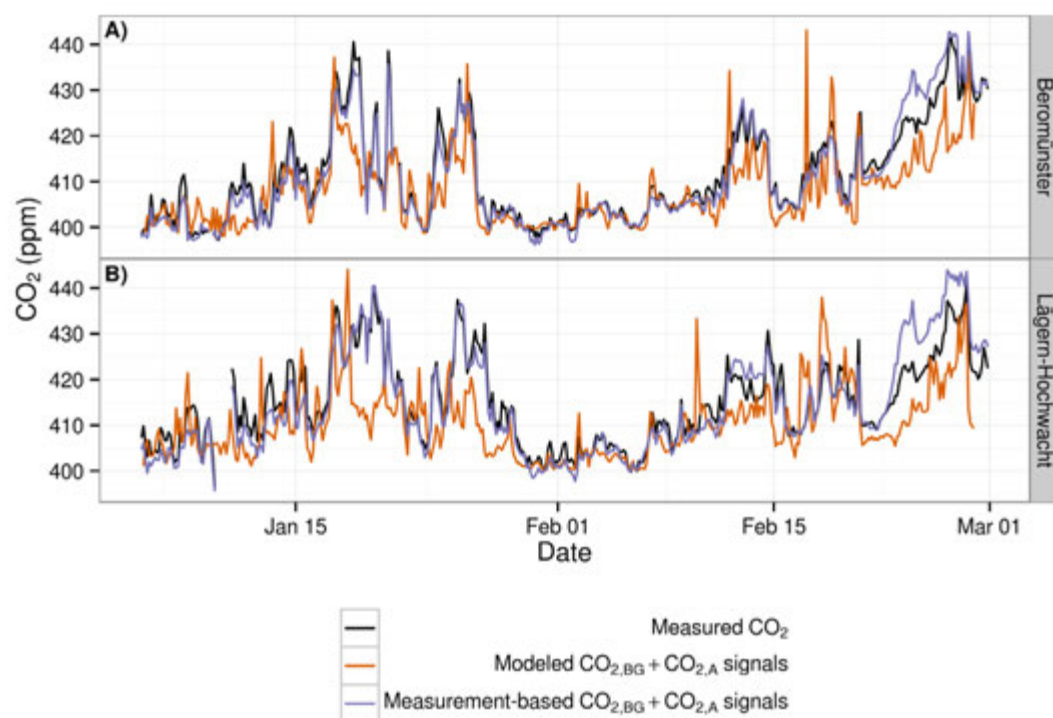


Figure 1. Time-series plot with the measured CO₂, modeled, measurement-based CO₂ during late wintertime at two CarboCount sites. It is assumed that the biogenic signal is negligible during winter.

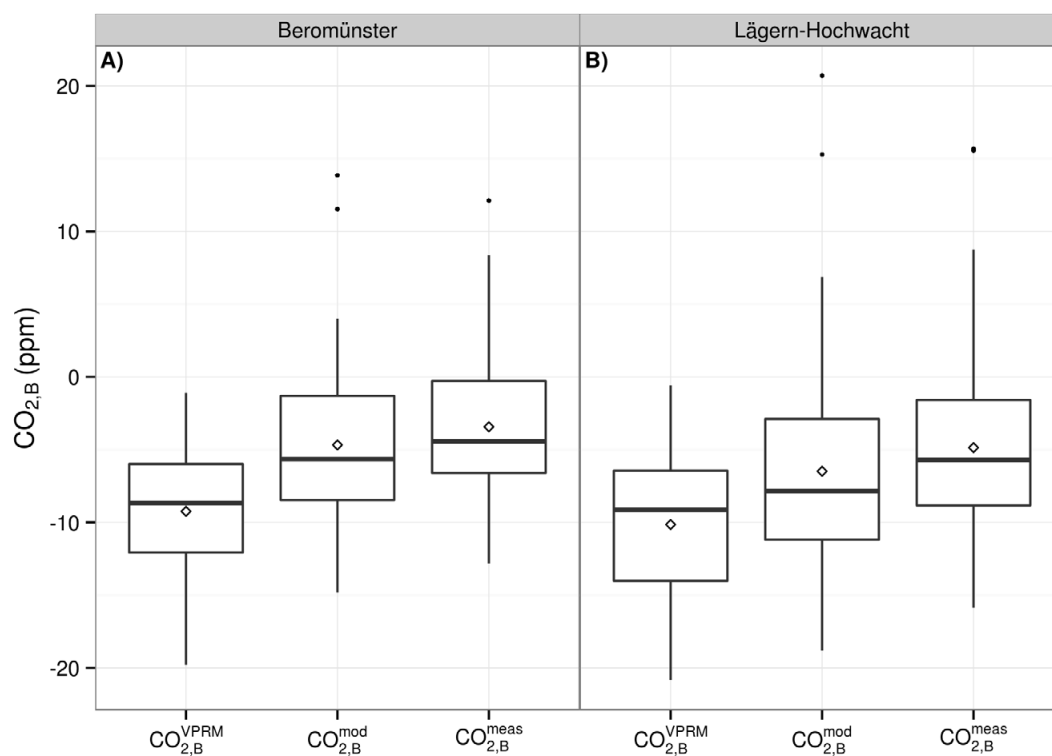


Figure 2. Summertime afternoon (1200-1500 UTC) biogenic signals ($\text{CO}_{2,B}$) at two CarboCount sites. The employed methods from left to right: directly modeled (VPRM), residual $\text{CO}_{2,B}$ using modeled $\text{CO}_{2,A}$ and $\text{CO}_{2,BG}$ (mod), residual $\text{CO}_{2,B}$ using $\text{CO}_{2,A}$ and $\text{CO}_{2,BG}$ derived from measurements (meas). The diamond points indicate the mean for each site and method.

15.11

Elemental mercury evasion from contaminated and background soils in Switzerland and Sweden

Stefan Osterwalder¹, Jonas Sommar², Jacqueline Riedi¹, Jen-How Huang¹, Staffan Åkerblom³, Mats B. Nilsson⁴, Kevin Bishop³, and Christine Alewell¹

¹ Department of Environmental Sciences, University of Basel, Bernoullistrasse 30, CH-4056 Basel
(stefan.osterwalder@unibas.ch)

² Institute of Geochemistry, Chinese Academy of Sciences, 46 Guanshui Road, 550002 Guiyang, China

³ Department of Aquatic Sciences and Assessment, Swedish University of Agricultural Sciences, Lennart Hjelms väg 9, SE-75236 Uppsala

⁴ Department of Forest Ecology and Management, Swedish University of Agricultural Sciences, Skogsmarksgränd, SE-901 83 Umeå

Mercury (Hg) is a potent neurotoxin and ubiquitous in the environment. Anthropogenic activities such as mining and burning of fossil fuels have significantly increased the global mercury cycling. In the atmosphere, elemental gaseous Hg (Hg^0) is the predominant form. This is transported and deposited to remote places far away from emission sources (Schroeder & Munthe, 1998). Re-emission of legacy Hg^0 from terrestrial surfaces has been reported to account for two-thirds of the worldwide Hg emissions (Streets et al., 2011). Aside from the Hg intake via seafood consumption, chronic or acute exposure by inhalation of Hg^0 in the air may be another important pathway (Syversen & Kaur, 2012). Thus, more comprehensive investigations about Hg^0 re-emission from different terrestrial surfaces are urgently required.

We quantified re-emission of Hg^0 from a background, anoxic mire soil ($< 0.1 \text{ mg Hg kg}^{-1}$) in northern Sweden as well as from contaminated, oxic soils ($1 - 200 \text{ mg Hg kg}^{-1}$) within settlement areas in Visp and Turtig, Switzerland. All-day measurements from 8 different plots in the boreal mire and 9 sites in Visp and Turtig were performed using dynamic flux chambers (DFCs) (details in Lin et al. 2012). In parallel, soil parameters (total Hg, soil temperature and soil moisture) and meteorological variables such as air temperature (inside and outside the DFC), relative humidity, solar irradiation wind speed and wind direction were measured to determine the factors influencing land-atmosphere Hg^0 exchange. By investigating Hg^0 fluxes in these very contrasting ecosystems, we wanted to first estimate the role of surface emission in regulating the pool of Hg in mires and the loading of methylmercury to surface waters. Secondly, we evaluated the potential of contaminated soils as sources to atmospheric Hg and furthermore to examine whether the current Hg evasion at contaminated sites in Visp and Turtig may cause public health problems.

The exchange of Hg^0 from the peatland surface was measured continuously during cloudless conditions in July 2014 and averaged $0.6 \pm 1.3 \text{ ng m}^{-2} \text{ h}^{-1}$. The flux revealed a significant diurnal pattern and a strong correlation with air temperature inside and outside the DFC. Preliminary results from ongoing measurements in Visp and Turtig highlight largely elevated Hg^0 fluxes ($30 - 2000 \text{ ng m}^{-2} \text{ h}^{-1}$), even though the DFC was shaded to ensure comparability among the different sites. In the contaminated sites we found a strong correlation between total Hg concentration in the soil and Hg^0 fluxes. Hg^0 air concentrations in northern Sweden reflected hemispheric background concentrations between 1 and 2 ng m^{-3} while up to 15 ng m^{-3} were measured in the air over the contaminated sites in Visp and Turtig.

The Degerö mire is hydrologically connected to downstream fresh waters and plays an important role in Hg and MeHg mobility. The estimated additional Hg export from Degerö via volatilization indicates that the time-span for reduced Hg emissions to translate into lower Hg levels in the soil are overestimated because up to now the emission of Hg from the mire surface to the atmosphere has not been considered.

The Hg contaminated soils in Visp and Turtig can be a major source of Hg^0 to the local atmosphere, which substantially elevated Hg^0 concentrations in the air one meter above the surface by a factor of 2 to 8. However a harmful chronic exposure of humans to Hg vapour is unlikely since all the Hg^0 concentrations are much smaller than workplace exposure limits (BAG, 2012)

REFERENCES

- Bundesamt für Gesundheit. 2012: Factsheet Quecksilber, available at: <http://www.bag.admin.ch/themen/chemikalien> (last access: 28.08.2015), 5 pp.
- Lin, C.-J., Zhu, W., Li, X., Feng, X., Sommar, J. & Shang, L. 2012: Novel dynamic flux chamber for measuring air-surface exchange of Hg^0 from Soils. *Environ. Sci. Technol.*, 46, 8910–8920.
- Schroeder, W.H. & Munthe, J. 1998: Atmospheric mercury - An overview. *Atmos. Environ.* 32, 809–822.
- Streets, D.G., Devane, M.K., Lu, Z., Bond, T.C., Sunderland, E.M. & Jacob, D.J. 2011: All-time releases of mercury to the atmosphere from human activities. *Environ. Sci. Technol.*, 45, 10485–10491.
- Syversen, T. & Kaur, P. 2012: The toxicology of mercury and its compounds. *J. Trace Elem. Med. Biol.*, 26, 215–226.

15.12

500 years of weather data for surfing

Christian Pfister¹

¹ *Oeschger Centre for Climate Change Research, University of Bern, Falkenplatz 16, CH-3012 Bern
(christian.pfister@hist.unibe.ch)*

The new data-base Euro-Climhist <http://www.euroclimhist.unibe.ch/de/> contains about 150'000 weather observations and climate data for Switzerland over the period since 1501, mostly for the period prior to the beginning of instrumental network observations in 1864. The paper presents the data base using examples of extreme events. Daily weather observations over the period 1684 to 1863 account for the lion's share of the evidence. Additional data are situated on the temporal level of months and seasons. Monthly weather reports are available from 1820 to 1999. The evidence is obtained from archival material and publications. The spectrum covers weather events in terms of wet, dry, cold and hot periods including impacts on agriculture, forestry and the wider economy (hailstorms, windstorms, frosts, droughts, wetness, snow, floods). Very long series, for instance about the number of rainy days (from 1684) and the sum of monthly precipitation (from 1706) are presented for the first time. Phenological observations mostly concerning phenophases of cereals, fruit and vines were frequently laid down prior to the late 19th century, because they were known to be temperature proxies close to people's experience. Systematic observations are available from the early 18th century. Johann Rudolf Rieter, a baker from Winterthur (Canton Zurich) has systematically laid down 19 phenological phases in his weather diary from 1721 to 1738. Very long series from the late 19th century to present are available for the flowering of snow-drop (*Galanthus nivalis*), hazel (*Corylus avellana*) and horse chestnut (*Aesculus hippocastanum*). For the first time, this wealth of different data may be accessed, cross-checked and used for follow-up investigations. In conclusion, may be said that most extremes of the instrumental period were exceeded once or several times within the period 1501 to 1863. This also concerns the hot summer of 2003.

15.13

New halogenated greenhouse gases in the atmosphere: from anesthetics to mobile air conditioning

Stefan Reimann, Martin K. Vollmer, Fabian Schoenenberger, Stephan Henne, Dominik Brunner & Lukas Emmenegger

Laboratory for Air Pollution and Environmental Technology, Empa, Swiss Federal Laboratories for Materials Science and Technology, Ueberlandstr. 129, CH-8600 Duebendorf (stefan.reimann@empa.ch)

Halogenated trace gases are typically categorized into 'generations' of compound classes following the evolution of the regulatory phases. Ozone-Depletion Substances (ODSs) comprise the first two generations, with the fully halogenated CFCs (chlorofluorocarbons) and halons defining the first generation and HCFCs (hydrochlorofluorocarbons, partially halogenated) defining the second generation. Both groups are regulated under the Montreal Protocol. They are followed by the F-gases, typically HFCs (hydrofluorocarbons) and PFCs (perfluorocarbons), which have no chlorine and bromine but exhibit high radiative forcing and hence are included in the Kyoto Protocol. In response to regulatory requirements to reduce the use of potent greenhouse F-gases (foremost the European F-gas regulation) a fourth generation of compounds is now being produced, which consists of short-lived fluorinated alkenes, so-called HFOs (hydrofluoroolefins).

Here we present first measurements of halogenated trace gases from different generations. From the second generation we have recently detected HCFC-31 (CH_2ClF) and improved our knowledge of HCFC-133a ($\text{CF}_3\text{CH}_2\text{Cl}$) in the global atmosphere (Schoenenberger et al., 2015; Vollmer et al., 2015a). Within the Montreal Protocol these substances are banned from usage in consumer products and their occurrence may therefore point to a violation of this treaty. However, our research suggests that they are released as by-products during the permitted production of HFCs. Nevertheless, calculated global emissions of several thousand tons per year are indicative of problems during the production of these HFCs.

We recently detected the third-generation compounds fluorinated anesthetics (isoflurane, desflurane, sevoflurane) in the atmosphere (Vollmer et al., 2015b). These compounds are released from operating theatres and were found from urban areas to the pristine Antarctic environment. Over the past decade, their emissions in the atmosphere have increased substantially and reached 0.6 million t CO₂-equivalent in 2014.

Finally, we report the first world-wide measurements of the newly-produced short-lived HFCs, so-called HFOs (4th generation halocarbons) from the high-Alpine site of Jungfraujoch and an urban site in Switzerland (Vollmer et al., 2015c). HFC-1234yf (CF₃CF=CH₂) is newly used in mobile air conditioners, HFC-1234ze(E) (t-CF₃CH=CHF) is used as a refrigerant and in foam-blowing, and HCFC-1233zd(E) (t-CF₃CH=CHCl) is used as a solvent (Fig. 1).

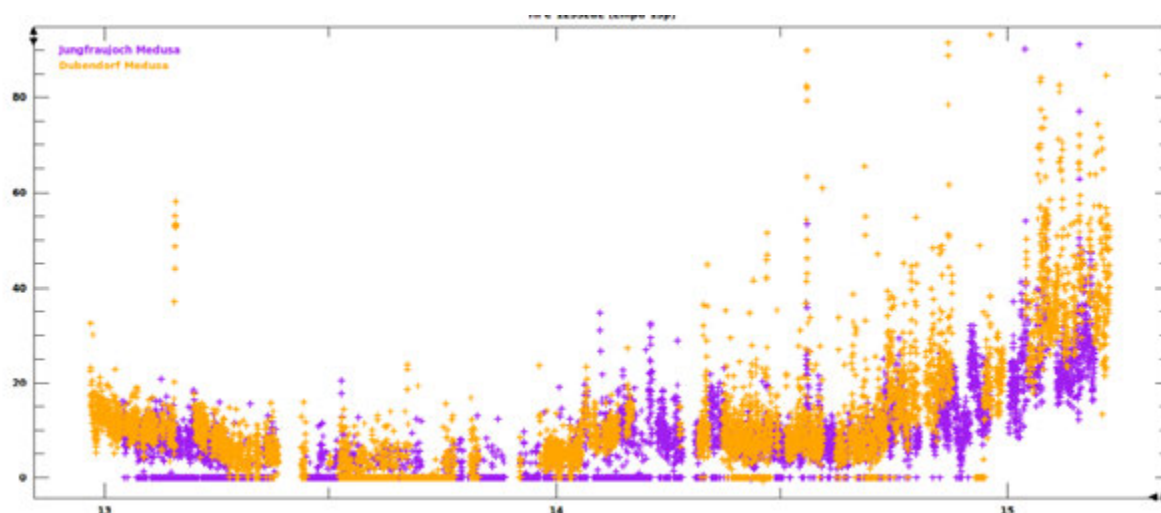


Figure 1: HCFC-1233zd(E) (t-CF₃CH=CHCl) at Jungfraujoch (violet) and Dubendorf (yellow) for 2013 – March 2015. Y-axis is dry air mole fraction in ppq (parts-per-quadrillion, 10⁻¹⁵). Many of the early measurements yielded undetectable mole fractions and a seasonal cycle is apparent. Mole fraction started to increase rapidly at the end of 2014.

REFERENCES

- Schoenenberger, F., M.K. Vollmer, M. Rigby, M. Hill, P.J. Fraser, P.B. Krummel, R.L. Langenfelds, T.S. Rhee, T. Peter & S. Reimann. 2015: First observations, trends and emissions of HCFC-31 (CH₂ClF) in the global atmosphere, *Geophys. Res. Lett.*, in press.
- Vollmer, M.K., M. Rigby, J.C. Laube, S. Henne, T.S. Rhee, L.J. Gooch, A. Wenger, D. Young, L.P. Steele, R.L. Langenfelds, C.A.M. Brenninkmeijer, J.L. Wang, C.F.O. Yang, S. A. Wyss, M. Hill, D. E. Oram, P.B. Krummel, F. Schoenenberger, C. Zellweger, P.J. Fraser, W.T. Sturges, S. O'Doherty & S. Reimann. 2015a: Abrupt reversal of HCFC-133a (CF₃CH₂Cl) in the atmosphere, *Geophys. Res. Lett.*, in review.
- Vollmer, M.K., T.S. Rhee, M. Rigby, D. Hofstetter, M. Hill, F. Schoenenberger, & S. Reimann. 2015b: Modern inhalation anesthetics: Potent greenhouse gases in the global atmosphere, *Geophys. Res. Lett.*, 42, 1606–1611.
- Vollmer, M.K., S. Reimann, M. Hill, & D. Brunner. 2015c: First observations of the fourth generation synthetic halocarbons HFC-1234yf, HFC-1234ze(E), and HCFC-1233zd(E) in the atmosphere, *Environ. Sci. Technol.*, 49 (5), 2703–2708.

15.14

Simulating air pollution on the city scale

Katrin Zink¹, Antoine Berchet¹, Dominik Brunner¹ & Lukas Emmenegger¹

¹ Empa, Swiss Federal Laboratories for Materials Science and Technology, Laboratory for Air Pollution/Environmental Technology, Überlandstrasse 129, CH-8600 Dübendorf (katrin.zink@empa.ch)

As more and more people are living in urban areas world wide, the importance of air quality monitoring and forecasting on the city scale is increasing. The concentrations of air pollutants depend both on local emission and on transport processes. Therefore, the temporal and spatial distribution of air pollutants is highly variable. As air pollution can seriously affect human health, it is desirable to have detailed knowledge about the occurrence of peak concentrations.

The Nano-Tera project OpenSense II addresses this issue both using a dense network of low-cost sensors and simulating air pollution using meteorological and dispersion models. In the framework of OpenSense II, we have set up the meteorological and dispersion model system GRAMM/GRAL for the cities of Lausanne and Zurich.

The wind fields for a larger domain around the two cities are simulated with a horizontal resolution of a 100 m using the meteorological model GRAMM. Land use and topography can be taken into account. Meteorological observations within the domain are used to drive the model. Taking these wind fields as input, the Lagrangian dispersion model GRAL is used to produce highly resolved concentration maps for different air pollutants. In a first step, GRAL modifies the wind fields to represent the flow around the buildings in the domain. In a second step, air pollutants are emitted and transported according to the modified wind fields taking into account detailed emission inventories.

We will give an overview of the model system including information about necessary input data and the different steps of the computational chain. Pollution maps for NO_x will be shown at a resolution of 5 m for different meteorological situations. The performance of the model system will be assessed based on comparisons between measured and simulated wind fields and concentrations of air pollutants.

15.15

Short-term weather variability is an important control of interannual variability in carbon and water fluxes in temperate forests

Jakob Zscheischler¹, Peter Blanken², Gil Bohrer³, Kenneth Clark⁴, Ankur Desai⁵, Simone Fatichi⁶, David Hollinger⁷, Trevor Keenan⁸, Kimberly A. Novick⁹, Sebastian Wolf¹⁰, and Sonia I. Seneviratne¹

¹ *Institute for Atmospheric and Climate Science, ETH Zurich, Universitätsstr 16, 8092 Zurich, Switzerland*

(jakob.zscheischler@env.ethz.ch)

² *University of Colorado, Boulder, CO, USA*

³ *Ohio State University, Columbus, OH, USA*

⁴ *USDA Forest Service, Northern Research Station, New Lisbon, NJ, USA*

⁵ *University of Wisconsin, Madison, WI, USA*

⁶ *Institute for Environmental Engineering, ETH Zurich, Zurich, Switzerland*

⁷ *USDA Forest Service, Northern Research Station, Durham, NH, USA*

⁸ *Prentice and Harrison Lab, Macquarie University, Sydney, Australia*

⁹ *Indiana University, Bloomington, IN, USA*

¹⁰ *Institute for Agricultural Sciences, ETH Zurich, Zurich, Switzerland*

Land surface models perform poorly for interannual variability in carbon and water fluxes, resulting in considerable uncertainty when estimating the land-carbon sink or making future projections. While many aggregated variables (e.g. growing season length, annual precipitation, growing season temperature, and phenology among others) have been suggested as predictors for the variability of annual sums in carbon fluxes, their explanatory power remains limited and uncertainties remain as to the relative contribution of each. Recent results suggest that the annual count of hours where evapotranspiration (ET) is larger than its 95th percentile (denoted as “good hours”) is highly correlated with the annual variability of ET and gross primary production (GPP) in an ecosystem model (Fatichi and Ivanov, 2014). This suggests that the occurrence of favourable conditions driven by short-term weather fluctuations have a strong influence on the annual carbon budget.

Here we analyse data from 8 forest sites of the AmeriFlux network, each having at least 8 years of continuous measurements. We show that for ET and all carbon fluxes (GPP, ecosystem respiration and net ecosystem exchange), counting “good hours/days” (i.e., hours/days when the flux exceeds a high percentile) correlates well with the respective annual sums (with correlations generally larger than 0.8). By exploiting this relationship and classifying hours/days as good or not good, interannual variability in ET and carbon fluxes can be predicted well by climate variables. We explore the implications of our results for understanding the dominant processes responsible for interannual variability in carbon and water fluxes.

REFERENCE

Fatichi, S., & Ivanov, V. Y. 2014: Interannual variability of evapotranspiration and vegetation productivity, *Water Resources Research*, 50, 3275-3294.

P 15.1

Predicting plant distribution in an heterogeneous Alpine landscape: does soil matter?

Aline Buri¹, Carmen Cianfrani¹, Jean-Nicolas Pradervand² & Antoine Guisan^{1,2}

¹ *Institute of Earth Surface Dynamics (IDYST), University of Lausanne, 1015 Lausanne, Switzerland (aline.buri@unil.ch)*

² *Department of Ecology and Evolution (DEE), University of Lausanne, 1015 Lausanne, Switzerland*

Topographic and climatic factors are usually used to predict plant distribution because they are known to explain their presence or absence. Soil properties have been widely shown to influence plant growth and distributions. However, they are rarely taken into account as predictors of plant species distribution models (SDM) in an edaphically heterogeneous landscape. Or, when it happens, interpolation techniques are used to project soil factors in space. In heterogeneous landscape, such as in the Alps region, where soil properties change abruptly as a function of environmental conditions over short distances, interpolation techniques require a huge quantities of samples to be efficient. This is costly and time consuming, and bring more errors than predictive approach for an equivalent number of samples.

In this study we aimed to assess whether soil proprieties may be generalized over entire mountainous geographic extents and can improve predictions of plant distributions over traditional topo-climatic predictors.

First, we used a predictive approach to map two soil proprieties based on field measurements in the western Swiss Alps region; the soil pH and the ratio of stable isotopes $^{13}\text{C}/^{12}\text{C}$ (called $\delta^{13}\text{C}$). We used ensemble forecasting techniques combining together several predictive algorithms to build models of the geographic variation in the values of both soil proprieties and projected them in the entire study area. As predictive factors, we employed very high resolution topo-climatic data. In a second step, output maps from the previous task were used as an input for vegetation regional models. We integrated the predicted soil proprieties to a set of basic topo-climatic predictors known to be important to model plants species. Then we modelled the distribution of 156 plant species inhabiting the study area. Finally, we compared the quality of the models having or not soil proprieties as predictors to evaluate their effect on the predictive power of our models.

In this study, we first showed that variation of soil proprieties can be modelled over large and complex areas at high resolution using predictive modelling techniques. Moreover, we also assessed that addition of predicted soil factors improved the predictive power of the 156 plant SDMs. The inclusion of soil factors improved the average area under the ROC curve (AUC) of the models by 3.5% and the poorest models experimented an AUC increase of 22%.

P 15.2

A Multiple Point Statistics Approach to Combine Weather Radar and Rain-Gauge Data

Gionata Ghiggi¹, Gregoire Mariethoz², Alexis Berne¹

¹ *Environmental Remote Sensing Laboratory, EPFL, CH-1015 Lausanne*

² *Institute of Earth Surface Dynamics, University of Lausanne, CH-1015 Lausanne*

Precipitation is a complex process, strongly varying over a large range of spatial and temporal scales. Rain gauges provide direct measurements of rainfall intensity but, unfortunately, with limited spatial representativity. On the other hand, weather radar systems cover extended areas with high spatial and temporal resolutions suitable to capture the dynamics of rainfall, providing however indirect estimates of rain rates that are affected by significant uncertainties. In topographically contrasted alpine environments such as Switzerland, it is therefore interesting to take advantage of both sources of information by merging them.

The published literature on the subject proves that geostatistical methods generally achieve better results than deterministic and simpler merging techniques (Goudenhoofdt and Delobbe, 2009). In the last decade several multivariate geostatistical methods have been introduced that focus on the estimation of hourly precipitation, based on Kriging with External Drift (KED) and Co-Kriging formulations (Haberlandt 2007, Velasco-Forero 2009, Sideris 2014).

The approach that we suggest in the present work is an alternative to classical geostatistical approaches and does not require the definition of a spatial variability model (correlogram or variogram). Guardiano and Srivastava (1993) proposed multiple-point statistics (MPS) for modelling subsurface heterogeneity. MPS characterizes the spatial structure by considering the configuration of several points within a training image, as opposed to two-point configurations with variogram approaches, enabling the reproduction of complex patterns. In this work, the Direct Sampling MPS algorithm (Mariethoz et al. 2010) has been used to generate stochastic fields representing complex statistical and spatial properties directly from the weather radar images.

The approach allows to correct errors and multiple biases present in radar images, which arise for example from non-uniform vertical profiles of reflectivity and conversion of radar reflectivity into rain rate (Z-R relationship), using rain-gauge measurements as conditioning data. Cumulated rainfall maps can be generated with customized temporal resolutions from 1 day up to 10 minutes, that is the integration time of the rain-gauges for the study case. Moreover, simulations can be generated over targeted regions and with different accuracy.

For stratiform events (see figure 1), cross-validation results show a mean correlation between simulated value and gauge data of 85 % with an increase of 30 % compared to the 55 % mean correlation between the radar product and the gauges. Meanwhile, for convective cases (see figure 2), the correlation ranges between 75 and 95 % depending on the spatial extent of the precipitation event that influences the number of rain-gauges available for the cross-validation analysis.

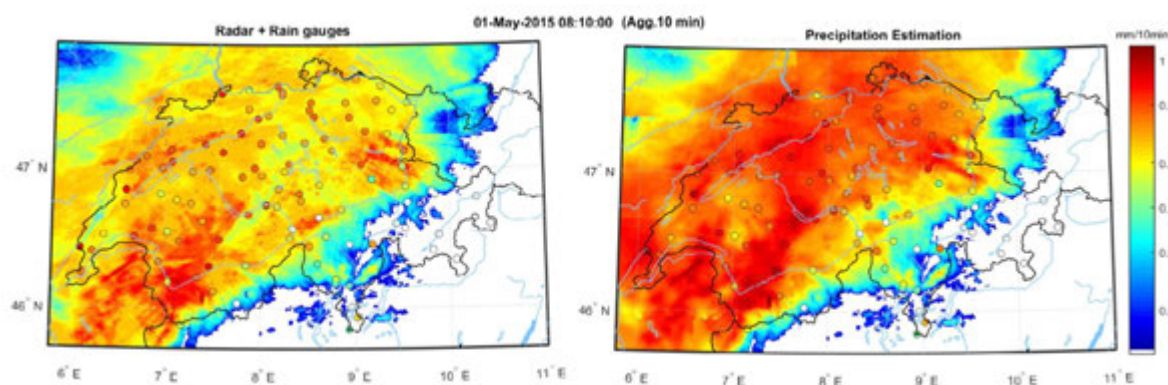


Figure 1. Comparison between radar, MPS estimates and rain-gauge measurements for a stratiform precipitation event over Switzerland (May 1, 2015).

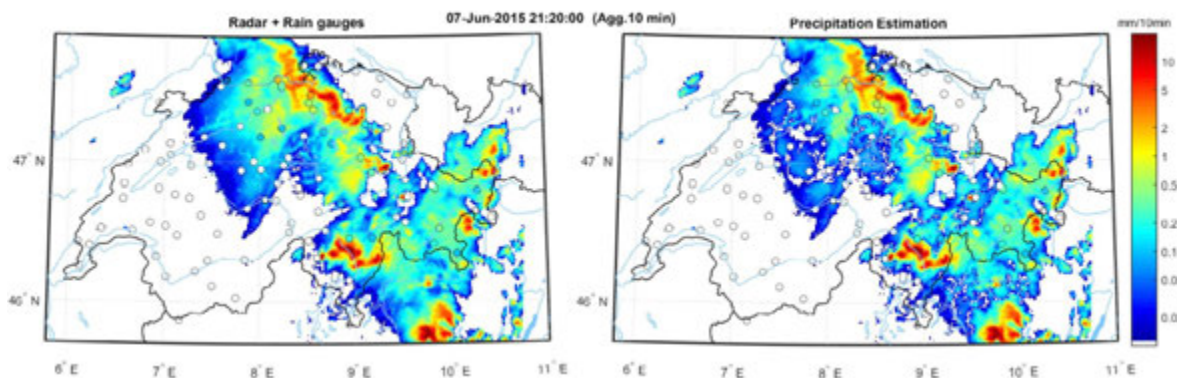


Figure 2. Comparison between radar, MPS estimates and rain-gauge data for a convective precipitation event over Switzerland (June 7, 2015).

In conclusion, the proposed approach allows to efficiently combine radar and rain-gauge observations, taking into account the nonstationarity and the intermittency of precipitation as well as to correct for possible errors present in radar composites, such as biases and wind drifts. Since it gives accurate estimates with both high temporal and spatial resolutions, the method could be useful for many hydrological applications such as flash flood forecasting.

REFERENCES

- Goudenhoofdt, E., Delobbe, L., 2009 : Evaluation of radar-gauge merging methods for quantitative precipitation estimates. *Hydrology and Earth System Sciences* 13, 195–203.
- Guardiano, F.B., Srivastava, R.M., 1993 : Multivariate Geostatistics: Beyond Bivariate Moments. *Geostatistics-Troia*, Vol. 1, 133–144.
- Haberlandt, U., 2007 : Geostatistical interpolation of hourly precipitation from rain-gauges and radar for a large-scale extreme rainfall event.
- Mariethoz, G., Renard, P., Straubhaar, J., 2010 : The Direct Sampling method to perform multiple-point geostatistical simulations. *Water Resources Research* 46.
- Sideris I. V., Gabella M., Erdin, R., Germann U., 2014 : Real-time radar-rain-gauge merging using spatio-temporal co-kriging with external drift in the alpine terrain of Switzerland. *Q.J.R. Meteorological Society* 140, 1097-1111.
- Velasco-Forero, C.A., Sempere-Torres, D., Cassiraga, E.F., 2008 : A non-parametric automatic blending methodology to estimate rainfall fields from rain gauge and radar data. *Advanced Water Resources* 32, 986–1002.

P 15.3

CO₂ and CH₄ exchange of a degrading fen, Seeland, Switzerland

Sonja Paul¹, Christof Ammann², Christine Alewell¹ & Jens Leifeld²

¹ *Umweltgeowissenschaften, University of Basel, Bernoullistrasse 30, CH-4056 Basel (sonja.paul@unibas.ch)*

² *Institut für Nachhaltigkeitswissenschaften, Agroscope, Reckenholzstrasse 191, 8046 Zürich*

Peatlands serve as important carbon sinks. Globally, more than 30% of the soil organic carbon is stored in organic soils, although covering only 3% of the land surface. On a long-term view, water saturated, peat accumulating bogs have a cooling effect on the climate (Frolking & Roulet 2007). The agricultural use of organic soils is usually accompanied by drainage that turns peatlands from a net carbon sink into a net source. Globally, about 2 to 3 Gt CO₂ are emitted from degrading organic soils (Joosten 2011; Parish et al. 2008) which is ca. 5% of the total anthropogenic emissions in 2013. A substantial part of these emissions could be avoided through rewetting of drained organic soils. In Switzerland, the biggest sequestration potential for soil organic carbon is attributed to the restauration of agriculturally used peatlands. However, in the context of climate protection these former fens and bogs are still neglected.

We study the potential saving of greenhouse gases from rewetting of a former agriculturally used fen near Cressier, Neuchatel, Switzerland. In addition, emission factors of CO₂ and CH₄ for improving the Swiss Greenhouse Gas Inventory will be generated.

The study site was under crop rotation until 2009 when it was converted to extensive grassland and became part of a newly extended nature reserve. After the present use as grassland, it will be rewetted in 2016. Since November 2014 we measure the carbon exchange of this grassland using the Eddy-Covariance method. Fast response gas concentrations are measured with open path devices (LI-COR LI7500A for CO₂ and H₂O; LI7700 for CH₄). The three-dimensional wind speed is measured with a sonic anemometer (Campbell CSAT-3). In addition, controlling parameters including global radiation, precipitation, soil temperature and humidity, and groundwater level are recorded. Soil and vegetation inventories are also included.

Results of the first measurement year will be presented illustrating the baseline year with active drainage system.

REFERENCES

- Frolking, S. & N.T. Roulet. 2007: Holocene radiative forcing impact of northern peatland carbon accumulation and methane emissions. *Global Change Biology* 13, 1079-1088.
- Joosten, H., 2011: Neues Geld aus alten Mooren: Über die Erzeugung von Kohlenstoffzertifikaten aus Moorwiedervernässungen. *Telma Beiheft* 4, 183-202.
- Parish, F., A. Sirin, D. Charman, H. Joosten, T. Minayeva, M. Silvius & L. Stringer (Eds.). 2008: Assessment on Peatlands, Biodiversity and Climate Change: Main Report. Global Environment Centre, Kuala Lumpur and Wetlands International, Wageningen

16. Phenology and seasonality

Martine Rebetez, Christian Rixen, This Rutishauser

Swiss Commission for Phenology and Seasonality (CPS)

TALKS:

- 16.1 Basler D.: Linking mixed temperate forest canopy closure to remote sensing phenology
- 16.2 D'Odorico, P., Buchmann N.: Land Surface Phenology – A good surrogate for photosynthesis seasonality?
- 16.3 Eugster M.: Seasons in my region (SIMR)
- 16.4 Körner C., Basler D., Hoch G., Kollas C., Lenz A., Randin C., Vitasse Y., Zimmermann N.: Phenology helps explaining the low temperature range limits of temperate tree species
- 16.5 Mazzoleni S., Cartenì F., Giannino F., Basile B., Gianni Pezzatti B., Conedera M.: A new process-based approach to model plant phenology based on carbon allocation
- 16.6 Prevéy J.S., Rixen C., Hollister R., Henry G., Welker J., Molau U., Høye T., Björkman A., Cannone N., Cooper E., Elberling B., Elmendorf S., Fosaa A., Jónsdóttir I.S., Klanderud K., Kopp C., Levesque E., Mauritz M., Myers-Smith I., Natali S., Oberbauer S., Post E., Rumpf S., Schmidt N.M., Schuur T., Semenchuk P., Troxler T., Vellend M., Wahren H., Wipf S.: The temporal niches of Arctic and alpine plants help explain phenological responses to climate warming
- 16.7 Vuffray Z., Deléglise C., Amaudruz M., Jeangros B., Mosimann E., Meisser M.: Evolving phenology of semi-natural meadows in the western part of Switzerland

POSTERS:

- P. 16.1 Rutishauser T., Brönnimann S., Rebetez M., Eugster W. and project collaborators: Climate impact science with citizens. First results of the «OpenNature.ch» project

16.1

Linking mixed temperate forest canopy closure to remote sensing phenology

David Basler¹

¹ *Institute of Botany, University of Basel, Schönbeinstrasse 6, CH-4056 Basel (david.basler@unibas.ch)*

Spring phenological events strikingly mark the onset of the growing season. So far, a variety of methods have been developed to assess plant phenology across different scales, ranging from site- and species-specific visual observations to regional greenup-estimates extracted from remote sensing data. Using time-series of hemispherical images collected along transects in a mixed hornbeam-oak forest and mixed beech-spruce forest in France and Switzerland, I quantified canopy closure and the associated increase in leaf area index (LAI) during a nine-week period in spring 2011 (Figure 1). These observations, together with traditional, species-specific phenological observations and quantitative measurements of leaf development in the dominant broadleaved tree species, were linked to remote-sensed (MODIS) NDVI of the same sites. For both forest types, the inflection-point of the spring-increase in NDVI coincides with the inflection-point of the increases of LAI values, while the loss in canopy transmission precedes this event. From these data I conclude that, at least in rather homogenous forests, the remote sensed start-of-season date is tightly linked to increase of the LAI of the forest canopy, rather than the earlier green-up of forest understory. In late spring observations, the variance between the individual ground observations points increases, and NDVI progressively saturates with increasing LAI. Using the developed image-analysis procedures, time-series of hemispherical images may be used for (automated) collection of valid ground-truth data for satellite based phenological observations.

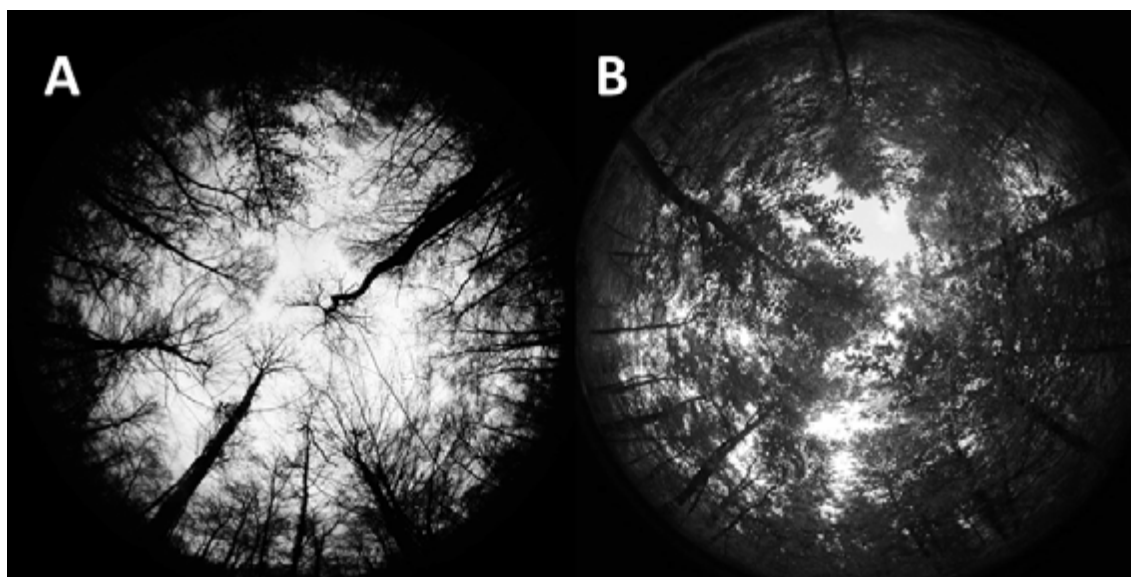


Figure 1. Example of hemispherical images of forest canopy before (A; end of March) and after leaf-out (B; end of April).

16.2

Land Surface Phenology – A good surrogate for photosynthesis seasonality?

Petra D'Odorico & Nina Buchmann

*Grassland Sciences Group, Institute of Agricultural Sciences, ETH Zurich, Universitätstrasse 2, 8092 Zurich, Switzerland
(petra.dodorico@usys.ethz.ch)*

Phenology remains one of the most difficult processes to parameterize in dynamic vegetation and ecosystem process models. Most current models employ simple functions derived from meteorological variables, modeling phenology as a contemporary climate-dependent process (Arora & Boer, 2005). However, the study of the underlying mechanisms and their adaptation to changing climates requires continuous regional and global scale observations of phenology. Remote sensing observations of seasonal canopy greenness dynamics represent a valuable means to study land surface phenology (LSP) at scales relevant for comparison with regional climate information. Which part of the vegetation phenological cycle is effectively captured by these remote sensing measurements and which is the link with distinct plant physiological and functional processes has however been largely overlooked.

Here we present the results of an investigation (D'Odorico et al., 2015) in which we assessed the match and mismatch between photosynthesis and remote sensing based land surface phenology for 19 deciduous broadleaf and mixed forest sites in the northern hemisphere over the period 2000-2012. Key LSP dates at the start and end of the season are obtained from three remote sensing products: Normalized Difference Vegetation Index (NDVI); Phenology Index (PI) (Gonsamo et al. 2012); MODIS Land Cover Dynamics Product based on the Enhanced Vegetation Index (EVI), and additionally from ground based digital cameras. Photosynthesis phenology dates are extracted from gross primary productivity (GPP) time series, derived from eddy covariance CO₂ flux measurements. Further, we report on the consistency among LSP dates obtained with different satellite remote sensing products and on their comparability with ground based digital camera estimates.

We find that LSP dates estimated by the three remote sensing products are not equivalent and differ in their sign and magnitude of lags with photosynthesis phenology dates. NDVI-derived phenology is characterized by shorter growing seasons, while EVI prolongs it by about two weeks compared to the photosynthesis phenology season length. PI start and end of season dates more closely match the start and end of photosynthesis phenology as estimated by GPP time series. We conclude that while many crop and conifer species exhibit coordinated development of leaf area and physiological capacity, deciduous forest canopies are known to show lagged and continued physiological development beyond full canopy leaf area development. For ecosystems exhibiting this developmental pattern, remote sensing products that are more sensible to canopy expansion might overestimate the onset of maximum physiological function if they do not account for a maturation period following the development of canopy leaf area.

REFERENCES

- Arora, V.K. & Boer, G.J., 2005: A parameterization of leaf phenology for the terrestrial ecosystem component of climate models. *Global Change Biology*. 11, 39–59.
- D'Odorico, P., A. Gonsamo, C.M. Gough, G. Bohrer, J. Morison, M. Wilkinson, P.J. Hanson, D. Gianelle, J.D. Fuentes, and N. Buchmann, 2015: The match and mismatch between photosynthesis and land surface phenology of deciduous forests. *Agricultural and Forest Meteorology*. 214–215, 25–38.
- Gonsamo, A., J.M. Chen, D.T. Price, W.A. Kurz, and C. Wu, 2012: Land surface phenology from optical satellite measurement and CO₂ eddy covariance technique. *Journal of Geophysical Research: Biogeosciences*. 117, G03032.

16.3

Seasons in my region (SIMR)

Markus Eugster

Sekundarschule, Schoentalstrasse 2, 9244 Niederuzwil (markus.eugster@schule-uzwil.ch)

In a nutshell

This is a worldwide long-term citizen science project to learn more about the timing of the seasons and how it responds to changing conditions.

Introduction

Seasons can be globally defined by astronomical facts. Locally however they often are greatly influenced by regional singularities as for example winds, relief, weather patterns and altitude. Many people observe nature closely and know reliable local phenomena that indicate the beginning of a season in their region. Thus the beginning of a season becomes a variable that integrates significant regional conditions and can be very sensitive to any changes.

Method

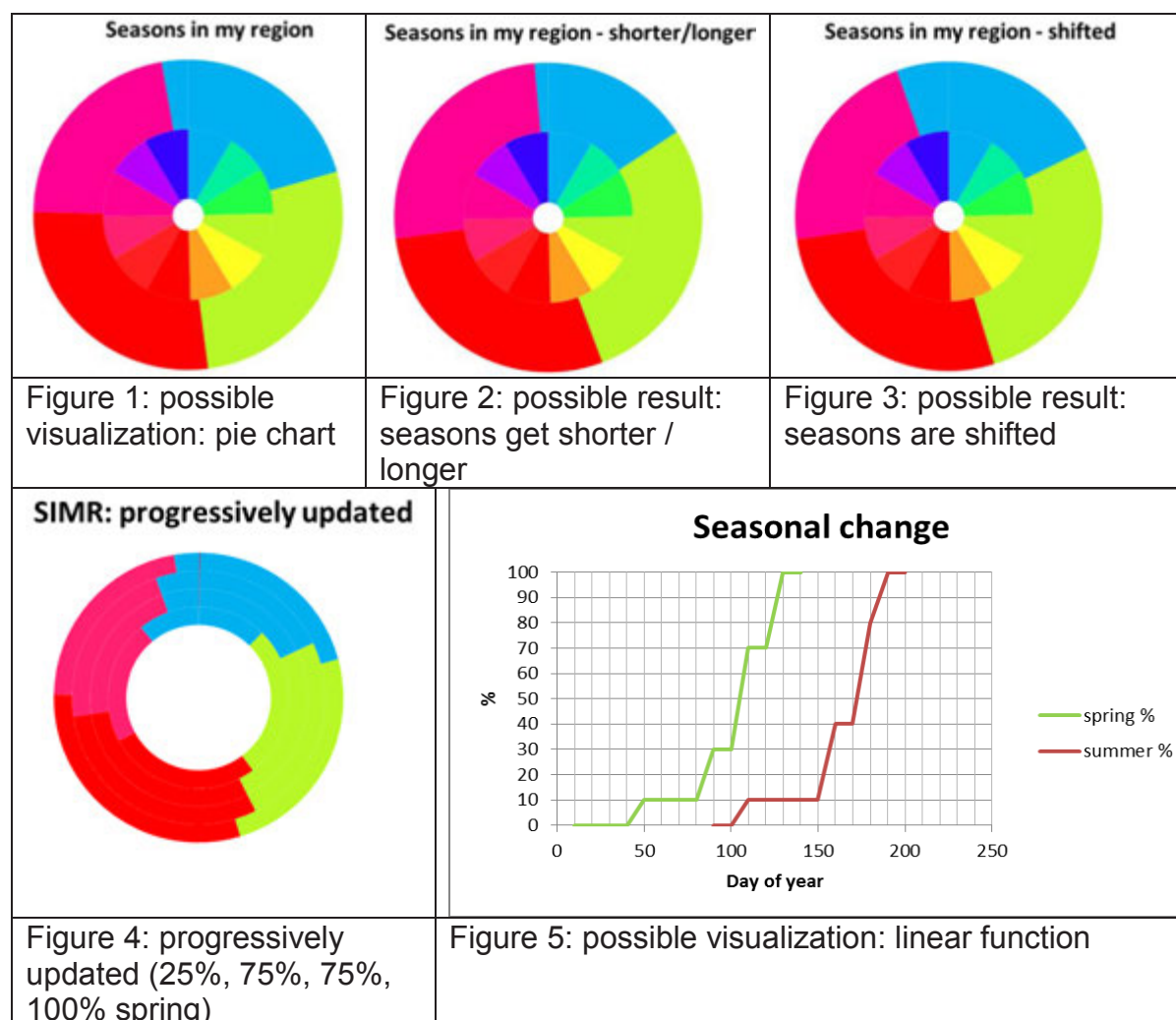
By defining indicators for seasons and their long-term observation with our senses and modern technical equipment we can document the changing conditions in a habitat and prove statements about these changes.

The method allows a synergy of scientific approaches and traditional knowledge, strengthens the attention and comprehension of observers of every age and gives ample scope for own observations and approaches, allowing the participants to be inquiringly active. The observations can give pleasure and be eye-opening, the results can be scientifically instructive and not least aesthetically attractive and thus be rewarding for scientists, laymen and outsiders.

Investigation (5 indicators)

1) Observer	<input checked="" type="checkbox"/>	name:	Markus Eugster				
	<input checked="" type="checkbox"/>	e-mail:	markus.eugster@schule-uzwil.ch				
	<input checked="" type="checkbox"/>	address:	Schöntalstrasse 2, CH-9244 Niederuzwil				
	<input type="checkbox"/>	date of birth					
2) Region		name:	Untertoggenburg				
		latitude	47.437	°	(N + / S -)		
		longitude	-9.131	°	(W + / E -)		
		altitude	580	m a. s. l.			
3) Seasons		indicators:	loading:	date:	%	pict	
3.1 spring	1	Willows in full bloom	1	14.03.2015			3101
	2	First chifffaff song	2	30.03.2015			3102
	3	Bird cherry in bloom	1	26.04.2015			3103
	4	General bloom of cowslips	1	16.04.2015			3104
	5	Beech leaves unfolding	2	30.04.2015			3105
3.2 summer	1	Wild cherries ready to harvest	2	10.07.2015			3201
	2	First wild strawberries	2	18.06.2015			3202
	3	First thunderstorm	1	19.05.2015			3203
	4	Air temperature above 30°C	2	04.07.2015			3204
	5	Linden tree in bloom	3	28.06.2015			3205

Visualization



Concept

- Be a researcher: the outcome is unknown and depends on your choice
- Work on something nobody has done before
- It's not only collecting data that is used by unknown people – if used at all
- Idea: open your eyes, be curious, bring in your own ideas
- Results in the first year already, new insights in following years
- Participants can steer the process themselves

Implementation and references

Test run: August 2015 – August 2016: send data sheets to simregion@gmx.ch

Link: <http://www.seasonsandbiomes.net/170simr.html>

Data sheet: <http://www.seasonsandbiomes.net/600links.html> (SIMR B5 or Bvar)

Official start of the SIMR project: August 2016

16.4

Phenology helps explaining the low temperature range limits of temperate tree species

Körner C., Basler D., Hoch G., Kollas C., Lenz A., Randin C., Vitasse Y., Zimmermann N.

Institute of Botany, University of Basel, Schönbeinstrasse 6, 4056 Basel

Attempts at explaining range limits of temperate tree species still rest on correlations with climatic data that lack a physiological justification. Here we present a synthesis of a project that aimed at resolving that question. We employed climatology, biogeography, dendrology, population and reproduction biology, stress physiology and phenology to provide an eco-evolutionary explanation of the low temperature limits of temperate tree species. We combine results from in situ elevational (Swiss Alps) and latitudinal (Alps vs Scandinavia) comparisons, from common garden and phytotron studies, as well as laboratory experiments, for 8 common European tree species. We show that absolute temperature minima in treetops can be predicted from weather station data, but such winter extremes do not explain range limits. The ranking of the range limits of species is similar across elevation and latitude. Recruitment is not limited at the current upper elevational limit of any species. Reciprocal common gardens revealed that environmental influences on growth and phenology of seedlings exceeded those of seed origin.

Spring flushing in adults trees turned out to be timed in such a way that the probability of freezing damage is minimized, with a uniform 80-year safety margin across elevations and taxa. More resistant species flush earlier than less freezing resistant species. Tree ring formation at the range limit is not related to season length, but to growing season temperature. Young trees, grown at temperatures colder than at their natural range limit, show incomplete lignification and maturation.

We conclude that the range limits of the examined taxa are set by the interactive influence of phenology, freezing resistance in spring, and the time required to mature tissues. Microevolution of spring phenology compromises between demands set by species-specific freezing resistance of immature tissue and evolutionary life history traits related to tissue maturation. Phenology, thus plays a central role in controlling species range limits, by timing key developmental steps in the annual life cycle of trees.

Funded by ERC advanced grant TREELIM

REFERENCES

- Basler D, Körner C (2012) Photoperiod sensitivity of bud burst in 14 temperate forest tree species. *Agric For Meteorol* 165:73-81
- Basler D, Körner C (2014) Photoperiod and temperature responses of bud swelling and bud burst in four temperate forest tree species. *Tree Physiol* 34:377-388
- Kollas C, Vitasse Y, Randin CF, Hoch G, Körner C (2012) Unrestricted quality of seeds in European broad-leaved tree species growing at the cold boundary of their distribution. *Ann Bot* 109:473-480
- Kollas C, Körner C, Randin CF (2014) Spring frost and growing season length co-control the cold range limits of broad-leaved trees. *J Biogeogr* 41:773-783
- Körner C, Basler D (2010) Phenology Under Global Warming. *Science* 327:1461-1462
- Lenz A, Hoch G, Vitasse Y, Körner C (2013) European deciduous trees exhibit similar safety margins against damage by spring freeze events along elevational gradients. *New Phytol* 200:1166-1175
- Randin CF, Paulsen J, Vitasse Y, Kollas C, Wohlgemuth T, Zimmermann NE, Körner C (2013) Do the elevational limits of deciduous tree species match their thermal latitudinal limits? *Glob Ecol Biogeogr* 22:913-923
- Vitasse Y, Hoch G, Randin CF, Lenz A, Kollas C, Körner C (2012) Tree recruitment of European tree species at their current upper elevational limits in the Swiss Alps. *J Biogeogr* 39:1439-1449
- Vitasse Y, Hoch G, Randin CF, Lenz A, Kollas C, Scheepens JF, Körner C (2013) Elevational adaptation and plasticity in seedling phenology of temperate deciduous tree species. *Oecologia* 171:663-678
- Vitasse Y, Lenz A, Körner C (2014) The interaction between freezing tolerance and phenology in temperate deciduous trees. *Front Plant Sci* 5:541

16.5

A new process-based approach to model plant phenology based on carbon allocation

Stefano Mazzoleni¹, Fabrizio Carteni¹, Francesco Giannino¹, Boris Basile¹, Gianni Boris Pezzatti², Marco Conedera²

¹ *Dipartimento di Agraria, University of Naples Federico II, Via Università 100, 80055 Portici (NA)*
(stefano.mazzoleni@unina.it)

² *WSL Swiss Federal Institute for Forest, Snow and Landscape Research, Community Ecology Research Unit, Via Belsoggiorno 22, CH-6500 Bellinzona*

The relationships between plant phenological processes and climate seasonality has been studied in both ecological and agricultural fields for either theoretical or applied purposes, what resulted in the development and use of different models aiming at predicting the timing of phenological phases (Cleland et al. 2007).

So far, most models have been based on the relationships between empirical observations of phenological events and climatic derived variables (Chuine et al. 2003), while in other cases photoperiod and hormonal status were also taken into account (Olsson et al. 2013). A drawback of phenological models based on either “cold” and “heat” units as explanatory mechanisms consist in the limited applicability which is restricted to the a specific geographical region and related climate on which it has been calibrated.

We propose a new approach linking the phenology to basic plant physiological processes such as photosynthesis, cell proliferation (mitosis) and tissue enlargement, all explicitly related to main environmental conditions (water status and temperature). Initial physiological assumptions of the new model are: photosynthesis produces non-structural carbohydrates (NSC) which are consumed by growth, whereas cell proliferation produces a growth inhibitory signal as reported in the case of yeast cell cultures (Mazzoleni et al. 2015). These processes respond differently to the environment (Fig. 1a, b) increasing or decreasing NSC and the inhibitory signals in the plant tissues. The central assumptions are then that bud burst is driven by limited NSC availability, bud setting by the accumulation of growth inhibitory signals, and leaf fall by NSC accumulation. Aboveground plant growth is represented by the explicit allocation of photosynthates to the three main compartments of leaves, green shoots and wood. Carbon partitioning between these compartments is driven by source-sink balance and related concentration gradients.

Theoretical simulations show the capability of the model to reproduce evergreen and deciduous behaviours in tropical and temperate climatic conditions and the occurrence of multiple vegetative phases, typical of Mediterranean environments. Furthermore, different species can be parameterised to represent different carbon allocation patterns and the physiological process-based nature of this model has the potential to provide a mechanistic explanation for observed trends of phenological behaviours under changing climatic conditions.

Future work will however be necessary to calibrate the model on to simulate and predict the phenology of several plant species in different environments.

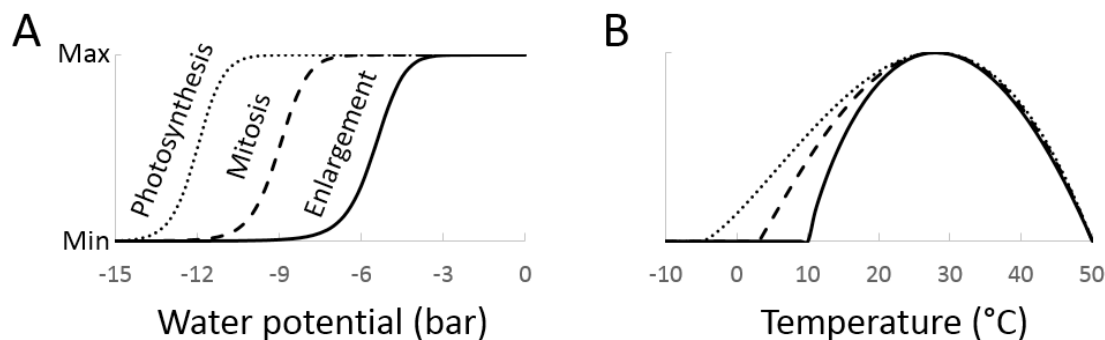


Figure 1. Different functional responses of photosynthesis, mitosis and enlargement to (a) water status and (b) temperature. These responses drive the seasonal changes of concentrations of non-structural carbohydrates and growth inhibitors that are assumed to regulate plant phenology.

REFERENCES

- Chuine, I., Kramer, K., Hanninen, H. 2003: Plant development models. In: Phenology: An Integrative Environmental Science (Ed by Schwartz, M.D.), Kluwer, pp 217–235.
- Cleland, E.E., Chuine, I., Menzel, A., Mooney, H.A. & Schwartz, M.D. 2007: Shifting plant phenology in response to global change, *Trends in Ecology and Evolution*, 22, 357–365.
- Mazzoleni, S., Landi, C., Carteni, F., de Alteriis, E., Giannino, F., Paciello L., Parascandola, P. 2015: A novel process-based model of microbial growth: self-inhibition in *Saccharomyces cerevisiae* aerobic fed-batch cultures, *Microbial Cell Factories*, 14, 109.
- Olsson, C., Jönsson A.M., Bolmgren, K., Lindström, J. 2012: Performance of tree phenology models along the bioclimatic gradient of Sweden, *Ecological Modelling*, 266, 103–117.

16.6

The temporal niches of Arctic and alpine plants help explain phenological responses to climate warming

J.S. Prevéy¹, C. Rixen¹, R. Hollister², G. Henry³, J. Welker⁴, U. Molau⁵, T. Høye⁶, A. Björkman⁷, N. Cannone⁸, E. Cooper⁹, B. Elberling¹⁰, S. Elmendorf¹¹, A. Fosaa¹², I.S. Jónsdóttir¹³, K. Klanderud¹⁴, C. Kopp¹⁵, E. Levesque¹⁶, M. Mauritz¹⁷, I. Myers-Smith¹⁸, S. Natali¹⁹, S. Oberbauer²⁰, E. Post²¹, S. Rumpf²², N.M. Schmidt²³, T. Schuur¹⁷, P. Semenchuk²², T. Troxler²⁰, M. Vellend²⁴, H. Wahren²⁵, S. Wipf¹

¹ WSL Institute for Snow and Avalanche Research SLF, Flüelastrasse 11, CH-7260 (janet.prevey@slf.ch)

² Biology Department, Grand Valley State University, MI, USA

³ Department of Geography, University of British Columbia, BC, Canada

⁴ Department of Biological Sciences, University of Alaska Anchorage, AK, USA

⁵ Department of Biology and Environmental Sciences, University of Gothenburg, Sweden

⁶ Arctic Research Centre, Aarhus University, Denmark

⁷ German Centre for Integrative Biodiversity Research, Leipzig, Germany

⁸ Department of Science and High Technology, Università degli Studi dell'Insubria, Como, Italy

⁹ Institute for Arctic and Marine Biology, University of Tromsø, Norway

¹⁰ Department of Geography, University of Copenhagen, Copenhagen, Denmark

¹¹ National Ecological Observatory Network, CO, USA

¹² Faroese Museum of Natural History, Faroe Islands

¹³ School of Engineering and Natural Sciences, University of Iceland, Iceland

¹⁴ Department of Ecology and Natural Resources, Norwegian University of Life Sciences, Norway

¹⁵ Department of Botany and Zoology, University of British Columbia, Vancouver, BC, CA

¹⁶ Université du Québec à Trois-Rivières, Québec, Canada

¹⁷ Center for Ecosystem Science and Society Center, Northern Arizona University, Flagstaff, AZ, USA

¹⁸ University of Edinburgh, Scotland

¹⁹ Woods Hole Research Center, Falmouth, MA, USA

²⁰ Department of Biological Sciences, Florida International University, FL, USA

²¹ The Polar Center and Department of Biology, Penn State University, University Park, Pennsylvania, USA

²² Institute for Arctic and Marine Biology, University of Tromsø, Norway

²³ Department of Bioscience, Aarhus University, Denmark

²⁴ Département de Biologie, Université de Sherbrooke, Sherbrooke, Québec

²⁵ Department of Agricultural Sciences, La Trobe University, Melbourne, AU

The phenology of vegetation in tundra regions is strongly affected by temperature, and thus is predicted to be particularly sensitive to climate warming. Previous studies have found that Arctic and alpine plants advance phenological events in response to warmer temperatures. However, responses differ between lifeforms, species, and locations, with some plants shifting dates of greenup, flowering, and senescence more than others. Identifying the underlying mechanisms for the varied phenological responses of tundra plants is integral for predicting how vegetation will respond to climate change in the future.

To identify factors that affect changes in tundra plant phenology at a global scale, we analyzed phenological responses of over 147 species at 22 sites from Arctic and alpine ecosystems around the world (Fig. 1). We analyzed data from both long-term monitoring plots and warming experiments. We predicted that plants which flower later in the season would advance phenological events more with warmer temperatures than early-flowering species. Phenology of late-flowering species may be more responsive to cumulative heat sums over the growing season, whereas phenology of early-flowering species probably depends more on timing of snowmelt. Preliminary results supported our predictions: phenology of late-flowering tundra plants was more sensitive to summer temperature change than phenology of early-flowering species. These divergent responses of late versus early-flowering species led to shorter community-level flowering seasons in warmer years. Our results suggest that the relative flowering time, or temporal niche, of plants can help predict phenological changes of species and plant communities across tundra ecosystems in response to climate warming.

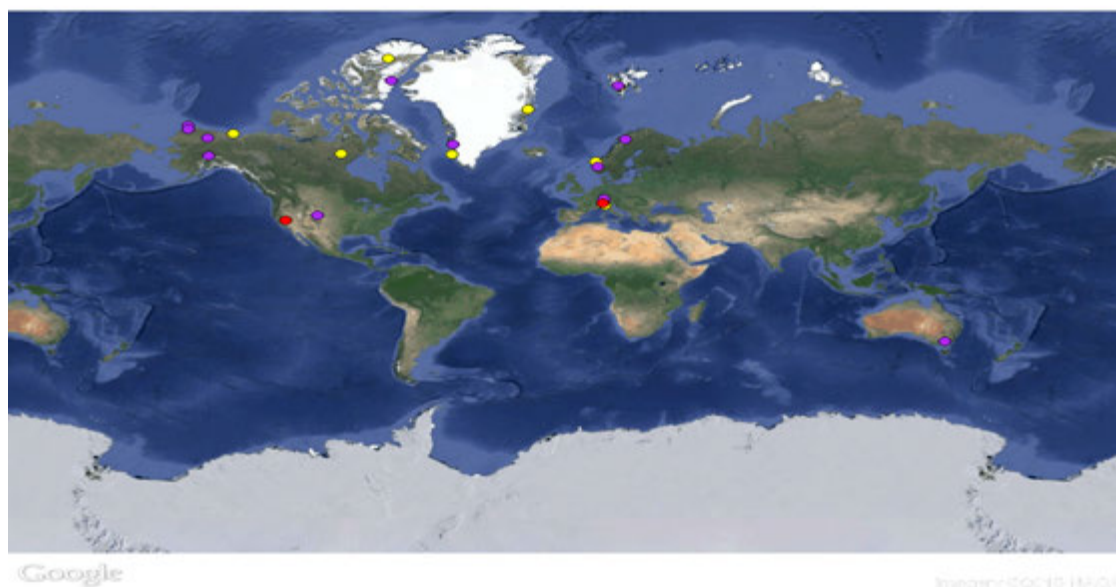


Figure 1. Locations of sites where phenological responses of tundra plants were observed. Yellow dots indicate sites with long-term monitoring plots, red dots indicate sites with warming experiments, and purple dots indicate sites with both.

16.7

Evolving phenology of semi-natural meadows in the western part of Switzerland

Zoé Vuffray¹, Claire Deléglise¹, Michel Amaudruz², Bernard Jeangros¹, Eric Mosimann¹ & Marco Meisser¹

¹ Agroscope Changins-Wädenswil Research Station ACW, CH-1260 Nyon 1, Switzerland

² Agridea Lausanne, CH-1000 Lausanne 6, Switzerland

The phenology of semi-natural meadows located at different thermal levels was observed in springtime between 1995 and 2015. The aim of this study is (i) to control the standardized method enabling the description of the developmental stage of meadows under various conditions and (ii) to study the variation of meadow's phenology earliness over the years.

Each year the phenological stages of ten common species differing in their earliness (five grasses, one legume and four forbs) were monitored over several weeks. Cocksfoot (*Dactylis glomerata*) was used as the reference species and the stages observed in other species were converted into 'equivalent cocksfoot stages' (ECS). The mean ECS, involving many species, allows the characterization of the stage of meadow development to be made on a standardized basis (Jeangros & Amaudruz 2005). This method is useful for agricultural advisory since meadow development stages are directly linked to fodder quality (ADCF 2006).

The main results of this study relates to changes affecting the phenology of meadows in the course of time. One of those changes involves variations in the realization date of the ECS 4 (full heading). The variations between the thermal levels and the years are shown in Figure 1. Inter-annual variations are slightly higher in colder zones than in warmer ones. Stage ECS 4 is delayed by 4 days on average for each altitude increase of 100 m.

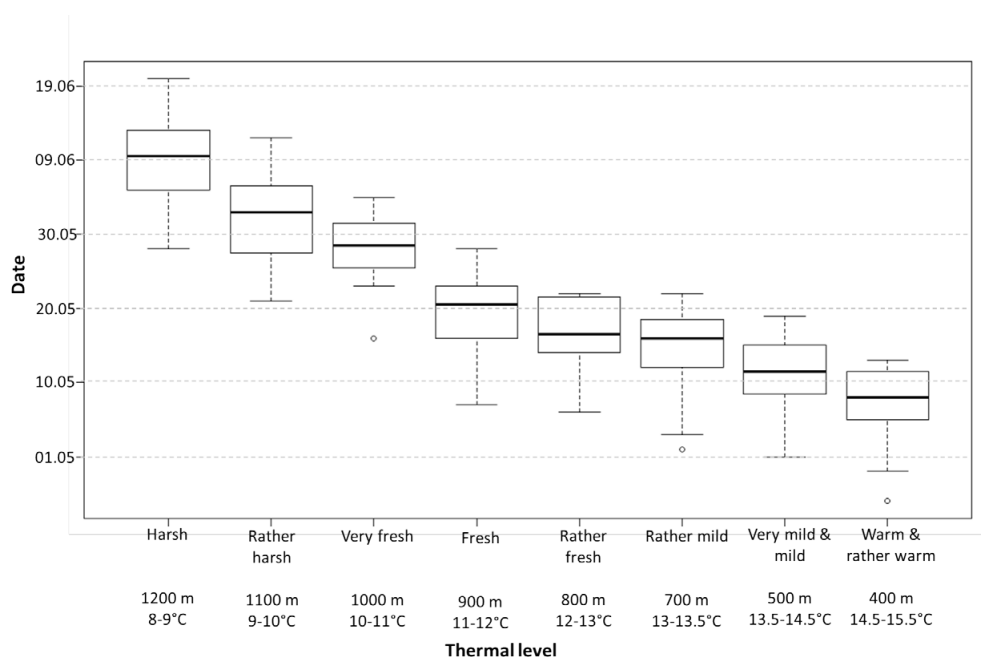


Figure 1. Variations in realization dates of equivalent cocksfoot stage 'full heading' (mean ECS = 4) for the different thermal levels, characterised by altitude and mean temperatures between April and October. Mean values for the period 1995 to 2014 (extreme values, first and third quartiles, median).

However, the difference between the earliest and latest years calculated over the period 1995-2004 is smaller than the variation over 2005-2014 (data not shown here). Thus, variations in the realization dates of stages increase over the years. The second main result is a trend to earliness, which is observed for all thermal zones unless for the *harsh* zone. Phenology of meadows occurs slightly earlier (between 1 and 3 days earlier every ten years): Figure 2 illustrates this fact for three zones.

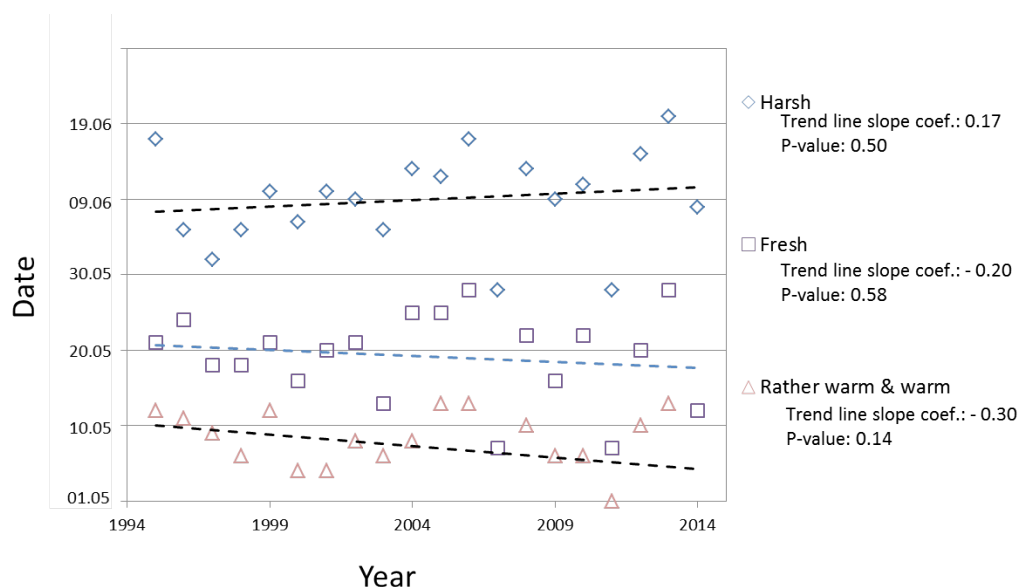


Figure 2. Pattern of periodicity in realization dates of equivalent cocksfoot stage 'full heading' (mean ECS = 4) for three thermal levels.

Phenology can be seen as an indicator of climate change (Defila 2010) since development stages are mostly linked to temperature (Gillet 1980). The trends observed in this study show that there is an earlier spring for almost all thermal zones, demonstrated as well by Claudio Defila (2007) on the phenology of cherry-tree in Liestal.

REFERENCES

- ADCF. 2006 : Estimation de la valeur du fourrage des prairies. Valeur nutritive et production de lait ou de viande. Fiche technique 2.7.1. 3e édition. ADCF. Nyon. Switzerland. 6 p.
- Defila, C. 2007 : Changements climatiques en Suisse. Office fédéral de l'environnement OFEV. Berne. Suisse. 46.
- Defila, C. 2011: Retrospective phénologique de l'année 2010. Recherche Agronomique Suisse 2 (5), 226-231.
- Gillet, M. 1980 : Les graminées fourragères: description, fonctionnement, applications à la culture de l'herbe. Gauthier-Villars.
- Jeangros, B. & Amaudruz, M. 2005 : Dix ans d'observations sur la phénologie des prairies permanentes en Suisse romande. Revue suisse d'agriculture 37 (5), 201-9.

P 16.1

Climate impact science with citizens. First results of the «OpenNature.ch» project

This Rutishauser¹, Stefan Brönnimann¹, Martine Rebetez², Werner Eugster³ & project collaborators⁴

¹ Institute of Geography and Oeschger Centre for Climate Change Research, University of Bern, Halerstrasse 12, CH-3012 Bern (rutis@giub.unibe.ch).

² University of Neuchâtel, Neuchâtel, and, Swiss Federal Institute for Forest, Snow and Landscape Research WSL, Lausanne.

³ Institute of Agricultural Sciences, ETH Zurich, Zurich.

⁴ <http://www.opennature.ch/partner>.

In spring 2015, the Swiss citizen science website OpenNature.ch was launched. The website aims at building awareness for science-based climate impact knowledge, collecting scientifically sound phenology and seasonality observations and understanding environmental change. The present project focuses on plants, animals, mushrooms, landscapes, and climate extremes. OpenNature.ch includes a news section presenting new scientific findings and shares the results on social media networks (@OpenNature_ch; www.facebook.com/OpenNature.ch).

Our contribution presents first results and key-learnings of the first half year after going public. Longterm observations of cherry tree flowering dates and snow cover duration are compared with OpenNature data from spring 2015 (Figure 1). We highlight the potential of OpenNature to continue data collection from ongoing observations programs such as BernClim (Jeanneret and Rutishauser 2011) and present options of planned applications. We illustrate successful and less promising experiences with examples from the newsblog and the associated social media sites. Financed by the Swiss National Science Foundation (SNF) science communication program AGORA 2012–2015, OpenNature.ch builds on existing observations programs and partnerships in Switzerland under the auspices of the Swiss Academy of Natural Sciences SCNAT. Future development will focus on the development of a more flexible visualisation of results and implementing continued news feed with contributions from scientists.

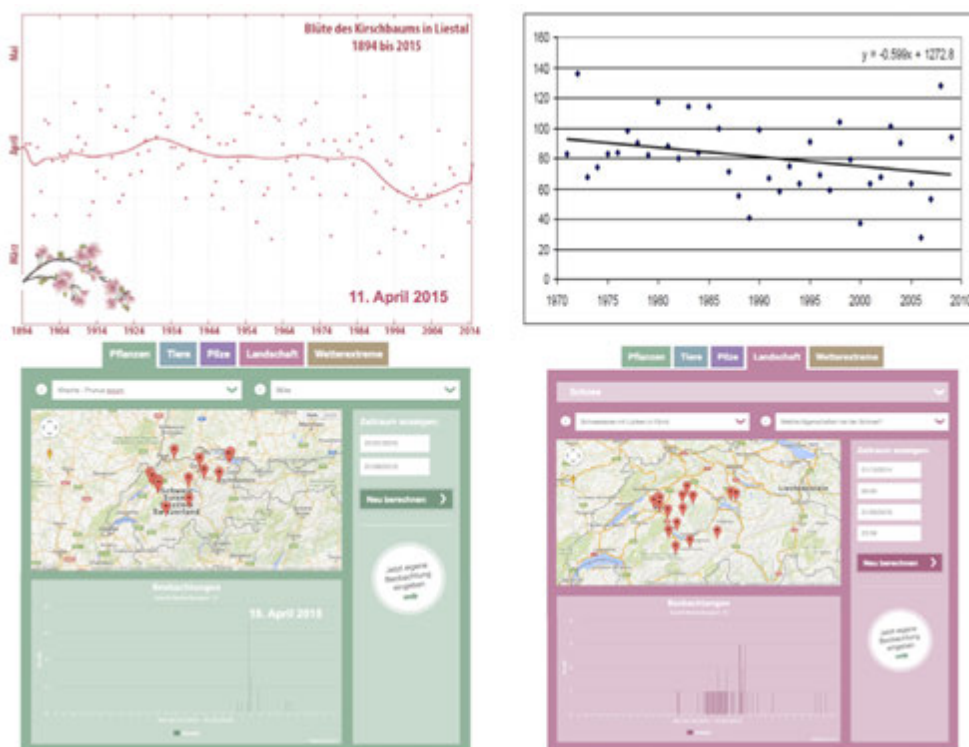


Figure 1. Observations of cherry tree flowering dates (left column) from one tree near Liestal, northern Switzerland, since 1894 (top left) and map and frequency plot of observations by citizen observers in spring 2015 (bottom left). Observations of the number of snow days since 1971 as recorded by a citizen of the «BernClim» network (top right) and OpenNature observations from 2015 (bottom right).

REFERENCES

www.OpenNature.ch

Jeanneret, F., & Rutishauser T. 2012: BernClim. Saisonalitäts-Monitoring – Jura, Mittelland, Alpen. Geographica Bernensia G87, pp. 111.

17. Earth Observation addressing key Earth System processes

Stefan Wunderle, Mathias Kneubühler, Brigitte Buchmann, Alain Geiger

*Swiss Commission for Remote Sensing,
Swiss Geodetic Commission*

TALKS:

- 17.1 Baffelli S., Frey O., Hajnsek I.: Observing the Bisele Glacier with Ku-band differential radar interferometry
- 17.2 Böhler J.E., Kneubühler M., Tuia D., Schaepman M.E.: Improved land cover assessment in agriculture with optical remote sensing data
- 17.3 Kuhlmann G., Hueni A., Damm A., Emmenegger L., Brunner D.: High-resolution remote sensing of NO₂ maps over Zurich with the Airborne Prism Experiment (APEX): new results
- 17.4 Lieberherr G., Riffler M., Wunderle S.: Lake Surface Water Temperature: Performance of split-window coefficients – a sensitivity analysis
- 17.5 Lohmann H.: Satellite images: The Weissenstein anticline is younger than the Jura foldbelt
- 17.6 Meusburger K., Alewell C.: Estimating vegetation parameters in an alpine catchment by means of WorldView-2 imagery
- 17.7 Milani G., Tonolla D., Robinson C., Kneubuehler M., Doering M., Schaepman M.: Classification of habitat diversity in two floodplains using UAVs
- 17.8 Wingate V.R., Phinn S.R., Scarth P., Kuhn N.: Mapping decadal land cover changes in the woodlands of north eastern Namibia using the Landsat satellite archive (1975-2014)

POSTERS:

- P 17.1 Bur P., Lieberherr G., Wunderle S.: Lake surface water temperatures derived from Landsat 8

17.1

Observing the Bisgletscher with Ku-band differential radar interferometry

Simone Baffelli¹, Othmar Frey^{*,1}, Irena Hajnsek^{o,1}

¹ *Institut for Umweltingenieurwissenschaften, ETH Zürich, Stefano-Franscini Platz 3, 8093 Zürich, (baffelli@ifu.baug.ethz.ch)*

^{*} *Gamma Remote Sensing AG, Worbstrasse 225, 3073 Gümlingen, (frey@ifu.baug.ethz.ch)*

^o *DLR, Microwaves and Radar Institute, Wessling, Germany*

The Bisgletscher is a steep, fast flowing glacier located above the village of Randa, on the western flank of the Mattertal, Canton of Valais. In the past, several ice falls and avalanches from the glacier caused considerable losses of human life and property.

Because an acceleration of the glacier has been related to rupture events (Faillettaz, Funk, and Vincent 2015), monitoring the glaciers velocity can be used to issue early warnings. Since 2012, an automatic camera is used to determine the glaciers velocity. However, this technique requires optical visibility; observations at night or with foggy weather are impossible. Ground based Radar interferometry (GBInSAR) offers all-weather, day and night capability and can continuously measure the line-of-sight component of the glacier velocity field (Monserrat, Crosetto, and Luzi 2014).

In summer 2014 the velocity of Bisgletscher was first measured by Ku-Band ground based differential radar interferometry (GB-DInSAR) from a fixed installation at the Domhütte. This location gives the best observation geometry under the constraints of operating a radar in an alpine environment. This campaign was successful: the estimated line of sight velocity was comparable to the reference measurements obtained with optical methods.

In this paper, we present first results of a ground-based radar measurement campaign that was held between June and September 2015. Each day, the glacier was scanned at daytime for the duration of 12 hours with an acquisition each 2:30 minutes. The dense temporal sampling reduces decorrelation between the acquisitions, minimizes phase wrapping and allows to capture the temporal evolution of the velocity. A full polarimetric ground based radar was used for this campaign; the data will be used to develop improved processing techniques that integrate the polarimetric information.

For the observation of glacier velocities, daily displacement maps were obtained by zero-baseline differential interferometry (Caduff, Strozzi, and Wiesmann 2013):

subsequent images were combined into interferograms; the phase referenced to a stable scatterer in the proximity of the glacier to mitigate atmospheric phase disturbances. The interferograms were unwrapped and the residual atmospheric phase screen was corrected with a quadratic polynomial estimated in stable areas. Finally, several corrected interferograms were averaged in order to further reduce the atmospheric disturbances, which are assumed to be a zero-mean random process (Wegmüller, Strozzi, and Tosi 2000). The velocity maps measured with GB-DInSAR agree with the existing knowledge on the Bisgletscher; the measured displacement in the fastest moving parts of the glacier is approximatively 2 meters per day.

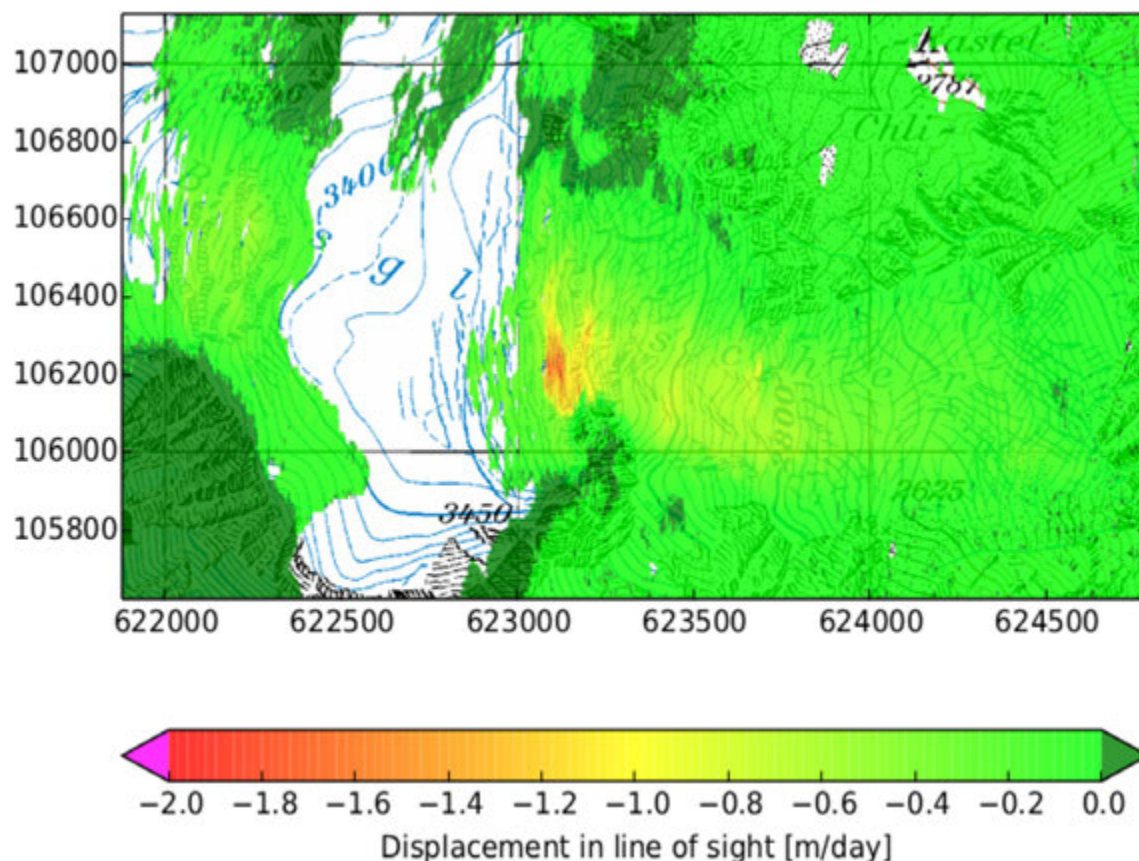


Figure 1: Daily average of the glacier velocity component in line of sight of the radar, for August 12, 2015.

REFERENCES

- Caduff, Rafael, Tazio Strozzi, and Andreas Wiesmann. 2013. "Erfolgreicher Einsatz Terrestrischer Radar-Interferometrie Zur Flächenhaften Vermessung von Ausserordentlichen Hangrutschungsbewegungen Im Gebiet Hintergraben (OW)." *Swiss Bulletin Für Angewandte Geologie* 18. doi:10.5169/seals-391152.
- Failetta, Jérôme, Martin Funk, and Christian Vincent. 2015. "Avalanching Glacier Instabilities: Review on Processes and Early Warning Perspectives: GLACIER INSTABILITIES." *Reviews of Geophysics* 53 (2): 203–24. doi:10.1002/2014RG000466.
- Monserat, O., M. Crosetto, and G. Luzi. 2014. "A Review of Ground-Based SAR Interferometry for Deformation Measurement." *ISPRS Journal of Photogrammetry and Remote Sensing* 93 (0): 40–48. doi:http://dx.doi.org/10.1016/j.isprsjprs.2014.04.001.
- Wegmüller, Urs, Tazio Strozzi, and Luigi Tosi. 2000. "Differential SAR Interferometry for Land Subsidence Monitoring: Methodology and Examples." In *Land Subsidence : Proceedings of the Sixth International Symposium on Land Subsidence*, 93–105. C.N.R., Gruppo nazionale per la difesa dalle catastrofi idrogeologiche.

17.2

Improved land cover assessment in agriculture with optical remote sensing data

Jonas E. Böhrer¹, Mathias Kneubühler¹, Devis Tuia², Michael E. Schaepman¹

¹ Remote Sensing Laboratories, Department of Geography, University of Zurich, Winterthurerstrasse 190, CH-8057 Zürich (jonas.boehler@geo.uzh.ch)

² Multimodal Remote Sensing, Department of Geography, University of Zurich, Winterthurerstrasse 190, CH-8057 Zürich

Land cover classification in agriculture is an important task in remote sensing. On the one hand statistical data on land cover, use and management is often available on administrative units and accessible regions only (De Wit & Clevers, 2004). On the other hand, monitoring of biodiversity has gained increasing importance over the past years. Among the ten recently proposed essential biodiversity variables are land cover and vegetation phenology (Skidmore et al., 2015). These variables are equally important when monitoring diversity as well as agriculture and can be provided with high spatial and temporal resolution by remote sensing sensors.

In this study, we present first classification results using Airborne Prism Experiment (APEX) imaging spectrometer data acquired over an agricultural area in May 2013. The area is located northwest of Lyss (Swiss midlands) and is composed of 300 fields of 10 different crop types in an early stage of phenology. We identified the ten crops present in the area under study with a Random Forest classifier, which is a nonparametric method for probabilistic classification (Breiman 2001). The overall accuracy (OAA) of the crop identification is of 72% (Fig. 1a). In order to include spatial information about the crops in neighboring pixels, we further processed this result by using a Markov Random Field model with a Potts pairwise smoothing term (Schindler, 2012), thus improving the OAA by 2% (Fig. 1b).

These results show the potential of imaging spectroscopy for precise crop classification and there is still large potential for further improvement by using spatial filters such as textural, morphological or bag of visual words features (Tuia et al., 2015).

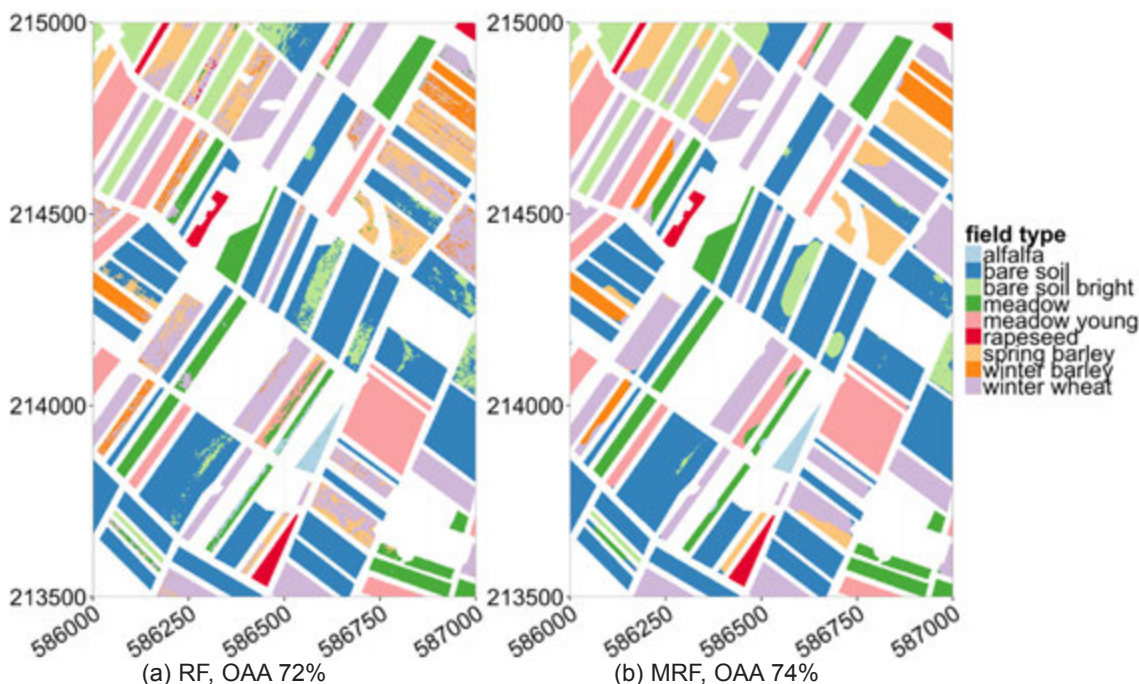


Figure 1. Classification results for Random Forest (a) and Markov Random Field (b) for 10 different crop types in Lyss (here only a part of the scene is shown).

REFERENCES

- Breiman, L. (2001). Random forests. *Mach. Learn.*, 45, 5-32.
- De Wit, a. J. W., & Clevers, J. G. P. W. (2004). Efficiency and accuracy of per-field classification for operational crop mapping. *Int. J Remote Sens.*, 25, 4091-4112.
- Schindler, K. (2012). An Overview and Comparison of Smooth Labeling Methods for Land-Cover Classification. *IEEE Trans. Geosci. Remote Sens.*, 50, 4534-4545.
- Skidmore, A. K., Pettorelli, N., Coops, N. C., Geller, G. N., Hansen, M., Lucas, R., ... Wegmann, M. (2015). Environmental science: Agree on biodiversity metrics to track from space. *Nature*, 523, 403-405.
- Tuia, D., Courty, N., Flamary, R. (2015). Multiclass feature learning for hyperspectral image classification: sparse and hierarchical solutions. *ISPRS J. Int. Soc. Photo. Remote Sens.*, 105, 272-285.

17.3

High-resolution remote sensing of NO₂ maps over Zurich with the Airborne Prism Experiment (APEX): new results

Gerrit Kuhlmann¹, Andreas Hueni², Alexander Damm², Lukas Emmenegger¹ & Dominik Brunner¹

¹ Empa, Swiss Federal Laboratories for Materials Science and Technology, CH-8600 Dübendorf, Switzerland
(gerrit.kuhlmann@empa.ch, lukas.emmenegger@empa.ch and dominik.brunner@empa.ch)

² Remote Sensing Laboratories, Irchel-Campus, University of Zurich, 8075 Zurich, Switzerland
(andreas.hueni@geo.uzh.ch and alexander.damm@geo.uzh.ch)

Since nitrogen dioxide (NO₂) concentrations have high spatial and temporal variability, high-resolution NO₂ maps are an important tool for urban air pollution assessment and epidemiological studies. These maps can be obtained with airborne imaging spectrometers such as the Airborne Prism Experiment (APEX) (Schaepman et al. 2015). APEX measures back-scattered solar irradiance in the visible and near-infrared (VNIR) with a spatial resolution of a few metres.

We present an improved version of the Empa APEX NO₂ retrieval (Popp et al. 2012). Our retrieval benefits from the newest APEX radiance product and better characterization of centre wavelength positions (CW) and full widths at half maximum (FWHM) of the slit function. Since the NO₂ retrieval requires accurate spectral calibration, we improved CW and FWHM accuracy for the VNIR channel (385-1000 nm) by aligning solar Fraunhofer lines and fitting atmospheric absorbers (H₂O and O₂). The NO₂ retrieval is a two-step procedure. In the first step, NO₂ slant column densities (SCD) were obtained using differential optical absorption spectroscopy (DOAS) between 440 and 510 nm. This is a larger fitting window than used previously which allowed us to include more absorbers such as the oxygen dimer (O₄), ozone, water vapour and liquid water to reduce cross-correlations. In addition, the first principle component of the residual spectra was fitted to include systematic instrument features not accounted for in the spectral calibration. An undersampling correction was applied to correct interpolation errors between reference and measurement spectrum. In the second step, air mass factors (AMF) were calculated to convert SCDs to vertical column densities (VCD) of NO₂, the final data product. The AMFs depend on solar position, instrument viewing direction, surface reflectance and atmospheric scattering due to air molecules, aerosols and clouds.

The improved retrieval was applied to an APEX flight over Zurich in August 2013 to obtain an NO₂ map with 50×50m² spatial resolution. The map shows the complex NO₂ distributions in the city with increased values in densely populated areas and low values over forests and hills surrounding the city. Furthermore, local features could be identified such as major roads and NO₂ emitted by a waste incinerator.

In conclusion, our revised retrieval is a significant step forward and reduces systematic and fitting errors as compared to the first version of the algorithm. Future analyses of APEX measurements already collected over Zurich and other locations will benefit from these improvements. The obtained maps will be used for further analysis such as comparison with urban-scale chemistry transport modelling.

REFERENCES

- Popp, C., Brunner, D., Damm, A., Van Roozendaal, M., Fayt, C., and Buchmann, B., 2012: High-resolution NO₂ remote sensing from the Airborne Prism Experiment (APEX) imaging spectrometer, *Atmos. Meas. Tech.*, 5, 2211-2225.
- Schaepman M.E. et al., 2015: Advanced radiometry measurements and Earth science applications with the Airborne Prism Experiment (APEX), *Remote Sens. Environ.*, 158, 207-219.

17.4

Lake Surface Water Temperature: Performance of split-window coefficients – a sensitivity analysis

Gian Lieberherr^{1,2}, Michael Riffler^{1,2}, Stefan Wunderle^{1,2}

¹ *Institute of Geography, University of Bern, Switzerland*

² *Oeschger Centre for Climate Change Research, University of Bern, Switzerland*

Lake surface water temperature (LSWT) is an important driver of lake ecosystems and it has been identified as an indicator of climate change. Available in-situ data for European LWT are heterogeneous in terms of spatio-temporal coverage and retrieval methods. Therefore they are not well suited for the study of climate induced change.

To solve that issue, a consistent satellite derived time series can serve as a baseline to standardise the available in situ data. The framework project of this study aims at compiling a homogeneous and consistent dataset of European LSWT. To ensure consistency, the same sensor type has to be used over a long period of time. The AVHRR sensor is mounted on NOAA/METOP satellites since the early 80ies, and therefore fulfils the requirements of climate relevant period as defined by the WMO.

The split-window method is the state of the art satellite temperature retrieval method. The principle is to empirically determine a relation between the surface temperature and the brightness temperatures measured at the satellite. This relationship, embodied within so called split window coefficients (SWCoefs), are then used to compute the LSWT. The precision of the method mainly depends on the quality of the SWCoefs. Therefore improving the method means that we need to understand the uncertainty sources during the SWCoefs determination process.

In general we assume that reducing the validity domain leads to more specific SWCoefs and thus to smaller errors. In the past, different split window approaches have been used, whereas the main difference amongst them lies in the way they determine the SWCoefs. For global applications (SST) the SWCoefs are determined with global validity but with limited temporal validity whereas for local studies (LSWT) the SWCoefs tend to have smaller spatial and larger temporal validity. However, there is no comparative study, quantifying and analysing the uncertainties related to the one or the other restriction of validity. Within a sensitivity analysis, the impact of the validity restricting parameters on the accuracy was quantified and compared. To improve the significance of the results, the analysis was performed on five different areas in Europe covering different climatic regions.

The results showed some interesting relationships and will help to design optimal validity parametrisations of the SWCoefs for each type of application. This will also be the basis for further improvements of the processing chain to generate the 30 years LSWT dataset of European lakes.

17.5

Satellite images: The Weissenstein anticline is younger than the Jura foldbelt

Hinrich Lohmann

Dorfstrasse 37, CH-4452 Itingen BL (h.lohmann@eblcom.ch)

The shape and development of the Jura foldbelt seem to be well understood, see for ex. Sommaruga (1997) or Becker (2000). Early steps in image interpretation of parts of the Jura foldbelt were undertaken by Laubscher (1981) and Berger (1994). The second named author stresses a straight N – S prolongation of the Upper Rhine graben. The present author disagrees and claims that the southern prolongation bends towards SW. This bend is best traceable along the eastern main border fault of the Rhine graben : From Lörrach via the E edges of the Laufen and Délemont basins to Gänsbrunnen, Lyss, and Payerne, possibly even Moudon. This may imply that the existence of the three lakes (Biel, Murten, Neuchâtel) is partly due to ongoing Rhine graben subsidence.

Generally all Jura folds and thrusts are konvex towards NW the only exception being the Chaumont, N of Neuchâtel. In the region between Ferrette – Liestal –Bretzwil – Biel – Saignelégier we see Rhine graben faults warp through the Jura folds and thrusts. This means: Within the circumscribed area (including the Weissenstein) we observe an interference pattern between rejuvenated Paleogene thick-skinned tectonics and Neogene thin-skinned tectonics.

This statement requires amplification: The Weissenstein anticline is unusually straight, WSW – ENE from Sonceboz to Hägendorf. It is broader than the curved Jura folds and shows on satellite images soft northern and southern flanks. While the Weissenstein gives a rather roof-like impression the Jura folds show only their crests plus minor SE flanks. Based on this interpretation one should consider the Weissenstein anticline as NOT being part of the Jura foldbelt. Which of the two elements is younger? It seems that the Chasseral fold and its NE extension CROSS the Weissenstein anticline at Grenchenberg and continue from there via Gänsbrunnen and Welschenrohr. This would mean: The Weissenstein anticline is younger than this part of the Jura foldbelt.

Bitterli (1990) reports strong indications for at least two tectonic phases in that part of the Weissenstein which he studied, between Oensingen and Wiedlisbach. He mentions the warp-through of Rhine graben tectonics and the south-vergent character required for proper section balancing. These observations support the idea of a young compressional event (post-Jura foldbelt, that means less than 5 million years ago) of thick-skin character. The Weissenstein anticline coincides with the S edge of the North Swiss Permocarboneous trough as described by Ustaszewski and Schmid (2007). We can explain the Weissenstein as a surface expression of a reactivated basement fault or – to say it differently –as a compressed extensional form, an inversion. – There is no significant alignment of recent seismic epicentres along the Weissenstein anticline.

REFERENCES

- Becker, A. 2000 : Der Faltenjura : Geologischer Rahmen, Bau und Entwicklung seit dem Miozän. – Jber.Mitt.Oberrhein geol. Ver., N.F.82, 317-336
- Berger, Z. 1994: Satellite hydrocarbon exploration. -330p. ; Springer, Berlin
- Bitterli, T. 1990 : The kinematic evolution of a classical Jura fold, a reinterpretation based on three-dimensional balancing technics (Weissenstein anticline, Jura mountains, Switzerland). – Eclogae geol.helv., 83(3), 493-511
- Laubscher, H. 1981: The 3-D propagation of décollement in the Jura. – In: Thrust and nappe tectonics; Geol.Soc.London, 311-318
- Sommaruga, A. 1997: Geology of the central Jura and the Molasse basin. –Mem.Soc.Neuchâteloise Sci.Nat., 12, 1-176
- Ustaszewski, K. and S.M.Schmid 2007: Neotectonic activity in the Upper Rhine graben-Jura mountains junction (northwestern Switzerland and adjacent France). – Swiss Bull. Appl.Geol., 12(1), 3-19

17.6

Estimating vegetation parameters in an alpine catchment by means of WorldView-2 imagery

Katrin Meusburger¹ & Christine Alewell¹

¹ *Environmental Geosciences, University of Basel, Bernoullistrasse 30, CH-4056 Basel (Katrin.Meusburger@unibas.ch)*

In alpine areas vegetation parameters are decisive for several earth surface processes such as erosion, runoff generation, land sliding, and snow gliding. To account for the typical small scale heterogeneity of the alpine landscape spatially high resolved imagery such as from QuickBird was found to be promising for the mapping of land cover types and fractional vegetation cover. However, the disadvantage of this spatially high resolved imagery, in general, is the small spectral resolution that causes difficulties in separating bare soil areas from non-photosynthetic vegetation and rock. The latter is mainly caused by the lack of short wave infrared channels that are important for mineral and rock discrimination. Thus, the objective of this study is to evaluate the suitability of WorldView-2 satellite (launched in October 2009) imagery that provides both 8 spectral bands (two of it in the near infrared) and high spatial resolution (1.8 m resolution at nadir) to map vegetation parameters. First results on the performance of land use classification and spectral unmixing of pixels to apportion vegetation and bare soil abundance will be discussed for the Bedretto- and Piora Valley in Ticino.

17.7

Classification of habitat diversity in two floodplains using UAVs

Gillian Milani¹, Diego Tonolla², Christopher Robinson³, Mathias Kneubuehler¹, Michael Doering², Michael Schaepman¹

¹ *Department of Geography, Remote Sensing Laboratories, University of Zurich, Winterthurerstrasse 190, Zurich, Switzerland (gillian.milani@geo.uzh.ch)*

² *Institute of Integrative Ecology, Zurich University of Applied Sciences ZHAW, Wädenswil, Switzerland*

³ *EAWAG, Swiss Federal Institute of Aquatic Science and Technology, Dübendorf, Switzerland*

River floodplains are among the most important ecosystems with respect to biodiversity despite their very small terrestrial coverage (Postel & Carpenter, 1997). They form an environment in which the aquatic and terrestrial components of the landscape interact closely. Since 1850 to 2002, 90% of pristine floodplains have disappeared in Switzerland. Even more, since 2010 two third of all aquatic vascular plants are on the red list of threatened species. Today, more than 4'000 km along rivers must be ecologically revitalised, among the 14'00 km of swiss rivers (Federal Council, 2015).

In this context, we suggest interdisciplinary work to improve the efficiency of planned restoration works and to integrate observational and modeling approaches. Remote sensing of floodplains has demonstrated impact combining ecological and hydraulic sciences as well as hydrological modeling. However, remote sensing of floodplains is challenging because of a particular state of vegetation: while some parts are comparable to tropical forests with mixed and layered structure, other parts are comparable to temperate forests with heterogeneous patches of species. Successful remote sensing techniques used in forest monitoring fail for riverine vegetation (Congalton et al., 2002). In general, observational requirements for floodplain monitoring using remote sensing are demanding in the spatial, temporal and spectral domains. Here, we propose the use of UAVs, combining high spatial resolution with flexible operating times.

Existing methods have largely been developed for landscapes not including heterogeneous floodplains, in particular taking into account restoration and monitoring aspects of floodplain dynamics. One of the main challenges is to apply a method allowing to reproduce approaches used by ecologists (Mertes, 2002). In this study, two very diverse floodplains are considered: the Saane river and the Sense river (Swiss plateau). The Saane river is exposed to substantial anthropogenic influence, whereas the Sense river is without hydrologic regulation. These different habitat dynamics can be observed using classification approaches for habitats. We use supervised classification based on spectral and textural information derived from ortho-images as well as 3D structure from point clouds generated using photogrammetric approaches. A preliminary classification example using a random forest classifier is presented in figure 1. The purpose of simultaneously

using texture and structural information is to increase the precision of the classification and allow a higher number of final classes. We aggregate pixels in individual data layers to increase the dimensionality of the classifier input. This allows to include texture to the classification procedure and – as a side effect – also reduces the computation load. Further metrics based on grey-level co-occurrence matrices are added to the input layers. Relative height and 3D structural information is added from the point cloud generated by photogrammetric methods from the UAV data. An independently generated digital elevation model is further used.

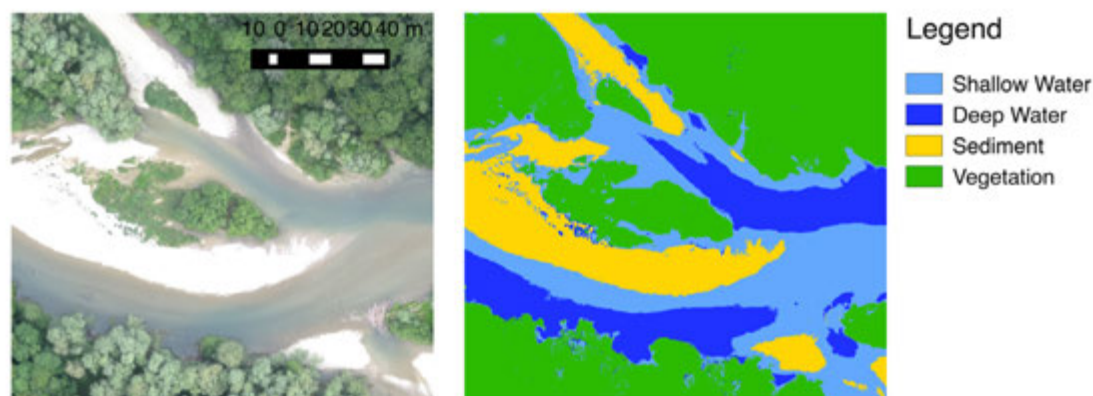


Figure 1. Coarse classification using only pixel-based spectral information.

Future work on floodplain classification will also make use of imaging spectrometer data (Torabzadeh et al., 2014). UAV data combined with imaging spectrometer data will allow to retrieve texture, 3D structural information as well as biochemical information, resulting in advanced habitat classification of floodplains.

REFERENCES

- Congalton, R. G., Birch, K., Jones, R., & Schriever, J. 2002: Evaluating remotely sensed techniques for mapping riparian vegetation. *Computers and Electronics in Agriculture*, 37, 113-126.
- Federal Council, 2015: Environment Switzerland 2015. State of the environment, 2015, 144.
- Mertes, L. A. K. 2002: Remote sensing of riverine landscapes. *Freshwater Biology*, 47, 799-816.
- Postel, S., & Carpenter, S. 1997: Freshwater ecosystem services. *Nature's services: Societal dependence on natural ecosystems*, 195.
- Torabzadeh, H., Morsdorf, F., & Schaepman, M. E. 2014: Fusion of imaging spectroscopy and airborne laser scanning data for characterization of forest ecosystems – A review. *ISPRS Journal of Photogrammetry and Remote Sensing*, 97, 25-35.

17.8

Mapping decadal land cover changes in the woodlands of north eastern Namibia using the Landsat satellite archive (1975-2014)

Vladimir R. Wingate ^{1,°}, Stuart R. Phinn ^{2,3†}, Peter Scarth ^{2,3†} and Nikolaus Kuhn ^{1†}

¹ *Physical Geography and Environmental Change, The University of Basel, Klingelbergstrasse 27 Basel 4056; Nikolaus.kuhn@unibas.ch*

² *Remote Sensing Research Centre, School of Geography, Planning and Environmental Management, The University of Queensland, St Lucia, QLD 4072, Australia; s.phinn@uq.edu*

³ *Joint Remote Sensing Research Program, School of Geography, Planning and Environmental Management, University of Queensland, St Lucia, QLD 4072, Australia; peter.scarth@gmail.com*

[†] *These authors contributed equally to this work.*

[°] *Author to whom correspondence should be addressed; E-Mail: Vladimir.wingate@unibas.ch; Tel.: +41-(0)-78-613-6259.*

Woodland savannahs provide essential ecosystem functions and services to communities. On the African continent, they are widely utilized and converted to intensive land uses. This study investigates the land cover changes of 108,038 km² in NE Namibia using multi-temporal, multi-sensor Landsat imagery, at decadal intervals from 1975 to 2014, with a post-classification change detection method and supervised Regression Tree classifiers. We discuss likely impacts of land tenure and reforms over the past four decades on changes in land use and land cover. These changes included losses, gains and exchanges between predominant land cover classes. Exchanges comprised logical conversions between woodland and agricultural classes, implying woodland clearing for arable farming, cropland abandonment and vegetation succession. The most dominant change was a reduction in the area of the woodland class due to the expansion of the agricultural class, specifically, small-scale cereal and pastoral production. Woodland area decreased from 90% of the study area in 1975 to 83% in 2014, while cleared land increased from 9% to 14%. We found that the main land cover changes are conversion from woodland to agricultural and urban land uses, driven by urban expansion and woodland clearing for subsistence-based agriculture and pastoralism.

Keywords: Deforestation; Tropical dry forest; Land degradation; Namibia; Remote Sensing; Landsat; Land cover change; Africa;

P 17.1

Lake surface water temperatures derived from Landsat 8

Patrick Bur, Gian Lieberherr, Stefan Wunderle

¹ *Institute of Geography, University of Bern, Hallerstrasse 12, CH-3012 Bern Switzerland (patrick.bur@students.unibe.ch)*

² *Institute of Geography, University of Bern, Hallerstrasse 12, CH-3012 Bern Switzerland (gian.lieberherr@giub.unibe.ch)*

³ *Institute of Geography, University of Bern, Hallerstrasse 12, CH-3012 Bern Switzerland (swun@giub.unibe.ch)*

Changes in Lake Surface Water Temperature (LSWT) can have strong impacts on the quality of the lake water, the concentration of dissolved gases, on the lake biology and chemistry. In addition, Global Climate Observing System (GCOS) lists lake water temperature as an essential climate variable (ECV). Regarding those aspects, LSWT-monitoring with satellite data is very promising. It can provide continuous long-term records of observation, as well as giving information on spatial patterns of LSWT variability.

The remote sensing group at the University of Berne provided a LSWT data set based on Advanced Very High Resolution Radiometer (AVHRR) of lakes located in or near the European Alps (Riffler et al. 2015). Based on that work, the goal of this master thesis is to compile a LSWT data set from Landsat 8 data. Compared to the AVHRR-sensors on the NOAA-satellites, the Landsat 8 sensors have a higher spatial resolution in the thermal infrared spectra (100m vs 1.1km resolution). Therefore, this work will focus in a large part on the difference between the two sensors. In particular on the Landsat 8 sensor performance compared to AVHRR. The project focuses on two or three Swiss lakes (for example Lake Constance). The method used to derive the LSWT is the linear Split Window Algorithm after Hulley et al. 2011.

The poster will feature a description of the master thesis, first results and plots for the lake surface water temperature of Lake Constance and a comparison to in situ measurements and AVHRR-data. Furthermore, the poster will give information's about the current state of the work and provide an outlook for the next steps.

REFERENCES

- Hulley G. C., Hook S. J., Schneider P. 2011: Optimized split-window coefficients for deriving surface temperatures from inland water bodies. *Remote Sensing of Environment* 115, 3758-3769.
- Riffler M., Lieberherr G., Wunderle S. 2015: Lake surface water temperatures of European Alpine lakes (1989-2013) based on the Advanced Very High Resolution Radiometer (AVHRR) 1 km data set. *Earth Syst. Sci. Data*, 7, 1–17.

18. Geoscience and Geoinformation - From data acquisition to modelling and visualisation

Nils Oesterling, Adrian Wiget, Massimiliano Cannata, Michael Sinreich

Swiss Geological Survey
Swiss Geodetic Commission
Swiss Geotechnical Commission
Swiss Geophysical Commission
Swiss Hydrogeological Society

TALKS:

- 18.1 Baumberger R., Herwegh M., Kissling E.: Derivation and verification of a structural 3D model of the Haslital (Aar massif, Switzerland) from remote sensing and field data
- 18.2 Baumeler A., Reber D., Sinreich M.: Der digitale hydrogeologische Datensatz 1:100000 als Teil einer massstabs-übergreifenden Raumdatenhaltung: Anforderungen und Potential
- 18.3 Brentini M., Favre S., Giuliani G., Lehman A., Moscariello A.: Information System for subsurface geological data: Overview of the situation in Europe
- 18.4 Brodhag S.H., Oesterling N., Baumberger R.: Data Management Strategy Based on Harmonised Data Models – An Example from Switzerland
- 18.5 Cannata M., Colombo M., Antonovic M., Cardoso M., Delucchi A., Gianocca G., Brovelli M.: I CAMMINI DELLA REGINA – Open Source based tools for preserving and culturally exploring historical traffic routes
- 18.6 Composto S., Bollinger D., Ingensand J., Patthey P., Eyholzer R., Heeb C.: An analysis of deer habitat on the Swiss Plateau
- 18.7 Leder R.M.: iDigBio vs. FOSSIL? Closing the gap and franking private fossil resources into professional databases
- 18.8 Marti U.: Gravity field modeling in Switzerland
- 18.9 Preisig G., Gischig V., Eberhardt E., Hungr O.: Hydromechanical versus seismic fatigue in progressive failure of deep-seated landslides
- 18.10 Schmidt S., Meusburger K., Panagos P., Alewell C.: Seasonal variability of rainfall erosivity across Europe and Switzerland

POSTERS:

- P 18.1 Zheng L., May D., Gerya T.: Deformation enhanced fluid distribution in the subduction interface: numerical modelling
- P 18.2 Spataro A., Hoffmann M.: Long range laserscanning for the Gneiss quarries survey

18.1

Derivation and verification of a structural 3D model of the Haslital (Aar massif, Switzerland) from remote sensing and field data

Roland Baumberger¹, Marco Herwegh², Edi Kissling³

¹ Federal Office of Topography, Swiss Geological Survey, Seftigenstrasse 264, CH-3084 Wabern
(roland.baumberger@swisstopo.ch)

² University of Bern, Institute of Geological Sciences, Baltzerstrasse 1+3, CH-3012 Bern

³ ETH Zürich, Institute of Geophysics, Sonneggstrasse 5; CH-8092 Zürich

Ideally, the three-dimensional (3D) representation of subsurface structures relies on both underground and surface data. Commonly, the former is scarcely available or entirely lacking. Therefore, 3D models often have to rely on surface data only, requiring the projection of geological surface information to depth. The prediction of subsurface continuation of rocks and structures represents an important task for general research and applied projects (e.g., underground constructions, deep geothermal energy, fossil energy and ore resources, CO₂ sequestration, and nuclear waste disposal). In the past years, powerful software tools have been developed to facilitate extrapolation of surface data to depth. Despite this progress in construction capabilities, development of 3D geological models still mainly depends on amount and quality of surface information available and related assumptions regarding the projection to depth. In this respect, estimations about quality and associated uncertainty of information projected to depth and transfer of this knowledge to the end user of the 3D model are crucial.

In this study we present an approach to investigate the large-scale 3D deformation pattern in the European Central Alps in Switzerland from surface data only combined with a thorough assessment of uncertainties related to input data, to extrapolation of surface data and the correlation of surface and underground information. We bank our approach on the mapping of lineaments by means of remote sensing and field work. Our uncertainty estimations concentrate on aspects related to both 2D (spatial resolution, digitization accuracy, angular resolution) and 3D input data (dip data extraction, extrapolation of surface data, extrapolation uncertainty). We introduce the concepts of the Central Extrapolation Surface (CES) and the Extrapolation Uncertainty Area/Volume (2D: EUA; 3D: EUV), which enable the valid projection of surface data to depth within a well-defined and data-constraint uncertainty range. In a subsequent stage, the accuracy of the projected data are evaluated using geological information from depth available from a gas pipeline tunnel. With this study we document, how geometrical correlations between surface and underground data within their respective EUA/EUV may be used to construct a valid 3D model and we demonstrate that this approach delivers geologically relevant results. The application of the suggested work flow allows the generation of validated 3D models of fault and shear zones, which will help for structural predictions at depth being helpful in the case of underground constructions but also for improved geodynamic understanding of mountain building processes.

18.2

Der digitale Hydrogeologische Datensatz 1:100000 als Teil einer massstabsübergreifenden Raumdatenhaltung: Anforderungen und Potential

Andreas Baumeler¹, Doris Reber² & Michael Sinreich³

¹ DIGIKARTO, Mythenquai 353, CH-8038 Zürich (andreas.baumeler@digikarto.ch)

² Geozeichen, Mythenquai 353, CH-8038 Zürich

³ Bundesamt für Umwelt BAFU, Abteilung Hydrologie, CH-3003 Bern

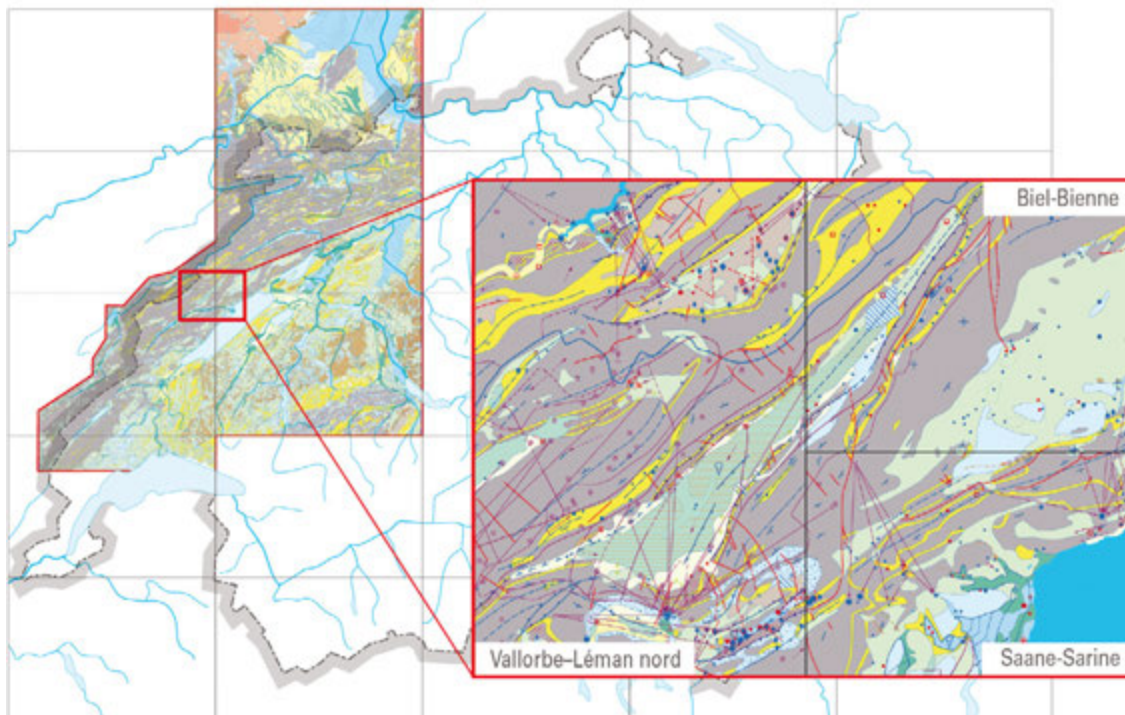
Im Herbst 2015 wird vom Bundesamt für Umwelt BAFU die digitale *Hydrogeologische Karte 1:100000 Nordwest-Schweiz* veröffentlicht. Dieser vektorielle Datensatz stellt einen weiteren wichtigen Teil einer massstabs-übergreifenden thematischen Raumdatenhaltung dar, mit der die Themen Hydrologie, Grundwasser und Geologie verknüpft werden (Figur 1). Er veranschaulicht die speziellen Anforderungen an Datenrückfassung und Digitalisierung, Generalisierung, blattschnittfreie Darstellung und insbesondere an die Massstabsfrage bei der Zurverfügungstellung von digitalen Geodaten.

In der Schweiz existieren auf Bundesebene sechs, auf kantonaler Ebene zwei offizielle Massstabsabstufungen (Figur 2). Diese wurden im vordigitalen Zeitalter als grundlegendes Instrument zur Erstellung und Nutzung geobasierter Daten eingeführt. Die bewusste Wahl eines Massstabs wurde damit zur ersten Frage jeder Datenerstellung. Die Festlegung auf einen Zielmassstab hat u.a. folgende wichtigen Funktionen:

- Erstellung von Atlaswerken
- Darstellung von Themen auf nationaler, regionaler und lokaler Ebene
- Benutzergerechte Publikation von Geodaten
- Verknüpfung von Themen
- Flächendeckende Darstellung von Themen mit geringem oder lückenhaftem Wissensstand (abgeleitete oder interpretierte Geodaten).

Bei gedruckten Karten wird die Aussagekraft der Daten von den meisten Nutzern intuitiv richtig eingeschätzt. Im Zuge der Digitalisierung und Nutzung der Daten am Bildschirm wird jedoch der Massstabsfrage deutlich weniger Gewicht geschenkt, wobei durch die Vergrößerungsfunktion der Detaillierungsgrad der Daten oft überschätzt wird. Prinzipiell hat aber jeder Datensatz – ob analog gedruckt oder digital in GIS-Systemen gehalten – bei der Erstellung und Aktualisierung einen Zielmassstab sowie einen Massstabsbereich, innerhalb dessen eine Nutzung der Informationen sinnvoll und zulässig ist.

Zur intuitiven Erfassung des Zielmassstabs erscheint es daher notwendig, neue grafische Werkzeuge zu entwickeln. Zudem gibt es konzeptionellen Bedarf sowie hinsichtlich der technischen Möglichkeiten, eine generalisierte Karte automatisch aus grossmassstäblichen Datensätzen abzuleiten. Im Sinne einer umfassenden digitalen Raumdatenhaltung wird dies im Zusammenhang mit den Hydrogeologischen Karten derzeit geprüft, da noch grosses Potential zur Inwertsetzung bereits vorhandener Daten im Bereich Grundwasser besteht.



Figur 1. Digitale Hydrogeologische Karte 1:100000 Nordwest-Schweiz: Für einen blattschnittfreien Datensatz wurden die publizierten Ausgangsdaten der Kartenblätter Vallorbe-Léman nord, Saane, Biel und Basel homogenisiert und angepasst.



Figur 2. Die Hydrogeologische Karte 1:100000 als Teil einer thematischen Raumdatenhaltung. In den Massstäben 1:25000 und 1:500000 ist eine interdisziplinäre Verknüpfung der hydrologischen mit den geologischen Informationen gegeben.

18.3

Information System for subsurface geological data: Overview of the situation in Europe

Maud Brentini¹, Stéphanie Favre², Gregory Giuliani², Anthony Lehmann² & Andrea Moscariello¹

¹ *Department of Earth Sciences, University of Geneva, Rue de Maraichers 13, CH-1205 Genève (maud.brentini@unige.ch)*

² *Institute for Environmental Sciences, University of Geneva, Boulevard Carl Vogt 66, CH-1205 Genève (stephanie.favre@unige.ch)*

The deep subsurface and its natural resources belong to the State. A detailed and accurate knowledge of them is therefore key to allow their effective exploitation and management.

GEothermie 2020 is a program piloted by the Service Industriels de Genève (SIG) and the State of Geneva. Its aim is to develop geothermal energy in the Geneva basin. Different themes must be approached to deal with the whole project. The topic of this paper concerns the challenges and issues regarding the organisation and effective management of subsurface data.

Funded and supported by the State of Geneva, this project focuses on centralization and valorisation of regional geological data. Building a database linked to a Geographic Information System (GIS) capable to manage two and three-dimensional (2D & 3D) geological information such as seismic lines, borehole logs, reports, outcrops and subsurface 2D and 3D models is therefore essential. In parallel a substantial work on the review and consolidation of basin stratigraphic definition and nomenclature has to be carried out in order to correlate all the data.

We first need to make an overview of the current geological data management practices in Europe. A literature research highlighted the different ways that geological surveys manage their surface and subsurface data (BRGM and SGF, 2014 ; Van der Meulen et al., 2013 ; EUREGEO, 2015). Geological surveys with a lot of data had to find a solution already some years ago, such as the BRGM (Bureau de Recherches Géologiques et Minières, France), the TNO (Geological Survey of the Netherlands) and the BGS (British Geological Survey).

In order to achieve an accurate overview and establish the state of the art on this subject a short structured question list will be sent to all european geological surveys. This survey will cover six themes ranging from IT, human and financial resources, management of geological data, GIS applications, cross-border collaboration and policy and legal framework. The collection of all this information will allow us to develop the Geneva Geological Information System using the best practices from european geological surveys.

The complete information system will be owned by the State of Geneva and will offer users (scientists, engineer and public) capabilities to find, extract, validate (relevance, quality), interpret, process and spread 2D and 3D geological data. Finally, it will provide tools for the State of Geneva to manage its subsurface resources like Geothermal energy!

REFERENCES

- BRGM and SGF. March 2014: Le référentiel géologique de la France, *Géochronique*, Magasine des géosciences, n°129, 56p.
- M.J. van der Meulen, J.C. Doornenbal, J.L. Gunnink, J. Stafleu, J. Schokker, R.W. Vernes, F.C. van Geer, S.F. van Gessel, S. van Heteren, R.J.W. van Leeuwen, M.A.J. Bakker, P.J.F. Bogaard, F.S. Busschers, J. Griffioen, S.H.L.L. Gruijters, P. Kiden, B.M. Schroot, H.J. Simmelink, W.O. van Berkel, R.A.A. van der Krogt, W.E. Westerhoff. 2013: 3D geology in a 2D country: perspectives for geological surveying in the Netherlands, *Netherlands Journal of Geosciences*, vol. 92, n°04, pp. 217–241.
- EUREGEO 2015: Geological 3D Modelling workshop, 8th EUREGEO – European Congress on REgional GEOscientific Cartography and Information Systems, 15-17.06.2015, Barcelona, Spain.

18.4

Data Management Strategy Based on Harmonised Data Models – An Example from Switzerland

Sabine H. Brodhag¹, Nils Oesterling¹ & Roland Baumberger¹

¹ *Federal Office of Topography swisstopo, Swiss Geological Survey, Seftigenstrasse 264, CH-3084 Wabern (sabine.brodhag@swisstopo.ch)*

The Swiss Confederation is based on a federal political system. Legislation is split between federal, cantonal and communal level. This system strongly affects the handling of geological surface and sub-surface data, which is why data capture, storage and supply is carried out by different federal levels mentioned above. Since Switzerland consists of 26 Cantons (and more than 2000 communes) and common standards for geological data are rare, the exchange of this data is difficult. For instance, national wide analyses are barely possible or can only performed with extensive manual work. The Swiss Geological Survey (SGS) identified this challenge already a couple of years ago. In order to face it, the SGS started developing common data models for various types of geological data. These models include geological maps, borehole data and 3D models. Further topics such as seismic data and geological reports are envisaged. For the data model development it turned out to be essential to integrate the relevant stakeholders in order to increase the acceptance of the respective model and to guarantee meeting its proper target. This participation practice is generally appreciated by the stakeholders. Furthermore, during the process of data model development, it became obvious that a clear strategy is crucial for efficient data management. Especially the target data (data of national relevance) and relevant stakeholders as well as duties and responsibilities have to be identified and defined.

On the basis of this strategy, underpinned by harmonised data models, target data of defined quality can be collected, stored and distributed. Furthermore, services such as a central platform for data capture or distribution can be established. As a result, geological data of various dimensions (from 0D to 4D) can be efficiently exchanged between different information systems from various data providers. Redundant storage of inconsistent and incomplete data is prevented.

18.5

“I CAMMINI DELLA REGINA” - Open Source based tools for preserving and culturally exploring historical traffic routes.

M. Cannata¹, M. Colombo, M. Antonovic¹, M. Cardoso¹, A. Delucchi¹, G. Gianocca¹, M. Brovelli²

¹ *Scuola Universitaria Professionale della Svizzera Italiana (SUPSI), Campus Trevano, CH-6952 Canobbio*

² *Politecnico di Milano, Como Campus, DICA, Via Valleggio 11, 22100 Como, Italy)*

“I CAMMINI DELLA REGINA” (The Via Regina Paths) is an Interreg project funded within the transnational cooperation program between Italy and Switzerland 2007-2013. The aim of this project is the preservation and valorization of the cultural heritage linked to the walking historically paths crossing, connecting and serving the local territories. With the approach of leveraging the already existing tools, which generally consist of technical descriptions of the paths, the project uses the open source geospatial technologies to deploy innovative solutions which can fill some of the gaps in historical-cultural tourism offers.

The Swiss part, and particularly the IST-SUPSI team, has been focusing its activities in the realization of two innovative solutions: a mobile application for the survey of historical paths and a storytelling system for immersive cultural exploration of the historical paths.

The former, based on Android, allows to apply in a revised manner a consolidated and already successfully used methodology of survey focused on the conservation of the historical paths (Inventory of historical traffic routes in Switzerland). Up to now operators could rely only on hand work based on a combination of notes, pictures and GPS devices synthesized in manually drawn maps; this procedure is error prone and shows many problems both in data updating and extracting for elaborations. Thus it has been created an easy to use interface which allows to map, according to a newly developed spatially enabled data model, paths, morphological elements, and multimedia notes. When connected to the internet the application can send the data to a web service which, after applying linear referencing and further elaborating the data, makes them available using open standards.

The storytelling system has been designed to provide users with cultural insights embedded in a multimedial and immersive geospatial portal. Whether the tourist is exploring physically or virtually the desired historical path, the system will provide notifications and immersive multimedia information that foster a new sight of the territory: award of the culture and history of the place thanks to attractive description of the geological, land use, historical and ethnographic contexts.

The technologies used for these developments are: mongoDB, tornado, Android SDK, geoserver, bootstrap, OpenLayers, HTML5, CSS3. The approach, methodologies and technical implementations will be discussed and presented.

18.6

An analysis of deer habitat on the Swiss Plateau

Sarah Composto¹, Dominique Bollinger¹, Jens Ingensand¹, Patrick Patthey², Roman Eyholzer³, Christian Heeb⁴

¹ G2C Institute, University of Applied Sciences Western Switzerland (HEIG-VD), Route de Cheseaux 1, CH-1401 Yverdon (VD) (sarah.composto@heig-vd.ch)

² Direction générale de l'environnement (DGE) – Forest, Ch. du Marquisat 1, CH-1025 St-Sulpice (Vaud)

³ Service des forêts et de la faune (SFF), Route du Mont Carmel 1, CH-1762 Givisiez (Fribourg)

⁴ Département de la faune de l'Etat de Berne, Schwand 17, CH-3110 Münsingen (Berne)

The red deer is a native species but at the beginning of the 20th century has been nearly extinct in Switzerland. Due to an improved protection the numbers of red deer are rising and in the last decades the species has recolonized many parts of Switzerland. The situation of the deer is sensitive. It is therefore important to weight environmental capacities and to manage deer populations in a balanced way. In order to manage deer populations it is first of all necessary to determine the deer's habitat potential which is the main focus of this project.

Currently several methods are used for the determination of deer habitat such as manual counts and mortality statistics. These methods however do not take into account various environmental aspects. We have therefore chosen to use the extended Ueckermann method (Bonney, 1991; Ueckermann, 1952, 1960) for the identification of deer habitat on the Swiss Plateau. This method has never been applied in Switzerland before and it is based on six criteria which are all independently evaluated on the basis of several environmental parameters such as the shape of forest patches or the kind of bedrock. Ueckermann's method yields an estimate of sustainable red deer densities regarding economical value of forests (between 1.5 and 4 deer / 100 hectares).

Several steps were required to apply this method. At first georeferenced datasets were acquired and analyzed in order to identify the data that fitted Ueckermanns criteria. Moreover data precision, reliability, homogeneity, malleability were important measures. Finally four data sets were selected:

The swissTLM3D (swisstopo) a large-scale topographical landscape database of Switzerland which includes land-use data
The geological 1:500'000 atlas of Switzerland (swisstopo)
Forest data from the cantons of Vaud (dendrometric data) and Fribourg (surfaces)

These data sets were used to implement a data analysis process in order to apply the extended Ueckermann method. Each criterion was processed independently and some hypothesis were established with the help of specialists. (Figure 1) In order to identify forest patches for instance, minimum dimensions had to be taken into account: A minimum distance of 100 meters that could fit in a surface of at least 25 hectares.

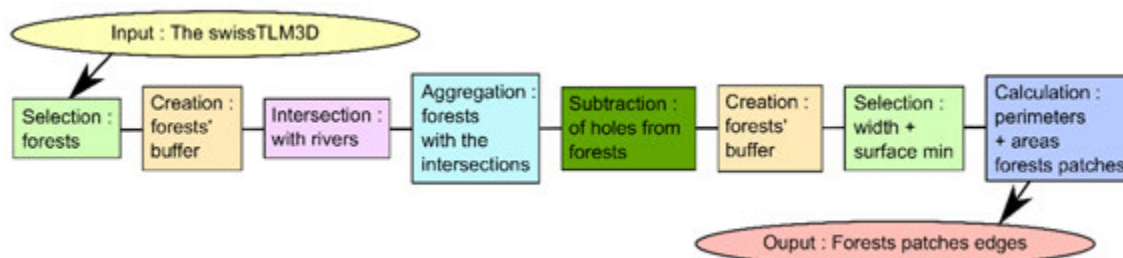


Figure 1. Example of processing steps of one criterion of the extended Ueckermann method.

Moreover as the trees' height information which is taken into consideration for an another criterion was missing, it had to be determined using other information such as the stage of forest development, the degree of closure, planned forest management and the availability of hardwood.

The main result of the data analysis is a synthetic map showing forest areas on the Swiss Plateau and highlighting potential deer habitat. For each habitat Ueckermanns criteria and points are specified (Figure 2). Although it is still necessary at this stage to control the results and to present them to forest and wildlife experts, this study demonstrated the applicability of Ueckermanns extended method on western Switzerland, despite the difficulty of merging together heterogeneous datasets. All generated data enables stakeholders to take decisions for the protection of this habitat and allows for a comparison with other data sets such as for instance deer observations.

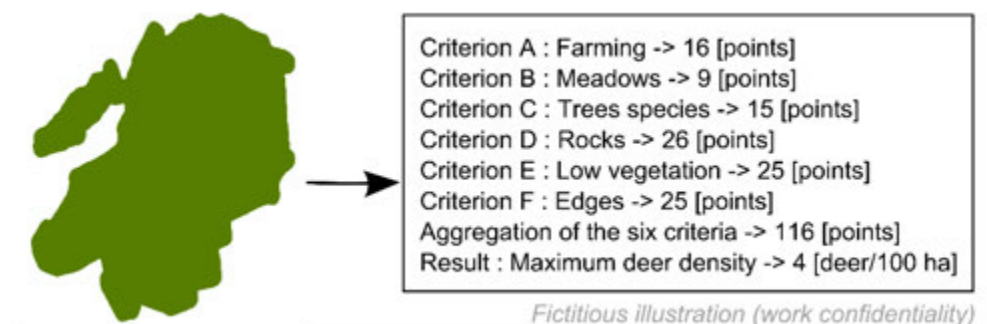


Figure 2. Illustration of a forest patch with different calculated criteria.

This study demonstrated the applicability of Ueckermanns extended method on Swiss data. However a main difficulty in the processing of data was the heterogeneity of data coming from the Swiss state and different cantons which can lead to potential inconsistencies. The approach that the authors have taken in order to apply Ueckermanns extended method can be used for the analysis of other species' habitat.

REFERENCES

- Bonney, G. & Klein, F. 1991: Le cerf. Paris : Hatier.
 Ueckermann, E. 1952: Rehwild und Standort. Graz : Der Anblick.
 Ueckermann, E. 1960: Wildstandsbewirtschaftung und Wildschadenverhütung beim Rotwild : ein Leitfaden für die erfolgreiche Rotwildhege. Berlin : Hamburg Berlin Parey.

18.7

iDigBio vs. FOSSIL? Closing the gap and franking private fossil resources into professional databases.

Dr. Ronny Maik Leder¹

¹ Florida Museum of Natural History, University of Florida, 1659 Museum Road PO Box 117800, Gainesville, FL 32611-7800, USA (leder.ronnymaik@flmnh.ufl.edu)

The great natural history collections in museums, universities and other academic institutions all over the world are the backbone of national and international research in taxonomy, biodiversity and evolution. But getting access to those resources is mostly limited to academics. The main goal of the Integrated Digitized Biocollections project, in short iDigBio, is to collect data and images for millions of biological specimens and make them available in electronic format for the research community, government agencies, students, educators, and the general public. It is the National Resource for Advancing Digitization of Biodiversity Collections (ADBC) funded by the National Science Foundation (NSF). The bulk of the collections, especially for fossils, has its origin in private engagement and was donated by private collectors and enthusiasts. Even the most iconic of fossils (e.g. *Archaeopteryx lithographica*, von Meyer 1861) stem from the playground of amateur paleontologists and private collectors. It is hard to imagine how much more may lie dormant unnoticed in private cabinets. The NSF funded FOSSIL project is focused on getting access to these treasures in building connections in the paleontological community. It is the core of a big network between amateurs and professionals. How can iDigBio and FOSSIL get along? While iDigBio is the big online collection for the bio-community, FOSSIL is part of this community. It helps the paleo-people getting together, communicate in a simple form and tear down borders between the academics and the public. It is focused on attracting fossil hunters of all ages and level of experience to participate in academic research in general and to provide professional digital databases like myFOSSIL and iDigBio with input that was recently mostly unreachable. To that end, the Fossil Project in partnership with iDigBio has begun training amateurs to fulfill all the requirements needed to not just get access into the databases but also to be part of the FOSSIL and iDigBio world in donating their treasures in digital form. As amateurs gain skills, we anticipate increased interest and participation in the international effort to digitize collections.

18.8

Gravity field modeling in Switzerland

Urs Marti

*Bundesamt für Landestopografie swisstopo, Bereich Geodäsie, Seftigenstrasse 264, CH-3084 Wabern
(urs.marti@swisstopo.ch)*

The Earth's gravity field has a major influence on all geodetic observation techniques. Classical observations, such as horizontal and vertical angles, distances and height differences (leveling) have to be corrected for works on a regional or national scale in order not to introduce systematic errors. But on GNSS measurements as well, the gravity field has an impact in form of disturbed satellite orbits and the obtained heights have to be reduced by the geoid undulation.

In other disciplines such as geophysics, geology or even archeology, the knowledge of the gravity is useful in the determination of the structure of the underground and the modeling of the interior of the Earth. In metrology, gravity values are needed for the calibration of high precision balances, pressure and force meters or atomic clocks. Hydrologists and glaciologists use gravity to study mass changes such as soil moisture, ground water level or ice melting. Oceanographers investigate the ocean currents by comparing the physical surface of the sea with the equipotential surface of the gravity field.

Global gravity field models today are usually constructed out of data from dedicated satellite missions such as GRACE or GOCE and have reached an accuracy of about 1 mGal. They have the advantage of global coverage, a uniform reference system and a homogeneous gravity datum. Satellite only models reach a resolution in the order of 50 km and are very useful for many studies on a global or continental scale. By combining satellite data with terrestrial data, as it is done for global models such as EGM2008, the resolution can be improved to around 10 km. The monthly GRACE solutions are a very versatile tool to study global mass change.

Due to the limited resolution of global models, local and national gravity field models are still useful and necessary for most applications. In Switzerland, the main source for gravity measurements is the database maintained by the University of Lausanne on behalf of the Swiss Geophysical Commission (SGPK). This data set was used to produce the gravimetric atlas 1:100'000 (Olivier et al. 2010). Further sources include the data of the Swiss Geodetic Commission (SGC), the Institute of Geophysics (ETH Zurich), the University of Lausanne, the University of Geneva, the University of Neuchâtel and NAGRA.

swisstopo is assembling all these various data sets into one single national database and maintains it in the future. Besides archiving the existing data since the 1950ies, further goals are the management of data distribution, the quality assessment, the detection of outliers, the application of recent reduction formulas and topographic models and to transfer the data to a modern and uniform reference system.

The actual gravimetric reference network (LSN2004) is based on recent absolute measurements on around 15 stations. The absolute measurements are repeated at least every 10 years. This basic network is densified by more than 100 relative stations which are mainly identical to the points of the base network SG95 (Arnet & Klingelé 1997) and are re-observed regularly. All observations since 1992 are treated in a rigorous least squares adjustment process and the results are published on the swisstopo website.

The newly compiled gravity data set together with the measured deflections of the vertical and the GNSS/leveling stations form the basis for a national 3D gravity field model in which the very low frequencies are taken from a global model, the middle frequencies are mainly given by the measurements and the highest frequencies are calculated out of a digital mass model.

With this national gravity field model it is possible to predict gravity values with an accuracy better than 1 mGal and vertical deflections better than 1 arcsec in most parts of the country. This is sufficient for most applications in geodesy and metrology without the necessity to perform in-situ measurements.

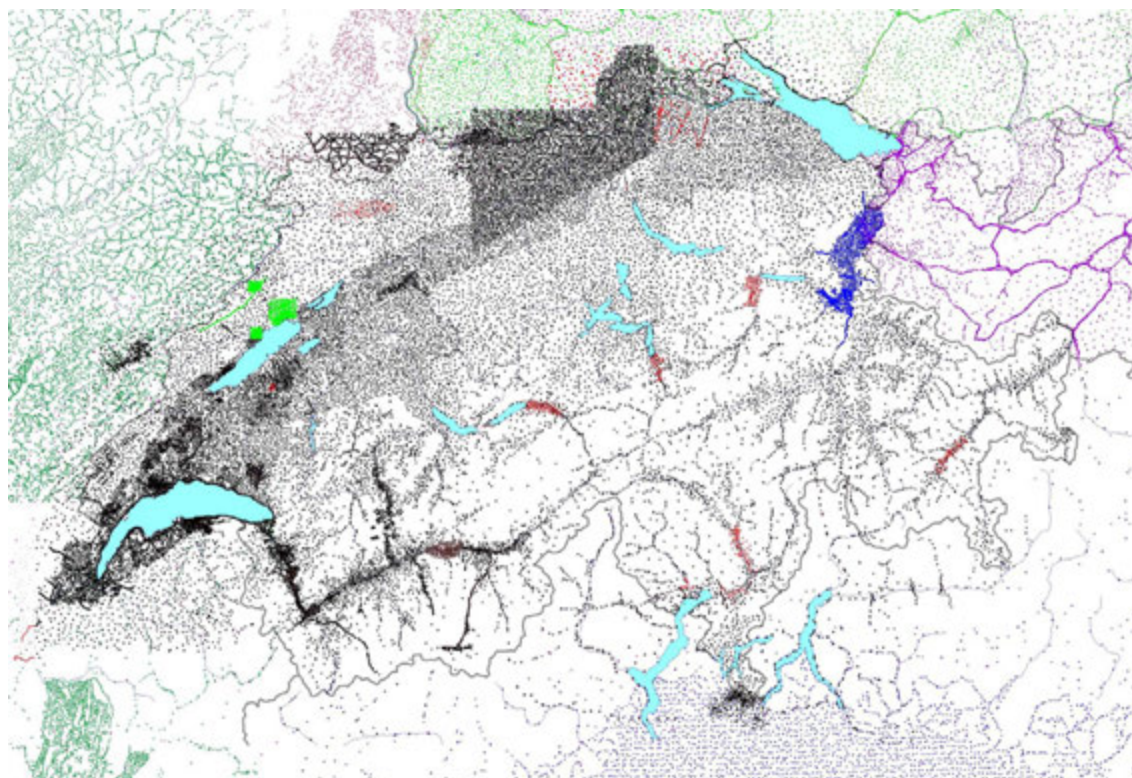


Figure 1. Gravity data of Switzerland and surrounding areas.

REFERENCES

- Arnet F. & Klingelé E. 1997: SG 95: Das Neue Schweregrundnetz Der Schweiz. Geodätisch-geophysikalische Arbeiten in der Schweiz Nr. 54.
- Olivier R., Dumont B. & Klingelé E. 2010: Atlas gravimétrique de la Suisse, Contribution to the Geology of Switzerland - Geophysics Nr. 43.

18.9

Hydromechanical versus seismic fatigue in progressive failure of deep-seated landslides

Giona Preisig^{1,2}, Valentin Gischig^{1,3}, Erik Eberhardt¹ & Oldrich Hungr¹

¹ EOAS – Geological Engineering, The University of British Columbia, 2207 Main Mall, V6T 1Z4 Vancouver BC, Canada (gpreisig@eos.ubc.ca)

² Swiss Geological Survey - swisstopo, Seftigenstrasse 264, CH-3084 Wabern bei Bern

³ ETH Zürich, Swiss Competence Center for Energy Research (SCCER-SoE) Sonneggstrasse 5, CH-8092 Zürich

Deep-seated landslides are characterized by slow time-dependent movements induced by constant gravitational creep, and periods of acceleration associated with stress changes within the rock and the pre-existing fracture network. Natural stress changes are typically caused by seasonal variations in surface temperatures and groundwater pressures, but also by rare and more violent events such as earthquakes. These processes are responsible for cyclic loading and unloading that leads to rock mass damage, fatigue and progressive failure with time, and may explain sudden, unexpected rock slope acceleration phases. In this work, we present a set of distinct-element models to investigate and compare the role of hydromechanical fatigue and seismic fatigue in the history of a deep-seated landslide. Hydromechanical fatigue arises from the fluctuation of pore pressure in fractures accompanying periods of significant groundwater recharge. In alpine areas, there are usually one or two cycles per year associated with snow melt and intense rainfall periods. In the presence of a deep confined aquifer within the rock slope, the amplitude of pressure fluctuations may reach values of 0.25-0.5 MPa. Hydromechanical models considering such pressure changes are able to reproduce observed slope accelerations-decelerations phases. Substantial accelerations may occur even in the absence of a cycle of exceptional amplitude, depending on the current state of fatigue. At a given time, one or more fractures may be critically-stressed, and a small change in applied stress is enough to cause local failure and induce a crisis of enhanced slope movement. Similar fatigue effects have also been proposed for repeated earthquake events in seismically active regions. Unlike hydromechanical stress changes that occur in a more localized portion of the rock slope, those induced by passing seismic waves involve the entire rock mass. Moreover, the frequency and amplitude of stress perturbations due to earthquakes are different than those induced by pore pressure variations, although both likely contribute in combination to the degradation and progressive failure of large deep-seated landslides when both are present. The results presented illustrate that: i) assessment of slope stability near critical infrastructure, e.g. hydroelectric reservoirs, should not only consider static stability, but also failure mechanisms related to fatigue that evolve over time and may result in an apparently stable slope progressing towards a critical state due to relatively small but repetitive stress changes; and that ii) characterization of fatigue processes affecting a deep-seated landslide requires multi-parametric continuous monitoring at different observation points.

18.10

Seasonal variability of rainfall erosivity across Europe and Switzerland

Simon Schmidt¹, Katrin Meusburger¹, Panos Panagos² & Christine Alewell¹

¹ *Institute for Environmental Geoscience, University Basel, Bernoullistrasse 30, 4056 Basel, Switzerland
(si.schmidt@unibas.ch)*

² *Joint Research Centre of the European Commission, Institute for Environment and Sustainability, Via E. Fermi 2749, 21027 Ispra, Italy*

Modelling soil erosion by water is crucially dependent on rainfall erosivity as a factor considering the erosive effect of rainfall amount and intensity. Widely used soil erosion models like USLE and its revised version RUSLE comprise the rainfall erosivity in form of the R-factor. Past studies commonly work on rainfall erosivity either with low time or spatial resolution of precipitation records as base data (Mikos et al., 2006; Verstraeten et al., 2006). Since a few torrential rainfall events predominantly control the R-factor and therefore soil erosion sediment yields, a high time resolution (60-1min) is required to consider short-term events adequately.

Objectives of recent studies are to establish an European-wide R-factor data base and map (Fig. 1) with time resolution of 30min in a dense network of 1541 gauging stations across Europe (Panagos et al. 2015) and special emphasis on 71 stations in Switzerland (10min resolution) (Meusburger et al. 2012). Beyond the mapping of long-term average R-factor, monthly R-factors are viable to identify seasonal patterns. Even more since monthly R-factors in Switzerland show significant increasing trends.

In aim of this study is to map monthly R-factors and identify its controlling factors across Switzerland. The results will further be discussed in a European context.

Congruent with the results found in Switzerland in almost all European countries (excluding Ireland, United Kingdom and North France), the seasonal variability of rainfall erosivity is high. Even though the spatial pattern varies: in summer the highest R-factor values are observed in the Northern and Central European countries, while for the Southern European countries highest R-factors occur from October to January. Identifying the most erosive season (month) decisively contributes to the mitigation of soil erosion by protecting soil with vegetation coverage and applying appropriate management practices. A “dynamic” RUSLE (considering the variability of vegetation cover and rainfall erosivity) accomplishes a more realistic time-dependent risk assessment and thereby selective erosion control practices and decision making.

The European R-factor map (Fig. 1) identifies lowest factors in Northern Europe (Scandinavia, western UK and eastern Germany) and highest rainfall erosivity in Mediterranean and Alpine regions. High R-factors areas are corresponding to localities with highest frequency of thunderstorms (van Delden 2001). Monthly Swiss R-factors in the months May to October show significant increasing trends within 1988 to 2010 (Mann-Kendall trend test) that correspond to climate change prognosis with the prediction of a reduction in average summer precipitation accompanied by intensified precipitation events for many parts of Central Europe and the Alps. Three out of six months (May, September and October) with increasing tendency correlate to periods of sparse or instable vegetation cover. Increasing soil erosion rates are expected converging rising R-factors and low C-factors (cover management).

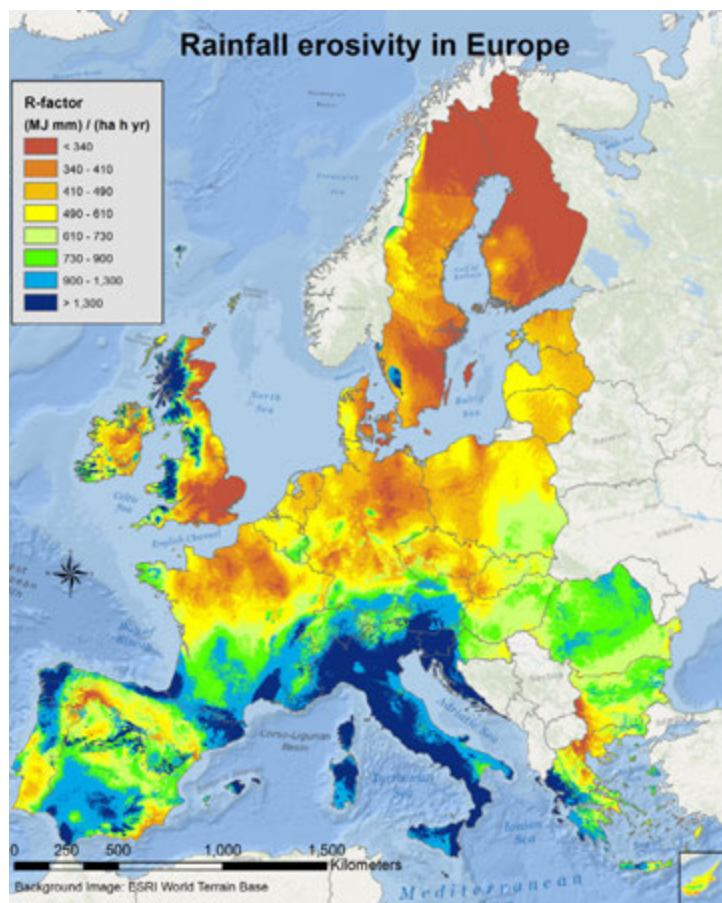


Figure 1. High-resolution (1-km grid cell) map of rainfall erosivity in Europe (time resolution 5-60min) (Panagos et al., 2015)

REFERENCES

- Meusburger, K., Steel, A., Panagos, P., Montanarella, L., and Alewell, C., 2012. Spatial and temporal variability of rainfall erosivity factor for Switzerland. *Hydrology and Earth System Sciences*, 16, 167-177.
- Mikos, M., Jost, D., and Petkovsek, G., 2006. Rainfall and runoff erosivity in the alpine climate of north Slovenia: a comparison of different estimation methods. *Hydrological Sciences Journal*, 51, 115–126.
- Panagos, P., Ballabio, C., Borrelli, P., Meusburger, K., Klik, A., Rousseva, S., Perčec Tadić, M., Michaelides, S., Hrabalíková, M., Olsen, P., Aalto, J., Lakatos, M., Rymaszewicz, A., Dumitrescu, A., Beguería, S., Alewell, C. 2015. Rainfall erosivity in Europe. *Science of the Total Environment* 511, 801-814.
- Van Delden, A., 2001. The synoptic setting of thunderstorms in western Europe. *Atmospheric Research* 56, 89-110.
- Verstraeten, G., Poesen, J., Demaree, G., and Salles, C., 2006. Long-term (105 years) variability in rain erosivity as derived from 10-min rainfall depth data for Ukkel (Brussels, Belgium): Implications for assessing soil erosion rates. *Journal of Geophysical Research - Atmospheres*, 111, 1-11.

P 18.1

Deformation enhanced fluid distribution in the subduction interface: numerical modelling

Liang Zheng¹, Dave May¹, Taras Gerya¹

¹ *Institute of Geophysics, ETH Zurich, Sonneggstrasse 5, 8092 CH-Zurich (liangzh.cug@gmail.com)*

Rock deformation enhanced fluid migration/distribution within the subduction interface is related to many geological/geophysical phenomena, such as serpentinization, tectonic slicing, episodic tremor, interseismic locking, etc. We study the fluid-rock interaction using a 2D hydro-mechanical model with the rock fracturing behavior under the poro-visco-plastic rheology. The math theory, numeric methodology, and numerical results will be shown. Our models generated two typical regimes, which are coupled and decoupled subduction interfaces. Systematic parameter study suggests that the yield stress is the key factor, which controls the faulting processes inside the subduction interface. Fluid content, fluid pore pressure and effective friction are closely related to the coupling and decoupling processes.

REFERENCES

- McKenzie, D., 1984, The generation and compaction of partially molten rock: *Journal of Petrology*, v. 25, no. 3, p. 713-765.
- Stevenson, D. J., and Scott, D. R., 1991, Mechanics of fluid-rock systems: *Annual review of fluid mechanics*, v. 23, no. 1, p. 305-339.
- Dymkova, D., and Gerya, T., 2013, Porous fluid flow enables oceanic subduction initiation on Earth: *Geophysical Research Letters*, v. 40, no. 21, p. 5671-5676.

P 18.2

Long range laserscanning for the Gneiss quarries survey

Alessio Spataro ¹, Marcus Hoffmann¹

¹ *Istituto scienze della Terra (IST), Scuola Universitaria Professionale della Svizzera Italiana (SUPSI), Campus Trevano, CH-6952 Canobbio (alessio.spataro@supsi.ch)*

Geological and geomorphological conditions of the Canton Ticino make it an favourable territory for the natural stone exploitation. In fact, the Canton records numerous historical sites where the stone has been extracted and processed since centuries, mainly for building construction.

Nevertheless, today, to protect the Ticino's environment, there is an urgent need to regulate and plan the quarries for the next decades. A fundamental step in this process is the geometric survey of the sites of exploitation that allows to extract information useful for defining effective strategies for the sustainable development of the sector.

In this context, the Institute of Earth Sciences at SUPSI is conducting Terrestrial Laser Scanning (TLS) surveys of some quarries of type Gneiss in the "Riviera" and "Vallemaggia" valleys. This work aims at testing the long range laser scanning Riegl VZ4000 to support landuse planning.

This scanner combines excellent specifications guaranteeing pure safety (laser class 1).

Relevant technical specifications are:

long range measurements up to 4 km;

high-speed scanning of up to 147,000 points / second;

a scanning range of 60° vertical and 360° horizontal;

the new V-line technology, based on the data acquisition, using reread differentiated signals "echos", which permit the classification of the surface relief even in the presence of obstacles such as vegetation.

The surveys of quarries of type Gneiss are conducted with the laser scanner Riegl VZ4000 from different measurement points that are aligned in post-processing.

The obtained results allow the extraction a series of geometric-dimensional values, like, for example, extracted volumes, storage volumes and terrain profiles. Data used to evaluate quarry management alternatives and ground stability. The laser scanning survey is the base for the interdisciplinary study of the exploitation of stone. Its ability to perform accurate surveys of long range measurements (in the project 1.5 to 4 km) provided tangible benefits to the project results in term of time and accuracy.

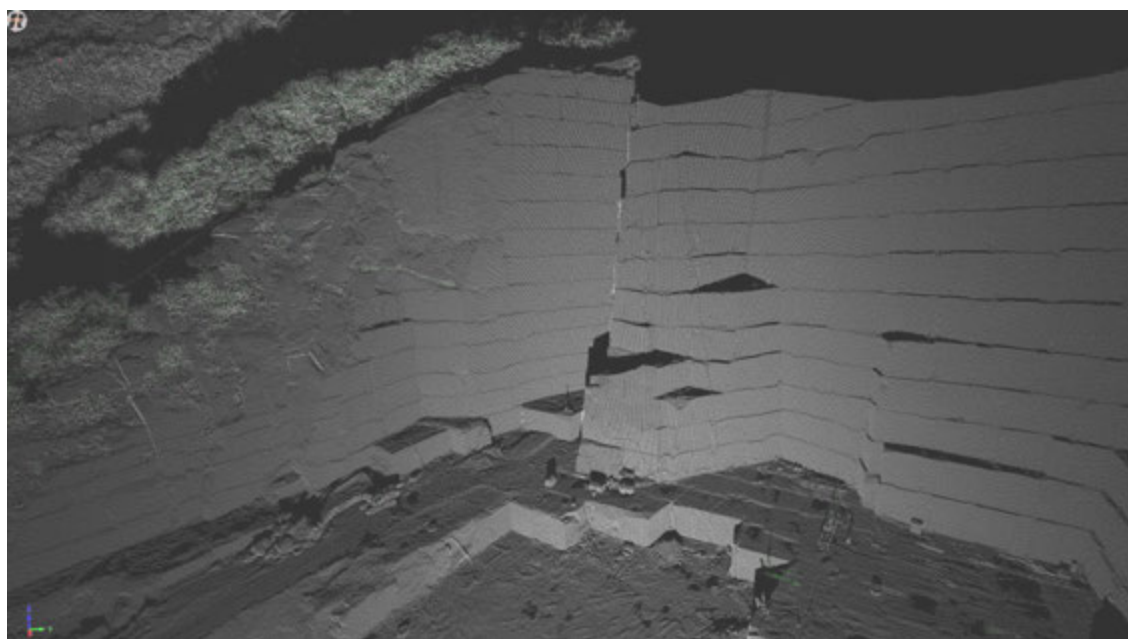


Figure 1. Particular of the scan position in the Lodrino cave